JOURNAL *of* CHROMATOGRAPHY

INTERNATIONAL JOURNAL ON CHROMATOGRAPHY, ELECTROPHORESIS AND RELATED METHODS

VOL. 55 1971

PRINTED IN THE NETHERLANDS

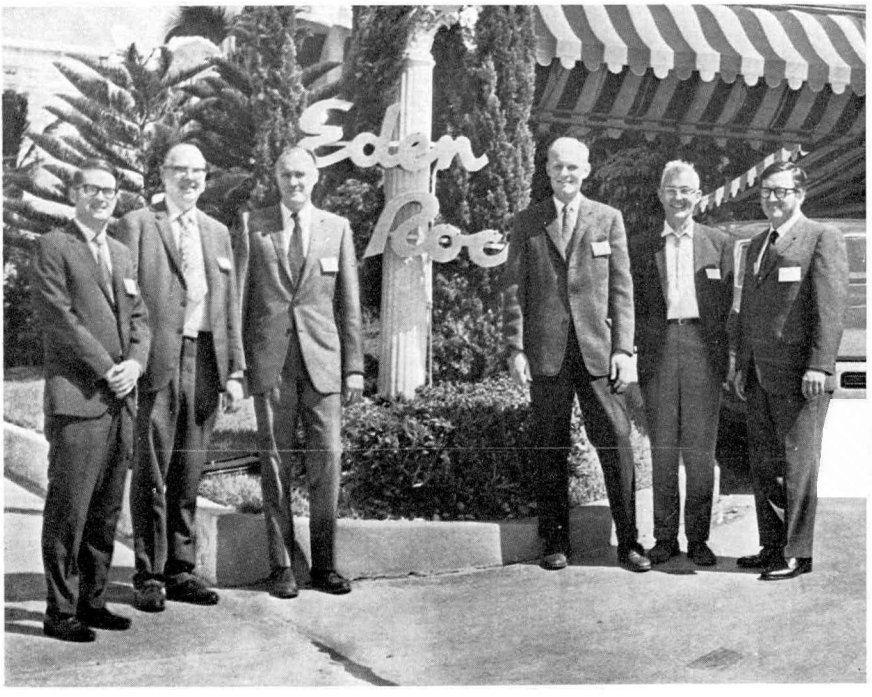

9th INTERNATIONAL GEL PERMEATION CHROMATOGRAPHY SEMINAR

Miami Beach, Florida, October 4–7, 1970

Edited by:

PH. W. ALMQUIST
(Waters Associates, Framingham, Mass.)

M. LEDERER
(Rome)

K. MACEK
(Prague)

The picture shows the principals in the 9th International Seminar on Gel Permeation Chromatography in front of the Eden Roc Hotel at Miami Beach. From left to right: Philip W. Almquist, General Chairman, 9th Seminar; Dr. Fred W. Billmeyer, Jr. — Session Chairman; James L. Waters — President, Waters Associates; Dr. Roger S. Porter — Session Chairman; John C. Moore — Session Chairman; Karl J. Bombaugh — Vice President, Director of R&D, Waters Associates.

9TH INTERNATIONAL GEL PERMEATION CHROMATOGRAPHY SEMINAR, MIAMI BEACH (FLORIDA, U.S.A.), OCTOBER 4–7, 1970.

NINTH INTERNATIONAL GEL PERMEATION CHROMATOGRAPHY SEMINAR

INTRODUCTION

The Ninth International Gel Permeation Chromatography Seminar was held October 4–7, 1970, at the Eden Roc Hotel, Miami Beach, Fla. The Eden Roc is located in the center of the famous Miami Beach resort hotel strip.

Scientists attended the seminar from the U.S.A., Canada and Europe. General plans are for these international seminars to be held alternately inside the U.S.A. and in some other international location. The following seminars were held to date:

1st January, 1965 — Cleveland
2nd September 16–17, 1965 — Boston
3rd May 19–20, 1966 — Geneva
4th May 22–24, 1967 — Miami
5th Summer, 1968 — London
6th October 7–9, 1968 — Miami
7th October 12–15, 1969 — Monaco
8th July 1–3, 1970 — Prague

The main program for the Ninth Seminar consisted of 34 technical papers given in five Technical Sessions. Each technical session was directed to a specific area or type of interest in gel permeation chromatography. The papers were grouped in the following five major topical areas:

1. Practical applications of gel permeation chromatography:

Most of these papers were devoted to problems in product development, product improvement, and quality control.

2. Calibration techniques:

In this session, presentations were made concerning refinements to existing techniques and new methods of simplifying calibration of gel permeation chromatography instrumentation.

3. Gel permeation chromatographic instrumentation and column packing materials:

Here, some evaluations of new and old packing and materials were given and new instrumentation discussed. Some interesting, possible future developments were also presented.

4. Computations in gel permeation chromatography:

This session consisted mainly of discussion of methods and hardware for processing and interpreting data obtained from gel permeation chromatographs.

5. Research studies, general considerations in gel permeation chromatography:

The last session was directed to studies on the gel permeation phenomenon itself, studies of the instrumentation and basic research studies on some specific materials.

The full technical program is given on pp. 2 and 3.

Technical session I

GPC of silicones	Fred N. Larsen Bendix Corp.
GPC analysis of plasticizer blends	Morgan R. Hallwachs, H. E. Hanson, W. E. Link, N. S. Salomons, C. R. Widder Ashland Chemical Company
GPC and polymer additive systems	Jesse M. Howard General Electric
The use of GPC in the development of high-quality graphite	J. M. Dickinson, E. M. Wewerka University of California, Los Alamos Scientific Laboratory
Chemical heterogeneity and composition of a modified poly(ethylene terephthalate)	Anthony L. Spatorico, O. E. Schupp, A. S. Marshall Eastman Kodak Company
Applications of GPC in the manufacture of epoxy-glass printed circuit laminates	E. A. Eggers, J. S. Humphrey, Jr. IBM Corp.
GPC investigation of irradiated copolymers	Edward C. Ferlauto Mobil Chemical Co.

Technical session II

GPC. II. Ana-Prep GPC fractionation and characterization of poly(methyl-methacrylate) for calibration in 2,2,2-Trifluoroethanol	Theodore Provder, James H. Clark, Esmond E. Drott Monsanto Company
Practical GPC column calibration for polymers	M. Zinbo, J. L. Parsons Ford Motor Company
Examination of polymer size parameters for universal calibration in GPC	J. V. Dawkins, J. W. Maddock, D. Coupe Imperial Chemical Industries Ltd.
GPC calibration for polymers making use of the universal calibration curve	M. C. Morris Goodyear Tire & Rubber Co.
Molecular weight analysis of block copolymer by GPC	F. S. C. Chang Borg-Warner Corporation
GPC elution behavior of branched alkanes	W. W. Schulz Esso Research
Preparative liquid chromatography	J. L. Waters Waters Associates

Technical session III

The effect of temperature on GPC separations	James N. Little, William J. Pauplis Waters Associates
Separation by flow and its application to GPC	E. A. DiMarzio, C. M. Guttman National Bureau of Standards

Applications of vinyl acetate gels	H. Bayer, D. Randau E. Merck oHG
Recent developments in GPC instrumentation	H. Felton, K. J. Bombaugh, R. Levangie Waters Associates
Precision improvements in GPC determinations of molecular weight averages and polydispersities of polymers	B. E. Hudson Esso Research
A comparative study of Porasil and Styragel as column supports for GPC	Jeanne M. Pacco Xerox Corp.

Technical session IV

An analysis of skewing in GPC chromatograms	T. Ishige, S. I. Lee, A. Hamielec McMaster University
GPC: Data treatment	J. A. May, Jr., G. W. Knight Dow Chemical Company
The use of fast, finite, Fourier transforms for the solution of Tung's equation. II. Theory and application	T. Vladimiroff Picatinny Arsenal
The instrument spreading correction in GPC. III. The general shape function using singular value decomposition with a nonlinear calibration curve	Edward M. Rosen Monsanto Co. Theodore Provder SCM Corp.
Characterization of low-molecular-weight difunctional polybutadienes	G. Perrault, M. Tremblay Defence Research Bd., Canada
GPC data acquisition with the PDP-8/I and AXO8 laboratory peripheral	L. D. Moore, Jr., J. R. Overton Tennessee Eastman Co.
Solution of Tung's axial dispersion equation by asymptotic search methods	S. I. Lee, T. Ishige, A. E. Hamielec McMaster University

Technical session V

GPC study of furfuryl alcohol resins	B. A. Petro, J. B. Barr, S. B. Walton Union Carbide Corp.
GPC: Diffusional phenomena in dilute polymer solutions flowing in capillaries	A. C. Ouano, J. A. Biesenberger IBM Corp.
Structural evaluation of copolymers using preparative GPC	A. Barlow, L. Wild, T. Roberts U.S. Industrial Chemicals
Some velocity profile effects in empty tubes	M. Hess, J. W. Tierney Koppers Co.
Application of GPC to studies of the functionality distribution of carboxy- and hydroxy-polybutadienes	Ronald D. Law Thiokol Chemical Co.
The application of preparative GPC to polyurethane foam technology	G. K. Baker Bendix Corp.
Causes of skewed molecular weight distributions in GPC separation of nylon resins	E. K. Walsh Allied Chemical Corp.

Session chairmen this year were Dr. FRED W. BILLMEYER, Jr., Professor of Analytical Chemistry of Rensselaer Polytechnic Institute, Troy, N.Y.; Dr. ROGER S. PORTER, Head, Polymer Science & Engineering, University of Massachusetts, Amherst, Mass. and Mr. JOHN C. MOORE, Basic Research Division, Dow Chemical Company, Freeport, Texas.

In addition, an introductory course in gel permeation chromatography was given on the day prior to the start of the technical sessions. This was intended to familiarize those new to the subject with general gel permeation chromatography. It was conducted by Dr. JAMES N. LITTLE and Mr. WILLIAM A. DARK of Waters Associates and contained such topics as:

1. Mechanism of separation
2. Discussion of theory, terminology
3. Calibration
4. GPC packings, solvents
5. GPC operating parameters
6. Applications — curve interpretation

A separate session was held after the technical session covering GPC instrument minor repair and preventive maintenance. This was conducted by JOHN SARRUDA of Waters Associates.

A new feature of the seminar was a "split session" on the first day of the technical session. Thus, a session was held in the morning; the afternoon was left free for informal discussions or elected activities and the second technical session was held in the evening.

Another feature of this seminar was an exhibition of a complete range of instrumentation for gel permeation chromatography. Photographs below show some informal scenes in the exhibit area.

In summary, the Seminar served as a forum for a broad range of work now being done by gel permeation chromatographers. It also gave some initial instruction in the practice of gel permeation chromatography and exhibited and discussed gel permeation chromatographic instrumentation both from an operational and a maintenance point of view.

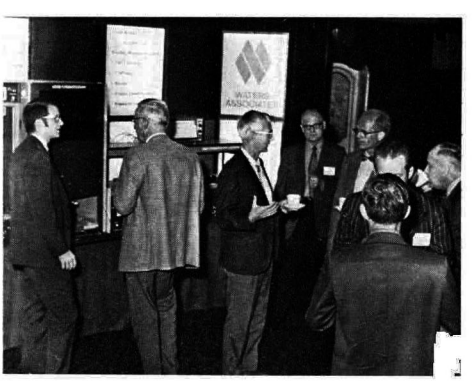

CHROM. 5116

CHEMICAL HETEROGENEITY AND COMPOSITION OF A MODIFIED POLY(ETHYLENE TEREPHTHALATE)

A. L. SPATORICO, O. E. SCHUPP AND A. S. MARSHALL
Research Laboratories, Eastman Kodak Company, Rochester, N.Y. 14650 (U.S.A.)

SUMMARY

A series of samples of a modified poly(ethylene terephthalate) has been characterized by gel permeation chromatography, ultraviolet spectrophotometry, differential thermal analysis, and nuclear magnetic resonance techniques. These samples were prepared in the melt phase by reaction of dimethyl terephthalate, ethylene glycol, 1,4-butanediol, and an ultraviolet absorbing monomer, dimethyl Z.

To determine if there were heterogeneity in composition as a function of molecular weight, samples were fractionated by preparative scale gel permeation chromatography, and selected fractions were analyzed by ultraviolet spectrophotometry. The composition was found to be relatively constant over the bulk of the distribution; however, the very low-molecular-weight region is appreciably richer in moiety Z. A portion of one of the samples, of *ca.* 1000 (polystyrene equivalent molecular weight), was submitted for mass spectral examination and found to be a mixture of cyclic dimers of moiety Z and the glycols.

The glass transition temperature of the highest molecular weight fraction from the preparative gel permeation chromatography fractionation had the same value (within experimental error) as that of the bulk polymer. This is interpreted as indicating (1) the cyclic dimer material does not act as a plasticizer lowering the glass transition temperature, (2) there is no dependence of glass transition temperature on molecular weight, and (3) no major variation exists in the glycol composition with molecular weight.

Two samples of this polymer were prepared using the same monomer feed ratios, temperature, catalyst, etc. These samples were found to have approximately the same viscosity and molecular weight distributions; however, their glass transition temperatures differed by *ca.* 10°. This difference was interpreted as indicating that one sample contained more butanediol than expected from the monomer feed concentration. This postulate was confirmed by nuclear magnetic resonance measurements on the bulk samples.

CHROM. 5117

GEL PERMEATION CHROMATOGRAPHY ANALYSIS OF PLASTICIZER BLENDS

M. R. HALLWACHS, H. E. HANSON, W. E. LINK, N. S. SALOMONS AND C. R. WIDDER
Ashland Chemical Co., Division of Ashland Oil, Inc., Bloomington, Minn. 55420 (U.S.A.)

SUMMARY

Plasticizer blends and components were analyzed using the technique of gel permeation chromatography. A technique is described for the identification of the plasticizer components and a method is given for obtaining the relative weight percent of each component in the blend.

INTRODUCTION

Gel permeation chromatography (GPC) permits size separations of polymers[1-4]. This technique has been applied to the separations of small molecules and low-molecular-weight polymers[5-9]. Blends of monomeric and polymeric plasticizers were separated by GPC. The components present in the blends were identified by comparing their peak elution volumes with those of known plasticizer standards. Relative weight percentage determinations of each component were obtained through a comparison of peak elution deflections.

EXPERIMENTAL

The blends and components were analyzed with a Waters Associates gel permeation chromatograph, Model 200. The gel permeation chromatograph operated at ambient temperature using tetrahydrofuran (THF) for the solvent with a flow rate of 1 ml/min. The samples were injected using an automatic sample injection system at a maximum weight concentration of 0.25 % in THF. The separations were performed with two Styragel column banks of 10^5, 10^4, 10^3, 60 and 100, 100, 60, and 60 Å porosities. The columns were checked for adsorption of polar molecules by injecting organic acids to detect any distortion in the chromatograms[10]. The 10^5, 10^4, 10^3, and 60 Å porosity column bank was calibrated using polystyrene standards supplied by Waters Associates for evaluation of the polymer component. The criteria for the selection of the ester, epoxy, and polyester components for investigation were their plasticizing functionality, commercial supply, and price.

Peak elution volumes of known standards were obtained (Fig. 1) and related to their molecular weight or chain lenth (Tables I and II). Elution volume reproducibility was checked with two plasticizers as shown in Table III. Since some components

had similar elution volumes, the 100, 100, 60, and 60 Å porosity column bank was used to enhance the separation of the low-molecular-weight components. The separating efficiency was evaluated using a blend of 2 esters as shown in Fig. 2. However, since the separation was not significantly improved, the 10^5, 10^4, 10^3, and 60 Å porosity column bank was used in all subsequent work. Further, the use of this latter column bank system permits the determination of weight average chain length ($\bar{A}_w$), number average chain length ($\bar{A}_n$), and peak elution volume of a polyester. The polyester's polydispersity (Table II) was narrow enough to relate peak elution volume to chain length.

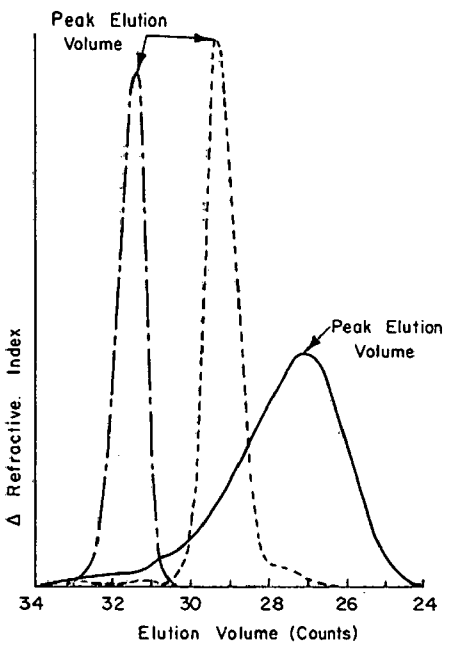

Fig. 1. Peak elution volume. Columns: 10^5, 10^4, 10^3, and 60 Å. Solvent: THF. Temperature: ambient. Concentration: 0.10 g/100 g solution for ester and epoxy; 0.25 g/100 g solution for polyester. ———, Polyester; —·—·—, ester; – – – –, epoxy.

Analysis of the polyester component shows low-molecular-weight material eluting in the elution volume range of the epoxy and ester standards as shown in Fig. 3. Very few polyesters of the large number analyzed exhibited large deflections in the overlapping area; therefore, it was possible to detect additional esters and/or epoxies as a result of deviation from the normal polyester distribution curve (Fig. 4).

A correlation was sought between the relative amount of each plasticizer component and peak deflection heights through an analysis of known mixtures. Table IV shows the results of the study.

DISCUSSION

The chromatograms of the esters exhibited symmetrical distributions, except for tributyl citrate which gave two peaks. The presence of monomeric plasticizers in

TABLE I

PEAK ELUTION VOLUMES AND MOLECULAR WEIGHTS OF STANDARDS

Standards	*Molecular weight*[a]	*Peak elution volume (counts)*
Dimethyl phthalate	194	34.50
Dibutyl phthalate	278	32.67
Butyl benzyl phthalate	312	32.67
Butyl cyclohexyl phthalate	304	32.86
Diphenyl phthalate	318	32.75
Dioctyl phthalate	390	31.68
Diisooctyl phthalate	391	31.67
Dinonyl phthalate	419	31.50
Dinoctyl *n*-decyl phthalate	419	31.42
Diisodecyl phthalate	446	31.25
Diundecyl phthalate	474	31.00
Ditridecyl phthalate	530	30.75
Trioctyl trimellitate	546	30.69
n-Octyl *n*-decyl trimellitate	582	30.33
Dioctyl adipate	370	31.50
Didecyl adipate	426	31.25
Diisodecyl adipate	426	31.00
Dioctyl azelate	413	31.00
Tributyl citrate	360	31.58 and 32.92
Dibutyl sebacate	314	31.83
Dioctyl sebacate	426	31.00
Tricresyl phosphate	368	32.41
Epoxidized tallate	530	31.02
Expoxidized soybean oil	1000	29.31
Expoxidized linseed oil	1120	29.04

[a] *Modern Plastics Encyclopedia 1967*, Vol. 44, No. 1A, 1966, McGraw-Hill, New York, N.Y.

TABLE II

PEAK ELUTION VOLUMES AND MOLECULAR PARAMETERS OF POLYESTER STANDARDS

Standards	$\bar{A}_w$	$\bar{A}_n$	$\bar{A}_w/\bar{A}_n$	*Peak elution volume*
Polyester No. 1	47.7	37.2	1.28	29.31
Polyester No. 2	78.3	54.1	1.45	28.15
Polyester No. 3	117	70.8	1.65	27.23
Polyester No. 4	131	78.1	1.68	27.08
Polyester No. 5	152	71.3	2.13	26.62
Polyester No. 6	184	116	1.59	26.54
Polyester No. 7	294	146	2.01	25.77

TABLE III

PEAK ELUTION VOLUME REPRODUCIBILITY

Compound	*Peak elution volumes*
Dioctyl phthalate	31.83, 31.65, 31.67, 31.68, and 31.68
Trioctyl trimellitate	30.75, 30.69, and 30.69

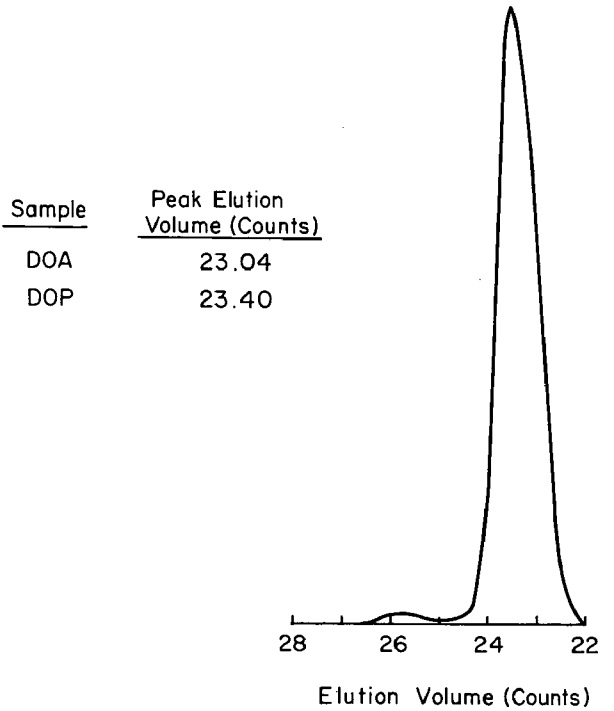

Fig. 2. Column separating efficiency. Column: 100, 100, 60, and 60 Å. Solvent: THF. Temperature: ambient. Concentration: 0.125 g/100 g solution. Sample: dioctyladipate (DOA)/dioctyl phthalate (DOP).

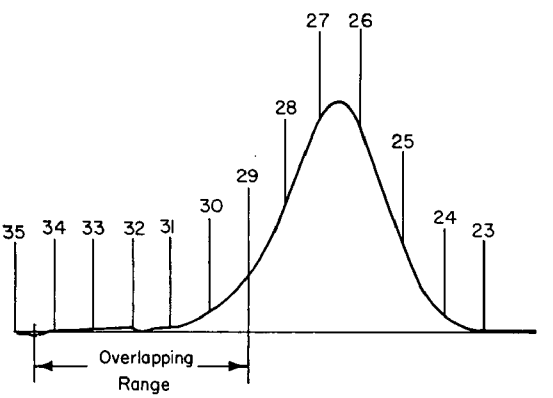

Fig. 3. Polyester elution range. Column: 10^5, 10^4, 10^3 and 60 Å. Solvent: THF. Temperature: ambient. Concentration: 0.25 g/100 g solution.

a blend was readily discernible due to the characteristic sharpness of their distribution curves. However, their chemical identification by GPC is difficult since esters of different chemical families have similar elution volumes, as shown in Fig. 5. The data in Table III show that small variations occur in elution volumes which lead to further difficulties in identifying components. These variations arise from aging of columns,

solvent pressure changes, and solvent flow changes. Such variations were corrected by injecting a known standard with the blends, and the standard's elution volume was then compared with elution volumes previously obtained.

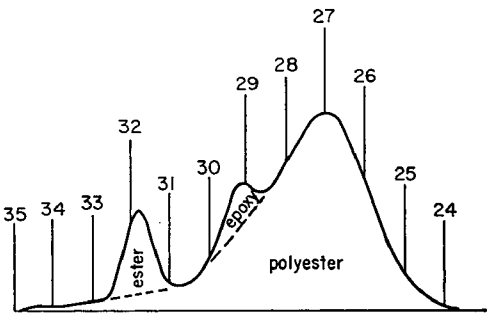

Fig. 4. Chromatograph of plasticizer blend. Column: 10^5, 10^4, 10^3, and 60 Å. Solvent: THF. Temperature: ambient. Concentration: 0.25 g/100 g solution.

TABLE IV

QUANTITATIVE ANALYSIS OF BLENDS

Blend	*Column*	*Known weight percentage*	*Experimental weight percentage*
Polyester	10^5, 10^4, 10^3	89	77
Diisodecyl phthalate	and 60 Å	4	10
Epoxidized linseed oil		7	13
Polyester	10^5, 10^4, 10^3	93	87
Epoxidized linseed oil	and 60 Å	7	13
Polyester	10^5, 10^4, 10^3	85	63
Diisodecyl phthalate	and 60 Å	8	25
Expoxidized linseed oil		7	12
Polyester	10^5, 10^4, 10^3	85	62
Dioctyl phthalate	and 60 Å	8	12
Epoxidized linseed oil		7	26
Dioctyl adipate	100, 100, 60	50	No separation
Dioctyl phthalate	and 60 Å	50	
Dioctyl adipate	100, 100, 60	50	No separation
Diisodecyl phthalate	and 60 Å	50	
Diisodecyl phthalate	100, 100, 60	50	45
Epoxidized linseed oil	and 60 Å	50	55
Dioctyl phthalate	100, 100, 60	50	42
Epoxidized linseed oil	and 60 Å	50	58

Fig. 2 shows that identification of the ester by GPC is not unequivocal, but many esters can be eliminated by comparison of peak elution volumes as shown in Table I. The remaining possibilities can be further narrowed through the consideration of the application and cost of the plasticizer blend. Finally, the suspected components can be subjected to the classical analytical method for identification.

The higher-molecular-weight epoxy components were easy to separate from the

esters, but they also eluted in the elution range of the polyester component as shown in Fig. 4. Recognition of this component was relatively easy in a blend, and the identification was not difficult as the only three epoxidized materials considered had widely different elution volumes.

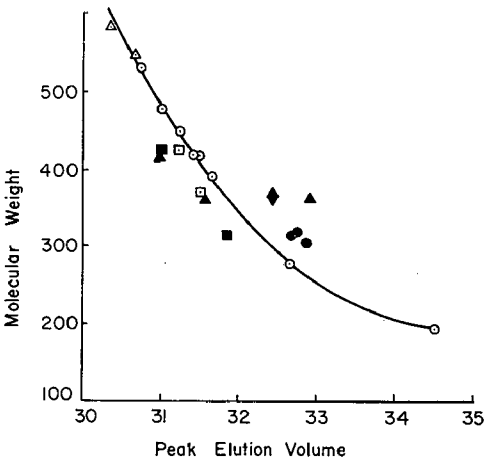

Fig. 5. Peak elution volume. ⊙, Aliphatic phthalates; ●, aromatic and cyclic phthalates; △, trimellitates; ▲, citrates; ⊡, adipates; ■, sebacates; ◆, phosphate.

The polyester component exhibits a distribution curve typical of most polymers. The $\bar{A}_w$ and $\bar{A}_n$ of the polyester, taken from Table II and supplemented with chemical identification, can help in the identification of the particular polyester.

Attempts to obtain relative amounts of each component in a blend were not successful using the method of peak height deflection (Table IV). This discrepancy is due to a combination of factors which include differences in refractive index of each component, determination of a base line, and the preparation of a blend on a weight basis instead of a molar basis.

CONCLUSION

The gel permeation chromatograph was used to separate and aid in the identification of esters, epoxies and low-molecular-weight polyesters in plasticizer blends through a comparison of elution volumes with elution volumes of known standard components. To test the validity of the procedure, known blends were prepared and analyzed by GPC. Attempts were made to obtain relative amounts of each component by comparing elution heights of the component.

GPC is useful in the separation of plasticizer blends and yields information which helps the analytical chemist in the characterization of the plasticizer. Furthermore, the technique makes it possible for the chemist to eliminate certain combinations from consideration and alerts him to the presence of blends and minor components.

REFERENCES

1 J. C. MOORE, *J. Polym. Sci.*, A2 (1964) 835.
2 J. C. MOORE AND J. G. HENDRICKSON, *J. Polym. Sci.*, C (1965) 233.
3 J. C. MOORE AND M. C. ARRINGTON, *Intern. Symp. Macromol. Chem., Tokyo and Kyoto, 1966.*
4 J. C. MOORE AND M. C. ARRINGTON, *Proc. 3rd Intern. Seminar Gel Permeation Chromatography, Geneva, 1966.*
5 J. CAZES AND D. R. GASKILL, *Proc. 4th Intern. Seminar Gel Permeation Chromatography, Miami Beach, 1967.*
6 J. CAZES AND D. R. GASKILL, *Proc. 6th Intern. Seminar Gel Permeation Chromatography, Miami Beach, 1968.*
7 J. G. HENDRICKSON, *Anal. Chem.*, 40 (1968)49.
8 J. G. HENDRICKSON AND J. C. MOORE, *J. Polym. Sci.*, A4 (1966) 167.
9 B. M. RUSHTON AND N. S. SALOMONS, *J. Appl. Polym. Sci.*, 13 (1969) 2341.
10 R. M. SCREATON AND R. W. SEEMANN, *Intern. Symp. Polymer Characterization, Columbus, 1967.*

CHROM. 5118

GEL PERMEATION CHROMATOGRAPHY AND POLYMER ADDITIVE SYSTEMS

J. M. HOWARD III
General Electric Company, AP 5-249, Appliance Park, Louisville, Ky. 40225 (U.S.A.)

SUMMARY

Chromatograms obtained on solvent extracts of polymer systems can be used to identify the vendor of the polymer in much the same manner as absorption spectra are used to identify the base polymer. The chromatogram in its entirety is compared to reference chromatograms obtained on similar extracts of known polymers from known vendors. The individual components can be identified by comparison of the individual peaks to chromatograms of known compounds. The same procedure can be used to follow depletion of additive components during environmental testing and/or field exposure by determining peak heights or peak areas. Quantitative determination of additives can be made by either or both of the above measurements. Chromatograms of the additive systems in several commercially available polymer compounds are shown along with quantitative calibrative curves for various additive components. Chromatograms illustrating the effects of processing and environmental conditioning on additive concentrations are also presented.

INTRODUCTION

Since its introduction by MOORE[1] gel permeation chromatography (GPC) has become a "laboratory word" in those laboratories engaged in the analysis and characterization of polymeric compounds. One normally associates GPC with the determination of molecular weight distributions (MWD), however the technique has been used successfully to separate the components of complex mixtures for subsequent identification by other means. BARTOSIEWICZ[2] has used it in the analysis of coating systems, LARSON[3] used it for the analysis of epoxides and SPELL[4] used GPC and infrared spectrophotometry in the separation and identification of the components in complex organic mixtures.

This paper illustrates how the chromatograms obtained on extracted polymer additive systems can be used in the identification of the commercial supplier of the polymer compound as well as in the identification of the individual components of the additive system. Chromatograms obtained in the same manner can be used in the evaluation of antioxidant and plasticizer systems during processing and/or environmental exposure. The chromatogram in its entirety is used, much like absorption spectra, to identify an additive system indicative of a particular supplier. The elution

volumes or count numbers of the individual peaks are used to identify the components and the peak area and/or height is used in determining the concentration of the components.

The additive system incorporated into a polymer should be carefully selected to give the best performance in the environment to which the finished product will eventually be exposed. This means that the supplier of polymeric compounds might use the same base resin for various end uses, changing only the additive system in order to meet specific requirements. It also means that the manufacturer of formed plastic parts probably inventories several types of polymer, differing only in the additive system. Screening a polymer-additive formulation for a specific end use can take up to a years' testing under environmental conditions. It is necessary, therefore, to insure that the parts being tested do contain the proper additive system and that the effects of the exposure on the system can be meaningfully monitored.

The normal procedure for monitoring such a system, if it can indeed be monitored, is to extract the additives from the sample and measure the concentration of the extracted components by appropriate instrumental techniques. This procedure is not only time consuming but in many cases just does not do the job. Additive systems can, and do, contain several components which cannot be individually determined or measured in such a procedure. The chromatographic procedure described herein allows one to analyze most additive systems in a rapid and straightforward manner.

EQUIPMENT

The equipment consists of a Waters Associates' Model 100 gel permeation chromatograph unit operated at room temperature (*ca.* 30°) using tetrahydrofuran (THF) at a flow rate of 2 cc/min. Nine 4-ft. stainless steel GPC columns packed with Poragel A-1 were used in the study. The columns were packed in this laboratory by filling with a THF–Poragel slurry (previously swollen in THF for a minimum of 24 h). The column to be packed was placed in an upright position, a vacuum applied to the lower end and the slurry slowly poured in the top. The column was constantly vibrated during the packing procedure. The nine columns in series have an interstitial volume of 100 ml (40 counts). The plate count for this system was calculated to be 460 using 1 % trichlorobenzene in THF and a 10-sec injection time. The molecular weight exclusion limit for Poragel A-1 is 1000.

EXPERIMENTAL

Reference chromatograms are obtained on additive systems of polymers received from known suppliers. For qualitative work the sample is cut into pea-size pieces, just covered with degassed solvent and allowed to stand overnight. For quantitative analyses the sample is preferably ground in a Wiley mill to pass a 20 mesh screen and 10 g of the powder is extracted with 20 ml of degassed THF overnight. Two milliliters of the extract is injected onto the columns. The sensitivity of the instrument is normally set at 2 ×.

Calibration curves (Fig. 1) for known compounds are made by plotting peak heights and/or peak areas, taken from chromatograms run on solutions of known

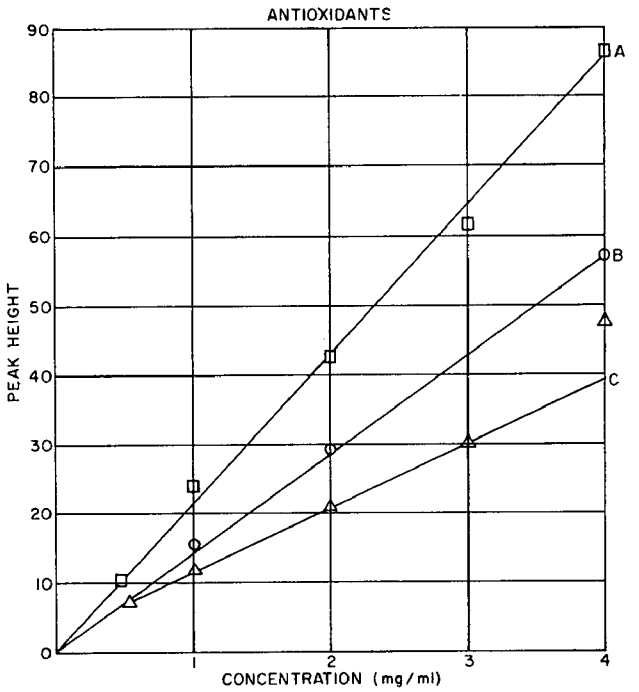

Fig. 1. Antioxidant calibration curve.

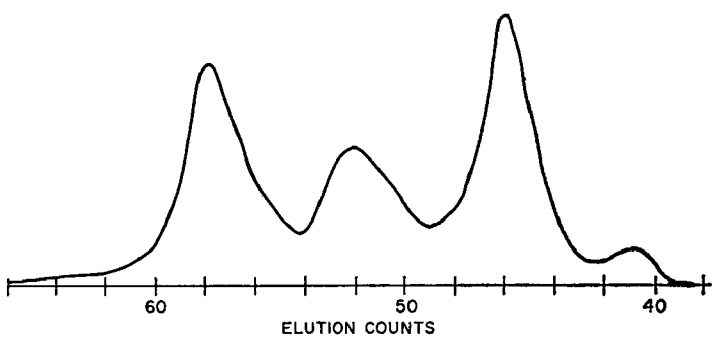

Fig. 2. Chromatogram of polymer A extract.

concentrations, against the concentration. Correlation charts showing different additive components and their elution volumes, or counts, can be made to facilitate the identification of additives in unknown polymers. Such charts are valid only for a specific set of columns and must be used with discretion.

Identification of suppliers

Figs. 2–5 show chromatograms obtained on the THF extracted additive systems in four commercial polypropylenes. One can see from these chromatograms that there

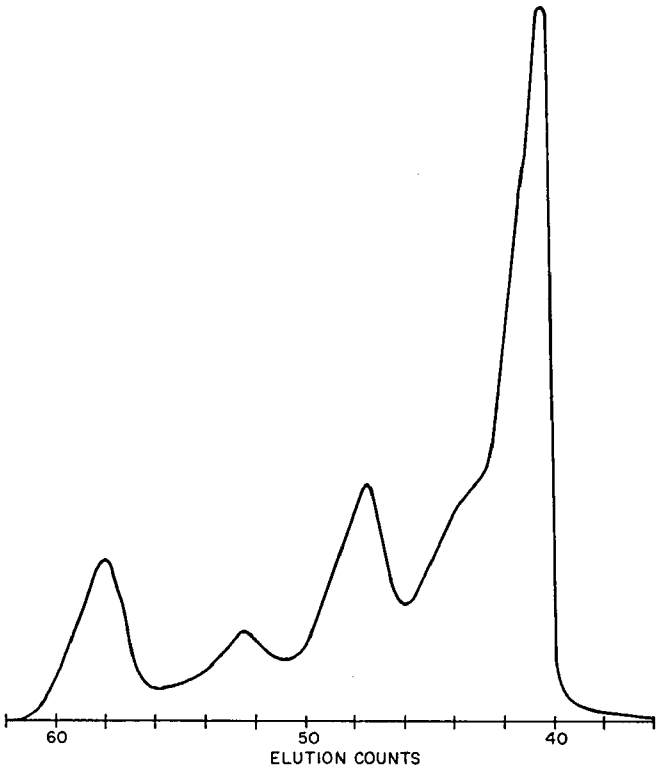

Fig. 3. Chromatogram of polymer B extract.

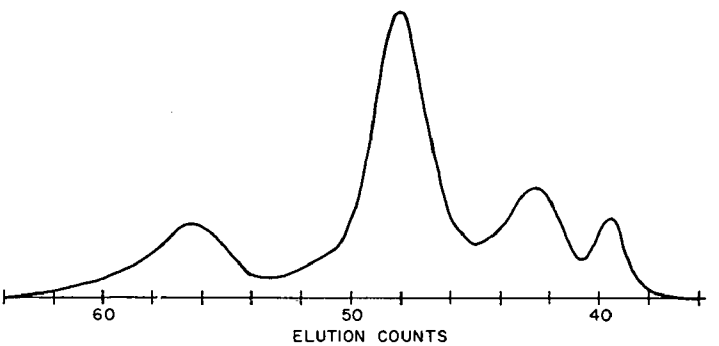

Fig. 4. Chromatogram of polymer C extract.

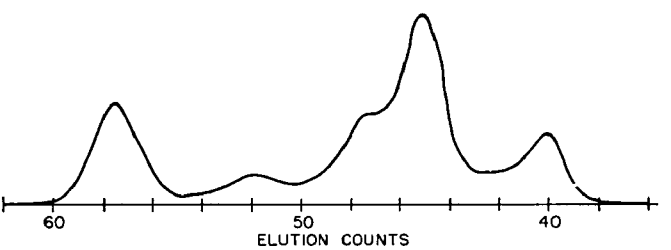

Fig. 5. Chromatogram of polymer D extract.

are significant differences in the additive systems which can be used as a basis for identification. Chromatograms such as these have been obtained on more than twenty commercially available polypropylenes and so far no two have had the same system. There is no rule of course saying that two or more suppliers cannot use an identical additive system. Should such a situation arise one would have to explore other techniques of identification before making a final decision. These other techniques might

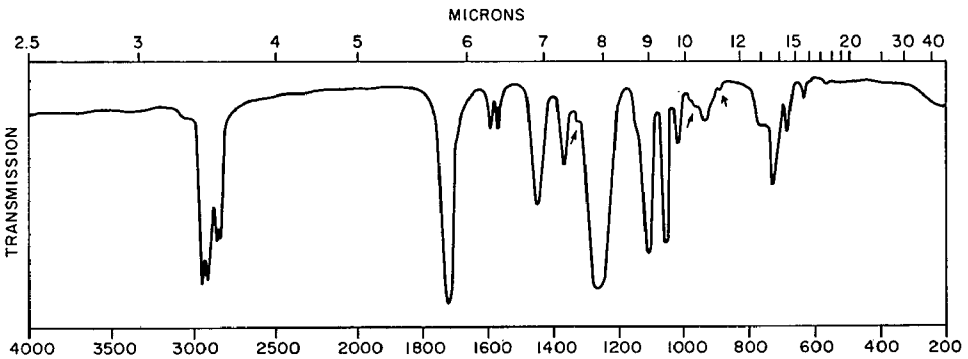

Fig. 6. PVC plasticizer system.

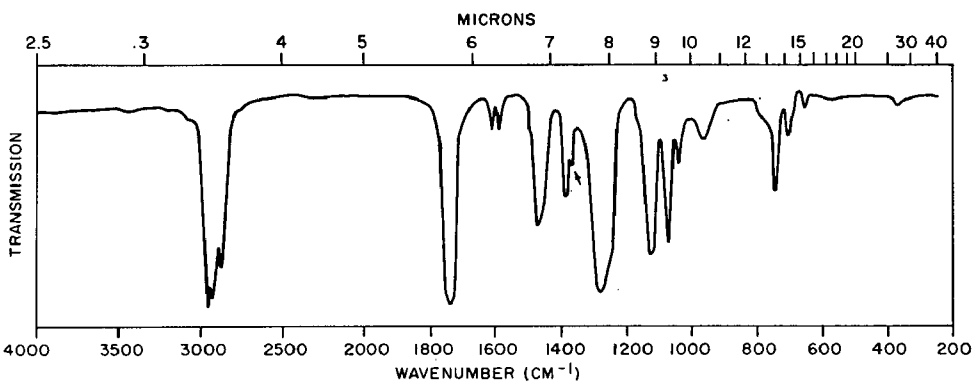

Fig. 7. PVC plasticizer system.

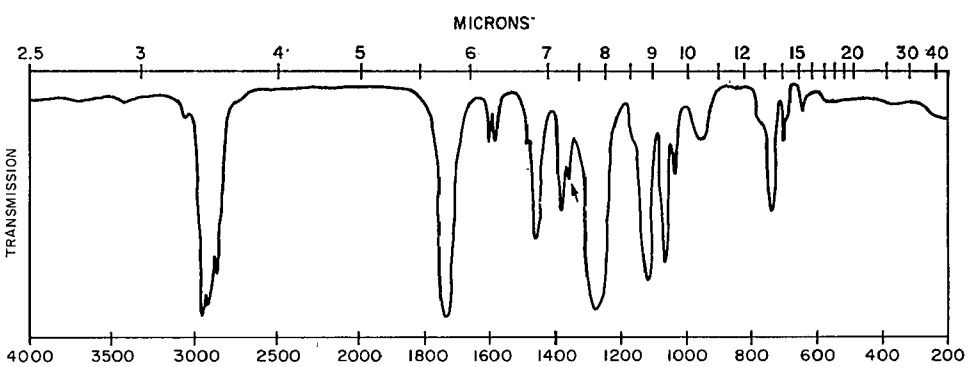

Fig. 8. PVC plasticizer system.

include analysis for catalyst residues, MWD etc. A thorough investigation of the sample history would certainly be helpful. In any event the chromatogram would have narrowed the search to two or three possibilities.

Figs. 6–8 show the infrared (IR) spectra of plasticizer systems extracted from poly(vinyl chloride) compounds supplied by different vendors. There are differences in these spectra (indicated by arrows) which might be used in distinguishing between them, however, after exposure to field environment these differences are often masked

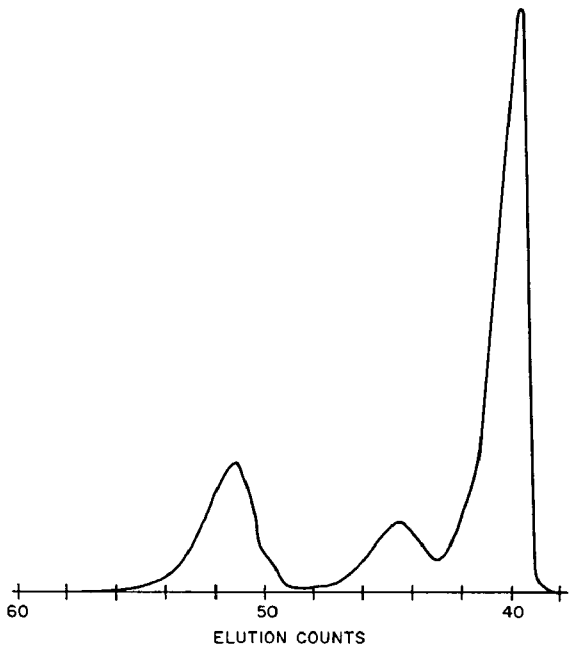

Fig. 9. Plasticizer from supplier A.

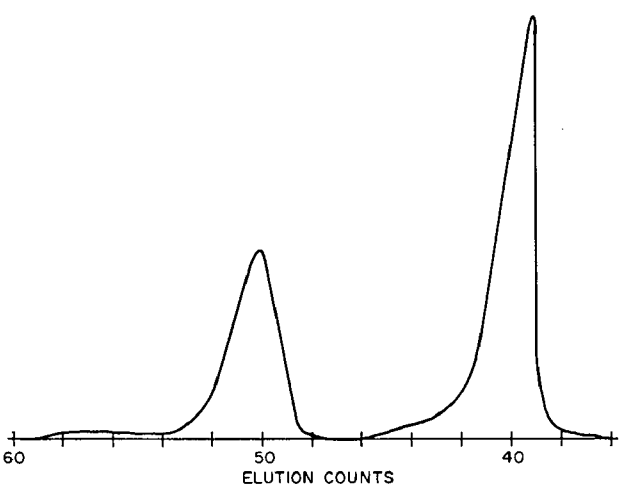

Fig. 10. Plasticizer from supplier B.

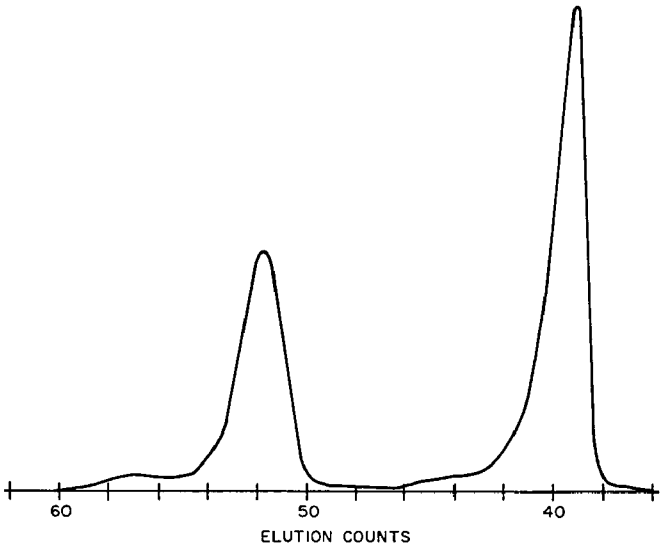

Fig. 11. Plasticizer from supplier C.

by contaminants or have actually vanished. Figs. 9, 10 and 11 show the chromatograms of these same three systems. It is quite obvious from these figures that there are indeed very significant differences in the compounds. The peak at 40 counts is PVC resin; the other peaks are plasticizer components. The IR spectra indicated the plasticizers to be phthalic acid derivatives, but it would be difficult to detect the second component in Fig. 9 (*ca.* 44 counts). IR analyses of GPC fractions show the phthalate in Figs. 9 and 10 to be di-isodecyl phthalate (50.3 counts) and in Fig. 11 to be di-octyl phthalate (52.3 counts). The second component in Fig. 9 is an epoxy derivative.

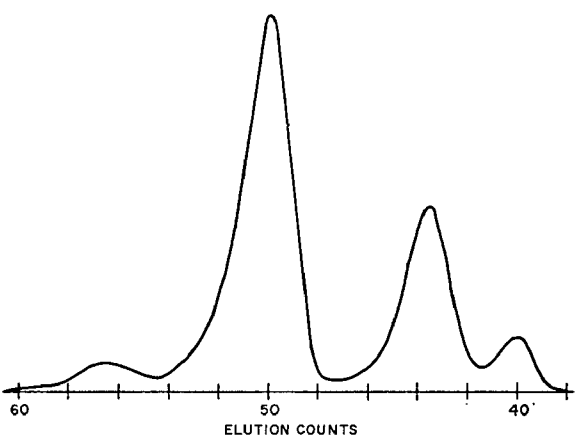

Fig. 12. PVC plasticizer system before exposure.

The procedure followed in our laboratory now for the identification of such plasticizer systems would be to determine by IR analysis that a phthalate system is present. A chromatogram would then be obtained on the extract and the identity of the specific phthalate would be determined by its elution count. The GPC fractions would be collected for subsequent positive identification by IR.

Environmental effects

Figs. 12–14 show one of the plasticizer systems previously discussed after various periods of environmental exposure. Perhaps the most interesting point here is not the decreasing phthalate peak (50.3 counts) but the increasing epoxy derivative peak at 43.5 counts. Calculations have shown that the increase in epoxy content of the sample cannot be attributed to the increase in PVC resin required to offset the phthalate ester loss. It is assumed from this information that the epoxy derivative is migrating to the phthalate-poor areas during exposure. Information such as this is invaluable in helping to choose the most satisfactory materials and designs for functional parts in consumer destined products.

Other additive systems can be followed in the same manner.

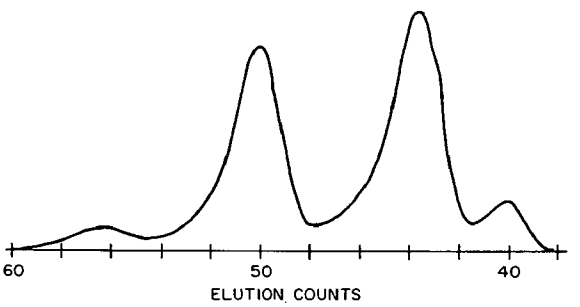

Fig. 13. PVC plasticizer system after short exposure.

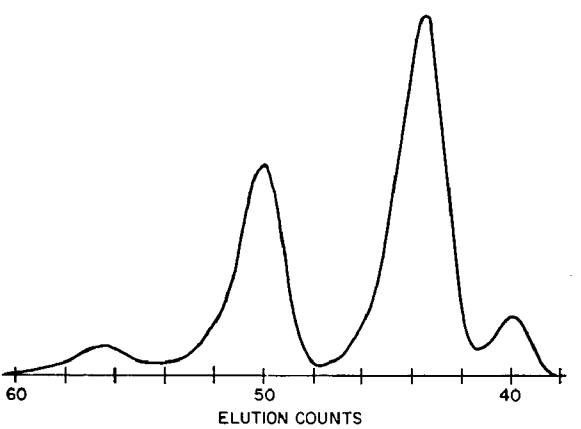

Fig. 14. PVC plasticizer system after long exposure.

Effects of processing

Figs. 15–17 show the effects of processing on a four component stabilizer system. Fig. 15 shows the chromatogram of the virgin material. The peaks are labeled as A, B, C and D. Fig. 16 shows the chromatogram of the same system after a short exposure to processing conditions. Peak "B" is diminishing whereas peaks A, C and D remain unchanged. In Fig. 17, peak "B" has almost completely disappeared while peaks A, C and D still remain unchanged. If the purpose of component "B" is to

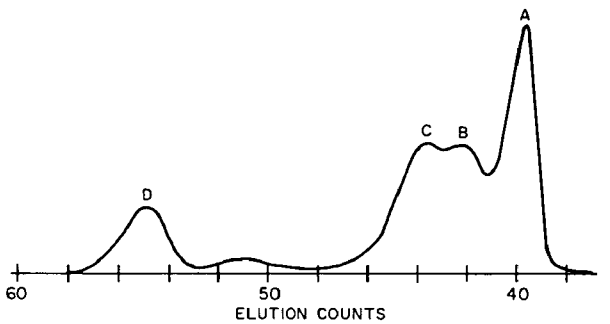

Fig. 15. Stabilizer system before processing.

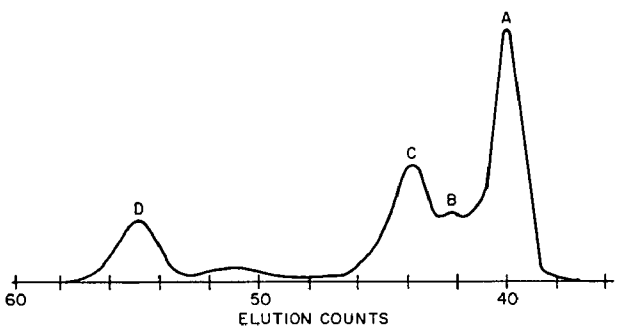

Fig. 16. Stabilizer system during processing.

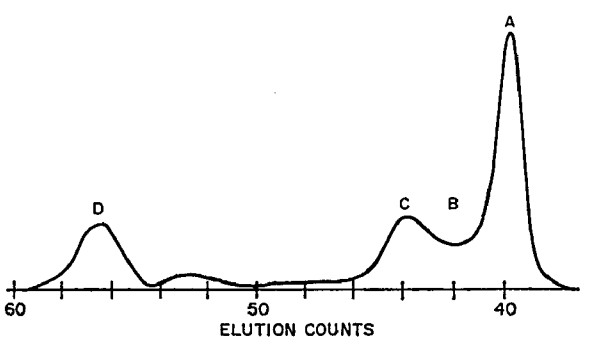

Fig. 17. Stabilizer system after processing.

protect the material during processing then it is apparently doing its job. On the other hand if it is added to give long-term protection then its use needs to be re-evaluated and a more permanent substitute found.

CONCLUSION

The use of a low porosity packing material (Poragel A-1) in GPC columns enables one to distinguish between various commercial polymers by characterizing the additive systems. The chromatograms in their entirety can be used to identify the supplier and the individual peaks can be used to identify the additive components. Chromatograms of additive systems obtained on samples from field use and processing areas can be used for evaluation of additive systems designed for specific applications.

REFERENCES

1 J. D. MOORE, *J. Polym. Sci.*, 2 (1964) 835.
2 R. L. BARTOSIEWICZ, *4th Intern. Seminar Gel Permeation Chromatography, Miami Beach, 1967.*
3 F. N. LARSON, *6th Intern. Seminar Gel Permeation Chromatography, Miami Beach, 1968.*
4 H. L. SPELL, *4th Intern. Seminar Gel Permeation Chromatography, Miami Beach, 1967.*

CHROM. 5119

THE USE OF GEL PERMEATION CHROMATOGRAPHY IN THE DEVELOPMENT OF HIGH-QUALITY GRAPHITE*

J. M. DICKINSON AND E. M. WEWERKA
Los Alamos Scientific Laboratory, University of California, Los Alamos, N.M. 87544 (U.S.A.)

SUMMARY

Many graphites to be used for nuclear, aerospace or high-temperature applications are now being made with synthetic components rather than with the traditional mixtures of coke filler and pitch binder. This additional control of raw materials results in a higher quality and more reproducible graphite. One class of synthetic polymers finding considerable use as graphite binder materials is furfuryl alcohol resins. The molecular size distributions of furfuryl alcohol resin binders as determined by gel permeation chromatography have been shown to play an important role in determining the physical properties of the resulting graphites. Gel permeation chromatographic data were related to graphite physical properties by two methods. In the first, the amount of material in a given molecular size interval was computed, and the effect of each size interval on the properties of graphite was determined using a graphical method. Secondly, the total molecular size distribution was then related to the physical properties of graphite by a statistical method, which was used to calculate parameters describing the gel permeation chromatographic data. The results of these studies have led to a more thorough understanding of the role played by furfuryl alcohol resins as related to their use in the manufacture of graphites, and to specifications for the synthesis of an improved furfuryl alcohol resin for use as a graphite binder material.

INTRODUCTION

Artificial graphites are usually made by molding or extruding a semi-plastic mass of petroleum coke and coal-tar pitch, and subsequently heating the piece, over a period of several months, to a temperature of 2500 to 3000°. Such graphites, which find wide spread use in the aluminum and steel manufacturing industries, usually have rather low densities, high conductivities and moderate strengths. By careful selection of materials, nuclear grade graphites have been and still are being manufactured from mixtures of coke and coal tar pitch[1]. However, the increasingly stringent demands being made on the purity and uniformity as well as on the properties of

* Work done under the auspices of the United States Atomic Energy Commission and with the support of National Aeronautics and Space Administration.

graphites for use in nuclear reactors have made it desirable to examine other raw materials.

Most of the materials that are used as binders in graphite are polymeric in nature and are chemically heterogeneous; *i.e.*, they usually contain many different kinds of chemical compounds. Coal tar pitch binders[2], for example, are composed of a myriad of distinct organic compounds, and often contain an assortment of extraneous impurities. In addition, they can vary considerably, both chemically and physically, from batch to batch. These factors make it difficult to control the reproducibility of graphite made using pitch binders.

Binder materials that are based entirely on synthetic polymers have distinct advantages. A number of such synthetic binder materials have been used; however, this discussion will be limited to the various furfuryl alcohol polymers which are used as binders.

Furfuryl alcohol polymers are also heterogeneous but they possess several desirable characteristics for the manufacture of high-quality graphite. In particular, the amounts of undesirable impurities can be kept to a minimum. They are liquid at room temperature, which greatly simplifies the mixing and fabrication operations; they result in high yields of carbon upon high-temperature pyrolysis; and they are thermosetting, which is desirable if complex shapes are to be fabricated. In addition, by controlling the degree of polymerization of the resins, a variety of viscosities and molecular size distributions can be reproducibly synthesized.

Considering the numerous purposes served by the binder material during the manufacture of graphite it has been suggested[3,4] that the molecular sizes, or more precisely the molecular size distribution, of the binder might be an even more important characteristic of it than its exact chemical composition. Based on this postulate, a study was undertaken to determine the effects of the molecular size distributions of furfuryl alcohol polymers on the properties of graphites made from them.

The molecular size distributions of the various furfuryl alcohol polymers were determined using gel permeation chromatography (GPC). The resulting data were treated using a statistical method which resulted in a numerical description of the molecular size distribution of the polymer. Correlations were made between the molecular size distributions of the binder polymer and the physical properties of the graphites made from them. These studies resulted in a better understanding of the relationships between the binder and the resulting graphite, and in a set of specifications for an improved furfuryl alcohol polymer for use as a binder in the manufacture of high-quality, high-density graphite.

EXPERIMENTAL

The furfuryl alcohol polymers were made by the polymerization of furfuryl alcohol in the presence of maleic anhydride by methods which have been reported elsewhere[5].

GPC was done with a Waters Model 200 gel permeation chromatograph which was equipped with a series arrangement of five 4-ft. polystyrene gel columns having maximum pore sizes of 3000, 500, 250, 250 and 60 Å. Samples for GPC analysis were either 0.5 or 1 % by weight in tetrahydrofuran (THF). These were injected for either 15- or 30-sec periods. A solvent (THF) flow rate of 1 ml/min was used.

Most of the polymer molecular size distributions used in this study were made by blending furfuryl alcohol resins of differing degrees of polymerization with one another or with furfuryl alcohol until the desired viscosity of 1600 cP was reached. This resulted in a number of polymer binders having equal viscosities and rather widely differing molecular size distributions. The resin viscosities were measured with a MacMichael-Fisher viscometer at 25°.

The graphites were manufactured using a mixture of 85 parts of graphite powder, 15 parts of carbon black, and 27 parts of one of the experimental furfuryl alcohol polymers that had been catalyzed with 4 % maleic anhydride. A manufacturing process that has been described earlier[6,7] was used. It involved a complex mixing and multiple extrusion procedure prior to making the final extrusion in the form of a 1/2 in. diameter rod. The rods were thermally set by heating them to 200° over a period of several days. Then the rods were heated slowly to 900° to carbonize the binder material. The carbonized rods were finally given a graphitization treatment at 2800°. This procedure has been demonstrated to be satisfactory for the production of an exceptionally uniform, high-quality graphite[6].

Property measurements were made on the graphitized rods, using standard methods, and these properties were related to the molecular size distributions of the polymers used to make the graphites.

MATERIALS

Furfuryl alcohol (Eastman white label), maleic anhydride (MCB standard quality) and tetrahydrofuran (Dupont commercial grade) were used in this study. The graphite powder was Great Lakes 1008S grade and the carbon black was Thermax, manufactured by the Thermatomic Carbon Company.

RESULTS

Correlations between molecular size regions of the polymer and the physical properties of the graphites

It has previously been shown that the binder viscosity, up to about 1600 cP, has a strong influence on both the manufacturing processes and the properties of the resulting graphite[8]. Consequently, the molecular-size-distribution studies were carried out using a series of furfuryl alcohol polymers all having viscosities of about 1600 cP. This value was chosen since at viscosities near 1600 cP a small change in the viscosity of the resin caused only minor changes in the properties of the graphite, while at lower viscosities a change in viscosity resulted in an appreciable change in properties. In addition, at viscosities much above 1600 cP fabrication difficulties increased appreciably.

The molecular size distributions of the furfuryl alcohol polymers were determined using GPC. The resulting elution curves were divided according to molecular size, and the size regions were numbered 1, 2, 3 and 4 as shown in Fig. 1. These divisions were chosen such that the first region represents the amount of monomer-size molecules in the resin; the second represents the low-molecular-weight species such as the dimer, trimer and tetramer; the third represents the medium-size molecules of molecular weights up to about 1000; and the fourth represents large molecules having molecular weights to about 5000.

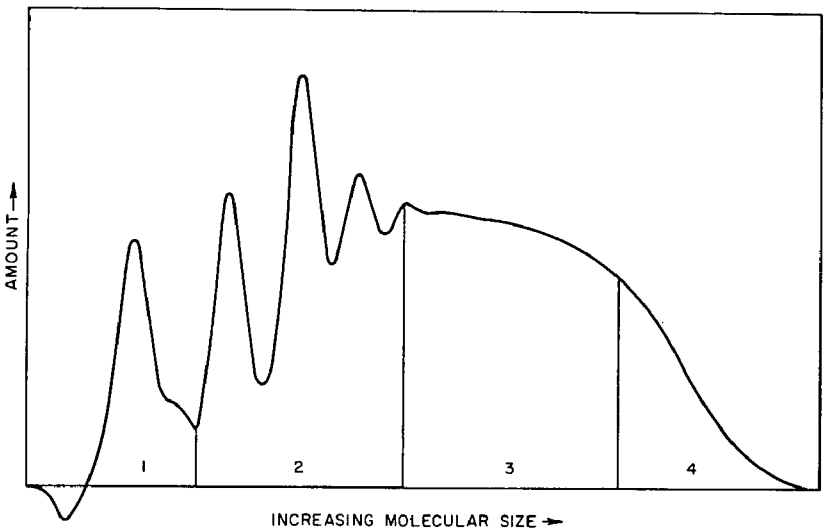

Fig. 1. A GPC trace of a furfuryl alcohol polymer showing the size intervals chosen for the molecular-size-distribution studies.

The amount of material in each of the numbered regions was estimated from the GPC curves using weight integration. These data, expressed as fractions of the total distribution of each resin, are shown in Table I. The relationships between the fraction of polymer in each of these regions and both the extrusion parameters and physical properties of the graphite were examined.

As the proportion of the distribution in region 1, monomer-size molecules, increased the extrusion characteristics changed appreciably, and the properties of the resulting graphite were affected. A distinct drop in the bulk density of the graphite rods occurred as the amount of monomer-size molecules in the resin used to make the graphite increased (Fig. 2). The drop in density appears to be due to a combination of factors, all related to the molecular size distribution and, in particular, to the

TABLE I

MOLECULAR SIZE DISTRIBUTIONS OF SOME FURFURYL ALCOHOL POLYMERS

Resin identification No.	*Fraction of polymer in each of the molecular size regions*			
	Number 1 (%)	*Number 2* (%)	*Number 3* (%)	*Number 4* (%)
1600	9.5	38.6	40.7	11.2
144	10.0	35.4	41.5	13.1
234 + 236	12.0	35.4	39.3	13.3
240 + FA	12.6	31.2	40.9	15.3
235 + 236	13.7	35.2	37.2	13.9
163 + 215	16.5	40.0	34.5	9.0
239 + FA	21.1	23.7	36.2	19.0
154 + FA	24.5	22.6	34.5	18.4
163 + FA	29.0	30.2	32.4	8.4
241 + FA	31.9	22.6	32.5	13.0

monomer-size molecules. These factors include a lowering of the extrusion pressure, the adhesiveness of the resin, and the carbon residue realized from the polymer upon pyrolysis.

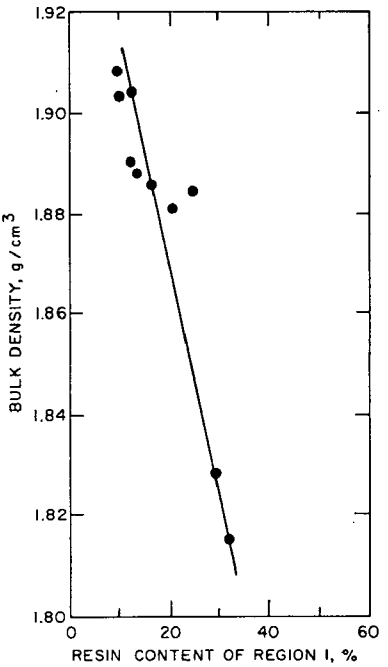

Fig. 2. The change in bulk density due to the amount of monomer-size molecules in the polymers.

Accompanying this large drop in density were corresponding changes in such properties as strength, modulus, and the thermal and electrical conductivities. Measurements of the preferred orientations of the rods using X-ray methods indicated that, in general, only minor changes occurred. These were too small to affect the properties that are sensitive to crystallographic orientation.

The amount of the polymer in the intermediate size regions, 2 and 3, of the distribution did not individually affect the properties of the graphites in a systematic manner. However, it was observed that in order to make a high density graphite it was necessary to have over 70 % of the molecular size distribution contained in these two regions (see Table I).

Increasing the amount of the largest polymer molecules did not appreciably increase the densities of the graphites, perhaps because such an increase necessitated a corresponding increase in the amount of the smaller molecules required to maintain the viscosity at 1600 cP.

Statistical descriptions of the polymer distributions and their relationship to the properties of the graphites

A non-functional statistical treatment[9] of the GPC data was used to obtain a numerical description of the molecular size distributions of the polymers. This

treatment has proven useful for handling porosity distributions[10] as well as particle-size distributions[9] and appears to be equally applicable to GPC data.

The molecular size intervals used for this study were selected as described earlier in this paper and are shown in Fig. 1. If comparisons between the polymers are to be valid, the same interval widths must be used for all of the distributions.

Since the sizes of the polymer molecules in each of the four intervals chosen for this study were not known accurately, the numbers 1, 2, 3 and 4 were used to represent the midpoints of the molecular size intervals. It would, of course, be more desirable to use the actual molecular sizes if they were available; however, useful comparisons can be made from data treated in this way.

The mean, $\bar{M}$, of the sample data for each distribution was calculated using eqn. 1, where W_i/W represents the fraction of the polymer present in the ith molecular size region, whose midpoint is represented by M_i, the number of the interval.

$$\bar{M} = \sum_{1}^{I} \frac{W_i}{W} M_i \tag{1}$$

Similarly, the variance, S^2, of the distribution was determined using eqn. 2.

$$S^2 = \sum_{1}^{I} \frac{W_i}{W} (M_i - \bar{M})^2 \tag{2}$$

A third statistic, the coefficient of variation, CV_d (ref. 9), which can be used to describe the distribution with a single numerical value, was determined using eqn. 3.

$$CV_d = \frac{S}{\bar{M}} \tag{3}$$

The means and variances of the molecular size distribution data are shown plotted against the bulk densities of the graphites in Fig. 3. Increasing the mean molecular size resulted in an increase in bulk density, while decreasing the variance resulted in an increase in density. It can be noticed that for polymers with nearly equal mean molecular sizes, those having the smaller variances result in graphites having higher densities.

This is further suggested by the curve shown in Fig. 4. The bulk density of a graphite increased if the coefficient of variation of the binder used to make the graphite decreased. This statistic, which relates the "average" molecular size of the polymer to the "width" of its molecular size distribution, has been particularly useful in examining relationships between binder materials and the graphites made from them. It points out that a low value of the variance coupled with a high value of the mean is desirable, and implies that a binder containing a single molecular size would be ideal. However, other factors such as the need of a certain amount of monomer to provide lubrication for the extrusion process, coupled with the 1600 cP viscosity requirement, limit the degree of monosizedness that is desirable. Also, from a practical standpoint, the manufacture of a polymer with monosized molecules and a specified viscosity, to say the least, presents substantial problems.

However, by minimizing the coefficient of variation, which can be done by choosing proper experimental conditions and by polymerizing directly to the desired viscosity, a superior furfuryl alcohol polymer binder can be made.

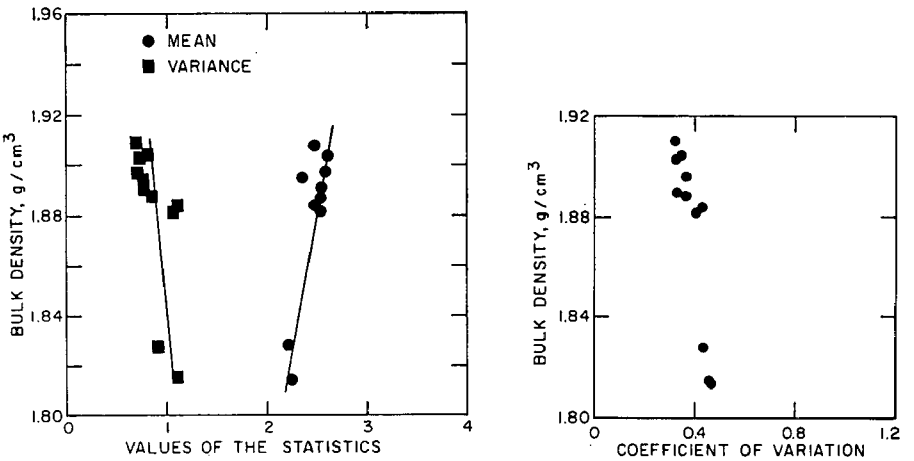

Fig. 3. The change in bulk density with statistical parameters describing the molecular size distribution of the polymers.

Fig. 4. The effect of the coefficient of variation of the polymers upon the bulk density of the graphite.

CONCLUSIONS

GPC has been used to determine the molecular size distributions of furfuryl alcohol polymers which were used as binders in the manufacture of high-density graphites. The GPC data were evaluated in such a way that a direct correlation could be made between the molecular size distributions of binder materials and the properties of graphites made from them. This led to a better understanding of the role played by the binder in graphite, and to the production of improved furfuryl alcohol polymer binders.

REFERENCES

1 R. E. NIGHTINGALE, *Nuclear Graphite*, Academic Press, New York, 1962.
2 J. R. HOOKER, *Pitch Binders for Graphite: A Survey of the Literature*, USAEC, Division of Technical Information, GA3985, General Atomics, San Diego, Calif., 1963.
3 E. M. WEWERKA, *Carbon*, 6 (1968) 93.
4 E. DE RUITER, J. F. M. OTH, V. SANDOR AND H. TSCHAMLER, *Characterization of Binders used in the Fabrication of Graphite Bodies*, WADD Technical Report 61-72, Vol. XI Supplement, Union Carbide European Research Associates, Brussels, 1964.
5 E. M. WEWERKA, *J. Appl. Polym. Sci.*, 12 (1968) 1671.
6 M. C. SMITH, *The Manufacture and Properties of an Extruded, Resin-Bonded Graphite, CMF-13 Lot AAQ1*, LA-3981, Los Alamos Scientific Laboratory of the University of California, Los Alamos, N.M. 1968.
7 P. WAGNER AND L. B. DAUELSBERG, *Carbon*, 7 (1969) 273.
8 J. M. DICKINSON AND E. M. WEWERKA, *Carbon*, 8 (1970) 249.
9 H. D. LEWIS AND A. GOLDMAN, *Theoretical Small Particle Statistics: A Summary of Techniques for Data Analysis with Recent Developments in Data Comparisons, Notations, and Mixture Theory*, LA-3656, Los Alamos Scientific Laboratory of the University of California, Los Alamos, N.M., 1968.
10 J. M. DICKINSON AND H. D. LEWIS, *Porosity Data Interpretation*, LA-3938, Los Alamos Scientific Laboratory of the University of Calif., Los Alamos, N.M., 1968.

CHROM. 5120

APPLICATIONS OF GEL PERMEATION CHROMATOGRAPHY IN THE MANUFACTURE OF EPOXY-GLASS PRINTED CIRCUIT LAMINATES

E. A. EGGERS AND J. S. HUMPHREY, JR.
Circuit Package Manufacturing — SMD, IBM Corporation, Endicott, N.Y. (U.S.A.)

SUMMARY

An IBM 1440 data processing system has been adapted to perform on-line data collection and analysis and has been applied to the analysis of an epoxy resin system used in printed circuit lamination. A feature of the computer program allows performance of independent calculations on selected portions of the chromatogram.

In practice, gel permeation chromatography has been effectively applied to monitor epoxy resin molecular distributions through each step of a laminating process to final gel. It has been shown that molecular weight distribution is a more useful parameter than epoxy equivalent weight for describing resin reactivity variations. Gel permeation chromatography also provides a convenient means of following resin advancement through the prepreg state. Studies of the "B" stage resin relate gel-time sensitivity to small changes in molecular weight distribution.

INTRODUCTION

Applications of gel permeation chromatography (GPC) to the characterization of epoxy resins are well known and have been previously discussed in the literature[1-3]. This paper describes the application of GPC to the study of performance factors, as related to molecular distribution, at several stages of epoxy-glass printed circuit laminate manufacturing. The computerized data acquisition and analysis system used for this work is also described.

Fig. 1 is a flow diagram describing the steps required to manufacture a glass-

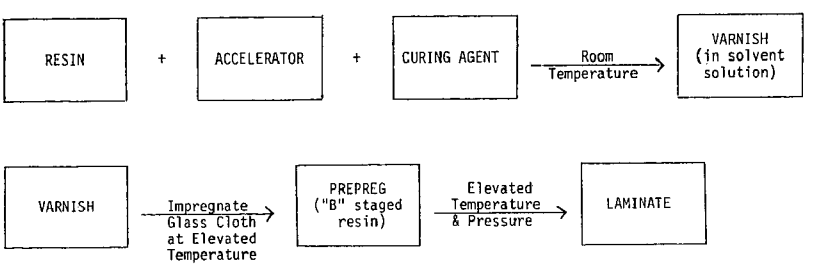

Fig. 1. Flow diagram for laminate manufacture.

filled epoxy laminate. The resin can be separated by gel chromatography at each step including prepreg manufacture. Prepreg is a dry, stable, and storable form of partially advanced or "B" staged resin on glass cloth. The resin in the cured or laminate form is too highly crosslinked for solvent solubilization. Discussion will center on (1) the relationship of molecular distribution to reproducible resin reactivity at constant epoxide equivalent weight (EEW) and (2) the effect of "B" stage advancement on the molecular distribution.

EXPERIMENTAL CONDITIONS

All samples were run on a Waters* Model 200 gel permeation chromatograph with automatic sample injection. The chromatograph is operated with tetrahydrofuran (THF) solvent at room temperature, a 1 ml/min flow rate, and a 2.5 ml syphon. Two mixed gel columns are included in an eight column configuration. Exclusion limits for the eight Styragel packed columns are 2000 to 700 Å (mixed), 700 to 50 Å (mixed), 500 Å, 350 Å, 250 Å, 250 Å, 100 Å, and 60 Å. Sample concentration is 0.25% by weight injected automatically from the 2 ml sample loop.

A calibration curve of effective chain length *versus* elution volume was prepared from three different types of molecules: *n*-alkanes, polypropylene glycols and polystyrenes. Four *n*-alkanes from Applied Science Laboratories, Inc.** were C_{12}, C_{20}, C_{25}, and C_{36}. Two polypropylene glycols of peak Å 56.9 and 84.4 (corrected for THF association) and four polystyrenes of peak Å 117, 244, 480, and 1,220 were obtained from Waters Associates'. The actual curve was constructed from two linear polynomial equation fits to the two most linear portions of the curve. Apparent molecular sizes for each 2.5 ml elution volume or single count were subsequently determined through substitution into the appropriate equation. Apparent molecular size was selected as the criteria for comparison. This method of calibration was considered adequate for the intended purpose of comparing similar polymers within the same laboratory.

The "gel time" is the time in seconds required for a solvent-containing varnish to reach a tack-free gel at 300°F. In practice there are many variations of this test but any reproducible test (± 3 sec) measuring the same approximate degree of crosslinking would suffice for the intended purpose of determining relative degree of reactivity.

Chromatographic characterization of resin

The starting brominated bisphenol A type resins used in this work were received in solvent solution and can be separated by gel chromatography without alteration. Fig. 2 is a typical chromatogram for this resin. Solvents are eluted beyond count 127 and do not interfere in the chromatogram analysis. The peak labeled $n = 0$ is the diglycidyl ether of bisphenol A (DGEBA) referred to as monomer. The probable sequence of steps in the synthesis of brominated bisphenol A type polymers requires an excess of DGEBA in the presence of brominated bisphenol A. This produces even numbered oligomers almost exclusively with alternating repeating units of brominated and nonbrominated bisphenol A units as shown in an idealized structure in Fig. 3. The small amount of $n = 1$ in Fig. 2 can be attributed to the nonbrominated starting

* Waters Associates, Inc., Framingham, Mass.
** Applied Science Laboratories, Inc., State College, Penn.

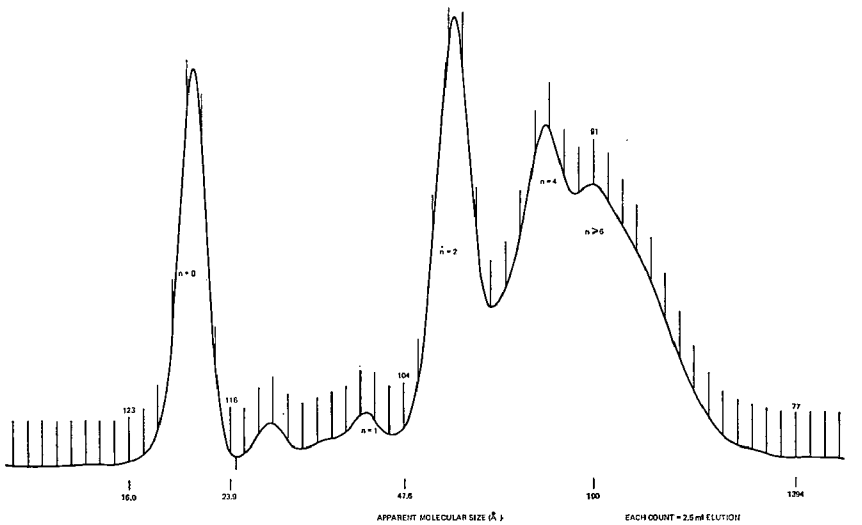

Fig. 2. Brominated bisphenol A resin.

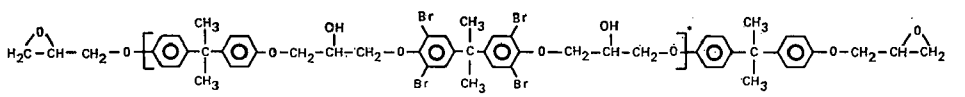

Fig. 3. Structure of brominated bisphenol A resin.

material which always contains a small quantity of all low-numbered oligomers. If $n = 0$ is considered monodisperse, then $n = 2$ closely approximates a monodispersed oligomer. Although not monodisperse, $n = 4$ and 6 are clearly defined oligomer peaks in the resin. Beyond this oligomers are not discernible but probably exist in small quantities as high as $n = 100$ or more.

DATA ACQUISITION SYSTEM

The data acquisition and reduction system consists of a modified IBM 1440 data processing system programmed for the specific application. The system program monitors the output from the GPC for a predetermined number of elutions, places the data in a table, and performs the following functions after the run is completed: (1) calculates linear base line drift and applies the correction to area accumulation and all molecular weight parameters; (2) calculates the molecular weight parameters of $\bar{A}_n$, $\bar{A}_w$, $\overline{M}_n$, $\overline{M}_w$, and $\overline{M}_w/\overline{M}_n$ for the overall chromatogram and, also for three independently designated portions or subareas of the same chromatogram; (3) performs area integration of the chromatogram based on a summation of concentration values

obtained from a signal reading every six seconds; and (4) records the run in histogram form giving chain lengths, accumulated areas, and accumulated weight percentages.

The semidedicated IBM 1440 data processing system was modified to accommodate the output of the Model 200 gel permeation chromatograph. Modifications include an altered serial I/O channel for attachment of nonstandard devices and the addition of a sense and operate matrix (SOM) with a single-level interrupt capability. These features enable the system program to control external equipment.

The IBM 1311 disc drive, indicated in Fig. 4, stores up to 12 previously entered calibration curves. Because the computer system is conveniently located with respect to the GPC, the IBM 1447 console is used as input for experiment initiation and exception message output. Elution and injection signals are cabled to the SOM and the analog signal from the differential refractometer is cabled to the SOM analog-to-digital converter. An IBM 1443 printer records all results in tabular and frequency polygram form. Figs. 5A and 5B are examples of a typical printout for an epoxy resin. The operator enters information for each sample as shown under "auto run". "Measurement range" designates the range for overall curve analysis. This feature allows overlap of samples for more efficient chromatographic usage. "Base range" designates the two counts from which linear baseline drift is calculated. "Skip areas" can include a maximum of three portions of the chromatogram that can be intentionally omitted from the analysis. These might be areas containing solvents or extraneous portions of polymers that interfere or do not contribute to the intended analysis. "Sub areas" can include three portions of the chromatogram for which independent calculations are made. The areas are designated by elution counts and may be wholly resolved peaks such as DGEBA in epoxy resins or portions of other broader distributions.

A preliminary chromatographic run of any unknown polymer is necessary to determine the run parameters for the program.

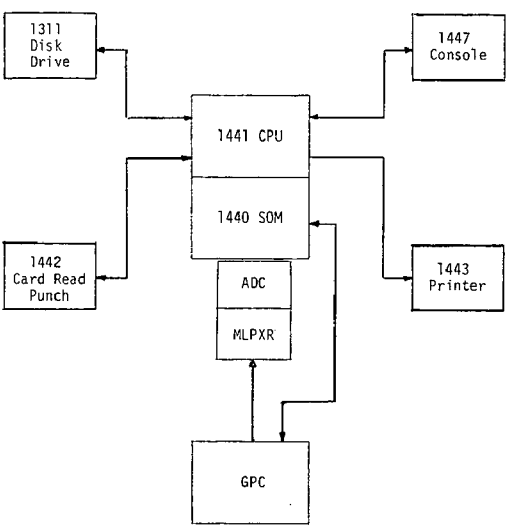

Fig. 4. 1440 System configuration.

SAMPLE NUMBER 0004

FLOW RATE - 1.0 ML/MIN
SYPHON SIZE - 2.5 ML
SAMPLE LOOP SIZE - 2.0 ML

CHART SPEED - 10 MIN/IN
SENSITIVITY - 8 TIMES
COLUMN SET B AUTO 2000 to 60

AUTO RUN
CALIBRATION CURVE 1
MEASUREMENT RANGE -077 123
SKIP AREAS -
SUB AREAS - 077 091-010/091 104-010/116 123-010

Q - 010
BASE RANGE -076 149
COLUMN TEMP -022 C

NAMS A N - 52.7
NAMW M N - 52.7
WAMS A W - 87.4
WAMW M W - 87.4
M W /M N - 1.66

SUB AREA 1

NAMS A N - 138.9
NAMW M N - 138.9
WAMS A W - 171.6
WAMW M W - 171.6
M W /M N - 1.24

SUB AREA 2

NAMS A N - 70.4
NAMW M N - 70.4
WAMS A W - 73.6
WAMW M W - 73.6
M W /M N - 1.05

SUB AREA 3

NAMS A N - 20.5
NAMW A N - 20.5
WAMS A W - 20.5
WAMW M W - 20.5
M W /M N - 1.00

CHAIN XXXXXX.X	COUNT XXX	CONCENTRATION 0 0 0 0 0 1 1 1 1 1 2 2 2 2 2 3 3 3 3 3 4 4 4 4 4 5 0 2 4 6 8 0 2 4 6 8 0 2 4 6 8 0 2 4 6 8 0 2 4 6 8 0 2 4 6 8 0	AREA XXX.XX	ACCUM WT SUB-AREA XXX.XX		ACCUM WT TOTAL XXX.XX
		* *				
16.56.0	INJ	*				
05.06.1	76	* BEGIN BASE DRIFT REF A * 054				
1394.0	77	* 000	0.00	100.00		100.00
1133.0	78	* 000	0.00	100.00		100.00
921.0	79	** 002	0.03	100.00		100.00
748.0	80	** 006	0.15	99.82		99.95
05.15.6	INJ	*				
608.0	81	** 009	0.34	99.26		99.81
494.0	82	* * 016	0.64	98.44		99.59
401.0	83	* * 030	1.16	96.96		99.21
326.0	84	* * 048	2.09	94.20		98.48
265.0	85	* * 071	3.54	89.79		97.33
215.0	86	* * 098	5.59	83.26		95.62
175.0	87	* * 121	8.26	74.24		93.26
142.0	88	* * 148	11.53	63.11		90.34
113.0	89	* * 164	15.15	49.49		86.78
106.0	90	* * 182	19.32	34.41		82.83
100.0	91	* * 192	23.87	17.66	100.00	78.44
94.8	92	* * 188	28.46	91.89		73.82
89.5	93	* * 198	33.04	83.94		69.29
84.5	94	* * 232	38.25	75.57		64.52
79.8	95	* * 212	43.74	65.77		58.94
75.4	96	* * 157	48.19	56.80		53.83
71.2	97	* * 121	51.50	50.17		50.05
67.2	98	* * 109	54.21	45.05		47.13
63.5	99	* * 160	57.26	40.45		44.51
59.9	100	* * 279	62.60	33.69		40.66
56.6	101	* * 287	69.53	21.89		33.94
53.4	102	* * 155	75.01	9.76		27.02
50.4	103	* * 055	77.42	3.21		23.29
47.6	104	* * 021	78.29	0.89		21.97
45.0	105	* * 021	78.77			21.46
42.5	106	* * 032	79.38			20.95
40.1	107	* * 033	80.20			20.18
37.9	108	* * 021	80.84			19.39
35.8	109	* * 016	81.28			18.88
33.8	110	* * 014	81.64			18.50
31.9	111	** 010	81.92			18.16
30.1	112	* * 016	82.20			17.92
28.4	113	* * 027	82.74			17.53
26.8	114	* * 021	83.37			16.88
25.1	115	** 006	83.68			16.38
23.9	116	** 007	83.81	100.00		16.23
22.6	117	* * 063	84.43	98.96		16.06
21.3	118	* * 224	87.79	89.61		14.55
20.2	119	* * 251	94.09	56.38		9.15
19.0	120	* * 097	98.32	19.14		3.11
18.0	121	* * 024	99.60	4.75		0.77
17.0	122	** 006	99.91	1.19		0.19
16.0	123	** 002	100.00	0.30		0.05
08.07.0	149	* END BASE DRIFT REF B * 045				
		* *				

Fig. 5. A and B, computer printout.

TABLE I

GPC DATA FOR BROMINATED RESINS

Sub area 1 = count 77–91; sub area 2 = count 91–104; sub area 3 = count 116–123.

Batch No.	*Overall distribution*			*Sub area 1 High molecular weight*				*Sub area 2 Mid molecular weight*				*Sub area 3 DGEBA (n = 0)*				*Gel time (sec)*
	$\bar{A}_n$	$\bar{A}_w$	$\bar{A}_w/\bar{A}_n$	$\bar{A}_n$	$\bar{A}_w$	$\bar{A}_w/\bar{A}_n$	*Weight (%)*	$\bar{A}_n$	$\bar{A}_w$	$\bar{A}_w/\bar{A}_n$	*Weight (%)*	$\bar{A}_n$	$\bar{A}_w$	$\bar{A}_w/\bar{A}_n$	*Weight (%)*	
15E	52.5	116.3	2.21	164	240	1.46	31.3	70.7	74.0	1.05	43.8	20.2	20.3	1.00	18.5	132
9F	52.3	91.6	1.75	143	191	1.34	23.5	69.8	73.4	1.05	53.5	20.5	20.6	1.00	15.8	148
85E	52.0	94.1	1.81	145	206	1.42	23.0	70.1	73.3	1.05	53.6	20.7	20.7	1.00	16.7	151
9E	50.8	85.2	1.68	139	180	1.30	21.0	69.6	73.0	1.05	54.6	20.4	20.5	1.00	16.5	157
8E	50.3	87.0	1.72	141	186	1.32	21.7	69.7	72.9	1.05	53.3	20.4	20.5	1.00	17.4	162
42E	50.0	85.7	1.72	140	188	1.35	20.2	69.5	72.7	1.05	55.3	20.5	20.5	1.00	17.8	165
95E	48.9	83.2	1.70	139	181	1.31	20.0	69.5	72.7	1.05	53.4	20.3	20.4	1.00	18.7	168
44E	49.2	77.0	1.57	132	160	1.21	17.7	69.3	72.4	1.05	57.5	20.5	20.5	1.00	17.7	175

RESULTS AND DISCUSSION

Molecular distribution areas of greatest interest in epoxy resin chromatograms are the monomer portion (sub area 1), middle molecular weight region from count 104 to 91 (sub area 2), and high-molecular-weight portion from count 91 to the interstitial volume at 77 (sub area 3) (see Fig. 2). Other chemical factors being equal, it is these areas that are the best indicators of the reproducible reactivity of an epoxy resin system. Table I gives the results for 8 different batches of the same brominated resin. All batches fall within a relatively narrow EEW range of 422 to 442. Data for all portions is shown although emphasis is on the columns of "overall distribution", "weight percent" of sub area 1, "weight percent" of sub area 2, and "weight percent" DGEBA. The data for batch 15E indicates it to be significantly different from the others. An 8 to 13 % increase in high-molecular-weight material, a like decrease in mid molecular weight, both reflected in the overall weight average, are the key indicators. Indeed, the chemical reactivity reflected in the gel time indicates it to be faster by 19 sec over its nearest neighbor. Although 15E best dramatizes the effect of increased quantities of high molecular weight material on gel time, the trend is apparent for the remaining batches. In general, as the weight average and/or weight percent of high molecular weight material increases, reactivity of the system increases resulting in lower gel times. Any variance in EEW within the range of 422 to 442 cannot account for the observed differences in reactivity. EEW is an average value only which cannot describe molecular distribution and is not a sufficient indicator of resin reactivity.

To demonstrate the effect on reactivity of a change in specific oligomeric content, DGEBA was sequentially added in known quantities to a base resin and the gel times obtained (Table II). As expected, increased quantities of low molecular weight epoxy material decreases the reactivity as indicated by longer gel times. It was necessary to demonstrate the molecular weight-reactivity relationship with low molecular weight materials because discrete oligomers of high molecular weight epoxies were not available.

In a varnish, see Fig. 6, the presence of the curing agent can be seen and quantified. The curing agent is dicyandiamide and is usually employed in quantities of 3 to 5 % by weight. Its appearance is at an approximate elution count of 124.5 and a simple calibration procedure corrects for its different refractive index response; therefore, it can be determined as a percentage of the varnish solids.

Resin from the glass impregnated prepreg in the advanced "B" stage state is soluble in THF and its molecular weight (size) distribution can be determined by

TABLE II

EFFECT OF INCREASED DGEBA CONTENT ON REACTIVITY

DGEBA content	*Gel time (sec)*
15.9%	164
17.2%	167
19.6%	172
22.5%	179

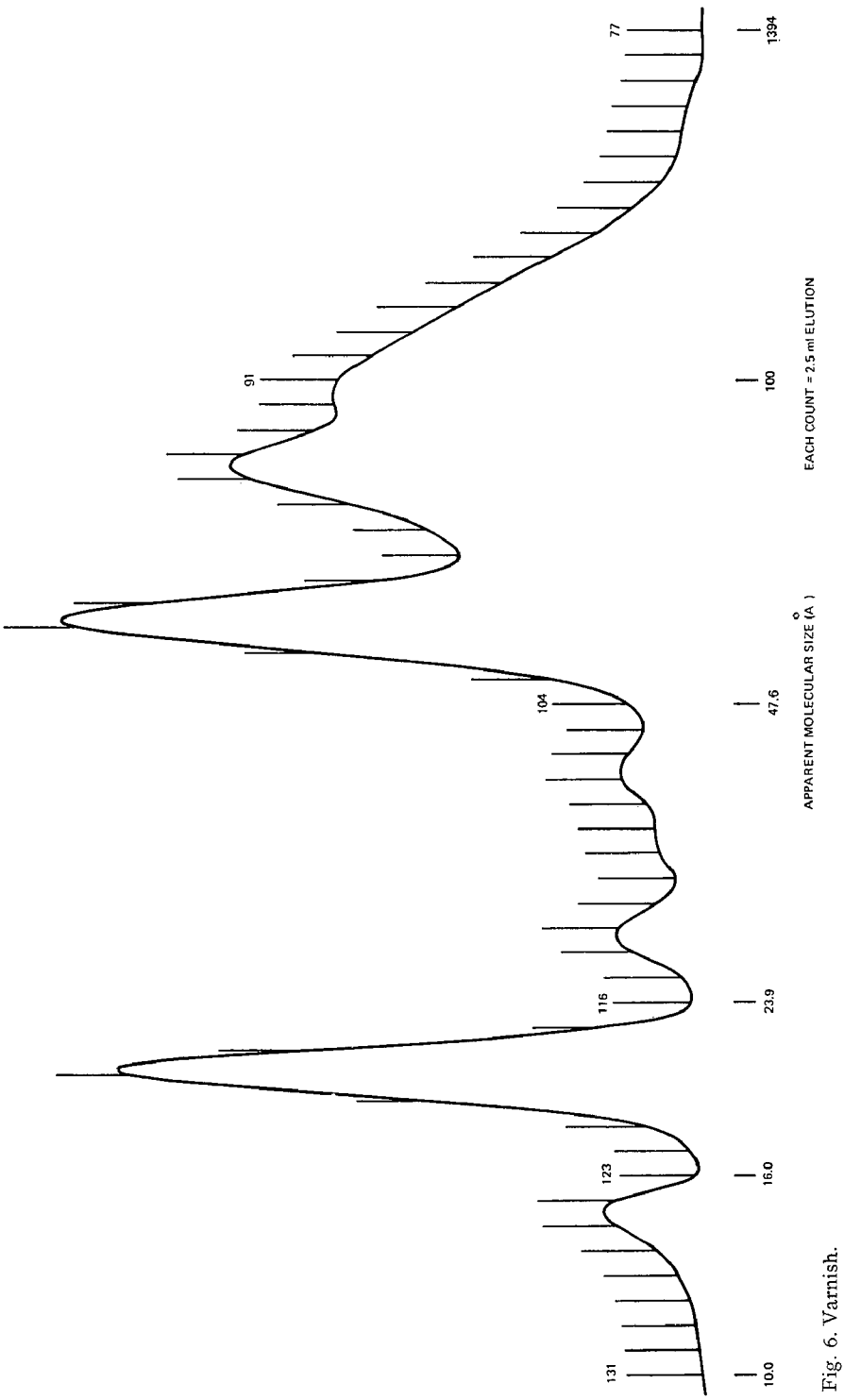

Fig. 6. Varnish.

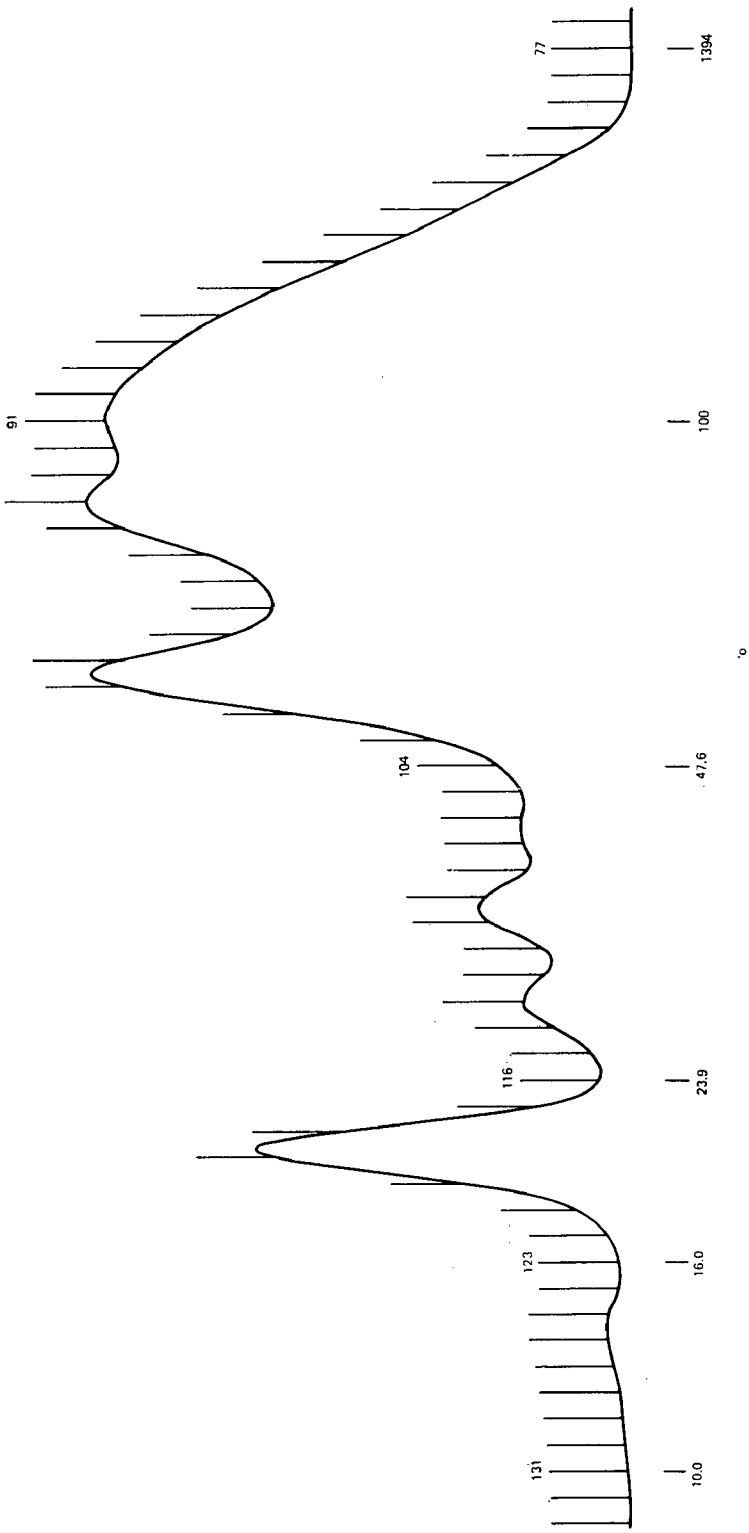

Fig. 7. Prepreg ("B" staged resin).

TABLE III

GPC DATA FOR PREPREG AND CORRESPONDING RESIN

Sub area 1 = count 77–91; sub area 2 = count 91–104; sub area 3 = count 116–123.

Sample	*Overall distribution*			*Sub area 1* *High molecular weight*				*Sub area 2* *Mid molecular weight*				*Sub area 3* *DGEBA* ($n = 0$)			
	$\bar{A}_n$	$\bar{A}_w$	$\bar{A}_w/\bar{A}_n$	$\bar{A}_n$	$\bar{A}_w$	$\bar{A}_w/\bar{A}_n$	*Weight* (%)	$\bar{A}_n$	$\bar{A}_w$	$\bar{A}_w/\bar{A}_n$	*Weight* (%)	$\bar{A}_n$	$\bar{A}_w$	$\bar{A}_w/\bar{A}_n$	*Weight* (%)
9E-Resin	50.8	85.2	1.68	139	180	1.30	21.0	69.6	73.0	1.05	54.6	20.4	20.5	1.00	16.5
9E-Prepreg	57.6	96.0	1.67	144	184	1.28	27.6	71.0	74.3	1.05	51.6	20.4	20.5	1.00	10.4
65E-Resin	50.0	81.7	1.64	172	172	1.27	19.6	69.7	72.9	1.05	54.7	20.4	20.6	1.00	17.2
65E-Prepreg	57.2	93.3	1.63	177	177	1.24	26.9	70.0	74.6	1.05	51.6	20.4	20.5	1.00	10.9

TABLE IV

GPC DATA FOR PREPREG

Sub area 1 = count 77–91; sub area 2 = count 91–104; sub area 3 = count 116–123.

Sample	*Overall distribution*			*Sub area 1* *High molecular weight*				*Sub area 2* *Mid molecular weight*				*Sub area 3* *DGEBA* ($n = 0$)				*Percent dicyandiamide of original concentration*
	$\bar{A}_n$	$\bar{A}_w$	$\bar{A}_w/\bar{A}_n$	$\bar{A}_n$	$\bar{A}_w$	$\bar{A}_w/\bar{A}_n$	*Weight* (%)	$\bar{A}_n$	$\bar{A}_w$	$\bar{A}_w/\bar{A}_n$	*Weight* (%)	$\bar{A}_n$	$\bar{A}_w$	$\bar{A}_w/\bar{A}_n$	*Weight* (%)	
150	51.9	83.3	1.61	136.5	164.5	1.21	22.26	70.5	73.7	1.05	53.27	20.2	20.3	1.00	13.94	57
200	54.9	88.1	1.60	139.0	170.4	1.23	24.39	70.7	74.0	1.05	52.91	20.4	20.5	1.00	11.99	35
250	56.3	92.0	1.63	141.5	177.3	1.25	25.87	70.8	74.1	1.05	52.18	20.4	20.5	1.00	11.08	29
300	56.7	96.6	1.70	145.2	188.0	1.29	27.26	71.0	74.4	1.05	50.41	20.3	20.4	1.00	10.63	26
350	58.0	96.0	1.66	144.3	180.9	1.25	28.06	71.1	74.5	1.05	50.52	20.3	20.4	1.00	10.05	20

GPC. The chromatogram in Fig. 7 indicates the nature of the distribution. At this point the free dicyandiamide content is less than one-third its original concentration in the varnish. Table III contains the data for two prepregs and their corresponding batches of raw resin. For each batch, the overall polydispersity remains constant but the weight and number averages are shifted to higher molecular weights. This is more clearly observed in the 6 to 7 % increase in high-molecular-weight material that indicates polymer advancement. A corresponding decrease in mid molecular weight and in DGEBA content occurs as expected.

It is possible to follow advancement of a resin through the prepreg state by means of GPC. Table IV provides data pertaining to distinct states of advancement. Relative stability of the overall weight-to-number average molecular weight material increases from 22 to 28 % while the amount of DGEBA decreases from 14 % to 10 %. These molecular distribution changes are comparable to those observed for raw resins that produced maximum gel time variations of 20 %. In the "B" stage, however, these molecular distribution changes produce considerably greater effects. Sample 350 required only one-half of the time to gel as sample 150. All of the advancement towards gel is apparently occurring through the reaction of the dicyandiamide curing agent that is being consumed at a similar rate. Whatever the mechanism, the conclusion reached is that the reactivity of "B" staged resin is particularly sensitive to small changes in molecular weight distribution.

ACKNOWLEDGEMENTS

Acknowledgement is made to Mr. T. B. WILLIAMS, CPM Test Engineering for his dedicated efforts in providing a data acquisition and analysis system suited to the needs of our laboratory. We also wish to thank Mr. W. J. SUMMA and Mr. G. H. HASTINGS, Jr. of CPM Chemical Technology for the prepreg samples and gel time data.

REFERENCES

1 G. D. EDWARDS AND Q. Y. NG, *J. Polym. Sci.*, Part C (1968) 105.
2 F. N. LARSEN, *6th Intern. Seminar of Gel Permeation Chromatography, Miami Beach, Fla., October, 1968.*
3 G. H. MILES, *National ACS Meeting, Chicago, Ill., 1965.*

CHROM. 5202

GEL PERMEATION CHROMATOGRAPHIC INVESTIGATION OF IRRADIATED COPOLYMERS

E. C. FERLAUTO

Mobil Chemical Company, Research Development and Engineering Laboratory, Edison, N.J. 08817 (U.S.A.)

SUMMARY

Hot melt samples of irradiated and non-irradiated ethylene–isobutyl acrylate copolymers and ethylene–vinyl acetate copolymers were examined with gel permeation chromatography and the gel content determined to investigate changes in polymer growth upon increasing radiation dosage. Variations in the molecular size and gel content of both copolymer systems studied suggested that the degree of cross-linking is inversely dependent upon the molecular size of the starting material and the rate of degradation is directly related to molecular size. It has been demonstrated that these techniques can be employed to determine the optimum initial molecular size and polymer composition for selection of a copolymer system for irradiation.

INTRODUCTION

Radiation studies have been reported most extensively for polyethylene and other polyolefins. Some general observations have been made with these systems which may act as a guide in the investigation of the effects of radiation for copolymers.

Radiation of polymeric materials can cause cross-linking (polymerization) and/or chain scission (degradation). KANG *et al.*[1] concluded that the cross-linking probability in polyethylene increases faster than the radiation dose while the chain scission probability remains directly proportional to dose. Based upon FLORY's equations for random cross-linking of a polymer[2], LYONS AND FOX[3] concluded that, at a specific molecular weight, the loss in material due to chain scission and to cross-linking will be exactly balanced by the gain due to scission of larger molecules provided the chain scission probability is relatively small compared with the cross-linking probability.

Cross-linking in polyethylenes is believed to involve carbon–hydrogen bond scission and subsequent coupling of resultant alkyl radical intermediates according to CHARLESBY[4,5]. He concluded that the radiolytic behavior of polyethylene and other polymers could be explained by assuming that both main-chain scission and cross-linking occur randomly along the polymer chain. More recently GEYMER[6] concluded, on the basis of kinetic considerations, that radiation-induced cross-linking of polypropylene involves free radicals.

The copolymer systems reported here, ethylene–isobutyl acrylate and ethylene–vinyl acetate, were investigated to aid in the application of radiation curing to commercial resins acceptable for coatings. Several interesting observations were made that define parameters to be considered in the selection of copolymer materials and radiation conditions to obtain optimum physical properties of the cross-linked copolymer. A study of relative molecular size distributions with gel permeation chromatography (GPC) and gel content of the irradiated copolymer is demonstrated to be of value in determining the conditions necessary for achieving optimum physical properties of the radiation products.

EXPERIMENTAL

Pressed films of copolymers consisting of ethylene–isobutyl acrylate and ethylene–vinyl acetate were cross-linked by irradiation with a cobalt-60 γ-radiation source and limited access to air. Composition effects were studied with films of similar molecular weight but varying monomer content. Effects due to differences in molecular weight were determined with films from resins of the same composition but of varying melt index.

Radiation dosages of 2.6, 10.6, and 22.3 Mrad were employed to cross-link the two different types of copolymers investigated, ethylene–isobutyl acrylate (Zetafax resins supplied by E. I. duPont Co.) and ethylene–vinyl acetate (Elvax resins supplied by Dow Chemical Co.). The copolymers were characterized as to composition, melt index, weight average ($\bar{A}_w$) and number average ($\bar{A}_n$) molecular size, percent crystallinity, and melting point. GPC was employed to determine $\bar{A}_w$ and $\bar{A}_n$ of the copolymers before irradiation and after each radiation dose. In addition, the gel content was determined and the observation of changes in the molecular size distribution parameters, $\bar{A}_w$ and $\bar{A}_n$, were compared with changes in gel content. These measurements were correlated with changes in physical properties investigated with an Instron Tester and included measurement of breaking stress (tensile strength), elongation at break, tensile modulus, and non-elastic deformation.

EQUIPMENT

Waters Associates Model 100 gel permeation chromatograph

GPC analyses were conducted with the copolymers dissolved in *o*-dichlorobenzene at 130°, with four columns in series packed with Styragel having exclusion limits of 10^6, 10^5, 10^4, 10^3 Å, respectively. The columns were calibrated with polystyrene standards having narrow molecular weight distributions.

Cobalt-60 source

Ten pencils of cobalt-60.

Ceric sulfate dosimeter

Film sections were extended between two points where equivalent dosage rates were observed and the total dosage was governed by exposure time.

Pasadena hydraulic press

Films of the polymers were made by pressing at a temperature of 300° F and

a pressure of 1880 lb./sq. in. They were cooled rapidly by running water through the platens of the press while the pressure was maintained. The films were placed between sheets of plate glass (3/64 in. thick) and sealed with pressure sensitive tape.

Instron tester Model TM

TEST METHODS

Gel content determination

A sample of polymer (1.25 g) was refluxed for 3 h with 150 ml of *o*-dichlorobenzene, cooled, and filtered through No. 41 Whatman paper with a Buchner funnel, washed with fresh solvent, and brought to the mark in a 250 ml volumetric flask. An aliquot was evaporated to dryness, placed in a vacuum oven at 60°C for 1 h, cooled and weighed. The gel content was calculated by difference based on the weight of polymer contained in the 25 ml aliquot of the filtered solution, and the weight of polymer contained in a 25 ml aliquot without filtering.

Tensile modulus

Determined with the Instron tester according to ASTM Method D-882.

Breaking stress and break elongation

Determined with the Instron tester in which samples of 2 in. gauge length were stretched 150% of original elongation at a rate of 1 in. per min, retracted, and repeated for three full cycles.

Computer calculations were employed to tabulate and establish the statistical significance of the data on mechanical properties.

RESULTS

The unique finding with the ethylene–isobutyl acrylate series of copolymers is that molecular size begins to increase rapidly at 2.6 Mrad, forms gel at 10.6 Mrad, but on continued radiation exposure the gel disappears. This could be explained if the main chain scission referred to by CHARLESBY[4,5] occurred to the point where sufficient main chain fragmentation took place to break up the network structure of the gel. The observation of events which were followed with GPC curves are shown for sample Z-1278 (20% IBA, 250 melt index (M.I.)) in Fig. 1 in which the curves are arranged so that their axes coincide. A fairly small fraction of high molecular size material can be seen before irradiation and an increase can be seen in the high molecular size end after irradiation at the 2.6 Mrad level. At 10.6 Mrad dosage, at which point gel formed, the high molecular size shoulder has disappeared. At 22.3 Mrad the gel fraction has disappeared and a distribution curve similar to the original material is observed including restoration of high and medium molecular size fractions. GPC indicates that cross-linking begins at low levels of irradiation. A gel is formed with continued radiation which is then degraded to almost restore the original system. The requirements for optimum radiation cross-linking was found to be a low molecular weight starting material (M.I. about 250) and an isobutyl acrylate content of 30% or higher.

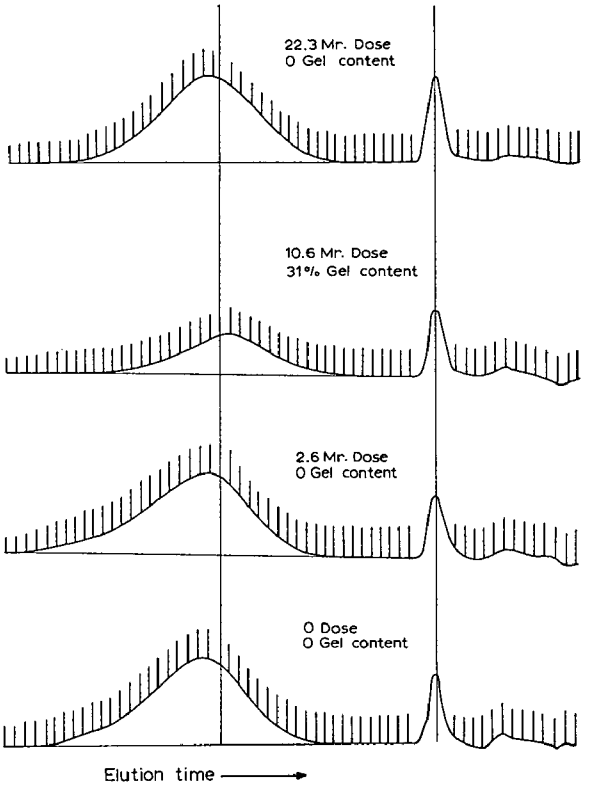

Fig. 1. GPC Molecular size distribution, ethylene–isobutyl acrylate copolymer γ-irradiated Dow Z-1278, 20% IBA, M.I. = 250.

GPC and gel content studies indicate a much lower degree of cross-linking at the extremes of molecular weight for the ethylene–vinyl acetate copolymers. The lowest molecular weight copolymer tested is probably too low in average molecular size to attain the proper size for gelation. The highest molecular weight copolymers tested are probably of too low mobility (similar to macro-Brownian movement) to allow access of active centers of adjacent molecules for cross-linking.

Ethylene–vinyl acetate copolymers having a vinyl acetate content of greater than 30 % but probably less than 42 % and in the molecular weight range 22–175 M.I. would be optimum for sensitivity to radiation.

Ethylene–isobutyl acrylate copolymers

The GPC data presented in Table I show that for the ethylene–isobutyl acrylate copolymers the highest weight average molecular size, $\bar{A}_w$, observed in *o*-dichlorobenzene solvent for each series of copolymers exists at a radiation dosage of 2.6 Mrad. A dramatic decrease in the weight average molecular size of the copolymer in solution is observed at the 10.6 Mrad level for the entire series of copolymers and is accompanied by the appearance of an insoluble portion (gel) as shown in Table II.

The next level of radiation dosage, 22.3 Mrad yielded a decrease in gel content for the three samples which contained gel at 10.6 Mrad. The gel content was observed

TABLE I

ETHYLENE–ISOBUTYL ACRYLATE COPOLYMERS: VARIATION OF WEIGHT AVERAGE MOLECULAR SIZE WITH RADIATION DOSAGE

Sample	*% IBA*	*M.I. (g/10 min)*	*Weight average molecular size ($\bar{A}_w$)*			
			Radiation dosage (Mrad)			
			None	*2.6*	*10.6*	*22.3*
Z-1278	20	250	3510	7 010	1510	2070
Z-1275	20	20	5540	16 700	2210	2770
Z-1270	20	2–3	7860	17 600	3490	3160
Z-1375	30	20	6880	21 500	2440	3870
Z-1370	30	2–3	8140	24 600	1330	2070

TABLE II

ETHYLENE–ISOBUTYL ACRYLATE COPOLYMERS: VARIATION OF GEL CONTENT WITH RADIATION DOSAGE

Sample	*% IBA*	*M.I. (g/10 min)*	*Gel content (%)*			
			Radiation dosage (Mrad)			
			None	*2.6*	*10.6*	*22.3*
Z-1278	20	250	0	0	30.9	0
Z-1275	20	20	0	0	12.8	0
Z-1270	20	2–3	0	0	0	0
Z-1375	30	20	0	0	2.2	16.0
Z-1370	30	2–3	0	0	3.5	0

to increase for sample Z-1375 (30 % isobutyl acrylate (IBA), 20 M.I.), which contains a higher isobutyl acrylate content (30 %), in the range from 10.6 to 22.3 Mrad. The weight average molecular size, $\bar{A}_w$, of this sample was also observed to increase significantly at the 22.3 Mrad radiation dosage compared with the 10.6 Mrad irradiated sample as shown in Table I. Sample Z-1370 (30 % IBA, 2–3 M.I.), which also has a higher isobutyl acrylate content, also exhibits a larger molecular size than the 20 % isobutyl acrylate samples in *o*-dichlorobenzene. The data indicate that molecular size increases with the isobutyl acrylate content upon irradiation.

Samples of series Z-1275 and Z-1375, each initially having a melt index of 20 (20 % and 30 % IBA respectively) exhibit a similar maximum gel content (13 % and 16 %) as shown in Table III. Sample Z-1278 which had a lower molecular size (M.I. 250

TABLE III

ETHYLENE-ISOBUTYL ACRYLATE COPOLYMERS: MAXIMUM GEL CONTENT OF IRRADIATED SAMPLES

Sample	*% IBA*	*M.I. (g/10 min)*	*Maximum gel content (%)*
Z-1278	20	250	30.9
Z-1375	30	20	16.0
Z-1275	20	20	12.8
Z-1370	30	2–3	3.5
Z-1270	20	2–3	0.0

and 20 % IBA) shows the highest gel content, 31 %, of the five samples investigated. This observation probably reflects greater tendency for the lower molecular weight starting material to increase in size.

Mechanical properties in general followed the cross-linking reaction. The variation of break stress (tensile strength) and gel content for sample Z-1278 with increased radiation dosage are seen in Fig. 2 to show correlation. It can be seen in Table IV that in general, the lower molecular weight polymers were observed to increase in strength with radiation. When the gel content of the lower molecular weight starting

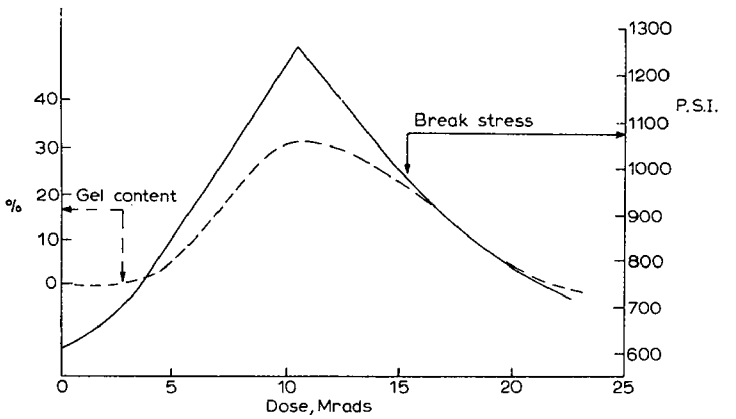

Fig. 2. γ-Radiation effect on breaking stress and gel content of ethylene–isobutyl acrylate copolymer. Dow Zetafax 1278, 20% IBA, M.I. = 250.

TABLE IV

ETHYLENE-ISOBUTYL ACRYLATE COPOLYMERS: EFFECT OF γ-IRRADIATION ON MECHANICAL PROPERTIES

Sample No.	*% IBA*	*Mole ratio E/IBA*	*M.I. (g/10 min)*	*Radiation dosage (Mrads)*	*Break stress (p.s.i.)*
Z-1270	20	18/1	2–3	0	2367
				2.6	2329
				10.6	2448
				22.3	2269
Z-1275	20	18/1	20	0	1571
				2.6	1691
				10.6	1683
				22.3	1751
Z-1278	20	18/1	250	0	635
				2.6	704
				10.6	1263
				22.3	735
Z-1370	30	11/1	2–3	0	2338
				2.6	2340
				10.6	2169
				22.3	2425
Z-1375	30	11/1	20	0	1284
				2.6	1406
				10.6	1409
				22.3	1387

material decreased or disappeared, a drop was observed in break stress but not back to the original level. It can be seen in Table IV that in general, the lower molecular weight polymers (Z-1278, Z-1275, and Z-1375) were observed to increase in strength with radiation up to the 10.6 Mrad dose level. The initially higher molecular weight samples, Z-1270 and Z-1370, showed slight but statistically significant losses in break stress at the 2.6 or 10.6 Mrad level.

The investigation of physical properties indicate that the higher initial molecular weight polymers are slightly adversely affected by irradiation while the lower initial molecular weight polymers show improvement in physical properties. In addition the copolymers which have a higher isobutyl acrylate content appear to be more susceptible to irradiation than those with lower isobutyl acrylate content. These findings corroborate the observations made with GPC and gel content studies.

Ethylene–vinyl acetate copolymers

The ethylene–vinyl acetate (VA) copolymers of varying initial molecular weight and varying composition generally showed an increase in molecular size with initial

TABLE V

ETHYLENE-VINYL ACETATE COPOLYMERS: MOLECULAR SIZE AND PERCENT GEL DATA

Sample No.	*VA (%)*	*M.I. (g/10 min)*	*Radiation dosage (Mrads)*	$\bar{A}_w \times 10^{-3}$	$\bar{A}_n \times 10^{-2}$	*Gel (%)*
E-40	39–42	45–65	0	3.83	9.92	0.0
			2.6	11.3	6.72	8.2
E-150	32–34	22–28	0	3.26	8.26	0.0
			2.6	4.63	7.38	23
E-210	27–29	340–370	0	1.69	5.47	0.0
			2.6	1.94	4.27	0.0
			10.6	1.74	6.83	1.2
			22.3	1.65	4.95	0.8
E-220	27–29	125–175	0	3.16	7.59	0.0
			2.6	4.51	7.05	3.5
			10.6	4.11	8.82	4.5
			22.3	2.49	5.16	33
E-240	27–29	22–28	0	3.79	8.16	0.0
			2.6	4.99	6.46	2.4
			10.6	3.44	5.72	6.3
			22.3	1.38	2.24	65
E-250	27–29	12–18	0	4.19	8.36	0.0
			2.6	5.01	6.99	0.0
			10.6	4.66	6.27	8.2
			22.3	6.44	6.48	5.6
E-260	27–29	5–7	0	5.14	1.21	0.0
			2.6	3.63	11.9	0.0
			10.6	5.61	6.93	2.2
			22.3	3.81	4.81	4.8
E-350	24–26	16–22	0	3.84	10.3	0.0
			2.6	3.53	9.89	0.0
E-460	17–19	2–2	0	5.78	11.8	0.0
			2.6	7.85	6.48	3.3

radiation at the 2.6 Mrad dosage level as shown in Table V. The next higher level of radiation dosage, 10.6 Mrad, generally showed a decrease in the molecular size of the copolymer in solution but was accompanied by an increase in the gel content. Sample E-250 (27-29 % VA, 12–18 M.I.) showed a drop in gel content between irradiation dosages of 10.6 and 22.3 Mrad. In the series of copolymers having the same composition (27–29 % VA), maximum sensitivity to irradiation was experienced in the medium to low molecular weight range. This can be seen for samples E-240 (M.I. 22–28) and E-220 (M.I. 125–175) in Table V. It can also be seen that the greatest response to irradiation seems to be with copolymers with vinyl acetate content greater than 30 % as judged by gel content and by increase in the weight average molecular size of the soluble fraction. The effect upon the weight average molecular size, $\bar{A}_w$, in solution is also shown in Fig. 3. A plot of melt index *vs.* gel content (Fig. 4) shows that sample E-240 (27–29 % VA, 22–28 M.I.) produces the greatest degree of cross-linking for copolymers of the same composition. Samples with lower melt index (higher initial molecular weight) show less polymer growth. This is attributed to degradation of the polymer and is best illustrated by sample E-250 (27–29 % VA, 12–18 M.I.) in Table V which shows a decrease in gel content between 10.6 and 22.3 Mrad.

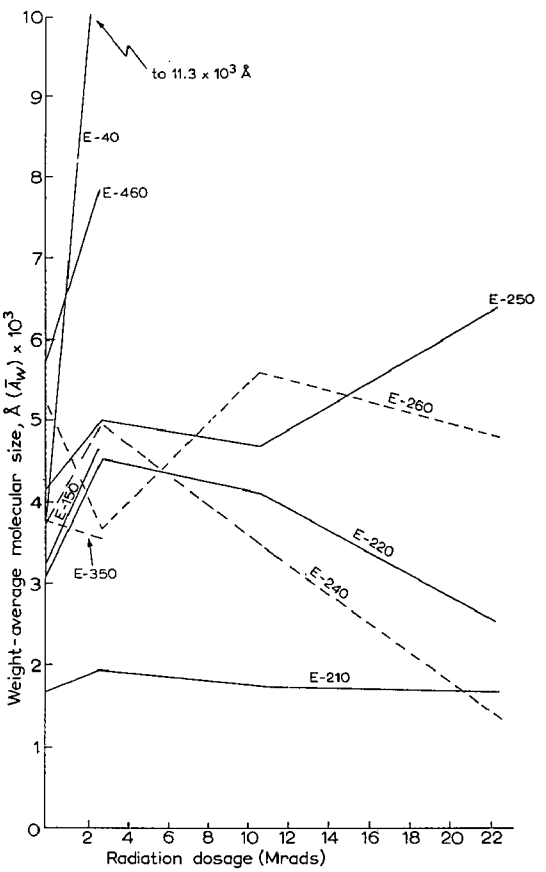

Fig. 3. Ethylene–vinyl acetate copolymers: molecular size *vs.* radiation dosage; *o*-dichlorobenzene solution.

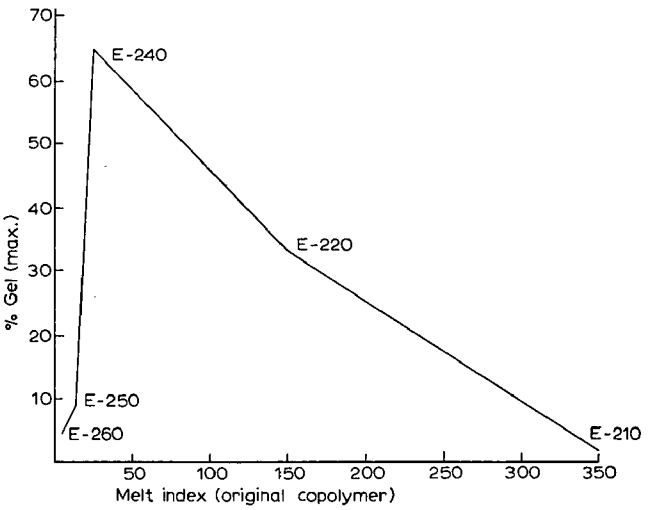

Fig. 4. Melt index *vs.* maximum gel content of ethylene–vinyl acetate copolymers containing 27–29% vinyl acetate.

TABLE VI

EFFECT OF γ-IRRADIATION ON MECHANICAL PROPERTIES

Ethylene–vinyl acetate copolymers: copolymers of varying molecular weight, same composition (28%, VA).

Sample No.	*M.I.* (*g/10 min*)	*Radiation dosage* (*Mrads*)	*Break stress* (*p.s.i.*)
E-210	340–370	0	511
		2.6	537
		10.6	582
		22.3	579
E-220	125–175	0	584
		2.6	1097
		10.6	1138
		22.3	1020
E-240	22–28	0	1179
		2.6	1245
		10.6	737
		22.3	2000
E-250	12–18	0	1371
		2.6	1312
		10.6	1395
		22.3	1122
E-260	5–7	0	2541
		2.6	2700
		10.6	2125
		22.3	1979

TABLE VII

EFFECT OF γ-IRRADIATION ON MECHANICAL PROPERTIES

Ethylene–vinyl acetate copolymers of similar molecular weight, varying composition.

Sample No.	*E/VA mole ratio*	*VA (%)*	*M.I. (g/10 min)*	*Radiation dosage (Mrads)*	*Break stress (p.s.i.)*	*Break elongation (%)*	*Tensile modulus (p.s.i. × 10^{-3})*
E-40	4.4/1	39–42	45–65	0	824	1247	0.35
				2.6	844	891	0.39
E-150	6.25/1	32–34	22–28	0	1026	1028	0.97
				2.6	917	698	0.95
E-240	8/1	27–29	22–28	0	1179	855	1.94
				2.6	1245	793	2.02
E-350	9.2/1	24–26	16–22	0	1679	921	2.80
				2.6	1755	836	2.72
E-460	14/1	17–19	2–3	0	2908	849	6.09
				2.6	3041	832	6.11

Samples E-250 and E-260, the higher molecular weight copolymers discussed above, showed significant losses in break stress (tensile strength) at 22.3 Mrad as shown in Table VI. Changes in breaking stress and tensile modulus were not significant at the 2.6 Mrad level for copolymers of similar molecular weight but varying composition (Table VII). However, the lessening in break elongation was significant except for sample E-460 (M.I. 2–3) which may have had little macro-Brownian movement to permit cross-linking due to the high molecular weight.

This study demonstrates that three parameters of radiation cross-linking of copolymers have been identified with molecular size distribution measurements conducted with GPC and gel content determinations. The three parameters are: (1) composition of copolymer, (2) molecular weight of starting material, and (3) radiation dosage. The cross-linking effect of each of these parameters can be deduced with these techniques which constitute a method for defining the optimum conditions for achieving a radiation cross-linked polymer. The validity of this approach is supported with measurements of physical properties which show correlation with the cross-linking effects observed with GPC and gel content studies.

ACKNOWLEDGEMENT

Data relating to mechanical measurements were supplied by P. R. BEUCHLER and R. E. BRAND. Chemical dosimetry measurements were conducted by J. P. GUARINO.

REFERENCES

1 H. Y. KANG, O. SAITO AND M. DOLE, *J. Amer. Chem. Soc.*, 89 (1967) 1980.
2 P. J. FLORY, *J. Phys. Chem.*, 46 (1942) 132.
3 B. J. LYONS AND A. S. FOX, *J. Polym. Sci., C*, 21 (1968) 159.
4 A. CHARLESBY, *Proc. Royal Soc. (London)*, A215 (1952) 187.
5 A. CHARLESBY, *Proc. Royal Soc. (London)*, A222 (1954) 60.
6 D. O. GEYMER, *Makromol. Chem.*, 100 (1967) 186.

CHROM. 5121

PRACTICAL GEL PERMEATION CHROMATOGRAPHIC COLUMN CALIBRATION FOR POLYMERS

M. ZINBO AND J. L. PARSONS
Scientific Research Staff, Ford Motor Company, Dearborn, Mich. 48121 (U.S.A.)

SUMMARY

A gel permeation chromatographic column calibration technique for polymers under a given set of operating conditions such as column, solvent, oven temperature, and elution rate is presented, using the exponent a of appropriate limiting viscosity number–molecular weight relationships of various polymers. The elution volumes V_e usually bear a linear, inverse relationship to the logarithms of molecular weight within a limited molecular weight range, permitting extrapolation to molecular weight unity as a measure of the apparent maximum elution volume V_m. A linear relationship between log V_m/V_e and log M over the linear range of log M *versus* V_e curves has been demonstrated for available polystyrene and polypropylene glycol standards for several given gel permeation chromatographic operating conditions. The indicated linear relationships for the polymer standards may be expressed by simple equations of the form $(V_m/V_e) = kM^{a'}$, where V_m and a' are constant for a given polymer under a given set of operating conditions and k is constant for a given operating condition. It seems likely that a' is a linear function of the exponent a of the limiting viscosity number–molecular weight relationship over the corresponding linear range of molecular weight. Thus, a given gel permeation chromatographic column system can be characterized for polymer samples by the column constant k and a conversion factor f between a and a'. The calibration technique is then of particular interest for polymers of different types than the available standards. An application of the technique to polyethylene oxide is presented.

INTRODUCTION

Calibration in gel permeation chromatography (GPC) has been one of the major problems for evaluating the chromatograms when the calibration curve for a given polymer sample in question is unknown. A functional relationship between the peak elution volume of a series of nearly monodisperse samples and their molecular weight is usually difficult to establish except for two series of commercially available polystyrenes (PS) and polypropylene glycols (PPG). It was apparent in the early stages of GPC development that the elution volume is not a function of molecular weight of the solute molecules alone, but that also interaction of GPC solvent with the polymer and chemical structure of the polymer play a role.

BENOIT *et al.*[1-3] have demonstrated that the logarithms of the products of molecular weight and intrinsic viscosity when plotted as a function of peak elution volumes for structurally different polymers yield a single curve. It is probably the most "universal calibration" to date which is independent of polymer type. The theoretical justification for using $M \cdot [\eta]$ or a similar quantity as a universal calibration function to transform the primary calibration curve into calibration curves for linear but structurally different polymers has been reported[4]. However, it should be noted that BENOIT's "universal calibration" procedure requires that intrinsic viscosities must be measured for each polymer sample, such as for a series of research-type polymers.

It was our primary objective to find a more practical way to calibrate a given solvent–column system for several different types of polymers, using available polymer standards and the reported values of the exponent a in the Mark-Houwink-Sakurada equation.

EXPERIMENTAL

Materials

The polystyrenes (PS) and polypropylene glycols (PPG) used were narrow-distribution samples supplied by Waters Associates (Framingham, Mass.). Carbowax 6000 and 20M were obtained from Applied Science Laboratories, Inc. and were characterized by NMR[5], osmometry, and viscosity. The standards employed for calibration and study are listed in Table I together with their intrinsic viscosities in several solvents. The root-mean-square average molecular weights or molecular weights at peak for PPG standards have been estimated by the "comparative technique" described by BLY[6].

Intrinsic viscosities

The instrument used was a modified Ubbelohde viscometer, originally described by CRAIG AND HENDERSON[7], equipped with a Hewlett Packard Model 5901B

TABLE I

POLYMER STANDARDS AND DATA

Standard No.	$\bar{M}_{rms}$	*Intrinsic viscosity, dl·g⁻¹ at 30.0°*			
		DMF	*p-Dioxane*	*Toluene*	*Benzene*
PS 1	4 800	0.0470	0.0578	0.0559	0.0587
2	10 000	0.0731	0.0888	0.0910	—
3	19 750	0.1110	0.1478	0.1487	0.1586
4	50 000	0.1971	0.2681	0.2800	—
5	97 200	0.2981	0.4237	0.4330	0.4748
6	171 000	0.4142	—	0.6610	—
7	402 000	0.6966	—	1.1069	1.2590
8	830 000	—	—	1.9040	—
9	1 987 000	—	—	3.5070	—
PPG 1	830	0.0300	0.0307	0.0215	—
2	1 280	0.0382	0.0410	0.0315	0.0448
3	2 100	0.0525	0.0573	0.0520	0.0620
4	4 100	0.0778	0.0932	0.0941	0.1012

autoviscometer read-out. Measurements were carried out at four or five different concentrations within a range of 0.1 to 1.3 $g \cdot dl^{-1}$. Reduced viscosities, η_{sp}/c, were plotted against c according to HUGGINS[8].

Gel permeation chromatography

A Waters' Ana-Prep Gel Permeation Chromatograph used in this work was slightly modified to prevent solvent evaporation from the syphon[9]. Operating conditions varied and are listed in Table II.

TABLE II

GPC COLUMN SET AND OPERATING CONDITION

GPC column set	*Waters' column designation, (Å)*	*Solvent*	*Oven temperature (°C)*	*Flow rate (ml/min)*
A	$10^4 + 10^3 + 10^2$	DMF	39	1.00
B	$10^2 + 10^3 + 10^4$	*p*-Dioxane	50	0.96
C	$10^4 + 10^3 + 10^2$	*p*-Dioxane	39	0.89
D	$10^4 + 10^3 + 10^5$	*p*-Dioxane	50	0.83
E	$10^4 + 10^3 + 10^5$	*p*-Dioxane	39	0.75
F	$10^5 + 10^4 + 10^3$	Toluene	50	0.89
G	$10^2 + 10^3 + 10^4$	Toluene	50	0.96
H	$10^4 + 10^3 + 10^5$	Benzene	36	0.86

RESULTS

Intrinsic viscosity–molecular weight relationships determined for PS and PPG standards in several solvents are summarized in Table III. There are some discrepancies of the exponent a with the values reported in the literature. The most likely source of error would be a difference in the polydispersity of samples for which the constants were measured.

Figs. 1(a), (b), (c) and (d) illustrate GPC calibration curves for PS and PPG

TABLE III

VISCOSITY–MOLECULAR WEIGHT RELATIONSHIPS, $[\eta] = K\bar{M}^a_{rms}$

All measurements were done at 30 ± 0.01°.

Standard	*Solvent*	$K \times 10^4$ *(dl/g)*	*a*	*Mol. wt. range* $M \times 10^{-3}$
Polystyrene	DMF	2.606	0.612	5–400
	p-Dioxane	2.241	0.655	5–100
	Toluene	1.786	0.680	5–2000
	Benzene	1.623	0.695	5–400
Polypropylene glycol	DMF	5.284	0.598	0.8–4
	p-Dioxane	2.247	0.715	1–4
	Toluene	0.447	0.920	0.8–4
	Benzene	3.241	0.686	1–4

standards with column sets A, C, F, and H. Both the logarithms of molecular weight and of the products of molecular weight and intrinsic viscosity are plotted against elution volume.

It was observed that the logarithm of $1/V_e$ is a linear function of the logarithm of M at peak position over the linear range of log M *vs.* V_e curves. Two examples are given in Fig. 2 (column set: A and B).

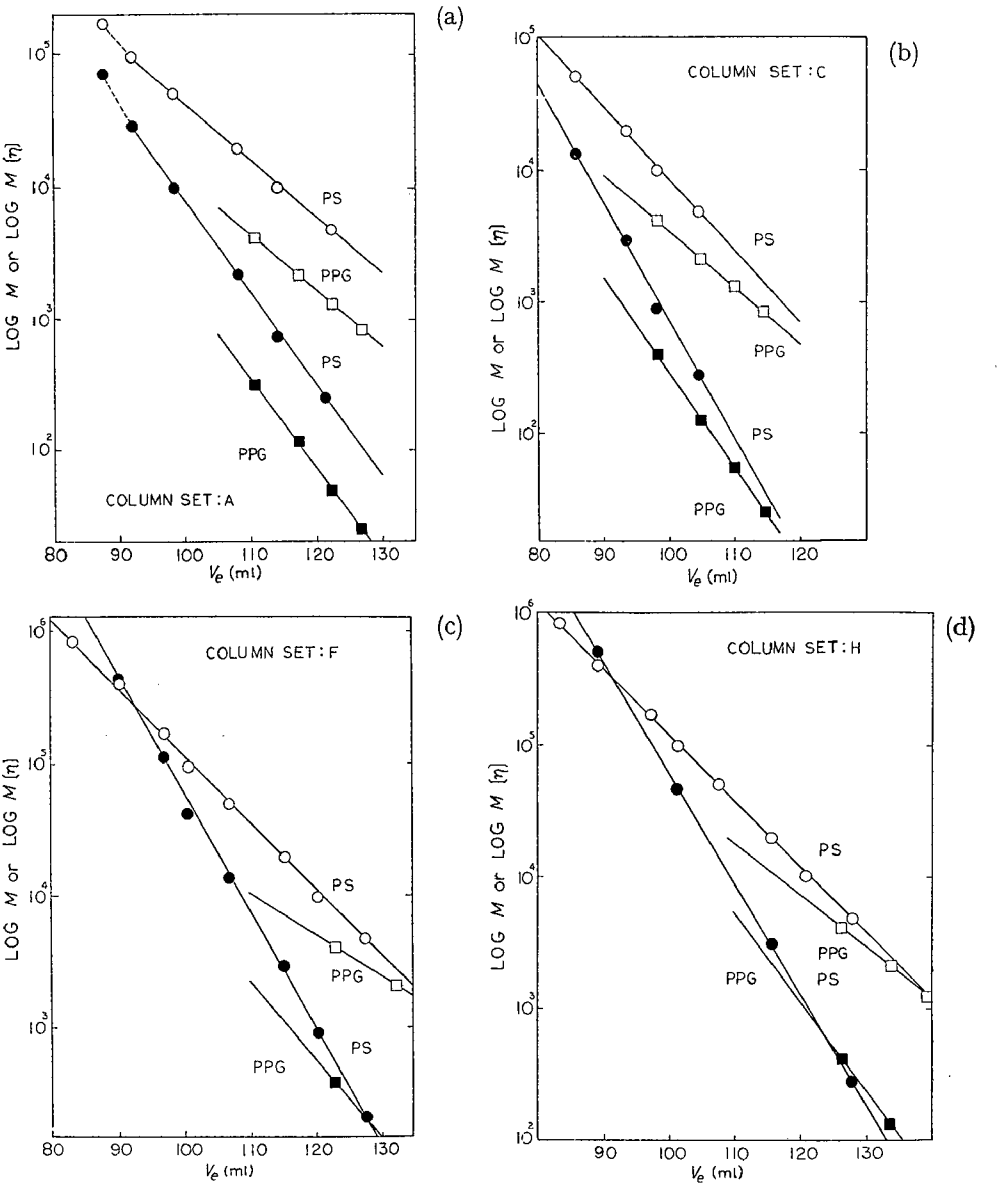

Fig. 1. (a) Calibration data for PS and PPG with column set A. (b) Calibration data for PS and PPG with column set C. (c) Calibration data for PS and PPG with column set F. (d) Calibration data for PS and PPG with column set H. ○, log M *vs.* V_e for PS; □, log M *vs.* V_e for PPG; ●, log $M \cdot [\eta]$ *vs.* V_e for PS; ■, log $M \cdot [\eta]$ *vs.* V_e for PPG.

An empirical constant V_m for both PS and PPG under a given set of operating conditions has been obtained by extrapolation of the linear range of log M *vs.* V_e calibration curves to molecular weight unity. Then another extrapolation to molecular weight unity of the plot of log V_m/V_e *vs.* log M for both PS and PPG standards

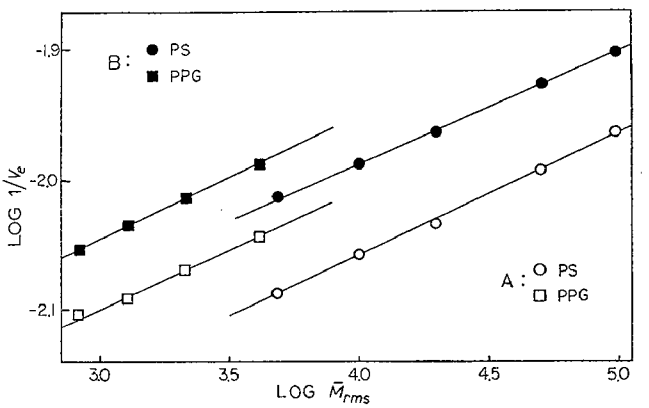

Fig. 2. Double logarithmic plots of M *vs.* $1/V_e$ in DMF and *p*-dioxane for PS and PPG. ○, PS with column set A; □, PPG with column set A; ●, PS with column set B; ■, PPG with column set B.

under the limited conditions described above comes to a point, giving another empirical constant, k. Figs. 3(a), (b), (c) and (d) illustrate the extrapolation described above for the column sets A, B, C, and G.

The indicated relationships for PS and PPG standards over the linear range of log M *vs.* V_e calibration curves may be expressed by simple equations of the form

$$(V_m/V_e) = k\bar{M}_{rms}^{a'}$$

where k and a' are constants determined, respectively, by the intercept and the slope of a plot of the type shown in Fig. 3 and V_m is a constant determined by extrapolation of the linear range of the log calibration curve to molecular weight unity. Empirical constants for the equation for both PS and PPG standards are summarized in Table IV together with the ratio between a and a'. The ratio f, which can be called a conversion factor, is assumed to be constant for any type of polymer within the following limitations:

(1) molecular weight must be within a linear range of the log calibration curve,
(2) intrinsic viscosity–molecular weight relationship should cover the linear range of the log calibration curve, and
(3) a given set of GPC operating conditions must be used.

The equation indicates that having one known standard, two average molecular weights or one average molecular weight with polydispersity less than 1.10 is sufficient to find the effective linear calibration over the range of the linear log calibration of standards.

The present calibration procedure was applied to an intermediate mol. wt. polyethylene oxide–Carbowax 20M with column sets A and B. Carbowax 6000,

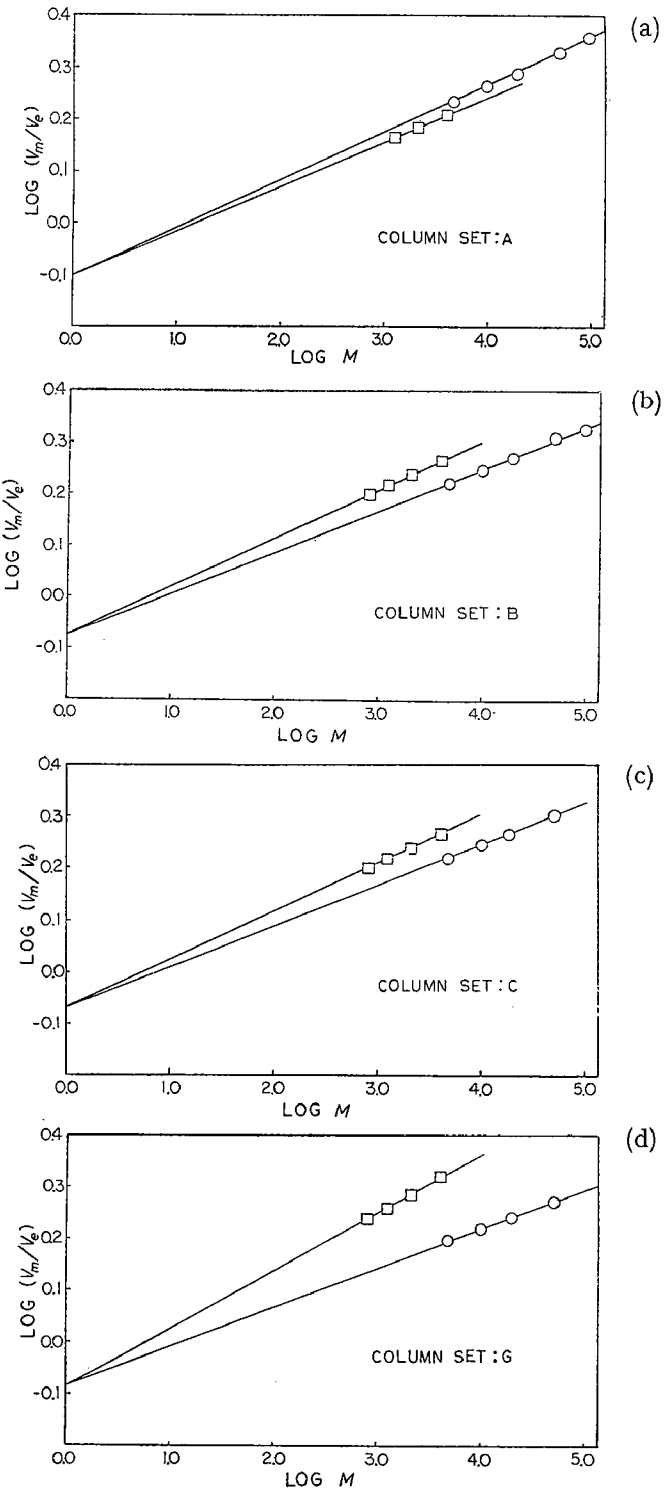

Fig. 3. (a) Double logarithmic plots of M *vs.* V_m/V_e for PS and PPG with column set A. (b) Double logarithmic plots of M *vs.* V_m/V_e for PS and PPG with column set B. (c) Double logarithmic plots of M *vs.* V_m/V_e for PS and PPG with column set C. (d) Double logarithmic plots of M *vs.* V_m/V_e for PS and PPG with column set G. ○, PS; □, PPG.

TABLE IV

EMPIRICAL CONSTANTS OF THE EQUATION $(V_m/V_e) = k\bar{M}_{rms}^{a'}$

GPC column set	*Standard*	V_m *(ml)*	a'	k	$f = a/a'$
A	PS	209.50	0.094	0.791	6.51
	PPG	179.50	0.092		6.50
B	PS	172.00	0.087	0.841	7.53
	PPG	178.25	0.095		7.53
C	PS	172.25	0.084	0.849	7.80
	PPG	181.75	0.092		7.77
G	PS	157.50	0.076	0.822	8.94
	PPG	199.20	0.112		8.21
H	PS	203.00	0.087	0.832	7.99
	PPG	210.20	0.086		7.98

$\bar{M}_w/\bar{M}_n = 7500/7300$, which had been characterized by NMR near end-group assay[10], vapor phase osmometry, and viscosity, was used as a single standard for the procedure. The viscosity–molecular weight relationships used for the exponent a were:

$$[\eta] = 0.02 + 24 \times 10^{-5} \cdot \bar{M}_w^{0.73}$$

$(1.0 \times 10^3 < \bar{M}_w < 3.0 \times 10^4$; DMF; at 25°) (see ref. 11)

and

$$[\eta] = 0.0075 + 35 \times 10^{-5} \cdot \bar{M}_n^{0.71}$$

$(6.0 \times 10 < M_n < 1.9 \times 10^4$; p-dioxane; at 20°) (see ref. 12).

The results are given in Figs. 4 (column set A) and 5 (column set B).

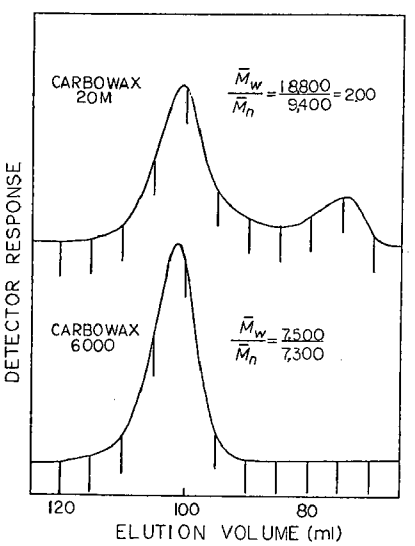

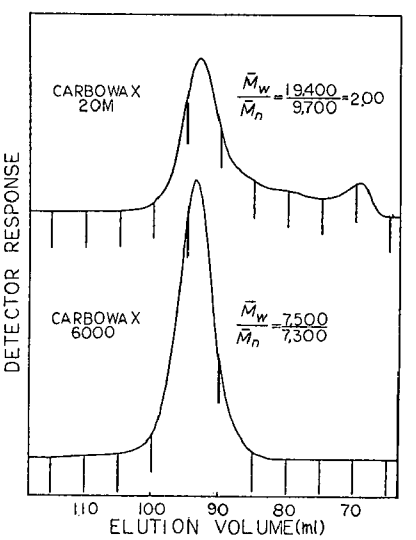

Fig. 4. GPC chromatograms of Carbowax 6000 and 20M. Column set A, $k = 0.791$, $f = 6.50$, $a' = 0.112$, and $V_m = 216.5$ ml.

Fig. 5. GPC chromatograms of Carbowax 6000 and 20M. Column set B, $k = 0.841$, $a' = 0.094$, and $V_m = 181.5$ ml.

DISCUSSION

It has been reported[13] that available PS and PPG standards below 5000 mol. wt. do not give calibration curves consistent with the Benoit "universal calibration". The same deviations have been observed by us in several given sets of GPC operating conditions (Fig. 1).

The viscosity of a polymer solution depends in the first place on the factors which determine the volume occupied by the dissolved macromolecule in solution (molecular weight, interaction of the solvent with the polymer, chemical structure of the polymer) and on the concentration of the solution. Thus, the intrinsic viscosity of a polymer solution itself is a measure of the capacity of a polymer molecule to enhance the viscosity, which depends on the size and the shape of the molecule as well as molecular weight. The intrinsic viscosity is widely used in polymer studies, as it provides a simple and easy method of molecular weight determination of polymers for which the dependence of intrinsic viscosity on molecular weight has been established experimentally. Intrinsic viscosity–molecular weight relationships for various polymers have been compiled[14].

It is generally assumed that both K and a in the viscosity–molecular weight relationship become insensitive to the temperature when a exceeds about 0.70, and that they may be used in a ten-degree range on either side of the temperature at which the constants were determined. Note should be made that the exponent a does not vary with the kind of average molecular weight when a series of polymer samples used for viscosity measurements possess the same degree of polydispersity, but the constant K does vary with the particular average molecular weight. Furthermore, the exponent a is not expected to vary with molecular weight for a linear polymer in a good solvent at a given temperature except at rather low molecular weight, where the long-range interactions are reduced to zero[15].

If we exclude specific interactions between the solute molecules and the Styragel in the GPC process, the factors related to the viscous properties of polymer solutions are also the major factors involved in size separation by the GPC process. The fingering effect[16] or other concentration effects can be minimized by appropriate choice of experimental conditions.

It is generally easy to choose the column combination[6] so that there is a linear log M *vs.* V_e region which covers the interested range of molecular weights. The linear log regions for polymers, which are tedious to obtain a series of well characterized samples, can be safely estimated by the commercially available PS and PPG standards for a given set of operating conditions. As shown in Table IV, the exponent a seems to be a linear function of the constant a' in the equation obtained for PS and PPG standards; however, the relation should be further verified with several additional series of well characterized polymer samples. Even though the exponent a determined in ordinary solvents is valid only within a rather limited range of molecular weights, the value can be useful to find the constant a' for the corresponding molecular weight range of a linear log M *vs.* V_e curve. Thus, a and a' can be related for the corresponding molecular weight–solvent–temperature system as follows:

$$a = \frac{\mathrm{d} \log [\eta]}{\mathrm{d} \log M} = f \cdot a' = \frac{\mathrm{d} \log (V_m/V_e)}{\mathrm{d} \log M} \cdot f$$

The column constant k can be obtained graphically as shown in Fig. 3; however, it is recommended that the method of least squares be used for a series of polymer standards.

Very recently the use of the apparent maximum elution volume, V_m, as a measure of the apparent effective internal solvent volume has been reported[17] for the reverse gel permeation process. The constant V_m for a polymer in a given set of GPC operating conditions would be defined as the apparent elution volume of molecular weight unity.

Polyethylene oxide has been chosen for the examination of the calibration method with the column sets of A and B. The results are shown in Figs. 4 and 5. Number-average molecular weight of Carbowax 20M, obtained by the NMR near-end group analysis[10], was found to be 10500. Most likely sources of error would be the instrumental spreading and the temperature difference between viscosity measurements and GPC operation. However, it seems that the agreement between number-average molecular weights obtained by the present method and by NMR is satisfactory.

DUERKSEN AND HAMIELEC[18] have reported the increasing importance of the resolution correction with increasing molecular weight and decreasing residence times. For the linear region of a given linear log calibration (log M *vs.* V_e), provided that efficient columns are used, resolution varies linearly with log M[19]. When the variation of resolution with molecular weight is known, the calculation of molecular weight parameters from the chromatogram *via* the calibration of a given polymer become valid. According to HAMIELEC[20], the specific resolution R_s derived by BLY[19] is consistent with the analytical solution of Tung's integral dispersion equation for symmetrical axial dispersion. Considering the present results and the specific resolutions derived by BLY and HAMIELEC, it is clearly indicated that different types of polymers have different specific resolutions at a given elution volume for a given set of GPC operating conditions. Thus we feel that the logarithm of molecular weight *versus* elution volume calibration for polymers should be used to evaluate chromatograms with valid molecular weight parameters, such as for resolution correction and for "analytical solution"[20].

CONCLUSION

It has been assumed that the conversion factor f and the empirical constant k for a given set of operating conditions are constant for any type of polymer. They are the key parameters for the present calibration technique. It has been felt that the constancy of k and f should be confirmed further with some different series of well characterized polymer samples. However, it seems that by using a series of well characterized polymer samples, a given set of operating conditions can be characterized by a column constant k and a conversion factor f over the corresponding linear range of molecular weight and temperature. Thus, by using a well characterized polymer sample with a known value of the exponent a from an appropriate viscosity–molecular weight relationship, the log M *vs.* V_e calibration can be obtained for the polymer by using the equation.

The application of this column calibration procedure to a specific polymer is straightforward and average molecular weights are simple to estimate when there is

a viscosity–molecular weight relationship and a well characterized polymer sample available. Such a polymer sample can be collected from the analytical column and characterized by classical methods.

Column calibration for a polymer for which the viscosity–molecular weight relationship is not available, will be reported in the near future.

ACKNOWLEDGEMENT

We wish to express our thanks to Dr. J. F. KINSTLE for valuable discussions of this work. We also wish to acknowledge the help of Mr. W. K. OKAMOTO and Miss A. W. TAUB in calculating the GPC data.

REFERENCES

1 H. BENOIT, Z. GRUBISIC, P. REMPP, D. DECKER, AND J. ZILLIOX, *J. Chim. Physiol.*, 63 (1966) 1507.
2 Z. GRUBISIC, P. REMPP AND H. BENOIT, *Polym. Lett.*, 5 (1967) 753.
3 H. BENOIT AND Z. GRUBISIC, *Proc. 5th Intern. Seminar Gel Permeation Chromatography, London, 1968.*
4 H. COLL AND D. K. GILDING, *J. Polym. Sci.*, A2, (1970) 89.
5 K. LIU, *Makromol. Chem.*, 116 (1968) 146.
6 D. D. BLY, *Proc. 6th Intern. Seminar Gel Permeation Chromatography, Florida, 1968.*
7 A. W. CRAIG AND D. A. HENDERSON, *J. Polym. Sci.*, 19 (1956) 215.
8 M. L. HUGGINS, *J. Amer. Chem. Soc.*, 64 (1942) 2716.
9 W. W. YAU, H. L. SUCHAN, C. P. MALONE AND S. W. FLEMING, *Proc. 5th Intern. Seminar Gel Permeation Chromatography, London, 1968.*
10 J. E. TANNER, private communication.
11 T. A. RITSCHER AND H. G. ELIAS, *Makromol. Chem.*, 30 (1959) 48.
12 C. SADRON AND P. REMPP, *J. Polym. Sci.*, 29 (1958) 127.
13 J. R. RUNYON, *159th ACS National Meeting Abstract, Cell-26, Houston, 1970.*
14 M. KURATA, M. IWAMA AND K. KAMADA, in J. BRANDRUP AND E. H. IMMERGUT (Editors), *Polymer Handbook*, ch. IV, Interscience, New York, 1967, pp. 7–46.
15 C. ROSSI, U. BIANCHI AND E. BIANCHI, *Makromol. Chem.*, 41 (1960) 31.
16 J. C. MOORE, *159th ACS National Meeting Abstract, Cell-21, Houston, 1970.*
17 L. F. MARTIN, F. A. BLOUIN AND S. P. ROWLAND, *159th ACS National Meeting Abstract, Cell-16, Houston, 1970.*
18 J. H. DUERKSEN AND A. E. HAMIELEC, *J. Polym. Sci.*, C, 21 (1968) 83.
19 D. D. BLY, *J. Polym. Sci.*, C, 21 (1968) 13.
20 A. E. HAMIELEC, in J. C. MOOR (Editor), *Gel Permeation Chromatography*, Appendix 1, St. Louis, 1969.

CHROM. 5122

EXAMINATION OF POLYMER SIZE PARAMETERS FOR UNIVERSAL CALIBRATION IN GEL PERMEATION CHROMATOGRAPHY

J. V. DAWKINS, J. W. MADDOCK AND D. COUPE
Imperial Chemical Industries Ltd., Petrochemical and Polymer Laboratory, The Heath, Runcorn, Cheshire (Great Britain)

SUMMARY

Various procedures for universal calibration in gel permeation chromatography with polystyrene gels are examined for polystyrene and poly(dimethylsiloxane) fractions. For *o*-dichlorobenzene at 138°, experimental intrinsic viscosity–molecular weight data show that the Mark-Houwink exponents are 0.70 and 0.57 for polystyrene and poly(dimethylsiloxane), respectively. In principle, this difference permits a distinction between the various polymer size parameters proposed for universal calibration. An interpretation of the experimental poly(dimethylsiloxane) calibration for *o*-dichlorobenzene at 138° requires a consideration of errors in average molecular weights and errors arising from the use of average molecular weight instead of peak molecular weight. When hydrodynamic volume and unperturbed dimensions calibration procedures are examined, the difference between them is comparable with experimental error. If the FLORY-FOX viscosity expression is employed, the perturbed end-to-end distance (or radius of gyration) gives an equivalent universal calibration to the hydrodynamic volume. The experimental data are sufficiently accurate to show that the perturbed dimension determined with the PTITSYN-EIZNER relation does not give an adequate universal calibration.

CHROM. 5123

MOLECULAR WEIGHT ANALYSIS OF BLOCK COPOLYMER BY GEL PERMEATION CHROMATOGRAPHY

FRANKLIN S. C. CHANG
Borg-Warner Corporation, Roy C. Ingersoll Research Center, Des Plaines, Ill. 60018 (U.S.A.)

SUMMARY

A method is introduced for converting the experimental elution volume to molecular weight of linear block copolymer by use of the calibration curves for homopolymers. The basis of this method is the linear relationship between the logarithm of molecular weight and the elution volume. In a comparison of the results obtained by this method and those calculated, according to a method recently suggested by RUNYON and coworkers[1], it has been found that this method gives lower molecular weight than the latter method does. In the case of styrene–butadiene block copolymer in tetrahydrofuran, the difference is negligible for all practical purposes. It can be deduced, however, that in some extreme cases the RUNYON correction can give a molecular weight 80 % higher than that calculated by the suggested method.

INTRODUCTION

Gel permeation chromatography (GPC) has been developed into a most convenient technique for the determination of molecular weight distribution (MWD) of polymers. For homopolymers the interpretation of experimental GPC curve is now standard procedure. The relation between the GPC curve of a block polymer and its MWD is yet to be established. The interpretation in this case is complicated by the presence of a composition distribution along with MWD. RUNYON and coworkers[1] have recently suggested a method to calculate the MWD of styrene–butadiene block polymer from GPC and UV data; the latter being obtained by adding a UV spectrometer to the GPC instrument. In this paper a slightly different method for calculating the molecular weight of block polymer from elution volume is introduced and compared with the above method.

PARALLEL CALIBRATION CURVES

The most useful part of a molecular weight *vs.* elution volume calibration curve from a gel permeation chromatogram is a straight line on a semi-log plot which can be expressed as

$$V - V_0 = k(\log M - \log M_0) \qquad (1)$$

where M is the molecular weight eluted at solvent volume V and k is a constant. The subscript zero designates the reference point. When the calibration curves for two homopolymers A and B are parallel to each other, *i.e.*, when they have the same slope, at any elution volume the following is true:

$$M_A = rM_B$$

where M_A and M_B are the molecular weights of A and B respectively at elution volume V and r is the ratio of M_A to M_B at the reference elution volume V_0. This relation shows that so far as elution volume is concerned M_A and rM_B are equivalent. Let us assume that this equivalence can be applied to the component blocks in a block copolymer. That is to say, it is assumed that a homopolymer with molecular weight M_A' will elute at the same solvent volume as a block copolymer $M_1 + M_2$ when $M_A' = M_1 + rM_2$, where M_1 and M_2 are the molecular weights of the blocks of monomers A and B respectively. Since the molecular weight of the block copolymer $M_c = M_1 + M_2$, $M_1 = W_1M_c$ and $M_2 = W_2M_c$, it follows that

$$M_c = M_A'/(1 + [r - 1]W_2) \tag{2}$$

where W_2 is the weight fraction of monomer B in the copolymer M_c. Therefore, the molecular weight of the block polymer can be calculated by (1) evaluating r from the two calibration curves for homopolymer, (2) reading M_A' at the elution volume of the homopolymer from the calibration curve for homopolymer A, (3) determining W_2 by UV spectrum in a case such as styrene–butadiene copolymer, and (4) calculating M_c by use of eqn. 2.

UNPARALLEL CALIBRATION CURVES

When the calibration curves of two homopolymers under the same experimental conditions are not parallel to each other, the case can be stated mathematically as follows:

$$\begin{aligned} V - V_0 &= k_1 (\log M_A - \log M_{Ao}) \\ &= k_2 (\log M_B - \log M_{Bo}) \\ k_1 &\neq k_2 \end{aligned} \tag{3}$$

It is assumed that the B block in the copolymer can be substituted by a block M_1' of monomer A, without changing the elution volume if

$$M_1' = \left(\frac{M_2}{M_{20}}\right)^{k_2/k_1} M_{10}$$

Then the homopolymer A having the same elution volume as the block polymer has a molecular weight M_A'.

$$M_A' = M_1 + \left(\frac{M_2}{M_{20}}\right)^{k_2/k_1} M_{10}$$

Subtracting $M_c = M_1 + M_2$ and rearranging terms, we have

$$k_3(W_2M_c)^{k_2/k_1} - (1 + W_2)M_c + M_A' = 0 \quad (4)$$

where $k_3 = M_{10}M_{20}^{-k_2/k_1}$ is a constant. With k_1, k_2 and k_3 calculated from the calibration curves of the two homopolymers, W_2 determined experimentally and M_A' read from the calibration curve at the same elution volume as the copolymer in question, eqn. 4 can be solved for M_c, the molecular weight of the block copolymer. For instance, when $k_2/k_1 = 2$, eqn. 4 is quadratic and can be solved. For other values of k_2/k_1, it may be more convenient to find M_c by trial and error. In the special case when $k_2 = k_1 = k$ the two calibration curves are parallel to each other and $k_3 = r$. Eqn. 4 reduces to eqn. 2.

Eqn. 3 can be rewritten as

$$\log M_B = \frac{k_1}{k_2} \log M_A + \log M_{B0}M_{A0}^{-k_1/k_2}$$

Based on the universal calibration curve and the Mark-Houwink equation it can be derived (*e.g.* see ref. 2)

$$\log M_B = \frac{1 + a_1}{1 + a_2} \log M_A + \frac{1}{1 + a_2} \log \frac{K_1 f(e_2)}{K_2 f(e_1)}$$

where K and a are the constants in the Mark-Houwink equation and $f(e)$ is a function of a. A comparison of these two equations reveals

$$\frac{k_1}{k_2} = \frac{1 + a_1}{1 + a_2}$$

and

$$M_{B0}M_{A0}^{-k_1/k_2} = [K_1 f(e_2)/K_2 f(e_1)]^{1/(1+a_2)}$$

In trichlorobenzene at 135°, the values of k_1/k_2 for poly-α-methylstyrene, polypropylene[2], and polyethylene, compared to polystyrene, are 1.021, 0.975, and 0.990 respectively — close enough to 1 to justify the use of eqn. 2 instead of eqn. 4, even though the calibration curves are not strictly parallel to each other. Since the value of a varies in a narrow range from 0.5 to 0.8 (ref. 3) one can anticipate that eqn. 2 can be applied to most solvent and block copolymers and eqn. 4 will be needed less frequently for higher precision.

DISCUSSION

Although the derivations are done for diblock polymers, the treatment can be readily extended to triblock cases. The third block is treated in the same manner as the second block. Thus, $M_A' = M_1 + r_2M_2 + r_3M_3$, and $M_c = M_A'/(1 + [r_2 - 1]W_2 + [r_3 - 1]W_3)$ for the ABC type of block polymer. It can be readily deduced that this treatment makes no distinction between ABA and ABAB types

TABLE I

COMPARISON OF CORRECTION FACTORS

W_2	$r = 2$		$r = 5$		$r = 10$	
	$W_2 \log r$	$\log (1 + W_2)$	$W_2 \log r$	$\log (1 + 4W_2)$	$W_2 \log r$	$\log (1 + 9W_2)$
0.20	0.061	0.079	0.140	0.255	0.20	0.447
0.30	0.091	0.114	0.210	0.342	0.30	0.568
0.40	0.121	0.146	0.280	0.415	0.40	0.663
0.50	0.152	0.176	0.349	0.477	0.50	0.740
0.60	0.182	0.204	0.419	0.531	0.60	0.806
0.70	0.212	0.230	0.489	0.580	0.70	0.863
0.80	0.242	0.255	0.559	0.623	0.80	0.914

of copolymers, both of which are treated as AB type diblock cases. If we carry this reasoning one step further, a random copolymer of comonomers A and B would be treated as an AB type block polymer. It would be interesting to find out experimentally whether GPC would not distinguish a random copolymer from a diblock or triblock polymer of the same composition and molecular weight.

This can be readily observed from eqn. 2, $M_c = M_A'/(1 + [r - 1]W_2)$. It shows that a homopolymer A of molecular weight M_A', if it is present in the block polymer sample, will be fractionated at the same elution volume as the block polymer M_c. Since this equation can be expressed in terms of M_B' as well, the homopolymer M_B' would be also separated at this elution volume. So will other structures of various values of W_2. For example, in a styrene–butadiene block polymer S(100 000), S(90 000) B(5000), S(88 000) B(6000) and B(50 000) would all be eluted at the same elution volume, if they are present. [S(m)B(n) stands for a polymer consisting of a block of polystyrene of molecular weight m and a block of polybutadiene of molecular weight n.] Therefore, what we have obtained from GPC fractionation is a GPC average molecular weight and a GPC average composition. Further work is needed to convert the GPC average MWD of block polymer to its true MWD. This is a subject being currently studied in our laboratory.

RUNYON and coworkers[1] suggested that the molecular weight of a block copolymer is related to the molecular weights of the homopolymers at the same elution volume according to the following equation:

$$M_c = {M_{A_1}'}^{W_1} {M_B'}^{W_2}$$

Since $W_1 + W_2 = 1$ and $M_A'/M_B' = r$,

$$M_c = M_A'/r^{W_2} \tag{5}$$

Comparing this equation with eqn. 2 one can see that the difference between the two corrections is in the form of the function of r. In one the correction factor is r^{-W_2}, and in the other it is $(1 + [r - 1]W_2)^{-1}$. A comparison is made in Table I of the actual values calculated according to these two methods for various values of r and W_2.

It can be seen from Table I that for low values of r, say $r = 2$, the two methods

of correction give almost the same results. The difference amounts to only 4 % at the most, probably well within experimental error. Only at high value of r the difference is appreciable. In the case of $r = 10$ and $W_2 = 0.20$, eqn. 5 will give a molecular weight about 80 % higher.

ACKNOWLEDGEMENT

The author expresses his gratitude to Borg-Warner Corporation for permission to publish this work.

REFERENCES

1 P. RUNYON, D. E. BARNES, J. F. RUDD AND J. H. TUNG, *J. Appl. Polym. Sci.*, 13 (1969) 2359.
2 H. COLE AND D. K. GILDING, *J. Polym. Sci. A2*, 8 (1970) 89.
3 P. J. FLORY, *Principles of Polymer Chemistry*, Cornell University Press, New York, 1953, p. 311.

CHROM. 5124

GEL PERMEATION CHROMATOGRAPHIC ELUTION BEHAVIOR OF BRANCHED ALKANES

W. W. SCHULZ
Esso Research and Engineering Company, P.O. Box 121, Linden, N.J. 07036 (U.S.A.)

SUMMARY

The conformation of a branched alkane molecule can be described by the average number of gauche arrangements (*Zg*) which the molecule can assume. A quantitative relation of great exactness has been shown to exist between *Zg* and such bulk properties of branched alkanes as refractive index, density and heat of combustion.

The present study extends *Zg*-related properties to include gel permeation chromatographic elution behavior of branched alkanes in the range of C_7-C_{11}. The same simple rules, which had been evolved earlier for precise calculations of refractive index values, can be employed to predict gel permeation chromatographic elution behavior via the molecular volume concept.

The results of the study further confirm that the gel permeation process is one of volume exclusion and that for small, non-polar molecules a description of molecular volume is apparently sufficient to explain elution behavior.

INTRODUCTION

The conformation of a branched alkane can be described by the average number of gauche arrangements (*Zg*) which the molecule can assume. A method for calculating *Zg*-values has been published and applied to the calculation of *Zg*-values of over one hundred singly and doubly branched alkanes[1,2].

A linear dependence of great exactness was observed between *Zg*-values and such bulk properties of branched alkanes as refractive index, density and heats of combustion. It was found that the increment in physical property values, which each gauche conformation affects, is constant for all isomeric hydrocarbons and inversely proportional to molecular weight for alkanes of different carbon numbers. The introduction of an additional tertiary carbon atom in the hydrocarbon chain produces a constant shift, equivalent to one gauche conformation. For doubly branched alkanes steric effects require corrections terms. However, these corrections were found to be systematic and applicable to all analogously branched alkanes.

The observed correlations were taken as confirmation of the quantitative relation that exists between molecular volume and conformation. The fact that each gauche conformer exerts an identically large effect on such bulk properties as density,

refractive index and heat of combustion was taken as evidence that the properties are primarily dependent on intra-molecular interactions; while properties, such as boiling point or gas chromatographic retention index, would presumably be more responsive to inter-molecular interactions and would not be expected to correlate. The absence of correlations between *Zg*-values of singly branched tridecane isomers and their experimentally determined boiling points or gas chromatographic retention indices was taken as support for this reasoning[2].

In contrast to gas chromatography, which is based on a gas/liquid partition process, gel permeation chromatography (GPC) is believed to operate by molecular volume exclusion from a porous stationary phase. For macromolecules, hydrodynamic volume or mean external length are molecular size parameters which successfully correlate size and GPC elution volume for a number of polymers[3–5]. For small molecules, HENDRICKSON AND MOORE[6] and HENDRICKSON[7] related GPC elution volume of a large number of hydrocarbons and substituted hydrocarbons to their extended chain length values. SMITH AND KOLLMANSBERGER[8] noted an improved correlation using molar volume rather than chain length for hydrocarbons and halogenated aromatic compounds. Similarly, CAZES AND GASKILL[9] found molar volume correlative with GPC retention volume for a number of small molecule hydrocarbons, acids and alcohols. The GPC behavior of more than a hundred polynuclear aromatic hydrocarbons[10] indicated that separation is a complex function of molecular size, shape and polarity with no readily apparent correlations. From a GPC study of phenyl- and benzo-substituted aromatic compounds, it was concluded that the more molecular dimensions are considered, the more accurately the elution volume can be predicted, and that a sufficient number of molecular dimensions may uniquely describe the elution volumes of a small group of compounds[11].

The feasibility of extending the existing correlations between molecular conformation and molecular volume of branched hydrocarbons to include GPC elution behavior was studied with the aim of finding systematic correlations between size, structure and GPC elution volume of small molecules. Such correlations would provide additional insight into GPC's separation mechanism, aid in the prediction of the elution behavior or structure of unknown hydrocarbons, and be helpful towards the quantitative evaluation of chromatograms of saturated hydrocarbon oligomers and low-molecular-weight polymers.

EXPERIMENTAL

Apparatus and procedure

All measurements of elution volume were performed by means of Waters' Gel Permeation Chromatograph Model 100, employing an R-4-type differential refractometer detector. Four 4-ft. columns in series were used with nominal pore sizes of 10^4 Å, 10^3 Å, 10^2 Å, 10^2 Å. A total plate count of 1178 P/ft. was determined, injecting dichlorobenzene and applying the usual procedure for chromatogram width measurement and plate count calculation. Elution volumes were measured at peak maxima.

The solvent was tetrahydrofuran and the instrument temperature 23°. Samples were manually injected for 10–15 sec as 0.25 wt. % solutions in tetrahydrofuran. Solvent flow rate was kept close to 1 ml/min and detector sensitivity at 4 ×. All elutions were performed in close succession over a 3-day period to minimize the possibility

of column performance or calibration changes. *Zg*-values and corrections for double branching were obtained from tables published by MANN and coworkers[1,2]. *Zg* corrections were introduced to refer all double-branched alkanes to a single-branch basis for comparison purposes.

Materials

Hydrocarbons were either API standards or purchased from the Chemical Samples Company. Tetrahydrofuran was obtained from Matheson Coleman & Bell and used without further purification.

TABLE I

ELUTION VOLUMES, AVERAGE NUMBER OF GAUCHE ARRANGEMENTS (*Zg*) AND CALCULATED MOLAR VOLUMES OF BRANCHED ALKANES

Compounds	*Elution volume (counts)*	*Zg*	*Zg corrections for double branching*				*Corr. Zg*	*Molar volume*
			Add. branch	*1,1*	*1,2*	*1,3*		
3-Ethylpentane	30.58	3.58					3.58	143.5
3-Methylhexane	30.30	2.47					2.47	145.8
2-Methylhexane	30.13	1.64					1.64	147.6
2,4-Dimethylpentane	30.05	2.00	−0.88			−0.11	1.01	149.0
3,3-Dimethylpentane	30.38	4.00	−0.88				3.12	144.5
2,3-Dimethylpentane	30.43	3.55	−0.88		+0.60		3.27	144.1
2-Methyl-3-ethylpentane	30.07	5.00	−0.88		+0.64		4.76	158.8
4-Methylheptane	29.85	2.65					2.65	162.1
3-Methylheptane	29.87	2.79					2.79	161.8
2,5-Dimethylhexane	29.59	2.34	−0.88				1.46	164.6
2,2-Dimethylhexane	29.61	2.38	−0.88	+0.14			1.64	164.2
2,4-Dimethylhexane	29.80	3.23	−0.88			−0.20	2.19	163.1
3,3-Dimethylhexane	29.92	4.00	−0.88	+0.14			3.26	160.9
2,3-Dimethylhexane	29.94	3.74	−0.88		+0.64		3.50	160.4
2-Methylheptane	29.71	1.93					1.93	163.6
2,2-Dimethylheptane	29.19	2.66	−0.88	+0.20			1.98	180.2
2,4-Dimethylheptane	29.35	3.38	−0.88			−0.20	2.30	179.6
2,6-Dimethylheptane	29.22	2.59	−0.88				1.71	180.7
3,5-Dimethylheptane	29.47	4.47	−0.88			−0.20	3.39	177.4
4,4-Dimethylheptane	29.54	4.00	−0.88	+0.20			3.32	177.7
3,3-Dimethylheptane	29.49	4.38	−0.88	+0.20			3.70	177.0
3-Ethylheptane	29.58	4.08					4.08	176.3
2-Methyloctane	29.23	2.22					2.22	179.9
3-Methyloctane	29.38	3.08					3.08	178.2
4-Methyloctane	29.41	2.97					2.97	178.6
4-Methylnonane	28.99	3.26					3.26	194.4
3-Methylnonane	29.05	3.38					3.38	194.2
2-Methylnonane	28.93	2.52					2.52	195.8
5-Ethylnonane	28.77	4.57					4.57	208.9
4-Methyldecane	28.60	3.56					3.56	210.7
3-Methyldecane	28.58	3.68					3.68	210.5
2-Methyldecane	28.60	2.82					2.82	212.1

RESULTS AND DISCUSSION

Elution volume correlations

Table I lists all measured elution volumes and calculated Zg-values as well as molar volumes. A plot of molar volume against Zg-values for all hydrocarbons studied results in a series of straight-line parallel curves, with a separate curve for each group of isomers (Fig. 1). The fact that the curves are of equal slope and equidistant from

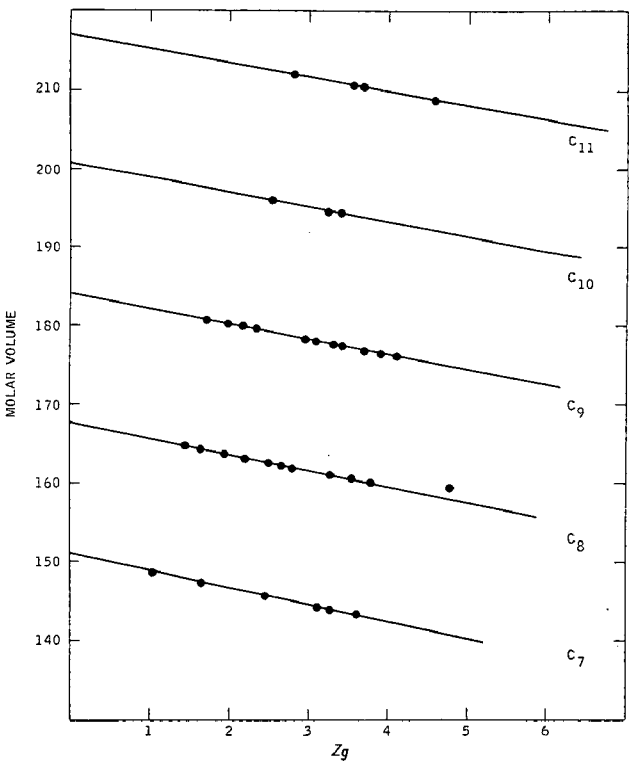

Fig. 1. Correlation of molar volume with average number of gauche conformers (Zg) and carbon number.

each other indicates that the contributions of carbon number and Zg to molar volume are independent and constant. The contribution of carbon number is 7.5 times greater than the conformational contribution. The plotted Zg-values have been adjusted to a comparable single-branch basis, using literature correction values for double branching[2].

The interdependence of molar volume (V_m), Zg, and carbon number (C) can be expressed in the following equation

$$V_m = aZg + b \cdot C + c \qquad (1)$$

The values of the constants were measured to be $a = -2.22$, $b = 16.5$ and $c = 35.8$. V_m is expressed in units of ml/mole.

Similarly, a plot of log Zg against GPC elution volume (V_e) presents a family

of linear curves which exhibit the same carbon number groupings and approximately equidistant shifts (Fig. 2). The data are not of a sufficiently wide range and precision to distinguish experimentally between equidistant spacings or spacings that

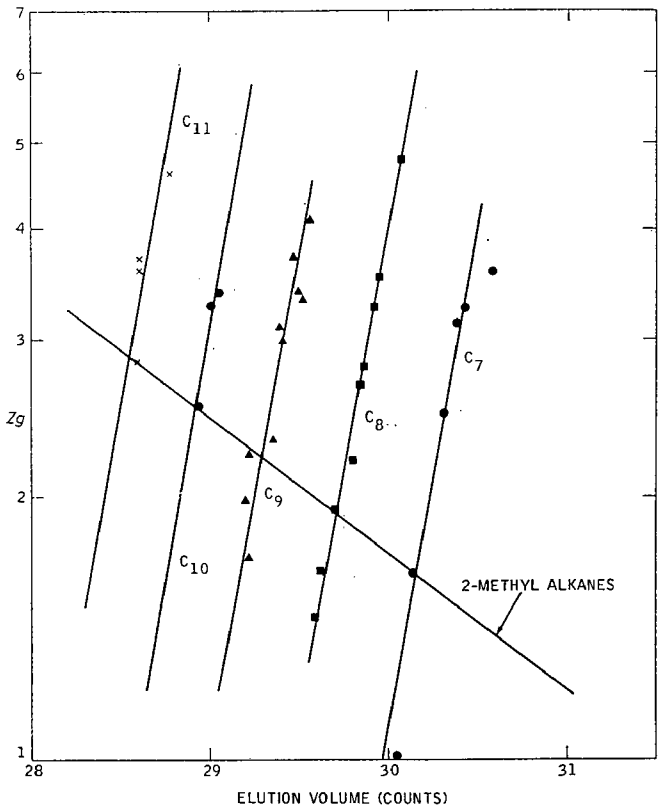

Fig. 2. Correlation of average number of gauche conformers (Zg) with GPC elution volume.

vary logarithmically with carbon numbers. The relation between V_e, Zg and C might be expressed in the following form:

$$V_e = a' \log Zg + b' \log C + c' \qquad (2)$$

The experimental values for the constants are: $a' = 1.0$, $b' = 9.3$, $c' = 37.8$.

If for any group of compounds one of the independently contributing factors of Zg and C can be related to the other, molar volume or GPC elution volume becomes a function of only Zg or C. Such is the case for a homologous series, for which the change in Zg with C appears to be constant. As an example, the increase of Zg for an additional methylene group for the 2-methyl branched hydrocarbon series is 0.30. Eqn. 2 reduces now to a linear variaton of V_e with log Zg. Experimental data for this series verify the prediction (Fig. 2). Alternately, a linear relation of V_e with log C (or molecular weight) would be expected. This is a familiar relation having been demonstrated many times before. It seems to be fundamental to the GPC separation process, holding true over a molecular weight range in which columns fractionate with equal efficiency.

The derivation of eqns. 1 and 2 was undertaken preliminary to relating V_e with V_m. The earlier equations predict V_e to be dependent on molar volume and carbon numbers. The prediction is borne out by the experimental data. Plots of V_e *vs.* log V_m result in the familiar group of isomeric compound curves (Fig. 3).

$$\log V_m = a''V_e + b'' \log C + C'' \tag{3}$$

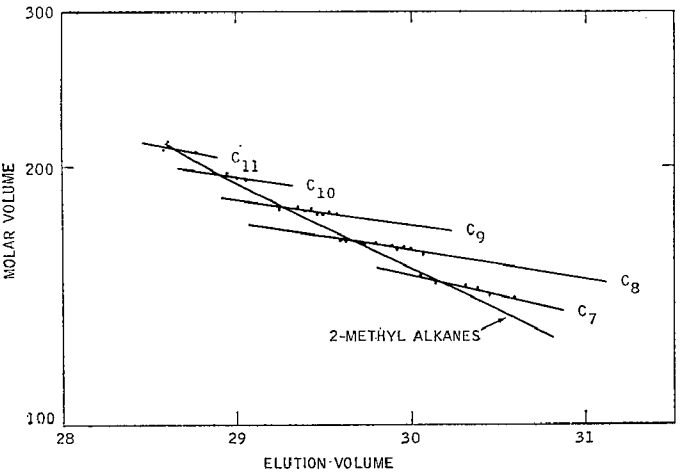

Fig. 3. Correlation of molar volume with GPC elution volume.

Again, the separate contributions of conformation and carbon number are visible from the group of curves. For the 2-methyl branched homologous series V_e varies linearly with log V_m (Fig. 3). The construction of a calibration curve, common to all hydrocarbons investigated, was attempted by parallel shifting of all isomeric curves to a common line (Fig. 4). The shifts amounted to a value of log 12 or multiples thereof.

The conclusion is that molar volume alone does not uniquely describe elution behavior of branched hydrocarbons unless carbon number is also considered. How-

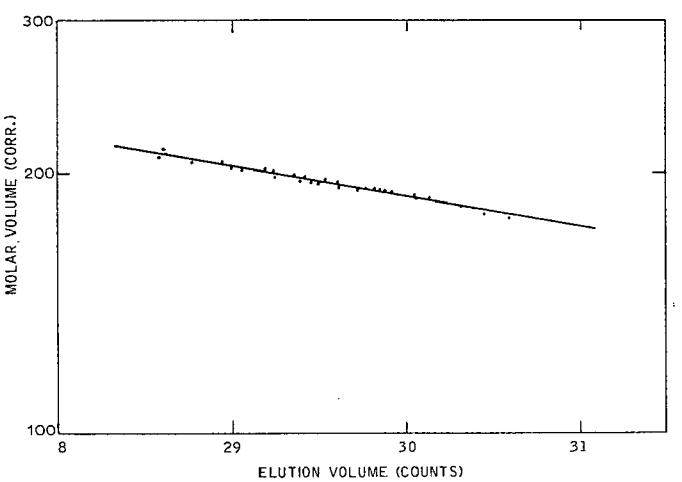

Fig. 4. Common GPC calibration curve for branched hydrocarbons.

ever, the same molecular packing factors which allow for the accurate prediction of molar volume, also permit the prediction of elution volume. The results constitute additional support for the GPC separation mechanism to be one of volume exclusion, dependent on the volume size of the solute molecule, in contrast to gas chromatography where such correlations could not be demonstrated.

Boiling point correlation

In an attempt to develop GPC for the determination of boiling point range distribution of petroleum fractions, the interdependence of elution volume, carbon number and boiling point of normal and 2-methyl-substituted alkanes was investigated[12]. The elution volumes for the two homologous series could be correlated with boiling points through two log-linear segments with a slope change at C_{12}.

Fig. 5 represents a plot of boiling points against elution volume of all C_8-isomers

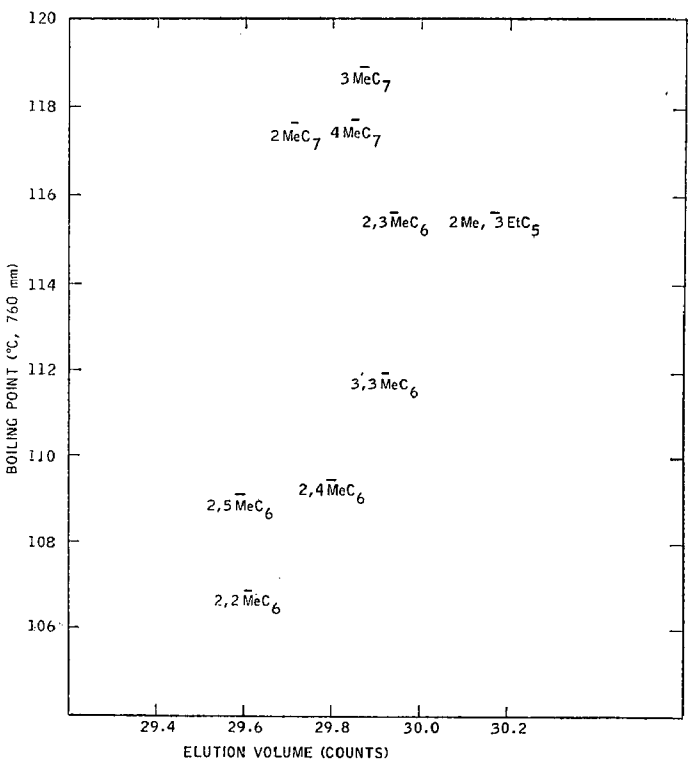

Fig. 5. Correlation of boiling point of octane isomers with GPC elution volume.

investigated. A correlation coefficient of only 0.47 was calculated. Boiling data were taken from API tables[13]. The absence of a boiling point correlation makes it doubtful that a simple approach to the use of GPC for the measurement of boiling point range distributions of petroleum fractions can be developed.

Detector response correlation

The common method of GPC effluent monitoring is through measurement of differential refractive index. While it is desirable for the detector response to be pro-

portional to mass of solute only, it will be affected also by changes in composition and molecular weight, particularly in the low-molecular-weight range.

The cited correlations between refractive index and structure of hydrocarbons have a direct bearing on detector response. For non-polar substances in solution, being essentially free of strong solute–solute and solute–solvent interactions, the Gladstone-Dale rule has been adequate in predicting specific refractive index increments (dn/dc) from bulk refractive indices[14]. The GPC detector response is expected to be inversely proportional to molecular weight for a homologous series and proportional to Zg for isomers. The extrapolated refractive index plots of Fig. 6 intersect at a common point,

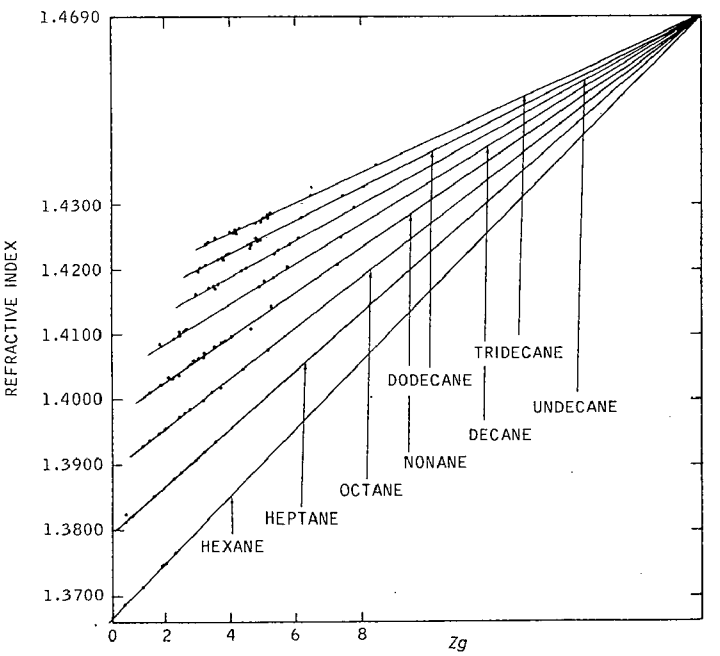

Fig. 6. Correlation of refractive index with average number of gauche conformers (Zg) and carbon number.

predicting that a limiting refractive index for saturated hydrocarbons be reached at a value of 1.47. At this point, refractive index would be insensitive to molecular weight and structure. The limiting Zg-value is approximately 20.

CONCLUSIONS

GPC elution volumes of branched hydrocarbons do not depend on hydrocarbon molar volume alone, but reflect the separate contributions that carbon number and average number of gauche conformers make to molar volume. The systematic contributions allow one to predict elution behavior of other branched alkanes. Similar systematic correlations between boiling point and GPC elution volume do not exist. The correlation of bulk refractive index with structure and molecular weight is useful for introducing detector response corrections in connection with the chromatogram evaluation of hydrocarbon mixtures.

REFERENCES

1 G. MANN, *Tetrahedron*, 23 (1967) 3375.
2 G. MANN, H. MÜHLSTÄDT, J. BRABAND AND E. DÖRING, *Tetrahedron*, 23 (1967) 3393.
3 H. BENOIT, Z. GRUBISIC, P. REMPP, D. DECKER AND J. G. ZILLIOX, *J. Chem. Phys.*, 63 (1966) 1507.
4 Z. GRUBISIC, P. REMPP AND H. BENOIT, *J. Polym. Sci. B*, 5 (1967) 753.
5 K. A. BONI, F. A. SLIEMERS AND P. B. STICKNEY, *J. Polym. Sci. A-2*, 6 (1968) 1579.
6 J. G. HENDRICKSON AND J. C. MOORE, *J. Polym. Sci. C 8*, (1965) 233; *ibid.*, A-1 4, (1965) 167.
7 J. G. HENDRICKSON, *4th Intern. Seminar Gel Permeation Chromatography*, Preprints, 1967, p. 139.
8 W. B. SMITH AND A. KOLLMANSBERGER, *J. Phys. Chem.*, 69 (1965) 4157.
9 J. CAZES AND D. R. GASKILL, *Separ. Sci.*, 2 (1967) 421.
10 T. EDSTROM AND B. A. PETRO, *J. Polym. Sci. C*, 21 (1968) 171.
11 R. E. THOMPSON, E. G. SWEENEY AND D. C. FORD, *J. Polym. Sci. A-1*, 8 (1970) 1165.
12 E. G. SWEENEY, R. E. THOMPSON AND D. C. FORD, *J. Chromatog. Sci.*, 8 (1970) 76.
13 *Selected Values of Hydrocarbons and Related Compounds*, Amer. Petrol. Inst., Project 44, Table 3A, Part 1, April 1956.
14 A. BELLO AND G. M. GUZMAN, *Europ. Polym. J.*, 2 (1966) 85.

CHROM. 5125

SEPARATION BY FLOW AND ITS APPLICATION TO GEL PERMEATION CHROMATOGRAPHY

EDMUND A. DIMARZIO AND CHARLES M. GUTTMAN
Polymers Division, National Bureau of Standards, Washington, D.C. 20234 (U.S.A.)

SUMMARY

When dilute solutions of finite size particles undergoing Brownian motion flow through a capillary, the larger particles have higher average velocities than the smaller particles. Thus one can obtain a separation of particles of different sizes due to fluid flow. The elution volumes of suspended particles or polymer molecules are derived for various tube geometries. Following TAYLOR, the effects of diffusional broadening of the volume elution peak for finite size particles are discussed and the process is shown to be chromatographic.

Models of a gel permeation chromatographic column are proposed in which there is fluid and particle flow through each of the beads as well as around them. Diffusion is allowed within and outside of the beads. Equations for the location of the volume elution peaks are computed for such models and shown to yield functional dependence on the polymer radius and column geometry very much like equations derived by previous workers for models of gel permeation chromatographic columns in which there was no flow allowed within the beads. Explicit formulae are given for the second and third moments for the above models. It is shown that for a monodisperse species the volume elution peak is always a gaussian of a finite width. It is shown that beads with open pores that allow for flow always have better separation capabilities than beads with pores that do not allow for flow.

I. INTRODUCTION

An isolated polymer molecule flowing down the inside of a thin capillary and undergoing Brownian motion will have an average velocity greater than that of the solvent. This is because the center of the particle (assumed to be a rigid sphere) cannot get any closer to the walls of the capillary than its radius. It therefore samples only those solvent velocities away from the walls. Since the solvent velocity is larger, the farther the distance from the wall, larger molecules will have larger average velocities than smaller molecules. See Fig. 1.

Suppose we now introduce particles of two different sizes simultaneously at the top of the column. The average distance between these particles will increase linearly with time as they flow through the tube because they have different average velocities. On the other hand the peak widths of the distribution of particle distances about

their mean value for each kind of particle increases as the square root of time. This is a characteristic of particle diffusion. It therefore follows that by waiting for sufficiently long periods of time the separation between peaks can be made large compared to the width of the peaks. The particles therefore separate into two groups.

These ideas have been placed on a firm quantitative foundation in a previous paper[1]. The main results for a single capillary are recapitulated in Section 2.

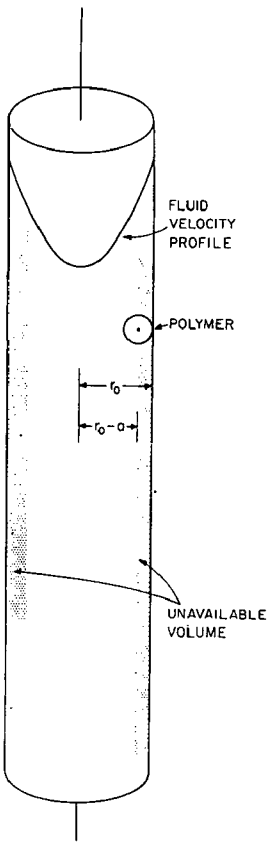

Fig. 1. Schematic of flow down a single tube. The fluid velocity profile causes polymer separation by virtue of the unavailable volume.

Because the elution characteristics of a single capillary are very much like those of gel permeation chromatographic (GPC) columns we were led to consider the elution properties of various networks of capillaries (combinations of capillaries in series and in parallel). The main results are summarized in Section 3. A complete paper on this aspect of the problem has appeared elsewhere[2].

A particular combination of tubes is considered as a model for GPC (see Fig. 2). In this model there are tubes of two diameters. The large tubes represent flow between the beads (interstitial flow) of a GPC column, and the small tubes represent flow through (intra-bead-flow) the beads. The idea that there is flow within the bead as well as around it is essential to the applicability of the separation by flow (SBF) concept to GPC. In Section 3 we also discuss the application of SBF to GPC.

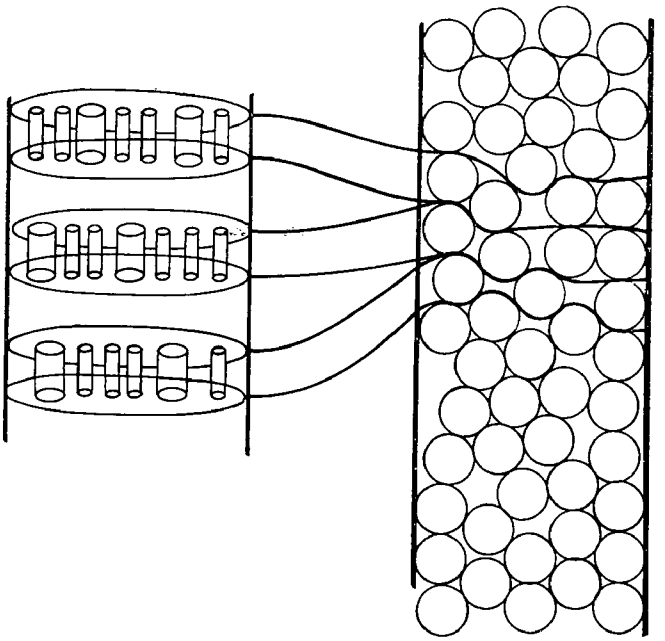

Fig. 2. The bank model of a GPC column. The large tubes in a given bank (on left) represent the totality of interstitial regions at that same level in the column (on right). The small tubes in this bank represent the totality of fine tubes within the beads at this same level. The space between banks serves as a mixing region and is not considered to have any volume.

2. SEPARATION BY FLOW IN A LONG THIN CAPILLARY

A. Volume elution

The velocity v_f of solvent flowing down a tube of radius r_0 under Poiseuille flow is

$$v_f = \frac{1}{4\eta}\frac{\partial p}{\partial l}(r_0^2 - r^2) \tag{1}$$

The velocity of the center of mass of a polymer molecule, v_p, has been derived under the free draining assumption[1].

$$\frac{v_f - v_p}{u_0} = \frac{2}{3}\left(\frac{s}{r_0}\right)^2 \tag{2}$$

where u_0 is the fluid velocity along the axis of the capillary.

The radius of gyration is s. It was found that the molecule does not migrate radially (unless there is diffusion), but is retarded by the amount in eqn. 2. HAPPEL AND BYRNE[3] have derived a relation for the slip at the axis of a cylindrical tube of radius r_0 for rigid impermeable spheres of radius s. They obtain

$$\left[\frac{v_f - v_p}{v_f}\right]_{r=0} = \frac{2}{3}\left(\frac{s}{r_0}\right)^2 \tag{3}$$

This relation is identical with ours if we identify the radius of the sphere with the radius of gyration of the molecule. Eqn. 3 has been confirmed experimentally by GOLDSMITH AND MASON[4]. We can now evaluate the average velocity and therefore the elution volume. Because of entropy forces a polymer molecule will tend to maintain its shape as it flows down the tube. That is to say, if we deform a polymer molecule from its spherical shape by means of an external force, a restoring force is set up by the polymer which acts in a direction so as to restore the shape. It is for this reason that the center of mass of the polymer molecule cannot approach too closely the walls of the tube down which it flows. We are thus led to define an effective radius, a, for the polymer. For flexible polymer molecules it has been shown that this radius is related to the radius of gyration, s, by

$$a = \frac{3}{\sqrt{\pi}} s \tag{4}$$

If Brownian motion in a direction perpendicular to the axis of the tube is allowed, then the center of mass of the polymer molecule will sample every possible horizontal position in the tube with equal probability, except for the fact that it cannot be closer than a distance, a, to the wall. We obtain then for $\langle v_p \rangle$, the average velocity of the polymer, in a circular cylinder

$$\langle v_p \rangle = u_0 \int_0^{r_0-a} \left[1 - \left(\frac{r_c}{r_0}\right)^2 - \gamma \left(\frac{a}{r_0}\right)^2\right] r_c \mathrm{d}r_c \Big/ \int_0^{r_0-a} r_c \mathrm{d}r_c$$

$$\langle v_p \rangle = u_0 \left[1 - \frac{(1 - a/r_0^2)}{2} - \gamma \left(\frac{a}{r_0}\right)^2\right] \quad \text{circular cylinders} \tag{5}$$

where

$$u_0 = \frac{\partial p}{\partial l} \frac{r_0^2}{4\eta}$$

We have let r_0 be the radius of the cylinder and r_c the distance from an axis down the center of the tube to the particle center of mass. It should be noted that u_0 as defined in eqn. 5 is the maximum velocity of the fluid in the tube. The γ in eqn. 5 is defined by

$$\gamma a^2 = 2s^2/3 \tag{6}$$

For flexible polymer molecules $\gamma = 2\pi/27$. However, in general, γ is a function of the shape of the particle as well as the density distribution within the particle. For this reason we retain γ as a parameter. In a similar manner we obtain for parallel plates

$$\langle v_p \rangle = u_0 \left[1 - \frac{(1 - a/z_0^2)}{3} - \frac{\gamma}{2} \left(\frac{a}{z_0}\right)^2\right] \quad \text{plates} \tag{7}$$

where for parallel plates

$$u_0 = \frac{\partial p}{\partial l} \frac{z_0^2}{2\eta}$$

The elution volume, $\bar{V}_e$, is the fluid volume flow rate, Q, times the time needed for passage of the polymer through the capillary, t. Thus, for a tube of length l

$$\bar{V}_e = Qt = Ql/\langle v_p \rangle \tag{8}$$

We obtain then

$$\bar{V}_e = \frac{\pi l r_0^2}{2\left[1 - \frac{(1-R)^2}{2} - \gamma R^2\right]} \quad \text{circular cylinders} \tag{9}$$

$$\bar{V}_e = \frac{z_0 l}{\frac{3}{4}\left[1 - \frac{(1-R)^2}{3} - \frac{\gamma}{2}R^2\right]} \quad \text{plates} \tag{10}$$

In eqn. 9, $R = a/r_0$, while in eqn. 10 it is $R = a/z_0$. Thus, the elution volume is equal to the elution volume of solvent times a factor which is a function only of R and the geometry of the capillary.

In Fig. 3 the effect of varying γ on the elution volume of a circular cylinder is given; for convenience we have let $\pi l r_0^2$ equal 1 in this figure. We have plotted V_e *vs.* 3 log R in the figure since R^3 is nearly proportional to the so-called hydrodynamic volume of the polymer. We pointed out previously[5] that the features of the curves given here are similar to the log hydrodynamic volume *vs.* volume elution curves of GRUBISIC *et al.*[6], found experimentally for a GPC column. We wish to emphasize here the similarity of the curves for $R < 0.2$. Clearly for this region we have an insensitivity to γ in the V_e *vs.* 3 log R plots.

In Fig. 4 we have plotted V_e *vs.* 3 log R for three different cross sections of tubes;

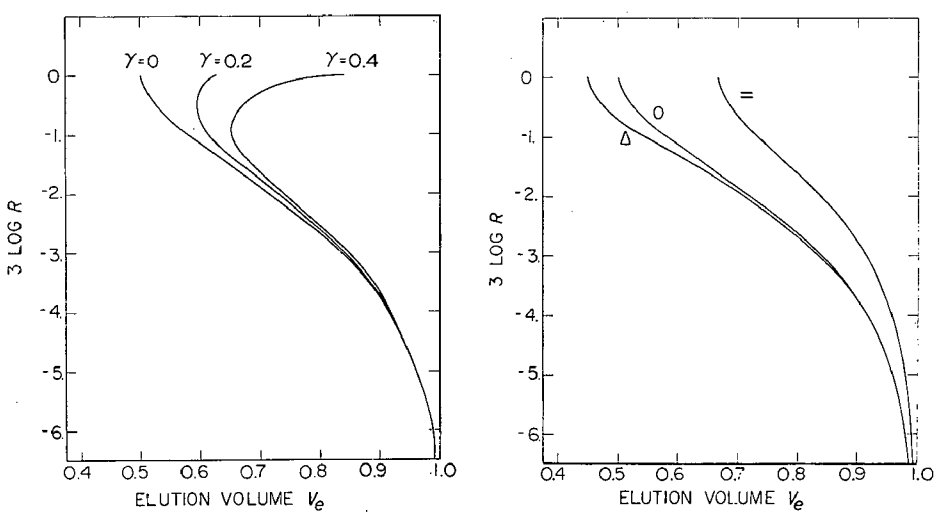

Fig. 3. A plot of the normalized elution volume *versus* the logarithm of the effective particle volume for separation in a single circular cylinder is shown. The effect of varying γ, the parameter relating to the magnitude of the retardation effect, is seen to be small below $R = 0.4$. R is defined as a/r_0.

Fig. 4. A plot of the normalized elution volume *versus* the logarithm of the effective particle volume (with $\gamma = 0$) for various tube geometries for a single tube is shown. Notice the general shape of the curve is insensitive to the geometry. R is defined as a/r_0.

we have normalized all the curves to $V_e = 1$ for $R = 0$. In this plot we see that although the parallel plates result is different from the others, the shape of the curves show a general insensitivity to cross section for smaller R's

Neglecting the retardation effect ($\gamma = 0$), the ratio of maximum to minimum elution volume is 2 for circular cylinders and 1.5 for parallel plates. It is interesting to compute this ratio for tubes of various other cross sections. This is done by computing the ratio of maximum velocity to average velocity. We obtain, for a square cross section 2.5, for an elliptical cross section 2.0 (independent of the eccentricity of the ellipse), and for equilateral triangle 2.2. Thus, one might expect the effect of different cross section on volume elution is a small one.

B. Dispersion in the volume elution peak due to diffusion

TAYLOR had addressed himself to the problem of dispersion of soluble matter in solvent flowing through a circular cylinder[7]. ARIS has extended the results to cylinders of arbitrary cross section[8]. Their problem is identical with ours except for one factor: the size of the molecule. They assumed that the soluble matter is made up of point particles, while we assume our soluble matter is made up of particles of finite size.

We have adopted their treatment to the solution of the problem for finite size molecules. The starting point is the three dimensional diffusion equation in a moving medium.

$$D\nabla^2 C = \frac{\partial C}{\partial t} + \vec{v}\cdot\nabla C \tag{11}$$

where C is the concentration of solute particles, $\vec{v}$ is their velocity, D their diffusion constant, and t time. Eqn. 11 is a generalization of the ordinary diffusion equation to a moving medium. The main result of TAYLOR and ARIS can be described as follows. Suppose we define C_m to be the mean concentration over the cross-sectional area whose normal is parallel to the axis of the cylinder. Then C_m is found to obey a one dimensional diffusion equation.

$$K\frac{\partial^2 C_m}{\partial x^2} = \frac{\partial C_m}{\partial t} \tag{12}$$

with an effective diffusion coefficient K,

$$K = D + \theta\frac{u_0^2 r_0^2}{D} \tag{13}$$

The coordinate system of eqn. 12 moves along with the average velocity of the particle and the direction along the tube is the x direction. θ is a number which depends on the cross sectional geometry and has value 1/192 for circular cylinders and 1/120 for parallel plates. For parallel plates one replaces r_0 by z_0; in both cases u_0 is the maximum fluid velocity in the tube. The effective diffusion coefficient K has an ordinary part D resulting from longitudinal diffusion and a part $\theta u_0^2 r_0^2/D$ which results from transverse diffusion and simultaneous smearing due to the fluid velocity profile. The shear gradient causes material at different levels in the tube to travel at different velocities thereby smearing the particles over large longitudinal distances.

Thus this effect increases with increasing u_0. However, the rate at which particles sample various levels is important; if the particle sampled quickly (D large) then there would be only a small amount of smearing since the longitudinal velocity of each particle is the average velocity. However, if the particle sampled the various levels slowly then there would be much smearing. This is the reason for the inverse dependence in D in the second term of eqn. 13. This term is the dominant one for many situations of interest. Thus, the larger the diffusion coefficient, the smaller the spreading in the elution volume peak!

The only effect of particle size is to scale the quantities u_0 and r_0, (z_0) as follows.

$$r_0 \rightarrow (r_0 - a)$$

$$u_0 \rightarrow u_0 \left(\frac{r_0 - a}{r_0}\right)^2 \text{ circular cylinders} \tag{14}$$

$$z_0 \rightarrow (z_0 - a)$$

$$u_0 \rightarrow u_0 \left(\frac{z_0 - a}{z_0}\right)^2 \text{ parallel plates} \tag{15}$$

Eqns. 12 and 13 are now applicable with the substitution afforded by eqns. 14 and 15.

C. Implications of the equations and further results

Separation by flow occurs in the capillary considered in sections 2 A and B. The average distance traveled by molecule i down a tube in time t is $\langle v_p \rangle_i t$; then the distance between peak centers for two substances 1 and 2 is

$$d_{12} = |\langle v_p \rangle_1 - \langle v_p \rangle_2| t \tag{16}$$

Because of diffusion, the elution volume peaks become spread out in time. But as is always the case for diffusion, the width of the peaks are proportional to $\sqrt{t}$ rather than t. Thus, if one waits for a long enough time, either by using a long tube or equivalently by recycling through one tube, one can always separate the two materials.

From eqns. 9 and 10 we observe that the elution volume peak is a function only of the effective radius of the particle and of the geometry of the tube. It is independent of both viscosity of the fluid and the diffusion coefficient of the molecules. It also does not depend on the pressure head and the flow rate through the tube. If we flow different molecules through the same tube then the only pertinent variable is the effective radius. We have already pointed out[1] that the effective radius cubed of a polymer is nearly proportional to its hydrodynamic volume. Presumably then we have a method of characterizing molecules on the basis of hydrodynamic volume alone. For rigid rods also, the only pertinent variable for volume elution is hydrodynamic volume[1].

The validity of the concept of separation by flow is independent of the detailed assumptions used in deriving the specific formulas. It is, for example, not necessary for us to have a quadratic dependence of fluid velocity in a circular cylinder. All that is required is that we have on the average a larger velocity toward the center than at the boundary of the tube. It is not necessary even to have Brownian motion. All that is needed is a mechanism whereby the particles sample various levels in the tube.

Turbulence for example might replace Brownian motion as the mode of sampling.

If one attempts to use a bundle of identical capillaries as a practical method of separating polymer molecules of molecular weight 10^6 or less one finds that it is impossible to choose reasonable values of the parameters, tube size, numbers, and length. One cannot have both good separation which requires narrow capillaries and large flow which requires wide capillaries. For this reason we were led to the study of combinations of large and small tubes in series and in parallel. The bank model discussed in the next section provides both excellent separation capabilities and large flow rates.

3. ELUTION CHARACTERISTICS OF NETWORKS OF CAPILLARIES; APPLICATION TO GPC

Ideally, we would like to solve the problem of flow through an arbitrary combination of tubes of various diameters, widths and numbers. We have not been able to do this. But we have solved the problem for a more restricted class of networks which we have called "bank models". These models are useful in their own right as objects to be constructed, and also because they seem to be good models for GPC columns.

A. Description of the models

In this section we shall describe some models for a GPC column. A GPC column is made up of fine gel beads (*ca.* 50 μ in diameter) packed together. The beads are porous; we assume that the pores go through the entire bead. Thus we assume the carrier fluid flows around, into and through the beads.

The surface of the beads divides the system into two regions; that within the beads and that outside. In this picture of the column the region within the beads is viewed, for the purpose of calculation and simplicity, as made up of small open cylinders, all of radius r_s, and all of length l. We assume, naively, that each cylinder is of uniform radii and that no cylinder intersects another. These cylinders are assumed aligned in one direction and this direction is chosen as the direction of fluid flow. The number of small tubes per unit volume is chosen so that the total volume within small tubes is the same as that available to solvent within the beads. Furthermore these tubes must be bunched together so that the distance between bunches is comparable to the size of the interstitial region between beads in the real column. Thus both flow and diffusion are allowed within the beads as well as within the interstitial region between beads. Initially, none of the tubes will be closed. Thus there is no stationary or stagnant volume in our system. This restriction is easily removed.

The above model does not yet specify a detailed geometry for the system. We have purposely maintained generality because the method used to compute the broadening and skewness does not require a detailed specification. However in order to calculate average elution volumes as is done we have need of a more specific model. This latter model is a series of banks of tubes separated by mixing regions (see Fig. 2). We shall refer to this model as the bank model. Each bank is made up of parallel arrays of right circular cylinders of different radii; the fluid flows through the cylinders (rather than around them). For concreteness one can view each bank as a membrane riddled with holes. For clarity of presentation we assume there are tubes of only two radii, r_l and r_s; their numbers in each bank are N_l and N_s and their length l. The

banks are thus all identical and there are n of them. This series of n banks is called a column.

The path of the particle through the column is as follows. A pressure head Δp forces the particle (which is suspended in carrier fluid) through the column from top to bottom. The particle emerges at time t later after having traversed np_l large tubes and np_s small ones. We assume that particles in the mixing region lose memory of the tubes they came out of. Accordingly the probability p_i of a particle jumping into and through the tubes of the next bank ($i = l,s$) is independent of which tube it emerged from. This assumption will be more valid for larger diffusion coefficients and less valid for smaller diffusion coefficients. Its validity is also a function of the actual geometry of the system. For example, if all the large tubes were bunched together at one end of the bank (membrane) and the small tubes at the other end, one would expect that by piling the banks in register one could have large tubes in one bank vertically above large tubes in the adjacent banks. Consequently, particles coming from large tubes would tend to go into large tubes and so on. One obviously minimizes this effect by mixing the tubes within each bank.

The above bank model can be viewed in its own right as an object of study, or as a model for GPC. As a model for GPC, the large tubes represent the flow region outside of and around the beads; the small tubes represent pores in the beads. Any particle emerging from a small tube has the option of choosing to go into a small tube again (into a bead) or into a large tube (flow around a bead). Thus the totality of small tubes in one bank represents all the pores in all the beads at one level in the GPC column, and the totality of big tubes in this bank represents all the regions between beads at this same level. The length of the tubes is proportional to the diameter of the beads.

B. The final formulae

The elution characteristics of the bank model have been calculated in our previous paper[2]. We have shown that the elution volume peak for a single species is Gaussian and have evaluated its first three moments. The procedure used is an adaptation of the method of HERMANS[9]. HERMANS allowed diffusion into and out of the beads while we have allowed both for flow through the beads and diffusion. Furthermore, we have evaluated the particle size dependence of the first moment (elution volume) in both the high fluid flow and low fluid flow (equilibrium) limits. One should consult ref. 2 for details. Here we will quote only the results.

$$\frac{\langle t\rangle}{x} = \left[1 + \frac{(1-\phi)}{k\phi}\right] \Big/ \langle v_p\rangle_{l'} \tag{17}$$

$$\frac{\mu_2}{x} = \frac{l(1-\phi)}{\phi k \langle v_p\rangle_s \langle v_p\rangle_{l'}} \mathcal{L}\left(\frac{l\langle v_p\rangle_s}{2D_s}\right) + \frac{2D_m}{\langle v_p\rangle_{l'}^3}\left[1 + \frac{(1-\phi)}{k\phi}\right]^2 \tag{18}$$

$$\frac{\mu_3}{x} = \frac{-3(1-\phi)l^2}{\phi k \langle v_p\rangle_s^2 \langle v_p\rangle_{l'}}\left[\frac{1}{\left(\frac{l\langle v_p\rangle_s}{2D_s}\right)^2} - \frac{1}{\sinh^2\left(\frac{l\langle v_p\rangle_s}{2D_s}\right)} - \frac{1}{3}\right] \tag{19}$$

$$+ \frac{6D_m}{\langle v_p\rangle_{l'}}\left(\frac{\mu_2}{x}\right)\left(\frac{\langle t\rangle}{x}\right)$$

$$\langle v_p \rangle_l' = \langle v_p \rangle_l \left[1 - \frac{(1-\phi)\langle v_p \rangle_s}{\phi k \langle v_p \rangle_l} \right] \tag{20}$$

$$D_s = D_a + \frac{u_s^2 (1 - a/r_s)^6 r_s^2}{192 D_a} \tag{21}$$

$\mathcal{L}$ in eqn. (18) is the Langevin function, $\mathcal{L}(x) = \coth(x) - 1/x$. The length of the column is x and $\langle t \rangle$ is the average time spent in it by the elutant. ϕ is the fraction of flowing volume in large tubes, $\langle v_p \rangle_l$ and $\langle v_p \rangle_s$ are the average velocities in large and small tubes. μ_2 and μ_3 are the second and third moments about the mean for the time spent in the column. l is the length of the capillaries (in each bank) of which there are two types of radius r_s and r_l and the number of banks is, of course, x/l. The diffusion coefficient of the molecule of radius a is D_a. The maximum velocity of solvent in the small tube is u_s and an expression identical to eqn. 21 with m replacing s holds for D_m. The value of the quantity k depends on the flow rate through the system. In the limit of slow flow we have

$$\begin{aligned} \frac{1}{k} &= K_e = (1 - a/r_s)^2 \qquad a \leqq r_s \\ K_e &= 0 \qquad\qquad\qquad\quad a \geqq r_s \end{aligned} \tag{22}$$

For other shapes of tubes one replaces $(1 - a/r_s)^2$ by the appropriate partition coefficient.

In the limit of fast flow one has

$$\begin{aligned} \frac{1}{k} &= K_f = 1 \Big/ \left[2 - (1 - a/r_s)^2 - 2\gamma \left(\frac{a}{r_s} \right)^2 \right] \qquad a \leqq r_s \\ K_f &= 0 \qquad\qquad\qquad\qquad\qquad\qquad\quad a \geqq r_s \end{aligned} \tag{23}$$

We have not been able to derive an expression for all flow rates, but an heuristic argument given previously suggests

$$\frac{1}{k} = K = K_f(1 - \exp(-u_s l/\beta D_a)) + K_e \exp(-u_s l/\beta D_a) \tag{24}$$

where β is a parameter near 1. The above moments (for the time it takes a particle to elute out of a column) are related to moments for the volume elution, V_e.

We obtain

$$\langle V_e \rangle = \bar{V}_e = g' V \left[\phi + \frac{1-\phi}{k} \right] \tag{25}$$

$$\frac{\langle (V_e - \bar{V}_e)^2 \rangle}{\bar{V}_e^2} = \frac{\mu_2}{\langle t \rangle^2} \tag{26}$$

$$\frac{\langle (V_e - \bar{V}_e)^3 \rangle}{\langle (V_e - \bar{V}_e)^2 \rangle^{3/2}} = \frac{\mu_3}{\mu_2^{3/2}} \tag{27}$$

$$g' = \frac{\left[1 + \frac{(1-\phi)}{\phi}\frac{u_s}{u_l}\right]}{1 - \left[\frac{(1-\phi)\langle v_p\rangle_s}{k\phi\langle v_p\rangle_l}\right]} \tag{28}$$

The quantity g' is always close to 1 for any system of interest. V on the right hand side of eqn. 25 is the total volume in small and large tubes. We have also shown that the elution volume peak is Gaussian.

C. Discussion of results

In Fig. 5 we have plotted $3\log(a/r_s)$, the logarithm of the cube of ratio of the particle radius to that of the small tube, *versus* the volume elution for various fractions of the volume available in the large tube, ϕ, in both the flow limit and equilibrium limit. The variable $(a/r_s)^3$ is proportional to the hydrodynamic volume of the polymer[10].

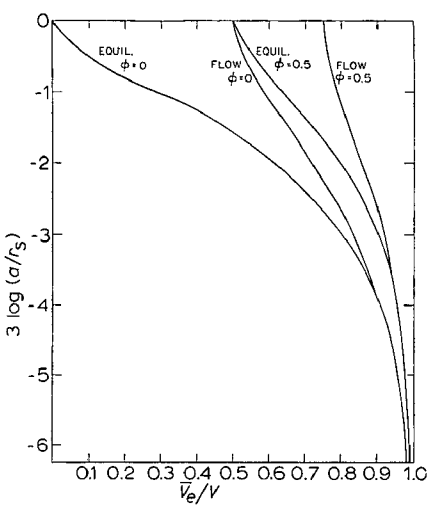

Fig. 5. Volume elution, $\bar{V}_e$, *versus* log size (hydrodynamic volume) for the bank model for both the equilibrium and the flow limit for various values of ϕ the fraction of volume in the interstitial region. V is total volume available to solvent.

The reader should notice that for small (a/r_s) the flow limit and the equilibrium limit are the same; one should also notice that the curves are similar in shape to experimental volume elution *versus* logarithm hydrodynamic volume curves of single column GPC systems. Clearly we could reproduce other experimental curves by suitable choice of a distribution of small tube sizes. (This statement is meant to suggest the sufficiency, not necessity, of the theory since others have produced such curves. Also see part D of this section.)

As we pointed out in Section 3 B, we have only derived the volume elution *versus* particle size equation in the limit of high flow and in that of low flow (equi-

librium). We also pointed out that from considerations of a single tube one might expect the more general volume elution equation as a function of flow rate $V_e(u_s)$ to be

$$V_e(u_s) = V + KV_s \tag{29}$$

$$K = \theta K_e + (1 - \theta)K_f$$

$$\theta = \exp(-u_s l/\beta D_a)$$

In Fig. 6 we have plotted $V_e - V_e(u_s = 0)$, (ΔV_e), for various a/r_s as a function of $u_s l/\beta D_a$ (we generally expect $\beta \cong 1$). For large molecules $u_s l/D_a$ is about 3 ($u_s = (r_s/r_l)^2 u_l = 10^{-4}$ cm/sec, $l = 30$ microns, $D_a = 10^{-7}$ cm^2/sec) while for small molecules $u_s l/D_a = 3 \times 10^{-2}$ (all parameters the same except $D_a = 10^{-5}$ cm^2/sec). Clearly except for large a/r_s we see very small changes in $\overline{V}_e$ as a function of flow except for a very high flow rate.

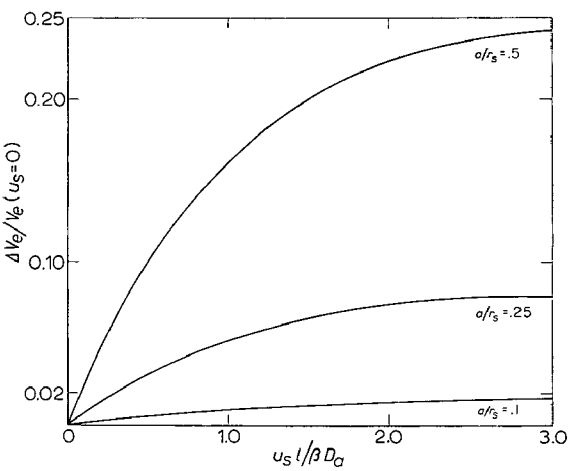

Fig. 6. Here we have plotted our estimate of the fractional change in volume elution as a function of $u_s l/\beta D_a$. ΔV_e is the difference between the actual volume elution and that at zero flow ($V_e(u_s = 0)$). For small a/r_s the change is minimal. These results are for a bank with only one size small tube; β is estimated to be one or two.

Our expression for the peak width eqn. 18 is similar to that derived by HERMANS[9] and indeed our expression includes the case of diffusion (diffusion only) as a limiting case. In Fig. 7 we have plotted the ratio of this expression to that obtained in the limit of zero flow. The ratio is always less than or equal to 1. This means that separation is always improved by using tubes with flow rather than tubes blocked up so that there is no flow.

The HETP (height equivalent theoretical plate) of a chromatographic column is normally defined as $(V_e - \overline{V}_e)^2/V_e$, the dispersion in the volume elution divided by the volume elution. For small $u_s l/D_a$ our expression for that part of the dispersion arising from the dispersion in small beads is similar to that obtained by others. For larger velocity and/or small diffusion coefficients the functional form changes dramatically. In Fig. 8 we have plotted the quantity $(V_e - \overline{V}_e)^2/[V_e(V_e - V_l)]$ *versus* $u_s l/2D_a$ for various ratios of bead size to small tube radius, l/r_s. The $(V_e - V_l)$ in

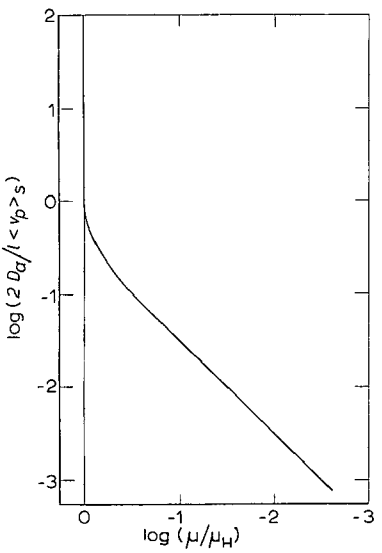

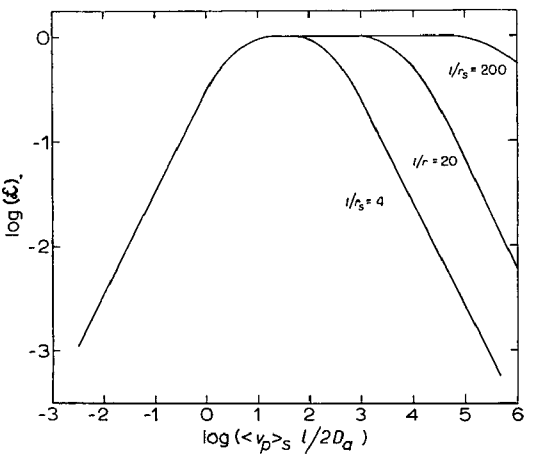

Fig. 7. Plot of the log of the ratio of second moment computed here to the second moment when no flow is allowed in the small tubes (the HERMANS limit) μ_H as a function of the log $(2D_a/l<v_p>_s)$ for l/r_s from 5 to 100. The quantity $(2D_a/l<v_p>_s)$ is essentially the ratio of the time for a particle to be flushed out of bead to the time it takes it to diffuse out. When that ratio is greater than one, the time to diffuse is smaller than the flush time. Our result goes to HERMANS' result. For this ratio less than one, the dispersion from our calculation is less than that from HERMANS'. (Notice this curve shows the ratio of μ/μ_H as a function only of $(2D_a/l<v_p>_s)$. This is true for the range of $(2D_a/l<v_p>)$ we have chosen. For $(2D_a/l<v_p>_s) > 10^{-3}$ effects of changes in r_s are seen).

Fig. 8. Plot of logarithm of the Langevin function $\mathcal{L}(<v_p>_s l/2D_s)$ (where $D_s = D_a + (u_s^2\, r_s^2/192\, D_a)$ *versus* $<v_p>_s l/2D_a$ for various l/r_s. The Langevin function is proportional to that part of the HETP arising from the dispersion inside the beads. Notice for small $<v_p>_s l/2D_a$ the curves are identical. This is the low velocity-high diffusion constant region and yields increasing dispersion as $<v_p>_s l/2D_a$ increases; in the high flow–small diffusion constant region, the dispersion decreases for increasing flow. The slopes of the shoulders of the curves are ± 1.

the dispersion expression is the difference between the V_e and V_l, the volume elution of particles to big to go into the small tube. With the inclusion of this term in the expression for the dispersion, the only variable for a column of a single size of small tubes is $\langle v\rangle_s l/2D_a$. Thus we might expect that for a single column (except for some weak size dependence in $\langle v_p\rangle_s/u_s$), u_s/D_a or, thus, u_l/D_a, the fluid velocity over the diffusion constant, is the important variable. One would expect the data for this part of the dispersion to scale that way.

The reader should notice that for small $l\langle v_p\rangle_s/2D_a$, the curves in Fig. 9 are identical. For larger $l\langle v_p\rangle_s/2D_a$ they clearly break away from each other; for all curves however as $l\langle v_p\rangle_s/2D_a$ gets above 1 the dispersion is either a constant or decreasing as $\langle v_p\rangle_s/D_a$ increases. This is in contradistruction to the results obtained at smaller $\langle v_p\rangle_s/D_a$. Thus one might expect for a given column system that the dispersion for small molecules would increase for increasing u_l while that for large molecules (low diffusion constant) would decrease or remain constant for increasing u_s. Such results have been observed[11].

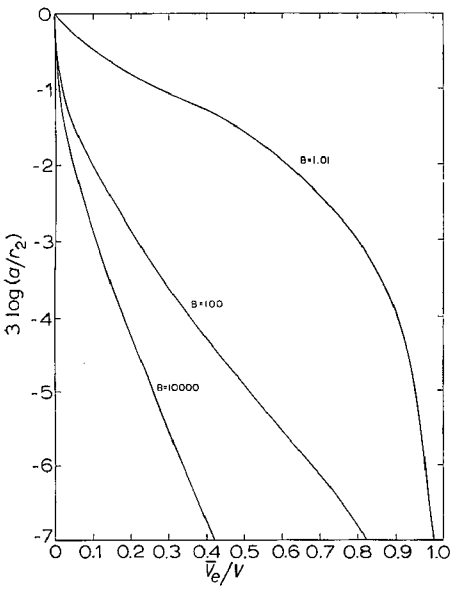

Fig. 9. A plot of the logarithm of the hydrodynamic volume *versus* $\bar{V}_e/V$ for $\phi = 0$ for a distribution of tube sizes (see eqn. 32). Notice as the ratio of the largest small tube to the smallest small tube, B, increases, the length of the linear portion of the curve increases, (For B = 10000 the curve is linear from 3 log $(a/r_s) = -3$ to 3 log $(a/r_2) = -13$).

D. Application to distributions of tube sizes

Our equations are easily modified to include distributions of tube radii for the small tubes in each bank. Denoting the normalized distribution by $g(r)$ so that $V_s g(r)\mathrm{d}r$ is the volume of cylinders of radius r within dr we have

$$\bar{V}_e = V_l + V_s \int_0^\infty g(r)K(a/r)\mathrm{d}r = V_l + V_s \int_a^\infty g(r)K(a/r)\mathrm{d}r \tag{30}$$

The use of a as the lower limit of integration is permissable because $K(a/r) = 0$ for $a > r$. Eqn. 30 is valid if most of the flow is in the big tubes (interstitial region of the beads) which are not part of the distribution function $g(r)$. It is obvious from eqn. 30 that the shape of the volume elution curve is very much dependent on $g(r)$ as well as $K(a/r)$. A choice of $g(r)$ which makes the equilibrium volume elution curve linear as a function of the logarithm of the hydrodynamic volume is

$$g(r) = 1/[r \ln (B)] \qquad r_1 \leqq r \leqq r_2 \tag{31}$$
$$= 0 \text{ elsewhere}$$

where

$$B = r_2/r_1$$

We obtain with use of eqn. 22,

$$\bar{V}_e = V_l + V_s \left[\frac{-\ln (a/r_2)}{\ln B} - \frac{(3 - a/r_2)(1 - a/r_2)}{2\ln B}\right] \qquad r_1 \leqq a \leqq r_2 \tag{32}$$

$$\bar{V}_e = V_l + V_s \left(1 - \frac{a}{\ln B}\left(\frac{1}{r_1} - \frac{1}{r_2}\right)\left[2 - \frac{a}{2}\left(\frac{1}{r_1} + \frac{1}{r_2}\right)\right]\right) \qquad a \leqq r_1$$

A plot of this function for various values of B is shown in Fig. 9. These curves have a much larger linear portion than those of Fig. 6. It is obvious from this example and the form of eqn. 30 that one can obtain a wide variety of elution volume curves by a judicious choice of $g(r)$.

There is an interesting insensitivity to the specific form of $K(a/r)$ that occurs when $g(r)$ is a very broad distribution function. This insensitivity is due to the step character of $K(a/r)$ (that is, that for $a > r$, $K = 0$, and for $a \ll r$ $K = 1$). Thus if $g(r)$ is so broad that most tubes have either $r < a$ or $r \gg a$ for all a then $\bar{V}_e$ of eqn. 30 will not be sensibly changed by use of a step function in place of the correct functional form. For example, with a step function for $K(a/r)$ and for the $g(r)$ given by eqn. 31 we obtain

$$\begin{aligned} \bar{V}_e &= V_l \qquad a \geqq r_2 \\ \bar{V}_e &= V_l + V_s \ln (r_2/a)/\ln (B) \qquad r_1 \leqq a \leqq r_2 \\ \bar{V}_e &= V_l + V_s \qquad a \leqq r_1 \end{aligned} \tag{33}$$

which is not much different from eqn. 32 over a wide range of values of a. To the extent that elution volume is insensitive to the difference between K and the step function $\theta(a/r)$ we can say that the exclusion aspects of the formulation dominate.

E. Generalization of the bank model to a combination of blocked and open capillaries

If one allows a certain fraction of the small capillaries to be blocked up so that diffusion into and out of them is allowed but flow through them is disallowed then one obtains a more general model. In general one would expect that in GPC columns cavities of both types occur in the beads.

The average elution volume of such a column is identical in the equilibrium (slow flow) limit with that of the model in which there are only open tubes. Eqns. 17 and 25 remain valid with the substitutions afforded by eqn. 22 for K_e. Thus average elution volume is insensitive to whether there is flow through the capillaries.

Our equation for the second moment is now replaced by a sum over the two kinds of tubes. For the open tubes $1 - \phi$ is replaced by the fraction of volume of tubes of the open type (ϕ which is the fraction of volume of big tubes is unchanged). For the closed tubes $1 - \phi$ is replaced by the fraction of volume of tubes of the closed type and also the Langevin is replaced by its argument. The effect of this replacement is to increase the broadening. This means that the elution characteristics are always improved by use of open-end pores rather than dead-end pores.

REFERENCES

1 E. A. DiMarzio and C. M. Guttman, *Macromol.*, 3 (1970) 131.
2 C. M. Guttman and E. A. DiMarzio, *Macromol.*, 3 (1970) 681.
3 J. Happel and B. J. Byrne, *Ind. Eng. Chem.*, 46 (1954) 1181.
4 H. L. Goldsmith and S. G. Mason, *J. Colloid Sci.*, 17 (1962) 448.
5 E. A. DiMarzio and C. M. Guttman, *J. Polym. Sci. B-7*, (1969) 267.
6 Z. Grubisic, P. Rempp and H. Benoit, *J. Polym. Sci. B-5*, (1967) 753.
7 G. Taylor, *Proc. Roy. Soc. (London)*, A219 (1953) 186.
8 R. Aris, *Proc. Roy. Soc. (London)*, A235 (1956) 67.
9 J. J. Hermans, *J. Polym. Sci. 2A*, (1968) 1217.
10 B. H. Zimm and W. H. Stockmayer, *J. Chem. Phys.*, 17 (1949) 1301.
11 K. J. Bombaugh and R. F. Levange, *Anal. Chem.*, 41 (1969) 1357.

CHROM. 5126

A COMPARATIVE STUDY OF PORASIL AND STYRAGEL AS COLUMN SUPPORTS FOR GEL PERMEATION CHROMATOGRAPHY

JEANNE M. PACCO
Materials Analyses Area, Xerox Corporation, Rochester, N.Y. (U.S.A.)

SUMMARY

Molecular weight data were compared using two different column supports, Styragel and Porasil. A series of poly(styrene) and poly(vinylchloride) materials were analyzed on a Model 100 gel permeation chromatograph. The results obtained from the Porasil-packed columns were consistently lower than those obtained using the Styragel-packed columns. Data from both methods were further compared to values determined by such classical techniques as light scattering and membrane osmometry. Two experimental parameters, concentration and injection time, were included in this evaluation.

INTRODUCTION

Since the advent of the term gel permeation chromatography (GPC) in 1964 by MOORE[1], workers in the field have utilized this technique to facilitate molecular weight polymer characterization. A few GPC chemists have experimented with more effective substrates for use as GPC column packing. COOPER AND JOHNSON[2] have published data which proves the complete elution of polystyrene and polyisobutene on porous glass column packings. They eliminated adsorptive effects by treating the porous glass with hexamethyldisilazane. LOCHMÜLLER AND ROGERS[3] compared the behavior of stable inorganic and organic species on several commonly used gel media on the basis of resolution and recovery. The gel media covered in their study included: Sephadex G-25, Sephadex LH-20 (Pharmacia, Sweden), Bio-Gel P-6 and Bio-Glas 200 (Bio-Rad Laboratories).

DE VRIES *et al.*[4] reported the evaluation of spherical porous silica beads (Porasil) as a GPC column packing material. The pure silica nature of this material lends itself to improved chemical inertness and heat-resistance over the commonly used organic polymeric supports. According to their observations, the Porasil packing improves column efficiency at decreased flow rates and narrowed particle size distribution. The authors concluded from this investigation that the highest inherent efficiency was obtained with Porasil packings of at least 100 μ average diameter.

In an other paper, LEPAGE *et al.*[5] described the characteristics of two types of calibration standards, polystyrene and polyvinylchloride. The polystyrenes covered

a molecular weight range of 600 to 1800000 and 6400 to 250000 in the case of the polyvinylchlorides.

The purpose of this paper is to compare data obtained using two column sets of four columns each, one packed with Styragel and the other with Porasil. Nineteen polymers of various molecular weights were analyzed on both systems and the resulting data compared and discussed.

EXPERIMENTAL

A Model 100 gel permeation chromatograph was the instrument used to carry out the analyses for the two column sets. Operating temperature was 37° using Eastman grade tetrahydrofuran as the carrier solvent. Each sample was dissolved in degassed solvent from the instrument's drain-out valve. The flow rate was regulated at a constant 1 cc per min.

The Styragel four column set, Set A, was obtained directly from the vendor, Waters Associates Inc. Precise column description is contained in Table I.

TABLE I

DESCRIPTION OF COLUMN SET A (STYRAGEL)

Porosity (Å)	*Plates/ft.*
1 000 000	860
400 000	920
10 000	1 345
1 000	824

TABLE II

DESCRIPTION OF COLUMN SET B (PORASIL)

Type	*Mesh*	*Pore diameter (Å)*
B	<150	100–200
C	<150	200–400
D	<150	400–800
E	<150	800–1500

The second column set, Set B, was packed with Porasil by our laboratory. Each of the four columns were hand-packed by adding the Porasil material in its original form to the column. An electric vibrator was used to aid in firm, even packing and eliminate air pockets. Table II contains the description of the Porasil packed column set, set B.

The polymers examined in this study are divided into three groups; first, the narrow distribution polystyrenes obtained from Waters Associates, Inc.; second, the broad molecular weight polystyrenes which were polymerized by our polymer synthesis group; and third, three polyvinylchloride samples distributed by ArRo Laboratories. Table III contains the absolute values obtained for use in this investigation. The data on the PS calibration standards were reported by Waters Associates and on

the polyvinyl chloride materials by ArRo Laboratories. The $\bar{M}_w$ values reported by ArRo Laboratories were obtained in THF at 25° by light scattering with $\lambda = 4360$ Å and a $dn/dc = 0.129$ ml/g. Their $\bar{M}_n$ values were obtained using a Mechrolab 503 high speed membrane osmometer in THF at 25° using Gel Cellophane 450 membranes.

TABLE III

ABSOLUTE VALUES ESTABLISHED FOR POLYMERS USED IN THIS STUDY

Sample	*Composition*	$\bar{M}_w$	$\bar{M}_n$	*MWD*	*Data source*
2.0K	Poly(styrene)	2 030	1 840	1.10	Pressure Chemical
5.0K	Poly(styrene)	5 000	4 600	1.09	Waters Associates Inc.
10.3K	Poly(styrene)	10 300	9 700	1.06	Waters Associates Inc.
19.8K	Poly(styrene)	19 800	19 600	1.01	Waters Associates Inc.
51K	Poly(styrene)	51 000	49 000	1.04	Waters Associates Inc.
98.2K	Poly(styrene)	97 200	96 200	1.01	Waters Associates Inc.
160K	Poly(styrene)	173 000	164 000	1.05	Waters Associates Inc.
411K	Poly(styrene)	411 000	392 000	1.05	Waters Associates Inc.
860K	Poly(styrene)	867 000	773 000	1.12	Waters Associates Inc.
2000K	Poly(styrene)	2 145 000	1 780 000	1.20	Waters Associates Inc.
A-1	Poly(styrene)	33 000	18 200	1.83	Xerox Corporation
A-3	Poly(styrene)	126 400	51 500	2.45	Xerox Corporation
A-4	Poly(styrene)	185 500	79 300	2.34	Xerox Corporation
A-5	Poly(styrene)	356 100	165 000	2.16	Xerox Corporation
400-2	Poly(vinyl chloride)	68 600	25 500	2.69	ArRo Laboratories
400-3	Poly(vinyl chloride)	118 000	41 000	2.88	ArRo Laboratories
400-4	Poly(vinyl chloride)	132 000	54 000	2.44	ArRo Laboratories

Using a Q factor of 25, GPC data was also obtained in THF at 25°. The column arrangement was designated 3×10^6, 10^5, 10^4, and 10^3 Å porosities. The samples were prepared at 0.5% w/v concentration and injected for 120 sec at a flow rate of 1.0 ml/min.

$\bar{M}_w$ values for the broad distribution polystyrenes, prepared in our polymer

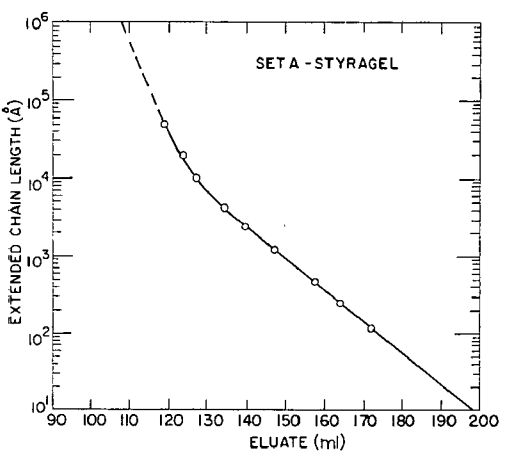

Fig. 1. GPC calibration curve, four Styragel column system, 1×10^6, 4×10^5, 1×10^4, and 1×10^3 Å, 0.5 to 0.25% in THF at 1×.

laboratory, were obtained from light scattering measurements at ambient temperature in MEK at a wavelength (λ) of 5460 Å. Our $\bar{M}_n$ values were obtained using a Mechrolab Model 501 high speed membrane osmometer in toluene at 37° using Schleicher and Schuell super dense 08 deacetylated acetyl cellulose membranes[6].

Each GPC column system was calibrated using the polystyrene standards from Waters Associates. The standards were dissolved in THF at 1/4 % w/v and injected for 120 sec. The calibration curve which resulted in Set A is illustrated in Fig. 1. The same procedure was followed in calibrating Set B and the resulting calibration curve is shown in Fig. 2. All GPC calculations made use of the values from the appropriate calibration curve.

The broad distribution polymers were analyzed at various concentration levels. All of them were run at the 1/2 % w/v in THF at a 120 sec injection time. This series was analyzed on Set A and compared with those run on Set B. The nine broad distribu-

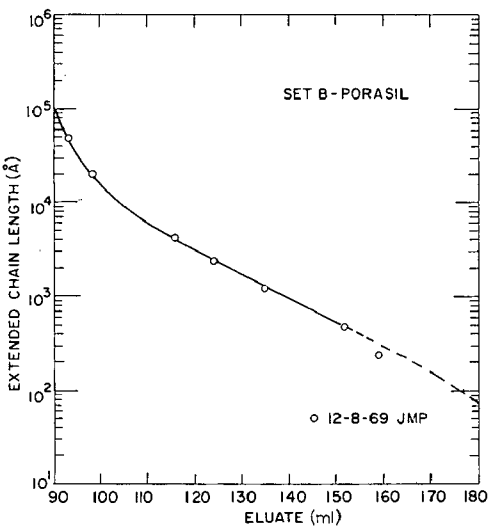

Fig. 2. GPC calibration curve, four Porasil column system, 0.25% in THF at 4 ×.

TABLE IV

GPC DATA FROM ANALYSIS OF PS STANDARDS

Standard PS	*Set A — Styragel*			*Set B — Porasil*		
	$\bar{M}_w$	$\bar{M}_n$	*MWD*	$\bar{M}_w$	$\bar{M}_n$	*MWD*
2.0K	3 400	3 100	1.10	7 050	6 600	1.07
5K	4 950	4 550	1.09	8 250	7 750	1.07
10.3K	11 000	9 800	1.12	13 400	12 350	1.08
19.8K	19 950	18 550	1.08	21 100	19 700	1.07
51K	53 650	49 050	1.09	52 100	47 300	1.10
98.2K	103 200	92 300	1.12	100 950	93 100	1.08
173K	157 450	137 700	1.14	174 600	157 300	1.11
411K	466 400	350 450	1.33	436 250	373 650	1.17
860K	1 007 500	666 200	1.51	931 950	662 300	1.41
2145K	2 165 200	1 134 550	1.91	1 795 400	918 900	1.95

TABLE V

GPC DATA ON BROAD PS MATERIALS

Sample code	*Set A — Styragel*			*Set B — Porasil*													
	1/2% — 2 min			*1/2% — 2 min*			*1/4% — 2 min*			*1/4% — 1 min*			*1/8% — 2 min*			*1/8% — 1 min*		
	$\bar{M}_w$	$\bar{M}_n$	*D*	$\bar{M}_w$	$\bar{M}_n$	*D*	$\bar{M}_w$	$\bar{M}_n$	*D*	$\bar{M}_w$	$\bar{M}_n$	*D*	$\bar{M}_w$	$\bar{M}_n$	*D*	$\bar{M}_w$	$\bar{M}_n$	*D*
A-1 (1)	34.16	17.14	1.99	32.55	21.60	1.51	31.75	20.55	1.54	29.90	20.50	1.46						
(2)	34.03	17.35	1.96	31.08	18.22	1.71	31.15	18.71	1.66	31.35	20.85	1.50						
(3)	34.00	17.25	1.97	30.13	17.88	1.68												
A-2 (1)	88.85	38.15	2.33	82.00	41.75	1.96	79.8	37.4	2.13	78.05	39.00	2.00						
(2)	91.96	41.49	2.22	86.34	39.77	2.17	95.07	39.35	2.42	86.05	27.60	3.12						
(3)							89.70	40.47	2.22	77.25	39.76	1.94						
A-3 (1)	113.3	51.2	2.21	103.35	56.95	1.81	98.40	49.50	1.99	97.12	48.79	1.99						
(2)	112.47	50.69	2.22	104.14	46.66	2.23	104.83	48.38	2.17									
(3)				100.11	45.72	2.19												
A-4 (1)	150.25	63.05	2.38	147.80	73.30	2.02	143.85	72.90	1.97	143.55	70.60	2.03						
A-5 (1)	316.90	101.40	3.12	275.15	109.55	2.51	278.10	111.80	2.49	281.62	126.44	2.23						
(2)	333.99	110.18	3.03	281.65	108.11	2.60	277.40	110.96	2.50									
(3)	331.26	99.73	3.32				277.13	110.39	2.51									
A-6 (1)	46.40	22.95	2.02	47.45	29.90	1.59	36.65	26.80	1.37	47.35	29.05	1.63	43.55	26.55	1.64	40.70	25.6	1.59
(2)	49.65	25.56	1.94							44.32	27.56	1.61	43.00	26.57	1.62	44.05	26.3	1.67
(3)	49.06	24.66	1.99													46.15	28.9	1.60

tion polymers were also run at 1/4 % w/w at 120 and 60 sec injection times on Set B. This phase of the work involved the effect of concentration on the Porasil packed columns. A-6 was analyzed at the 1/8 % w/v using 120 and 60 sec injection times. The precision levels for these analyses were calculated.

All of the GPC data were calculated following the usual peak height at the elution mark method with no corrections made for inherent curve errors.

RESULTS AND DISCUSSION

Table IV illustrates the molecular weight data obtained for the narrow distribution polystyrene calibration standards. The Porasil data generally indicated narrower distribution ratios as compared to the Styragel data. Even in the low-molecular-weight range the dispersity values are around 1.1 for the Porasil data. Reliable data is seen on Set B above 20K but overall better agreement with established values was attained by Set A throughout the entire molecular weight range of 2K to 2 million.

Table V illustrates the GPC data from the analysis of our own polystyrene materials. Again the distribution ratios are lower for the Porasil set than those for Styragel. A comparison of the results obtained for Porasil substrate show no significant change in molecular weight as a function of concentration or injection time.

Table VI shows the GPC data resulting from the analysis of the 3 polyvinyl

TABLE VI

GPC DATA ON POLY(VINYLCHLORIDE) SAMPLES

Sample code	*Set A — Styragel*			*Set B — Porasil*								
	1/2% — 2 min			*1/2% — 2 min*			*1/4% — 2 min*			*1/4% — 1 min*		
	$\bar{M}_w$	$\bar{M}_n$	D	$\bar{M}_w$	$\bar{M}_n$	D	$\bar{M}_w$	$\bar{M}_n$	D	$\bar{M}_w$	$\bar{M}_n$	D
400-2 (1)	59.75	26.10	2.29	53.40	25.62	2.08	58.22	26.01	2.24	49.65	24.9	1.99
(2)				55.51	24.84	2.23	55.73	24.61	2.26			
(3)				58.45	25.00	2.34						
400-3 (1)	100.25	47.90	2.09	96.93	50.03	1.94				80.70	38.70	2.08
(2)				98.43	43.02	2.29						
400-4 (1)	152.30	59.50	2.56	104.53	42.96	2.43	140.5	56.55	2.48	94.15	34.10	2.76
(2)	165.52	64.48	2.57	102.72	46.76	2.20						

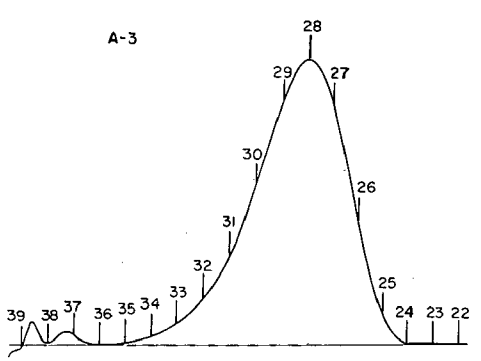

Fig. 3. A-3 polystyrene, 0.5% at 4 × on Set A. 112 k $\bar{M}_w$, 50 k $\bar{M}_n$; 2.22 ratio.

chloride polymers. For the third time Porasil data yields narrower distributions and lower $\bar{M}_w$ and $\bar{M}_n$ values than the Styragel data.

Typical chromatograms of sample A-3 are shown by Figs. 3 and 4, analyzed on

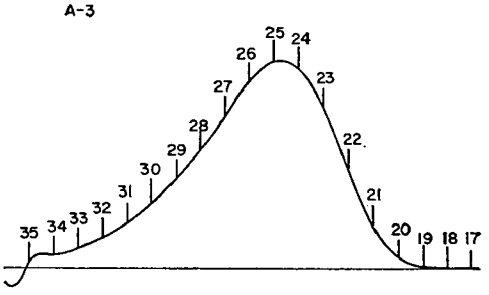

Fig. 4. A-3 polystyrene, 0.5% at 4 × on Set B. 100 K $\bar{M}_w$, 45 K $\bar{M}_n$; 2.19 ratio.

TABLE VII

COMPARISON OF GPC DATA (SET A) TO ABSOLUTE VALUES ON PS STANDARDS

Standard	*Absolute data*			*GPC data — Set A*			*Comparisons*			
	$\bar{M}_w$	$\bar{M}_n$	*MWD*	$\bar{M}_w$	$\bar{M}_n$	*MWD*	$\Delta\bar{M}_w$	*Diff.* (%)	$\Delta\bar{M}_n$	*Diff.* (%)
2.0K	2 030	1 840	1.10	3 400	3 100	1.10	1 370	67.5	1 260	68.5
5K	5 000	4 600	1.09	4 950	4 550	1.09	50	10.0	50	10.8
10.3K	10 300	9 700	1.06	11 000	9 800	1.12	700	6.8	100	10.3
19.8K	19 800	19 600	1.01	19 950	18 550	1.08	150	0.7	1 050	5.3
51K	51 000	49 000	1.04	53 650	49 050	1.09	2 650	5.2	50	0.1
98.2K	97 200	96 200	1.01	103 200	92 300	1.12	6 000	6.2	3 900	4.0
160K	173 000	164 000	1.05	157 450	137 700	1.14	15 550	8.9	26 300	16.0
411K	411 000	392 000	1.05	466 400	350 450	1.33	55 400	13.5	41 550	10.6
860K	867 000	773 000	1.12	1 007 500	666 200	1.51	140 500	16.2	106 800	13.8
2145K	2 145 000	1 780 000	1.20	2 165 200	1 134 500	1.91	20 200	0.9	645 450	36.3

TABLE VIII

COMPARISON OF GPC DATA (SET B) TO ABSOLUTE VALUES ON PS STANDARDS

Standard	*Absolute data*			*GPC data — Set B*			*Comparisons*			
	$\bar{M}_w$	$\bar{M}_n$	*MWD*	$\bar{M}_w$	$\bar{M}_n$	*MWD*	$\Delta\bar{M}_w$	*Diff.* (%)	$\Delta\bar{M}_n$	*Diff.* (%)
2.0K	2 030	1 840	1.10	7 050	6 600	1.07	5 020	247.2	4 760	258.7
5.0K	5 000	4 600	1.09	8 250	7 750	1.07	3 250	65.0	3 150	68.5
10.3K	10 300	9 700	1.06	13 400	12 350	1.08	3 100	30.1	2 650	27.3
19.8K	19 800	19 600	1.01	21 100	19 700	1.07	1 300	6.6	100	0.5
51K	51 000	49 000	1.04	52 100	47 300	1.10	1 100	2.2	1 700	3.5
98.2K	97 200	96 200	1.01	100 950	93 100	1.08	3 750	3.8	3 100	3.2
173K	173 000	164 000	1.05	174 600	157 300	1.11	1 600	0.9	6 700	4.1
411K	411 000	392 000	1.05	436 250	373 650	1.17	25 250	6.1	18 350	4.7
860K	867 000	773 000	1.12	931 950	662 300	1.41	64 950	7.5	110 700	14.3
2145K	2 145 000	1 780 000	1.20	1 795 400	918 900	1.95	349 600	16.3	861 100	48.8

Set A and Set B, respectively. As seen by the curves, Set A's chromatogram elutes in 12 elution counts while the one from Set B elutes in 16 counts. Visual examination of the two curves leads one to suspect a broader distribution for the Porasil analysis. The calculated data shows almost identical ratios; 2.22 *versus* 2.23. Since low-molecular-weight tailing is prominent in Set B's curve and not corrected in the calculations, it seems interesting that the ratios agree so closely.

The GPC data were compared to absolute values established for the PS standards and the resulting data from Set A and Set B are contained in Tables VII and VIII, respectively. One notes the need for correcting the higher-molecular-weight chromatograms due to viscous fingering effects[7].

Tables IX and X contain the comparisons of GPC data to classical values determined by our laboratory for four out of six samples evaluated by Set A and Set B, respectively. Better agreement is attained by Set A, generally speaking, in particular with $\bar{M}_w$ values determined by light scattering measurements.

TABLE IX

COMPARISON OF GPC DATA (SET A) TO ABSOLUTE VALUES ON BROAD PS SAMPLES

Sample	*Absolute values*		*GPC data — Set A*			*Comparisons*			
	$\bar{M}_w$ (*light scattering*)	$\bar{M}_n$ (*osmometry*)	$\bar{M}_w$	$\bar{M}_n$	*MWD*	$\Delta\bar{M}_w$	*Diff.* (%)	$\Delta\bar{M}_n$	*Diff.* (%)
A-1	33 000	18 200	34 060	17 250	1.97	1 060	3.2	950	5.2
A-3	126 400	51 500	112 880	50 940	2.22	13 520	10.7	560	1.1
A-4	185 500	79 300	150 250	63 050	2.38	35 250	19.0	16 250	20.5
A-5	356 100	165 000	327 380	103 700	3.16	28 720	8.1	61 300	37.1

TABLE X

COMPARISON OF GPC DATA (SET B) TO ABSOLUTE VALUES ON BROAD PS SAMPLES

Sample	*Absolute values*		*GPC data — Set B*			*Comparisons*			
	$\bar{M}_w$ (*light scattering*)	$\bar{M}_n$ (*osmometry*)	$\bar{M}_w$	$\bar{M}_n$	*MWD*	$\Delta\bar{M}_w$	*Diff.* (%)	$\Delta\bar{M}_n$	*Diff.* (%)
A-1	33 000	18 200	31 250	19 230	1.63	1 750	5.3	1 050	5.8
A-3	126 400	51 500	102 530	49 780	2.06	23 870	18.9	1 720	3.3
A-4	185 500	79 300	147 800	73 300	2.02	37 700	20.3	6 000	7.6
A-5	356 100	165 000	278 400	108 830	2.56	77 700	21.8	56 170	34.0

TABLE XI

COMPARISON OF GPC (SET A) TO VENDOR'S GPC DATA

Sample	*GPC data (ArRo)*			*GPC data (Xerox) Set A*			*Comparisons*			
	$\bar{M}_w$	$\bar{M}_n$	*MWD*	$\bar{M}_w$	$\bar{M}_n$	*MWD*	$\Delta\bar{M}_w$	*Diff.* (%)	$\Delta\bar{M}_n$	*Diff.* (%)
400-2	62 350	25 160	2.48	59 750	26 100	2.29	2 600	4.2	940	3.7
400-3	107 166	45 195	2.37	100 250	47 900	2.09	6 916	6.4	2 705	6.0
400-4	117 800	48 850	2.41	158 910	61 990	2.56	41 110	34.9	13 140	26.9

TABLE XII

COMPARISON OF GPC DATA (SET B) TO VENDOR'S GPC DATA

Sample	*GPC data (ArRo)*			*GPC data (Xerox) Set B*			*Comparisons*			
	$\bar{M}_w$	$\bar{M}_n$	*MWD*	$\bar{M}_w$	$\bar{M}_n$	*MWD*	$\Delta\bar{M}_w$	*Diff.* (%)	$\Delta\bar{M}_n$	*Diff.* (%)
400-2	62 350	25 160	2.48	55 780	25 150	2.22	6 570	10.5	10	0.03
400-3	107 166	45 195	2.37	97 680	46 525	2.12	9 486	8.9	1 330	2.9
400-4	117 800	48 850	2.41	103 625	44 860	2.32	14 175	12.0	3 990	8.2

TABLE XIII

COMPARISON OF GPC DATA (SET A) TO VENDOR'S ABSOLUTE DATA

Sample	*Absolute data*		*GPC data — Set A*			*Comparisons*			
	$\bar{M}_w$ (*light scattering*)	$\bar{M}_n$ (*membrane osmometry*)	$\bar{M}_w$	$\bar{M}_n$	*MWD*	$\Delta\bar{M}_w$	*Diff.* (%)	$\Delta\bar{M}_n$	*Diff.* (%)
400-2	68 600	25 500	59 750	26 100	2.29	8 850	12.9	600	2.4
400-3	118 000	41 000	100 250	47 900	2.09	17 750	15.0	6 900	16.8
400-4	132 000	54 000	158 910	61 990	2.56	26 910	20.4	7 990	14.8

TABLE XIV

COMPARISON OF GPC DATA (SET B) TO VENDOR'S ABSOLUTE DATA

Sample	*Absolute data*		*GPC data — Set B*			*Comparisons*			
	$\bar{M}_w$ (*light scattering*)	$\bar{M}_n$ (*membrane osmometry*)	$\bar{M}_w$	$\bar{M}_n$	*MWD*	$\Delta\bar{M}_w$	*Diff.* (%)	$\Delta\bar{M}_n$	*Diff.* (%)
400-2	68 600	25 500	55 780	25 150	2.22	12 820	18.7	350	1.4
400-3	118 000	41 000	97 680	46 525	2.12	20 320	17.2	5 525	13.5
400-4	132 000	54 000	103 625	44 860	2.32	28 375	21.5	9 140	16.9

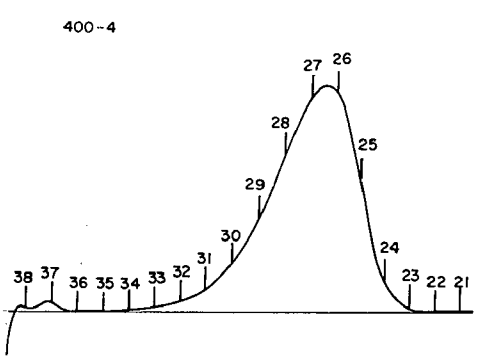

Fig. 5. 400-4 polyvinyl chloride, 0.25% at 16× on Set A. 158.9 K $\bar{M}_w$, 62 K $\bar{M}_n$; 2.56 ratio.

In comparing the GPC data from the analysis of the polyvinylchloride polymers, two approaches were taken. Tables XI and XII compared GPC data from Set A and Set B, respectively to the vendor's GPC data. This comparison indicates better

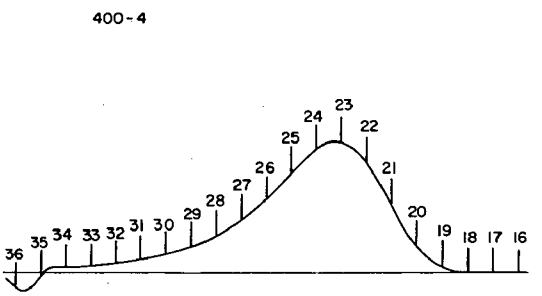

Fig. 6. 400-4 polyvinyl chloride, 0.5% at 4 × on Set B. 103.6 K $\bar{M}_w$, 44.8 K $\bar{M}_n$; 2.32 ratio.

TABLE XV

COMPARISON OF THE PRECISION BETWEEN THE TWO SUBSTRATES

	$\bar{X}_{M_w}$	$\bar{X}_{M_n}$	$\bar{X}_{MWD}$
Set A			
A-1	34.06 ± 0.351	17.246 ± 0.275	1.97 ± 0.089
A-6	48.37 ± 4.29	24.39 ± 3.286	1.98 ± 0.112
Set B			
A-1	31.25 ± 2.99	19.23 ± 5.10	1.63 ± 0.26
A-6	43.63 ± 6.82	26.93 ± 4.31	1.62 ± 0.146

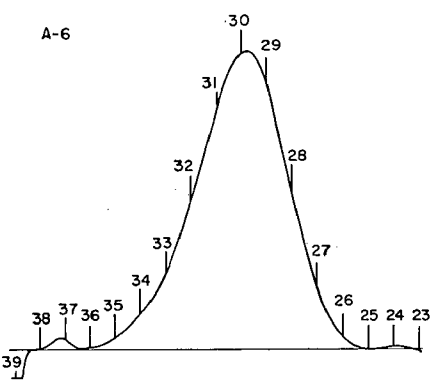

Fig. 7. A-6 polystyrene, 0.5% at 4 × on Set A. 34.06 K $\bar{M}_w$, 17.24 K $\bar{M}_n$; 1.97 ratio.

agreement is found in Set B especially with $\bar{M}_n$ values, $<10\%$ even at the highest $\bar{M}_n$ value. The highest difference in $\bar{M}_w$ for Set B was 12% as opposed to 34.9% for the same sample on Set A. The second approach was to compare the GPC data to the vendor's absolute data from light scattering and osmometry. The results of this comparison are shown in Tables XIII and XIV. Set A shows better $\bar{M}_w$ agreement than Set B for each sample with somewhat higher discrepancies than seen in Table XI. The opposite effect was observed with the $\bar{M}_n$ values in Set B which had

fewer differences than Set A. Figs. 5 and 6 illustrate chromatograms of 400-4 as analyzed on Set A and Set B, respectively.

Two samples, A-1 and A-6, which had been analyzed three times each on Set A and Set B were used to establish precision limits. Table XV contains the results of

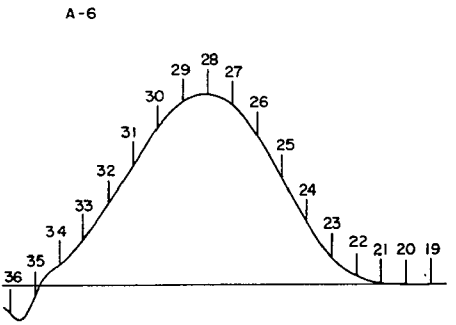

Fig. 8. A-6 polystyrene, 0.5% at 4 × on Set B. 31.25 K $\bar{M}_w$, 19.23 K $\bar{M}_n$; 1.63 ratio.

the precision evaluation. The average precision of Set A was better than Set B. Chromatograms of A-6 analyzed on Set A and Set B are shown in Figs. 7 and 8, respectively.

Reviewing all the data and considering no error corrections made for axial dispersion, diffusion or adsorption, it was difficult to see any great advantage of one substrate over the other. Set A yielded more precise molecular weights in the range evaluated in this study. Set B could be improved by using smaller angstrom packing of higher surface area which was not available at the time this study was initiated. A column packed with the smaller porosity substrate would increase resolution power in the low-molecular-weight region and extend the separation range of the Porasil.

REFERENCES

1 J. C. MOORE, *J. Polym. Sci. A-2*, (1964) 835.
2 A. R. COOPER AND J. F. JOHNSON, *J. Appl. Polym. Sci.*, 13 (1969) 1487–1492.
3 C. H. LOCHMÜLLER AND L. B. ROGERS, *Anal. Chem.*, 41 (1969) 173.
4 A. J. DE VRIES, M. LEPAGE, R. BEAU AND C. L. GUILLEMIN, *Anal. Chem.*, 39 (1967) 935–939.
5 M. LEPAGE, R. BEAU AND A. J. DE VRIES, *J. Polym. Sci. C*, 21 (1968) 119.
6 D. F. ALLIET, *J. Appl. Polym. Sci.*, 8 (1969) 41.
7 J. C. MOORE, *159th National Amer. Chem. Soc. Meeting, Houston, Texas, February 25, 1970.*

CHROM. 5127

GEL PERMEATION CHROMATOGRAPHY: DATA TREATMENT

J. A. MAY, JR. AND G. W. KNIGHT
Dow Chemical Co., B-1216 Bldg., Freeport, Texas 77541 (U.S.A.)

SUMMARY

Since the advent of gel permeation chromatography it has been difficult to compare molecular weight distributions of samples analyzed on different gel columns or under different experimental conditions. Corrections are described herein which convert gel permeation chromatographic curves to absolute molecular weight distributions. Good agreement of corrected molecular weight distributions for several samples analyzed on different column sets was obtained.

INTRODUCTION

Because gel permeation chromatographic (GPC) curves are graphs of Δ refractive index/Δ volume *vs.* elution volume, it is virtually impossible to superimpose GPC curves for identical samples from two different column sets. Even if the area under the curves is normalized, it is invalid to merely substitute molecular weights (from the calibration curves) for elution volumes. Furthermore the instrument spreading will most likely vary from instrument to instrument. To reiterate, in most cases there will be three significant differences between the chromatograms for the same sample analyzed under widely divergent experimental conditions, as follows: (1) identical elution volumes will not correspond to identical molecular weights, (2) the degree of instrument spreading will be different for each instrument or column set, and (3) polymer peaks will be of different size.

The first step in the correction process is the establishment of a calibration curve. Elution volumes of the peaks of twelve narrow distribution polystyrene standards were graphed *versus* the logarithm of the molecular weight at the peak. This calibration curve was fitted by a least-squares procedure to a fifth-order polynomial function. As a check of the validity of the calibration curve, the weight- and number-average molecular weights were calculated for the polystyrene standards for comparison with the reported values.

The values of the instrument spreading factors, σ_{GPC}, were determined by also using the polystyrene standards and the method proposed by HENDRICKSON[1]. The relationship $\sigma_{GPC} = (\sigma_{obs}^2 - \sigma_{dist}^2)^{1/2}$ was employed, where σ_{obs}, the observed spreading, is one-half the volume between the chromatogram peak and the baseline intercept of a tangent (theoretically the tangent at the first inflection point) to the leadside of the chromatograms, and where σ_{dist} is the volume (obtained from the calibration curve) corresponding to the difference between the molecular weight at the peak and the molecular weight (Table I) at the first inflection point.

The chromatograms were corrected for spreading using a third generation version of SMITH'S[2] computer program. This correction procedure assumes a molecular weight component at each particular volume increment. The chromatogram is then considered to be an envelope of the sums of the individual components, each of which has a gaussian shape due to spreading. The spreading factors, σ_{GPC}, can vary with molecular weight or can be unequal (for unsymmetrical, skewed peak shapes). Initially the amount of each component at each particular elution volume is set proportional to the chromatogram height at that particular elution volume. Then an iterative procedure is begun in which an envelope of the sums of the individual components is calculated, considering the contribution of neighboring components to each other due to gaussian spreading. The amount of each component is then adjusted by a ratio of the height of the chromatogram to the height of the calculated envelope. This procedure is repeated for a specified number of times or until the chromatogram and the calculated envelope agree within specified ("gate value") limits. Frequently CHANG AND HUANG'S[3] smoothing subroutine is used in conjunction with the spreading correction to smooth spurious baseline noise in the original chromatogram.

The replot technique proposed by YAU AND FLEMING[4] was used to correct for non-linear calibration curves. The weight fraction per volume increment (obtained from the chromatogram) is multiplied by the reciprocal of the slope of the calibration curve to obtain the corrected value of weight fraction per log molecular weight increment ($dW/d(\log M) = (dW/dV) \times dV/d(\log M)$). Finally the molecular weight distributions are normalized so that there are equal areas under every distribution.

After the chromatograph has been calibrated and all the various corrections made to a chromatogram, the inevitable question arises, just how accurate is the molecular weight distribution that one obtains? A good check of the validity of the corrections would be to analyze several duplicate samples on different chromatographs using different columns, apply the various corrections, and then compare the MWD from each chromatograph for identical samples.

EXPERIMENTAL

Results were obtained using Waters Associates Gel Permeation Chromatographs. Two instruments were used in this study, GPC-4 and GPC-3. Both chromatographs had been modified for operation at high temperature, for automatic injection, and for column reversing. GPC-4 is a Model 100 with a null-balance differential refractometer operating at 135° using the solvent 1,2,4-trichlorobenzene (TCB) and a flow rate of 1 ml/min. GPC-4 utilized three 4 ft. columns in series (2500 plates/ft.) of permeabilities 10^4, 2×10^5, and 10^6 Å. GPC-3 is a Model 200 with an R-4 differential refractometer operating at 145° also using the solvent TCB and a flow rate of 1 ml/min. GPC-3 utilized four 4 ft. columns in series (3000 plates/ft.) of permeabilities 10^4, 2×10^5, 2×10^5, and 10^6 Å.

All samples were injected onto the columns 46.5 sec. Below mol. wt. 300 000 all calibration samples were 1.0 mg/ml. Above mol. wt. 300 000 all calibration samples were 0.5 mg/ml and fresh samples made the day they were injected. Above mol. wt. 10^6 polystyrene solutions in TCB appear to degrade upon long standing, as the peaks broaden and elute later. Above mol. wt. 10^6 the concentrations may be slightly overloaded. However, due to the limits of instrument sensitivity, the concentration could not be reduced further.

RESULTS AND DISCUSSION

Calibration curves were constructed for GPC-3 and GPC-4 by graphing log molecular weight *vs.* elution volume for twelve narrow distribution polystyrene standards. Smooth curves were drawn through the twelve points. Readings every milliliter were taken from this curve and the readings were fitted by a least-squares procedure to a fifth-order polynomial ($\log M = a + bv + cv^2 + dv^3 + ev^4 + fv^5$, where v = volume) by computer program CALJAM. The values of spreading factors were determined from the leadside of the polystyrene standards using values by MOORE[5] (Table I).

TABLE I

MOLECULAR WEIGHT VALUES[a] FOR DETERMINATION OF SPREADING DUE TO THE DISTRIBUTION (σ_{dist})

Standard	*Peak molecular weight*	*Molecular weight at 1st inflection*
PS4190042	11 700	14 290
PS4190039	19 500	24 400
PS4190041	51 200	57 800
PS41984	170 600	178 200
PS4190037	411 000	428 000
PS4190038	990 000	1 042 000
PS61970	2 000 000	2 150 000

[a] See ref. 5.

Then, using the analytical calibration curve and the experimentally-determined spreading factors, weight- and number-average molecular weights as well as the polydispersity ratios ($\bar{M}_w/\bar{M}_n$) were calculated for the polystyrene standards using computer program JAMGPC. In general the calculated molecular weights were zero to ten percent low. The calibration curve was then shifted upwards the corresponding zero to ten percent and a revised calibration curve calculated. An example of the agreement between the twelve experimental points and the revised analytical calibration curve is shown in Fig. 1. In order to check the spreading correction, the reported polydispersities were compared with the calculated polydispersities. The reported polydispersities were less than the calculated polydispersities which were uncorrected for spreading, but more than the calculated polydispersities which were corrected for spreading. This indicated that the experimentally-determined spreading factors, σ_{GPC}, were too large. Fig. 2 shows the experimental variation of spreading factors with elution volume for GPC-3 and GPC-4. Lesser arbitrary values of spreading factors, also shown in Fig. 2, gave better agreement with reported polydispersity data and were used in all subsequent calculations. Table II includes reported polydispersities, weight-, and number-average molecular weights of the polystyrene standards, as well as the calculated values from GPC-3 and GPC-4 using the revised calibration curves and spreading factors.

Having established valid calibrations for GPC-3 and GPC-4, as evidenced by the good agreement of reported and calculated molecular weight values for the standards, it is possible to calculate valid molecular weight distributions from GPC-3 and

GPC-4. Fig. 3 is a comparison of MWD for a medium broad distribution ($\bar{M}_w/\bar{M}_n = 1.95$) polystyrene sample obtained from GPC-3 and GPC-4. The chromatograms were smoothed prior to spreading corrections in order to minimize baseline noise. The agreement of MWD from different chromatographs (Fig. 3) appears to be about as good as the agreement of MWD from repeat analysis on the same chromatographs (Fig. 4). The agreement even seems better when one realizes that the area under the curves in Figs. 3 and 4 is approximately six times the area of the original chromatograms, which has the effect of magnifying the differences approximately six times.

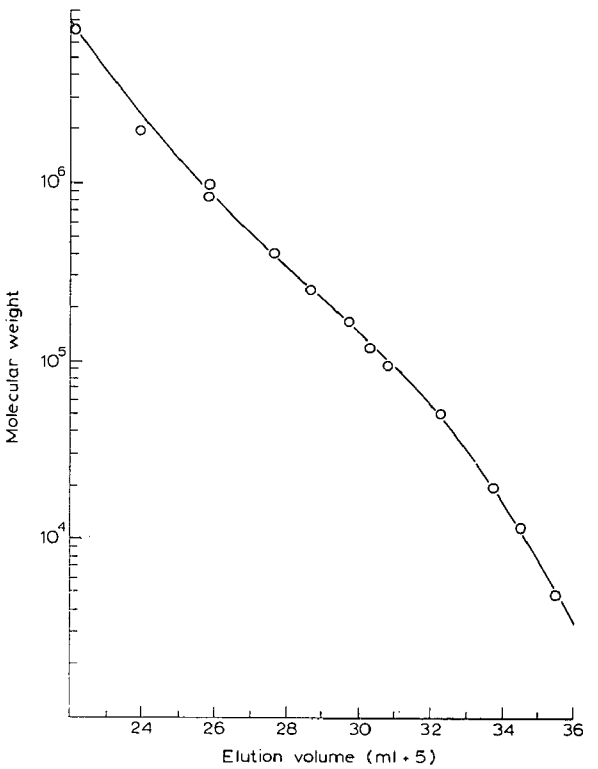

Fig. 1. Calibration curve for the polystyrene standards. The line represents the revised analytical function.

Prior computer programs give accurate spreading corrections when the molecular weight distributions are broad and the spreading is relatively small. However, when the distributions are narrow and spreading is relatively large, most programs over-accentuate baseline noise and suffer from artificial oscillations, especially on the leading and trailing edges. Several of the prior-published spreading corrections oscillate badly and yield negative values for weight fraction of polymer at times. Most of these computer programs can not adequately handle multipeaked distributions. DUERKSON AND HAMIELEC[6] have done a good review of the currently used computer programs. Fig. 5 shows the chromatograms from GPC-3 and GPC-4 of a blend of five narrow distribution polystyrene standards which was prepared to rigorously test our present correction program. The two chromatograms are similar in shape, but cannot

TABLE II

POLYSTYRENE STANDARDS DATA

No.	*Sample*	*Reported*			*GPC-3*			*GPC-4*		
		$\bar{M}_w$	$\bar{M}_n$	$\bar{M}_w/\bar{M}_n$	$\bar{M}_w$	$\bar{M}_n$	$\bar{M}_w/\bar{M}_n$	$\bar{M}_w$	$\bar{M}_n$	$\bar{M}_w/\bar{M}_n$
a	PS4190040	5 000	4 600	1.08	4 630	4 310	1.075	4 905	4 660	1.053
b	PS4190042[a]	10 790	9 970	1.083	10 710	9 960	1.076	11 080	10 180	1.089
c	PS4190039[a]	20 340	19 410	1.048	19 860	18 800	1.056	17 446	14 550	1.199
d	PS4190041[a]	52 770	51 860	1.018	52 450	50 849	1.018	50 660	48 234	1.050
e	PS41995	98 200	96 200	$\leq$1.06	100 190	98 540	1.017	98 322	95 730	1.027
f	PS103	125 000	119 000	1.05	123 396	112 900	1.093	—	—	—
g	PS41984[a]	169 020	167 170	1.011	164 880	162 000	1.018	164 660	160 270	1.027
h	PS4190037[a]	404 850	383 390	1.056	404 620	395 090	1.024	412 070	394 080	1.046
i	PS4190038[a]	870 530	778 780	1.118	886 540	849 840	1.043	839 800	790 510	1.062
j	PS61970[a]	1 667 000	1 149 910	1.459	1 656 000	1 137 000	1.45	2 021 300	1 815 800	1.113
k	PS, blend of c, d, e, f, and PS108	114 590	54 460	2.10	102 810	50 850	2.02	99 140	46 950	2.11

[a] Ref. 5.

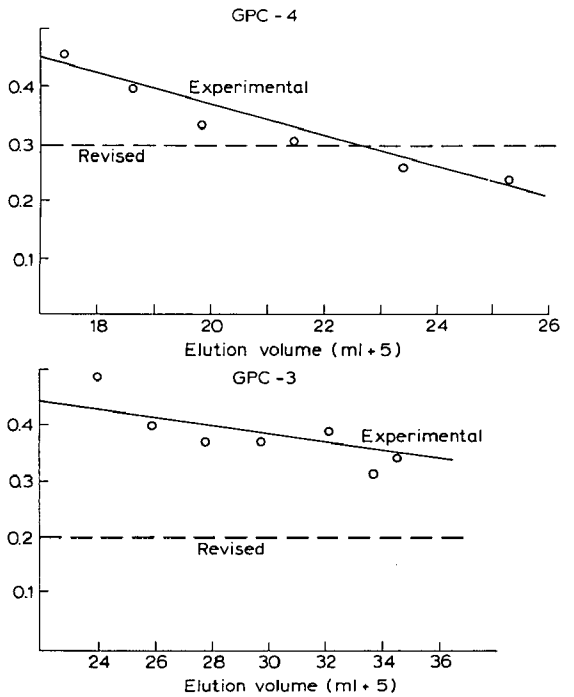

Fig. 2. Spreading factors *vs.* elution volume for GPC-3 and GPC-4. The revised spreading factors (dashed lines) gave better agreement with the reported values of $\bar{M}_w/\bar{M}_n$.

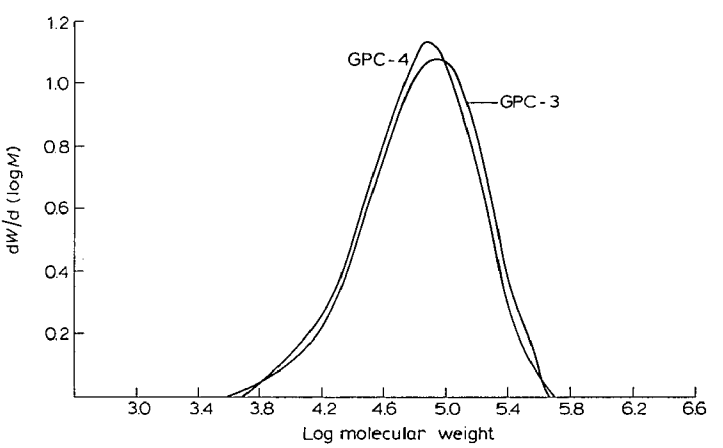

Fig. 3. Comparison of molecular weight distributions for polystyrene sample PS-6 obtained from GPC-3 and GPC-4.

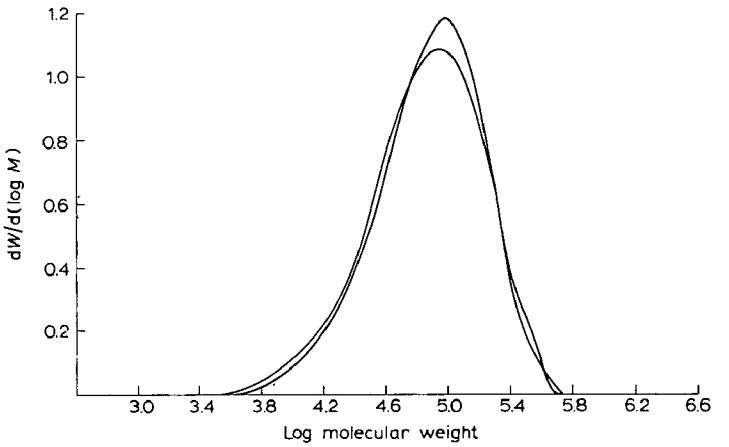

Fig. 4. Repeat analysis of polystyrene sample PS-6 on GPC-3.

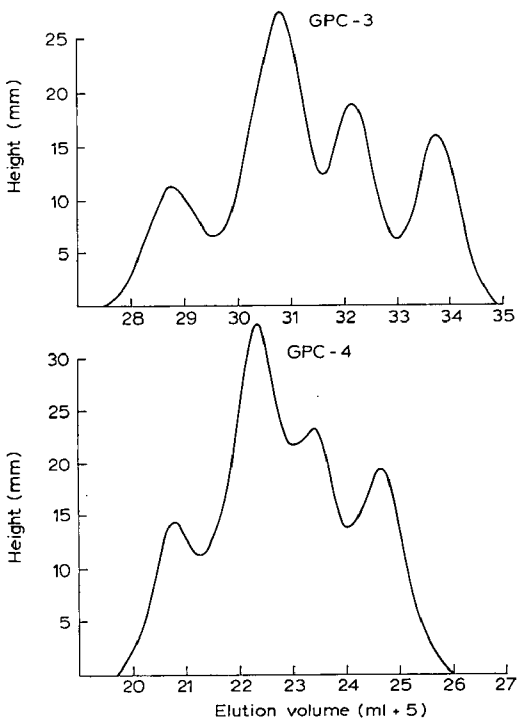

Fig. 5. Chromatograms of a five-component blend run on GPC-3 and GPC-4.

be readily visually compared. However, after these chromatograms have been corrected and plotted (Fig. 6) as weight fraction per log M increment *vs.* log mol. wt., the MWDs are very nearly the same. The area under the curves in Fig. 6 is approximately four times the area under the original chromatograms. The data were not smoothed prior to spreading corrections for Fig. 6. MWD (using smoothed data)

obtained from GPC-3 and GPC-4 for another blend of five narrow polystyrene standards is shown in Fig. 7. In this case the five peaks are so close together that the blend could not be resolved by the chromatographs into separate peaks.

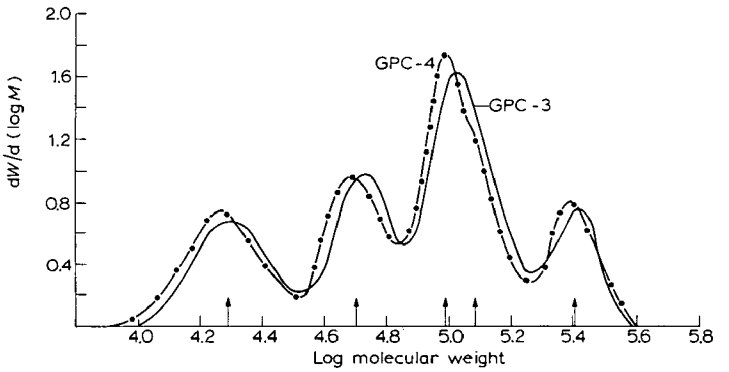

Fig. 6. Molecular weight distribution of the blend shown in Fig. 5. The arrows represent the peak elution volumes of the five components.

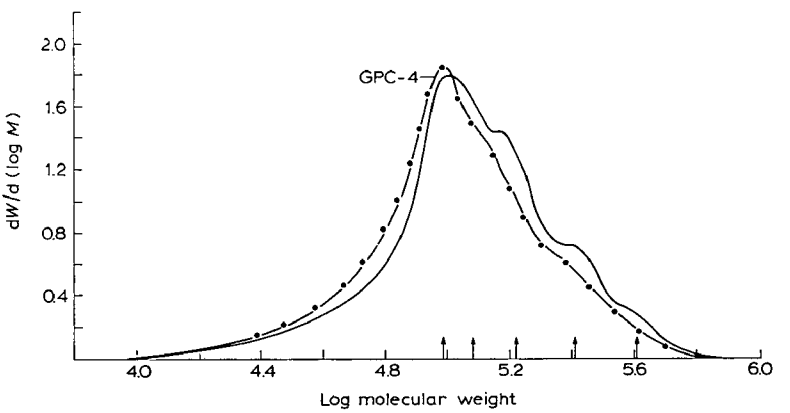

Fig. 7. Molecular weight distribution for a second blend run on GPC-3 and GPC-4. The arrows represent the peak elution volumes of the five components.

With respect to the spreading correction, there are two important questions. First, how large should the "gate value" be and second, when should the data be smoothed to remove baseline noise? If the gate value is too large, the spreading will not be corrected for. If the "gate value" is too small, the iterative program will overcorrect, magnifying anomalies and attempting to place a peak at every minor inflection or bump in the chromatogram. This can be disastrous if there is any baseline noise or short-term baseline drift. The best value for the "gate value" seems to be a value corresponding to the precision with which one can measure the curve height, or a value corresponding to the magnitude of baseline noise. For the present spreading corrections, the value of 1 mm was used as the "gate value", discounting smaller inflections as inconsequential. The smoothing of data can be used in most instances. The difference between smoothed and unsmoothed data in most cases was less than

1 mm. However, when few data points are taken and peaks are sharp, the smoothing routine will round off peaks and destroy essential detail. This loss of detail is a result of the inherent nature of the smoothing procedure. The smoothed height at a particular elution volume is the height at that elution volume of the best cubic curve through the point and the three data points on each side of the considered point, or in other words, a seven point cubic smoothing function is used. Therefore, if enough points are not taken and a smooth cubic curve cannot be placed through any seven neighboring points, the smoothing routine should not be used. The data shown in Fig. 5 were not smoothed because data was collected every milliliter, and therefore the peaks and valleys would have been rounded off.

In conclusion, a good procedure has been described for obtaining accurate molecular weight distributions, independent of the columns and experimental conditions (assuming the columns are good and of the applicable porosity range). However, when very minute and subtle differences are to be examined between two samples, the easiest and best method still is to chromatograph the samples consecutively under the same conditions and merely compare the chromatograms. Nevertheless, instances arise when one has earlier chromatograms of samples, but none of the samples to chromatograph consecutively.

CONCLUSIONS

1. Good agreement of corrected molecular weight distributions for identical samples analyzed on different column sets was found.

2. Narrow, multipeaked, as well as broad, simple molecular weight distributions were dealt with successfully in peak spreading corrections.

3. Criteria for the use of data smoothing prior to the spreading correction, and criteria for choosing a "gate value" in spreading corrections were discussed.

4. When extremely small differences in molecular weight distributions between two samples are to be examined, it is still best to chromatograph the samples on the same columns and compare the uncorrected chromatograms.

REFERENCES

1 J. G. HENDRICKSON, *J. Polym. Sci. A-2*,6 (1968) 1903.
2 W. N. SMITH, *J. Appl. Polym. Sci.*, 11 (1967) 639, modified by J. C. MOORE AND J. A. MAY, Jr.
3 K. S. CHANG AND R. Y. M. HUANG, *J. Appl. Polym. Sci.*, 13 (1969) 1459.
4 W. W. YAU AND S. W. FLEMING, *J. Appl. Polym. Sci.*, 12 (1968) 2111.
5 J. C. MOORE, private communication. Molecular weight values were from calculations by MOORE on data from L. H. TUNG.
6 J. H. DUERKSON AND A. E. HAMIELEC, *J. Polym. Sci. C*, 21 (1967) 83.

CHROM. 5128

CHARACTERIZATION OF LOW-MOLECULAR-WEIGHT DIFUNCTIONAL POLYBUTADIENES

G. PERRAULT, M. TREMBLAY, R. LAVERTU* AND R. TREMBLAY*
Defense Research Establishment Valcartier, Quebec (Canada)

SUMMARY

Hydroxylesterification and esterification reactions were made on α,ω-dicarboxypolybutadiene polymers and the products characterized by both analytical and preparative gel permeation chromatography. The choice of a calibration curve to study transformation of polymers is discussed, as well as the reasons for adopting the MOORE calibration curve relating size of polymers to elution volume. An automatic Fortran program was used to calculate number-average and weight-average sizes of polymers from the chromatograms. Problems associated with changes in the distribution of a polymer during a reaction are examined. To relate sizes of polymers in solution to molecular weight, measurements were made by vapor phase osmometry, light scattering and viscosity. The constancy of the refractive index increments with polymer size has been verified.

INTRODUCTION

Many problems are encountered in the characterization of low-molecular-weight polymers, polymers with molecular weight lower than about 5000. While the number average molecular weight ($\overline{M}_n$) can be measured easily by several well-known methods, the weight average molecular weight ($\overline{M}_w$) and the distribution of these polymers are very difficult if not impossible to obtain. Gel permeation chromatography (GPC) has become a well established technique for the characterization of high-molecular-weight polymers, and it is often possible to extract all the information required from only one chromatogram. It has been used with low-molecular-weight compound[1–6] but with less success, the main difficulty being the construction of a valid calibration curve.

The first part of this paper will deal with attempts to obtain a suitable calibration curve for low-molecular-weight polymers. In the second part, results obtained in analyzing some low-molecular-weight functionally terminated polybutadienes will be presented.

Calibration of GPC

The calibration of GPC for high-molecular-weight polymers has been fully

* In part.

described[7]. The calibration curve most often used relates the elution volume (V) to the logarithm of the molecular weight (M).

This calibration procedure presents two main difficulties. Firstly, well-characterized molecular weight standards are needed. These are not readily available for low-molecular-weight polymers. Secondly, a separate calibration curve is required for each polymer type studied. To solve this second problem, universal calibration curves have been proposed[8,9] which, however, do not seem to be valid for low-molecular-weight polymers[6].

The best solution so far proposed and used by most workers in this field is based on elution volume (V) *versus* molecular size (Å) calibration curve. A typical calibration curve of this relationship obtained using four columns of 10^5, 10^4, 10^3, and 10^2 Å, respectively, is given in Fig. 1. Standard polystyrene and polyethers, from

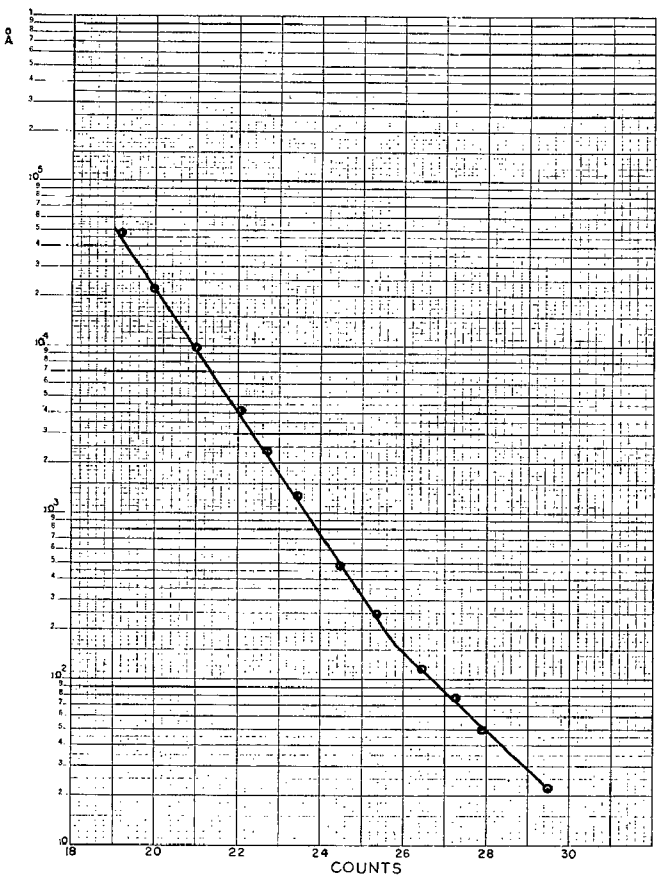

Fig. 1. Calibration curve.

Waters Associates, were used with an Ana-Prep instrument from the same company to obtain the curve. The reproducibility of this curve varied little from month to month giving only small parallel displacements. As can be seen, the curve is made up the most part of two straight line portions. A Fortran computer program was

used to calculate the number average molecular sizes ($\overline{A_n}$) (eqn. 1), and the weight average molecular sizes ($\overline{A_w}$) (eqn. 2), as defined by CAZES[10].

$$\overline{A_n} = \Sigma H_i/\Sigma(Hi/Ai) \tag{1}$$

$$\overline{A_w} = \Sigma HiAi/\Sigma Hi \tag{2}$$

where

Hi = height of a given segment

Ai = Å size corresponding to this segment on the calibration curve.

This program used is quite similar to the one suggested by Waters[11] except that the baseline is found in a different manner. In our technique, the computer begins at the maximum of the peak of the chromatogram and considers values on each side of the distribution curve in a three point sequence until it encounters values which are either similar or increasing. The computer then compares separately the values obtained on both sides of the base and if these do not differ by more than 5 % draws a straight line between them to give the base line. The computer does this with readings of the curve taken at 30 sec intervals by a digital curve translator.

The ratio of average sizes gives a measure of the polymer distribution (p) which is written with a subscript A (eqn. 3) to indicate that this distribution was obtained from measurements of the sizes of the polymer in solution. The terminology "volumetric distribution" is proposed for P_A.

$$P_A = \overline{A_w}/\overline{A_n} \tag{3}$$

To obtain an appreciation of the validity of the results from this method, some curve parameters were examined. The resolution factor (h) and the skewing factor (SK) were examined on calibration curves of standard monodisperse products. Our intention was to work under conditions where the resolution would remain constant and skewing negligible. To evaluate measurements on unknown polymers, changes in resolution and skewing must be considered but it is also important to check the constancy of the refractive index increment (dn/dc) over the entire molecular weight range studied.

Resolution and skewing

The Fortran program was extended to calculate the variance (σ) as well as the first and second moment (B_1 and B_2) of the distribution. The usual mathematical definition for these values are given in eqns. 4–6.

$$\sigma = \int_{-\infty}^{\infty} (x - \mu_1')^2 \mathrm{d}F \tag{4}$$

$$B_1 = (b_1)^{1/2} = m_3/m_2^{3/2} \tag{5}$$

$$B_2 = m_4/m_2^2 \tag{6}$$

where

x = one point on the chromatogram

μ_1' = the arithmetic average of the theoretical distribution

$$F = \int_{-\infty}^{\infty} x(f(x))\,dx$$

$$m_n = (1/N) \sum_{i}^{N} = 1^{(x_i - \bar{x})n}$$

n = an integer

N = sampling size

$\bar{x}$ = arithmetic average of a sample with N points $= \frac{1}{N} \sum_{i=1}^{N} x_i$

In the equations above, the variance is related to the resolution of the system, the first moment, B_1 is a coefficient of symmetry equal to 0 for a perfect gaussian distribution, and the second moment B_2 is an acuity coefficient equal to 3 in an ideal case. The results of the calculation for the standard products are given in Table I. As usual, the reduced surface of the peak was also calculated to provide a check on the chromatogram.

TABLE I

POLYESTER AND POLYSTYRENE STANDARDS AT 0.1–0.15% IN TETRAHYDROFURAN

Samples (Å)	*Reduced surface* (*ml/mg*)	σ	B_1	B_2	$\overline{A_n}$ (Å)	$\overline{A_w}$ (Å)
20 000	65.5	3.24	0.33	3.25	17 700	22 600
9 800	64.1	3.24	0.34	3.31	9 300	11 400
4 160	63.1	2.74	0.15	2.99	3 800	4 500
2 360	62.0	2.52	0.18	2.95	2 250	2 650
1 250	62.6	2.46	0.12	2.94	1 220	1 380
1 220	59.6	2.47	0.11	2.94	1 228	1 390
480	61.5	2.79	0.18	3.06	470	550
241	61.3	2.72	0.06	2.83	258	293
117	60.7	3.30	0.71	4.10	115	130
78	16.2	2.39	0.16	2.95	77	81
50.5	15.7	2.56	0.14	2.95	51	55

As can be seen, σ is fairly constant for the polystyrene standards smaller than 4160 Å, except for the 117 Å sample. In this range, 50.5 to 4160 Å, B_1 is quite low giving an indication of a very small skewing effect toward the low-molecular-weight side of the distribution. B_2 is also very near to an ideal gaussian distribution. The overall results indicate that very small corrections are to be made. Nevertheless, as is shown in Table II, without any correction, the distributions p_A obtained are higher than the true distribution ($p(t)$) calculated from $\overline{M_n}$ and $\overline{M_w}$ measured by two independent techniques.

In order to obtain a better appreciation of the magnitude of the corrections that should be made for skewing and for the resolution power of the columns, the skewing factor (SK) and the resolution factor (h) were calculated as suggested by HAMIELEC[12] using eqns. 7–9 in their molecular size versions.

$$SK = \frac{A_1(t)}{A_1(\infty)} + \frac{A_2(t)}{A_2(\infty)} - 2 \tag{7}$$

$$h = 1/2\sigma^2 \tag{8}$$

$$A_k(h,SK) = A_k(\infty)\left(1 + \frac{SK}{2}\right) \exp\,(3 - 2K)D_2^2/4h \tag{9}$$

where

$A_1(t)$ = true average size at peak height for standard 1

$A_1(\infty)$ = measured size at peak height for standard 1

K = 1, 2 ... where $\overline{A_1} = \overline{A_n}$ and $\overline{A_2} = \overline{A_w}$

D_2 = slope of the calibration curve.

TABLE II

POLYETHER AND POLYSTYRENE STANDARDS AT 0.1–0.15% IN TETRAHYDROFURAN

Samples (Å)	$p(t)$	P_A	$p(\infty)$
4160	1.05	1.18	1.06
2360	1.00	1.18	1.06
1250	1.04	1.13	1.02
1220	1.04	1.13	1.02
480	1.01	1.17	1.05
241	1.06	1.14	1.08
117	1.09	1.13	1.07
78	—	1.05	1.00
50.5	—	1.08	1.03

TABLE III

SKEWING FACTORS OF STANDARD PRODUCTS

$A_1(t)$ (Å)	$A_2(t)$ (Å)	*SK*	
4160	2360		0
2360	1250		−0.055
1250	480		−0.08
480	244		−0.04
244	177		−0.05
117	78		−0.04
78	50.5		−0.01
		Average SK =	−0.04

Table III gives the skewing factors obtained from two consecutive points along the valid part of the calibration curve. These results are the average of two determinations as calculated from eqn. 7. These values give for the skewing portion of the corrective eqn. 9 (*i.e.* $1 + SK/2$), an average value of 0.98 which, as was expected, is very small.

The resolution factors calculated with eqn. 8 for each standard product, as

determined from the chromatograms in the forward flow mode are given in Table IV and are constant at 2.25. However, the resolution portion of eqn. 9, exp. $(3\text{-}2K)$ $D_2^2/4h$, gives different values because of the change in slope of the calibration curve. This gave values of 1.08 for A_n for the first part of the calibration curve with a slope (D_2) of 0.84, and a correction for symmetrical dispersion, and 0.92 for A_w. The second part of the calibration curve of slope 0.535 gave a correction of 1.03 A_n and 0.97 A_w.

TABLE IV

RESOLUTION FACTORS OF STANDARD POLYMERS FOUND IN THE FORWARD FLOW MODE

Samples (Å)	*h* (*from the chromatogram*)
4160	2.04
2360	2.41
1250	2.58
480	1.88
244	1.92
117	—
78	2.52
50.5	2.41
Average h =	2.25

However, if these values are used to obtain the true distribution, an overcorrection results giving distributions lower than unity. If the resolution constant is taken to be constant at about twice the value found in Table IV ($h = 4.5$), the results obtained for the distributions of the whole series would be very good as shown in Table II under $p(\infty)$.

Refractive index increment

The main conclusions that can be drawn from the results obtained with unknown polymers concern the constancy of dn/dc. For this, carboxyl-terminated and hydroxyl-terminated polybutadienes (OH polymer made from COOH polymer) were fractionated by preparative GPC in methylene chloride and their dn/dc measured at 25° with a differential refractometer (Model BP-2000 V, Phoenix Precision Instrument Company).

For the carboxyl-terminated polybutadiene, the results as shown in Table V

TABLE V

dn/dc OF FRACTIONATED CARBOXYL-TERMINATED POLYBUTADIENE

Fraction No.	dn/dc *THF*	$[\eta]$[a]	
		Benzene	*THF*
1	0.140	0.42	—
2	0.144		—
3	0.138	0.18	0.25
4	0.130	0.15	0.21
5	0.132	0.11	0.18
6	0.146	0.09	0.16

[a] $[\eta]$: as determined by the one-point method.

indicate a nearly constant value of dn/dc. The intrinsic viscosity, as determined by the one-point method, is also given in this table.

The results for the hydroxyl-terminated polymer are given in Table VI. These are discussed in more detail in the second section. The first conclusion was that while separation against molecular sizes was obtained, it did not produce a polymer of significantly narrower distribution than the starting product. Secondly, the dn/dc is nearly constant for the first ten fractions obtained at about the same value as for the carboxyl-terminated polymer, but the remaining fractions gave values which are lower and scattered. This was probably caused by the presence of products formed during secondary reactions.

TABLE VI

dn/dc OF FRACTIONATED HYDROXYLESTER–TERMINATED POLYBUTADIENE

Fraction No	$\overline{A_n}$ (Å)	$\overline{A_w}$ (Å)	dn/dc *THF*	$\overline{M}_n$ (*VPO*)
1	458	806	0.142	
2	387	588	0.147	
3	320	493	0.159	
4	284	477	0.140	
5	284	533	0.157	
6	308	560	0.104	
7	315	536	0.140	
8	314	539	0.137	4600
9	308	511	0.126	
10	288	470	0.133	
11	269	443	0.090	4200
12	240	397	0.097	4100
13	229	386	0.073	3700
14	204	347	0.095	3300
15	196	329	0.130	2900
16	181	307	0.100	2200
17	171	300	0.096	
18	157	268	0.142	

Finally, our study on the validity of the calibration curve has shown that a very small correction for skewing is needed. The resolution factor must be reevaluated but indications are that it is probably a constant. Quite good gaussian chromatograms were obtained with standard polymers in the 4160 Å to 50.5 Å range. The dn/dc ratio appeared to be constant in the molecular range of the polybutadienes examined.

APPLICATION OF GPC TO LOW-MOLECULAR-WEIGHT POLYBUTADIENE

Carboxyl-terminated polybutadiene

First the instrument was used to study lot-to-lot variation of carboxyl-terminated polybutadienes (HC-434) as received from the manufacturer (Thiokol Corporation). The results in Table VII show that lot 90M is quite different from the others because of a wider distribution. Lot 93M has average sizes slightly larger than the others in Table VII but has a narrow distribution. The six remaining lots show a slight

tendency towards narrower distributions especially in the last lots. These values are lower than those published[4] for lot 30M (1.81, 2.07 and 1.73). In the latter work, however, the authors experienced some difficulties with absorption of the carboxyl-end-groups on the polystyrene gel.

TABLE VII

LOT-TO-LOT VARIATIONS FOR HC-434[a]

Lot	$\overline{A_n}$ (Å)	$\overline{A_w}$ (Å)	P_A	M_n (*VPO*)
39M	234	376	1.61	3200
84M	247	423	1.71	3400
90M	253	491	1.94	3600
92M	235	402	1.71	
93M	259	412	1.59	
100M	249	410	1.66	
121M	238	374	1.57	
127M	233	354	1.52	

[a] Four columns of respective pore sizes, 10^3, 10^3, 10^4 and 10^5 Å.

Hydroxyl-terminated polybutadienes

Difficulties arose during the development phase of a study initiated in our laboratory on the hydroxylesterification (reaction 1) of a carboxyl-terminated polybutadiene (PB) (I), using alkene oxides.

$$\underset{\text{I}}{\text{HOOC–PB–COOH}} + \underset{\text{II}}{\text{RCH–CH}_2\text{O}} \rightarrow \text{RCHOHCH}_2\text{OOC–PB–COOCH}_2\text{–CHOHR} \qquad \text{(Reaction 1)}$$

This reaction was first followed by acid number titration and bulk viscosity measurements on a Rotovisco Haake rotating viscometer giving the pattern shown in Fig. 2. In the first part of the reaction, the viscosity of the isolated polymer decreases slowly from an initial value of 200 P to about 150 P as the acid number is lowered to 2% of its initial value. Upon further reaction, the viscosity increases abruptly to 1000 P or more.

Various hypotheses are possible to explain this viscosity increase. However, GPC appeared to be a good technique to investigate what was happening to the polymer molecules as the reaction was proceeding.

If polymer I is reacted with ethylene oxide (II, R=H) and the resulting isolated polymer is analyzed by GPC at different reaction times, the changes of $\overline{A_n}$ and $\overline{A_w}$ shown in Fig. 3 are found.

These curves can be separated into two portions similar to the viscosity curve (Fig. 2). In the first part, small increases in sizes are measured as the $\overline{A_n}$ is increased by 8 Å from the starting product to its extrapolated value at nil acidity number, and the $\overline{A_w}$ increased by 33 Å. The second part shows an abrupt increase to 380 Å for $\overline{A_n}$ and 845 Å for $\overline{A_w}$. An important aspect of the results, which is not possible to

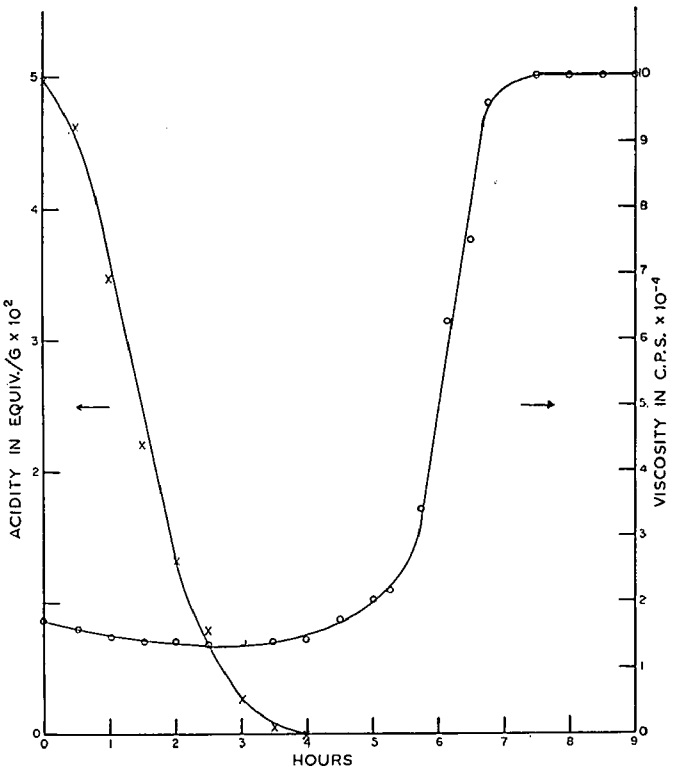

Fig. 2. Viscosity and acidity changes during hydroxylesterification reaction.

TABLE VIII

GPC OF THE PRODUCTS OF THE REACTION BETWEEN CARBOXYL-TERMINATED POLYBUTADIENE AND ETHYLENE OXIDE

Samples No.	*Reduced surface (ml/mg)*	σ	$\overline{A_n}$ (Å)	$\overline{A_w}$ (Å)	P_A
1	75.8	5.4	236	387	1.64
2	77.7	5.7	255	468	1.83
3	73.1	5.5	244	407	1.67
4	76.3	5.5	243	408	1.68
5	74.8	5.5	238	396	1.66
6	77.0	5.5	248	419	1.69
7	79.0	5.6	240	403	1.68
8	78.6	5.7	243	420	1.73
9	75.2	5.5	250	420	1.68
10	77.0	6.0	303	589	1.94
11	74.1	6.5	381	845	2.2

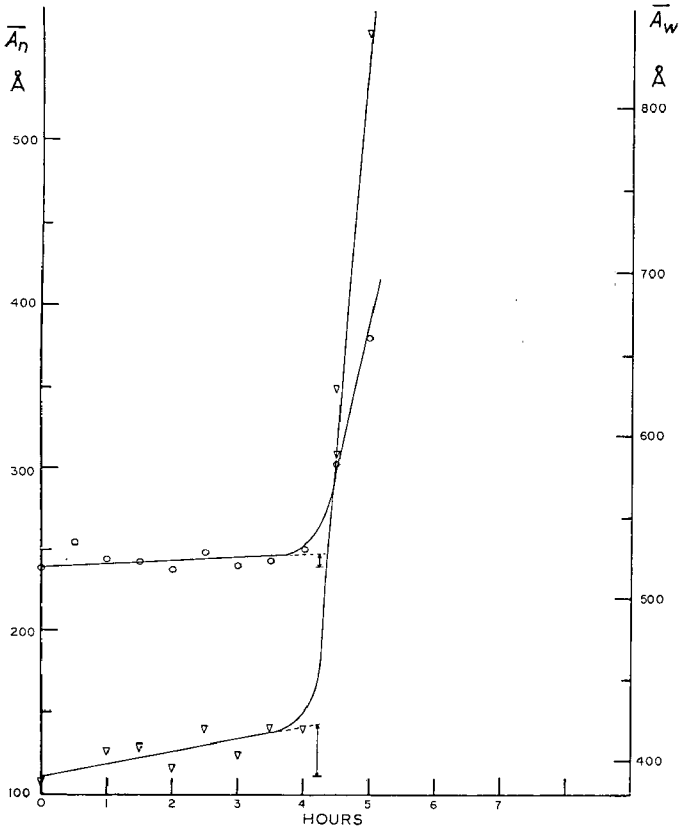

Fig. 3. Hydroxylesterification by ethylene oxide.

visualize from this figure but which is easily noted from Table VIII, is that the distribution values remain nearly constant, except for sample 2, from the first to the ninth sample, after which there was a sharp increase. This can also be observed with the variance of the chromatogram as the increase in size is accompanied by an increase of the width of the distribution curve.

Secondly the reaction with propylene oxide (II, R=CH_3) was examined. In this case, any possible effect of the solvent evaporation on reacted polymer was also investigated. The polymer fractions taken out of the reaction kettle at different reaction times were measured, both in the presence of solvent (unevaporated polymer) and after stripping out all volatile products (evaporated polymer). The results for the $\overline{A_n}$ and $\overline{A_w}$ are shown in Fig. 4.

It was found that the size values were always slightly higher for the evaporated polymers than for the unevaporated ones. However, this effect was so small and so regular that we were led to think that it could have been caused by a slight shifting in the calibration curve. In any case, these curves can also be divided into two portions. The first one shows an increase of 9 Å for the $\overline{A_n}$ and 39 Å for the $\overline{A_w}$ at zero acidity number. The second portion increases rapidly as was the case with the ethylene oxide adduct, but this time, as the reaction was investigated further, a leveling off appeared

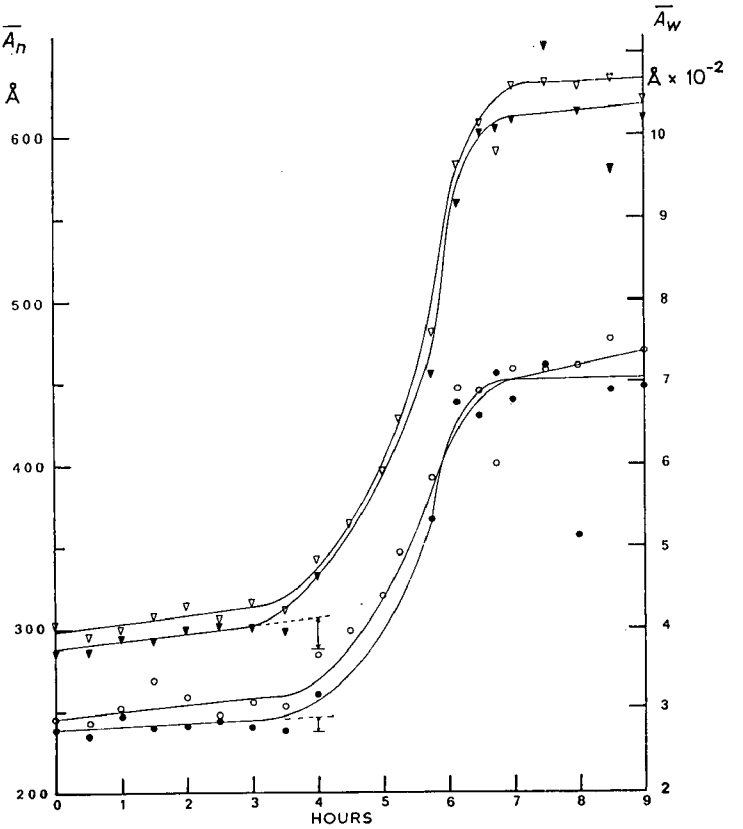

Fig. 4. Hydroxylesterification by propylene oxide. ○ = $\overline{A_n}$ not evaporated; ● = $\overline{A_n}$ evaporated; ▽ = $\overline{A_w}$ not evaporated; ▼ = $\overline{A_w}$ evaporated.

TABLE IX

GPC OF THE PRODUCTS OF THE REACTION BETWEEN CARBOXYL-TERMINATED POLYBUTADIENE AND PROPYLENE OXIDE

Samples No.	*Reduced surface (ml/mg)*	σ	$\overline{A_n}$ (Å)	$\overline{A_w}$ (Å)	P_A
1	73.7	5.1	239	371	1.55
2	76.3	5.2	248	396	1.60
3	74.1	5.5	241	403	1.67
4	77.1	5.5	241	406	1.68
5	77.0	5.8	260	468	1.80
6	73.5	5.9	367	712	1.94
7	74.8	6.6	430	1004	2.33
8	77.6	6.6	439	1021	2.33
9	82.1	7.6	357	1032	2.89
10	93.7	6.5	446	1022	2.29

for an $\overline{A_n}$ of about 460 Å, which is almost double the initial value, and for an $\overline{A_w}$ value of about 1050 Å. In Table IX, the distribution and variance values are seen to increase slowly from the first to the eighth sample before rising to a significantly higher value.

The same effect was noticed when the reaction with butylene oxide (II, R= C_2H_5) was considered. Fig. 5 summarizes these results. In this case, there was no evidence of an increase of molecular sizes caused by evaporation in the first portion of the curve, but large differences were noted in the leveling-off portion. The first part of the curve gives an increase in $\overline{A_n}$ values of 14 Å and for $\overline{A_w}$, of 40 Å. The second part shows increases of about the same extent as those found for the propylene oxide transformed polymer at least for the unevaporated samples. Values of Table X show very small effects on the distribution from the first to the ninth sample. For the other sample, the distribution increases to a value higher than 2.

A summary of the GPC results is given in Table XI. These results, as well as the

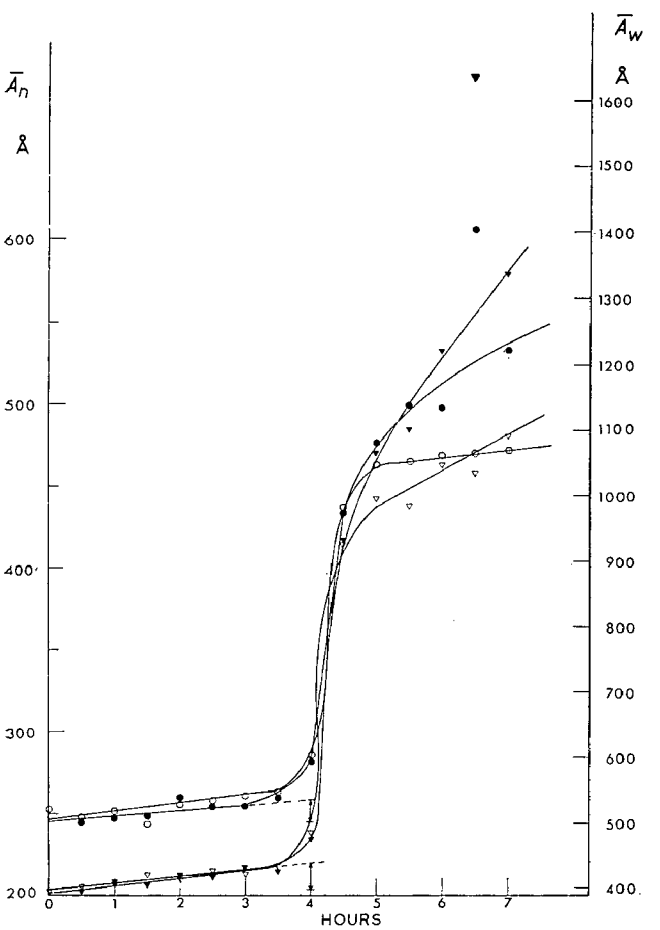

Fig. 5. Hydroxylesterification by butylene oxide. ○ = $\overline{A_n}$ not evaporated; ● = $\overline{A_n}$ evaporated; ▽ = $\overline{A_w}$ not evaporated; ▼ = $\overline{A_w}$ evaporated.

TABLE X

GPC OF THE PRODUCTS OF THE REACTION BETWEEN CARBOXYL-TERMINATED POLYBUTADIENE AND BUTYLENE OXIDE

Samples No.	*Reduced surface (ml/mg)*	σ	$\overline{A_n}$ (Å)	$\overline{A_w}$ (Å)	P_A
1	77.8	5.3	245	395	1.61
2	81.3	5.4	248	409	1.65
3	77.4	5.4	248	404	1.63
4	75.8	5.2	260	419	1.61
5	77.0	5.3	257	416	1.62
6	80.0	5.5	255	433	1.70
7	76.5	5.3	260	425	1.63
8	77.9	5.5	283	487	1.72
9	75.1	6.2	435	932	2.14
10	75.0	6.4	477	1063	2.23
11	70.7	6.3	500	1100	2.20
12	75.5	6.7	498	1221	2.45
13	78.1	7.0	606	1641	2.71
14	71.9	6.8	533	1346	2.52

TABLE XI

SUMMARY OF THE RESULTS OF HYDROXYL ESTER-TERMINATED POLYBUTADIENES

Reacting epoxides	*First part of the curves*			*Final equilibrium state*		
	$\Delta\overline{A_n}$ (Å)	$\Delta\overline{A_w}$ (Å)	P_A	$\overline{A_n}$ (Å)	$\overline{A_w}$ (Å)	P_A
Ethylene	8	33	1.7	—	—	—
Propylene	9	39	1.7	460	1050	2.3
Butylene	14	40	1.7	470	=1050	2.3

fact that almost identical infrared and NMR spectra are obtained for all these products, agree with the hypothesis that the first portion of the curves corresponds to the hydroxyl esterification reaction. As the acidity decreases close to zero, a secondary transesterification reaction (reaction 2) takes place rapidly doubling the molecular sizes and widening the distribution until an equilibrium state is reached.

$$2\text{PB}(\text{COOCH}_2\text{CHOHR})_2 \rightleftarrows$$
$$\text{RCHOH–CH}_2\text{OOC–PB–COOC(R)CHCH}_2\text{–OOC–PB–COOCH}_2\text{–CHOHR} + \text{RCHOHCH}_2\text{OH}$$

(Reaction 2)

The summary of Table XI does point out some additional problems. It must be emphasized at this point that the results are presented at their present stage of study, and not fully resolved.

The increases in size were calculated from the values of HENDRICKSON AND MOORE[1] and HENDRICKSON[3] with the hypothesis that the polymer is difunctional and that every functional group reacts ideally. The calculated increases in sizes were compared to measured values in Table XII. The comparison is very good considering the

TABLE XII

SIZES OF THE SUBSTITUENTS

Substituents	*Calculated* (Å)	*Measured* (Å)
$-CH_2CH_2O-$	11.6	8
$-CH_2CH(CH_3)O-$	14.2	9
$-CH_2CH(C_2H_5)O-$	16.6	14

possibility of changes in the association between solvent molecules and functional groups. However, if the reaction were to take place in the ideal manner as these first results indicate, it would lead to corresponding calculated increases of $\overline{A_w}$ situated between 4 to 8 Å. These values are lower than the ones obtained (33–40 Å).

The obvious answer to this lack of agreement is that near the end of the hydroxyl esterification a transesterification reaction begins to take place and by doubling molecular sizes, it produces a more noticeable effect on the $\overline{A_w}$ than on the $\overline{A_n}$, as the $\overline{A_w}$ is more sensitive to high-molecular-weight polymers. More information on the initial stage of the transesterification reaction is needed to resolve the statistical calculations.

It was thought that more information could be obtained by not only looking

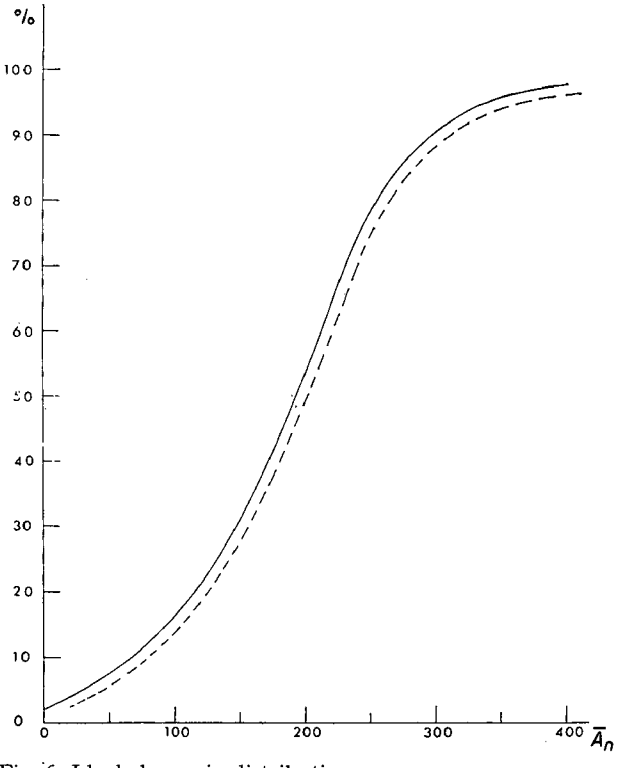

Fig. 6. Ideal change in distribution curve.

at the added results of the average sizes but by looking at the changes in sizes all along the distribution curves. Ideally (Fig. 6) two parallel distribution curves should be obtained, or at least the differences between the distribution of the starting product and that of a polymer obtained at a given stage of the reaction should vary regularly. However, the results of Fig. 7 were obtained showing important irregularities in the curves.

Evidently, it is important to determine if these irregularities are technical artifacts or if they are significant. To get a clearer picture of the reaction mechanism a model reaction was needed, and an esterification of carboxyl groups by an excess of alcohol was chosen.

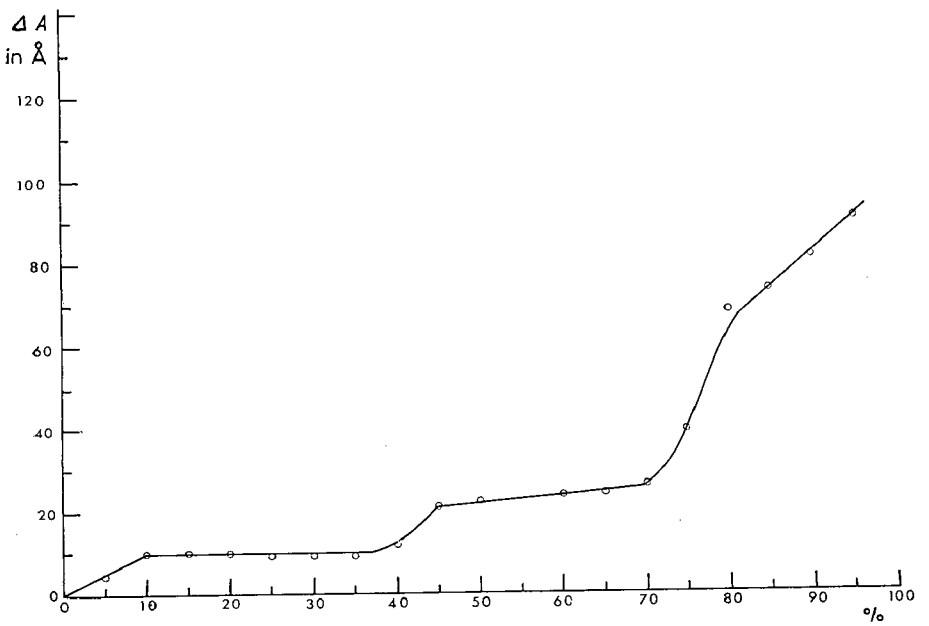

Fig. 7. Distribution difference between initial and isolated polymer.

Ester-terminated polybutadiene

GPC studies on the methyl esters of various carboxyl-terminated polybutadienes have been published[2]. They give increased or decreased sizes after esterification depending on the polymer used, but good reproducibility of distribution values are obtained.

Two different carboxyl-terminated polybutadienes (HC-434, Thiokol Corporation and Telagen CT 2000, General Tire) were esterified with various alcohols. The GPC results on the esterified HC-434 are given in Table XIII. With the exception of the ethyl ester product, it is seen that the sizes increase slowly with the length of the ester chain. However, the size decreases with the more compact end-groups such as alcohol containing side substituents. The results of the esterified Telagen are in Table XIV. Again mean sizes increased with the length of the ester chain but this time more slowly than was the case with HC-434. The butanol adduct does not reflect the general

TABLE XIII

GPC OF ESTERIFIED CARBOXYL-TERMINATED POLYBUTADIENES (HC-434)

Types of ester end-group	*Reduced surface (ml/mg)*	σ	$\overline{A_n}$ (Å)	$\overline{A_w}$ (Å)	P_A
—	75.18	5.4	237	399	1.68
Methyl	75.69	5.25	242	403	1.67
Ethyl	78.31	5.3	224	378	1.69
Propyl	71.62	5.2	251	423	1.69
Butyl	74.10	5.1	257	429	1.67
Isopropyl	78.00	5.2	229	379	1.65
sec.-Butyl	77.37	5.3	233	399	1.71
tert.-Butyl	71.56	5.3	235	395	1.68

TABLE XIV

GPC OF ESTERIFIED CARBOXYL-TERMINATED POLYBUTADIENE (TELAGEN)

Types of ester end-group	*Reduced surface (ml/mg)*	σ	$\overline{A_n}$ (Å)	$\overline{A_w}$ (Å)	P_A
—	72.20	5.0	142	218	1.53
Methyl	72.35	4.6	143	206	1.44
Ethyl	74.05	4.8	144	216	1.50
Propyl	71.32	4.4	146	207	1.42
Butyl	72.20	5.0	142	218	1.53
Isopropyl	73.11	5.0	148	234	1.58
sec.-Butyl	71.12	4.5	149	212	1.42
tert.-Butyl	71.86	4.9	146	221	1.52

trend. Surprisingly, compact end-groups (isopropanol, etc.) gave a greater increase of the total polymer size than other products.

Differences all along the distribution curves are now under consideration and will be decreased in later papers.

REFERENCES

1 J. G. HENDRICKSON AND J. C. MOORE, *J. Polym. Sci. A-1*, 4 (1966) 167.
2 D. C. VAN LANDUYT AND C. W. HUSKINS, *J. Polym. Sci. B-6*, (1968) 643.
3 J. G. HENDRICKSON, *Anal. Chem.*, 40 (1968) 49.
4 R. M. SCREATON AND R. W. SEEMANN, *J. Polym. Sci. C*, 21 (1968) 297.
5 R. D. LAW, *J. Polym. Sci. A-1*, 7 (1969) 2097.
6 F. N. JARSEN, *J. Polym. Sci.*, 18 (1969) 111.
7 Waters Associates, Technical Information Bulletin.
8 K. A. BONI, F. A. SLIEMERS AND P. B. STICKNEY, *J. Polym. Sci., A-2* (1967) 221.
9 Z. GRUBISIC, P. REMPP AND H. BENOIT, *J. Polym. Sci. B-5*, (1967) 753.
10 J. CAZES, *J. Chem. Educ.*, 43 (1966) A567.
11 Three-Channel Digital Curve Translator. Instruction Manual, Waters Associates Inc.
12 A. E. HAMIELEC, *Amer. Chem. Soc. Educ. Course on Gel Permeation Chromatography, St.-Louis, Mo., April 25, 26, 1969.*

CHROM. 5129

GEL PERMEATION CHROMATOGRAPHY DATA ACQUISITION WITH THE PDP-8/I AND AXO8 LABORATORY PERIPHERAL

L. D. MOORE, JR. AND J. R. OVERTON
Research Laboratories, Tennessee Eastman Company, Division of Eastman Kodak Company, Kingsport, Tenn. 37662 (U.S.A.)

SUMMARY

A PDP-8/I with an AXO8 laboratory peripheral (Digital Equipment Corp.) has been programmed and interfaced for simultaneous direct data acquisition from two Waters gel permeation chromatographs. Analog-to-digital conversions are made at a variable but set rate from both instruments. A cathode ray tube is used to display sample identification, the contents of any location within the computer core, a graph of the contents of the data buffer, and a plot of the data storage table (*i.e.*, the gel permeation chromatographic curve). A permanent record of the data is obtained on punched paper tape. Two or more gel permeation chromatographic curves (from tapes obtained earlier) can be displayed on the cathode ray tube for direct comparison. Also, the data can be corrected for base line drift by "drawing" in a base line on the cathode ray tube display. The base line is then subtracted, and a corrected paper tape is obtained for further processing. Final data reduction is carried out on an IBM 1130 equipped with paper tape reader and CalComp plotter. A number of convenience options are included in the data reduction program, such as corrections for axial dispersion and various ways of plotting the data. This approach to data handling has reduced operator time for data treatment about 80% and improved the quality of the results.

INTRODUCTION

In laboratory analysis, it is becoming increasingly fashionable to automate collection and manipulation of raw data by means of computers. In this paper we describe an effort to apply these techniques to gel permeation chromatography (GPC). It is particularly worthwhile to develop automatic data acquisition for GPC. Once one is exposed to the tedium of reading a hundred data points from a GPC trace and becomes aware of the probability of human error under such circumstances, the need is obvious, and justification need not be in terms of fashion.

In our approach, a small dedicated computer, the PDP-8/I from Digital Equipment Corp. was used in conjunction with Digital's AXO8 Laboratory Peripheral unit for this purpose. The AXO8 has a 9-bit analog-to-digital (A/D) converter (precision is 1 part in 512), a multiplexer for 4 input channels, two clocks, and three event

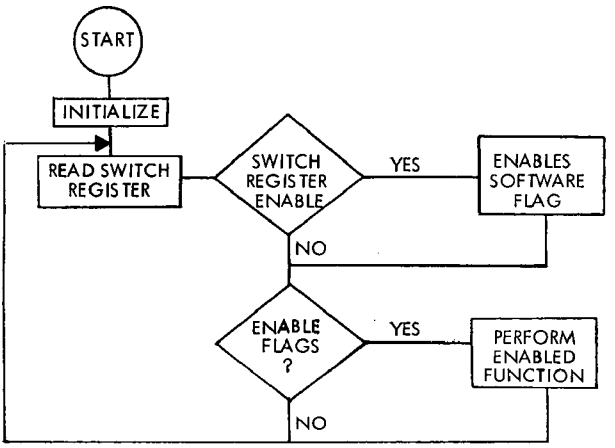

Fig. 1. Schematic of program.

markers known as Schmitt triggers. A programmable 'enable' register and the computer's 'interrupt' capability allow one to interrupt the program at appropriate times to handle the collection and averaging of raw data.

SOFTWARE

Programming was done in assembler language (PAL III) by using DEC's symbolic editor and the PAL III symbolic assembler. A general schematic of the program is shown in Fig. 1. When the program is started, an initialization routine is

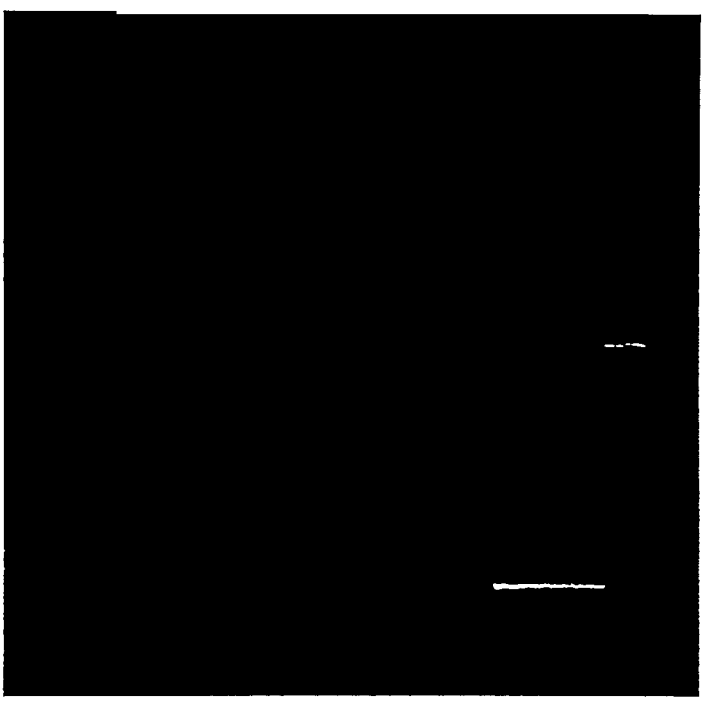

Fig. 2. CRT display of data buffer.

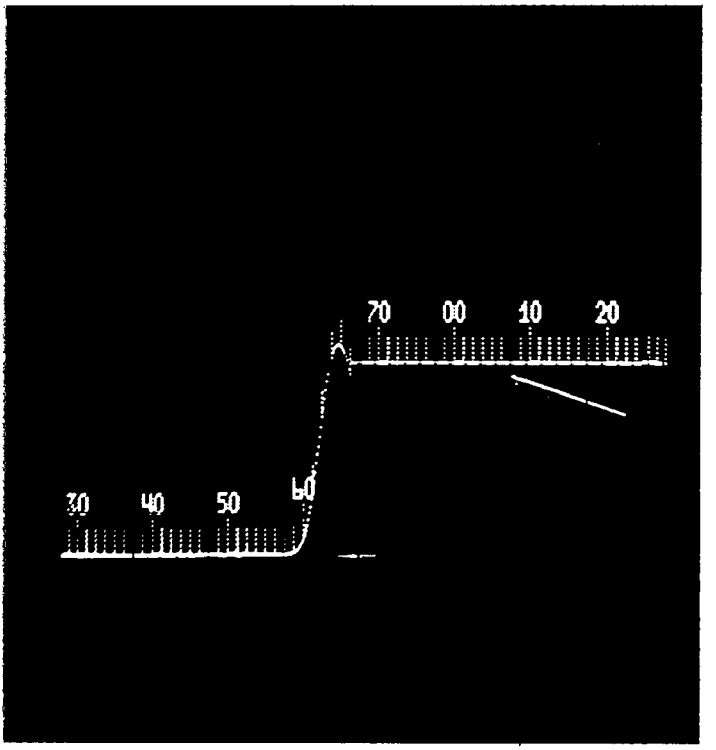

Fig. 3. CRT display of typical GPC run in progress.

performed. This routine includes setting the AXO8 enable register and establishing the use of the computer interrupt capability. The AXO8 register is put in the following configuration: The clock flag is set after each 32 oscillator pulses, the frequency of which can be varied; setting this flag initiates an A/D conversion, *i.e.*, a data point is taken. The program is interrupted when the ADC done flag is set (*i.e.*, when the A/D conversion is complete) and when the signal from the GPC siphon dump activates a Schmitt trigger.

The program is controlled by manipulating the switch register (SR) at the computer console. The settings on the SR allow the following functions to be performed: (1) typing in input data (sample identification and conditions of data collection) and initiating the run, (2) displaying the input data on the cathode ray tube (CRT), (3) displaying data buffer on CRT, (4) displaying data table (GPC curve) on CRT, (5) punching paper tape, (6) drawing baseline for the GPC curve, (7) displaying baseline on CRT, (8) correcting GPC data for baseline and displaying corrected curve, (9) reading in paper tape of some previous run, (10) integrating between two specified siphon dumps and typing out area, (11) displaying (CRT) the contents of any location in computer, and (12) clearing all software flags.

FEATURES AND CAPABILITIES OF COMPUTER PROGRAM

By adjusting the oscillator frequency of the clock, data may be collected over a wide range of rates. A typical example would be A/D conversions at the rate of

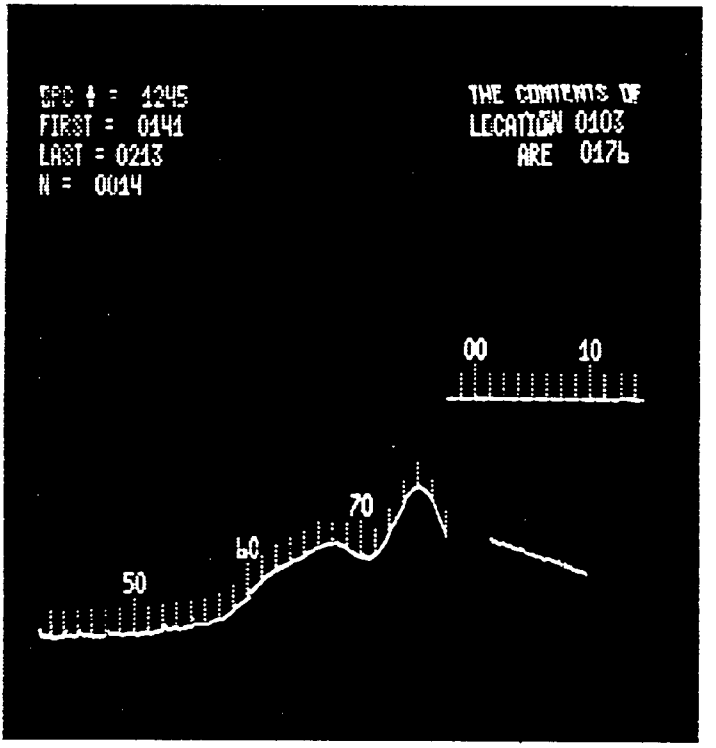

Fig. 4. CRT display of run in progress.

100 sec^{-1}. A total of 64 conversions are averaged to produce a single data point, which in turn is stored in the data buffer. This buffer may be displayed on the CRT as shown in Fig. 2. The bias control of the signal amplifier can then be adjusted to put the signal in an appropriate position on the scope. The data buffer will hold up to 128 points, and when full, it simply ignores additional data. In general, the clock is adjusted so that approximately 100 points are collected between each 1-ml dump.

When the siphon dumps, a Schmitt trigger is activated. A program interrupt results, and the computer treats the data in the buffer to produce the appropriate

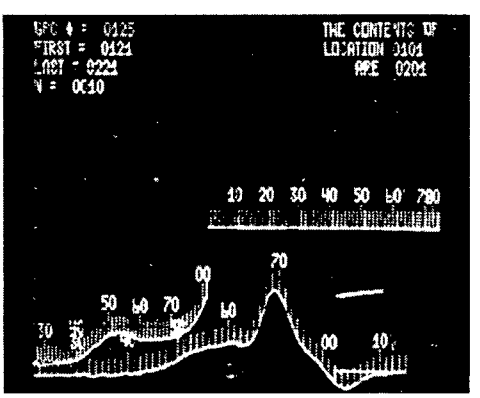

Fig. 5. CRT display during data acquisition from two instruments.

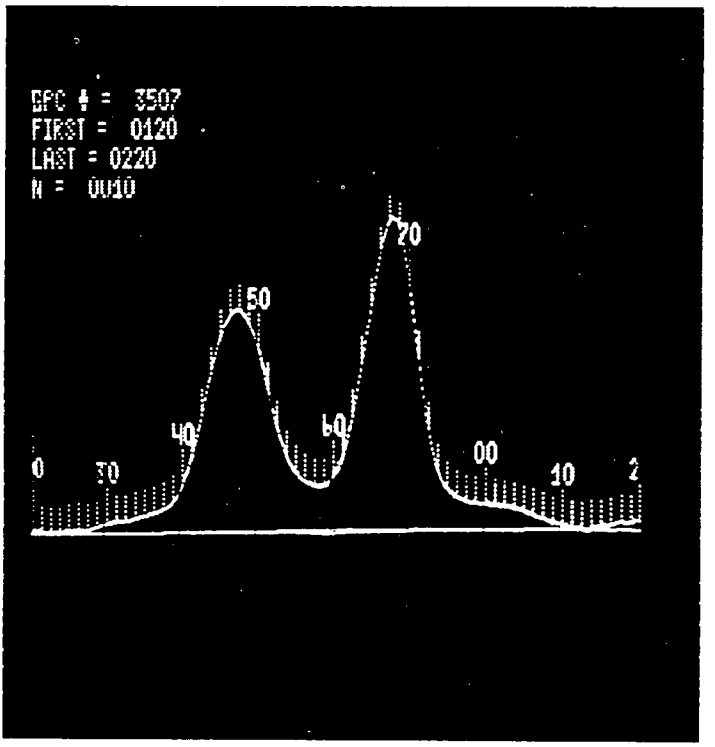

Fig. 6. Incorrect baseline.

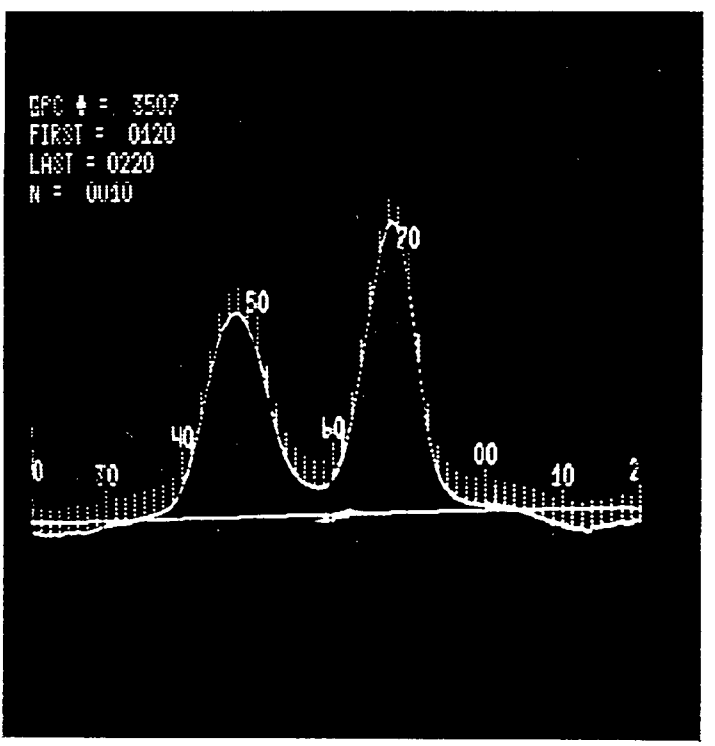

Fig. 7. Correct baseline.

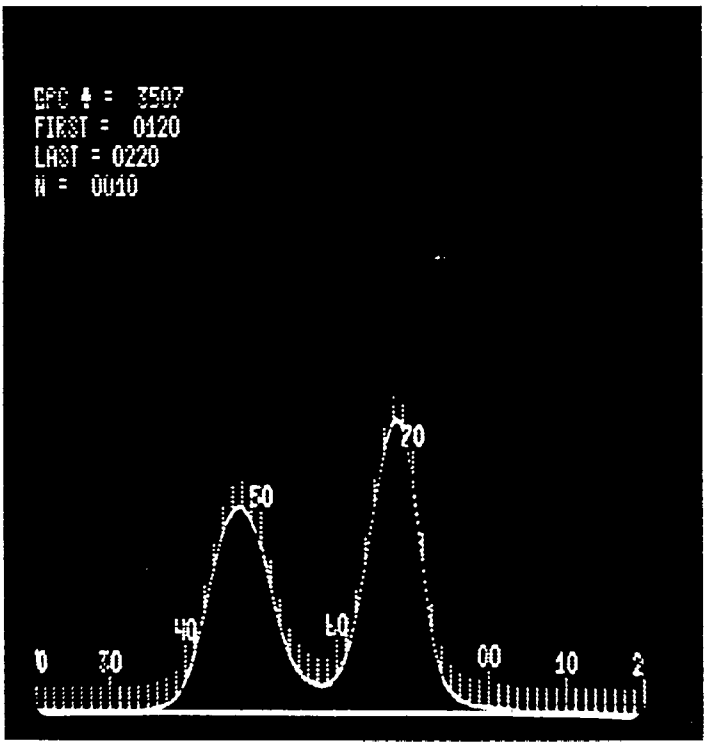

Fig. 8. GPC curve corrected for baseline.

number of points defining the GPC trace between the last two dumps. The number of points defining the curve between dumps can be adjusted over a wide range. These points are stored in a data table which will hold up to 512 points. A typical GPC curve might be defined by 64 dumps with 8 points per dump, as shown in Fig. 3.

To initiate a run, appropriate switches are set on the console and the teletype responds by requesting input data. Input data consist of (1) the GPC number for sample identification, (2) the first and last dumps between which data are collected, and (3) the number of points to be collected per dump. The input data are in octal format. When the sample is injected, striking a certain teletype key initiates the run. The computer keeps a record of the number of dumps but discards the GPC data until the point where data are to be collected is reached. Fig. 4 illustrates a display of input data for a run in progress. Also shown in the upper right are the contents of the location of a counter keeping track of the number of dumps since the run was initiated. This feature allows one to inspect almost any location in core while the run is in progress. This capability is quite useful in keeping track of a run, and it was particularly useful in debugging the original program.

```
THE AREA BETWEEN 0133 & 0157 FR 1 IS PROP.TO 00025406
THE AREA BETWEEN 0157 & 0203 FR 1 IS PROP.TO 00030621
THE AREA BETWEEN 0133 & 0203 FR 1 IS PROP.TO 00056227
```

Fig. 9. Teletype output displaying integration.

```
GPC INSTRUMENT =,   C.

GPC CURVE NUM.=  676.

FIRST DATA POINT TAKEN AT  58.ML

LAST DATA POINT TAKEN    AT 122.ML

   8.DATA POINTS TAKEN PER ML.

THE POLYSTYRENE CALIBRATION CURVE FOR THIS SYSTEM
EXTENDS FROM   7CML TO  105ML
PDP DATA FOR THIS SYSTEM    COVERS THE RANGE 58.0TO122.0ML

          ONLY THAT PORTION FALLING WITHIN THE CALIBRATION
          CURVE IS USED FOR COMPUTATION

THE TOTAL AREA IS PROPORTIONAL TO    2251.9
HE POLYSTYRENE EQUIVALENT NUMBER AVERAGE IS    25675.

THE POLYSTYRENE EQUIVALENT WEIGHT AVERAGE IS    28914.

THE RATIO OF WEIGHT TO NUMBER AVERAGE IS      1.12
```

Fig. 10. IBM 1130 output.

As in normal GPC operation, a second run can be started while the current run is in progress. The computer monitors both runs simultaneously. It is only necessary that the first run be complete prior to storing data from the second run. This requirement is tantamount to not having the elution volumes of the two samples overlap — a routine restriction. After the last dump which completes the first run, a paper tape is automatically punched. This tape contains the input information and data table, *i.e.*, the 512 points defining the GPC curve. Subsequently, the input data and dump count for the second run are transferred to the locations previously used. A third run can then be initiated. With the present 4K of core, this machine can monitor two GPC instruments simultaneously with two runs in progress on each. Additional core and/or a disk will allow expansion of this capability.

Fig. 5 shows a run in progress (upper curve) with trichlorobenzene at 130°; a Waters Associates Model 100 gel permeation chromatograph is being used. Data are being stored at the rate of five points per dump. Location 101 shows that a total of 201 (octal) dumps have occurred since injection of the sample. Note the display

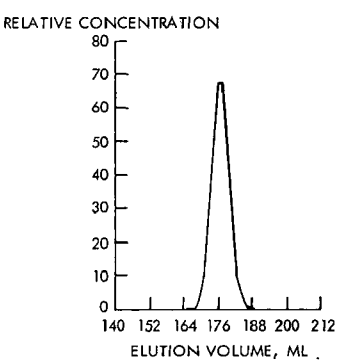

Fig. 11. Calcomp plot of data from paper tape.

of the data buffer (A) at the right. The information at the upper left refers to the lower curve, which is being collected from the analytical side of an Ana-Prep located in another laboratory some 200 ft. from the computer. The data buffer (B) for this curve is also shown. This sample is being run in tetrahydrofuran at room temperature. Data are being stored at the rate of 10 (octal) points per dump. At the time this picture was taken, additional samples had been injected into both instruments, so that four runs were being monitored.

After the paper tape has been generated, it may be read back into the computer and displayed on the CRT if a run is not in progress on both instruments. In this way, two curves may be directly compared. Also the program allows the curve to be corrected for the baseline position. This operation is illustrated in Figs. 6–8. The baseline is drawn by drawing a straight line between any two points at the extreme left and extreme right of the scope. The vertical position of the points is manually controlled at the console. Visual selection of a baseline is preferable to dependence on some mathematical algorithm. For example, the curve shown in Fig. 6 was obtained when the baseline was known to be unstable. The baseline shown could easily have been determined by an appropriate extrapolation algorithm, but it is incorrect. In reality, because of temperature drift, the correct baseline is curved and that shown in Fig. 7 is a better approximation in the area of interest than the baseline shown in Fig. 6. When the baseline has been selected, it is subtracted from the curve via a subroutine activated at the console. Fig. 8 shows the corrected curve. A corrected paper tape is then punched for data processing on a larger computer.

An additional capability built into the program allows integration between any two dump marks on the curve. Fig. 9 shows the teletype output comparing the areas under the two peaks of Fig. 8.

The paper tape from the baseline corrected curve is used as input data for conventional GPC computational schemes which we carried out with an IBM 1130 equipped with a CalComp plotter and tape reader. One has the usual flexibility at this point to treat the data as befits the situation. The program which we use routinely does not include corrections for so-called 'axial dispersion'.

The primary options incorporated into our standard data processing program, through the use of data switches on the 1130 console, are related to ways of plotting the data. Calibration data are included on punched cards and run with the object deck. The GPC curve is integrated via trapezoidal integration, and the weight average and number average molecular weights are calculated. Representative 1130 output and a plot from the CalComp plotter are shown in Figs. 10 and 11.

CONCLUSION

In conclusion, we find that automatic data acquisition by means of a small computer can be made quite flexible through proper programming. Such systems minimize error and eliminate much of the tedium associated with gel permeation chromatography.

CHROM. 5061

GEL PERMEATION CHROMATOGRAPHY

DIFFUSIONAL PHENOMENA IN DILUTE POLYMER SOLUTIONS FLOWING IN CAPILLARIES*

AUGUSTUS C. OUANO AND JOSEPH A. BIESENBERGER**
IBM Research Laboratory, San Jose, Calif. 95114 (U.S.A.)

SUMMARY

This work is concerned with the dispersion of high-molecular-weight solutes in dilute solutions flowing through empty capillary tubing, such as that which is found between chromatographic columns and detectors, etc., in gel permeation or liquid chromatographs.

Residence time distributions of solvent as well as solutes were measured simultaneously. This was done for both pulse and step solution inputs using a two-cell detection system. The solutes, *o*-nitrotoluene and narrow-distribution polystyrene (gel permeation chromatographic standards), were monitored with an ultraviolet detector while hexane (hexane–chloroform (20:80) was used to dissolve the polymer solutes) was monitored with a refractometer in a chloroform mobile phase. Polystyrene concentrations were 0.20 percent and 0.15 percent. Three tubing lengths and two flow rates were studied.

The results indicate that polymer molecules have residence time distributions which are different from those of small molecules. This lends support to our belief that molecular entanglements occur among the polymer molecules which causes radial concentration non-uniformities and virtual two-phase flow.

INTRODUCTION

All fluid solutions which are transported through capillaries by bulk flow have a radial velocity distribution which, in the total absence of molecular diffusion, gives rise to dispersion which is rather broad and extremely unsymmetrical. We have named this extreme case the segregated flow regime[1].

Only when radial molecular diffusion is permitted to occur to a sufficient degree does this dispersion become symmetrical or Gaussian. This phenomenon has been studied by TAYLOR and is called TAYLOR diffusion. We have named the symmetrical case the TAYLOR regime[2].

The region between these extremes is of special importance in all types of chro-

* For a preliminary report, see *J. Polym. Sci., A2*, in press.
** Stevens Institute of Technology, Hoboken, N.J., U.S.A.

matography employing liquid solutions, and in particular gel permeation chromatography (GPC) because the latter involves polymeric solutes which have very low molecular diffusion coefficients.

In our previous studies[1,3] we have shown that, while maintaining capillary tubing as short as possible causes dispersion to remain narrow in width, the capillary tubing also gives rise to severe skewing, even with small solute molecules and certainly with polymeric solutes. On the other hand, long tubing tends to reduce skewing while increasing the width of dispersion. It is clear that skewed chromatograms are not desirable, since they do not conform to most theories in chromatography which assume Gaussian behavior.

We have also shown that not only can skewing perhaps never be totally eliminated in polymer solutes flowing in capillaries, but that polymer dispersion does not exhibit the behavior expected of small molecules. Rather, polymer solutes exhibit anomalous dispersion and give rise to bimodal chromatograms. Moreover, some recent preliminary studies with recycle GPC have shown that skewness, rather than disappearing with increasing number of recycles, is severely compounded with polymer solutions in the recycle mode.

As a possible explanation of the anomalous dispersion behavior of polymer solutes in capillaries, we have proposed that molecular entanglements occur among the polymer molecules. These entanglements cause them to aggregate near the tube center and to have residence time distributions which are different from those of the solvent, as well as any other small molecule solutes which might be present in solution.

We are in essence proposing that something similar to two-phase flow exists in which polymer clusters behave virtually like a separate phase, independent of the remaining solution consisting of small-molecule solutes and solvent.

If this picture is accurate, then the solvent residence time distribution, which is equivalent to a newtonian, parabolic velocity profile in the segregated flow regime, should be different from that of the polymer solute. Similarly, TAYLOR diffusion among the small-molecules in the TAYLOR regime should proceed more or less independently of the polymer solute.

Thus, we believe that the results of the present study, which consist of simultaneous measurement of polymer solute and solvent residence time distributions, contribute new experimental evidence in support of our interpretation of the anomalous flow phenomenon.

EXPERIMENTAL PROCEDURE

The independent measurement of the elution time (or elution volume) of a polymer solute and solvent through a small diameter tubing with no packing, was done using a standard DuPont Model 820LC liquid chromatograph which was equipped with an ultraviolet (UV) photometer (254 nm) connected in series to a Fresnel Type refractometer (RI) detector (UV ahead of RI). Polystyrene dissolved in a mixture of hexane–chloroform (20:80) is a good choice of solvent, since both hexane and chloroform have very low UV extinction coefficients (at 254 nm) relative to polystyrene. The RI detector, on the other hand, can be made insensitive to polystyrene by using a much higher concentration of hexane (relative to polystyrene) in the polystyrene–hexane–chloroform solution. Consequently, when the polystyrene solution containing hexane is injected into a chloroform mobil phase, the UV and the

RI detectors become specific for monitoring the elution of polystyrene and hexane, respectively.

The chromatographic column of the DuPont 820LC was replaced with stainless steel tubing by modifying the septum injection port. The modification consisted of replacing the chromatographic column with a 2 in. × 1/4 in. O.D. brass tubing with an I.D. of 0.047 in. To the brass tubing, 4 in. × 1/16 in. O.D. tubing with an I.D. of 0.047 in. was silver-soldered to act as the connector for the 0.047 in.-I.D. tubing being tested.

Polystyrene (Pressure Chemical Co., $\bar{M}_w/\bar{M}_n$ of 1.02–1.10 with molecular weights of 600, 10,000, 20,400, and 97,200) and *o*-nitrotoluene were each dissolved in a 20–80 (5:95 for step input) by volume hexane–chloroform solvent mixture to 0.2 % (0.15 % for step input) solutions. Lower concentrations of hexane and polystyrene were necessary for the step input to prevent the recorder from going off scale at the highest detector attenuation.

For the pulse input mode, two tubing lengths (39 in. and 146 in.) and flow rates (1.9 ml/min and 1.0 ml/min, respectively) were used. The test conditions covered both segregated flow and TAYLOR diffusion dispersion ranges. Sample volume injected was between 4 to 6 μl. For the step input mode, only the segregated flow dispersion region was studied. This corresponds to 17 in. of tubing at 1.0 ml/min flow rate.

In order to accommodate a large amount of solution in the injection port which is required for the step injection mode, the septum type sample injection port was replaced by the Waters Associates' six-port sample injection valve. The regular 2 ml sample loop which comes as standard equipment with the Waters' sample injection valve was replaced by a 7 ml sample loop.

DISCUSSION OF RESULTS

Fig. 1 shows the elution curves of 20,400 and 97,200 molecular-weight polystyrene (PS) solutions along with the corresponding elution curve of hexane, which was

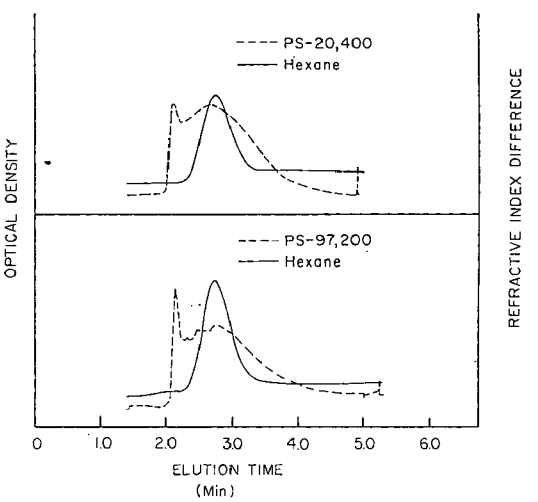

Fig. 1. Pulse input elution curve of PS-97,200 and 20,400 through a 146 in. long by 0.047 in. I.D. stainless steel tubing at 1 ml/min flow rate. – – – –, UV optical density; ———, refractive index difference.

injected with the polymer into the chloroform solvent stream through 146 in. of 0.047 in. I.D. stainless steel tubing. It is evident that the bimodal anomaly occurs in the polystyrene elution, but not in hexane. Furthermore, the hexane elution curve approaches the Gaussian shape which agrees with the theoretical curve based on TAYLOR diffusion[2] in tubing.

The possibility of a malfunctioning UV photometer cell, which can cause anomalies in the elution curve of polystyrene, was checked by substituting PS-600 and *o*-nitrotoluene for high-molecular-weight polystyrene. Fig. 2 shows the elution curve of *o*-nitrotoluene and PS-600 (detected by the UV photometer) to be free of the bimodal anomaly. The elution curve of PS-10,000, however, is beginning to show the anomaly. This indicates that the bimodal elution curve of high-molecular-weight polystyrene is not an artifact but is highly dependent on the molecular weight of the solute.

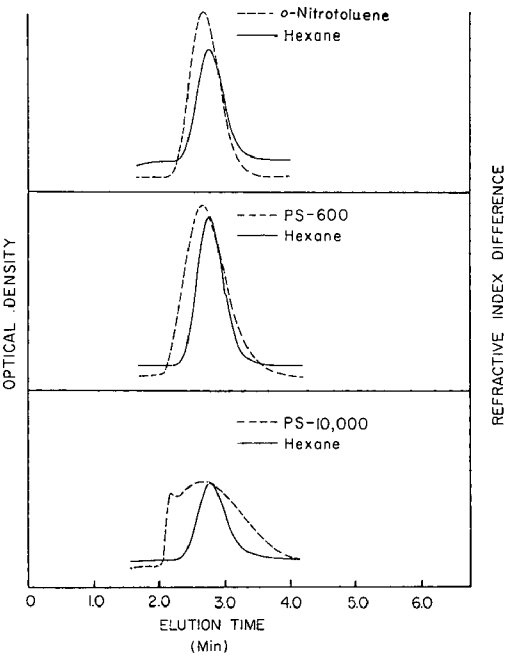

Fig. 2. Pulse input elution curve of PS-10,000, PS-600 and *o*-nitrotoluene through a 146 in. long by 0.047 in. I.D. stainless steel tubing at 1 ml/min flow rate. – – – –, UV optical density; ———, refractive index difference.

For a better comparison of the elution curves of hexane, *o*-nitrotoluene, and the various molecular weight polystyrenes, a normalized curve is presented in Fig. 3. It shows that elution curves of *o*-nitrotoluene and hexane fall within the shaded area, which is Gaussian as predicted by a model based on TAYLOR diffusion[3]. Since the elution curves of high-molecular-weight polystyrene and hexane were measured independently in the solution, the difference in their elution curves indicates that a two-phase flow in dilute polystyrene solution may actually be taking place. This flow condition may be similar to that of a dilute pulp slurry (0.1 %) flowing in pipes[4]. In the pulp suspension experiment, it was observed that the pulp fibers tend to flow

as an entangled mass with a velocity profile considerably flatter than the water suspending medium. The pulp fibers were also observed to concentrate at the axis of the pipe. This phenomenon can perhaps be more directly shown if shorter tubing length and higher flow rates are used such that the segregated flow condition is met.

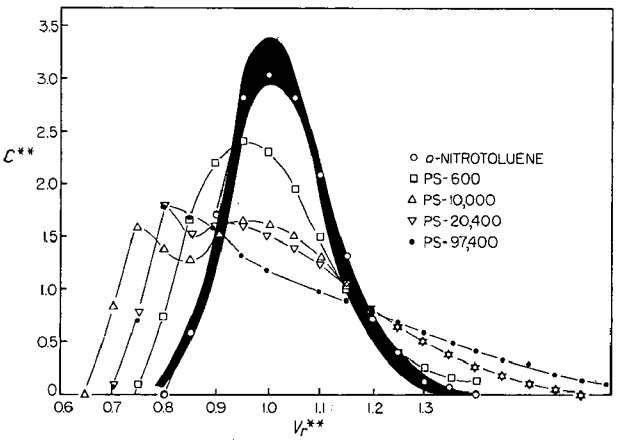

Fig. 3. Normalized pulse input elution curve of high- and low-molecular-weight polystyrenes and *o*-nitrotoluene through a 146 in. long by 0.047 in. I.D. stainless steel tubing at 1 ml/min flow rate.

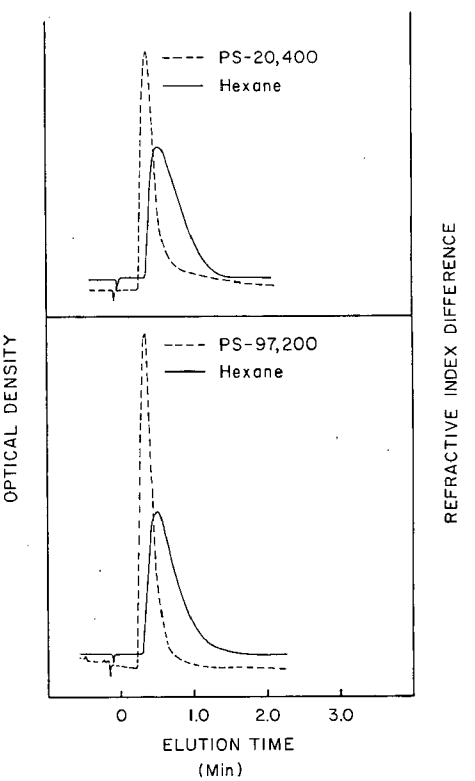

Fig. 4. Pulse input elution curve of PS-97,200 and PS-20,400 through a 39 in. long × 0.047 in. I.D. stainless steel tubing at 1.9 ml/cm flow rate. – – – –, UV optical density; ———, refractive index difference.

Figs. 4 and 5 show the elution curves of PS-97,200, PS-20,400, PS-10,000, PS-600 and *o*-nitrotoluene through a 39 in. stainless steel tubing. The dependence of the elution curve on molecular weight is again apparent. The higher molecular weight polystyrenes show a sharper elution curve than that of hexane and *o*-nitrotoluene. The shape of the elution curves of high-molecular weight polystyrenes seems to approach a sharp spike (pulse response to pulse input), which is associated with a "plug-like" velocity profile. The contrast in the shape of polystyrene and hexane elution curves is more readily seen in Fig. 6, which is a normalized elution curve of PS-97,200, PS-600 and *o*-nitrotoluene and hexane. The shaded area in Fig. 6 includes the data points for hexane and *o*-nitrotoluene.

The elution curves (for a step input of solutions) of PS-97,200, PS-20,400,

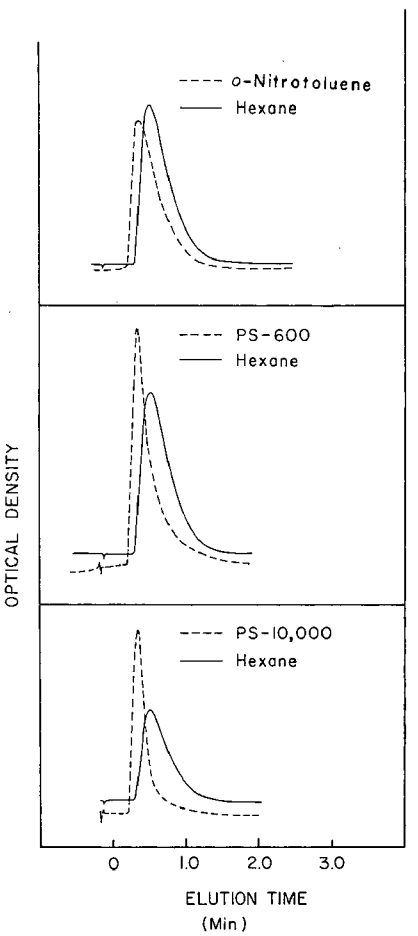

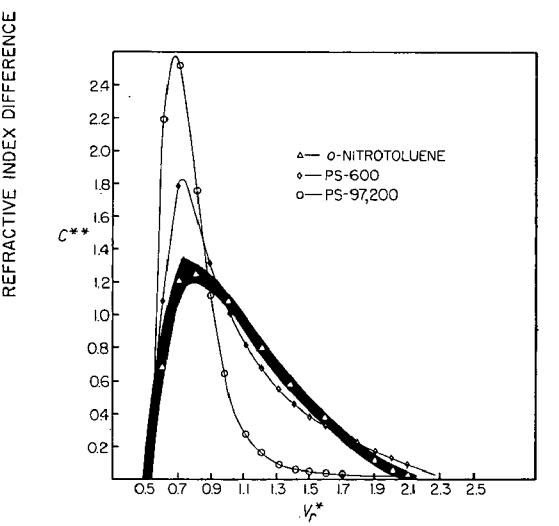

Fig. 5. Pulse input elution curve of PS-10,000, PS-600 and *o*-nitrotoluene through a 39 in. long by 0.047 in. I.D. stainless steel tubing at 1.9 ml/min flow rate. – – – –, UV optical density; ———, refractive index difference.

Fig. 6. Normalized pulse input elution curve of high- and low-molecular-weight polystyrene and *o*-nitrotoluene through a 39 in. by 0.047 in. I.D. stainless steel tubing at 1.9 ml/min flow rate.

PS-600 and *o*-nitrotoluene through stainless steel tubing (17 in.) are shown in Figs. 7 and 8. The plug-like flow of the high-molecular-weight polystyrene is again evident. The "step-like" elution curve of high-molecular-weight polystyrene reveals its "plug-like" velocity profile. An elution curve of a model based on parabolic velocity profile (segregated flow condition) along with normalized experimental curves for PS-97,200, PS-600 and *o*-nitrotoluene are shown in Fig. 9. It is clear in this plot that the elution curve of high-molecular-weight polystyrene does not reflect a parabolic velocity profile, since it is much steeper than the model curve. The deviation of the *o*-nitrotoluene elution curve from the model curve can perhaps be explained by molecular diffusion of *o*-nitrotoluene (small, but nevertheless finite), for which the segregated flow model does not account (assumes molecular diffusivity to be zero).

If one assumes plug flow for the high-molecular-weight solute and parabolic

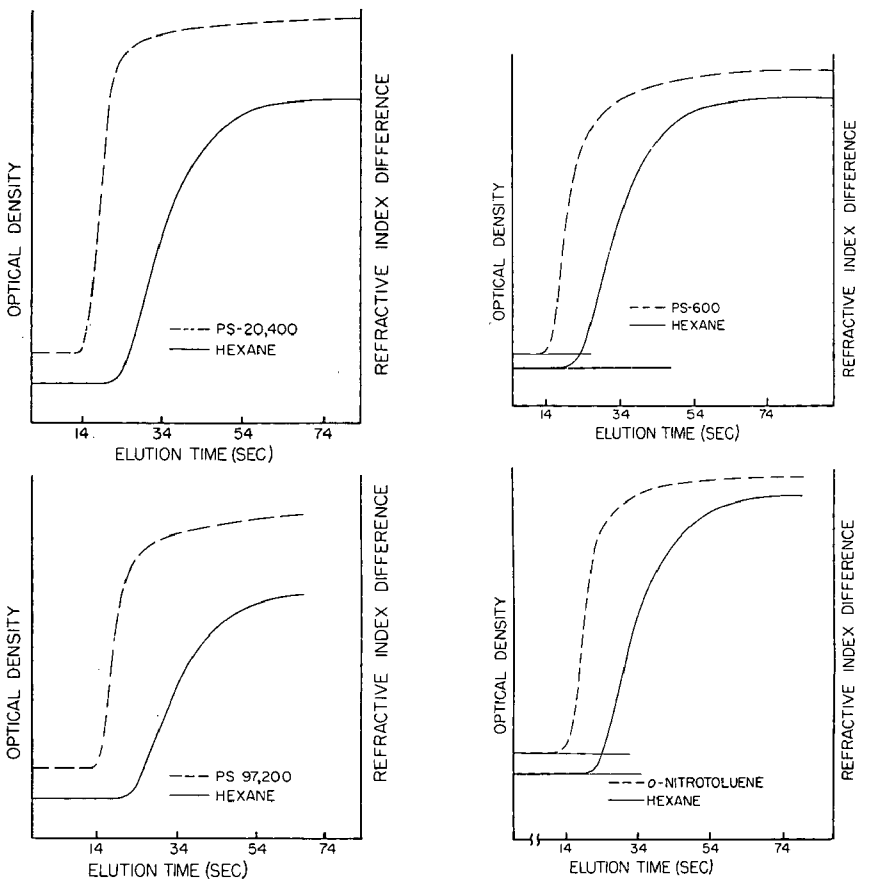

Fig. 7. Step input elution curve of PS-97,200 and PS-20,400 through a 17 in. long by 0.047 in. I.D. stainless steel tubing at 1 ml/min flow rate. – – – –, UV optical density; ———, refractive index difference.

Fig. 8. Step input elution curve of PS-600 and *o*-nitrotoluene through a 17 in. long by 0.047 in. I.D. stainless steel tubing at 1 ml/min flow rate. – – – –, UV optical density; ———, refractive index difference.

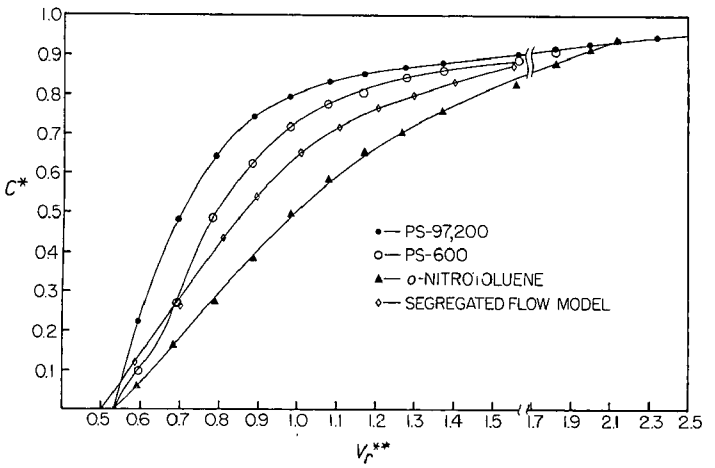

Fig. 9. Normalized step input elution curve of high- and low-molecular-weight polystyrene and *o*-nitrotoluene through a 17 in. long by 0.047 in. I.D. stainless steel tubing at 1 ml/min flow rate.

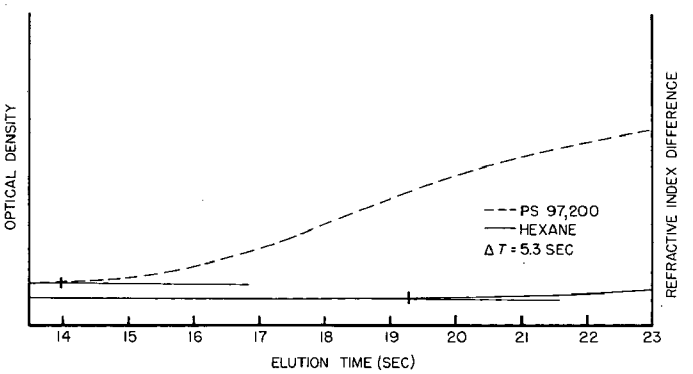

Fig. 10. High speed (recorder speed = 1 in./sec) recording of the step input elution curve of *o*-nitrotoluene and hexane through a 17 in. long by 0.047 in. I.D. stainless steel tubing at 1 ml/min flow rate. – – – –, UV optical density; ———, refractive index difference.

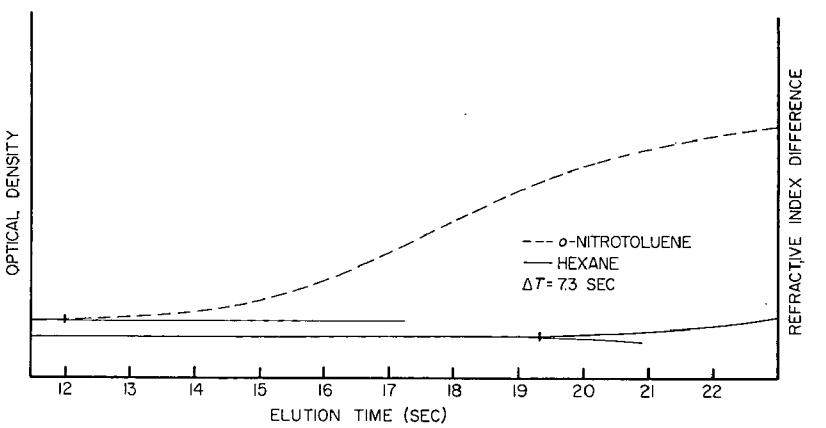

Fig. 11. High speed (recorder speed = 1 in/sec) recording of the step input elution curve of PS-97,200 and hexane through a 17 in. long by 0.047 in. I.D. stainless steel tubing at 1 ml/min flow rate. – – – –, UV optical density; ———, refractive index difference.

flow for the solvent, then a difference in minimum elution time between the polystyrene and hexane curves should exist. The hexane/*o*-nitrotoluene difference is due to detector configuration only, while that of hexane/PS-97,200 is due to detector configuration and velocity profile difference. This difference has been observed directly by comparing the difference between the minimum elution time of *o*-nitrotoluene/hexane and PS-97,200/hexane solutions. This difference is illustrated in Figs. 10 and 11. Although the difference in elution times of *o*-nitrotoluene/hexane and PS-97,200/hexane is only 2 sec, this is significant when one considers the length of the tubing used, which was 17 in.

A summary of the experimental evidence presented in this paper suggests that there is some inhomogeneity in the flow of dilute polymer solutions in small-diameter tubing. It also indicates that a two-phase flow similar to that observed in dilute pulp slurries flowing in pipes[4] may take place in dilute solutions of polymers with sufficiently high molecular weight. Although a good molecular model which can explain this anomalous behavior is at the moment not available, a qualitative speculation as to its cause is perhaps in order.

When a polymer solution is injected into a solvent stream, it is thought that intermolecular interaction between polymer solute molecules causes them to flow with a "plug-like" velocity profile. It is also proposed that, because of the shear gradient in laminar flow, a polymer solute molecule is more highly perturbed by a neighboring polymer molecule which is closer to the tubing axis than another neighboring polymer molecule which is closer to the tubing wall. This results in a radial migration of polymer solute toward the tubing axis. Furthermore, there is a critical radial distance, R, which is a function of shear rate, polymer concentration and molecular weight, from the tubing axis where the polymer solute is essentially unperturbed by the neighboring polymer molecules (no radial migration). The net result of the above proposal is a polymer solute concentration profile which has a maximum near the tube axis and a minimum in an annular region (R distance from the tubing axis). If the above explanation is accepted, the bimodal elution curve becomes evident when one superimposes the velocity profile with the above distorted concentration profile.

APPENDIX

A = Area of elution curve
C_o = Concentration of injected sample
$\bar{C}$ = Instantaneous concentration at the cell
C^* = $\bar{C}/C_o$ = dimensionless concentration (step input)
$C^{**} = \dfrac{\bar{C}V_e}{A}$ = dimensionless concentration (pulse input)
V = Detector cell volume
V_t = Volume of tubing
V_e = $V_t + V$ (total system volume)
V_r = Retention volume
$V_r^{**} = \dfrac{V_r}{V_t}$

ACKNOWLEDGEMENTS

The authors wish to extend appreciation to Mrs. B. Dawson who helped in obtaining most of the data in this paper and to Drs. R. J. GRITTER and T. L. SMITH for their helpful suggestions in reviewing this manuscript.

REFERENCES

1 J. A. BIESENBERGER AND A. C. OUANO, *J. Appl. Polymer Sci.*, 14 (1970) 471.
2 G. I. TAYLOR, *Proc. Roy. Soc. (London)*, A219A (1953) 186.
3 A. C. OUANO AND J. A. BIESENBERGER, *J. Appl. Polym. Sci.*, 14 (1970) 483.
4 J. W. DAILY AND G. BUGLIARELLO, *Ind. Eng. Chem.*, 51 (1959) 887.

CHROM. 5130

STRUCTURAL EVALUATION OF COPOLYMERS USING PREPARATIVE GEL PERMEATION CHROMATOGRAPHY

A. BARLOW, L. WILD AND T. ROBERTS
U.S. Industrial Chemicals Co., Research Division, 1275 Section Road, Cincinnati, Ohio 45237 (U.S.A.)

SUMMARY

A detailed structural evaluation of a copolymer, or a resin exhibiting a branched structure, is only possible through the analysis of fractions from the parent resin. A description is given of a preparative GPC unit which operates at elevated temperatures and thus may be used in the structural analysis of a wide range of resin types including copolymers. Examples are given of the use of this preparative gel permeation chromatographic technique in the study of ethylene–vinyl acetate copolymers and styrene–butadiene rubbers. Through analysis of fractions by infrared, solution viscosity and analytical gel permeation chromatography, a comprehensive structural evaluation is derived which serves to illustrate the potential of preparative gel permeation chromatography in resin structure studies.

INTRODUCTION

In attempting to obtain polymer structure information one needs to fractionate the polymeric material into its differing molecular weight components on a scale large enough to allow further analysis of the fractions by the many techniques presently available, such as osmometry, solution viscosity, infrared (IR), gel permeation chromatography (GPC), nuclear magnetic resonance (NMR), etc., in order to define the structure and composition of sample. The most commonly used fractionation method has been gradient elution chromatography[1] in which the eluent composition is varied to produce the molecular weight separation. This method has proved very useful but does suffer from some disadvantages such as: (a) the lack of resolution of very high-molecular-weight species, (b) the difficulty of fractionating copolymers such as ethylene–vinyl acetate copolymers or rubber which may differ in composition, as well as molecular weight, and hence have variable solubility, (c) the fact that each different polymer system requires individually tailored solvent/non-solvent mixtures.

GPC with its separation based on the hydrodynamic volume of molecules in solution, provides a very attractive alternative to the gradient elution fractionation method and generally does not suffer from the above problems. For the most part, however, the GPC method has been used as an analytical procedure, fractionating very small samples; only occasionally[2,3] has the method been applied to large scale

fractionation. In this present paper a description is given of the operation of a high temperature preparative GPC which combines the advantages of the GPC method of separation with those of a preparative technique. Examples are given of how the preparative GPC technique has been used in the study of the structural characteristics of ethylene–vinyl acetate (EVA) copolymers and styrene–butadiene rubbers (SBR).

In designing the preparative GPC described below, the objective was to produce a system which could be readily operated at differing temperatures and with various solvents so as to be suitable for application to a wide range of resins. The ability to provide fractions of sufficiently large size for subsequent study was considered very important. To facilitate the handling of replicate fractionations necessary to produce the required sample sizes, an in-line solvent stripper has been incorporated into the system to reduce the large volumes of the eluent fractions.

EXPERIMENTAL

Construction and operation of preparative gel fractionation equipment

A diagram of the preparative gel fractionation (PGF) equipment is shown in Fig. 1. The solvent is fed, by gravity, to the degasser and then to the metering pump; the flow rate is 40 ml/min. The solvent then flows through the preheater, which is set at the same temperature as the oven and can be varied from ambient to 150°. Two electrically operated solenoid valves switch the solvent stream either through the sample loop to inject a sample, or to bypass the loop as in normal operation. The solvent stream passes through a filter and then through the fractionation columns; these are Waters' preparative GPC columns which measure 4 ft. by 2.4 in. O.D. and are packed with 'Styragel' of differing porosities (see Fig. 1). The solvent stream then passes through a 'Rototherm' ¼ square ft. thin film evaporator, removing approximately 75% of the solvent in the form of vapor, which is condensed and recycled. The concentrated solution is then fed to a fraction collector operating in a time mode, *i.e.*, fractions are collected for 5 min intervals rather than according to volume, so that any fluctuation in rates of evaporation will not influence the fraction collection procedure which is of importance when combining the fractions from several runs.

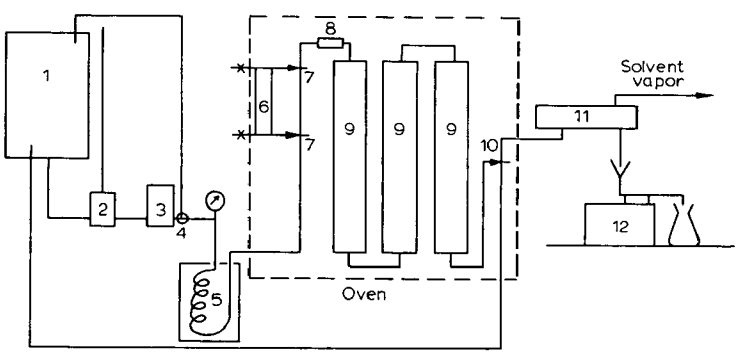

Fig. 1. Schematic diagram of preparative gel fractionator. 1 = Solvent reservoir; 2 = degasser; 3 = metering pump; 4 = pressure relief valve; 5 = preheater; 6 = sample injection system; 7 = 3-way solenoid valves; 8 = filter; 9 = styragel columns, 5×10^3–1.5×10^4, 5×10^4–1.5×10^5, 7×10^5–5×10^6 Å porosity; 10 = 3-way air-operated recycle and fail-safe valve; 11 = solvent stripper; 12 = automatic fraction collector.

The fractions obtained are recovered and then analyzed in the usual manner by IR, GPC, solution viscosity and other relevant methods. Since a refractometer or other detection device is not used to monitor the effluent, the choice of solvent depends upon the material being examined, *i.e.*, the best solvent for the polymer can be used which aids in fractionating the materials since the molecules are then fully expanded. The styrene–butadiene rubbers were consequently fractionated using benzene at room temperature and the ethylene–vinyl acetate copolymers were fractionated in xylene at 60°. The materials to be fractionated are made up as 1.5% solutions in the appropriate solvent, filtered, and introduced into the sample loop. The sample is then injected into the solvent stream by energizing the solenoid valves; approx. 1 g of polymer is fractionated at a time.

Polymers to be fractionated are, first of all, analyzed by GPC so that the upper and lower elution volume limits can be determined. The optimum number of fractions to be combined at the beginning and end of the fractionation, to provide sufficiently large samples for analysis, are also determined from this data.

Calibration

In order to calibrate the equipment a mixture of polystyrene, having a broad molecular weight distribution ($M_w/M_n = 30.7$), was fractionated. The fractions were precipitated, dried, weighed, and analyzed by GPC.

The elution volumes of the fractions were then plotted as a function of their extended chain length to provide the calibration curve shown in Fig. 2. In addition,

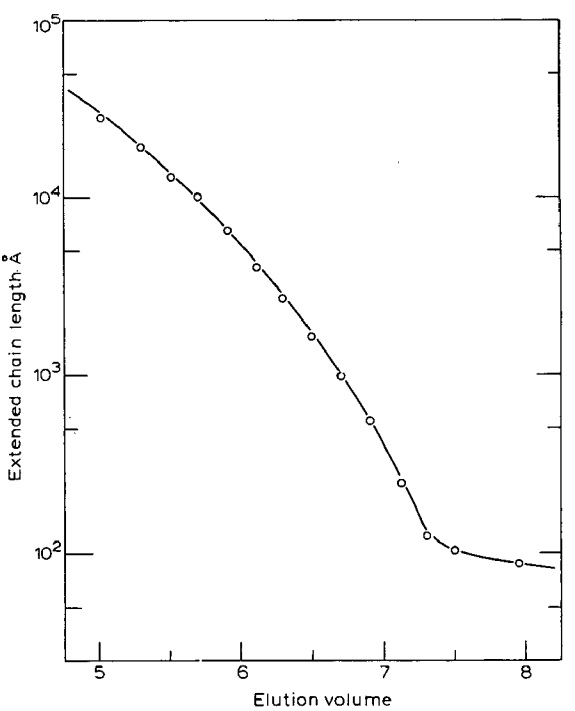

Fig. 2. Calibration curve for preparative gel fractionation using polystyrene in benzene at 25°.

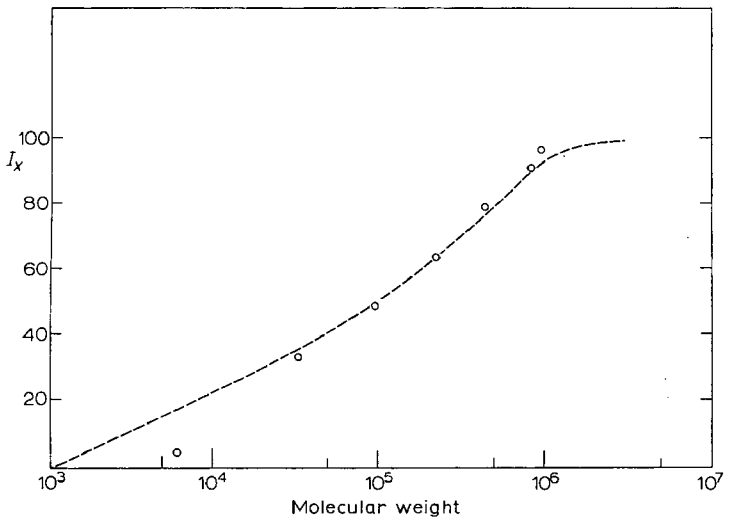

Fig. 3. Comparison of MWD data for polystyrene obtained by analytical GPC and preparative gel fractionation. ○ = Preparative gel fractionation; - - - - - = analytical GPC.

an integral weight *vs.* molecular weight curve was drawn (Fig. 3) and compared with the similar data obtained by GPC analysis of the polystyrene mixture. It is readily apparent that the fractionation achieved by the PGF is quite satisfactory with the possible exception that there is insufficient resolution at the low molecular weight end. (It is planned to install a lower porosity column to rectify this situation.)

CHARACTERIZATION OF FRACTIONS

GPC analysis

A Waters Associates' GPC Model 200 was used to analyze the EVA copolymer fractions. The operating temperature was 140° using trichlorobenzene (TCB) as solvent at a flow rate of 1 ml/min. The porosities of the columns are (1) 7×10^5–5×10^6 Å, (2) 5×10^4–1.5×10^5 Å, (3) 5×10^3–5×10^4 Å, and (4) 5×10^3–1.5×10^4 Å.

The rubber fractions were analyzed on a Model 100 GPC using tetrahydrofuran (THF) as solvent at a temperature of 40° and flow rate of 1 ml/min. Five columns were used in this instrument; the porosities of the first three columns were the same as above and the others were (4) 700–2000 Å, and (5) 500/250/100/60 Å.

Solution viscosity measurements

Viscosities were determined as inherent viscosities using a modified Ubbelohde. The viscosities of the EVA fractions were determined in TCB at 140° and of the SBR fractions in THF at 40°.

Molecular weight measurements

The molecular weights of the EVA fractions were determined as number average molecular weights (M_n), by osmometry in toluene at 85° in a Hallikainen automatic osmometer.

Infrared analysis

The ethylene–vinyl acetate copolymers were analyzed for vinyl acetate content by dissolving the material in carbon tetrachloride and measuring the characteristic absorption of the carbonyl group at 5.8 μ. The styrene content of the SBR fractions was determined by dissolving the material in carbon disulphide and measuring the absorption band characteristic of various types of unsaturation and also phenyl from which the styrene content and microstructure were calculated.

RESULTS AND DISCUSSION

The two resin types included in this study, ethylene–vinyl acetate copolymer and styrene–butadiene rubber, were chosen as ones which prove difficult to fractionate by gradient elution chromatography. The value of the preparative GPC should be therefore clearly apparent if it proves possible to achieve successful fractionations through its use. The fractionated samples produced by the preparative GPC have been analyzed from the point of view of demonstrating that the technique produces effective molecular weight fractionation while also attempting to determine whether the resins exhibit any structural heterogeneities, such as variations of copolymer content or the presence of long-chain branching.

Examination of ethylene–vinyl acetate copolymers

The first copolymers to be examined were ethylene–vinyl acetate (EVA) resins synthesized in an autoclave reactor. Two resins of differing copolymer content but similar melt index were included in the study: Resin A, containing 16.5% VA and Resin B, with 25.5% VA. By analogy with low-density polyethylenes made by the same process, it was considered likely that these resins would exhibit long-chain branching (LCB) — possibly to differing degrees — and perhaps variations in comonomer content. Certainly simple analytical GPC data (Fig. 4) for the two resins show differences which may be associated with differences in the degree of LCB. In the case

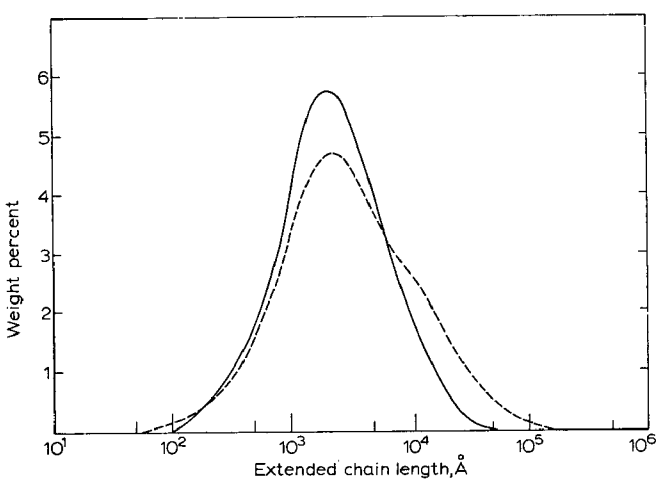

Fig. 4. Molecular size distribution of ethylene–vinyl acetate copolymers A and B. - - - - - = EVA copolymer A; ——— = EVA copolymer B.

TABLE I

STRUCTURAL DATA FOR ETHYLENE–VINYL ACETATE COPOLYMER A

Fraction	*Inherent viscosity* $\{\eta\}$ dl/g	*Measured* $M_n \times 10^{-4}$	*Computed* $M_n \times 10^{-4}$	$M_w \times 10^{-4}$	*R*	*Percent VA*
1	2.36	—	112.3	252.7	2.24	11.0
2	2.07	—	57.5	87.0	1.51	13.8
3	1.76	—	39.0	65.3	1.67	15.3
4	1.57	—	20.1	38.1	1.88	16.4
5	1.35	16.8	14.8	26.8	1.80	16.2
6	1.08	9.03	8.06	15.6	1.93	16.3
7	1.02	8.63	7.23	15.0	2.07	16.8
8	0.898	4.84	4.69	10.1	2.14	16.8
9	0.667	2.32	1.92	4.8	2.68	16.8
10	0.488	1.72	1.34	3.34	2.48	16.2
11[a]	0.354	1.49	1.26	1.76	1.39	—
12[a]	0.186		0.54	0.77	1.41	17
Whole polymer		3.09	1.86	14.4	7.70	16.5

[a] Gradient elution fractions.

of low-density polyethylenes, for example, it has been shown[4] that a distinct high molecular weight shoulder in the GPC trace as shown in the case of Resin A, is usually associated with a high degree of LCB. Consideration of synthesis conditions suggests also that differences in degree of LCB are likely to be present in the two EVA resins.

Fractionation of the EVA resins using the preparative GPC produced fractions which were analyzed by IR, solution viscosity, osmometry, and analytical GPC. The results obtained for fractions from Resin A and Resin B are shown in Tables I and II, respectively. The molecular weight separation is seen to be good except in the low-molecular-weight region, possibly due to the absence of a low porosity column. Because of this difficulty, two or three low-molecular-weight fractions obtained through a gradient elution fractionation[7] have been included to complete the structural information. The data from these materials are also included in Tables I and II.

TABLE II

STRUCTURAL DATA FOR ETHYLENE–VINYL ACETATE COPOLYMER B

Fraction	*Inherent viscosity* $\{\eta\}$ dl/g	*Measured* $M_n \times 10^{-4}$	*Computed* $M_n \times 10^{-4}$	$M_w \times 10^{-4}$	*R*	*Percent VA*
1	1.70		42.97	60.97	1.41	24.0
2	1.35	16.1	18.24	32.24	1.76	—
3	1.27	10.4	13.32	20.44	1.53	—
4	1.16		9.01	15.25	1.69	26.1
5	0.879	6.66	5.64	9.72	1.72	26.0
6	0.743		3.72	6.47	1.74	25.8
7[a]	0.679		3.91	5.49	1.40	24.7
8	0.659	2.93	3.36	6.56	1.94	26.8
9	0.573	1.62	1.78	3.83	2.16	26.1
10	0.503		1.41	3.58	2.54	26.0
11[a]	0.432	1.78	1.29	2.66	2.05	26.1
Whole polymer		2.70	2.78	10.9	3.90	25.5

[a] Gradient elution fractions.

The IR analysis of the fractions shows that the vinyl acetate content is practically constant and exhibits only a very slight decrease in the highest-molecular-weight species. Information of this sort is important when analyzing copolymers by GPC since variations in comonomer content could lead to variations in the refractive index which would give rise to erroneously high or low concentration values and hence yield an erroneous molecular size distribution. It is thought that in this case the fluctuation in vinyl acetate content would have an insignificant influence upon the GPC data. The homogeneous incorporation of the vinyl acetate into the polymer chain as indicated by the copolymer content data is a confirmation of kinetic studies which indicate that ethylene and vinyl acetate are equally reactive with each other at high temperatures and pressures.

If long-chain branching is present in a polymer, the conversion of GPC data into molecular weight distribution (MWD) data becomes complicated because LCB influences the hydrodynamic volume. BENOIT *et al.*[5] have proposed a Universal Calibration for GPC which takes into account the influence of LCB. It has been demonstrated that this Universal Calibration (elution volume, (C) *vs.* $[\eta]M$) is applicable to both linear and branched polyethylenes[6] and should therefore be suitable for EVA resins also.

This Universal Calibration has been applied to fractions from the two EVA resins. A computer program has been set up for this purpose through which values of $[\eta]M_w$ are derived from elution volumes for fractions which allows one to determine M_w using measured values of $[\eta]$. The program is not described here but it does include an iterative analysis aimed at accounting for the presence of polydispersity within the fractions. Analysis of a series of fractions provides information which allows the derivation of a molecular weight calibration (C *vs.* M) for the particular resin sample being studied from which complete MWD, and hence all molecular weight averages, for fractions and whole polymers, can be computed.

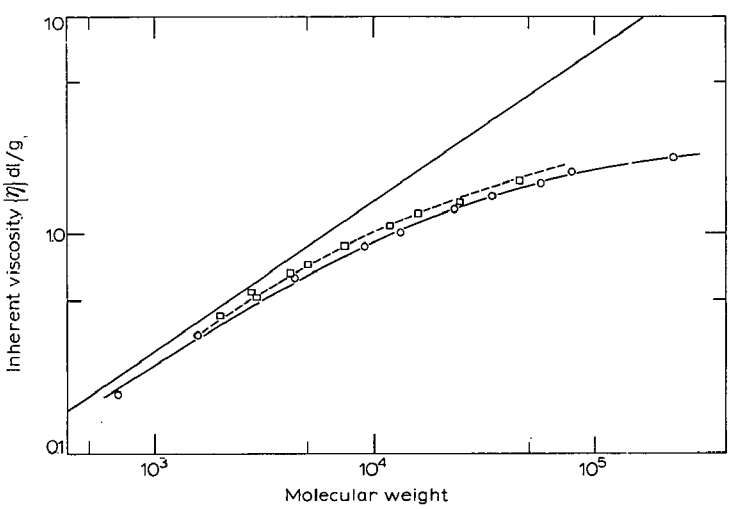

Fig. 5. Solution viscosity–molecular weight relationship for ethylene–vinyl acetate copolymers in TCB at 140°. ——— = linear polymer; ○—○ = copolymer A; □ --- □ = copolymer B.

TABLE III

STRUCTURAL DATA FOR STYRENE–BUTADIENE RUBBER Y

Fraction	*Inherent viscosity* $\{\eta\}$ *dl/g*	$M_n \times 10^{-4}$	$M_w \times 10^{-4}$	R	*Percent styrene*
1	5.90	57.0	130.0	2.28	—
2	4.70	47.7	94.0	1.97	
3	3.86	32.6	67.5	2.07	19.1
4	3.47	17.2	50.5	2.94	19.9
5	2.68	16.2	40.4	2.50	—
6	2.15	11.3	26.7	2.36	—
7	1.86	7.4	23.7	3.21	27.7
8	1.40	4.7	17.1	3.62	—
9	1.04	2.9	14.0	4.81	32.8
10	0.98	1.8	12.0	6.56	32.9

TABLE IV

STRUCTURAL DATA FOR STYRENE–BUTADIENE RUBBER X

Fraction	*Inherent viscosity* $\{\eta\}$ *dl/g*	$M_n \times 10^{-4}$	$M_w \times 10^{-4}$	R	*Percent styrene*
1	3.71	52.4	73.3	1.4	14.8
2	3.34	30.9	64.9	2.1	18.5
3	2.50	26.7	48.7	1.8	20.8
4	1.95	18.2	23.0	1.3	21.9
5	1.41	11.4	16.4	1.4	22.0
6	1.09	9.4	13.3	1.4	22.1
7	0.99	7.8	11.3	1.4	23.1
8	0.84	6.2	7.9	1.3	24.1
9	0.82	5.9	7.5	1.3	24.3
10	0.78	4.9	7.0	1.4	25.2

Molecular weight data computed in this manner is included in Tables I and II. Also given in these tables are the measured number average molecular weights of the fractions which are found to be in close agreement with the computed values and confirm that the analytical and mathematical procedures used are capable of giving realistic results. From this information the solution viscosity-molecular weight relationship may be determined and compared with the relationship derived for corresponding linear material to show the presence or absence of long-chain branching.

In practice the most suitable way of making such a comparison is by adjusting the EVA data to that for a hypothetical polyethylene using a linear polyethylene $[\eta]$–M_w relationship as the reference line. This has been done and the resultant relationships are shown in Fig. 5.

From this data one concludes that the EVA copolymers exhibit relatively high degrees of LCB and in addition that, as expected, the level of LCB present in Resin A is greater than in Resin B.

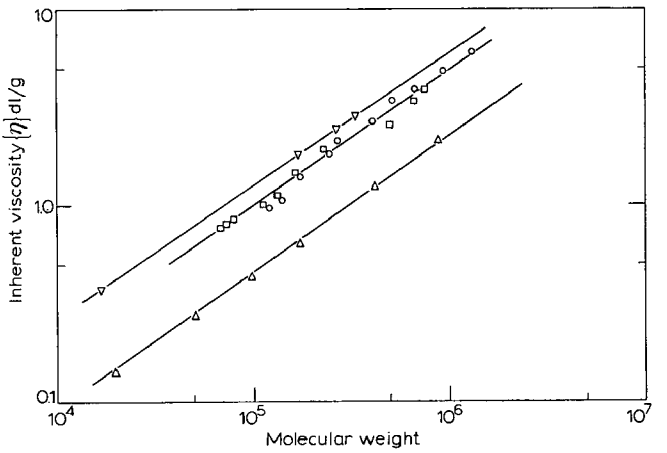

Fig. 6. Solution viscosity–molecular weight relationship for polybutadiene, polystyrene and SBR in THF at 40°. □ = Rubber X; ○ = rubber Y; ▽ = polybutadiene standards; △ = polystyrene standards.

STYRENE–BUTADIENE RUBBER

The two styrene–butadiene rubbers (Resin X and Resin Y) were synthesized using different initiator systems; both rubbers contained approximately 25% styrene. In this case it was again of interest to know whether the comonomer content varied with molecular weight and also whether either of the resins contained any LCB.

Both rubbers were successfully fractionated using the PGF and the fractions analyzed using techniques similar to those used on the EVA copolymers, with the exception of the osmometry measurements.

The information obtained is given in Tables III and IV. It is apparent from the IR analysis of the fractions that the comonomer content of both materials varies considerably and shows a marked decrease in the amount of styrene present as the molecular weight increases. This, of course, means that the raw GPC data for the whole polymer could be misleading because of the unknown influence comonomer content has on the refractive index. Once it has been established that the comonomer content and refractive index vary with molecular weight, then the data may be corrected either by calculation or through measurements on the fractions. This has not been done here and close inspection of Fig. 6 shows a tendency for the copolymer line to converge with that for the polybutadiene at high molecular weight.

It was assumed that the fractions were sufficiently narrow in molecular weight distribution that the slight variation in refractive index within the fraction is negligible, consequently reliable molecular weights are computed via the Universal Calibration iterative analysis procedures.

Using the data presented in Tables III and IV, the molecular weight–solution viscosity relationships for the Rubbers X and Y have been plotted (Fig. 6) together with the similar relationship for polybutadiene and polystyrene. Both the polybutadiene and the polystyrene were polymerized anionically so that they are known to be linear molecules. The fact that the curve for the rubbers falls in between the curves

for polybutadiene and polystyrene and is practically parallel to both, shows that these styrene–butadiene rubbers are also linear materials and do not contain any detectable long-chain branching.

CONCLUSION

The studies described above demonstrate the usefulness of preparative GPC in providing fractions of materials which were previously very difficult, if not impossible, to fractionate by the classical fractional precipitation techniques based on differences in solubility of the fractions. They also illustrate the great potential of the preparative GPC when used in conjunction with a suitably calibrated analytical GPC, as the basis for a rapid and comprehensive structural evaluation for soluble polymers.

REFERENCES

1 M. J. R. CANTOW, *Polymer Fractionation*, Academic Press, N.Y., 1967.
2 K. J. BOMBAUGH, W. A. DARK AND R. N. KING, *4th Intern. Seminar Gel Permeation Chromatography, Miami, 1967*, reprints, p. 25.
3 R. D. LAW, *J. Polym. Sci. A-1*, 7 (1969), 2097.
4 L. WILD AND R. GULIANA, *6th Intern. Seminar Gel Permeation Chromatography, 1968*, reprints, p. 55.
5 H. BENOIT, P. REMPP AND Z. GRUBISIC, *J. Polym. Sci. B* 5, (1967) 753.
6 L. WILD AND R. GULIANA, *J. Polym. Sci. A-2*, 5 (1967) 1087.
7 P. M. KAMATH AND L. WILD, *22nd Ann. Tech. Conf. of the Society of Plastics Engineers, Montreal, Canada, 1966*, SPE Technical Papers, 12 (1966) XVII-6.

CHROM. 5131

SOME VELOCITY PROFILE EFFECTS IN EMPTY TUBES

MARTIN HESS* AND JOHN W. TIERNEY

University of Pittsburgh, Department of Chemical and Petroleum Engineering, Pittsburgh, Pa. 15213 (U.S.A.)

SUMMARY

Several investigators have observed that macromolecular solutes deviate from the dispersion behavior predicted on the basis of a parabolic velocity profile. These experimental observations are discussed in the light of numerical computations on unsteady state mass and momentum-transport with concentration-dependent viscosity.

INTRODUCTION

The viscosity of macromolecular solutions is rather sensitive to the molecular weight and concentration of the solute. It seemed desirable to determine the extent to which changes in viscosity might alter the velocity profile of dilute macromolecular solutions during laminar flow in empty tubes and to consider the effect of such changes in the velocity profile on the dispersion of macromolecules. In this paper, some results of a numerical study of this problem are presented. These results are of particular interest in connection with axial dispersion of solute in the injection system of gel permeation chromatographs.

DISPERSION OF SMALL SOLUTE MOLECULES

TAYLOR[1] demonstrated in 1953 that a solute flowing in the laminar regime in a tube is dispersed longitudinally about a plane that moves at the average velocity of the fluid as though it were diffusing about that plane in accordance with Fick's law of molecular diffusion, but with a dispersion coefficient defined by the expression

$$E = \frac{a^2 U^2}{48D} \tag{1}$$

In terms of the flow rate, the longitudinal dispersion coefficient is given by the equivalent expression

$$E = \frac{Q^2}{48\pi^2 a^2 D} \tag{2}$$

* Present address: Koppers Company, Inc., Monroeville, Pa. 15146, U.S.A.

According to these equations, longitudinal dispersion is enhanced by high velocities and large tube diameters and is diminished by large molecular diffusion coefficients.

ARIS[2] generalized TAYLOR's expression to include extremely slow flows, when molecular diffusion in the axial direction may become significant. When this is the case,

$$E = \frac{a^2U^2}{48D} + D \tag{3}$$

However, in most practical flow situations, and especially with macromolecular solutes, D is negligible with respect to the first term. ARIS further generalized this expression by substituting a parameter $\varkappa$ for the constant factor 1/48. The resulting expression for the dispersion coefficient is no longer restricted to a tubular geometry nor to a parabolic velocity profile:

$$E = \varkappa\frac{a^2U^2}{D} + D \tag{4}$$

For a parabolic velocity profile in a tube, $\varkappa = 1/48$ as found by TAYLOR. For perfect plug flow, $\varkappa = 0$ and there is no dispersion due to flow.

Axial dispersion arises then because of the existence of a velocity profile which causes material at the core of the tube to move faster than the average velocity, while material near the wall moves more slowly than the average velocity. In particular, when a Newtonian fluid of constant density and constant viscosity flows in a tube, material at the centerline moves at twice the average velocity, material in contact with the wall has zero velocity and intermediate velocities define a parabola. In the absence of molecular diffusion, this parabolic velocity profile causes material injected over a short time span to leave the tube over a longer time interval. Solute traveling near the centerline exits early, while material traveling near the wall exits considerably later.

However, when there is appreciable molecular diffusion, the situation is not quite as unfavorable. Near the tip of the velocity front, solute diffuses radially from the core into the more dilute periphery, and is slowed down. Small solute molecules, which have large molecular diffusion coefficients, thus exhibit smaller axial dispersion than they would in the pure convection regime. This is in accordance with the predictions of TAYLOR's equation.

THE DISPERSION OF MACROMOLECULES

ANANTHAKRISHNAN *et al.*[3] determined the regions of applicability of the TAYLOR and ARIS equations on a map having as coordinates a dimensionless time parameter ($\tau = Dt/a^2$) and the Peclet number ($N_{Pe} = 2aU/D$). Because of the small molecular diffusion coefficients of macromolecules, the flow of macromolecular solutions tends to be characterized by large Peclet numbers, and convective effects dominate. However, in most practical situations, the time interval involved is such that numerical solutions must be used, since the analytical pure convection solution applies only up to very short times.

Most macromolecular solutes have molecular diffusion coefficients that are one to two orders of magnitude smaller than those of small solute molecules, and the TAYLOR–ARIS equations, as well as the numerical solution of the convective diffusion equation with a constant velocity profile, predict that macromolecules should be dispersed more than small solute molecules. However, some experimental evidence reported in the literature runs contrary to this expectation. BILLMEYER AND KELLEY[4] removed all gel columns from a Waters gel permeation chromatographic (GPC) apparatus and studied the dispersion in the injection–detection system for two solutes: a low-molecular-weight solute, *o*-dichlorobenzene (ODCB), dissolved in tetrahydrofuran (THF) and a 0.1 % solution of monodisperse polystyrene of molecular weight 160000 also dissolved in THF. They studied the dispersion of both solutes at a number of flow rates and found that in all cases the ODCB was dispersed more than the polystyrene, but they offered no definite explanation for this result. Inasmuch as TAYLOR's equation has been shown to be valid for small molecules by many investigators, one might conclude from KELLEY's experimental results that TAYLOR's equation does not apply for macromolecular solutes during laminar flow in tubes. More recently a considerable amount of valuable experimental data was presented by BIESENBERGER AND OUANO[5]. These authors obtained data on the dispersion in empty tubes of lengths ranging from 18 in. to 285 in. for both step and pulse inputs. Their data include solutions in toluene of *o*-dichlorobenzene and of narrow molecular weight distribution polystyrenes (PS) having molecular weights of 900, 20400, 97200 and 160000. They observed that the concentration and molecular weight of the polymer solute had a profound influence on dispersion in the empty tubing. As the concentration was increased from 0.03 g/dl to 0.6 g/dl, the concentration response to a step input increasingly resembled plug flow. Furthermore, at a given concentration, the behavior approximated plug flow more closely at the higher molecular weight (97200) than at the molecular weight of 20400. Finally, BIESENBERGER AND OUANO found that reducing the tube diameter from 0.1 cm to 0.048 cm yielded a closer approach to plug flow.

NUMERICAL STUDY

A numerical study of the dispersion of macromolecules during laminar flow has recently been completed at the University of Pittsburgh[6]. The results of this study are being reported in detail elsewhere[7]. Only aspects of the study specifically related to GPC injection will be discussed here. A computer program based on the simultaneous unsteady state solution of the convective diffusion equation and of the momentum equation was written and used to simulate the dispersion of a macromolecular solute during flow in a tube. The viscosity of the solution was assumed to follow the Huggins equation:

$$\eta = \eta_s(1 + [\eta]c + k'[\eta]^2c^2) \tag{5}$$

and Newtonian behavior was assumed to apply.

Computations for a step signal of a macromolecular solution displacing pure solvent indicated that the velocity distribution shifts from a parabolic profile to a flatter one as illustrated in Fig. 1. This shift is a transient phenomenon: the profile changes in time as well as along the tube length (Fig. 2). At the front of the step, the

profile flattens with time from a parabolic one to one that is intermediate between fully developed and plug flow. The rate at which this change occurs depends on the solute molecular weight and concentration, as well as on the tube diameter and flow rate. The flattening of the velocity profile is caused by the existence of a significant radial viscosity gradient. When there is such a gradient, the assumptions of constant viscosity and invariant velocity profile introduce error into the dispersion calculations. The concentration gradients, which give rise to viscosity gradients, increase as the Peclet number increases; and in accordance with the Huggins equation, radial concentration gradients give rise to significant viscosity gradients when the product $[\eta]c_0$ of the intrinsic viscosity times the solute concentration is sufficiently large.

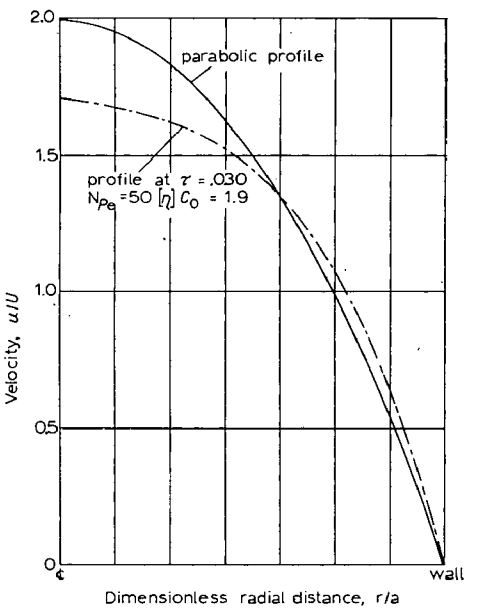

Fig. 1. Velocity profile.

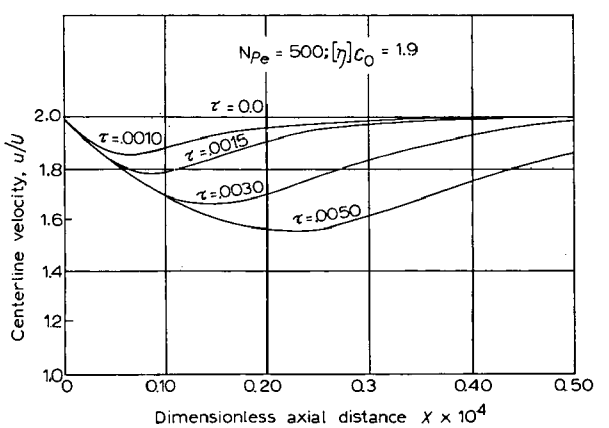

Fig. 2. Velocity profile in a tube of finite length.

Dimensional analysis indicates that the rate at which the velocity profile flattens depends on the Reynolds (N_{Re}) and Schmidt (N_{Sc}) numbers and on the dimensionless product $[\eta]c_0$. When these numbers are sufficiently large, the velocity profile predicted by our computations flattens rapidly and plug flow behavior is approached. At intermediate values, the velocity profile flattens more slowly and reaches an equilibrium value that is nearer to a parabolic profile. At very low Peclet numbers or small $[\eta]c_0$ values, changes in the velocity profile may be negligible.

Table I gives the results of computer simulations of the flow of polymer solutions of several molecular weights and concentrations. The conditions correspond to those used by BIESENBERGER AND OUANO in their experimental work (tube diameter 0.1 cm, flow rate 0.95 cm³/min). The solvent used by these authors was toluene and the solutes were a series of anionic polystyrenes of narrow molecular weight distribution available from the Pressure Chemical Company. Our computations included in addition polystyrene of 860 000 mol. wt.

TABLE I

COMPUTED PERCENT DECREASE IN CENTERLINE VELOCITY DURING FLOW OF POLYSTYRENE SOLUTIONS

Mol. wt.	$[\eta]$	*0.15 g/dl*	*0.30 g/dl*	*0.60 g/dl*
20 400	0.12	0.42		1.66
97 200	0.27	0.94		3.61
160 000	0.34		2.26	4.35
860 000	0.79	2.40	4.70	8.60

Table I shows that there is some decrease in the centerline velocity even at relatively low polymer concentrations and molecular weights. The effect of this flattening of the velocity profile is in qualitative agreement with the results reported by BIESENBERGER AND OUANO. With a parabolic velocity profile and the low molecular diffusion coefficient characteristic of macromolecules, the first solute molecules would be expected to emerge at a dimensionless retention volume of 0.5.

With a flatter velocity profile, the first solute molecules should emerge later, but the rise in concentration should be sharper. These effects are expected to be insignificant at very low molecular weights and small solute concentrations, but should become more significant as solute molecular weight and concentration increase. The calculations also predict that the step input elution curves for the smaller (0.05 cm diameter) tube should break through later and should be steeper than for the larger (0.1 cm diameter) tube. However, even though these results offer a qualitative explanation, these computations do not predict effects of the magnitude observed by BIESENBERGER AND OUANO at these molecular weights and concentrations.

NON-NEWTONIAN EFFECTS

FOX *et al.*[8] studied the effect of the rate of shear on the viscosity of dilute solutions of polyisobutylene. Their results and those of other investigators indicate that most polymer solutions are Newtonian at very low and very high shear rates, but deviate from Newtonian behavior at intermediate shear values. Such deviations are very important at high molecular weights and moderate to large concentrations,

as shown for instance by SEGAL AND GRAESSLEY[9] for solutions of polystyrenes in benzene. Deviations from Newtonian behavior at the relatively high shear rates prevailing near the tube wall would reinforce the flattening of the velocity caused by the radial concentration gradient.

For a power law fluid, the laminar velocity profile is given by the expression:

$$u = U\left(\frac{3n+1}{n+1}\right)\left[1-\left(\frac{r}{R}\right)^{\frac{n+1}{n}}\right] \tag{6}$$

The flow index n is 1.0 for Newtonian fluids, but is less than 1.0 for pseudoplastic polymer solutions.

The differential equation for pure convection

$$\frac{\partial c}{\partial t} + u\frac{\partial c}{\partial x} = 0 \tag{7}$$

with step input boundary conditions, has the solution

$$C_m = \left(1-\frac{X}{\tau}\right)^{2n/(n+1)} = \left(1-\frac{x}{\left(\frac{3n+1}{n+1}\right)Ut}\right)^{2n/(n+1)} \tag{8}$$

This equation tends to be valid for short tubes, but increasingly large deviations from the pure convection solution are to be expected as the tube length is increased. In deriving eqn. 8, it was assumed that the fluid which is displaced also has flow index n. Fig. 3 shows a plot of this solution for several values of the flow index n.

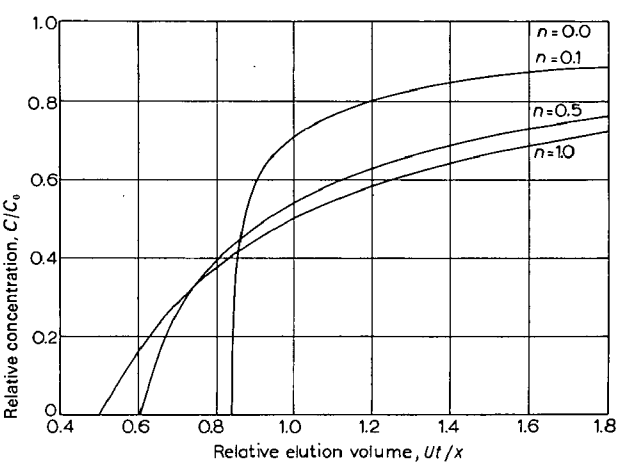

Fig. 3. Pure convection solution.

As the flow index decreases, the behavior of the elution curves is reminiscent of the results obtained by BIESENBERGER AND OUANO at the higher concentrations and molecular weights. However, published data on the shear rate dependence of the viscosity lead to the expectation that higher molecular weights and concentrations would be required for significant non-Newtonian effects. Additional numerical work is in progress at the present time to determine to what extent velocity profile effects might account for the observed anomalies.

With a pulse signal normally used in GPC, the effects are even more complex than for a step signal, as there are two discontinuities in concentration instead of the single discontinuity present with a step. Our computer program has provisions for a pulse input and numerical computations are planned for this type of signal.

CONCLUSIONS

The dispersion of macromolecular solutes during laminar flow in an empty tube has been studied numerically for a step input assuming Newtonian behavior and no chain entanglements. The computations predict a flattening of the velocity profile which provides at least a partial explanation of the experimental results of BILLMEYER AND KELLEY[4], and of BIESENBERGER AND OUANO[5]. However, the computed decrease in dispersion was of considerably lesser magnitude than the experimental results reported in the literature. Any deviation from Newtonian behavior at high shear rates would cause a further flattening of the velocity profile and a further decrease in dispersion.

NOTATION

a = tube radius, cm
c = concentration, g/dl
c_0 = concentration of step signal
C_m = average concentration over a cross-section
D = molecular diffusion coefficient, cm²/sec
E = axial dispersion coefficient, cm²/sec
k' = Huggins constant, dimensionless
n = flow index, dimensionless
N_{Pe} = Peclet number, $2aU/D$, dimensionless
N_{Re} = Reynolds number, $2aU/\nu$, dimensionless
N_{Sc} = Schmidt number, ν/D, dimensionless
Q = volumetric flow rate, cm³/sec
r = radial distance from tube centerline, cm
U = average velocity, cm/sec
u = velocity, cm/sec
x = axial distance, cm
X = dimensionless axial distance, x/aN_{Pe}

GREEK SYMBOLS

η = viscosity of solution, poises
η_s = viscosity of solvent, poises
$[\eta]$ = intrinsic viscosity, dimensionless
$\varkappa$ = factor in ARIS equation, dimensionless
ν = kinematic viscosity, cm²/sec ($= \eta/\rho$)
τ = dimensionless time, Dt/a^2

REFERENCES

1 G. I. TAYLOR, *Proc. Roy. Soc. (London), Ser. A*, 219 (1953) 186.
2 R. ARIS, *Proc. Roy. Soc. (London), Ser. A*, 235 (1956) 67.
3 V. ANANTHAKRISHNAN, W. N. GILL AND A. J. BARDUHN, *Amer. Inst. Chem. Engrs. J.*, 11 (1965) 1063.
4 F. W. BILLMEYER, JR. AND R. N. KELLEY, *J. Chromatog.*, 34 (1968) 322.
5 J. A. BIESENBERGER AND A. OUANO, *Division of Petroleum Chemistry, Inc., Amer. Chem. Soc. Meeting, Houston, February 22–27, 1970.*
6 M. HESS, *The Dispersion of Macromolecules in Laminar Flow*, Ph.D. Diss., University of Pittsburgh, 1970.
7 M. HESS AND J. W. TIERNEY, *Ses. Transp. Properties Polym. Syst., 63rd Ann. Meet. of Amer. Inst. Chem. Engrs., Chicago, November 29–December 3, 1970.*
8 T. G. FOX, JR., J. C. FOX AND P. J. FLORY, *J. Amer. Chem. Soc.*, 73 (1951) 1901.
9 L. SEGAL AND W. W. GRAESSLEY, *Symp. Mol. Struct. Aspects Rheology, 60th Ann. Meet. Amer. Inst. Chem. Engrs., New York, N.Y., November 26–30, 1967.*

CHROM. 5132

THE APPLICATION OF PREPARATIVE GEL PERMEATION CHROMATOGRAPHY TO POLYURETHANE FOAM TECHNOLOGY

G. K. BAKER
The Bendix Corporation, Kansas City Division, Kansas City, Mo. (U.S.A.)

SUMMARY

Both the polyol resin component and the isocyanate component of a rigid, molding polyurethane foam system were fractionated by preparative gel permeation chromatography. The fractionation of the polyol provided information about the structure of the polymeric resin which allowed the derivation of a convenient method for following the kinetics of the synthesis of the polyol by analytical gel permeation chromatography. The structure and reactivity of various fractionated isocyanate species in the polymeric polyaryl isocyanate component were studied and correlated to the behavior of this material in the production of rigid urethane foams.

CHROM. 5133

THE USE OF FAST, FINITE, FOURIER TRANSFORMS FOR THE SOLUTION OF TUNG'S EQUATION

II. THEORY AND APPLICATION

T. VLADIMIROFF
Propellants Laboratory, Picatinny Arsenal, Dover, N.J. 07801 (U.S.A.)

SUMMARY

Recently it has been suggested that fast finite Fourier transforms be employed for the solution of TUNG's integral equation. The COOLEY AND TUKEY algorithm used in the present work is much faster than the usual Fourier method since the length of computation is proportional to $N \log_2(N)$ rather than N^2. This saves computer time and also enables a larger number of points to be used in order to facilitate computer plotting of the corrected chromatogram. First some of the basic properties of finite Fourier transform are presented in order to familiarize the reader with the approximations involved. Then several chromatograms, both analytical and simulated experimental are considered and some of the problems inherent in processing experimental chromatograms are discussed.

INTRODUCTION

Gel permeation chromatography (GPC)[1] is becoming popular for the characterization of molecular weight distributions of polymers. However, as a result of axial diffusion spreading occurs in the GPC instrument so that the molecular weight averages obtained from the chromatograms can be significantly different from the absolute molecular weight averages[2]. As a result some interest has been generated in developing methods by which the experimental chromatograms can be corrected for this effect[3–9]. Central to this endeavour is the solution of the integral equation:

$$z(t) = \int_{-\infty}^{\infty} x(t-\tau)y(\tau)\,\mathrm{d}\tau \qquad (1)$$

which was first suggested by TUNG[3]. This equation relates z, the observed chromatogram to the true chromatogram y which is being spread by the function x. t and τ represent elution volumes. When x is a function of $t-\tau$ only, eqn. 1 can be solved using Fourier transforms[9,10]. The use of this type of solution in conjunction with numerical integration is not only slow but also seems to work better on analytical examples than on experimental data[2,11]. For this reason we have undertaken to investigate the use of fast finite Fourier transforms (FFFT)[12] as recently suggested by VLADIMI-

ROFF[13]. With this technique the length of computation becomes proportional to $N \log_2(N)$ rather than N^2. Even for a 32 point transform, this reduces the required computer time by a factor of 6. If large numbers of chromatograms must be processed the savings in money can be substantial. For the purposes of plotting, 32 points is really not enough as can be seen in Fig. 1. To obtain better plots, a larger number of points must be used resulting in greater savings when FFFT is employed. It was also suspected that this method might be used to investigate the nature of some numerical difficulties encountered by investigators attempting to process experimental chromatograms.

THEORY

Although a detailed theoretical analysis of the computational simplifications involved in the FFFT will not be presented here, some of the basic properties of the finite Fourier transforms (FFT) will be discussed in order to introduce the notation and to give the reader a feeling for the method. A more detailed discussion can be found elsewhere[14].

If $X(j)$, $j = 0, 1, \ldots, N-1$ is a sequence of N complex numbers, the finite Fourier transform of $X(j)$ is defined as:

$$A(n) = 1/N \sum_{j=0}^{N-1} X(j) e^{-2\pi i nj/N}$$

where $i = (-1)^{1/2}$. If $W_N = \exp(2\pi i/N)$ then:

$$A(n) = 1/N \sum_{j=0}^{N-1} X(j) W_N^{-uj}.$$

We also have the inverse finite transform:

$$X(j) = \sum_{n=0}^{N-1} A(n) W_N^{uj}.$$

This is a consequence of the orthogonality relationship of W_N^{uj}:

$$\sum_{j=0}^{N-1} W_N^{uj} W_N^{-mj} = \sum_{j=0}^{N-1} W_N^{(n-m)j} = N \text{ if } n = m \text{ Mode } N$$
$$= 0 \text{ otherwise}$$

A double arrow connecting two functions *i.e.* $X(j) \leftrightarrow A(n)$ is used to indicate a finite Fourier pair. The exponential function W_N is periodic in both n and j:

$$W_N^{nj} = W_N^{(n+N)j} = W_N^{n(j+N)}.$$

Therefore, $A(n)$ and $X(j)$, as defined by their finite transforms, are periodic in N. Also the convolution theorem holds:

$$1/N \sum_{k=0}^{N-1} X_1(k) X_2(j-k) = 1/N \sum_{k=0}^{N-1} X_1(j-k) X_2(k) \leftrightarrow A_1(n) A_2(n).$$

In this paper we are particularly interested in using the finite Fourier transform to approximate the Fourier integral:

$$a(f) = \int_{-\infty}^{\infty} x(t)e^{-2\pi ift}\,dt.$$

If $a(f)$ is sampled at intervals of length Δf and expressed at sampling points $n\Delta f$, $n = 0, \pm 1, \pm 2, \ldots$ then:

$$a(n\Delta f) = \int_{-\infty}^{\infty} x(t)e^{-2\pi int/T}\,dt,$$

where $T = 1/\Delta f$. $\mathrm{Exp}(-2\pi\, int/T)$ is a periodic function of t with period T. By changing the variables of integration it is possible to obtain:

$$a(n\Delta f) = \int_{0}^{T} x_p(t)e^{-2\pi int/T}\,dt,$$

where

$$x_p(t) = \sum_{k=-\infty}^{k=+\infty} x(t + kT).$$

The subscript p on a function will denote the periodic function formed by superposition of the non-periodic function shifted by all multiples of the fundamental period. This is the approximation introduced when the infinite transform is replaced by the finite transform. If $x(t)$ is zero outside certain limits so that $x_p(t) \approx x(t)$ this is a good approximation and the finite transform can be used to replace the infinite transform.

For the convolution integral of eqn. 1, the convolution theorem of Fourier theory states that if:

$$x(t) \leftrightarrow a(f)$$

$$y(t) \leftrightarrow b(f)$$

$$z(t) \leftrightarrow c(f),$$

then $c(f) = a(f)b(f)$. If $y(\tau)$ in eqn. 1 equals zero for $|\tau| > T_y$ then:

$$z(t) = \int_{-T_y}^{T_y} x(t-\tau)y(\tau)d\tau.$$

Approximating this integral by the trapezoidal rule gives:

$$z(j\Delta t) = \Delta t \sum_{k=-K}^{k=K} x((j-k)\Delta t)y(k\Delta t),$$

where $\Delta t = T/N$, $K = T_y/\Delta t$ and $j = 0, 1, 2, \ldots, N-1$. By the theorem on the convolution of FFT this will be approximated by $\Delta t NA(n)B(n)$. There is a wrap-around

error in this procedure. This is because values of X in the range $X(-K)$ to $X(N+K)$ must be used and the convolution is computed as though $X(j)$ repeated itself outside the $(0, N-1)$ interval. To avoid this type of difficulty it is necessary to include at least K zeroes on either side of x and y.

In other words the FFT can be introduced in two ways. One is through the observation that if $x_p(t) \approx x(t)$, then the FFT is a good approximation to the Fourier integral. The other is to approximate the integral in eqn. 1 using the trapezoidal rule and then employing the convolution property of FFT to obtain the desired result. Both these methods are related since they depend on the functions involved being small outside a certain region.

ANALYTICAL RESULTS

As we have seen, there are two justifications for employing FFFT. Actual application requires a judicious choice of F, T and N. In this respect it is important to take into account the relationships between these quantities:

$$N\Delta t = T \qquad 1/T = \Delta f$$

$$N\Delta f = F \qquad 1/F = \Delta t.$$

Usually T is determined by the experimental chromatogram, allowing a certain number of zeroes on both sides to keep from introducing wrap-around errors. N is then determined by having $F \approx 1$. Extending the calculation further into the frequency domain has no practical value since rounding errors will predominate. Once the transform of y is obtained using the formula $B(n) = C(n)/A(n)$, zeroes can be added at the end of B in order to increase N to N'. Δf and hence T is kept constant. The resulting inverse FFFT using N' points produces $Y(j)$ with a much smaller $\Delta t = T/N'$. This enables the computer to plot $Y(j)$. Otherwise a smooth curve must

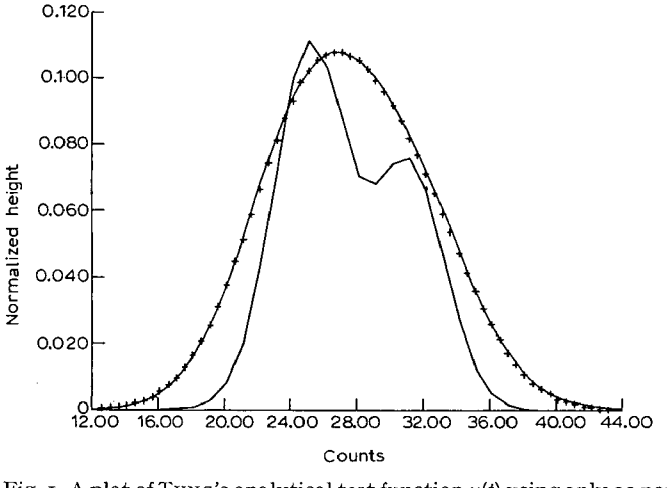

Fig. 1. A plot of TUNG's analytical test function $y(t)$ using only 32 points. ($\times\times\times$) $z(t)$; (———) $y(t)$.

be fitted through the processed points to avoid the type of plot illustrated in Fig. 1.

To explore the method analytically, the synthetic, two-peak distribution:

$$y(\tau) = (0.325/\sqrt{\pi})\,[0.6e^{-(0.325)^2(\tau-25)^2} + 0.4e^{-(0.325)^2(\tau-31)^2}]$$

suggested by TUNG[9] was utilized. A simple Gaussian of the form $x(\tau) = h(\pi)^{-1/2}$ $\exp(-h^2\tau^2)$ was used as the spreading function. This example is advantageous since

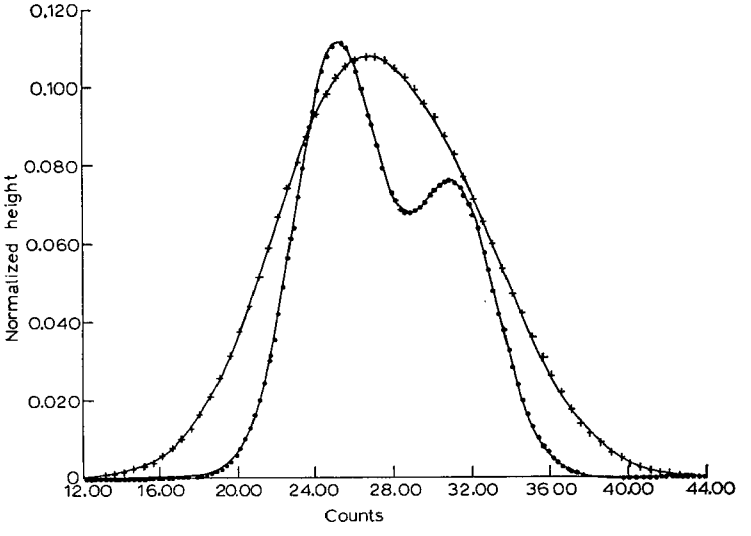

Fig. 2. A comparison of the exact $y(t)$ with $y_F(t)$ computed by FFFT with $h = 0.4$. (+++) $z(t)$; (·····) $y(t)$; (———) $y_F(t)$.

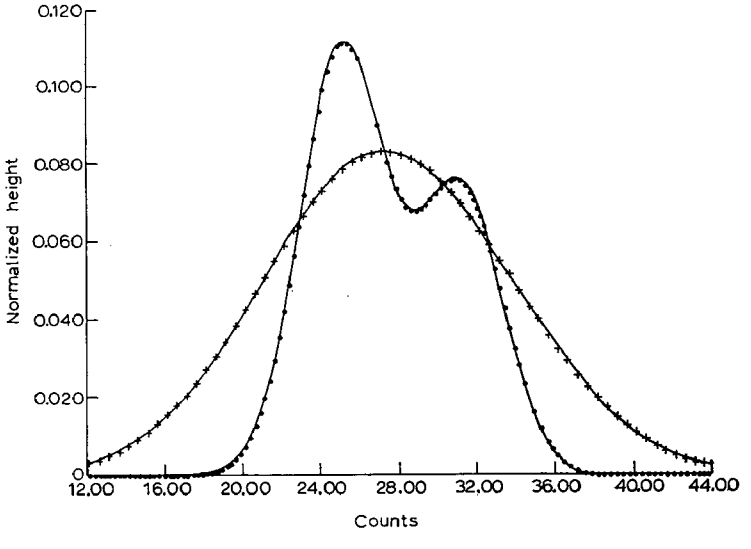

Fig. 3. A comparison of the exact $y(t)$ with $y_F(t)$ computed by FFFT with $h = 0.2$. (+++) $z(t)$; (·····) $y(t)$; (———) $y_F(t)$.

all the integrals of interest can be computed exactly and used for the purposes of comparison. Figs. 2 and 3 illustrate the plotted $y(\tau)$ obtained with $h = 0.4$ and $h = 0.2$, respectively, using a value of $N' = 1024$. For the case of $h = 0.2$ the results are worse since F had to be reduced to 1/2 and only 32 points were used from $z(t)$. However when the results are plotted, in Fig. 3 they can not be distinguished from the true values.

Once it had been established that the method and the relevant computer

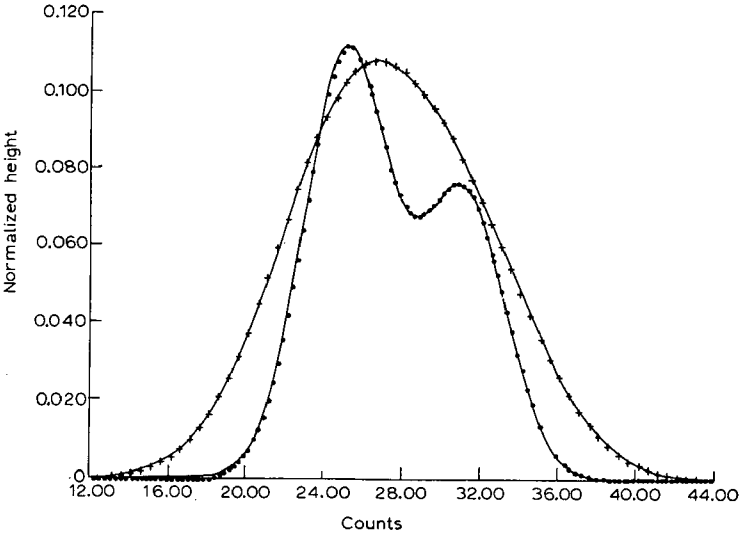

Fig. 4. A comparison of the exact $y(t)$ with $y_F(t)$ computed by neglecting values of $z(t) < 0.001$ $(z(t))_{max}$ with $h = 0.4$. (+++) $z(t)$; (·····) $y(t)$; (———) $y_F(t)$.

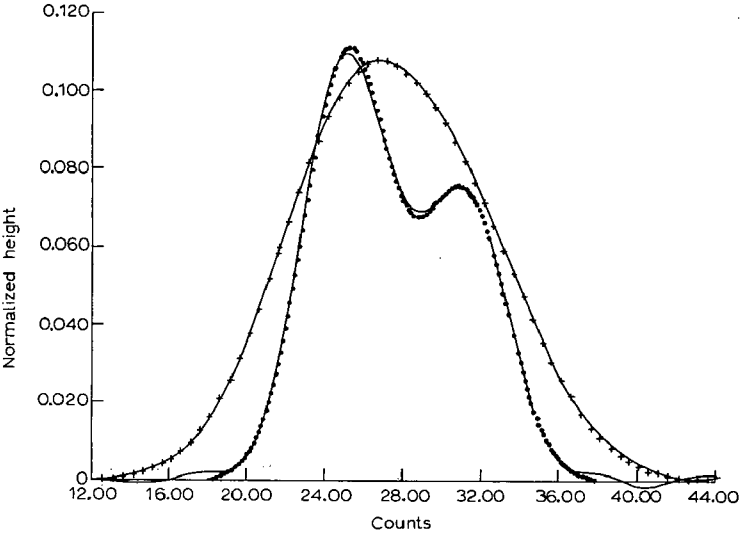

Fig. 5. A comparison of the exact $y(t)$ with $y_F(t)$ computed by neglecting values of $z(t) < 0.005$ $(z(t))_{max}$ with $h = 0.4$. (+++) $z(t)$; (·····) $y(t)$; (———) $y_F(t)$.

programs worked well on this example, an attempt was made to process more realistic chromatograms. In particular it was desired to establish practical limits on F and to investigate the oscillations in y encountered by other workers[2, 11].

The limit on the acquisition of data is the signal to noise ratio (S/N). In a typical GPC experiment one can not expect a value much in excess of 1000 to 1. With the FFFT method, the transform is computed to a certain number of decimal places. The exact number of places depends on the accuracy of the input data and

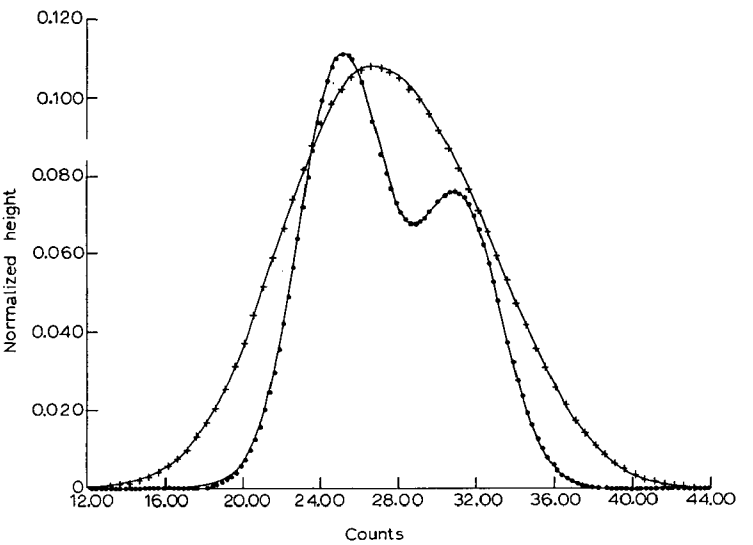

Fig. 6. A comparison of the exact $y(t)$ with $y_F(t)$ computed by rounding all values of $z(t)$ to 0.001 with $h = 0.4$. (+++) $z(t)$; (·····) $y(t)$; (———) $y_F(t)$.

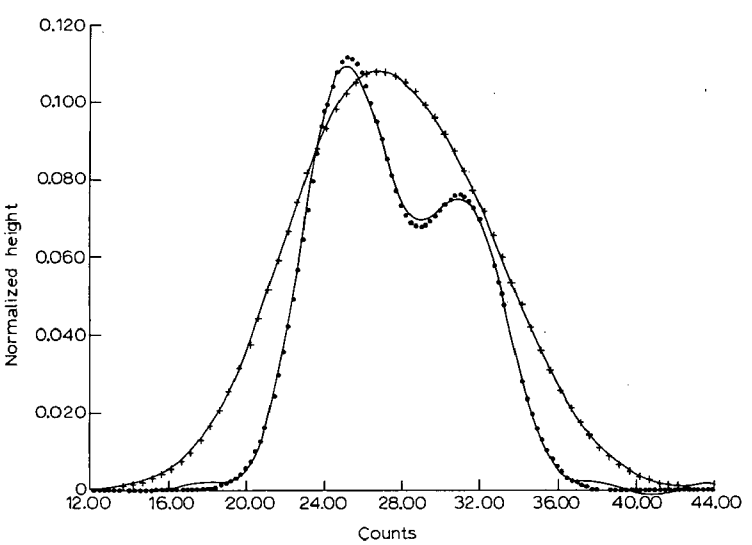

Fig. 7. A comparison of the exact $y(t)$ with $y_F(t)$ computed by rounding all values of $z(t)$ to 0.005 with $h = 0.4$. (+++) $z(t)$; (·····) $y(t)$; (———) $y_F(t)$.

on the number of significant figures retained by the computer. In the case of GPC, the signal to noise ratio of the input data becomes the limiting factor so that the transform can not be calculated more accurately than one part in a thousand. Unfortunately this means that the smallest numbers in the transform never get much smaller (in absolute value) than 10^{-3} times the largest number. Thus $C(n)$ does not appear to approach zero asymptotically as it should. On the other hand the Gaussian is analytic and its transform can be calculated quite accurately. Since the transform of a Gaussian is itself a Gaussian it approaches zero rapidly. To obtain the transform of Y we divide by the transform of X. The division by small numbers produces large meaningless numbers which completely dominate the Fourier synthesis of Y. This can be easily illustrated by setting all the values of Z smaller than 0.1 % of the largest Z equal to zero.

To compensate this type of error, it was decided to set all elements of the transform of Z smaller than 0.1 % of the largest equal to zero since elements of this order of magnitude could not be computed accurately. This calculation for $h = 0.4$ is plotted in Fig. 4 and compared with the exact result. If the cut-off point is set at 0.5 %, the somewhat inferior fit of Fig. 5 is obtained.

Not only are the wings of real chromatograms affected by the noise but all the data are limited in accuracy. To simulate this all the values of Z were rounded to 0.1 %. The results were plotted in Fig. 6. With this S/N ratio no oscillations are seen to appear. When Z was rounded to 0.5 %, the plot of Fig. 7 was obtained. The results are similar to those of Fig. 5 and probably represent the limiting value of S/N which can be handled successfully by this method.

CONCLUSIONS

When the spreading function is not strongly dependent on elution volume the FFFT is an efficient method of solving TUNG's equation. It also becomes possible to employ enough points for the computer to plot the end product. It seems practical to allow the spreading function to determine F as has already been suggested[2], although this is not critical in the FFFT method. Providing a cut-off for the transform of Z which goes inversely as S/N seems to be reasonable on the basis of the few examples examined in this paper. However, this could probably be optimized further in individual cases. The possibility of processing chromatograms with a S/N greater than 200/1 without producing an unsatisfactory loss of accuracy is suggested. It should also be noted that since the FFFT method uses $\log_2(N)$ operations to compute a point rather than N operations, errors in the input data do not accumulate as rapidly[14] as in the usual method.

REFERENCES

1 J. C. MOORE, *J. Polym. Sci. A-2*, (1964) 835.
2 E. M. ROSEN AND T. PROVDER, *Amer. Chem. Soc. Div. Petrol. Chem. 159th Nat. Amer. Chem. Soc. Meeting*, Houston, Texas, 1970.
3 L. H. TUNG, *J. Appl. Polym. Sci.*, 10 (1966) 375.
4 W. N. SMITH, *J. Appl. Polym. Sci.*, 11 (1967) 639.
5 M. HESS AND R. F. KRATZ, *J. Polym. Sci. A-2*, 4 (1966) 731.
6 H. E. PICKETT, M. J. R. CANTOW AND J. F. JOHNSON, *J. Polym. Sci. C*, 21 (1968) 67.
7 S. T. BALKE AND A. E. HAMIELEC, *J. Appl. Polym. Sci.*, 13 (1969) 1381.

8 P. E. PIERCE AND J. E. ARMONAS, *J. Polym. Sci., C*, 21 (1968) 23.
9 L. H. TUNG, *J. Appl. Polym. Sci.*, 13 (1969) 775.
10 G. ARFKEN, *Mathematical Methods for Physicists*, Academic Press, New York, 1966, p. 533.
11 S. T. BALKE AND A. E. HAMIELEC, *6th Intern. Seminar on Gel Permeation Chromatog., Miami Beach, October 1968*.
12 J. W. COOLEY AND J. W. TUKEY, *Math. of Comput.*, 19 (1965) 297.
13 T. VLADIMIROFF, *J. Appl. Polym. Sci.*, 14 (1970) 1397.
14 J. W. COOLEY, P. A. W. LEWIS AND P. D. WELCH, *The Fast Fourier Transform Algorithm and Its Applications*, Research Paper RC1743 IMB Watson Research Center, Yorktown Heights, N.Y., February 9, 1967.

CHROM. 5135

PRECISION IMPROVEMENTS IN GEL PERMEATION CHROMATOGRAPHIC DETERMINATION OF MOLECULAR WEIGHT AVERAGES AND POLYDISPERSITY OF POLYMERS

B. E. HUDSON, JR.
Esso Research and Engineering Company, P.O. Box 121, Linden, N.J. 07036 (U.S.A.)

SUMMARY

Illustrative repeatability data taken before and after certain instrument modifications are presented. Modifications include repiping and optimal adjustment of automatic injection valve, installation of evaporation control device, and insertion of optical diffusor plates in the refractometer sensor. A precision target of 10% relative (2 sigma, 95% confidence) has been consistently surpassed in the case of $\bar{M}_w$, but not quite reached in the case of $\bar{M}_n$. Typical 2-sigma limits for moderately skewed distributions are $\bar{M}_w$: 6–8%, $\bar{M}_n$: ~15%.

INTRODUCTION

Gel permeation chromatography (GPC) has exhibited a phenomenal growth rate as a technique for characterizing the molecular weight distribution (MWD) of polymers. The inherent capability of GPC in graphically presenting in differential form the fine details of complex distributions surpasses by far virtually all other fractionation techniques. In many areas of application, however, the precision with which moderately broad distributions can be characterized numerically in terms of the common molecular weight averages is of prime importance. Long-term as well as short-term repeatability is essential in sustained quality studies of experimental and/or commercial polymer products. Improved and automated data handling systems and the incorporation of correction techniques to enhance accuracy place further emphasis on the need for maximal precision of the initial or raw GPC data. Without reciting an extensive check list for routine maintenance of GPC equipment, the present paper describes three items of adjustment, modification, and addition to standard equipment found necessary in our laboratories to achieve an acceptable degree of short- and long-term precision in the quantitative characterization of polymers. These items include rearrangement and optimal adjustment of the automatic sample injector, installation of optical diffusor plates in the photoelectric detector of the refractometer, and installation of an evaporation control device at the solvent collector siphon.

SPECIFIC INSTRUMENT MODIFICATIONS

Automatic sample injector

Two sources contributing to poor repeatability of GPC results were traced to the manner in which the automatic sample injector system was originally connected in the GPC unit and to the necessity for individually and optimally adjusting six "stop" detents of the loop selector portion of the automatic system. The former led to a persistent difference in GPC peak positions, and consequently mol. wt. averages, according to whether the sample was injected manually or automatically. The latter affected high molecular weights selectively and was manifest as a variation in peak position according to "loop number" of the automatic injector.

In the original arrangement of the automatic and manual injection valves (upper portion, Fig. 1) the effective volume contained in the tubing leading from the loop selector to the auto inject valve and thence to the manual injector served to delay the emergence of all automatically injected samples relative to those injected manually. Interchanging the position of the manual and automatic valves with respect to solvent flow sequence makes it possible to adjust the length of tube (a) in Fig. 1 so that, volumetrically, flow path (a) and flow path (b) are precisely equivalent. Thenceforth, peak emergence volumes (V_e) of manually and automatically injected samples remain precisely equal ($\pm$ 0.03 count) when tested with low molecular weight polymers ($\ll 10^5$) or discrete substances.

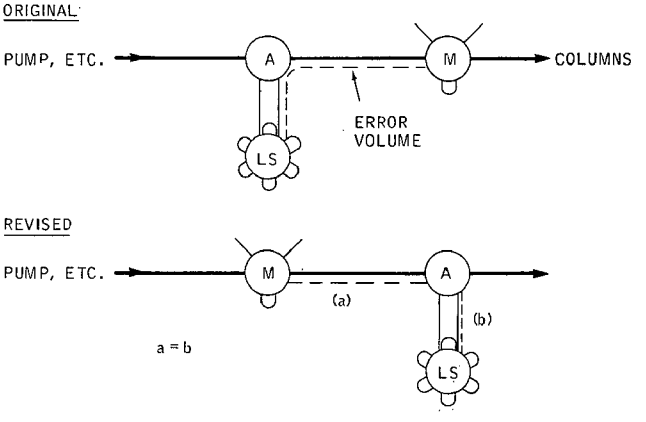

Fig. 1. Rearrangement of GPC injection valves. A = Automatic injection; LS = loop selector; M = manual injection.

Maladjustment of the loop selector valve with respect to the setting of individual position "stops" can lead to molecular shearing of very high-molecular-weight polymers even in dilute solution. This results in larger V_e values (0.05–2.0 counts) for automatically injected aliquots than for manual injections of the same polymer solution. Furthermore, when such a state of maladjustment exists, variations in V_e from one automatic sample loop to another can be observed, as well as poor reproducibility for repetitive injections from the same loop. The effect is greatest at high molecular weights, and a minor maladjustment becomes clearly evident only

if polymers of about 10^7 molecular weight are used for testing. Optimal adjustment of individual position stops of the loop selector overcame this problem.

With the loop selector valve disconnected from the GPC system, compressed nitrogen was supplied to the normal solvent inlet port of the selector through a needle valve, pressure regulator, and T-connected pressure gage. Individual stops were adjusted to halt the loop selector rotation at the center of the region of maximum gas perveyance (lowest indicated pressure). This assures proper registry of internal passageways in normal operation and guards against forcible injection of polymer solutions through partially open passageways. It has been the experience in our laboratory that the newer loop selector valves are less critical with regard to optimal adjustment of individual position stops than was the earlier design (conical insert).

Optical diffusors in differential refractometer

Precise recording of polymer molecular weight distribution curves, as rendered by the GPC column system, requires perfect performance of the strip-chart recorder, the current amplifier preceding it, and the differential refractometer which serves as a polymer concentration (wt./vol.) analyzer. By virtue of the design of the photodetector within the R-4 type refractometer, accuracy and repeatability of polymer molecular weight become rather entirely dependent on micro-uniformity of photocell response over small increments of the sensitive area.

To remove this direct dependence of the accuracy of recorded polymer distribution curves upon individual proporties, optical diffuser plates were installed in front of the photocells. Discs (0.265 in. diameter) of Eastman Kodak opal glass, placed white side toward oncoming light, served as diffusor elements.

While it can be reasoned that the use of optical diffusors in the refractometer is essential in high-precision GPC measurements, it is also difficult to demonstrate advantages in a simple way. In our laboratory, however, installation of the diffusors immediately and apparently permanently eliminated a type of baseline error describable as "post-peak undershoot". More generally, it is felt that greater fidelity of the recorded GPC curve and baseline is assured by the use of the diffusors. Longer photocell life appears to be an added bonus.

Evaporation control

To obtain long- or short-term intercomparability of GPC molecular weight averages of $\pm$ 10 % at the 95 % confidence level requires an overall operating standard deviation (one sigma) of 3.6 %. This must include factors relating to calibration stability and to the fidelity of recording in individual scans. Typically, a set of four columns, 10^6, 10^5, 10^4 and 10^3 Å, exhibiting a resolution index of about 2.5 "counts" per mol. wt. decade is readable to about 2 % in mol. wt. This corresponds to a chart readability (peak position) of 0.03 count and implies a reliability of volumetric accounting equivalent to 0.1 % of solvent (or better) over long as well as short periods of time.

A review of calibration data collected over a two-year period, using the same set of columns, indicated that our precision target was not generally being met, even over selected shorter periods of time. Results of a partial statistical analysis are given in Table I.

Four to nine polystyrene calibrants were monitored over three different time

TABLE I

STATISTICS OF CALIBRATION INSTABILITY

Polymer monitored	*Period duration*	*Number of mol. wt. levels*	*Percent standard deviation, peak mol. wt.*	*Range extremes, % mol. wt.*
PS	2 years	9	13	45 (average of 9)
PS	4 months	4	4	15 (average of 4)
PS	2 months	5	8	33 (average of 5)
PIB	1 month	1	9	29 (max.)

spans and one polyisobutylene calibrant was monitored (daily) for one month. Standard deviation and range are expressed as percent of molecular weight. Only for one 4-month period did the peak position stability approach our target for overall precision of calculated molecular weight averages. More detailed analysis of the accumulated data failed to reveal any long-term trends *versus* time, nor differences in peak position repeatability of high *versus* low molecular weights.

The preceding data were obtained with a Model 100 (R4) GPC instrument operating at ambient temperature in an air-conditioned room. All sample injections were made manually, and the siphon box door kept closed. It became increasingly evident, however, that additional safeguard against variable solvent loss by evaporation at the siphon was necessary. In Table II, column A assumes zero solvent evaporation at the time of calibration. Column B assumes 2 % loss at time of calibration and indicates positive and negative errors in the readout of peak molecular weights from the calibration chart as evaporation increases and decreases. An average evaporation of 2 %, slowly varying from 1 % to 3 %, could indeed explain the peak position variations observed and discussed earlier.

TABLE II

CALCULATED EFFECT OF VARIABLE SOLVENT EVAPORATION

Assumed solvent loss (%)	*Δ GPC (counts)*	*Δ % Mol. wt.*	
		A	*B*
0	0	0	−60
1	−0.3	+ 28	−32
2	−0.6	+ 60	0
3	−0.9	+100	+40

Simple experiments in which the column outlet tube was raised above and lowered into the neck of the glass siphon confirmed the approximate magnitude (and direction) of the effects of evaporation on calibrant peak positions. Further, a crude anti-evaporation device consisting of a two-hole cork connecting the chromatograph outlet tube to the siphon neck, and a solvent-saturated breather bottle gave immediate short-term improvement of GPC peak position stability (Table III).

In view of the five-fold short-term precision improvement achieved, a more

TABLE III

SHORT-TERM TEST OF ANTI-EVAPORATION DEVICE

Five sequential runs.

	Without evaporation control	*With evaporation control*	
		1st Test	*Again (1 week later)*
Average deviation (% mol. wt.)	10	2.0	2.2

permanent evaporation control device was installed as shown in Fig. 2. A 60-day test confirmed that an order of magnitude greater stability of peak position was being obtained with the use of the evaporation control device. Variations were of the order of chart readability (0.03 count, 2 % mol. wt.), and seldom more than double this.

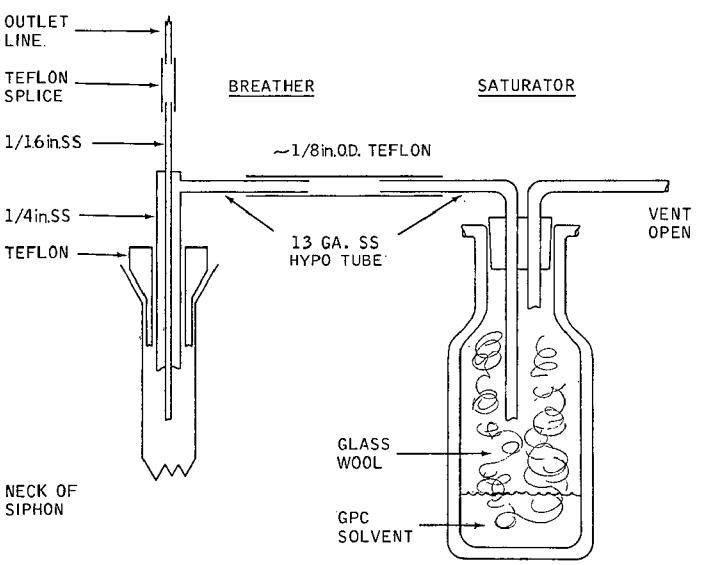

Fig. 2. Anti-evaporation device — GPC siphon.

REPEATABILITY OF MOLECULAR WEIGHT AVERAGES AND POLYDISPERSITY INDEX

In our laboratories, one Model 100 (R4) GPC instrument is utilized exclusively for the characterization of experimental and commercial specimens of polyisobutylene and butyl rubber. The latter is a copolymer of isobutylene with, usually, very small amounts of isoprene. For this application, the GPC instrument is operated at ambient temperature in an air-conditioned room (constant temperature, 23°). The solvent is tetrahydrofuran (THF). The instrument is calibrated directly in molecular weight units through the use of a series of polyisobutylene standards covering the mol. wt. range 500 to 2×10^6.

Features of quality control system

To determine impartially the precision of molecular weight averages and polydispersity as rendered by the GPC method, a statistical analytical quality control system is employed. Four polymer specimens, differing from each other in mean (peak) molecular weight and/or polydispersity were selected to bracket in general the corresponding properties of "unknown" specimens to be characterized. These quality control (QC) standards are then encoded as unknowns and randomly interspersed with genuine unknowns by the submitters. A submitter may maintain his own QC chart for the quality control standards he submits. All results from all QC standards are, however, relayed to a central group who monitor not only GPC, but numerous other instrumental and chemical analytical methods currently in use. Here, floating mean values of M_w, M_n and M_w/M_n are logged along with the average range based on successive pairs of results. From these data the standard deviation (one sigma) is derived, and an allowable spread (2.77 sigma) between successive results is computed. Deviation of a single result from the mean by more than three sigma, or a difference between successive results of more than 2.77 sigma constitutes an out-of-control signal. Possible causes are then investigated.

Characteristics of QC standard samples and calibration stability

Table IV gives the characteristics of the four QC standards in terms of mol. wt. averages and polydispersity. The values given represent the grand average (mean) of all GPC runs performed over a period of one year. The indicated number of runs per sample approaches a target schedule of one run per QC standard per week. In the lower part of the table, the percentage change of mean values from one three-month period to the next (averaged for the four standards) is indicated to be of the order of 1 % (0.6–1.1), *i.e.*, less than chart readability. The range over the year is indicated to be nearer 2 % (1.4–2.5). Detailed examination of quarterly data showed, however, that this comparatively large shift (comparable to chart readability) occurred, in each instance, between the first 3-month period and the second. Generally a high degree of stability was exhibited over the last three-quarters of the year.

TABLE IV

CHARACTERISTICS OF POLYISOBUTYLENE GPC QUALITY CONTROL STANDARDS AND STABILITY OF MEAN VALUES OVER 1 YEAR

Standard sample	*No. of runs*	$\bar{M}_w \times 10^{-5}$	$\bar{M}_n \times 10^{-5}$	$\bar{M}_w/\bar{M}_n$
A	32	20.5	7.55	2.72
B	50	10.6	1.37	7.87
C	46	8.51	2.60	3.27
D	36	6.54	2.28	2.88
% Average Δ/3 months		0.6	1.0	1.1
% Range/year[a]		1.4	2.5	2.4

Chart readability ~ 2 % (mol. wt.)

[a] Not a progressive drift, originated principally during 1st 6 months (1st 3 months *vs.* 2nd 3 months).

Replication precision: $\bar{M}_w$, $\bar{M}_n$ *and* $\bar{M}_w/\bar{M}_n$

While long-term calibration stability is a necessary prerequisite, many other factors enter into the quantitative repeatability of GPC characterization of polymer specimens. The recipient of final data is genuinely interested in its general degree of correctness, especially with regard to repeatability for a given sample and the precision limits to be considered when comparing data from different samples. (It seems reasonable to suppose, or at least tentatively assume, that accuracy and precision are commensurate when GPC calibrations are based on carefully evaluated specimens of the same type polymer as the unknowns being characterized.)

The precision data derived from repetitive GPC runs in our quality control program are summarized briefly in Table V. Here "sigma" has its usual statistical definition and significance. In general, the $\bar{M}_w$ precision was well within our arbitrary target (95 % confidence, 2 sigma = 10 %), but in the case of $\bar{M}_n$ and therefore $\bar{M}_w/\bar{M}_n$, this target was not quite met. In a collective sense ($\bar{M}_{\mathrm{rms}}$, $2\sigma = 9\,\%$), the target may be said to have been closely approximated. It is pertinent to note that 1.2 sigma corresponds to the average *de-facto* difference between successive runs. Out of 164 GPC runs performed collectively on four different QC standards, three runs were judged "out of control" (value reported deviated from pre-established mean by more than 3 sigma). Theory predicts two.

In Table VI the precision data for the four QC polymer standards are separately listed. In conjunction with the characteristics of the four standards (Table IV), it will be noted that the $\bar{M}_w$ reproducibility is slightly poorer at the highest mol. wt. level (A, $\bar{M}_w = 2.0 \times 10^6$) than at lower levels. Also, $\bar{M}_n$ reproducibility is notably poorer when polydispersity is large ($\bar{M}_w/\bar{M}_n > 3$). Although the effects of asymmetry of distribution on precision are not discussed here, it should be stated that all four

TABLE V

GPC PRECISION, ONE SIGMA AVERAGE FOR FOUR QC STANDARDS, 164 GPC RUNS, 3 "OUT OF CONTROL"

$\bar{M}_w$	$\bar{M}_n$	$\bar{M}_w/\bar{M}_n$
3.0 %	7.9 %	7.8 %

TABLE VI

GPC PRECISION LIMITS FOR A ONE-YEAR PERIOD AS DETERMINED ON FOUR QUALITY CONTROL STANDARDS

Standard sample[a]	*Standard deviation, one sigma (% of mean)*		
	$\bar{M}_w$	$\bar{M}_n$	$\bar{M}_w/\bar{M}_n$
A	4.0	6.4	5.9
B	2.8	8.7	10.0
C	2.6	10.0	9.0
D	2.4	6.5	6.2
Average	3.0	7.9	7.8

[a] Characteristics of individual standards and number of GPC runs each are given in Table IV.

QC standards were, in varying degrees, perceptibly asymmetric. One might expect that for moderately narrow and symmetric distributions, $\bar{M}_w$ and $\bar{M}_n$ precision would be nearly equal. It is felt that the consistently poorer precision of $\bar{M}_n$ is associated with uncertain baseline interpolation, especially in the low-molecular-weight region of the overall distribution. Further work, in our laboratories and/or others, may determine whether computer methods for baseline estimation can be superior to manual procedures.

NOTE

A solvent flow rate of 1.0 ml/min through the sample columns was maintained throughout the present work. Previously, in studying the effect of flow rate on GPC column performance, LITTLE *et al.*[1] and YAU *et al.*[2] applied corrections for evaporative solvent loss, especially at low flow rates. The latter investigators utilized, in some instances, a vapor feedback device to minimize evaporative loss.

REFERENCES

1 J. N. LITTLE, J. L. WATERS, K. J. BOMBAUGH AND W. J. PAUPLIS, *Polym. Preprints*, 10 (1968) 326.
2 W. W. YAU, H. L. SUCHAN AND C. P. MALONE, *J. Polym. Sci. A-2*, 6 (1968) 1349.

CHROM. 5136

CAUSES OF SKEWED MOLECULAR WEIGHT DISTRIBUTIONS IN GEL PERMEATION SEPARATION OF NYLON RESINS

E. K. WALSH
Allied Chemical Corporation, P.O. Box 309, Morristown, N.J. 07960 (U.S.A.)

SUMMARY

Gel permeation separations of nylon resins using phenol type solvents are characterized by extended tailing in the low-molecular-weight region. Number average molecular weights ($\bar{M}_n$) calculated from these chromatograms are abnormally low. The resultant molecular weight distributions ($\bar{M}_w/\bar{M}_n$ ratios) are broad.

This report contains investigations of possible causes for tailing of low-molecular-weight nylon species. Studies include thermal and oxidative degradations of resin solutions, flow rate, overloading and elution temperature levels. While none were found to cause tailing, the latter does effect the extent to which the tail is formed. Work with fractions and small molecule homologs of nylon and their comparisons with other resin types in universal calibration plots shows adsorption of low-molecular-weight species on the styrogel separating medium to be the primary cause of tailing. The degree of adsorption is shown to be a function of the ratio of polar ends to polymer chain length.

INTRODUCTION

Gel permeation chromatographic (GPC) separations of nylon 6 resins using phenol solvents in these laboratories have consistently shown tailing of low-molecular-weight species. Similar skewness in the distributions of polyamide resins is evident in the chromatograms shown in published literature[1,2]. Abnormally low number average molecular weights are calculated from these chromatograms. These low values produce broad molecular weight distributions (large weight to number average molecular weight ratios). Molecular parameters measured on nylon resins by classical techniques show nominal values of 2.0 for this ratio. The latter measurements confirm theoretical predictions based on kinetic studies of nylon resin polymerizations.

Broadening in gel permeation defined molecular weight distribution is common to all materials. It is caused by a diffusional process inherent in this type of chromatography. The broadening evident in GPC separations of nylon resin appears substantially different (1) in chromatogram shape from other resin types and (2) in excess of that due to dispersion processes.

Both theoretical and classical definitions of molecular weight distributions in nylon polymerizations have firm foundations. An explanation for molecular weight

distribution broadening, other than that due to a dispersion process, was sought. Verification of an obvious cause, resin adsorption on the styrogel separating medium, was not easily established. To ascertain the cause, all parameters which might conceivably contribute to molecular weight distribution broadening of nylon resins except inherent dispersion, were investigated. This paper relates the results of this investigation.

EXPERIMENTAL

Nylon separations were accomplished with a Waters Associates Inc. Model 200 GPC instrument. Orthochlorophenol was used to prepare and elute solutions of polymers through the instrument. The solvent was distilled under vacuum prior to use. It was continuously purged with purified nitrogen while in the reservoir of the GPC unit. Degassed at 150°, the solvent was metered through the styrogel columns at a 1 cc/min flow rate. Injection port, oven, refractometer and collection areas were maintained at 100°. A Hallikainen temperature controller regulated the temperature of the refractometer heat exchanger.

Two sets of styrogel columns purchased from Waters Associates were used in this work. The majority of separations were accomplished with three columns designated 10^5, 10^4 and 10^3 Å. Comparisons were made with a second set of three columns designated 10^6, 5×10^4 and 5×10^3 Å.

Five tenth percent (0.5 %) concentrations of nylon resin in *o*-chlorophenol, prepared at ambient temperature, were forced through a Waters filter unit maintained at 100°. Prior to injection, the solutions were held for approx. 20 min in an oven maintained at 105°. A 90 sec injection time, 7.5 mg loading, and a 2 × amplification was adopted as standard procedure in this work.

A Brice Phoenix Model 1000 light scattering photometer was used to measure the weight average molecular weights of polymer samples. Nylon whole resins and fractions were dissolved in 90 % formic acid buffered with 0.5 *M* potassium chloride. Measurements were made at ambient temperatures at a wavelength of 546 mμ. The majority of values were calculated from scattered light intensities measured at 90° and 0° angles. Very small corrections for scattering dissymmetry, measured at 45° and 135°, were applied. Multiangle scattered light intensity measurements on three nylon samples gave molecular weights equivalent to those obtained by 90° and 0° angular measurements.

Differential refractive index measurements were obtained with a Brice Phoenix unit. High temperature measurement capability was provided by circulating fluid to the insulated cell area from a bath maintained at the desired level.

Viscosities of polymer solutions were measured in No. 75 Cannon Ubbelohde viscometers at 100°. Flow times of *o*-chlorophenol were 100 sec or greater. No kinetic energy corrections were applied. Initial polymer concentrations of 0.5 g/dl were diluted in three steps to a final concentration of 0.125 g/dl. Intrinsic viscosities were defined by extrapolating four point viscosity-concentration plots to zero concentration.

RESULTS AND DISCUSSIONS

Typical GPC chromatograms of medium- and high-molecular-weight hydrolytically polymerized nylon 6 resins are shown in Figs. 1 and 2. Tailing in the low-

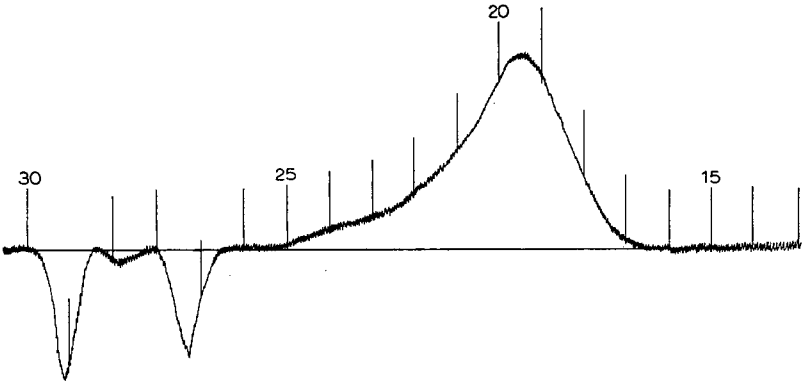

Fig. 1. Nylon 6, 19 500 g/m, water extracted and dried 0.5%, 90 sec, 1 cc/min, 2 ×, *o*-chlorophenol at 100°. Columns: 10^6, 5 × 10^4, 5 × 10^3 Å.

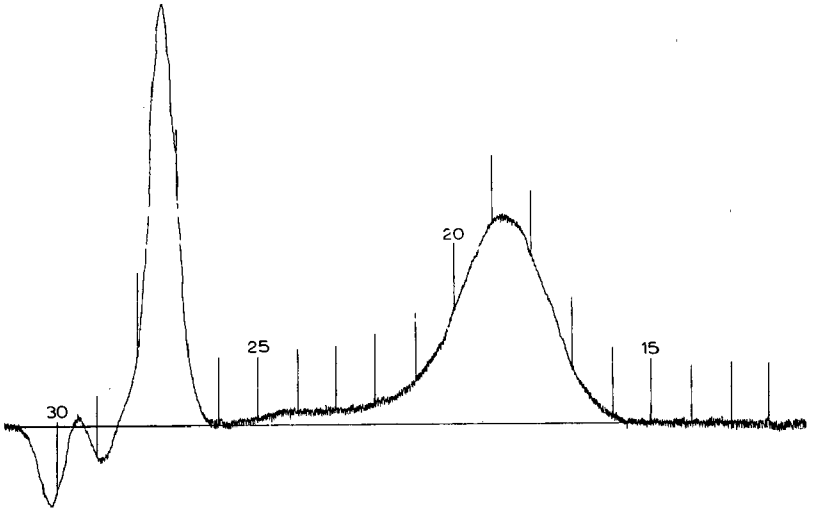

Fig. 2. Nylon 6, 44 000 g/m, water extracted and dried 0.5%, 90 sec, 1 cc/min, 2 ×, *o*-chlorophenol at 100°. Columns: 10^6, 5 × 10^4, 5 × 10^3 Å.

TABLE I

NYLON 6 MOLECULAR WEIGHT PARAMETERS DEFINED BY GPC AND CLASSICAL TECHNIQUES

Sample	*GPC*			*Classical*		
	$\bar{M}_w$	$\bar{M}_n$	$\bar{M}_w/\bar{M}_n$	$\bar{M}_w$[a]	$\bar{M}_n$[b]	$\bar{M}_w/\bar{M}_n$
Medium $\bar{M}$ nylon 6	44 000	9 300	4.7	38 000	19 500	1.9
High $\bar{M}$ nylon 6	97 700	16 500	5.9	88 700	44 000	2.0

[a] Determined by light scattering techniques.
[b] Determined by end group and osmotic techniques.

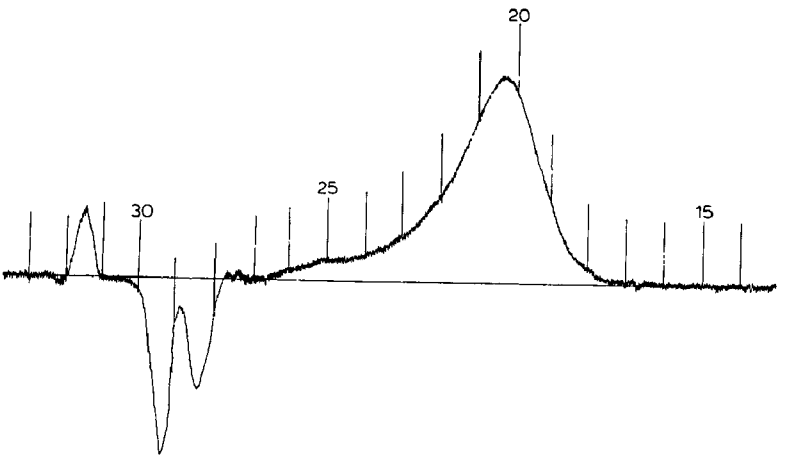

Fig. 3. Nylon 6, 19500 g/m, water extracted and dried 0.5%, 90 sec, 1 cc/min, 2 ×, *o*-chlorophenol at 100°. Columns: 10^5, 10^4, 10^3 Å.

molecular-weight region appears as the predominant characteristic of these chromatograms. Weight and number average molecular weights calculated from these chromatograms and from classical measurements are shown in Table I. These values illustrate the extent of molecular weight distribution broadening in GPC separations of nylon resins. Since the styrogel columns used in this work were calibrated with nylon fractions, one would expect differences in molecular parameters to be due solely to the inherent diffusional character of the styrogel columns. Yet comparisons with other resins, polystyrene for example, show the nylon resins to be excessively broadened during elution.

In our limited experience, the use of a different column set shown in Fig. 3 did not effect the shape of the low-molecular-weight portion of the chromatogram. Nor could impurities present in the *o*-chlorophenol account for the observed tailing. Such impurities always eluted at retention volumes 5 cc or more (1 or more counts) removed from the area of interest. They have, however, been previously cited as a major contributor to the imperfection of polyamide GPC distributions[1].

One would expect tailing of low-molecular-weight species to be exaggerated in chromatograms of both a low-molecular-weight nylon fraction and the lowest-molec-

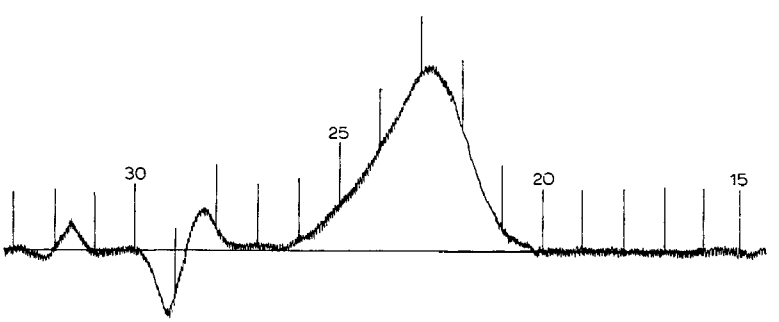

Fig. 4. Nylon 6 fraction, 6900 g/m, 0.5%, 90 sec, 1 cc/min, 2 ×, *o*-chlorophenol at 100°. Columns: 10^5, 10^4, 10^3 Å.

ular-weight nylon homolog, aminocaproic acid. Chromatograms obtained with 5.0 mg loadings of aminocaproic acid are totally obscured by solvent impurities. The results obtained with higher loadings are discussed in a later section of this report. The chromatogram of the lowest-molecular-weight nylon fraction, isolated by preparative scale fractionation techniques, is shown in Fig. 4. Surprisingly little evidence of tailing is observed in this chromatogram. Since no explanation for low-molecular-weight tailing was obtained from this work, it was thought that the problem was caused by some operational variable. An investigation of parameters which could possibly cause molecular-weight distribution broadening in nylon resins was initiated. The parameters studied were degradation, overloading, flow rate and temperature. Of these, only the latter gave an indication of causing change in the molecular weight distribution of nylon resins.

Solution degradation of nylon 6 resin in *o*-chlorophenol at 100° was evaluated by viscosity measurements. Three solutions prepared at ambient temperature, each consisting of 0.5 % concentrations of a high-molecular-weight nylon 6 resin, were maintained at 100°–105° for ~ 30 h. Viscosities measured at various time increments over this period decreased at a rate of 0.8 to 1.0 % per h for the first 3 to 4 h and at < 1.0 % per h for the remaining time period. Since the time required to complete elution of nylon species in GPC separations is ~ 3 h, the estimated maximum degradation possible is of the order of 3 %. Degradations of this type are known to be random. Their contribution to extended low-molecular-weight tailing must be minor. In addition, chromatograms of solutions of resins held 4 to 6 h at 100° prior to injection, show no significant difference from chromatograms obtained on samples injected into the system in the normal manner.

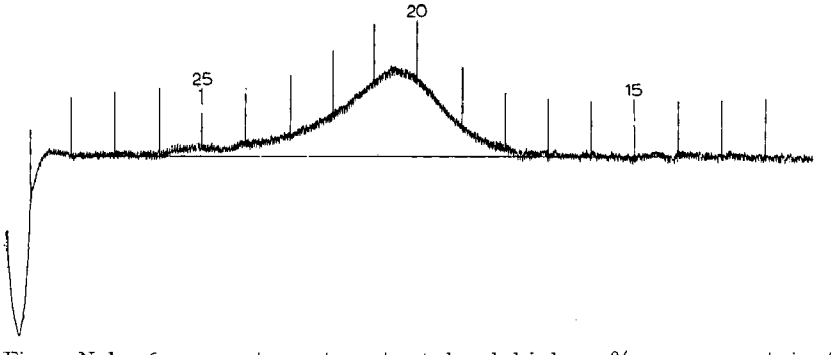

Fig. 5. Nylon 6, 19500 g/m, water extracted and dried 0.25 %, 90 sec, 1 cc/min, (3.75 mg), 2 ×, *o*-chlorophenol at 100°. Columns: 10^5, 10^4, 10^3 Å.

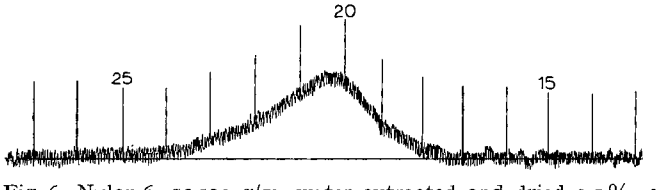

Fig. 6. Nylon 6, 19500 g/m, water extracted and dried 0.1 %, 90 sec, 1 cc/min; (1.5 mg), 4 ×, *o*-chlorophenol at 100°. Columns: 10^5, 10^4, 10^3 Å.

Chromatograms illustrating the effect of various load levels of nylon 6 resins are shown in Figs. 3, 5 and 6. A normal loading of 7.5 mg is shown in Fig. 3. Figs. 5 and 6 show 1/2 (3.75 mg) and 1/5 (1.5 mg) of normal loading level, respectively. Both reduced load levels show definite evidence of low-molecular-weight tails, although close inspection is required to distinguish the tail at the 1.5 mg load level. It is of interest to note that integral plots of data derived from chromatograms obtained using the 7.5 and 3.5 mg loadings are equivalent within experimental error. Overloading effects typified by polystyrene eluted with tetrahydrofuran show a shift in the peak elution volume, but give little or no evidence of tailing.

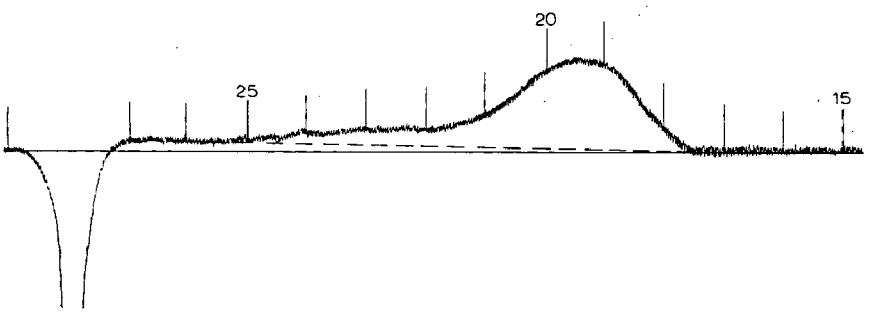

Fig. 7. Nylon 6, 19500 g/m, water extracted and dried 0.5%, 90 sec, 0.27 cc/min, 2 ×, *o*-chlorophenol at 100°. Columns: 10^5, 10^4, 10^3 Å.

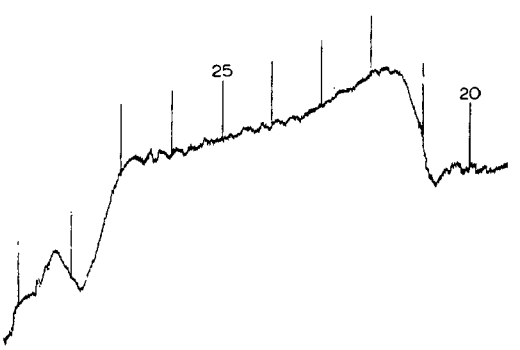

Fig. 8. Nylon 6, 19500 g/m, water extracted and dried 0.5%, 60 sec, 0.85 cc/min, 2 ×, *o*-chlorophenol at 40°. Columns: 10^5, 10^4, 10^3 Å.

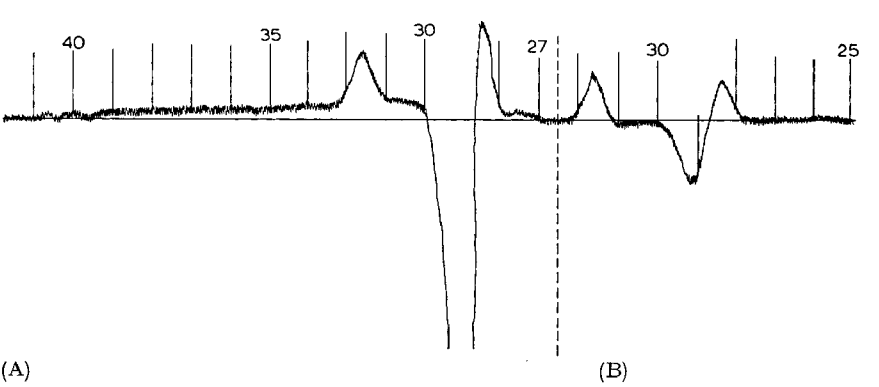

(A) (B)

Fig. 9. Aminocaproic acid. (A) 1%, 90 sec, 1 cc/min, 2 ×, *o*-chlorophenol at 100°. Columns: 10^5, 10^4, 10^3 Å. (B) Solvent; *o*-chlorophenol at 100° C, 90 sec, 1 cc/min, 2 ×. Columns: 10^5, 10^4, 10^3 Å.

A chromatogram illustrating the effect of change in flow rate is shown in Fig. 7. The flow has been reduced to 0.27 ml/min. It is quite clear from this chromatogram that low-molecular-weight tailing persists at this low flow rate.

The effect of temperature on nylon chromatographic separations is shown in Fig. 8. This reduced temperature level necessitated the use of maximum available pressure to maintain the 1 cc/min flow rate. The high pressure made base line stability untenable. The chromatograph obtained, however, shows evidence of both a delayed response and a drawn out shape. Both are indicative of an absorptive type mechanism.

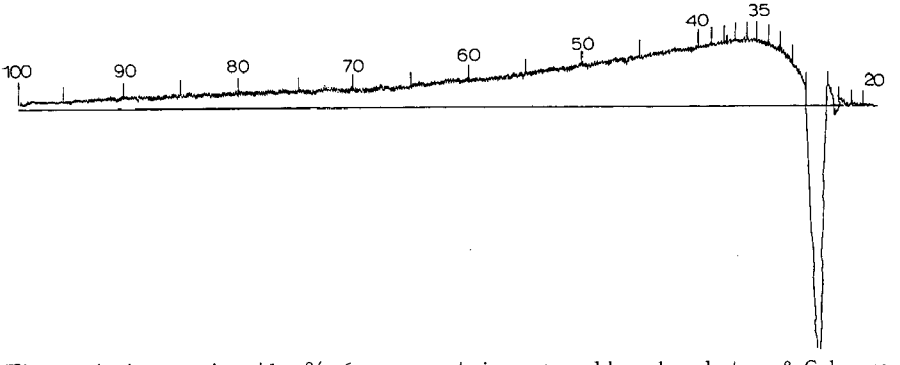

Fig. 10. Aminocaproic acid, 5%, 60 sec, 1 cc/min, 2 ×, *o*-chlorophenol at 100°. Columns: 10^5, 10^4, 10^3 Å.

None of these parameters, either alone or in combination, can explain the cause of tailing in GPC separations of nylon resins. If the cause is due to adsorption, as indicated by chromatogram shifts with temperature change, it must be evident in the chromatograms of the lowest-molecular-weight homolog of nylon 6 resins, aminocaproic acid. As stated previously, a loading of 5.0 mg shows little more than solvent impurity effects. Both, unfortunately, elute at approximately the same retention volume. Chromatograms of higher aminocaproic acid loadings, 15 and 50 mg, are shown in Figs. 9 and 10. Included in Fig. 9 is a chromatogram of the impurities in the *o*-chlorophenol solvent, collected at the same time and treated in the same manner as that used to prepare the aminocaproic acid solution. Both chromatograms of aminocaproic acid are equivalent, the higher loading being an exaggerated copy of the lower loading. Their interpretation is difficult since both down and up scale re-

TABLE II

EFFECT OF POLAR END–DEGREE OF POLYMERIZATION

	Ratio on GPC response			
	A.C.A.	*Nylon 6 fraction*	*Nylon 6 resin*	*Lactam*
$\bar{M}_w$	131	6900	40 000	113
Polar ends/DP	2	0.03	0.005	0
D.R.I.[a]	+0.035–0.040	+0.048	+0.050	+0.040–0.045
GPC response[a]	absorbed on gel	retention volume deviates from U.C.C.	broad distribution	retention volume fits on U.C.C.

[a] *o*-Chlorophenol at 100°.

fractive index changes are clearly evident. Such differences in solute refractive index indicate the presence of two materials having different structures. Their proportion, estimated from Fig. 10, is 15 and 85 %. Yet the use of essentially pure aminocaproic acid was indicated from melt temperature and IR spectral analysis. Also, if the material responsible for the down scale refractive index change is due to aminocaproic acid then its refractive index is appreciably different from the nylon polymer and from caprolactam, both of which show up scale refractive index changes. Such differences or similarities in solute–solvent refractive indexes should be capable of resolution by use of the Brice Phoenix differential refractometer. Table II contains the results of such measurements on aminocaproic acid, a low-molecular-weight fraction of nylon 6, the whole nylon 6 resin and caprolactam. *o*-Chlorophenol was used to prepare all solutions. Measurements were made at 100°. These conditions are equivalent to those used in GPC separations. The positive sign is placed before all the differential refractive index values to indicate that the refractive index of all solutes were observed in these measurements to have values greater than the solvent. The apparent discrepancy between aminocaproic acid values obtained from the two respective measurements, the GPC detector and the Brice Phoenix unit, seems to be a function of the proportions of the two materials present. This ratio is believed affected by the difference in solution residence time at temperature required for each measurement. Solution preparation and measuring time with the Brice Phoenix instrument is approximately one-eighth of that required for GPC measurements. Such time–temperature studies using the Brice Phoenix instrument, however, were inconclusive. Difficulties experienced in accurate measurements of these low values precludes the possibility of establishing a definite conclusion.

The data presented indicates that the material causing the sharp down scale refractive index change in the GPC chromatogram of aminocaproic acid is caused by a reaction product of aminocaproic acid and the solvent. The unreacted aminocaproic acid is responsible for the upscale refractive index change in the chromatogram. It is readily evident from Fig. 10, that this unreacted aminocaproic acid portion is being slowly desorbed from the styrogel separating medium.

It has been shown in Fig. 4, that very little evidence of low-molecular-weight tailing can be observed in a low-molecular-weight fraction of a nylon 6 resin. Tailing, however, is readily evident in the chromatograms of both the whole nylon resin and its lowest-molecular-weight homolog, aminocaproic acid. The GPC response to varying chain length nylon species is shown in Table II on lines 2 and 4. One would normally expect increased adsorption with an increase in functional groups per unit polymer chain length. A convenient means of relating the two parameters, GPC response and functional or polar groups per unit chain length, is provided by the universal calibration concept initially demonstrated by BENOIT *et al.*[3]. Its main tenet implies that if diffusion is the sole mechanism operating in the GPC separation process, then the hydrodynamic volume or size of random coiled polymers is the controlling factor in determining the retention volume at which a given chain length species will elute. A relative measure of the hydrodynamic size is provided by the product of the intrinsic viscosity and molecular weight. Retention volume is the volume measured from sample inject to the peak of the chromatogram. Such measurements are shown in Table III for fractions of polystyrene, polyoxazoline and nylon 6 resins and for caprolactam. Peak retention volumes are given in terms of counts. Molecular weights

TABLE III

RETENTION TIME MOLECULAR WEIGHT DATA

Material	*Count*	$\bar{M}_w$	$[N]$[a]	$[N]\bar{M}_w$
PMA[b]	16.55	541 000	1.21	655 000
PMA[b]	17.525	209 000	0.80	167 200
PS[c]	16.16	860 000	1.82	1 565 000
PS[c]	17.11	340 000	0.95	323 000
PS[c]	18.77	89 000	0.39	34 700
PS[c]	21.95	10 300	0.09	1 000
Nylon	18.24	169 000	1.24	210 000
Nylon	18.4	132 000	1.05	138 500
Nylon	18.66	115 000	0.968	115 000
Nylon	19.6	62 000	0.624	38 600
Nylon	21.6	20 600	0.275	5 700
Nylon	23.3	6 900	0.12	827
Caprolactam	26.5	113	0.03	3.39

[a] [N] = intrinsic viscosity.
[b] PMA = polyethyloxazoline.
[c] PS = polystyrene.

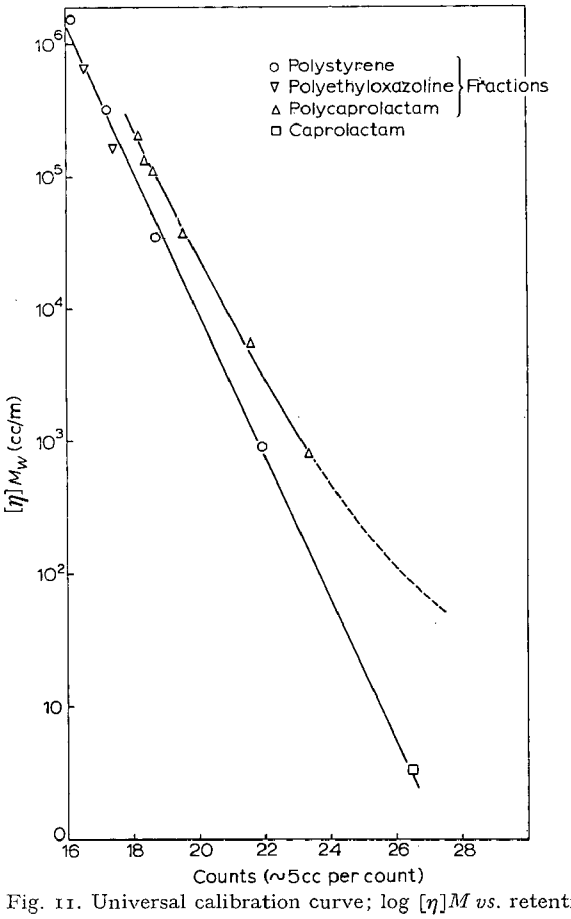

Fig. 11. Universal calibration curve; log $[\eta]M$ *vs.* retention volume.

shown are weight average values. Intrinsic viscosities of polymer fractions were determined in *o*-chlorophenol at 100°, the same conditions used to obtain their GPC chromatograms. A plot of this data is shown in Fig. 11. Readily evident is the conformity of fractions of the non-polar resins, polystyrene, polyoxazoline and of caprolactam, to a common curve in this universal calibration plot. Diffusion is indicated as the sole separation mechanism for these materials. Nylon fractions are displaced from this curve by 0.6 of a count (~ 3.0 cc) at a hydrodynamic volume of 10^5 cc/m. This displacement increases to approximately 2.3 counts (~ 11.5 cc) at a hydrodynamic volume of 10^2 cc/m.

These results show that in addition to dispersion another mechanism is controlling the separation of varying chain length species of nylon resins in styrogel media. The delayed response and extended low molecular weight tailing support an adsorption type mechanism. Both long and short chain length species of nylon resins are adsorbed on styrogel separation media. The strength of the adsorption bond increases as the functional group per unit chain length increases.

Adsorption of a similar type was described in GPC analysis of carboxy terminated polybutadienes[4]. It was reduced by selecting those styrogel columns which by trial and error elution experiments showed little or no adsorption of the resin. It is possible that a similar selection of styrogel columns could affect a reduction, or perhaps elimination, in the adsorption of nylon resins. Our experience with the use of different styrogel columns in this laboratory is very limited.

CONCLUSION

Adsorption accompanied by slow release of molecular weight species in 5000 to 2000 g/m range is primarily responsible for the tailing observed in GPC chromatograms of nylon resins.

ACKNOWLEDGEMENTS

I would like to express my appreciation to A. CLARK and T. CHOU for the GPC and intrinsic viscosity measurements used in this report and to Allied Chemical Corporation for permission to publish this data.

REFERENCES

1 J. D. GOVIER, L. G. PRINCE AND H. E. STAPELFELDT, *6th Intern. Seminar Gel Permeation Chromatog., Miami Beach, 1968.*
2 C. V. GOEBEL, *Proc. 4th Intern. Seminar Gel Permeation Chromatog., Miami Beach, 1967.*
3 Z. GRUBISIC-GALLOT, P. REMPP AND H. BENOIT, *J. Polym. Sci., B*,5 (1967) 753.
4 R. M. SCREATON AND R. W. SIEMANN, *J. Polym. Sci., C*, 21 (1968) 297.

CHROM. 5139

GEL PERMEATION CHROMATOGRAPHIC CALIBRATION FOR POLYMERS MAKING USE OF THE UNIVERSAL CALIBRATION CURVE*

M. C. MORRIS
Goodyear Tire and Rubber, 142 Goodyear Boulevard, Akron, Ohio 44316 (U.S.A.)

SUMMARY

It is usually difficult to obtain narrow molecular weight distribution samples of a given polymer for calibrating the gel permeation chromatographic instrument in the conventional way. The literature reports several methods which have been used to obtain instrument calibrations with samples of broad distribution polymer. However, these methods generally must assume a linear calibration of the logarithm of molecular weight *versus* elution volume. This assumption may lead to significant errors in precise molecular weight distribution computations. It is possible to avoid this assumption by making use of the universal calibration curve proposed by BENOIT without the necessity of defining this curve by any mathematical function. A number of methods have been developed for combining the universal calibration curve with measurable parameters of the polymeric material (such as intrinsic viscosity, number average molecular weight and weight average molecular weight) to calculate molecular weight distributions.

Results will be reported on a careful evaluation of the accuracy and reproducibility of several of these methods.

INTRODUCTION

In order to provide quantitative data from gel permeation chromatographic (GPC) traces it is necessary to have an instrument calibration, *i.e.*, a relation between elution volume and molecular weight eluted. For a given GPC apparatus such a calibration will depend upon the chemical nature of the polymer. The most direct method of calibration consists of using narrow distribution samples of the same chemical nature as the experimental samples to be analyzed. The application of such a method is limited by lack of readily available narrow distribution samples of different chemical structures. An attempt to make allowances for differences in chemical structure was the Q factor approach[1,2] which stated that the molecular species eluting at a given point is related to the size of the polymer chain. The size of the chain is assumed to be proportional to its molecular weight by a constant factor which depends on chain structure. Thus, having determined a calibration curve for one polymer type, say polystyrene using narrow distribution samples, the use of an appropriate Q factor allows a calibration to be calculated for another polymer type. However, this approach

* Contribution No. 461 from the Goodyear Tire and Rubber Co., Research Laboratory, Ohio.

has not been found to be sufficiently accurate for most work[3]. However, an alternate and only slightly more complicated scheme for obtaining calibrations has been made possible by new developments in GPC theory. It was observed by BENOIT *et al.*[4] that for all polymers studied, a plot of molecular weight times intrinsic viscosity *versus* elution volume gave data that fell on a common curve. Thus, the calibration for any polymer may be defined by knowledge of the universal calibration for the column set involved along with the relationship between molecular weight and intrinsic viscosity for the particular polymer type involved. If the Mark-Houwink relationship is considered adequate the problem resolves itself into finding a way to establish the Mark-Houwink constants K and a from data on broad molecular weight distribution materials. An interesting method for accomplishing this has been reported[5], the mathematical basis for the method will be presented followed by an experimental test of the usefulness and validity of the technique.

MATHEMATICAL BASIS FOR CALIBRATION[5]

For the purpose of simplification and use of the universal calibration curve the parameter J is defined as the product of the intrinsic viscosity times the molecular weight:

$$J_i = [\eta]_i M_i \tag{1}$$

The function J with elution volume is considered to be independent of polymer type[4] and hence may be provided from a calibration curve with narrow distribution polystyrene samples. Making use of the Mark-Houwink relationship:

$$[\eta]_i = KM_i^a \tag{2}$$

and taking for the whole polymer:

$$[\eta] = \Sigma_i W_i [\eta]_i \tag{3}$$

where W_i $[\eta]_i$ and M_i are the weight fraction, viscosity and molecular weight respectively of the i-th species, then it follows directly that:

$$[\eta] = K^{1/(a+1)} \Sigma_i W_i J_i^{a/(a+1)} \tag{4}$$

and:

$$M_n = K^{-1/(a+1)} / \Sigma_i (W_i / J_i^{1/(a+1)}) \tag{5}$$

Use of intrinsic viscosities with GPC curves to obtain calibration

By taking two polymers of broad distribution and the same chemical nature but with different viscosities and measuring their intrinsic viscosities and GPC traces in the same solvent, then from eqn. 4:

$$\frac{[\eta]_1}{[\eta]_2} = \frac{\Sigma W_{i1} J_i^{a/(a+1)}}{\Sigma W_{i2} J_i^{a/(a+1)}} \tag{6}$$

In the equation W_i values are obtained from the ordinate of the GPC trace and hence a may be determined since it is the only unknown. The parameter K may then be determined through eqn. 4 using data from one of the polymers.

The use of the intrinsic viscosity and number average molecular weight to obtain calibration

By combining eqns. 4 and 5 we obtain:

$$[\eta]M_n = \Sigma_i W_i J_i^{a/(a+1)} / \Sigma(W_i / J_i^{1/(a+1)}) \quad (7)$$

The corresponding result published by WEISS AND COHN-GINSBERG[5] contains a typographical error.

By taking a single polymer sample of broad distribution and known number average molecular weight and intrinsic viscosity and obtaining a GPC trace, the application of eqn. 7 allows a to be calculated followed by K from eqn. 5.

It should be noted that in eqns. 6 and 7 there is not a simple analytical solution for a. In practice the right hand side of eqn. 6 or eqn. 7 is evaluated for several values of a and an interpolation is performed to find the value of a which yields the desired value of the function. The actual calculations are carried out using a computer program.

EXPERIMENTAL

Universal calibration with polystyrene

The narrow molecular weight distribution polystyrene standards made by the Pressure Chemical Co and furnished to us by Waters Associates were used to establish the universal calibration curve. The viscosities of these standards were determined in THF at 30° using a Cannon dilution type micro-viscosimeter. All solutions and solvent were filtered through a glass frit before entering the viscosimeter. The original concentrations were adjusted so that the longest flow time was less than twice the solvent flow time. The results of the viscosity determinations are given in Table I. A plot of the logarithm of viscosity *versus* the logarithm of molecular weight is given as Fig. 1. Data points from the work of BENOIT *et al.*[4] are plotted as triangles. These are seen to be in good agreement with this work.

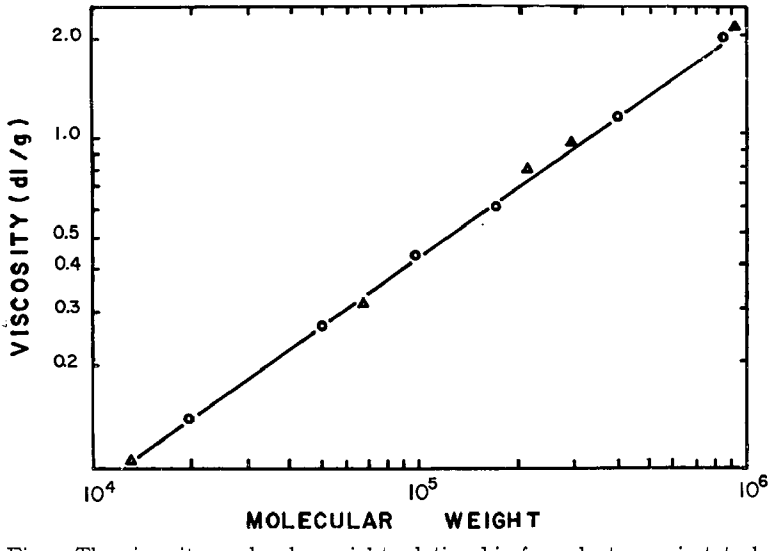

Fig. 1. The viscosity–molecular weight relationship for polystyrene in tetrahydrofuran at 30° from this work, ○ and from BENOIT[4], ▲.

TABLE I

MOLECULAR WEIGHTS AND INTRINSIC VISCOSITIES FOR POLYSTYRENE STANDARDS

Waters Standard No.	M_w	M_n	$[\eta]$
4 190 038	867 000	773 000	2.002
4 190 037	411 000	392 000	1.158
41 984	173 000	164 000	0.625
41 995	98 200	96 200	0.442
25 170	51 000	49 000	0.270
4 190 039	19 850	19 165	0.141

The line drawn represents the Mark-Houwink relation, eqn. 2, with $K = 1.25 \cdot 10^4$, and $a = 0.707$. The elution volume for each molecular weight was taken as the peak position of the GPC curve. Thus, the value of J *versus* elution volume was established. Fig. 2 shows the universal calibration curve for the four column set consisting of $1.5 \cdot 10^6$, 10^6, 10^5, and 10^4 Å columns. The unit for elution volume is counts (1 count = 5 cc). The concentrations used for GPC were about 0.1 % for the 411 000 and higher-molecular-weight standards and about 0.25 % for the lower molecular weight standards.

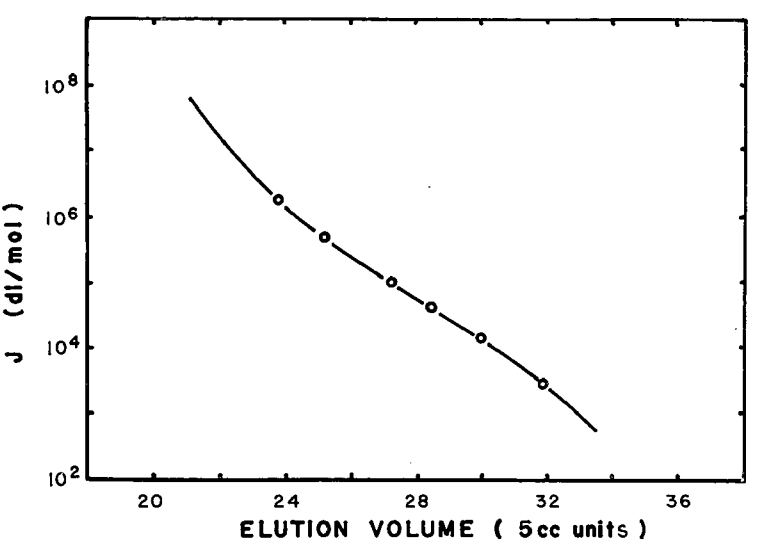

Fig. 2. The universal calibration curve for a styragel column set consisting of $1.5 \cdot 10^6$, 10^6, 10^5 and 10^4 Å columns.

Application to SBR polymers

In order to test these methods, intrinsic viscosities and number average molecular weights from osmometry were determined on two SBR polymers and GPC traces were obtained. The polymers were emulsion polymerized styrene–butadiene copolymers of about 23 % styrene.

The theory given allows the calculation of the molecular weight–intrinsic viscosity relation for a particular polymer and consequently its GPC calibration curve. Using various combinations of data Mark-Houwink parameters have been calculated and are shown in Table II. In addition, various molecular weight averages and in-

TABLE II

APPLICATION OF UNIVERSAL CALIBRATION METHODS TO SBR

Calibration method	*Standard sample and computed results*	*SBR*	*Calculated from GPC curve*		$[\eta]$
			M_n	M_w	
Using eqn. 7 with $[\eta]$ and M_n one sample one GPC curve	Case A				
	SBR 1808	1808	114 800[a]	453 500	2.47[a]
	$K = 0.2984 \cdot 10^{-3}$				
	$a = 0.7043$	1507	88 360	308 700	1.89
	Case B				
	SBR 1507	1808	111 100	475 700	2.38
	$K = 0.5463 \cdot 10^{-3}$				
	$a = 0.6545$	1507	84 900[a]	320 000	1.85[a]
Using eqn. 6 two $[\eta]$ two GPC curves	Case C				
	SBR 1808				
	SBR 1507	1808	129 700	445 600	2.47[a]
	$K = 0.8066 \cdot 10^{-4}$				
	$a = 0.8021$	1507	101 100	310 000	1.85[a]

[a] Indicates directly measured value used in establishing calibration.

trinsic viscosities have been calculated from the GPC curves and are listed in Table II. All number average molecular weights are seen to fall within a total range of about 20 %. The worst case is case C of Table II where the calibration curve was obtained from Eqn. 6 without reference to a molecular weight measurement on an SBR sample.

Weight average molecular weights fall within a range of 10 %. While the Mark-Houwink parameters K and a shown in Table II vary in the three cases, low values of a are compensated by high values of K so that the mid-range of the calibration checks out very well. The calibration curves are tabulated in Table III for comparison.

Application to butyl rubber

It was desirable to take several well characterized rubber samples and obtain replicate GPC traces on each in order to better establish the reproducibility and accuracy of the molecular weight averages. For this reason, five replicate GPC curves were obtained for each of three samples of butyl rubber, one control and two unknowns.

Using the calibration procedures demonstrated earlier and using eqn. 7 with

TABLE III

COMPARISON OF CALIBRATIONS FOR SBR SAMPLES

Elution volume (counts)	*Molecular weight*		
	Case A	*Case B*	*Case C*
16	35 100 000	41 100 000	28 300 000
20	1 772 000	1 894 000	1 677 000
24	145 400	144 200	157 700
28	30 150	28 520	35 600
32	5 369	4 822	6 962
36	645	544	939

TABLE IV

BUTYL CALIBRATIONS FROM CONTROL REPLICATES

Replicate	No. 1	No. 2	No. 3	No. 4	No. 5
$K \times 10^4$	0.8540	1.597	0.7789	1.287	0.8580
a	0.746	0.700	0.755	0.716	0.747
Elution volume (count)	Molecular weight corresponding to elution volume				
19	37.9×10^6	42.0×10^6	36.6×10^6	40.7×10^6	37.7×10^6
23	1.40×10^6	1.41×10^6	1.37×10^6	1.42×10^6	1.39×10^6
27	178 900	171 400	177 400	174 600	177 800
31	31 200	28 500	31 200	29 500	31 000
35	4 046	3 501	4 090	3 693	4 025
M_w	526 000	513 000	504 000	534 000	519 000
M_z	1 890 000	1 610 000	1 630 000	2 340 000	1 880 000

$[\eta] = 1.42$ and M_n 172600 for the control polymer, five sets of K and a values were obtained. They are listed in Table IV. Also listed are molecular weight values at specific elution volumes which result from use of the K and a values with the universal calibration curve. As with the SBR polymers, while the K and a values vary considerably, a high value of K is compensated by a low value for a so that the molecular weight values in the mid-range of the calibration are very simular.

In Table V, typical number average molecular weight results are given for calculating each of the sample replicates against the various control replicates. Thus, going across the table horizontally for a given sample, the standard deviation over different controls is about 4100 or 2.2 % of the average value. Comparing the values vertically, the standard deviation for different butyl No. 1 replicates over the same control runs about 1.2 %. Since 95 % confidence limits run about twice the standard deviation, we find confidence limits of about ± 5 % for variation in M_n due to the uncertainty of controls and about 2.5 % due to the uncertainty in the sample trace.

In Table VI the averages and standard deviations are summarized for both butyl unknowns. For number average molecular weights, the results for the second butyl rubber shows slightly more deviation over different sample traces. The variations

TABLE V

NUMBER AVERAGE MOLECULAR WEIGHTS FROM GPC FOR BUTYL NO. 1

Sample	*Control replicate*						
	1	*2*	*3*	*4*	*5*	*Average*	*S.D.*
1	192 400	181 500	191 300	186 000	191 200	188 480	4137
2	191 900	181 100	190 800	185 500	190 700	188 000	4104
3	187 600	176 700	186 500	181 100	186 400	183 660	4150
4	187 500	176 700	186 400	181 100	186 400	183 620	4117
5	191 900	181 100	190 800	185 500	190 800	188 020	4117
Average	190 260	179 420	189 160	183 840	189 100	Overall 186 356	
S.D.	2 220	2 226	2 220	2 245	2 211		

TABLE VI

STATISTICAL RESULTS

Sample replicate	*Vary calibration, fixed sample*							
	Butyl No. 1				*Butyl No. 2*			
	$\bar{M}_n$	*S.D.*	$\bar{M}_w$	*S.D.*	$\bar{M}_n$	*S.D.*	$\bar{M}_w$	*S.D.*
1	188 500	4137	552 000	4455	209 500	4198	558 300	4484
2	188 000	4104	542 200	4258	214 200	4172	556 000	4310
3	183 700	4150	557 600	4620	204 600	4211	551 200	4253
4	183 600	4117	545 700	4420	212 400	4061	529 600	3803
5	188 000	4117	543 500	4258	199 400	4156	541 100	4141
		~ 2.2%		~0.8%		~ 2.0%		~ 0.8%
Calibration	*Fix calibration, vary sample replicate*							
	Butyl No. 1				*Butyl No. 2*			
	$\bar{M}_n$	*S.D.*	$\bar{M}_w$	*S.D.*	$\bar{M}_n$	*S.D.*	$\bar{M}_w$	*S.D.*
1	190 300	2220	549 900	5749	211 600	5063	546 500	11 205
2	179 400	2226	551 200	6004	200 500	5042	547 100	11 686
3	189 200	2220	540 600	5610	210 200	4989	537 400	10 930
4	183 800	2245	553 100	5934	205 100	5087	549 200	11 577
5	189 100	2211	546 200	5680	210 300	5014	542 900	11 138
		~1.2%		~1.0%		~2.5%		~2.1%

Overall: $\bar{M}_n$ = 186360; $\bar{M}_w$ = 548200; osmotic M_n = 186000.

Overall: $\bar{M}_n$ = 207540; $\bar{M}_w$ = 544600; osmotic M_n = 212000.

due to calibration are almost identical for the two unknowns as would be expected. In terms of accuracy the average M_n values are in excellent agreement with osmotically determined values.

The standard deviations for the M_w values given in Table VI are seen to be smaller than those for M_n. Estimated 95% confidence limits are ± 2% due to calibration and ± 4% due to sample trace variation.

The values for the Z average molecular weight cover a range of about ± 10% the average values. The M_z values found for the two rubbers were not significantly different having average values of 1707000 and 1604000, respectively. The larger deviations for M_n and M_z reflect their greater reliance upon the extremes of the calibration curves where the calibrations are least accurate and reproducible.

CONCLUSION

Intrinsic viscosities in THF at 30° were determined on six of the standard polystyrene samples furnished by Waters Associates. The viscosity values made it possible to set up the universal calibration curve which was successfully applied in obtaining specific polymer calibrations.

The results shown with SBR served to check different cases of the theory. Satisfactory agreement of calculated M_n values with the osmotic pressure values was found for SBR. The work with butyls served as an independent test of the theory and

also as an examination of the reproducibility to be expected. Again the calculated M_n values were in good agreement with osmotically determined values. Reproducibility was determined to be very good and it was estimated that one can expect to be able to differentiate between samples having M_n values 5 % or more apart when the GPC traces are run against the same calibration.

However, certain assumptions are made in the derivation which results in the following restrictions. The Mark-Houwink viscosity relation must apply to the polymer. Use of the ordinate of the GPC curve as the measure of concentration means that all the material involved should be of the same refractive index. Therefore the method would not be expected to apply to mixtures of polymers or non-random copolymers and grafts.

The methods presented are especially attractive for routine use with GPC work since intrinsic viscosities and number average molecular weights are relatively easily obtainable. Also a distinct advantage comes about through the use of Mark-Houwink parameters K and a. It should be possible to apply the K and a values to obtain specific polymer calibrations for other similar column sets. This may be expected to facilitate comparison of results from different instruments or to correct for calibration drift of one instrument. Work is presently proceeding along these lines.

ACKNOWLEDGEMENTS

The author acknowledges helpful discussions and suggestions from Dr. G. S. TRICK and Dr. K. W. SCOTT. Thanks are also due to Mrs. NANCY DOTSON for the osmotic pressure measurements and GPC work.

REFERENCES

1 D. J. HARMON, *J. Polym. Sci. C*, 8 (1965) 243.
2 L. E. MALEY, *J. Polym. Sci. C*, 8 (1965) 253.
3 J. F. JOHNSON, R. F. PORTER AND M. J. CANTOW, *Macromol. Chem.*, 1 (1966) 393.
4 Z. GRUBISIC, P. REMPP AND H. BENOIT, *Polym. Lett.*, 5 (1967) 753.
5 A. R. WEISS AND E. COHN-GINSBERG, *Polym. Lett.*, 7 (1969) 379.

CHROM. 5137

THE EFFECT OF TEMPERATURE ON GEL PERMEATION CHROMATOGRAPHIC SEPARATIONS

JAMES N. LITTLE AND WILLIAM J. PAUPLIS
Waters Associates Inc., 61 Fountain Street, Framingham, Mass. 01701 (U.S.A.)

SUMMARY

In three previous studies[1–3] we reported the effect of several operational parameters on separations by gel permeation chromatography. These studies included the effects of (a) solvent flow rate, (b) sample concentration, (c) sample molecular weight, (d) particle size, and (e) operating temperature. In this present study, we extended the operating temperature limit to temperatures above the normal boiling point of the solvent. At these temperatures, polymer solutes will have smaller diffusion coefficients (solute moves faster) and the solvent will be less viscous. Both of these effects enhance the mass transfer of the solute and lead to more efficient separations.

A modified Waters Associates gel permeation chromatograph, Model 200, was operated with toluene solvent. The instrument was modified to include pre-columns for heating the solvent and a restrictor and cooling bath (before the inner heat exchanger of the refractor) to keep the solvent in the liquid state. The restrictor is necessary when operating above the boiling point of the solvent.

Two 4 ft. × 0.305 in. I.D. columns containing 10^5 Å Styragel were used for all studies. A siphon calibration curve was used to correct inaccuracies in the siphon dump volume. Samples were injected at a concentration of 0.5 % (weight/volume). A constant sample volume of 1 ml was used for all test samples. Samples of polystyrene standards were evaluated at 32, 80, 135 and 200° and at flow rates ranging from 1 to 10 ml/min. Elution volumes were found to decrease with temperature since the solute molecules are more fully expanded and occupy a larger volume at the higher temperatures. Peak widths decreased with temperature due to the better mass transfer. The column system gave a plate count (ODCB) of 3000 plates/ft. when operating at 1 ml per min and 135°. By increasing the temperature from 32° to 135°, the flow rate could be increased six-fold and maintain constant resolution. Since the solvent viscosity is much lower, the increased temperature and flow rate only increases the pressure drop by a factor of three. The data for all the standards and conditions were compared on a resolution (R), time (t), R/t and pressure drop basis.

REFERENCES

1 J. N. LITTLE, J. L. WATERS, K. J. BOMBAUGH AND W. J. PAUPLIS, *J. Polym. Sci. A-2*, 7 (1969) 1775.
2 J. N. LITTLE, J. L. WATERS, K. J. BOMBAUGH AND W. J. PAUPLIS, *J. Polym. Sci. Div. of Petrol. Chem.*, Preprints, 15 (1970) 121.
3 J. N. LITTLE AND W. J. PAUPLIS, *Separ. Sci.*, 4 (1969) 519.

CHROM. 5138

INDUSTRIAL PREPARATIVE LIQUID CHROMATOGRAPHY

J. L. WATERS
Waters Associates Inc., Framingham, Mass. 01701 (U.S.A.)

SUMMARY

This paper discusses the uses and requirements for narrow polymer fractions and pure chemical compounds separated by liquid chromatography. The ready availability of material fractions opens new opportunities for systematic investigation and research. It is now practical to separate quantities of several grams at extremely high resolution up to quantities of 20,000 g at moderately high resolution.

INTRODUCTION

Polymers and large molecules have, for many years, been preparatively fractionated by electrophoresis, sand column fractionation, and liquid chromatography employing affinity or size. Recent technical advances in liquid chromatography permit the fractionation of larger quantities of material with higher resolution. Waters Associates Inc. is now offering a custom fractionation service for liquid chromatography separations. In this paper the uses and applications for separated materials and the separation resolution attributable will be discussed.

USES AND APPLICATIONS FOR SEPARATED FRACTIONS

There are many needs and uses for narrow polymer fractions, individual chemical separations and pure chemical compounds. Table II briefly outlines some of these uses. The sources of material to be fractionated and uses for separated materials are listed.

SEPARATION TECHNOLOGY

Preparative liquid chromatography separations are required when a separation is difficult. This occurs when the components are degraded under the conditions for other separation methods or where they are very similar and, as a result, require the ultimate in resolution. Examples are separations where the temperature required degrades the molecule or where complex isomers or polymers must be separated. Liquid chromatography separations are generally made from a distribution of polymers or chemical mixtures. These mixtures are complex and contain similar compounds differing in either functionality or size and often in both.

The separation of a mixture of two or three compounds is a special distribution case and is generally an easier separation than one requiring the separation of many components.

There are four frequently used modes of liquid chromatography: (A) Molecular size separation is based on the relative size of the solute molecules in relation to the pore size of the column packing. (B) Liquid–liquid partition separation utilizes the relative solubilities of the sample components in the stationary and mobile liquid phase. (C) Liquid–solid separation involves the relative adsorptivity of the sample components on an active solid support. (D) Ionexchange separation is based on the reversible exchange of ions between the solid ionexchange resin and the eluting liquid.

The yield and resolution and hence the complexity of a separation is affected by the following factors: (A) A narrower polydispersity of a polymer fraction or higher purity of a separated chemical species increases the complexity. (B) A lower sample viscosity permits a higher sample concentration. Thus, lower molecular weight materials can be fractionated with higher yield and less complexity. (C) A greater compound similarity increases the complexity of a separation. Materials similar in size and functionality are difficult to separate. (D) A lower concentration of the desired material in the mixture increases complexity. If the desired component is present in a concentration of 0.1 % and several grams are required, it is necessary to fractionate several thousand grams to obtain the desired quantity of material.

The separation resolution (available from Waters Associates) is shown in Table I.

TABLE I

	Easy	*Difficult*	*Very difficult*
M_1/M_2	1.4	1.02	1.005
M_w/M_n	1.3	1.005	1.001
α	1.1	1.006	1.0015

M_1/M_2 represents the molecular weight ratio of two compounds separated by molecular size. M_w/M_n is the heterogenity index of the resulting polymer fractions. α is the ratio of the chromatographic elution volumes of two compounds separated by affinity chromatography. For example, two compounds having elution volumes of 10 and 11 liters have an α of 1.1.

For comparative purposes, preparative gas chromatography of α's of 1.1 or less is considered difficult. The increased resolution for preparative liquid chromatography separation is the result of the use of a liquid phase separation instead of a gas phase separation.

Separations of 2 to 20,000 g quantities are available now. Larger quantity separations will be available in the near future.

Table II is an outline of the uses for fractionated material. The uses listed in the table can be divided into two general classes: those involving the separation of a known material and those involving an unknown material. The separations of known materials result in an improved understanding of the material, an improvement in the end product for specific applications, or the direct use of the fractions.

TABLE II

Typical sources of material

(A) Research material:
1. Polymer synthesis
2. Chemical compound synthesis

(B) Production material:
1. Impurity removal
2. Manufacture of special property materials
3. High purity compounds

(C) Materials from other sources:
1. Natural products
2. Vendor products
3. Competitor products

Uses for separated materials

(A) Analysis by the identification of fractions using:
1. Infrared spectra
2. Gas chromatography
3. Mass spectra
4. NMR spectra
5. Ultra violet spectra
6. Thermal analysis
7. Elemental analysis
8. Atomic absorption
9. Thin-layer chromatography
10. Liquid chromatography

(B) Evaluation of properties of a single fraction and of a blend of fractions:
1. *Mechanical properties*
   (a) Molding
   (b) Milling
   (c) Extruding
   (d) Toughness
   (e) Plasticity
   (f) Melt index
   (g) Creep
   (h) Hardness
   (i) Impact strength
   (j) Tensile strength
   (k) Viscosity
2. *Thermal properties*
   (a) Heat degradation
   (b) Cold resistance
   (c) Flow characteristics
3. *Electrical properties*
   (a) Dielectric constant
   (b) Conductivity
   (c) Electrical breakdown
4. *Permeability properties*
   (a) Oxygen
   (b) Moisture
5. *Chemical and physical properties*
   (a) Solubility
   (b) Melting point
   (c) Infrared spectra
   (d) Ultra violet spectra
   (e) NMR
   (f) Mass spectra
6. *Biological activity*
   (a) Toxicity
   (b) Metabolism
   (c) Pharmaceutical activity
   (d) Insecticidal activity
   (e) Herbicidal activity

(*Continued on p. 216*)

TABLE II (*continued*)

7. *Degradation properties*
   (a) Time
   (b) Temperature
   (c) Radiation
   (d) Electrical discharge
   (e) Oxidation — ozone
   (f) Mechanical
      (i) Molding
      (ii) Milling
   (g) Chemical
8. *Miscellaneous properties*
   (a) Uniformity of degree of copolymerization
   (b) Degree of branching
   (c) Adhesion
   (d) Rheology
9. *Uses for separated materials as intermediates*
   (a) Chemical synthesis
   (b) Polymer synthesis
   (c) New product engineering for optimum performance
   (d) Rules of mixture for properties of combinations
   (e) Degradation of fractions

Two direct uses for fractions are as synthesis intermediates and as standards. Standards are vital for the identification of unknowns and the calibration of analytical instruments, such as mass spectrometers, infrared, NMR, GPC and other instrumental techniques.

Standards for molecular weight are an example of the usefulness of fractions. Until recently, the principal standards available for GPC were a series of polystyrene standards from 900 to 2 million molecular weight. Because of the lack of availability of other polymer standards, there has been a considerable effort to develop a universal calibration which will relate the polystyrene standards to all other polymer systems. This has been difficult and time-consuming. With the availability of preparative separation techniques having high resolution, it is now possible to prepare GPC calibration standards in a wide variety of polymer materials. Waters Associates will offer, in the near future, an extensive line of GPC calibration standards in many difficult polymer systems.

A series of linear polyethylenes are being fractionated by Waters for the National Bureau of Standards for characterization and distribution by NBS as primary polymer standards.

A more specialized standard is the ultra narrow distribution polymer. Using high resolution recycle preparative chromatography technology[1,2] extremely narrow polymer standards have been prepared. A set of polystyrene standards is now available from Waters Associates having molecular weights from 900 to 800,000. Typical polydispersities for these materials range from 1.0025 to 1.009. These narrow polystyrene standards are used to determine the properties of very narrow distributions, cross-calibrate osmotic pressure and light scattering instruments and investigate the mechanism of gel permeation chromatography.

In the past, there have been no high molecular weight standards above 2 million. Material separations make possible the preparation of extremely high molecular weight standards. Anionic polymers of 2 million molecular weight or greater are very

broad. GPC is used to separate at high resolution polymers greater in molecular weight than 2 million.

A particularly interesting field for separated materials is the degradation of compounds and polymers. Usually, degradation is studied by degrading a product and measuring the change in its overall properties. Although this method is often adequate, there are many cases when due to the complexity of the product, it is impossible to obtain an adequate understanding of the degradation process by this method.

Several techniques are used to overcome this problem. The starting material is fractionated and the individual fractions are degraded. The material resulting from the degradation of each fraction is measured as a whole material and it can, in turn, be fractionated and further measured as fractions. Alternatively, the whole material is degraded and fractionated. The original mixture fractions are then compared with the degraded material fractions to identify changes.

Obviously, degradation is a complex investigation. Fractionation of either the starting material or the degradation product offers a powerful tool to increase the understanding of the degradation mechanism. An example of this type of problem is the determination of the resistance of a polymer to radiation or chemical degradation. The polymer is first fractionated into reasonably narrow distribution fractions. Each fraction is then subjected to radiation and the resulting molecular weight distribution determined. On the other hand, when degradation is by chemical means, it is often desirable to fractionate the degraded material. The end group composition of each fraction of the degraded material is then measured to develop a better understanding of the mechanism.

Narrow polymer distribution materials and pure species are also important in the determination of physical properties. The properties listed in Table II can be examined for both pure materials and narrow polymer distributions. In this way, the interrelationship between chemical structure and the property of interest can be developed.

The study of complex mixtures is another important area. Mixtures such as asphalts, natural oils, polymers and resins have been optimized for performance by synthesizing different distributions, or combining material from different sources. The fractionation of a broad distribution and the blending of the individual fractions to obtain a desired blend of properties provides a greater range of adjustment and control of end product properties than the adjustment of a distribution or the blending of different distributions. As a general rule, the blending of individual fractions enables the research worker to obtain more combinations and develop more data in a given period of time. His examination of the range of properties and the optimization of performance can, as a result, be greatly expedited.

An example of this application is the fractionation of a broad distribution of lubricating oil. Appropriate blends of individual fractions are then run in an engine to determine the optimum combination of properties such as wear resistance, chemical stability, temperature resistance, etc.

Another example is the development of a new polymer where the synthesis technology is difficult to develop. For example, when preliminary data indicates that the high molecular weight end of the polymer has a valuable property and when it is difficult to make a reasonably narrow high molecular weight distribution, it is much easier to fractionate a broad polymer to obtain high molecular weight fractions.

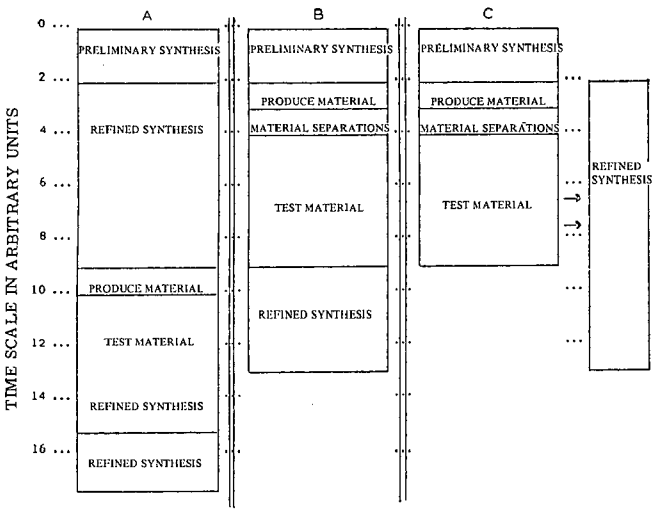

Fig. 1. Time sequence diagram.

Testing the fractions then indicates whether or not further work on the project will yield a useful product.

Fig. 1 is a time sequence diagram for a typical development project. The sequence is: (1) Development of a preliminary synthesis method. (2) Refinement of the synthesis method to produce a desired material. (3) Synthesis to obtain the test material. (4) Testing of the new compound or polymer to identify and optimize desirable properties. (5) Continuing refinement of the synthesis method to produce the desired product.

Most developments of this type require that these operations be done in sequence because each operation is dependent upon success in the previous one. This method has two major disadvantages: (1) It requires the time-consuming development of a refined synthesis method in order to produce enough material to determine whether or not the end product will be useful. If the end product is not useful, the development of a synthesis method represents a loss of development effort. (2) The fact that the synthesis method must be improved in order to produce test material requires that the two stages must be conducted in series. Hence, the total time between conception of the project and introduction to the marketplace is substantially longer than if the two are conducted in parallel.

Material separations permit two modifications in the normal development procedure. These are shown in Figs. 1B and 1C. In each of these cases, as soon as preliminary synthesis method has been developed, enough material is produced to prepare fractions for end product testing. If the end product evaluation is negative, the time-consuming development of a refined synthesis method can be omitted.

If a crash project is appropriate, the refinement of the synthesis method can proceed in parallel with the testing programme. In this way, the results of the test can be fed back into the refinement of the synthesis method development in order to direct it quickly and profitably to the best result.

The advantages of the use of separated materials are that they reduce the total

cost of the project. (1) If the end product is unsuccessful, a saving of unnecessary development efforts is made by reversing the order of development. (2) If the testing indicates a successful product, the refinement of the synthesis method will be better directed to the actual product desired. (3) If parallel development is appropriate, the material separation will shorten the time of development by permitting simultaneous material testing and refinement of the synthesis method.

A second major area for fractionations is in the examination of unknown materials. Natural products, new synthesis compounds, defective production batches and products manufactured by competitors and vendors are the usual sources of unknowns. The identification of the individual components of these materials leads to a better understanding of the nature of the mixture and to subsequent product improvement.

The first major classification for this type of product is the identification of the components of the mixture. The identification is made by standard instrumental techniques. Chemical structure involves the use of standard laboratory procedures, such as infrared spectra, NMR, GPC, gas chromatography and mass spectrometry.

One of the major applications for fractionation of unknown materials is copolymers. Copolymers can be extremely complex. In addition to having different degrees of copolymerization with change in size of the polymer molecule, they can also have differences in the degree of randomness, blocking and tatic properties. The mechanism of reaction as well as the temperature and reaction vessel geometry affect these properties.

Material separation makes possible the separation of a copolymer distribution into individual size fractions which are then further examined by analytical techniques to increase the knowledge of the reaction mechanism. In some cases, it is desirable to take the individual size fractions and further fractionate them using an affinity separation. In this case, they will be separated according to the chemical nature of the reactive groups on the polymer molecule. The complexity of copolymers requires the use of a separation fractionation for the development of a complete understanding of the mechanism.

In a biologically active product, the determination of toxicity and activity of each component present in a mixture are of vital concern. The development of a new drug requires the analysis of all of the unknown impurities present in the final product. The concentration of many of these components is very low. They must be identified and if their properties have not previously been determined, their properties must be determined. Material separations are used to rapidly separate and identify trace impurities which might have a deleterious effect on the product.

REFERENCES

1 K. BOMBAUGH, W. DARK AND R. LEVANGIE, *J. Chromatog. Sci.*, 7 (1969) 43.
2 J. L. WATERS, *J. Polym. Sci.*, 8 (1970) 411.

CHROM. 5201

GEL PERMEATION CHROMATOGRAPHY OF SILICONES

FRED N. LARSEN
Bendix Corp., Kansas City, Mo. (U.S.A.)

SUMMARY

The utility of gel permeation chromatography to characterize silicone materials is presented. Distribution profiles and analytical parameters are described for a wide variety of commercially available silicone fluids, gums and formulated compounds. The use of a calibration curve prepared from a series of dimethyl siloxane fluids and the quantitation of a specific silanol in a formulation are also described. Comparative data is shown for several silicones eluted with different solvents.

CHROM. 5157

EFFICACY OF THE CORRECTIONS APPLIED IN THE RESOLUTION OF OVERLAPPING CHROMATOGRAPHIC PEAKS BY THE PERPENDICULAR DROP METHOD

J. NOVÁK, K. PETROVIĆ* AND S. WIČAR

Institute of Instrumental Analytical Chemistry, Czechoslovak Academy of Science, Brno (Czechoslovakia)

(Received November 10th, 1970)

SUMMARY

Systematic errors associated with the use of the perpendicular drop method for the determination of the areas of incompletely resolved chromatographic peaks were evaluated experimentally for various peak size ratios and degrees of overlap. The experimentally determined errors were compared with those estimated theoretically using the Gaussian peak shape model. A theoretical analysis was carried out on the applicability of the model of a triangular peak to the mathematical resolution of overlapped chromatographic peaks.

INTRODUCTION

Detection and resolution of incompletely separated peaks is an important step in quantitative analysis by gas chromatography (GC). The commonly used empirical resolution techniques of perpendicular drop and triangulation[1] give satisfactory results only in favourable cases, characterised by Gaussian or near Gaussian peaks, moderate overlaps, and not very high ratios of the sizes of the larger and smaller peak. In more complex cases, where it may be impossible even to detect visually the true number of the component peaks in the incompletely resolved portion of a chromatogram, curve-fitting techniques[2–7] may be effective. Owing to the iterative character of the above techniques, a practical approach to this problem is possible only with the aid of computers. Besides digital procedures the application of analogue techniques to the resolution of overlapping peaks has been described[8].

A common feature of all curve-fitting techniques is the necessity of defining an adequate peak shape model; procedures involving models of Gaussian, bi-Gaussian as well as non-Gaussian peaks have been published. In practice, however, it happens frequently that even the computer-based procedures of mathematical peak resolution are inapplicable. Such cases occur when the unresolved segment of the

* Present address: Crude Oil Refinery, Pančevo, Yugoslavia.

chromatogram is composed of peaks of generally different shapes or when peaks of so different sizes are present in the segment that the dimensions of the smaller peak and of the asymptotic parts of the larger one, on which the smaller peak is superimposed, become comparable. In such situations, the most reliable solution of the resolution problem is the decision made by a skilled chromatographer, consisting in drawing adequate images of the component peaks. At this point, however, the matter becomes more or less an art.

The methods of mathematical resolution were also employed to determine the systematic errors incidental to the component peak area determination by the methods of perpendicular drop and triangulation[9]. In virtue of the concepts similar to those employed in the above cited work, PROKSCH *et al.*[10] have calculated a system of factors for correcting the component peak areas determined by the perpendicular drop method to obtain the respective true peak areas. In both cases mentioned above[9,10], a Gaussian curve was adopted as a peak shape model. KAISER AND KLIER[11] have recommended a procedure based on a model of triangular peak for the mathematical resolution of overlapped peaks.

The procedure involving the use of the above correction factors combines the simplicity of the perpendicular drop method with the exactness of the methods of mathematical peak resolution. This rational approach undoubtedly may provide for quick and accurate determination of the true component peak areas, however, the accuracy is again determined by the extent to which the model peak shape chosen in calculating the correction factors approximates the real chromatographic peaks. The present paper is an experimental check-up of the applicability of the correction factors of PROKSCH *et al.* in the above sense. Attention is also given to KAISER AND KLIER'S triangular model.

THEORETICAL

Determination of the empirical correction factors

The choice of a Gaussian peak shape model makes it possible to express the correction factors as functions of merely two parameters, A_2'/A_1' and Rs, where A_2' and A_1' are the apparent areas of the larger and of the smaller segment of the composite peak, respectively, as determined by the perpendicular drop method, and Rs stands for the degree of resolution defined by $\Delta/\bar{\sigma}$ where Δ is the distance between the maxima of the two component peaks and $\bar{\sigma}$ denotes the average standard deviation of the latter. Hence, the appropriate correction factors may be readily found for any particular case of two overlapping peaks, assuming the latter are Gaussian. However, the correction factors may also be determined directly from two chromatograms of a given binary mixture if one of the chromatograms consists of overlapping peaks and is evaluated by the perpendicular drop method while the other is run under conditions permitting complete separation of the components, thus rendering directly the true peak areas. These empirical correction factors are obviously independent of the peak shape and, therefore, the comparison of the factors obtained by both procedures, for the given mixture and degree of overlap, may give a measure of the applicability of the theoretical correction factors.

Let us consider a chromatogram of a pair of incompletely resolved peaks where A_2 and A_1 designate the true areas of the larger and of the smaller peak, A_2' and A_1'

stand for the areas found for the larger and for the smaller segment of the composite peak area divided by the separation perpendicular, and S is the total composite peak area, respectively. The true area fractions, a_2 and a_1, are given by

$$a_2 = A_2/(A_2 + A_1) = A_2/S \quad (1)$$
$$a_1 = A_1/(A_2 + A_1) = A_1/S \quad (2)$$

Eqns. 1 and 2 imply the calculation of a_2 and a_1 from the images of true peaks 2 and 1 in the composite chromatogram. However, these peak area fractions may be determined from the corresponding chromatogram where peaks 2 and 1 have been completely resolved, which is facilitated by the fact that area fractions are independent of the absolute sizes of the respective areas.

The correction factors have been defined[10] by the equations

$$f_2 = A_2/A_2' \quad (3)$$
$$f_1 = A_1/A_1' \quad (4)$$

which may be rewritten, on combining them with eqns. 1 and 2, to read

$$f_2 = a_2S/A_2' \quad (5)$$
$$f_1 = a_1S/A_1' \quad (6)$$

The above equations provide for calculating the correction factors from directly measured experimental data. In order to distinguish between the theoretical factors obtained from PROKSCH's tables and the empirical factors calculated by eqns. 5 and 6, we shall use the designation f_t and f_e for the theoretical and for the empirical factors, respectively.

Systematic errors of the peak area determination with the use of the theoretical factors

The relative systematic error of the determination of the true peak areas by applying the perpendicular drop method without any corrections at all, δ, may be expressed by

$$\delta_2 = (A_2' - A_2)/A_2 \quad (7)$$
$$\delta_1 = (A_1' - A_1)/A_1 \quad (8)$$

Upon substituting for A_2 and A_1 from eqns. 3–6, eqns. 7 and 8 may be rewritten to read

$$\delta_2 = (1/f_{e2}) - 1 = (A_2'/a_2S) - 1 \quad (9)$$
$$\delta_1 = (1/f_{e1}) - 1 = (A_1'/a_1S) - 1 \quad (10)$$

where the subscript e indicates that the empirical factors have been employed.

Assuming that the products $A_2'f_{e2}$ and $A_1'f_{e1}$ represent the true areas A_2 and A_1, it is possible to express also the errors that will affect the results when using PROKSCH's theoretical factors. Thus, denoting the above errors by δ_G (Gaussian peak shape model), we can write

$$\delta_{G2} = (A_2'f_{t2} - A_2'f_{e2})/A_2f_{e2} = (f_{t2}/f_{e2}) - 1 \quad (11)$$
$$\delta_{G1} = (A_1'f_{t1} - A_1'f_{e1})/A_1'f_{e1} = (f_{t1}/f_{e1}) - 1 \quad (12)$$

The applicability of KAISER AND KLIER's triangular model may be checked by carrying out an appropriate comparison of the latter with the more realistic Gaussian

model. With this end in view, a pair of overlapping triangles specified by the parameters of KAISER AND KLIER's model was analysed in terms of a Gaussion curve. The analysis was based on the following concept. Let us consider two triangles with the heights h_2 and h_1 (subscript 2 again denotes the larger component), equal base widths, d, and with the apexes separated from each other by a horizontal distance Δ. It can be shown that the horizontal distance (x) between the perpendicular separating the true areas of the triangles and the apex of the smaller triangle is given by

$$x = \frac{d + \Delta(h_1/h_2)^{\frac{1}{2}}}{1 + (h_1/h_2)^{\frac{1}{2}}} - \frac{d}{2} \tag{13}$$

Now, let us suppose that the pair of the triangles is substituted by a pair of Gaussian curves with the same height ratio and the same horizontal distance between the peak maxima, the standard deviations of the curves amounting to one fourth of the triangle base width. Provided the smaller peak is considered as that with the lower retention time, the individual Gaussian curves may be described by the equations

$$\varphi_1(t) = h_1 \exp[-8(t - t_1)^2/d^2] \tag{14}$$

$$\varphi_2(t) = h_2 \exp\{-8[t - (t_1 + \Delta)]^2/d^2\} \tag{15}$$

the corresponding composite peak being defined by

$$\varphi_3(t) = \varphi_1(t) + \varphi_2(t) \tag{16}$$

The symbol t in eqns. 14–16 stands for time, t_1 denoting the time corresponding to the maximum of the smaller peak. In this context, the abscissa x is related to the time corresponding to the separation perpendicular, t_s, by

$$t_s = t_1 + x \tag{17}$$

provided x is expressed in time units. It can be shown that the combination of eqns. 13 and 17 is an equivalent of KAISER AND KLIER's formula for determining the separation line between the two triangles[11]. The true areas of peaks 1 and 2 are obviously given by

$$A_1 = \int_0^\infty \varphi_1(t)\mathrm{d}t \tag{18}$$

$$A_2 = \int_0^\infty \varphi_2(t)\mathrm{d}t \tag{19}$$

while the areas that will be obtained according to the procedure suggested by KAISER AND KLIER are

$$A_1' = \int_0^{t_s} [\varphi_1(t) + \varphi_2(t)]\mathrm{d}t \tag{20}$$

$$A_2' = \int_{t_s}^\infty [\varphi_1(t) + \varphi_2(t)]\mathrm{d}t \tag{21}$$

Thus, eqns. 18–21 afford the estimation of the relative systematic error of the peak

areas determined in virtue of the triangular model, the estimate being of course referred to the Gaussian model. The above error is designated by $\delta_{K(G)}$ (cf. Table III).

EXPERIMENTAL

The experimental material was obtained by chromatographing on columns of different lengths a series of binary mixtures of various proportions of the components, thus obtaining a system of chromatograms with the peak area ratios and degrees of peak overlap ranging within appreciably wide limits. One of the chromatograms of each mixture presented completely resolved peaks.

The model substances were *m*-xylene and *o*-xylene of analytical grade purity (Koch-Light Laboratories Ltd., Great Britain). The mixtures were chromatographed on stainless-steel columns filled with a packing of 10 wt. % of Apiezon L on Chromosorb W 60/80 mesh and kept at 100°. The internal diameter of the columns was 3 mm and their lengths varied within 25–120 cm, as required for the particular degree of resolution. The above system rendered fairly symmetrical peaks for both components.

All measurements were carried out on a Hewlett-Packard high efficiency gas chromatograph, Model 402 (U.S.A.), employing flame ionisation detection. The flow rates of the carrier gas (N_2), hydrogen, and air were set to about 30, 40, and 400 ml/min, as measured at the detector outlet, respectively. The injection port and the detector were kept at a temperature of 150°. The sample charges amounted to some tenths of a microliter and were injected by a Hamilton 7001 N (1 μl) syringe (Hamilton Co., Whittier, Calif., U.S.A.), at appropriate sensitivity attenuations. The recorder chart speed was varied so as to obtain peaks of comparable widths with the columns of different lengths. The peak areas were determined from the records provided by a Disc chart integrator, Model 229-A (Disc Instruments, Inc., Santa Anna, U.S.A.). Three chromatograms were recorded and processed in all cases.

RESULTS AND DISCUSSION

When processing the results obtained by evaluating the chromatograms it became necessary to take into consideration also the sequence of the peaks in the chromatogram, which is obviously at variance with the theory based on the Gaussian peak model. Therefore, the results have been assorted accordingly.

Table I contains the data concerning the cases in which the smaller peak precedes the larger one. In these cases, the experimentally determined systematic errors due to neglecting the corrections are negative for the smaller peak and positive for the larger one. The above finding as well as the trends displayed by the bias upon varying the peak area ratio and the degree of overlap are in compliance with the above-mentioned theory. Therefore, the application of the factors of PROKSCH *et al.* appreciably lessens the systematic error in this case. The I_2 and I_1 in Tables I and II are the percentage coefficients of variation of the experimental correction factors f_{e2} and f_{e1}, respectively, and have been quoted to characterise the reliability of the respective data. The values of the factors represent the averages of three independent determinations, and the coefficients of variation have been expressed for the average values by the method of DEAN AND DIXON[12].

The results concerning the cases with the smaller peak located after the larger

TABLE I

DATA CONCERNING THE CASES WITH THE SMALLER PEAK PRECEDING THE LARGER ONE

A_2'/A_1'	$\Delta/\bar{\sigma}$	f_{e2}	f_{e1}	δ_2 (%)	δ_1 (%)	I_2 (%)	I_1 (%)	f_{t2}	f_{t1}	δ_{G2} (%)	δ_{G1} (%)
1.5	5.4	1.002	0.997	−0.2	0.3	0.137	0.525	1	1	−0.2	0.3
1.6	4.8	0.979	1.035	2.1	− 3.4	0.525	1.074	0.999	1.002	2.0	−3.2
1.7	3.4	0.957	1.075	4.5	− 7.0	0.382	0.568	0.986	1.025	3.0	−4.7
1.7	2.9	0.958	1.064	4.4	− 6.0	0.329	0.327	0.969	1.054	1.1	−0.9
2.6	5.4	0.997	1.009	0.3	0	0.335	0.750	1	1	0.3	−0.9
2.7	4.8	0.984	1.040	1.6	− 3.8	0.227	0.309	0.998	1.003	1.4	−3.6
2.8	3.8	0.980	1.055	2.0	− 5.2	0.330	0.472	0.989	1.031	0.9	−2.3
3.5	2.5	0.926	1.260	8.0	−20.6	0.160	0.562	0.917	1.290	−1.0	2.4
5.5	5.4	1.004	0.977	0.4	− 2.4	0.285	0.268	0.999	1.003	−0.5	2.7
6.0	4.3	0.992	1.050	0.8	− 4.8	0.145	0.289	0.996	1.031	0.4	−1.9
6.3	3.8	0.985	1.096	1.5	− 8.8	0.048	0.609	0.988	1.080	0.3	−1.5
6.1	3.6	0.990	1.077	1.0	− 7.1	0.242	0.592	0.983	1.103	−0.7	2.4
12.8	5.6	0.999	1.008	0.1	− 0.8	0.133	0.568	1	1.006	0.1	−0.2
14.5	4.0	0.991	1.127	0.9	−11.3	0.044	0.630	0.992	1.115	0.1	−1.1
16.0	3.7	0.987	1.240	1.3	−19.4	0	0.693	0.988	1.199	0.1	−3.3
16.6	3.3	0.982	1.287	1.8	−22.3	0.217	1.443	0.977	1.389	−0.5	7.9
29.6	3.7	0.995	1.222	0.5	−18.2	0.043	5.132	—	—	—	—
34.2	3.5	0.991	1.410	0.9	−29.1	0.042	1.443	—	—	—	—
39.3	3.4	0.988	1.614	1.2	−38.0	0.210	0	—	—	—	—
44.5	2.5	0.984	1.817	1.6	−45.0	0.339	1.924	—	—	—	—

TABLE II

DATA CONCERNING THE CASES WITH THE SMALLER PEAK FOLLOWING THE LARGER ONE

A_2'/A_1'	$\Delta/\bar{\sigma}$	f_{e2}	f_{e1}	δ_2 (%)	δ_1 (%)	I_2 (%)	I_1 (%)	f_{t2}	f_{t1}	δ_{G2} (%)	δ_{G1} (%)
1.2	5.2	1.039	0.956	−3.8	4.6	1.032	1.122	1	1	−3.8	4.6
1.2	4.8	1.027	0.977	−2.6	2.4	0.464	0.548	0.999	1.001	−2.7	2.5
1.2	4.1	1.041	0.948	−3.9	5.5	0.467	0.650	0.998	1.003	−4.1	5.8
1.1	3.1	1.007	0.920	−7.1	8.7	1.056	1.001	0.995	1.006	−7.6	9.3
2.1	5.6	1.013	0.955	−1.3	4.7	0.202	0.713	1	1	−1.3	4.7
2.2	5.4	1.004	0.991	−0.4	0.9	0.267	0.297	1	1	−0.4	0.9
2.2	3.6	1.010	0.974	−1.0	2.7	0.589	0.291	0.987	1.029	−2.3	5.6
1.8	2.7	1.085	0.845	−7.8	18.3	0.419	0.380	0.955	1.081	−12.0	29.5
4.2	5.3	1.018	0.922	−1.8	8.5	1.001	0.453	0.999	1.003	−1.9	8.8
4.0	3.9	1.029	0.882	−2.8	13.4	0.537	1.076	0.990	1.041	−3.8	18.0
4.3	3.5	1.018	0.928	−1.8	7.8	0.159	0.679	0.980	1.086	−3.7	17.0
7.5	5.3	1.016	0.882	−1.6	13.4	0.198	1.117	0.999	1.006	−1.7	14.1
6.8	5.0	1.028	0.812	−2.7	23.2	0.700	2.001	0.999	1.010	−2.8	24.4
6.7	4.9	1.032	0.788	−3.1	26.9	1.345	2.276	0.998	1.012	−3.3	28.4
7.7	4.5	1.013	0.902	−1.3	10.9	0.829	2.196	0.996	1.028	−1.7	14.0
12.8	5.0	1.012	0.831	−1.2	20.3	0.277	1.215	0.999	1.018	−1.3	22.5
15.9	4.9	1.003	0.953	−0.3	4.9	0.233	2.211	0.998	1.026	−0.5	7.7
13.7	3.4	1.016	0.781	−1.6	28.0	0.187	1.920	0.979	1.291	−3.6	65.3

one are summarised in Table II. It is evident from the values of f_{e2} and f_{e1} as well as δ_2 and δ_1 that the actual situation is just contrary to that predictable by virtue of the properties of Gaussian curves. In all these cases the systematic error of the uncorrected area of the smaller peak is positive whereas the area of the larger peak has a negative error. The consequence of the above situation is the introduction of an additional error by applying the correction factors of PROKSCH *et al.* which is apparent from the comparison of the values of δ_2 and δ_1 with those of δ_{G2} and δ_{G1}.

The above situation may be explained as follows. A chromatographic peak, even when it represents a concentration region falling into a linear part of the respective sorption isotherm, is always modified by a convolution component, irrespective of the other sources of peak skew. The above convolution component leaves a major part of the peak practically unskewed, except the tail occurring just at the foot of the trailing part, which becomes enlarged by the exponential decay component. As this enlargement is proportional to the peak size, it is insignificant with the smaller peak and, therefore, plays a small role if this peak is before the larger one. However, when a small peak follows closely after a large one, the former, being actually superimposed upon the convolution tail of the large peak, renders excessive values rather than deficient ones when evaluated by the perpendicular drop method. The above enlargement of the smaller segment is obviously to the detriment of the segment of the larger peak.

Under the above conditions, the true correction factors will vary significantly with even slight variations in the extent of the exponential decay component, especially as concerns the smaller peak. Therefore, minor experimental irregularities, particularly those incidental to injecting the sample, may be critical in the above respect. This is probably why it was not possible to find any correlation between the experimental correction factors and the respective values of A_2'/A_1' and $\Delta/\bar{\sigma}$, though the former have been determined with fair precision.

TABLE III

DATA CONCERNING THE MODEL OF A TRIANGULAR PEAK

A_2'/A_1'	$\Delta/\bar{\sigma}$	$\delta_{K(G)2}$ (%)	$\delta_{K(G)1}$ (%)	f_{t2}	f_{t1}	δ_{G2} (%)	δ_{G1} (%)
3	5.40	−0.54	1.63	1	1	0	0
	4.20	−1.31	4.06	0.994	1.017	0.60	−1.67
	3.00	−2.16	6.77	0.959	1.123	4.28	−10.95
	1.80	−2.39	7.54	—	—	—	—
6	5.40	−0.77	4.72	0.999	1.004	0.10	−0.40
	4.20	−1.66	10.34	0.994	1.037	0.60	−3.57
	3.00	−2.60	16.46	0.956	1.263	4.60	−20.82
	1.80	−3.00	19.14	—	—	—	—
9	5.40	−0.92	8.43	0.999	1.006	0.10	−0.60
	4.20	−1.79	16.70	0.994	1.054	0.60	−5.12
	3.00	−2.70	25.75	0.959	1.371	4.28	−27.06
	1.80	−3.14	30.18	—	—	—	—
15	5.40	−1.09	16.70	0.999	1.009	0.10	−0.89
	4.20	−1.89	29.51	0.995	1.082	0.43	−7.58
	3.00	−2.70	42.87	0.963	1.531	3.84	−34.68
	1.80	−4.08	66.60	—	—	—	—

Table III presents some selected data illustrating the errors associated with the use of the corrections according to KAISER AND KLIER's model. The values of $\delta_{K(G)_2}$ and $\delta_{K(G)_1}$ were calculated by eqns. 7 and 8, A_2' and A_1' being expressed by means of eqns. 20 and 21, respectively. The errors designated δ_{G_2} and δ_{G_1} are the theoretical errors of the uncorrected area segments, expressed under the presumption that the composite peak consists of Gaussian components; the δ_G values were calculated by $\delta_G = (A' - A'f_t)/A'f_t = (1/f_t) - 1$. Hence, the whole case has been referred to the Gaussian model. It is apparent from the data in Table III that the separation perpendicular determined by the formula derived in virtue of the triangular model is generally false. The application of this method leads to errors of the absolute values roughly comparable with the errors brought about by neglecting the corrections, but having opposite signs. Owing to the above-mentioned findings, this situation actually applies in cases where the smaller peak precedes the larger one. In the converse cases, the error associated with the application of KAISER AND KLIER's procedure will be about twice as large as that for the uncorrected data. These great discrepancies appear to be due to the fact that it is not possible to allow for the asymptotic parts of the peak by means of the triangular model, while it is just these parts that represent one of the main sources of the correction problems, particularly in cases of moderate overlaps.

CONCLUSIONS

The applicability of the factors defined in virtue of the Gaussian peak shape model to the correction of the areas determined by the perpendicular drop method is limited to the cases where the larger peak is preceded by the smaller one. If the smaller peak follows the larger one, excessive values of the area of the smaller peak and deficient values of that of the larger peak are obtained by the above method even when the composition peak consists of fairly symmetrical components. As this situation is just contrary to that expected by the theory based on the Gaussian peak model, additional systematic errors would be introduced by applying the correction factors in the above case. The discrepancies between the theory and reality appear to stem from the tailing effects, the significance of which rises with increasing peak size.

The application of the triangular model in locating the separation perpendicular leads generally to false results; the areas obtained by the plain perpendicular drop method are mostly more accurate than those determined by virtue of the above model.

REFERENCES

1 R. L. PESCOK, *Principles and Practice of Gas Chromatography*, John Wiley, New York, London, 1959, p. 145.
2 R. B. D. FRASER AND E. SUZUKI, *Anal. Chem.*, 38 (1966) 1770.
3 A. B. LITTLEWOOD, A. H. ANDERSON AND T. C. GIBB, in C. L. A. HARBOURN (Editor), *Gas Chromatography 1968*, Inst. Petrol., London, 1969, p. 297.
4 A. H. ANDERSON, T. C. GIBB AND A. B. LITTLEWOOD, *Anal. Chem.*, 42 (1970) 434.
5 A. H. ANDERSON, T. C. GIBB AND A. B. LITTLEWOOD, in A. ZLATKIS (Editor), *Advances in Chromatography*, University of Texas, Houston, 1970, p. 75.
6 H. A. HANCOCK, JR., L. A. DAHM AND J. F. MULDOON, *J. Chromatog. Sci.*, 8 (1970) 57.
7 H.-D. METZGER, *Chromatographia*, 3 (1970) 64.

8 K. ABEL AND F. W. NOBLE, *Anal. Chem.*, 36 (1964) 1856.
9 A. W. WESTERBERG, *Anal. Chem.*, 41 (1969) 1770.
10 E. PROKSCH, H. BRUNEDER AND V. GRANZNER, *J. Chromatog. Sci.*, 7 (1969) 473.
11 R. KAISER AND M. KLIER, *Chromatographia*, 2 (1969) 559.
12 R. B. DEAN AND W. J. DIXON, *Anal. Chem.*, 23 (1951) 636.

CHROM. 5162

SEPARATION AND IDENTIFICATION OF DIHALOCYCLOALKANES BY GAS CHROMATOGRAPHY

D. S. ASHTON, J. M. TEDDER AND J. C. WALTON
Department of Chemistry, The University, Purdie Building, St. Andrews (Great Britain)

(First received September 21st, 1970; revised manuscript received November 16th, 1970)

SUMMARY

Mixtures of dichlorocyclobutane, -cyclopentane, -cyclohexane and -cycloheptane isomers, and of chlorofluoro-, bromofluoro-, bromochloro- and dibromocyclohexane isomers have been separated by gas chromatography on a tritolyl phosphate column. The order of elution of the isomers is the same for each set of dihalocyclo alkanes except for the fluoro compounds, and individual isomers can be quickly identified from their retention times.

INTRODUCTION

As part of a detailed investigation into the kinetics of chlorination and bromination of halocycloalkanes, the dichloro isomers of C_4 to C_7 cycloalkanes have been prepared, and some other series of dihalocyclohexanes. The isomer configurations have been established by synthesis, NMR spectroscopy and mass spectrometry, and as a result it has been possible to establish a relationship between relative retention volumes and isomer structures.

The relative retention volumes may be used for identifying the isomers, and as a guide to establishing the structure of similar types of dihalo compound.

EXPERIMENTAL

Materials

1,1-Dichlorocyclohexane was prepared from cyclohexanone and PCl_5 (ref. 1). *trans*-1,2-Dichlorocyclohexane was prepared from cyclohexane and chlorine, and *cis*-1,2-dichlorocyclohexane from 2-chlorocyclohexanol[2]. *cis*- and *trans*-1,3-dichlorocyclohexane were obtained by preparative gas–liquid chromatography (GLC), of a mixture of dichlorocyclohexanes. *cis*- and *trans*-1,4-dichlorocyclohexane were prepared from *cis*- and *trans*-1,4-cyclohexanediol and HCl (ref. 3) and separated by spinning band distillation. All isomers were purified by preparative GLC and characterised by NMR spectroscopy[4].

1,1-Dichlorocyclopentane, *cis*- and *trans*-1,2-dichlorocyclopentane and *cis*-

and *trans*-1,3-dichlorocyclopentane were prepared by methods analogous to those for the corresponding dichlorocyclohexanes. Pure 1,1 *cis*-1,3-, *trans*-1,4-, *cis*-1,4- and *cis*-1,2-chlorofluorocyclohexanes were prepared by chlorination of fluorocyclohexane, and preparative GLC on the resulting mixture. *trans*-1,2-Chlorofluorocyclohexane was prepared by addition of HF to 1-chlorocyclohexane. The dichlorocyclobutane and dichlorocycloheptane isomers were prepared by chlorination of chlorocyclobutane and chlorocycloheptane respectively. Bromofluoro-, bromochloro- and dibromocyclohexane isomers were prepared by bromination of fluorocyclohexane, chlorocyclohexane and bromocyclohexane respectively.

Method

Preparative GC was carried out using a Pye 105 chromatograph, with a flame ionisation detector. The column was 20 ft. × 3/8 in. O.D. coiled glass packed with 15% w/w tritolyl phosphate on 60–100 mesh Embacel.

Analytical data were obtained from a Griffin and George D6 instrument with gas density balance detector using a 6 ft. × 3/16 in. O.D. stainless U-tube column packed with 15% w/w tritolylphosphate on 60–100 mesh Embacel. The column had a resolution of about 1100 theoretical plates based on *trans*-1,2-dichlorocyclohexane. The retention volumes of the dihalocycloalkanes were measured relative to that of *trans*-1,2-dichlorocyclohexane which has a retention volume near the middle of the range covered. Chromatography conditions varied widely depending on the mixture to be separated and are given as follows for each series of isomers: (a) Dichlorocyclobutanes; column temperature 90°, nitrogen flow rate 50 ml/min, inlet pressure 8.0 lbs./in^2. (b) Chlorofluorocyclohexanes: column temperature 85°, nitrogen flow rate 50 ml/min, inlet pressure 8.0 lbs./in^2. (c) Dichlorocyclopentanes; column temperature 90°, nitrogen flow rate 55 ml/min, inlet pressure 9.0 lbs./in^2. (d) Dichlorocyclohexanes and bromofluorocyclohexanes: column temperature 115°, nitrogen flow rate 60 ml/min, inlet pressure 10.5 lbs./in^2. (e) Dichlorocycloheptanes: column temperature 120°, nitrogen flow rate 70 ml/min, inlet pressure 12.0 lbs./in^2. (f) Bromochlorocyclohexanes: column temperature 125°, nitrogen flow rate 60 ml/min, inlet pressure 10.5 lbs./in^2. (g) Dibromocyclohexanes; column temperature 150°, nitrogen flow rate 200 ml/min, inlet pressure 25.0 lbs./in^2.

RESULTS AND DISCUSSION

The relative retention volumes, corrected for column dead space, V_r' of the isomers of dichlorocyclobutane, dichlorocyclopentane, dichlorocyclohexane and dichlorocycloheptane are given in Table I. The internal standard used was *trans*-1,2-dichlorocyclohexane which has a retention volume near the middle of the range. The pressure corrected specific retention volume V_g' for *trans*-1,2-dichlorocyclohexane corresponding to the particular column conditions used for each set of isomers is also given in Table I. A plot of the log V_g' values for *trans*-1,2-dichlorocyclohexane against $1/T$ °K gave an excellent straight line, confirming that this standard substance is well behaved with respect to the temperature.

The relative retention volumes for the chlorofluoro-, bromofluoro-, dichloro-, bromochloro- and dibromocyclohexane isomers are given in Table II, together with

TABLE I

RELATIVE RETENTION VOLUMES OF DICHLOROCYCLOALKANES ON 15% TTP

trans-1,2-Dichlorocyclohexane used as the internal standard, all retention volumes corrected for column dead volume.

Compounds	*Isomer*							*Conditions*	V_g' *(ml/g)*
	1,1	*t-1,2*	*t-1,3*	*t-1,4*	*c-1,3*	*c-1,4*	*c-1,2*		
$C_4H_6Cl_2$	0.058	0.13	0.15		0.21		0.40	(a)	1840
$C_5H_8Cl_2$	0.070	0.093	0.17		0.32		0.65	(c)	1890
$C_6H_{10}Cl_2$	0.48	1.00	1.26	1.33	1.63	2.03	2.73	(d)	860
$C_7H_{12}Cl_2$	0.74	1.26	1.95	2.30	2.42	3.02	3.76	(e)	700

the corresponding values of the specific retention volume of *trans*-1,2-dichlorocyclohexane.

The results form a coherent and regular overall pattern. Thus the order in which the isomers are eluted is the same for all compounds studied, with the exception of *cis*-1,3- and *trans*-1,4-chlorofluoro- and bromofluorocyclohexanes, which are interchanged relative to the other series. The 1,1 isomer is eluted first, followed by the *trans* isomers and then the *cis* isomers. In all cases the *cis*-1,2 isomer was eluted last.

A plot of log V_r' against boiling point is shown in Fig. 1 for all the isomers with known boiling points. Values of the retention for *cis*-1,2-bromochloro- and dibromocyclohexane used in the figure have been estimated as shown below.

There is a broad overall linear correlation between log V_r' and boiling point, but the detail of the graph reveals several interesting trends. The 1,1 and *trans* isomers of each set of compounds appear to lie on straight lines, but curvature of each line appears with the *cis*-1,4 isomer and becomes very marked with the *cis*-1,2 isomer. Clearly some specific interaction between the solute molecules and the weakly polar tritolylphosphate solvent, in addition to the normal solvent–solute forces, becomes important with the *cis* isomers and particularly with the *cis*-1,2 isomers. The straight line portions of the graphs are approximately parallel for the *trans* dichlorocyclopentane and *trans* dichlorocyclohexane isomers, indicating that solvent–solute interactions are of about the same magnitude. The straight line portion of the graph of the bromochlorocyclohexane isomers is steeper, and of the dibromocyclohexane

TABLE II

RELATIVE RETENTION VOLUMES OF DIHALOCYCLOHEXANES ON 15% TTP

Compound	*Isomer*							*Conditions*	V_g' *(ml/g)*
	1,1	*t-1,2*	*t-1,3*	*t-1,4*	*c-1,3*	*c-1,4*	*c-1,2*		
$C_6H_{10}FCl$	0.062	0.151	0.151	0.243	0.209	0.283	0.324	(b)	2250
$C_6H_{10}FBr$	0.193	0.602	0.602	1.01	0.844	1.01	—	(d)	860
$C_6H_{10}Cl_2$	0.48	1.00	1.26	1.33	1.63	2.03	2.73	(d)	860
$C_6H_{10}ClBr$	1.03	1.39	1.89	2.01	2.49	3.06	—	(f)	620
$C_6H_{10}Br_2$	2.84	3.21	4.65	4.88	6.03	7.40	—	(g)	290

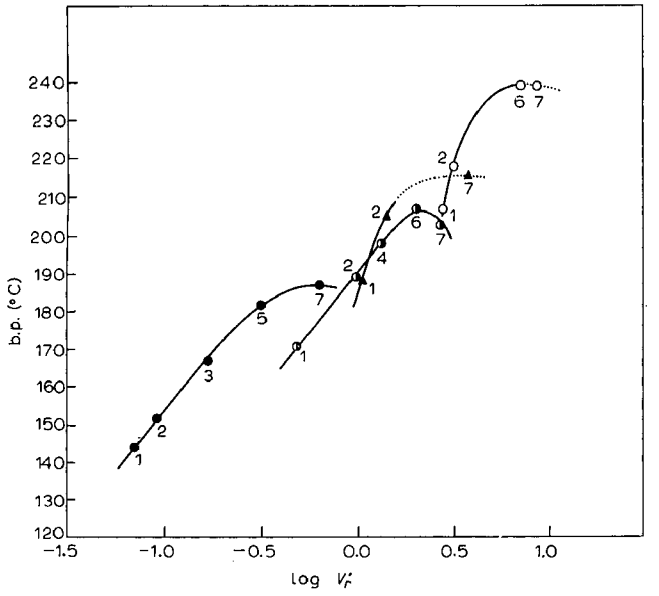

Fig. 1. Plot of log V_r' against b.p. at atmospheric pressure for various dihalocycloalkane isomers. ● = dichlorocyclopentane isomers; ◑ = dichlorocyclohexane isomers; ▲ = bromochlorocyclohexane isomers; ○ = dibromocyclohexane isomers. Dotted line indicates estimated retention volume data. 1 = 1,1 isomers; 2 = *trans*-1,2 isomers; 3 = *trans*-1,3 isomers; 4 = *trans*-1,4 isomers; 5 = *cis*-1,3 isomers; 6 = *cis*-1,4 isomers; 7 = *cis*-1,2 isomers.

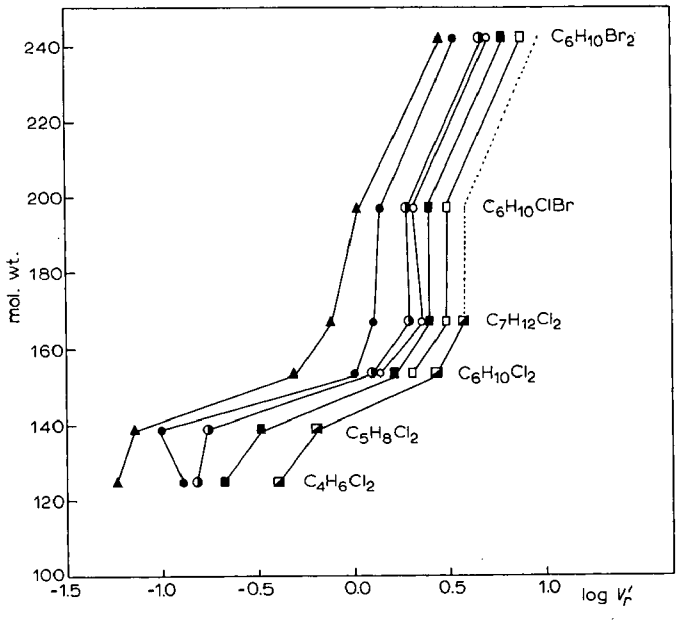

Fig. 2. Plot of log V_r' against molecular weight. ▲ = 1,1 isomers; ● = *trans*-1,2 isomers, ◑ = *trans*-1,3 isomers; ○ = *trans*-1,4 isomers; ■ = *cis*-1,3 isomers; □ = *cis*-1,4 isomers; ◪ = *cis*-1,2 isomers. Dotted line indicates the method of estimation of V_r' for *cis*-1,2-bromochloro, and dibromocyclohexane.

isomers steeper still, so that solvent–solute interactions become weaker with these molecules, possibly because of the decreased electronegativity.

In Fig. 2 a plot of $\log V_r'$ against molecular weight is shown. The values for the chlorofluoro and bromofluoro compounds have been omitted since they give anomalously low V_r' values due to the presence of fluorine. The dotted line in the figure indicates the method of estimation of V_r' for *cis*-1,2-bromochloro- and dibromocyclohexane. The line connecting all the points of isomers with the same nominal structure follows approximately the same path for each set of isomers, but there is no linear correlation. More specifically the points for the C_4 to C_7 dichlorides do not lie in a straight line. Presumably this is because the configuration of a particular isomer, say *trans*-1,3, differs greatly from the C_4 to the C_7 compound and the positions of the chlorine atoms, with respect to each other are very different. Configurational differences alone are not sufficient to explain the non-linearity however, since the three dihalocyclohexanes also do not lie on a straight line, although the configuration of a particular isomer differs little from one C_6 dihalo compound to another. This is further evidence therefore that the interaction between solute and solvent depends on the nature of the halogen atoms involved and that since the relative orientation of the halogen atoms is important, both halogens take part in the interaction, with the possible exception of the 1,1 isomers.

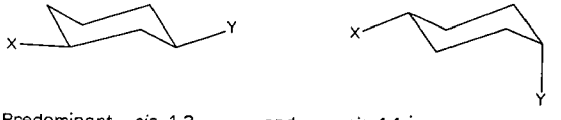

Predominant *cis*-1,3 and *cis*-1,4 isomers

Quantitatively the relation between compound structure and relative retention volume can be easily rationalised. Halogen orientation plays an important part thus the *cis* isomers, where both halogens are available on the same side of the molecule for interaction with the tritolyl phosphate solvent, are eluted last. The *trans* isomers, where two halogens on opposite sides of the molecule are available are eluted earlier, and the 1,1 isomer, where the relative orientation of the two halogens is fixed and independent of the ring conformation is eluted first. The interhalogen distance also affects the interaction between compound and solvent. The *cis*-1,2 isomer, in which both halogens are available close together on the same side of the molecule interacts most strongly with the solvent and is eluted after the *cis*-1,3 and *cis*-1,4 isomers. Models of the *cis*-1,3 and *cis*-1,4 dihaloisomers of cyclohexane in the energetically most favourable conformations[6], suggest that the interhalogen distance is slightly greater for the *cis*-1,3 isomer, which would explain why it is eluted before the *cis*-1,4 isomer.

In the case of the same isomers of cycloheptane the interhalogen distance is greater for the *cis*-1,4 isomer, but here the relative orientation of the two halogens is much less favourable for the *cis*-1,4 isomer so that the order of elution is still *cis*-1,3 followed by *cis*-1,4. For the *trans* isomers, the closer the halogens are together the less readily are they both available for interaction with the solvent so that the *trans*-1,2 isomer is eluted before the *trans*-1,3 and *trans*-1,4 isomers. It seems probable that

for the 1,1 isomers the two halogens are so close together that only one can interact with the solvent and hence they are eluted first.

The chlorofluoro- and bromofluorocyclohexane isomers are less rigidly fixed in any particular conformation, because of the small size of the fluorine atom. Hence the halogen orientation and interhalogen distance, which affect the availability of the halogens for interaction with the solvent, are more variable. Consequently the spread of retention volume values is less for these compounds, and more coincidences (*e.g. trans*-1,2- and *trans*-1,3-chlorofluoro- and bromofluorocyclohexane) and reversals of order are observed.

REFERENCES

1 B. CAROLL, D. G. KUBLER, H. W. DAVIS AND A. M. WHALEY, *J. Amer. Chem. Soc.*, 73 (1951) 5382.
2 M. S. NEWMAN AND C. A. VAN DER WEFF, *J. Amer. Chem. Soc.*, 67 (1945) 233.
3 W. KWESTROO, F. A. MEIJER AND E. HAVINGA, *Rec. Trav. Chim.*, 73 (1954) 717.
4 G. A. RUSSELL, I. AKILUHO AND R. KONAKA, *J. Amer. Chem. Soc.*, 85 (1963) 2988.
5 L. PAULING, *The Nature of the Chemical Bond*, 2nd. ed., Cornell University Press, 1948, p. 64.
6 J. MCKENNA, *Roy. Inst. Chem. Lect. Ser.*, No. 1 (1966) 33.

CHROM. 5142

A VACUUM ULTRAVIOLET ATOMIC EMISSION DETECTOR

QUANTITATIVE AND QUALITATIVE CHROMATOGRAPHIC ANALYSIS OF TYPICAL C, N, AND S CONTAINING COMPOUNDS*

W. BRAUN, N. C. PETERSON**, A. M. BASS AND M. J. KURYLO***

Photochemistry Section, Physical Chemistry Division, U.S. Dept. of Commerce, National Bureau of Standards, Washington, D.C. 20234 (U.S.A.)

(Received October 29th, 1970)

SUMMARY

Vacuum ultraviolet atomic emission detection of effluent gases from a chromatographic column is a very sensitive and selective method for qualitative and quantitative elemental analysis of carbon, nitrogen, and sulfur compounds. A low pressure microwave discharge through helium, with added trace amounts of molecular oxygen, produced complete fragmentation of all compounds used and generated intense atomic emissions in the vacuum ultraviolet. Photometric measurement of these monochromator-isolated atomic emissions was successfully used to establish absolute concentration calibrations for the elements carbon, sulfur and nitrogen in various compounds. This detection method is sensitive, highly selective, and has a range of linearity greater than four decades.

INTRODUCTION

Atomic and molecular emission detection has been successfully used by a number of groups in gas chromatographic (GC) applications[1–8]. This detection method is highly sensitive and frequently very selective. The technique consists of introducing chromatographic column effluents containing trace quantities of compounds into a discharge excited either by means of microwave power or high voltage d.c. or a.c. Fragmentation of the compound by electron bombardment and by collision processes involving rare gas metastable species produces electronically excited atoms as well as electronically excited diatomic fragments. Emissions from these species, isolated by means of a monochromator, are used to detect the presence of the compound in the effluent rare gas stream. Thus, the emitted spectral wavelength is frequently an indication of the elemental composition of the effluent compound. Various methods of

* Supported in part by NBS Measures for Air Quality Program.

** Visiting Scientist, 1969–1970. Permanent address: Chemistry Department, Polytechnic Institute of Brooklyn, Brooklyn, N.Y. 11201, U.S.A.

*** NRC-NBS Postdoctoral Research Associate, 1969–present.

producing discharges, the nature of the rare gas, column materials, and pressure conditions have been investigated in order to evaluate the linearity, sensitivity, and selectivity of this detection method[1-8].

Our interest in vacuum UV atomic emission sources has prompted this investigation of vacuum UV chromatographic detection as a means for performing both qualitative and quantitative elemental analysis. Previous work has been confined to the visible and near-UV region of the spectrum, posing some limitation on the elements that can be measured. Our main goal has been to employ atomic emission measurements to obtain quantitative measurement of total atomic content in the effluent compound. Unfortunately, oxygen and hydrogen analyses were not possible, but many other common elements (*e.g.*: C, N, S, Cl, Br, I, P, etc.) were detectable through measurement of vacuum UV resonance and non-resonance atomic transitions.

In the present work only C, N and S were extensively investigated. These are particularly important elements in air pollutants. Instrumental calibrations (of typical air contaminants) are difficult or impossible for standard mixtures which are unstable or difficult to store, (SO_2, NO_2, etc.). Conditions are described below in which essentially complete fragmentation of the compound can be achieved in a rare gas discharge and linearity between emission signal and atom content in the molecule can be realized. It is thus possible to establish concentration calibrations for a particular atom using a stable and easily stored compound. This calibration is then valid for many other compounds containing the same element.

EXPERIMENTAL

The experimental design is schematically shown in Fig. 1. Experiments were performed in basically two different configurations. Samples were analyzed through their vacuum UV emission spectra either continuously (configuration I) as shown in

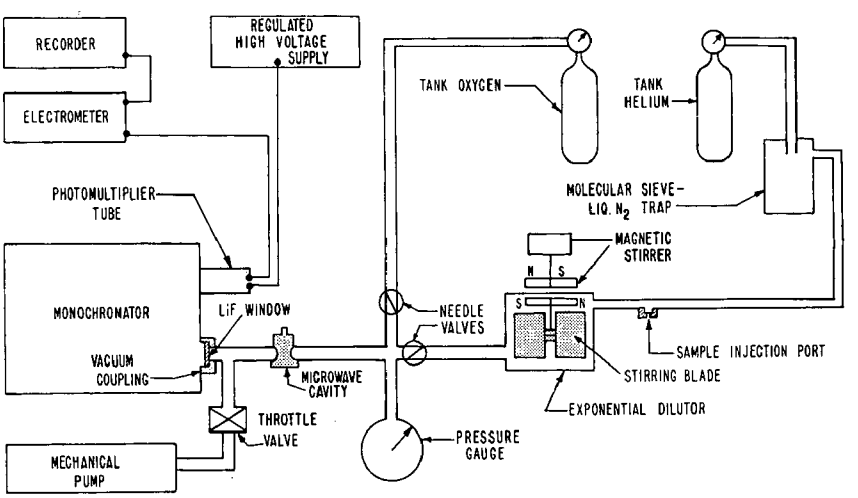

Fig. 1. Schematic drawing of apparatus showing essential components. In this configuration (I) the lamp is connected directly to the outlet of the exponential dilutor. With a chromatographic column replacing the dilution (configuration II) the apparatus is used as a chromatographic detector.

Fig. 1 or by passing them through a chromatographic column (configuration II). In the latter method the LOVELOCK[9] exponential dilutor was replaced by a temperature-controlled chromatographic column, all other components remaining the same. In either configuration a 1 or 5 ml sample diluted with He was injected into the injection port.

The essential components of the apparatus consist of a vacuum monochromator ($f/10$) used to isolate atomic-line wavelength positions below 2000 Å, a liquid N_2-trapped mechanical pump required to evacuate the discharge (lamp) section, and helium purified to remove trace carbon and nitrogen impurities such as CO, N_2, CO_2, by means of a bakeable (2000 cm^3) trap containing 5 Å molecular sieve cooled to liquid nitrogen temperature. The helium discharge is excited by means of a 2450 MHz microwave (diathermy) unit employing a small, tuneable EVENSON microwave cavity[10]. The chromatographic column or exponential dilutor was operated at 1 atm pressure of He. The inlet to the lamp consists of a variable flow needle valve which can be adjusted so that the pressure in the lamp discharge is about 2 Torr total pressure (1 Torr = 133.32 $N \cdot m^{-2}$). At this pressure a stable discharge through helium can be maintained. The microwave cavity, in this configuration, is about 10 cm from the entrance slit of the monochromator and the discharge in the 10 mm I.D. quartz tube is viewed end-on through a lithium fluoride window.

The pressure in the lamp is measured with a precision-dial Bourdon gauge (0–20 Torr) and the volume flow is monitored by venting the exhaust of the mechanical pump through a soap bubble flowmeter.

The various intense atomic line spectral positions and electronic transitions appearing in the vacuum UV have been previously determined and tabulated[11] under experimental conditions somewhat similar to those employed here. For most of the experiments, the carbon 1930.9 Å ($^1P^\circ_1 \rightarrow {}^1D_2$) line was used to monitor carbon containing compounds, the 1742.7 Å nitrogen line ($^2P_1 \rightarrow {}^2P_0$) line for nitrogen containing species, and 1826.3 Å sulfur line ($^3S^\circ_1 \rightarrow {}^3P_0$) for sulfur. The monochromator entrance slit setting was generally 0.05 mm; a LiF-window, CsTe photomultiplier was used to measure the line emission through a 0.05 mm exit slit. The electrometer time constant was about 1 sec. Carbon and nitrogen background signals from the helium carrier gas flowing through the lamp were subtracted out using the electrometer offset circuit. The liquid nitrogen-cooled molecular sieve trap was found to significantly lower carbon and nitrogen background signals, and considerably helped the signal-to-noise ratio. The response of the lamp section to compounds eluting from the GC column was sufficiently fast due to the almost thousand-fold pressure drop between the column and detector that the rather large detector (lamp) volume of 50 cm^3 produced adequate detector response time and resolution.

An additional feature of the detection system shown in Fig. 1 is the oxygen supply inlet. It was found that carbon and sulfur compounds eventually left deposits on the walls of the lamp. This was particularly noticeable for longer-chain hydrocarbon and other oxygen-free compounds. Molecular oxygen was introduced upstream of the discharge at a very low flow rate relative to the helium (O_2 pressure = 10–100 mTorr) but in large concentrations relative to those of the effluent compounds. Oxygen atoms produced in the microwave discharge were found to be very effective in keeping all of the carbon and sulfur in the discharge zone by rapidly removing deposits from the walls.

With the LOVELOCK exponential dilutor in line with the emission lamp the injected sample was diluted at a constant rate with He and the response at a particular spectral position was monitored as a function of a known concentration of sample passing through the lamp section. The dilution was calculated from

$$C = C_0 \cdot e^{-Kt} \tag{1}$$

where C is the concentration at time t; C_0, the concentration at $t = 0$; and the constant K, obtained from slope of a semilog plot of C against t, is related to the volume of the dilution flask $V(cm^3)$, and the volumetric flow rate, φ (cm^3sec^{-1}), through

$$K = \varphi/V \tag{2}$$

Both V and φ can be accurately measured. If the response of the detector is truly linear with the concentration of sample exiting from the dilution flask, then a linear plot of $\log(s)$ *vs.* t is obtained where s is the photomultiplier current and the value of K obtained from the slope will agree with the value of K calculated from eqn. 2.

In configuration II, with the chromatographic column replacing the exponential dilutor of Fig. 1, samples were prepared as follows. A gas syringe of 1 ml volume, filled to atmospheric pressure with a particular compound was injected into the exponential dilutor (external to the detection apparatus) at the He inlet side through a "T" fitting equipped with a rubber septum seal. At set time intervals, 1- or 5-ml samples were extracted from the exit side of the dilutor (vented to the atmosphere) and these were injected into the injection port inlet to the GC column. In this way chromatograms were developed for large variations in sample size, and the absolute concentrations could be estimated from the known (measured) flow rate through the dilutor and the volume of the dilution flask (300 cm^3). Linearity of the detector in the chromatographic mode of operation could again be verified by plotting $\log(s)$ *vs.* t and comparing the slope with the calculated slope attained from eqn. 2 using the flow rate through the dilution flask. Mixtures of two or more compounds were prepared in sample flasks equipped with a rubber septum at known dilution in helium. These were sampled at atmospheric pressure with a 1 ml syringe and injected into the chromatograph.

Although several column materials were employed, depending on the compounds investigated, the majority of experiments were performed with Porapak-N in a 1/4 in. × 1 ft. long stainless-steel column. Only experiments with this column are reported below. It should be noted, however, that other column packing materials, *e.g.*, molecular sieve, silica gel, and squalane gave equally satisfactory results. The column temperature was controlled by means of a water bath, the temperature of which was measured by a mercury immersion thermometer. Employing a 160,000 cm^3sec^{-1} mechanical pump, unthrottled, and maintaining about 1–2 Torr pressure in the lamp section of the detector resulted in flow rates of about 200 atm cm^3sec^{-1} through the chromatographic column in configuration II. In configuration I, with the exponential dilutor replacing the column, typical flows averaged about 100 atm cm^3sec^{-1}. In both modes of operation the pressure in the column or the dilutor was slightly over 1 atm.

RESULTS

Configuration I: Lovelock dilutor

Experiments employing the apparatus in configuration I (shown in Fig. 1), were designed to test the linearity of the detector as well as to test the response of the detector as a function of atomic composition of a test compound. A plot of the log of photomultiplier currents against time according to eqn. 1 should yield a straight line

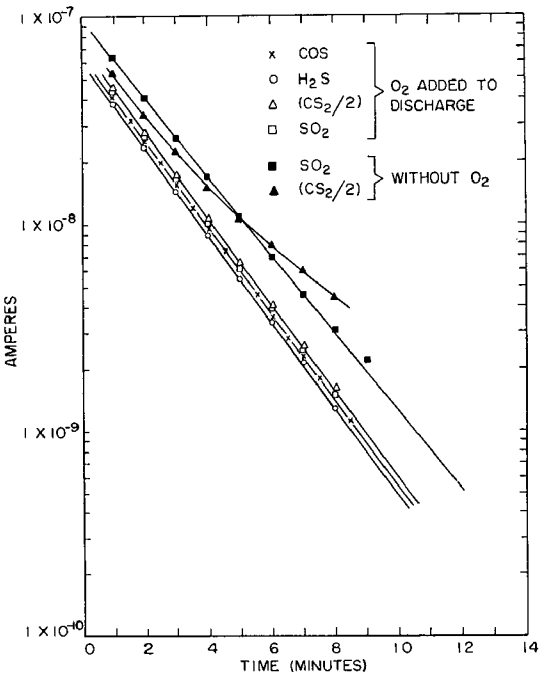

Fig. 2. Detector response S (A) at the sulfur 1826.3 Å line as a function of dilution time (min). Initial sample size the same for each compound, 4×10^{-9} moles ($\sim 10^{-4}$ cm³atm). Slope calculated from flow rate and dilutor volume, 0.52 min^{-1}; slope measured from lower family of curves, 0.39 min^{-1}; figure shows the effect of oxygen added to discharge (lower curves); absence of oxygen (upper curves) shows non-linear behavior.

plot. Linear behavior on a semilogarithmic plot in itself, however, does not demonstrate detector linearity unless the slope agrees with that obtained through eqn. 2.

Fig. 2 displays detector response using the sulfur 1826.3 Å emission line for various sulfur containing compounds: COS, H_2S, SO_2, and CS_2. The K values obtained from the slopes agree within experimental error $\pm 5\%$ with the calculated value (eqn. 2) provided that a supplementary oxygen flow is maintained. In the absence of oxygen, the initial response toward sulfur is somewhat larger. The Schumann-Runge absorption bands of molecular oxygen account for the attenuation in signal when O_2 was added. The slope for sulfur atom response without added oxygen is considerably lower than the value calculated from the volume of the dilution flask and the helium flow rate. Sulfur polymers deposit on the walls of the lamp and are removed very slowly, thus accounting for a delayed response and smaller slope. The

effect is much more pronounced for CS_2 than for SO_2, and distinct curvatur can be noted on the semi-logarithmic plot (Fig. 2). A distinct light brown film was observed to develop over long operating times. After operating the lamp without oxygen for some time, addition of oxygen to the discharge was found to cause a rapid removal of the deposit with a sudden development of a very large sulfur atom emission signal. By continuously passing oxygen through the discharge no deposit forms and the response to the sulfur number in the parent compound is linear. The relative response of the signal is approximately the same for COS, SO_2, H_2S, and (CS_2/2) as shown by the lower family of curves (Fig. 2). The total spread of these (10%) is in fair agreement with the precision of preparing the standard mixtures and syringe sampling (~5–10%).

The choice of the emission line may affect linearity between the atomic emission signal and atom concentration. Emission lines from transitions terminating on the ground electronic state of the atom can be strongly reversed due to self-absorption by the ground state atoms in the discharge. In the limit of high concentration the atomic emission signal may be slowly varying or may even be invariant with increasing atom concentration[12], whereas in the limit of low atom concentration it is always a linearly increasing function. Both oxygen and hydrogen atomic emissions, for example, observed at the 1303 Å and 1216 Å resonance lines, respectively, exhibit essentially negligible response toward oxygen and hydrogen containing compounds added to the discharge. This behavior results from the high background of hydrogen and oxygen atoms in the "pure" helium discharge since it is essentially impossible to remove trace amounts of water from the lamp and connecting tubing.

Fig. 3 demonstrates two distinctly different response characteristics to sulfur

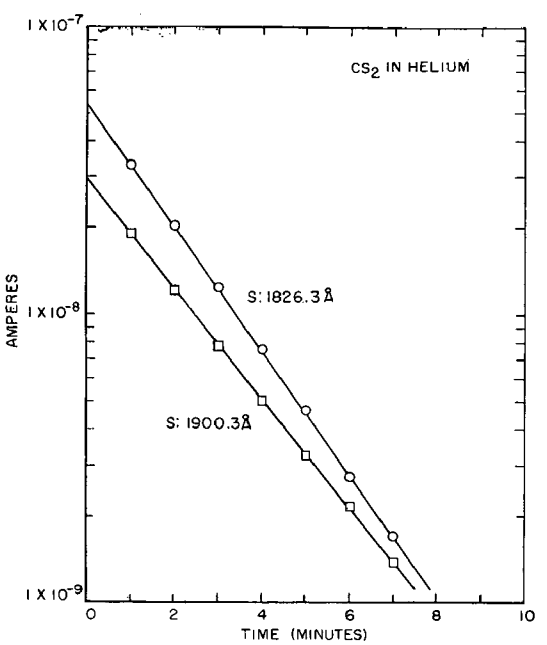

Fig. 3. Effect of line reversal on linearity: detector response at 1826.3 Å (J = 0) sulfur line and at the 1900.3 Å (J = 2) sulfur line. The upper curve (1826.3 Å) yields a slope which agrees exactly with the calculated slope (from flow rate and dilutor volume) *i.e.* demonstrates linear response.

atoms depending on the choice of the sulfur emission line. The sulfur 1826.3 Å line responds properly, *i.e.*, the slope agrees with the value calculated from eqn. 2. The 1900.3 Å sulfur emission line, however, is apparently not linearly dependent on sulfur atom (or sulfur compound) concentration but depends approximately on the 0.9 power of concentration. Both sulfur emission lines terminate on the ground electronic state of the sulfur atom; however, the 1826.3 Å terminates on the $J = 0$ state, while the 1900.3 Å line connects to the $J = 2$ state. The latter is the lower energy level, *i.e.*, the most populated level. If the multiplets are populated according to Boltzmann statistics, at room temperature the relative populations of the $J = 0$, 1, 2 levels are respectively about 1, 10, 100. Since the Boltzmann distribution is approximately obtained in the discharge, the emission line terminating on the least populated ground electronic state multiplet level ($J = 0$) is considerably less self-reversed than the most populated level ($J = 2$). The slope of the exponential dilution plot for 1900.3 Å (Fig. 3) should slowly change and in the limit of very low concentration approach that of the 1826.3 Å curve.

Complications of this type can be completely avoided if line transitions are chosen which do not connect to the ground electronic state of the atom. While this criterion can be realized for C, S, and N atoms using the respective 1930.9 Å, 1826.3 Å, 1742.7 Å emission lines, the only observable emissions for oxygen (1303 Å) and hydrogen (1216 Å) in the vacuum UV terminate on the ground state and preclude analysis for these atoms in this spectral range. The strong Balmer-α line ($n = 2$, 6562 Å) in the visible region of the spectrum, however, has been used successfully to measure hydrogen atom concentrations in hydrogen and deuterium mixtures[13,14].

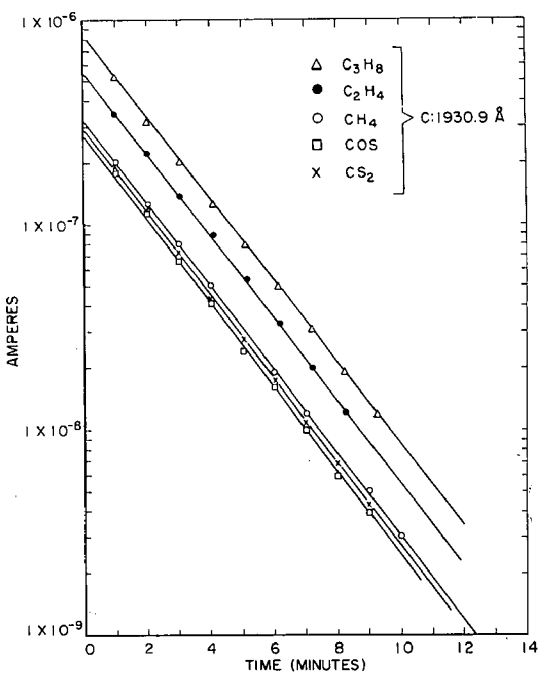

Fig. 4. Configuration I; demonstrates detector linearity and linearity on carbon number in compound. Initial sample size the same for each measurement, 4×10^{-9} moles ($\sim 10^{-4}$ cm^{3}atm).

Fig. 4 demonstrates the detection linearity for various carbon compounds. These curves were developed with an oxygen flow maintained. As found for sulfur compounds, the slopes for carbon compounds agree with the value calculated from the volume flow and the volume of the dilutor. The relative response also appears independent of the carbon containing compound (*e.g.*, COS, CS_2, CH_4) but follows closely the number of carbon atoms in the compound, (*e.g.*, equal amounts of CH_4, C_2H_4, and C_3H_8 give responses in the ratios 1:2:3). Deviations from linearity were observed also as in the sulfur case, although the deviations were somewhat less pronounced. Non-linearity in signal *vs.* carbon atom number in the carbon compound was observed in absence of supplementary oxygen flow. Deviations from linearity were severest for the higher molecular weight hydrocarbons.

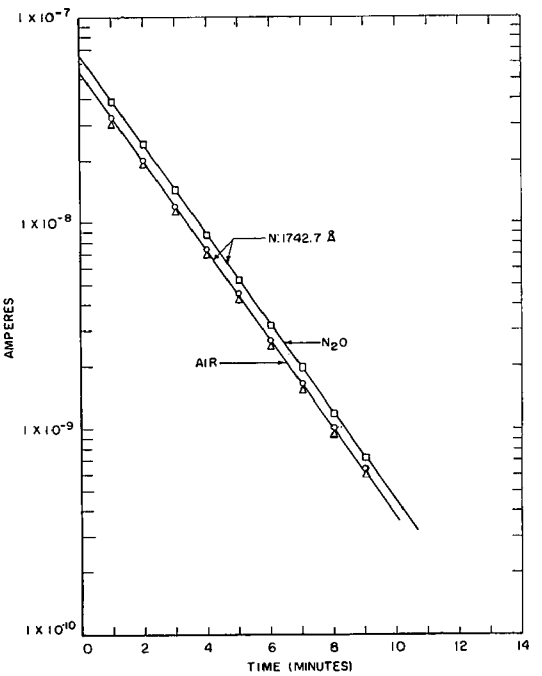

Fig. 5. Configuration I, equal volume samples of air in helium and N_2O helium. Initial sample size 4×10^{-9} moles (10^{-4} cm^3atm). Correcting for oxygen in air demonstrates equal response to nitrogen content for both samples.

Response to nitrogen, using the 1742.7 Å N emission line, is depicted in Fig. 5 for two compounds containing two nitrogen atoms, N_2O and N_2. As expected, equal sensitivities were realized as well as linear detector response. Dependence of detector linearity on oxygen flow for these two compounds was not evident.

Configuration II: chromatographic column application

Typical chromatograms are shown in Fig. 6. GC traces of a multi-component mixture containing approximately equimolar amounts of H_2S, COS, N_2O, cyclopropane (*c*-C_3H_6) and in addition containing the impurities air plus CO_2, are shown with the monochromator peaked on the nitrogen, sulfur, and carbon emission lines. At a

constant amplification throughout, the various traces show that there is no apparent response toward sulfur and carbon compounds at the nitrogen emission line. Further amplification by two orders of magnitude reveals a response toward both carbon and sulfur compounds about 10^{-3} times less than the photometric response toward nitrogen. Similarly, response toward carbon, *e.g.* *c*-C_3H_6, at the sulfur position is between 5×10^{-2} and 1×10^{-3} times the response toward sulfur, *e.g.*, H_2S or COS. Selectivity is here defined in the usual way, *i.e.*, the relative response to H_2S at the

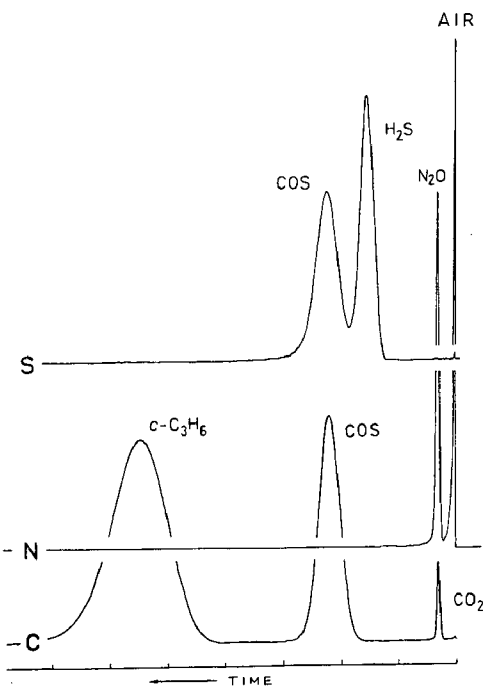

Fig. 6. Configuration II, equimolar mixtures of COS, H_2S, N_2O, and cyclopropane: 2×10^{-7} moles ($\sim 5 \times 10^{-3}$ cm^{3}atm) containing trace air and CO_2 impurities. Detector response at the sulfur 1826.3 Å (top), nitrogen 1742.7 Å (middle) and carbon 1930.9 Å (bottom) atomic line positions.

sulfur emission line position compared to the response at the sulfur position to a compound containing only carbon, *e.g.*, *c*-C_3H_6. Molecular emissions of CO, NO, and O_2, are minimal in this wavelength range and do not coincide with the atomic wavelength positions so that the selectivity, to a good approximation is limited by light scattering in the monochromator. Selectivity values of about 10^3 to 10^4 are expected from the stray radiation properties of the monochromator.

Selectivity values lower than 10^3 are sometimes observed which depend on the sample size, column, the composition of the gas mixture, and the oxygen flow rate. While oxygen removes essentially all of the sulfur and carbon passing through the lamp a displacement effect is sometimes noticeable for multi-component samples. For example, a carbon-containing compound passing through the lamp can liberate trace quantities of sulfur from the walls due to a sulfur compound which has just previously eluted from the column and formed deposits. This can result in selectivity

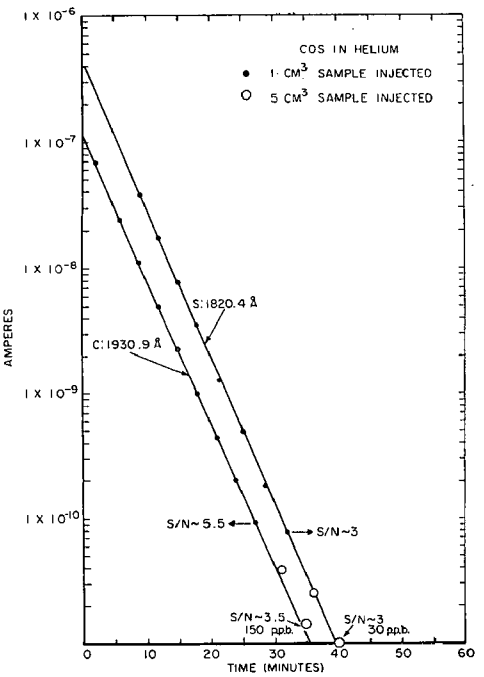

Fig. 7. Sulfur and carbon response from COS using exponential dilutor plus column. Semilog plot of peak height (A) *vs.* time. Column Porapak-N, $^1/_4$ in. × 1 ft., 25°, helium carrier. Carbon atomic emission at 1930.9 Å; sulfur atomic emission at 1820.4 Å 0.05 mm slits. Photomultiplier dynode voltages 2.5 kV and 3.0 kV for C and S respectively. Helium flow rate in exponential dilution flask = 90 cm³/min, volume = 300 cm³. Initial injection 0.5 ml COS into mixing flask.

values as low as 200. In general, selectivities observed here are in the 10^3 range or better, when an oxygen flow is maintained.

Fig. 7 demonstrates linearity of the column plus detection system. Samples of COS taken as a function of time from the exponential dilutor were injected into the chromatograph injection port and the peak heights, measured in amperes, were plotted on semilog paper. Both carbon and sulfur atomic emissions were monitored. This test of linearity examines not only the detector linearity but also the sampling from the dilutor plus column. Once again, K obtained from the slope agrees within several percent of the value calculated from eqn. 2 using the flow rate through the dilutor and the dilutor volume. The range of linearity appears to be at least four orders of magnitude, ranging from large sample sizes 10 Torr cm³ to sample sizes less than 10^{-3} Torr cm³.

The detection limit of the present apparatus, sampling at the lowest concentration limit with a 5 ml injection syringe, is about 100 p.p.b. for carbon and about 30 p.p.b. for sulfur. The limit, for this instrument, is arbitrarily fixed as a measurement which can be made at a signal to noise ratio of about 3:1. Sulfur determinations are somewhat more sensitive than carbon because of a lower background level for sulfur than for carbon with only "pure" helium flowing through the lamp.

A number of parameters affect the ultimate sensitivity; these were only qualitatively investigated. They include the distance of the discharge to the monochromator slit, the slit width, the tuning of the microwave cavity (which affects back-

ground noise of fluctuations), the pressure in the discharge, and the microwave power level. The best discharge can be maintained in the lamp at a pressure of about 1 to 5 Torr. At higher pressures in the lamp a higher concentration of eluting compound can be achieved with a potential increase expected in signal. In fact at low pressures in the discharge the detector signal increases linearly with increasing pressure. However, the emission signal becomes insensitive to increasing pressure at pressures greater than about 10 Torr where the microwave coupling is impaired.

Most experiments were performed with 0.05 mm slits. However, as expected, the absolute signal intensity increased with increasing slit width and a somewhat improved signal to noise ratio could be obtained at the larger slit settings. Little dependence of signal on microwave power level settings was observed. An increase in power level of about a factor of two produced an increase in signal by less than 20%. Therefore very constant sensitivity ($\pm 5\%$) was obtained for various sample sizes for many hours and even days at a fixed microwave power setting.

The microwave power level had little effect on the relative sensitivity *vs.* number of atoms in the compounds with oxygen flow maintained. In the absence of oxygen flow, however, higher molecular weight compounds containing more than one particular atom, as previously noted, produced less than a linear response with increasing atom content. Higher microwave power levels tended to improve linearity undoubtedly due to greater fragmentation and less polymer formation on the discharge tube walls. To ensure complete fragmentation of effluent compounds the helium flow direction was maintained from the back toward the front of the lamp *i.e.* toward the direction of the monochromator slit.

As previously noted, the percentage of oxygen introduced in the lamp is not critical. For very small sample sizes the polymer build-up problem is less severe and very little oxygen flow is required to achieve precise linearity between signal and atomic concentration. At higher concentrations, oxygen pressures as high as 50 mTorr are required to maintain linearity. In the absence of oxygen, with large sample size, large satellite peaks were frequently observed for carbon and sulfur containing compounds. These satellite peaks came immediately following the compound peak position. The satellite resulted from carbon and sulfur slowly eroding from the walls of the discharge tube after compounds had eluted from the column. Addition of oxygen produced larger initial peaks and completely eliminated the satellite peaks.

The precision obtainable with this detection system can be roughly assessed from the various figures. Fig. 5, for example, displays two separate determinations of an air sample with several hours between separate injections. The long term reproducibility is well within the precision of syringe sampling and presumably with a more precise sample injection technique the detection system reproducibility should at least match deviations of individual points from the straight line dilution curves ($\sim$2–5%).

DISCUSSION

The first systematic investigations of UV-visible atomic emission chromatographic detection were reported by BACHE AND LISK[4–7]. Selective analysis of drugs and pesticide residues was demonstrated by using the most intense phosphorous, sulfur, chlorine, bromine, and iodine lines in the UV-visible spectrum. In addition to achieving sensitive and highly selective qualitative detection, they were also able to

attain a fair degree of linearity of detector response for different organic compounds containing various amounts of a given element and different types of chemical bonds. This was achieved by analyzing very small concentrations of sample and by employing high power densities in a capillary discharge lamp. Reasonably intense atomic emissions were achieved through the use of helium carried gas. Earlier experiments by these workers with argon carrier gas resulted in intense molecular and somewhat weaker atomic emissions.

Here we have extended their work to detection in the vacuum UV region and demonstrated nitrogen and carbon analysis. We have been concerned primarily with precise chromatographic detection of simple gaseous systems useful in physical-chemical, photochemical, and air pollution applications. The range of linearity of the detection systems and linearity with atom number found in the present work suggests a potential use rivaling the flame ionization detector. The detection sensitivity utilizing atomic vacuum UV emissions compares favorably with flame-ionization detection.

Detection limits obtained by BACHE AND LISK[4–7], using visible and near UV atomic emission lines are somewhat smaller than those found in this work. Selectivity, however, appears to be better in the vacuum UV than in the visible, limited principally by light scattering in the spectrometer. No attempt has been made to achieve maximum sensitivity. Molecular fragment detection (as opposed to atomic detection) obtainable under higher pressure conditions by other workers appears to be as much as several orders of magnitude more sensitive than atomic emission detection. However, molecular emission detection is frequently not linear and requires separate calibration for each compound. Sensitivity varies markedly with the type of fragment emission measured and frequently requires the presence of impurities in the discharge (*e.g.* nitrogen, to obtain CN emission from hydrocarbons). For quantitative purposes, therefore, atomic emission appears to be potentially more useful in spite of the lower limits of detection possible by other means.

REFERENCES

1 A. J. MCCORMACK, S. C. TONG AND W. D. COOKE, *Anal. Chem.*, 37 (1965) 1470.
2 R. S. JUVET AND R. DURBIN, *J. Gas Chromatog.*, 1 (1963) 14.
3 R. S. BRAMAN, *Anal. Chem.*, 38 (1966) 734.
4 C. A. BACHE AND D. J. LISK, *Anal. Chem.*, 37 (1965) 1477.
5 C. A. BACHE AND D. J. LISK, *Anal. Chem.*, 38 (1966) 1757.
6 C. A. BACHE AND D. J. LISK, *Anal. Chem.*, 38 (1966) 783.
7 C. A. BACHE AND D. J. LISK, *Anal. Chem.*, 39 (1967) 786.
8 R. S. BRAMAN AND A. DYNAKO, *Anal. Chem.*, 40 (1968) 95.
9 J. E. LOVELOCK, *Anal. Chem.*, 33 (1962) 162.
10 F. C. FEHSENFELD, K. M. EVENSON AND H. P. BROIDA, *Rev. Sci. Instrum.*, 36 (1965) 294.
11 D. DAVIS AND W. BRAUN, *Appl. Opt.*, 7 (1968) 2071.
12 W. BRAUN AND T. CARRINGTON, *J. Quant. Spectrosc. Radiat. Transfer*, 9 (1969) 1133.
13 H. P. BROIDA AND J. W. MOYER, *J. Opt. Soc. Amer.*, 42 (1952) 37.
14 H. P. BROIDA AND G. H. MORGAN, *Anal. Chem.*, 24 (1952) 799.

CHROM. 5141

GAS CHROMATOGRAPHIC DETERMINATION OF LEVELS OF ALDADIENE IN HUMAN PLASMA AND URINE FOLLOWING THERAPEUTIC DOSES OF SPIRONOLACTONE

J. CHAMBERLAIN
Searle Scientific Services, Lane End Road, High Wycombe, Bucks. (Great Britain)

(Received October 29th, 1970)

SUMMARY

A specific and sensitive procedure for the determination of aldadiene in human plasma and urine after therapeutic doses of spironolactone has been developed. The method involves extracting the metabolite from the plasma or urine into dichloroethane with subsequent separation and detection on a gas chromatograph equipped with an electron-capture detector. Androst-4-ene-3,6,17-trione is used as an internal standard for quantitation by the relative peak height technique.

INTRODUCTION

Spironolactone (3-(3-oxo-7α-acetylthio-17β-hydroxyandrost-4-en-17α-yl)propionic acid-γ-lactone) is a synthetic steroid which provides effective treatment for resistant oedema and ascites by blocking the action of aldosterone. One of its principal metabolites is aldadiene[1] (3-(3-oxo-17β-hydroxyandrosta-4,6-dien-17α-yl)propionic acid-γ-lactone). A fluorescence technique has been used to determine the metabolite in plasma and urine[2]. This fluorescence method lacks specificity and it was thought that gas chromatography (GC) would offer a more reliable and rapid method for monitoring levels of aldadiene in plasma and urine. Preliminary experiments showed that aldadiene was a strong absorber of thermal electrons, thereby offering a means of sensitive and specific detection after GC.

EXPERIMENTAL

Reagents

The internal standard, androst-4-ene-3,6,17-trione, was prepared by chromium trioxide oxidation[3] of dehydro-*epi*-androsterone in the presence of air. A standard solution of 1 μg/ml in ethanol was prepared. Aldadiene was obtained from our own collection of reference steroids. All other reagents and solvents were obtained from Hopkin & Williams Co. Ltd., Chadwell Heath, Essex, Great Britain, and were not further purified prior to use.

Gas chromatography

A Pye 104 chromatograph equipped with a single ^{63}Ni electron-capture detector and injection point heater was used. Silanised glass columns (1.5 m long × 4 mm I.D.) were packed with 2% OV-1 on CQ 80–100 mesh (JJ's (Chromatography) Ltd., Hardwick Trading Estate, Kings Lynn, Norfolk, Great Britain) and conditioned overnight in a slow stream of nitrogen at 250°. Chromatography was at 250° with a carrier of oxygen-free nitrogen (120 ml/min).

Extraction procedure

Plasma. To each analysis tube was added 200 μl of the internal standard solution, 1 ml plasma, 0.1 ml 0.25% sodium hydroxide and 5 ml dichloroethane with shaking after each addition. After the layers had been allowed to separate the top (aqueous) layer was removed and the organic extract washed with a further 1 ml of water, dried by filtration through Whatman No. 1 filter paper and evaporated to dryness. The residue was dissolved in 1 ml ethanol and 10–15 μl was used for GC.

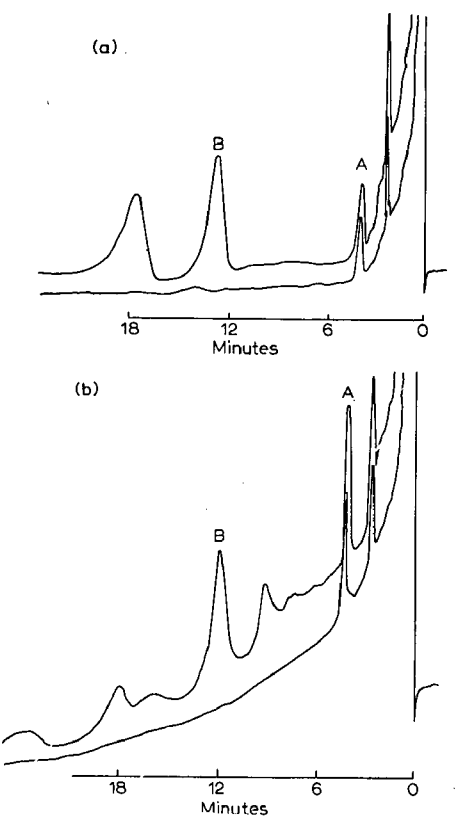

Fig. 1. (a) Gas chromatogram of a dichloroethane extract of urine from a volunteer who had ingested 100 mg spironolactone. (b) Gas chromatogram of a dichloroethane extract of plasma from the same volunteer. In each case the lower trace is from extracts of samples obtained prior to medication. A is the internal standard, androst-4-ene-3,6,17-trione. B is aldadiene corresponding to 3 mg/l in urine (a) and 14.0 μg/100 ml in plasma (b).

Urine. The procedure was as above using 5 ml urine and omitting the 0.25% sodium hydroxide.

Measurement

The retention times of androst-4-ene-3,6,17-trione and aldadiene under the conditions described were 4 and 12 min, respectively (Fig. 1). A linear response, as judged by the relative peak height technique, was observed for the range 0–15 mg/l urine and 0–150 μg/100 ml plasma. (Fig. 2).

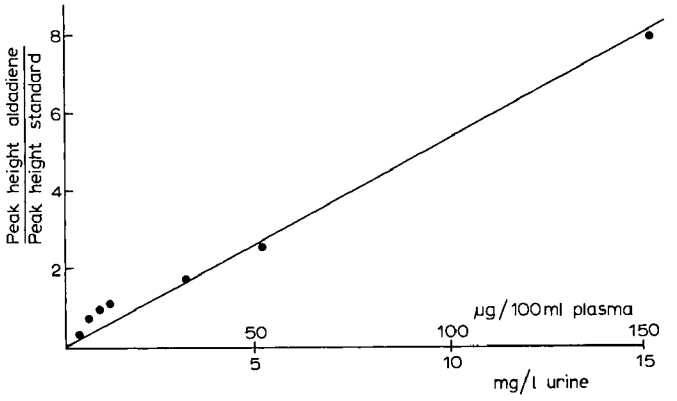

Fig. 2. Calibration curve for quantitation of aldadiene in plasma and urine.

Accuracy

Varying amounts of aldadiene were added to urine and plasma and the mixtures assayed by the present technique. The mean recovery was 96% (range 89–101%) with a standard deviation of $\pm$ 4.

Specificity

The detector used is specific for electron-absorbing molecules. Fig. 1 shows chromatograms obtained from plasma and urine extracts before and after treatment with spironolactone. Table I shows a comparison of values obtained from the analysis of urine and plasma samples assayed by the present technique and the fluorescence technique of GOCHMAN AND GANTT[2]. The lower values obtained by the present technique may be due to the higher specificity obtained by the GC separation from aldadine of other fluorescent metabolites.

Application

Plasma and urine were collected from male volunteers who ingested 100 mg spironolactone (Aldactone-A, G.D. Searle & Co. Ltd.). Venous blood samples were drawn at 0, $\frac{1}{2}$, 1, 2, 4, 6 and 24 h; urine was collected at 0, 2, 4, 6 and 24 h.

RESULTS AND DISCUSSION

Plasma levels of aldadiene reached a peak of 10–15 μg/100 ml approximately 3 h after administration of Aldactone-A (Fig. 3). GANNT *et al.*[4] reported peak plasma

TABLE I

COMPARISON OF PRESENT METHOD (A) AND FLUORESCENCE METHOD (B) FOR ESTIMATION OF ALDADIENE IN PLASMA AND URINE

Plasma (μg/100 ml)		*Urine (mg/l)*	
A	*B*	*A*	*B*
0	0	0	0
3.6	3.5	2.6	4.0
15.7	31.0	2.5	5.6
12.5	18.0	2.0	3.9
1.5	3.0	1.27	1.9
0.7	2.0	0.15	0
3.3	5.5	2.00	2.2
15.3	23.0	3.00	7.3
14.2	15.0	2.44	6.0
24.3	28.0	1.27	1.6

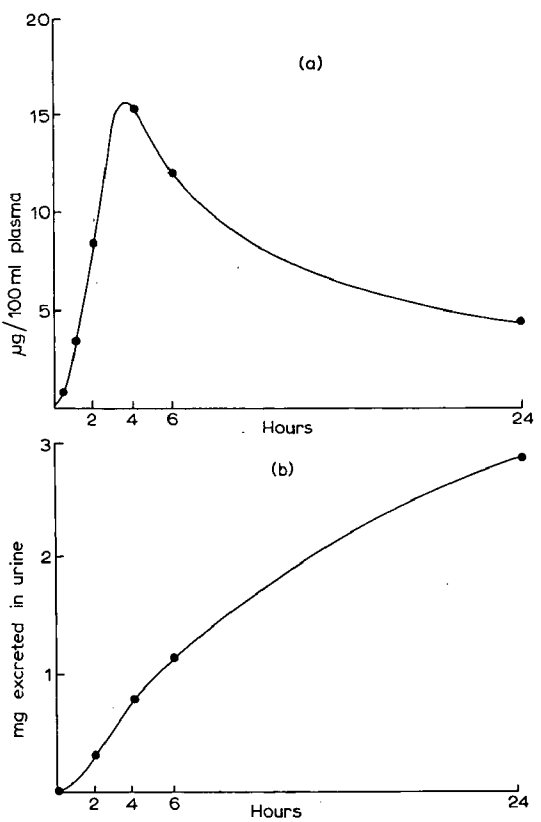

Fig. 3. (a) Plasma concentration–time curve indicating levels of aldadiene found in a male subject after an oral dose of Aldactone-A containing 100 mg spironolactone. (b) The corresponding urine levels of aldadiene in the same subject.

levels at three h of 40 μg/100 ml after a 200 mg dose of Aldactone-A, using the fluorescence technique. The lower values observed in the present study could be attributed to the greater specificity of the GC method.

Urinary excretion of aldadiene reflects the plasma levels of the metabolite (Fig. 3). About 4 mg is excreted in the 24 h after a 100 mg oral dose, and this is in agreement with figures quoted by GANTT *et al.*[4]

Inspection of the gas chromatograms obtained (Fig. 1) reveals the presence of several compounds after spironolactone treatment, in addition to the aldadiene usually measured to monitor levels of the drug. It is not clear, at present, whether these compounds are also metabolites of spironolactone or whether they represent increased excretion of natural products due to the action of spironolactone. This is being investigated.

In recent years it has become apparent that the increased specificity and potency of modern drugs requires very careful control of dose levels. For some drugs there may be considerable individual variation in absorption, metabolism and elimination and dosages are best individualised by monitoring blood levels, or in some cases urinary excretion, of the drug or its metabolites. The present technique provides a rapid, specific and sensitive procedure for correlating plasma and urine levels of aldadiene with biological activity of spironolactone.

ACKNOWLEDGEMENTS

Dr. M. J. TIDD inspired the present investigation and appropriate plasma and urine samples would not have been so readily available without his enthusiasm. I also wish to acknowledge the interest and encouragement of Drs. P. J. LEONARD and R. F. PALMER during the development of the assay.

REFERENCES

1 J. D. H. SLATER, A. MOXHAM, R. HURTER AND J. D. N. NABARRO, *Lancet*, ii (1959) 931.
2 N. GOCHMAN AND C. L. GANTT, *J. Pharmacol. Exp. Ther.*, 155 (1962) 312.
3 K. BOWDEN, I. M. HEILBRON, E. R. H. JONES AND B. C. L. WEEDON, *J. Chem. Soc.*, (1946) 39.
4 C. L. GANTT, N. GOCHMAN AND J. M. DYNIEWICZ, *Lancet*, i (1961) 486.

CHROM. 5155

ROUTINE IDENTIFICATION OF DRUGS OF ABUSE IN HUMAN URINE

I. APPLICATION OF FLUOROMETRY, THIN-LAYER AND GAS–LIQUID CHROMATOGRAPHY

S. J. MULÉ

New York State Narcotic Addiction Control Commission, Testing and Research Laboratory, Brooklyn, N. Y. 11217 (U.S.A.)

(Received November 2nd, 1970)

SUMMARY

The methods described in this report were developed for the rapid analysis of over 500 urines per day for psychoactive drugs. These techniques involve extraction of the drugs from biological material, scanning the extract by automated spectrofluorometry, extensive use of thin-layer chromatography coupled with sequential chromogenic spraying and application of gas–liquid chromatography as an adjunct method for positive identification and confirmation.

The urinalysis laboratory requires a 50–60 ml sample from which a 2 ml aliquot is subjected to fluorometric analysis. The positive morphine and/or quinine samples were then acid hydrolyzed, extracted at pH 9 and the extracts applied to thin-layer plates and the presence of morphine and quinine confirmed by R_F values and reactions with specific chromogenic spray reagents. A 15 ml aliquot of the urine was extracted at pH <1 for barbiturates, diphenylhydantoin and glutethimide. The extract was applied to chromagram sheets developed and sprayed with reagents that provide reactions with these acidic drugs. A 25 ml aliquot of the urine was extracted at pH 10–11 for opiates, opioids, amphetamines, phenothiazines and tranquilizers. The organic extract was divided into A and B fractions, and these fractions developed on separate thin-layer silica gel plates. The A fraction was sprayed with chromogenic reagents primarily to detect amphetamine and analogues. The B fraction was sprayed with reagents to detect opiates, opioids, tranquilizers and phenothiazines. However, the reactions and R_F values on the A and B plates were usually cross compared for the various drugs of abuse.

The methods and techniques were relatively simple to perform and the psychoactive drugs could be detected in the range of 1 to 5 μg/ml of urine.

INTRODUCTION

The techniques[1] used for the determination and identification of psychoactive drugs are essentially those routinely used in analytical chemistry for the character-

ization of chemical structures. Unfortunately, many of the analytical techniques are only effective with pure material. This, of course, is seldom the situation with drugs and/or metabolites extracted from biological material. Therefore, although many methods[1-8] are available for the determination of drugs of abuse none completely fulfills the requirements of a rather large urine monitoring control program. In essence the only technique that can fully meet the needs of a control program monitoring urines for drugs of abuse is complete automation, consisting of continuous flow extraction, photometric detection and computerized data processing. Until technological development can achieve this goal the laboratory today must develop rapid methodology for the detection of drugs of abuse to meet the present requirements of the drug abuse problem.

This communication describes the methods utilized and developed in our laboratory to analyze 500 or more urines per day for psychoactive drugs. These techniques include: extraction from biological material; semiautomated spectrofluorometry; extensive use of thin-layer chromatography (TLC) with sequential chromogenic spraying for detection and use of gas–liquid chromatogrpahy (GLC) as an adjunct tool for positive identification and confirmation.

METHODS AND MATERIALS

The urinalysis laboratory requires a 50–60 ml urine sample from which the following aliquots and analyses are performed:

Spectrofluorometric analysis

2 ml of urine were placed in 15 ml glass stoppered centrifuge tubes and pH adjusted to 9–10 with 3.7 *N* NH_4OH. 4 ml of chloroform–isopropanol (3:1) was added to each tube and the samples shaken by hand for 30 sec–1 min. A two-thirds aliquot of the lower organic phase was removed for the morphine assay and the remaining one-third for the quinine assay. The automated turret spectrofluorometric (ATS) assay for morphine and quinine was then performed as described by MULÉ AND HUSHIN[9]. Those urine samples positive for morphine and/or quinine were subsequently acid hydrolyzed and analyzed by TLC as described below.

Thin-layer chromatographic analysis

Acid hydrolysis of urine. 15 ml of urine in a 40 ml glass stoppered centrifuge tube was autoclaved at 120° for ½ h in 2.3 *N* HCl (final normality) at 18–20 lb. pressure. The samples were rapidly cooled in dry ice and filtered. The filtrate was washed at the acidic pH with 15 ml of ethyl acetate by shaking for 5 min in an Eberbach shaker. The upper organic phase was aspirated off and the pH of the aqueous phase adjusted to about 9 with 9.5 *N* NaOH. 5 ml of 2.3 *M* K_2HPO_4, pH 9.3 (1 of NaCl) and 15 ml of chloroform–isopropanol (3:1) were added to each tube and the tubes shaken for 10 min in the Eberbach shaker. Following centrifugation at 2500 r.p.m. the upper aqueous phase was aspirated off. The organic phase was filtered and evaporated to dryness in a water bath at 85° under a stream of air. The residue was dissolved in 25–50 μl of methanol and applied to 0.25-mm silica gel TLC plate (E. Merck A.G., Darmstadt, G.F.R.). The plates were developed in ethyl acetate–methanol–ammonia (85:10:10) and oven dried at 100° for 15 min. Chromogenic sequential spraying

consisted of 0.5% H_2SO_4 (v/v), followed by viewing the plates under short and long wave UV light; iodoplatinate reagent, followed by mild heating and lastly ammoniacal silver nitrate followed by heating the plates for 10–15 min at 100°.

Urine extraction for barbiturates, diphenylhydantoin and glutethimide at pH <1. To 15 ml of urine in a 40 ml glass stoppered centrifuge tube was added 0.3 ml of 9 *N* H_2SO_4 and 15 ml chloroform. The samples were shaken for 10 min on the Eberbach shaker, centrifuged and the upper aqueous phase removed by aspiration. The organic phase was filtered and the filtrate evaporated to dryness on a water bath at 85° under a stream of air. The residue was taken up in 25–50 μl of methanol or chloroform and applied to Eastman Chromagram sheets (No. 6060 silica gel with fluorescent indicator). The Chromagram sheets were developed in ethyl acetate–methanol–ammonia (85:5:2.5). The sheets were air dried and subjected to the following chromogenic spray sequence: 10% NH_4OH (v/v) followed by visualization with short and long wave UV light; 0.1% $KMnO_4$; 1.0% silver acetate and finally with 0.1% diphenylcarbazone in chloroform.

Urine extraction at pH 10–11 for opiates, opioids, tranquilizers, phenothiazines, phenethylamines and related analogues. Transfer a 25 ml aliquot of urine to a 50 ml glass stoppered centrifuge tube, adjust pH to 10–11 with 6.2 *N* NaOH. Add 5 ml of potassium phosphate pH 10.3 and 12 ml of 25% ethanol in chloroform (v/v), shake for 10 min in the Eberbach shaker, aspirate most of the upper aqueous phase, add 12 ml of 25% ethanol in chloroform to each tube, shake by hand for 1 min and centrifuge if required. Remove the remaining aqueous phase by aspiration, add 100 μl of 6 *N* HCl in ethanol to the organic extract. Filter the organic phase and divide the filtrate into equal fractions (A and B). Evaporate the organic extracts to dryness in a water bath at 75° under a stream of air. Dissolve the residue in 25–50 μl of methanol and apply *fraction A* to 0.25 mm Silica Gel F_{254} thin-layer plates (E. MERCK A.G.). Develop the thin-layer plates in chloroform–methanol–ammonia (90:10:1). The residues labeled *fraction B* were applied to 0.25 mm Silica Gel F_{254} plates and developed in ethyl acetate–methanol–water–ammonia (85:10:3:1). The plates following development were dried in an oven for 15 min at 100° and *fraction A* plates treated as follows: viewed under short and long wave UV light; sprayed with 0.4% ninhydrin in acetone and irradiated for 5–10 min under long wave UV light; followed by 0.5% H_2SO_4 (v/v); 1.0% iodine in methanol; 0.5% H_2SO_4 (clears TLC plate); and iodoplatinate reagent. *Fraction B* plates were treated as follows: viewed under short and long wave UV light; sprayed with 5.0% H_2SO_4 (v/v) and the plates viewed under long wave UV; sprayed with iodoplatinate reagent and lastly ammoniacal silver nitrate followed by heat. In order to detect meprobamate the A and/or B plates were sprayed with furfural followed by conc. HCl and heat.

Gas–liquid chromatographic analysis

The GLC detection of drugs of abuse in the urinalysis laboratory was utilized only as an adjunct or confirmatory technique following routine TLC analysis of the urine extracts.

Apparatus. A Perkin-Elmer Model 900 gas chromatograph equipped with dual flame ionization detectors including dual channel wide dynamic range amplifier. The chromatograph was connected to a Leeds and Northrup model W/L dual channel potentiometer recorder with 1 mV range.

Columns. (1) A 6-ft. borosilicate glass coiled column of 1/4 in. O.D. was packed with Gas-Chrom Q (100–200 mesh) and coated with 3% SE-30; (2) A second glass column (6 ft. × 1/4 in. O.D.) was packed with Chromosorb G A/W DMCS (80–100 mesh) and coated with 10% Apiezon-L and 10% KOH. Both columns were conditioned at 200° for a period of 12 h.

For the *barbiturate analysis* the operating conditions with the 3% SE-30 column were: column 180°; injector 250°; manifold 225°; hydrogen at 20 lb. in.$^{-2}$; air at 30 lb. in.$^{-2}$; nitrogen carrier flow rate at 40 ml/min.

For the *opiate analysis* the operating conditions with the 3% SE-30 column were the same as for the barbiturate analysis except a column temperature of 205° was maintained.

For the *phenethylamine and related analogues analysis* the operating conditions with the 10% Apiezon-L, 10% KOH column were: column 160°; injector 200°; manifold 200°; hydrogen at 20 lb. in.$^{-2}$; air at 30 lb. in.$^{-2}$; nitrogen carrier flow rate at 40 ml/min.

Procedure. A 0.1% solution of the commercially available drug was prepared in either methanol, ethyl acetate or acetone. 2–25 μg of the drug was directly injected into the gas chromatograph with a Hamilton microliter syringe. GC analysis of the drugs extracted from urine was accomplished as described for the pure drug by injecting a suitable aliquot (1–5 μl) of the extract dissolved in 50 μl of methanol. In some cases cochromatography was performed by adding the suspected drug to the unknown extract and gas chromatographing the mixture.

Controls. Composite drug standards ranging in concentrations from 10–20 μg of each drug was directly applied to the TLC plates. A urine extractable drug standard consisting of 2–5 μg/ml was utilized with every 50 unknown urines analyzed.

Sensitivity. The limiting sensitivity of most drugs detected was in the range of 1–5 μg/ml of urine.

Reagents. All chemicals were of reagent grade and obtained through J. T. Baker Chemical Company or Fisher Scientific Company. Specially prepared spray reagents were: (1) iodoplatinate. 1 g of platinic chloride in 10 ml of water was mixed with 10 g of potassium iodide in 200 ml of water. The mixture was diluted to 500 ml with water and stored in a refrigerator; (2) ammoniacal silver nitrate, prepared by mixing just prior to use 30 ml of 5 *N* NH_4OH and 30 ml of 50% $AgNO_3$. If cloudy add drop by drop 5 *N* NH_4OH until solution clears. All other spray reagents described were simple percentages either (v/v) or (w/v) of the commercial reagent.

Potassium phosphate buffer, pH 10.3. Prepared by mixing 350 g of anhydrous K_2HPO_4 with 50 g of $K_3PO_4 \cdot H_2O$ and dissolving in 1 l of distilled water.

Thin-layer chromatographic plates. The 0.25 mm silica gel plates with or without fluorescent indicator (F_{254}) were made by E. Merck A.G. Darmstadt, G.F.R. and distributed by EM Reagents, Division of Brinkman Instruments, Inc., Westbury, N.Y. The Eastman Chromagram sheets (silica gel) were made by Eastman Kodak Company, Rochester, N.Y., U.S.A.

RESULTS AND DISCUSSION

Acid hydrolysis of urine and extraction at pH 9.0

Table I summarizes the data obtained following acid hydrolysis of the urine

TABLE I

ACID HYDROLYSIS OF URINE AND EXTRACTION OF DRUGS AT pH 9

Drug	$R_F \times 100$	*Spray reagent color reactions*		
	Ethyl acetate–methanol–ammonia (85:10:10)	*0.5% H_2SO_4 followed by long wave UV visualization*	*Iodoplatinate*	*Ammoniacal silver nitrate*[d]
Morphine	40	green[c]	blue-purple	black
Codeine	75	—	blue	—
Quinine[a]	88	bright blue fl.	blue	—
Nicotine[b]	34	—	blue-black	—
d-Propoxyphene (Darvon)	95	—	red-blue	—
Meperidine (Demerol)	95	—	red-blue	—
Methadone (Dolophine)	96	—	red-blue	—

[a] Quinine provides several products in this fraction with $R_F \times 100$ values of 92, 88, 85, 77, 73, 69, 62, 54, 42, 27, 23 and 15. The colors observed under UV following 0.5% H_2SO_4 range from bright blue through orange, yellow and green. Some of these products were metabolites and some degradation products due to acid hydrolysis.

[b] A minor metabolite of nicotine may be observed at R_F ($\times$ 100) 68 following the iodoplatinate spray. The $R_F \times 100$ of the nicotine standard (unhydrolyzed, unextracted) was 91.

[c] A green fluorescence was observed with visualization under long wave UV light when morphine was present in high concentrations.

[d] Heat at 100° for several minutes was required after spraying.

and extraction at pH 9 as described under methods. The urines in this fraction were analyzed provided a positive result with the fluorometric assay for morphine or quinine was obtained[9]. The principle emphasis in this fraction was thus placed upon confirmation of the routine fluorometric screen for morphine and/or quinine. It is quite obvious that a clear separation of the narcotic analgesics, meperidine, methadone and *d*-propoxyphene was not achieved with this solvent system. This, of course, is not important in this system since an effort to identify these drugs is made in the basic pH 10–11 extraction. Codeine, however, may be readily identified following the iodoplatinate reaction. Morphine, the most important drug in this fraction, was easily identified especially after treating the plate with ammoniacal silver nitrate. Quinine is also confirmed in this system, however, hydrolysis does degrade this compound. Nicotine and its metabolites are important in this system since a vast majority of the urines contain this compound and its metabolites which react with the iodoplatinate spray and thus might cause some confusion with the positive identification of a narcotic analgesic.

Urines extracted at pH <1

The data obtained on R_F values and color reactions following sequential chromogenic spraying for barbiturates, diphenylhydantoin and glutethimide extracted from urine appears in Table II. It is quite obvious that difficulty was encountered in separating amobarbital, pentobarbital and secobarbital by TLC. Secobarbital, however, is readily identified by the bright yellow reaction observed following the 0.1% $KMnO_4$ spray. Amobarbital and pentobarbital metabolites may be

TABLE II

EXTRACTION OF DRUGS FROM URINE AT pH < 1

Drug	$R_F \times 100$[a]	*Spray reagent color reactions*			
	Ethyl acetate–methanol–ammonia (85:5:2.5)	*10% NH_4OH, UV visualization*[b]	*0.1% $KMnO_4$*[c]	*1.0% Silver acetate*[d]	*0.1% Diphenyl-carbazone*[e]
Phenobarbital (Luminal)	40	blue	—	white	blue
Amobarbital (Amytal)	77	blue	—	white	blue
Pentobarbital (Nembutal)	75	blue	—	white	blue
Secobarbital (Seconal)	72	blue	yellow	white	blue
Diphenylhydantoin (Dilantin)	61	—	pale spot	white	—
Glutethimide (Doriden)	89	—	pale spot	white	—

[a] Metabolites of pentobarbital and amobarbital occur at R_F (× 100) 39, 28 (observed as white spots after the silver acetate spray). Metabolites of secobarbital occur at 42 and 32 (observed after $KMnO_4$ spray). A metabolite of glutethimide occurs at R_F 81 (observed after silver acetate spray).

[b] No reaction observed with the nonfluorescent indicator TLC plates. However, with the chromagram fluorescent indicator plates the barbiturates appear blue on an orange background under short wave UV light.

[c] The permanganate spray also provided light yellow spots with the metabolites of secobarbital. Glutethimide and diphenylhydantoin appeared as pale spots on a pink background.

[d] The silver acetate reacting compounds quench the fluorescent indicator TLC plates when visualized under short wave UV light.

[e] The barbiturates and metabolites appear blue on a yellow background after diphenylcarbazone spray (DPC). The metabolite of glutethimide R_F 81 turns blue following the DPC spray. Glutethimide itself, however, does not.

TABLE III

THIN-LAYER CHROMATOGRAPHIC DATA ON VARIOUS BARBITURATES

All chromatography was performed on Eastman Chromagram Sheets with fluorescent indicator. Detection of drugs was as described under METHODS AND MATERIALS. The concentration of each drug was usually 10 μg. Solvent systems utilized (v/v) were: S_1, chloroform–acetone (90:10); S_2, ethyl acetate–methanol–ammonia (85:10:5); S_3, ethanol–dioxane–benzene–ammonia (5:40:50:5); S_4, hexane–ethanol (90:10); S_5, ethyl ether–chloroform (90:10); S_6, chloroform–isopropanol–ammonia (45:45:10); S_7, ethyl acetate–methanol–ammonia (85:10:25).

Barbiturate	$R_F \times 100$						
	S_1	S_2	S_3	S_4	S_5	S_6	S_7
Hexobarbital (Ortal)	85	89	87	62	90	86	89
Phenobarbital (Luminal)	67	57	45	18	96	54	66
Amobarbital (Amytal)	81	83	81	29	96	84	83
Pentobarbital (Nembutal)	80	81	82	31	98	80	84
Secobarbital (Seconal)	82	83	85	31	97	82	82
Aprobarbital (Alurate)	82	76	76	27	91	84	87
Allylisobutylbarbituric acid	83	75	76	32	91	84	87
Barbital (Veronal)	75	66	66	20	91	67	82

observed as white spots following the silver acetate spray ($R_F \times 100$ of 39 and 28). Diphenylhydantoin (Dilantin) as well as glutethimide (Doriden) provide discernible reactions with the silver acetate spray (white) and may be differentiated from barbiturates on the basis of R_F values. Furthermore, a metabolite of glutethimide ($R_F \times 100$ of 81) appears *blue* after the diphenylcarbazone spray reaction.

A small study on the detection and metabolism of barbiturates was initiated with two human volunteers following an ingestion of 100 mg of pentobarbital at 11 p.m. in the evening and urines obtained at about 7 a.m. the following morning. The parent compound (pentobarbital) was easily detected along with metabolites at $R_F \times 100$ of 38 and 27. A similar experiment was conducted whereby 100 mg of amobarbital was ingested and the parent drug as well as a metabolite at $R_F \times 100$ of 39 was easily detected following extraction and analysis for barbiturates.

In Table III the data appears on several barbiturates with various chromatographic solvent systems. It is quite obvious that no single solvent system was available in separating amobarbital, secobarbital and pentobarbital. Phenobarbital, however, is quite easily separated from the other barbiturates and usually exhibits a lower R_F value.

Urines extracted at pH 10–11

In Table IV appear the results obtained with amphetamine and related drugs (A fraction) as well as the data on opiates, tranquilizers and phenothiazines (B fraction). The S_3 solvent system was primarily used with the A fraction extracts and the S_1 solvent system with the B fraction extracted compounds. The S_2 solvent system was used occasionally for amphetamine and related analogues and proved to be effective in separating ecgonine from cocaine and benzoylecgonine.

Normally the TLC plates following development were viewed under short wave and long wave UV light. This provided for an initial evaluation of those drugs that fluoresce under long wave UV light and those that quench under short wave UV light with the fluorescent indicator plates (F_{254} nm). This procedure was followed whether the plates were sprayed with the A or B series of chromogenic reagents.

The drugs primarily extracted from urine in the A fraction and detected with the A series of spray reagents allows for the following comments: (1) Ninhydrin followed by UV irradiation for 10 min was only effective in detecting the primary amines, amphetamine and phenylpropanolamine; (2) Spraying with 0.5% H_2SO_4 usually intensified the ninhydrin reaction; (3) Iodine was in general a universal reagent so that almost all the compounds present on the plate provided a yellow-brown spot with this reagent; (4) Careful use of known standard reference drugs was required to identify the iodine reacting compounds; (5) The second application of 0.5% H_2SO_4 was used to clear the plate following the iodine spray; (6) The thin-layer plates were then sprayed with the iodoplatinate reagent which provided relatively good reaction with the opiates, opioids, phenothiazines and tranquilizers, but in general no reaction with amphetamine and related analogues. A reaction with iodoplatinate for the amphetamine-like compounds appears to depend upon levels of the drug present.

The drugs extracted from urine in the B fraction and detected with the B series of chromogenic reagents allows for the following comments: (1) With 5% H_2SO_4 the phenothiazine compounds appeared quite readily as redish-pink to blue spots; (2) Quinine and metabolites after this reagent when viewed under long wave UV light

TABLE IV

EXTRACTION OF DRUGS FROM URINE AT pH 10–11

Solvent systems used (v/v) were: S_1, ethyl acetate–methanol–water–ammonia (85:10:3:1); S_2, methanol–ammonia (99:1); S_3, chloroform–methanol–ammonia (90:10:1).

Drug	$R_F \times 100$			*UV light*		*Spray reagents color reactions*[a]						
						A fraction					*B fraction*	
	S_1	S_2	S_3	*Long wave*	*Short wave*	*Ninhydrin + UV irradiation*	*0.5% H_2SO_4*	*1% Iodine*	*0.5% H_2SO_4*	*Iodoplatinate*	*5% H_2SO_4*	*Iodoplatinate*
Morphine	18	44	23	green fl.	Q[e]	—	—	yellow-brown	—	purple	—	blue
Codeine	30	46	70	—	Q	—	—	yellow-brown	—	purple	—	blue
Methadone (dolophine)	80	83	80	—	Q	—	—	yellow-brown	—	purple	—	red-blue
Meperidine (Demerol)	62	63	87	—	Q	—	—	yellow-brown	—	purple	—	blue
d-Propoxyphene (Darvon)	94[d]	82	97	—	Q	—	—	yellow-brown	—	purple	—	red-blue
Pentazocine (Talwin)	77	59	60	—	—	—	—	yellow-brown	—	red-blue	—	red-blue
Cyclazocine	57	49	52	green fl.	—	—	—	yellow-brown	—	red-blue	—	red-blue
1-Methorphan	10	13	61	—	Q	—	—	yellow-brown	—	blue	—	blue-black
Hydroxyzine (Vistaril)	96	—	90	blue fl.	Q	—	—	yellow-brown	—	blue	—	blue
Quinine	42[d]	63	49	blue fl.	Q	—	—	yellow-brown	—	purple	bright blue[f]	blue
Cocaine	90	77	92	—	Q	—	—	yellow-brown	—	red-blue	—	red-blue
Ecgonine[b]	—	32	—	—	—	—	—	—	—	blue		blue
Benzoylecgonine[b]	—	78	—	—	Q	—	—	—	—	red-blue	—	red-blue
d-Amphetamine (Dexedrine)	42	52	73	—	Q	purple	increased intensity	yellow-brown	—	—	—	—[g]
Methamphetamine (Methedrine)	28	40	66	—	Q	—	—	yellow-brown	—	—	—	—[g]
Ephedrine	19	38	25	—	Q	—	—	yellow-brown	—	—	—	—
Phenmetrazine (Preludin)	46	67	83	—	Q	—	—	yellow-brown	—	—	—	—
Methylphenidate (Ritalin)	76	78	96	green fl.	Q	—	—	yellow-brown	—	—	—	—

Phenylpropanolamine	31	54	27	—	Q	light purple	increased intensity	yellow-brown	—	—	—	—
Chlorpromazine (Thorazine)	72	60	90	blue fl.	Q	—	—	yellow-brown	—	blue-brown	redish-pink	purple-red
Promethazine (Phenergan)	70	69	91	—	Q	—	—	yellow-brown	light yellow	blue-brown	pink	purple
Prochlorperazine (Compazine)	52	68	87	blue fl.	Q	—	—	yellow-brown	light yellow	blue-brown	blue	purple
Thioridazine (Mellaril)	73	—	88	blue fl.	Q	—	—	dark-brown	dark yellow	blue-yellow	blue	purple
Nicotine	56[d]	66	81	—	Q	—	—	yellow-brown	yellow brown	black-brown	—	blue
Diazepam (Valium)	92	84	92	green fl.	Q	—	—	yellow-brown	—	light red-blue	—	red-blue
Chlordiazepoxide (Librium)	68	82	75	green fl.	Q	—	—	yellow-brown	—	brown-blue	—	red-blue
Meprobamate[e] (Equanil)	81	85	41	—	—	—	—	—	—	—	—	—
Amitriptyline (Elevil)	79	77	95	—	Q	—	—	yellow-brown	—	purple	—	purple
Tripelenamine (Pyribenzamine)	60	51	80	blue fl.	Q	—	—	yellow-brown	—	dark-blue	blue	blue
Chlorpeniramine (Chlortrimeton)	33	34	57	green fl.	Q	—	—	yellow-brown	—	blue	—	blue

[a] Chromogenic sprays utilized under A were primarily for the detection of amphetamines and analogues and used only with the A extract. Those utilized under B were primarily for the detection of opiates and used only with the B extract.

[b] These metabolites of cocaine may be detected by following the iodoplatinate reagent with 5% H_2SO_4 and mild heating. In the ethyl acetate–methanol–NH_3 (85:10:10) solvent system, R_F (× 100) values of 95, 3 and 12 were obtained for cocaine, ecgonine and benzoylecgonine, respectively.

[c] Meprobamate is detected by finally spraying the plates with furfural followed by conc. HCl. A dark black spot appears after subjecting the plates to heat (100°) for a few minutes.

[d] In the S_1 solvent system metabolites of quinine were observed at R_F (× 100) 30, 23, 07; for nicotine at 36, 22; for methadone at 58, and for *d*-propoxyphene a streak was observed from the origin that provided an R_F of 38. Methadone standard generally provided an R_F of 95 in the S_1 or S_3 solvent system, however, in the composite standard the R_F values were identical to the urine extracted compound. Furthermore in the S_3 system a metabolite of methadone was observed at R_F 40. Combining the data from S_1 and S_3 provided excellent confirmatory data for methadone.

[e] The fluorescent indicator TLC plates fluoresce at 254 nm under short wave UV light. Q denotes the drugs which quench the fluorescence. The plates were viewed under UV light prior to spraying with either the A or B sequence of chromogenic reagents.

[f] Must be viewed under long wave UV light.

[g] *d*-amphetamine and methamphetamine may react with iodoplatinate when present in high concentrations (50 μg or more) and provide a blue color reaction.

vividly fluoresced as bright blue, green or orange spots. The presence of quinine was quite characteristic following the sulfuric acid spray; (3) The primary detecting reagent, however, with this group of drugs was iodoplatinate and it was quite effective in detecting the opiates, phenothiazines, tranquilizers, cocaine and its metabolites.

It is important to note that in some instances a different R_F value was obtained with a drug extracted from urine as compared to the nonextracted reference standard drug. An example of this was methadone which could in effect not be separated from *d*-propoxyphene when applied separately on a TLC plate. However, methadone and metabolite extracted from urine provided R_F values different from the standard reference methadone as well as *d*-propoxyphene (see Table IV). The urinary extracted methadone did agree with methadone in the composite standard which contains several narcotic drugs.

Meprobamate was easily detected by spraying the A fraction with furfural and conc. HCl after the iodoplatinate reagent. The presence of this drug was confirmed with the B fraction TLC plate that was sprayed with ammoniacal silver nitrate (detection of morphine) and then followed by furfural and conc. HCl. A characteristic brown-black reaction (spot) for meprobamate was obtained with furfural reagent.

Cocaine presented a rather difficult problem. In order to effectively detect the usage of this drug it was decided to attempt to identify the primary metabolites, ecgonine and benzoylecgonine[10]. If the urine was acid hydrolyzed and then extracted, neither cocaine nor any degradation product was detected indicating destruction under the conditions of acid hydrolysis. However, cocaine and metabolites may be extracted through the procedure used for the extraction of urine at pH 10–11. Neither ecgonine nor benzoylecgonine moves from the origin in solvent systems S_1 and S_3. In solvent system S_2 ecgonine may be separated from benzoylecgonine and cocaine. The metabolite, benzoylecgonine, may be separated from cocaine and ecgonine by using the solvent system ethyl acetate–methanol–ammonia (85:10:10) (see Table IV).

Methamphetamine and codeine also present a rather difficult problem with the solvent systems used in Table IV. A good iodoplatinate reaction with the A sequence of reagents would indicate codeine, however, high levels of methamphetamine may also provide a reaction with iodoplatinate. It is necessary to observe the metabolite of methamphetamine (amphetamine), or the metabolite of codeine (morphine) or resort to either GLC and/or other solvent systems for a definitive identification of these two drugs.

Gas–liquid chromatography of drugs of abuse

The retention time data obtained with various drugs of abuse appears in Table V. The barbiturates may be effectively separated by GLC whereas complete separation by TLC (*i.e.* amobarbital and pentobarbital) was not achieved. In all cases the retention time for the barbiturates was quite short ranging from 1.10 for barbital to 4.31 for hexobarbital. The change in retention time for the barbiturates did not appear to be directly correlated with the size or chain length substitution on barbituric acid. Glutethimide, a sedative hypnotic drug, may also be detected by GLC (retention time of 3.75).

Amphetamine and related analogues were chromatographed (Table V) on an Apiezon column. A fairly good separation was achieved with this column for these

TABLE V

GAS–LIQUID CHROMATOGRAPHIC RETENTION TIME DATA ON VARIOUS DRUGS OF ABUSE[a]

Drug	*RT*	*RRT*[b]
Barbiturates		
Pentobarbital (Nembutal)	2.62	1.00
Barbital (Veronal)	1.19	0.45
Secobarbital (Seconal)	3.43	1.31
Amobarbital (Amytal)	2.25	0.86
Phenobarbital (Luminal)	5.75	2.19
Aprobarbital (Alurate)	1.75	0.67
Hexobarbital (Ortal)	4.31	1.64
Allylbarbituric acid (Sandoptal)	2.25	0.86
Glutethimide (Doriden)[c]	3.75	1.43
Amphetamine and related analogues		
d-Amphetamine (Dexedrine)	4.12	1.00
Methamphetamine (Methedrine)	5.62	1.36
Methylphenidate (Ritalin)	—	—
Phenylpropanolamine	6.37	1.55
Phenmetrazine (Preludin)	3.87	0.94
Ephedrine	5.15	1.25
Narcotic analgesics		
Codeine	8.87	1.00
Morphine	10.50	1.18
d-Propoxyphene (Darvon)	5.19	0.58
Methadone (Dolophine)	5.25	0.59
Meperidine (Demerol)	1.31	0.15
Pentazocine (Talwin)	6.75	0.76
Cyclazocine	5.75	0.65
Cocaine[d]	7.50	0.84
Benzoylecgonine[d]	15.12	1.70
Ecgonine[d]	3.37	0.38

[a] The conditions whereby the drugs were analyzed appear under METHODS AND MATERIALS.
[b] The RRT (relative retention time) refers to pentobarbital for the barbiturates, *d*-amphetamine for the amphetamines and codeine for the narcotic analgesics.
[c] Not a barbiturate.
[d] Not a narcotic analgesic.

drugs. The retention time of each drug except for phenmetrazine was greater than *d*-amphetamine.

Data on the retention time of narcotic analgesics also appears in Table V. The data obtained was quite similar to that reported previously[1] where a much larger number of narcotic drugs were separated by gas chromatography. In essence all the drugs had a shorter retention time than codeine except for morphine and benzoylecgonine. It is of interest to mention that cocaine was easily separated from its metabolites (ecgonine and benzoylecgonine). However, relatively large concentrations of ecgonine and benzoylecgonine (10–20 μg) were required for sufficient detection with the SE-30 column.

ACKNOWLEDGEMENTS

The author expresses his appreciation for the technical assistance provided by P. L. HUSHIN, H. SHAH, E. SAFFER, R. MAST and R. GEISER.

REFERENCES

1 S. J. MULÉ, *Anal. Chem.*, 36 (1964) 1907.
2 S. J. MULÉ, *J. Chromatog.*, 39 (1969) 302.
3 J. COCHIN AND J. W. DALY, *Experientia*, 18 (1962) 294.
4 B. DAVIDOW, N. LIPETRI AND B. QUAME, *Amer. J. Clin. Pathol.*, 50 (1968) 714.
5 J. M. FUJIMOTO AND R. I. H. WANG, *Toxicol. Appl. Pharmacol.*, 16 (1970) 186.
6 G. F. PHILLIPS AND J. GARDNER, *J. Pharm. Pharmacol.*, 21 (1969) 793.
7 A. H. BECKETT, G. T. TUCKER AND A. C. MOFFAT, *J. Pharm. Pharmacol.*, 19 (1967) 273.
8 I. SUNSHINE, *Amer. J. Clin. Pathol.*, 40 (1963) 576.
9 S. J. MULÉ AND P. L. HUSHIN, *Anal. Chem.*, in press.
10 F. FISH AND W. D. C. WILSON, *J. Pharm. Pharmacol.*, 21 (1969) 135S.

CHROM. 5174

APPLICATIONS OF A GAS–LIQUID CHROMATOGRAPHIC METHOD FOR AMINO ACID ANALYSIS

A SYSTEM FOR ANALYSIS OF NANOGRAM AMOUNTS*

ROBERT W. ZUMWALT**, KENNETH KUO*** AND CHARLES W. GEHRKE§
University of Missouri, Columbia, Mo. 65201 (U.S.A.)

(Received November 23rd, 1970)

SUMMARY

The quantitative gas–liquid chromatographic determination of the protein amino acid content of biological substances has been clearly demonstrated with analyses of corn grain, soybean oil meal, blood plasma, and human urine. The precision and accuracy of the gas–liquid chromatographic technique was found to be equal to that of classical ion-exchange chromatography, and superior in some instances.

Further, an instrumental-chromatographic system has been invented which allows the injection of 100 μl or more on a standard analytical column. This device eliminates the TFA peak during analysis of amino acids on the EGA column; results in a more stable baseline due to the decreased amount of solvent and reagents traversing the column; greatly simplifies analysis for nanogram amounts of amino acids; and should find a wide range of applications in many gas–liquid chromatographic and gas chromatography–mass spectrometry investigations. A superior mixed phase chromatographic column is reported for the separation of His, Lys, Arg, Trp and Cys.

INTRODUCTION

A recent manuscript published in this journal[1] described in detail a gas–liquid chromatographic (GLC) method for quantitative analysis of amino acids in complex biological substances. The complete sample preparation procedures were described, including removal of protein, cation- and anion-exchange cleanup, derivatization to the amino acid N-trifluoroacetyl *n*-butyl esters, GLC analysis, and comments on critical points in the method. Also, initial studies on semimicro and micro methods

* Contribution from Missouri Agricultural Experiment Station Journal Series No. 6120. Approved by the Director. Supported in part by grants from the National Aeronautics and Space Administration (NGR 26-004-011-S5), the National Science Foundation (GB 7182), and the Experiment Station Chemical Laboratories.

** National Science Foundation Predoctoral Fellow, University of Missouri-Columbia.
*** Chemist, Experiment Station Chemical Laboratories, University of Missouri-Columbia.
§ Professor and Supervisor of the Experiment Station Chemical Laboratories, University of Missouri-Columbia.

for the derivatization and GLC analysis of amino acids were reported. A general review of this subject has also been presented recently by GEHRKE *et al.*[2].

This paper presents results obtained in two areas: (a) the application of the total analytical procedure described previously[1], demonstrating the analytical potential of the complete method, and (b) the development of a GLC instrumental system that greatly simplifies the analysis for nanogram amounts of amino acids.

To demonstrate the quantitative GLC determination of the amino acid content of corn grain and soybean oil meal, hydrolysates of each were analyzed by both GLC and classical ion-exchange chromatography. The chromatograms of the corn grain and soybean meal, obtained with simultaneous operation of the EGA and OV-17 columns, are presented in Figs. 1 and 2. The data resulting from these analyses are presented in Tables I and II, and the GLC and ion-exchange methods are seen to be in close agreement.

Fig. 3 presents the chromatogram obtained from the analysis of free amino acids in blood plasma. Again, good agreement of the GLC and ion-exchange techniques was achieved, as seen in Table III.

The corn grain, soybean meal, and blood plasma samples were amenable to GLC analysis after cation-exchange cleanup, however, both cation and anion-exchange cleanup were necessary prior to the analysis of human urine. An extensive

TABLE I

AMINO ACID ANALYSIS OF CORN GRAIN

Hydrolyzed for 22 h at 110° in a closed tube with 6 *N* HCl under N_2, cation-exchange cleaned. All percentages are given in w/w%.

Amino acid	*Gas–liquid chromatography*[a]		*Average*	*Ion-exchange chromatography*[b]		*Average*
Alanine	0.650	0.656	0.653	0.628	0.602	0.615
Valine	0.415	0.437	0.426	0.467	0.431	0.449
Glycine	0.328	0.333	0.331	0.329	0.322	0.326
Isoleucine	0.284	0.300	0.292	0.277	0.279	0.278
Leucine	0.967	0.965	0.966	0.969	0.937	0.953
Proline	0.890	0.916	0.903	0.952	0.824	0.888
Threonine	0.330	0.338	0.334	0.328	0.314	0.321
Serine	0.476	0.482	0.479	0.468	0.431	0.449
Methionine	0.190	0.186	0.188	0.178	0.189	0.184
Hydroxyproline	0.041	0.027	0.034	trace	trace	trace
Phenylalanine	0.391	0.399	0.395	0.384	0.394	0.389
Aspartic acid	0.516	0.522	0.519	0.540	0.513	0.527
Glutamic acid	1.409	1.389	1.399	1.549	1.413	1.481
Tyrosine[c]	0.235	0.137	0.186	0.229	0.153	0.191
Ornithine	trace	trace	trace	0.004	0.006	0.005
Lysine	0.278	0.236	0.257	0.245	0.225	0.235
Arginine	0.355	0.376	0.363	0.377	0.346	0.362
Cystine	0.044	0.044	0.044	0.061	0.057	0.059
Histidine	0.357	0.339	0.348	0.305	0.296	0.301
Tryptophan[d]	—	—	—	—	—	—
Total	8.070	7.980	8.025	8.279	7.748	8.014

[a] Two independent analyses, *n*-butyl stearate as internal standard.
[b] Two independent analyses, norleucine as internal standard.
[c] Partially destroyed during 6 *N* HCl hydrolysis.
[d] Destroyed during 6 *N* HCl hydrolysis.

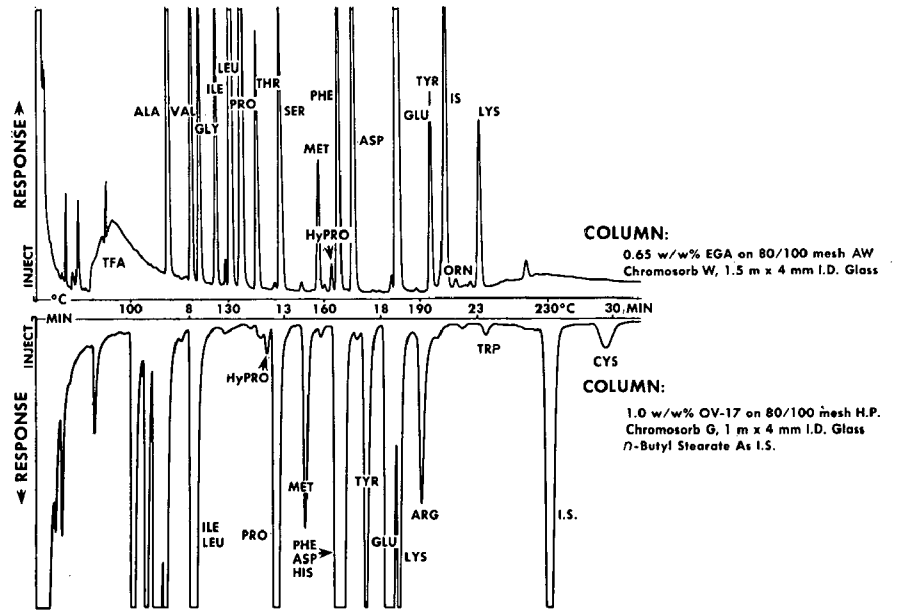

Fig. 1. GLC analysis of corn grain hydrolysate. 50 mg hydrolyzed with 6 *N* HCl, 110°, 22 h, cation-exchange cleaned. Final acylation volume, 2 ml; injected, 5 μl; *ca.* 5 μg total amino acids injected; attenuation, 8 × 10^{-10} A.F.S.; initial temperature, 70°; program rate, 6°/min; final temperature, 230°.

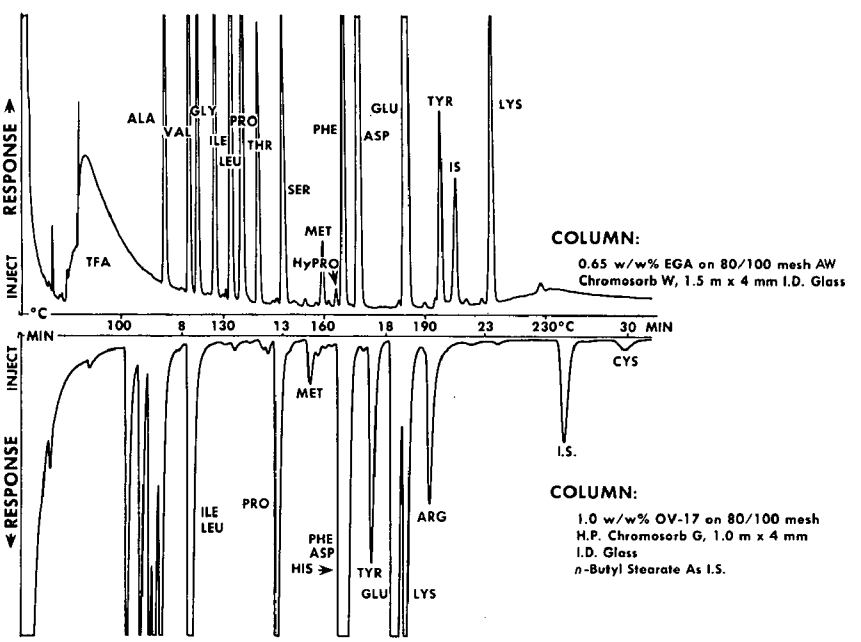

Fig. 2. GLC analysis of soybean meal hydrolysate. 25 mg hydrolyzed with 6 *N* HCl, 110°, 22 h, cation-exchange cleaned. Final acylation volume, 2 ml; injected, 5 μl; *ca.* 5 μg total amino acids injected; attenuation, 8 × 10^{-10} A.F.S.; initial temperature, 70°, program rate, 6°/min; final temperature, 230°.

study of the GLC analysis of urine was presented earlier[1], but since that study, improved chromatography now results in typical GLC analyses as seen in Fig. 4. The data obtained from the GLC and ion-exchange chromatography may vary somewhat, mainly due to the presence of small amounts of extraneous substances, with the level of these substances being dependent on the composition of the original urine sample. These interfering substances are eluted at different relative positions by GLC and ion-exchange chromatography, and thus are responsible for data variation as these substances interfere with different amino acids by GLC and ion-exchange chromatography. The differences in the data obtained by these techniques are generally small[1], but can be significant depending on the particular sample.

TABLE II

AMINO ACID ANALYSIS OF SOYBEAN MEAL

Hydrolyzed for 22 h at 110° in a closed tube with 6 *N* HCl under N_2, cation-exchange cleaned. All percentages are given in w/w%.

Amino acid	*Gas–liquid chromatography*[a]		*Average*	*Ion-exchange chromatography*[b]		*Average*
Alanine	2.181	2.159	2.170	2.096	2.111	2.104
Valine	2.348	2.304	2.327	2.368	2.497	2.433
Glycine	2.002	2.047	2.025	1.944	1.963	1.954
Isoleucine	2.127	2.092	2.110	2.088	2.196	2.142
Leucine	3.453	3.442	3.448	3.496	3.618	3.557
Proline	2.816	2.903	2.860	2.728	2.554	2.641
Threonine	1.850	1.885	1.868	1.856	1.822	1.839
Serine	2.739	2.829	2.785	2.752	2.616	2.684
Methionine	0.438	0.512	0.475	0.352	0.386	0.369
Hydroxyproline	0.093	0.099	0.096	trace	trace	trace
Phenylalanine	2.338	2.331	2.335	2.320	2.504	2.412
Aspartic acid	5.323	5.141	5.232	5.312	5.160	5.236
Glutamic acid	8.180	7.815	8.050	8.220	7.879	8.050
Tyrosine	1.384	1.288	1.336	1.312	1.426	1.369
Ornithine	trace	trace	trace	0.040	0.027	0.034
Lysine	3.080	2.384	2.957	2.816	2.788	2.802
Arginine	3.476	2.883	3.180	3.192	3.438	3.315
Tryptophan[c]	—	—	—	—	—	—
Cystine	0.264	0.264	0.264	0.232	0.295	0.264
Histidine	1.639	1.515	1.577	1.440	1.536	1.448
Total	45.730	44.343	45.037	44.564	44.816	44.690

[a] Two independent hydrolysates, *n*-butyl stearate as internal standard.
[b] Two independent analyses, norleucine as internal standard.
[c] Destroyed during 6 *N* HCl hydrolysis.

Table IV presents the data obtained on the analysis of a urine sample containing a relatively large amount of interfering material. The ion-exchange data were obtained from a single column, 10 h analyses, with the GLC analyses requiring *ca.* 45 min to complete. As noted in Table IV, the GLC and ion-exchange results for isoleucine, threonine, serine, methionine, ornithine, lysine, and histidine were somewhat divergent. Therefore, a careful study was made of the chromatograms to determine if one technique was generally more susceptible to interferences than the other. By the classical ion-exchange technique, definite interferences were noted for isoleucine,

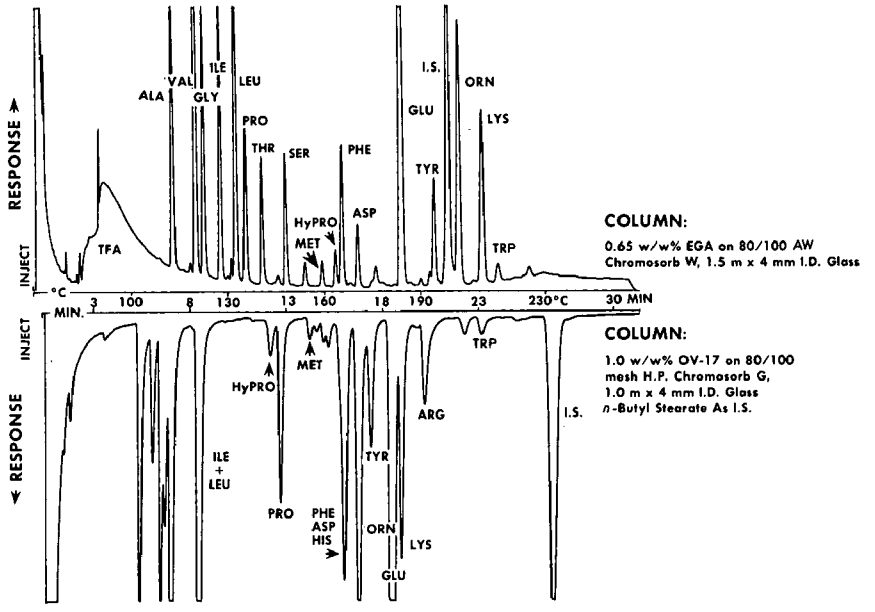

Fig. 3. GLC analysis of bovine blood plasma. 10.0 ml of plasma deproteinized with 40 ml of 1% picric acid, cation-exchange cleaned. Final acylation volume, 2 ml; injected, 5 μl; *ca.* 5 μg total amino acid injected; attenuation, 8 × 10^{-10} A.F.S.; initial temperature, 70°; program rate, 6°/min; final temperature 230°.

TABLE III

AMINO ACID ANALYSIS OF BOVINE BLOOD PLASMA

Blood plasma was cleaned by cation-exchange.

Amino acid	*mg/100 ml of plasma*					
	Gas–liquid chromatography[a]		*Average*	*Ion-exchange chromatography*		*Average*
Alanine	1.51	1.45	1.48	1.49	1.53	1.52
Valine	2.66	2.72	2.69	2.67	2.79	2.73
Glycine	1.38	1.44	1.42	1.41	1.53	1.47
Isoleucine	1.29	1.31	1.27	1.21	1.20	1.21
Leucine	1.81	1.83	1.82	1.79	1.81	1.80
Proline	0.91	0.94	0.93	0.91	0.95	0.93
Threonine	0.71	0.73	0.72	0.75	0.73	0.72
Serine	0.80	0.81	0.80	0.80	0.81	0.80
Methionine	0.22	0.22	0.22	0.24	0.22	0.23
Hydroxyproline	0.22	0.23	0.23	0.26	0.27	0.27
Phenylalanine	0.71	0.74	0.73	0.70	0.71	0.70
Aspartic acid[b]	0.32	0.32	0.32	0.10	0.10	0.10
Glutamic acid[b]	4.07	4.21	4.14	2.37	2.42	2.40
Tyrosine	0.63	0.61	0.62	0.59	0.60	0.59
Ornithine	1.04	1.10	1.07	1.08	1.09	1.09
Lysine	1.43	1.45	1.44	1.23	1.30	1.27
Arginine	1.38	1.40	1.39	1.44	1.47	1.46
Tryptophan	0.29	0.27	0.28	0.23	0.24	0.23
Cystine	trace	trace	trace	trace	trace	trace
Histidine	0.74	0.76	0.75	0.78	0.79	0.79
Total	22.13	22.53	22.33	20.01	20.56	20.29

[a] N-TFA *n*-butyl esters.

[b] GLC values include $AspNH_2$ and $GluNH_2$.

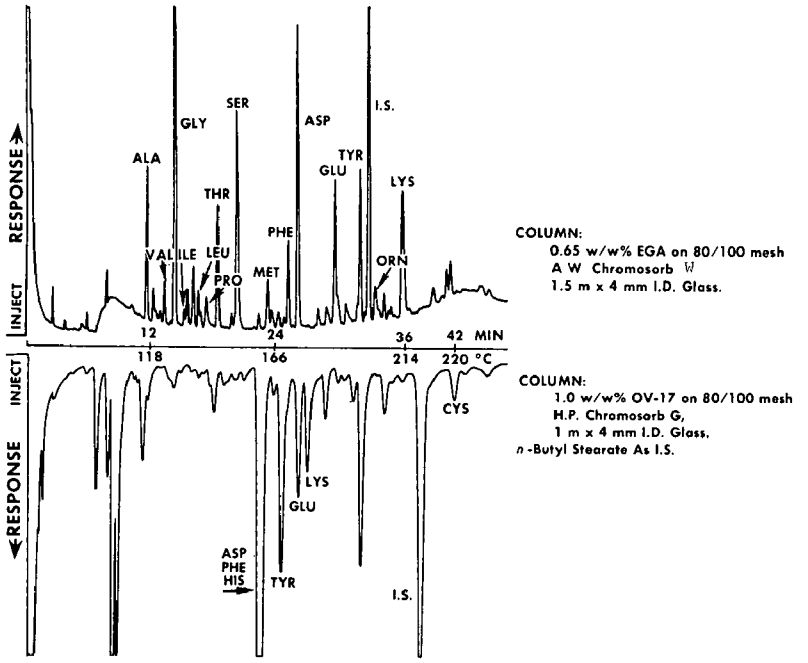

Fig. 4. GLC analysis of human urine. 4.5 ml of human urine hydrolyzed with 1 N HCl 110°, 2 h, final acylation volume, 2 ml; injected, 5 μl; *ca.* 2 μg of total amino acids injected; initial temperature, 70°; program rate, 4°/min; final temperature, 220°; attenuation, 8 × 10^{-10} A.F.S.

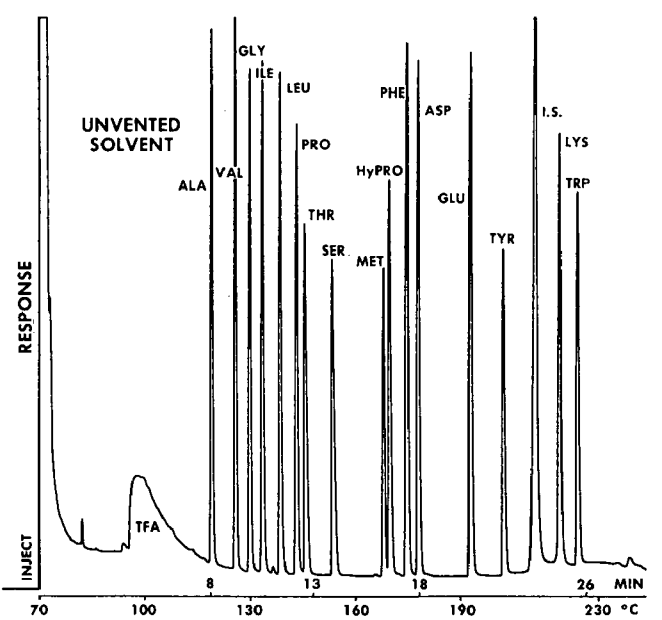

Fig. 5. GLC analysis of standard amino acid mixture. Standard mixture, 200 μg each amino acid; final acylation volume, 3 ml; injected, 15 μl; *ca.* 1.0 μg of each amino acid injected; initial temperature, 70°; injection port temperature, 180°; program rate, 6°/min; final temperature, 230°; attenuation, 32 × 10^{-10} A.F.S. Column, 0.65 w/w% EGA on 80/100 mesh AW Chromosorb W, 1.5 m × 4 mm I.D. glass. Pre-column, 1.0 w/w% OV-17 on 80/100 mesh H.P. Chromosorb G, 4 in. × 4 mm I.D. n-butyl stearate as I.S.

TABLE IV

AMINO ACID ANALYSIS OF HUMAN URINE

Cleaned by cation- and anion-exchange, and hydrolyzed with 1 *N* HCl, for 2 h at 110°.

Amino acid	*mg/100 ml of urine*					
	Gas–liquid chromatography[a]		*Average*	*Ion-exchange chromatography*		*Average*
Alanine	1.512	1.458	1.485	1.480	1.460	1.470
Valine	0.313	0.300	0.307	0.360	0.280	0.320
Glycine	5.968	5.900	5.934	—	5.160	5.160
Isoleucine	0.121	0.115	0.118	0.180[e]	0.160[e]	0.170[e]
Leucine	0.297	0.278	0.288	0.360	0.240	0.300
Proline	0.390	0.439	0.415	—	0.540[g]	0.540[g]
Threonine	1.484	1.473	1.479	0.920[d]	1.340[d]	1.130[d]
Serine	3.641	3.538	3.590	3.360[e]	3.240[e]	3.300[e]
Methionine	0.895	0.911	0.903	—[e]	—[e]	[e]
Phenylalanine	0.824	0.865	0.846	0.900	0.800	0.850
Aspartic acid	3.025[f]	2.948[f]	2.987[f]	2.740	2.140	2.440
Glutamic acid	1.841[f]	1.568[f]	1.705[f]	1.180	1.080	1.130
Tyrosine	1.880	1.763	1.822	1.860	1.700	1.780
Ornithine	0.289[d]	0.291[d]	0.290[d]	0.240	0.240	0.240
Lysine	2.284[e]	2.308[e]	2.296[e]	1.080	0.920	1.000
Arginine[b]	—	—		—	—	
Tryptophan[c]	—	—		—	—	
Cystine	1.015	0.903	0.959	1.280	0.880	1.080
Histidine	3.252	2.736	2.994	4.340	5.000	4.670

[a] N-TFA *n*-butyl esters.
[b] Not recovered from anion-exchange cleanup.
[c] Destroyed during hydrolysis.
[d] Not completely resolved.
[e] Intefering peak(s).
[f] Includes $AspNH_2$ and $GluNH_2$.
[g] Manual calculation, 440 nm.

threonine, serine, and methionine, with methionine being incalculable due to the presence of two unidentified interfering peaks. The GLC analyses gave interferences at the elution positions of ornithine and lysine, with a minor interference of isoleucine. Also, a minor interference of leucine was noted with both GLC and classical ion-exchange chromatography; however, the disparity of the histidine values could not be explained. Under these analytical conditions, it was observed that GLC resulted in a better resolution of the amino acids from interfering substances than did ion-exchange chromatography.

The amount of interference observed with the two analytical methods is dependent on the level and nature of the extraneous substances, with GLC and ion-exchange chromatography exhibiting comparable levels of interferences, although a pre-analysis cation and anion-exchange cleanup of the urine sample was made.

EXPERIMENTAL

A solvent–chromatographic venting system—nanogram analysis

In 1968, GEHRKE *et al.*[3] published a monograph describing in detail a derivatization method for submicrogram amounts of amino acids which included a discussion

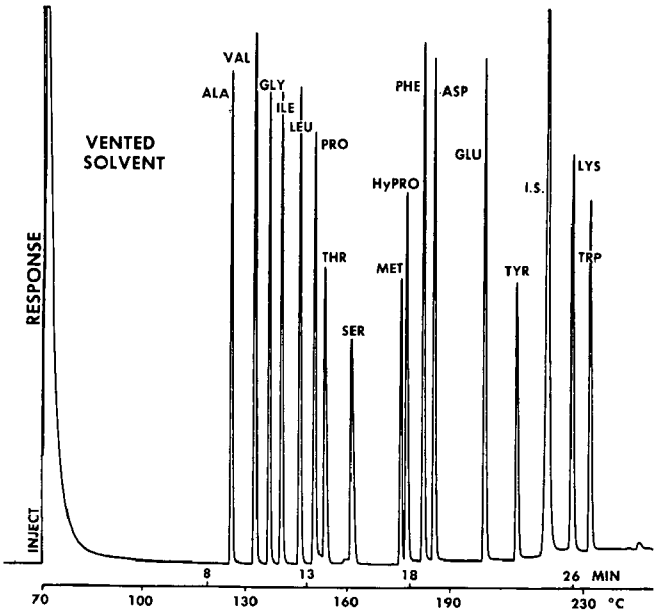

Fig. 6. GLC analysis of standard amino acid mixture. Standard mixture, 200 μg each amino acid, final acylation volume, 3 ml; injected, 15 μl; *ca.* 1.0 μg of each amino acid injected; initial temperature, 70°; injection port temperature, 180°; solvent vent time, 15 sec; program rate, 6°/min; final temperature, 230°; attenuation, 32 × 10^{-10} A.F.S. Column, 0.65 w/w% EGA on 80/100 mesh AW Chromosorb W, 2.5 m × 4 mm I.D. glass. Pre-column, 1.0 w/w% OV-17 on 80/100 mesh H.P. Chromosorb G, 4 in. × 4 mm I.D. *n*-butyl stearate as I.S.

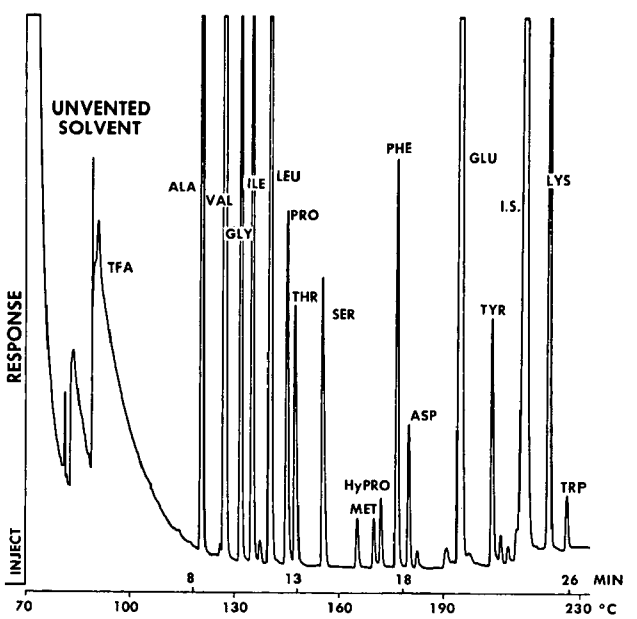

Fig. 7. GLC analysis of bovine blood plasma. 10 ml of plasma deproteinized with 40 ml of 1% picric acid; cation-exchange cleaned; final acylation volume, 2 ml; injected, 5 μl; *ca.* 5 μg total amino acid injected; initial temperature, 70°; injection port temperature, 180°; program rate, 6°/min.; final temperature, 230°; attenuation, 8 × 10^{-10} A.F.S. Column, 0.65 w/w% EGA on 80/100 mesh AW Chromosorb W, 1.5 m × 4 mm I.D. glass. Pre-column, 1.0 w/w% OV-17 on 80/100 mesh H.P. Chromosorb G, 4 in. × 4 mm I.D. *n*-butyl stearate as I.S.

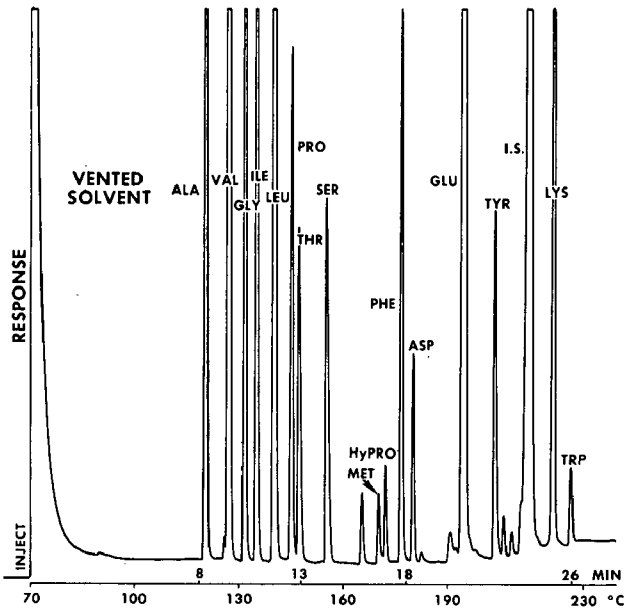

Fig. 8. GLC analysis of bovine blood plasma. 10 ml of plasma deproteinized with 40 ml of 1% picric acid; cation-exchange cleaned; final acylation volume, 2 ml; injected, 5 μl; *ca.* 5 μg total amino acid injected; initial temperature, 70°; injection port temperature, 180°; solvent vent time, 25 sec; program rate, 6°/min; final temperature, 230°; attenuation, 8 × 10^{-10} A.F.S. Column, 0.65 w/w% EGA on 80/100 mesh AW Chromosorb W, 1.5 m × 4 mm I.D. glass. Pre-column, 1.0 w/w% OV-17 on 80/100 mesh H.P. Chromosorb G, 5 in. × 4 mm I.D. *n*-butyl stearate as I.S.

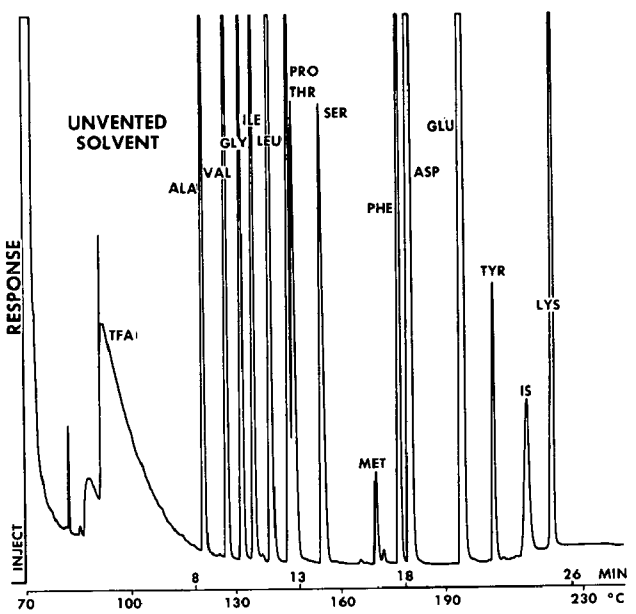

Fig. 9. GLC analysis of soybean meal hydrolysate. 25 mg of soybean meal, hydrolyzed 22 h, 110°, cation-exchange cleaned, final acylation volume, 3 ml; injected, 6 μl; *ca.* 18 μg total amino acid injected; initial temperature, 70°; injection port temperature, 180°; program rate, 6°/min; final temperature, 230°; attenuation, 32 × 10^{-10} A.F.S. Column, 0.65 w/w% EGA on 80/100 mesh AW Chromosorb W, 1.5m × 4 mm I.D. glass. Pre-column, 1.0 w/w% OV-17 on 80/100 mesh H.P. Chromosorb G, 4 in. × 4 mm I.D. *n*-butyl stearate as I.S.

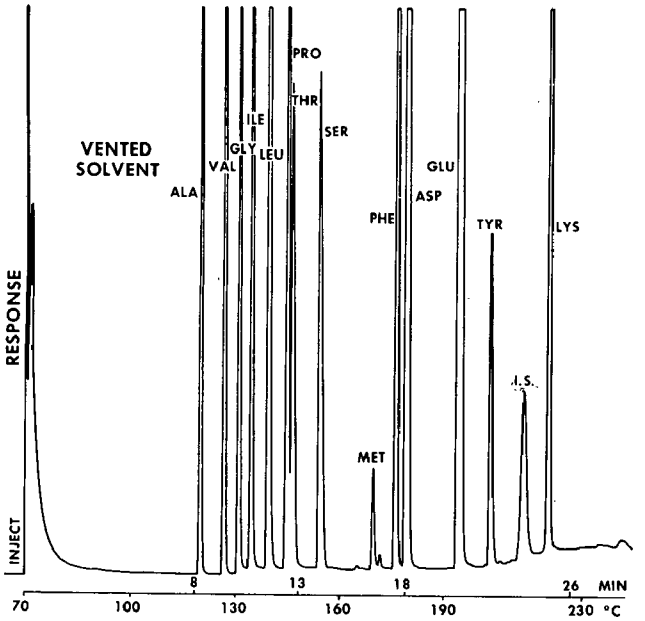

Fig. 10. GLC analysis of soybean meal hydrolysate. 25 mg of soybean meal, hydrolyzed 22 h, 110°, cation-exchange cleaned; final acylation volume, 3 ml; injected, 6 μl; *ca.* 18 μg total amino acid injected; initial temperature, 70°; injection port temperature, 180°; solvent vent time, 30 sec.; program rate, 6°/min.; final temperature, 230°; attenuation, 32 × 10^{-10} A.F.S. Column, 0.65 w/w% EGA on 80/100 mesh AW. Chromosorb W, 1.5 m × 4 mm I.D. glass. Pre-column, 1.0 w/w% OV-17 on 80/100 mesh H.P. Chromosorb G, 4 in. × 4 mm I.D. *n*-butyl stearate as I.S.

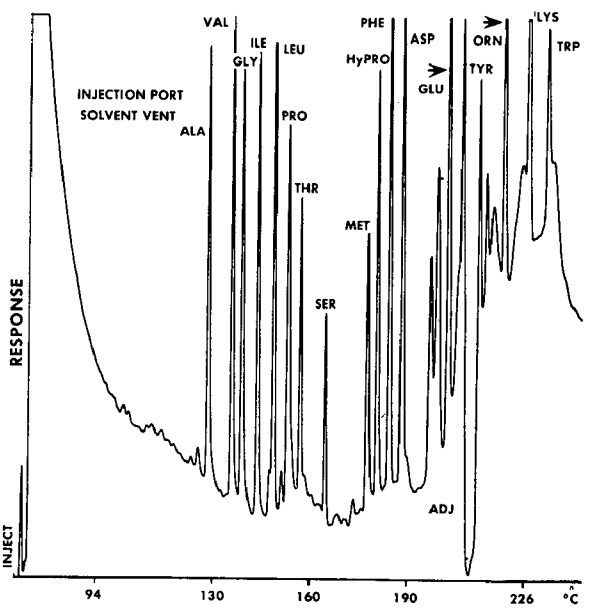

Fig. 11. Derivatization and GLC analysis of 100 ng of each amino acid. Derivatization; esterification, 150 μl of *n*-butanol with 3 *N* HCl, 100°, 30 min; acylation, 100 μl CH_2Cl_2–TFAA (2:1), 100°, 10 min; GLC analysis, sample injected, 50 μl; solvent vent time, 15 sec; injection port temperature, 180°; initial temperature, 70°; program rate, 6°/min; final temperature, 230°; attenuation, 8 × 10^{-11} A.F.S. Column, 0.65 w/w% EGA on 80/100 mesh AW Chromosorb W, 1.5 m × 4 mm I.D. glass. Pre-column, 1.0 w/w% OV-17 on 80/100 mesh H.P. Chromosorb G, 4 in. × 4 mm.

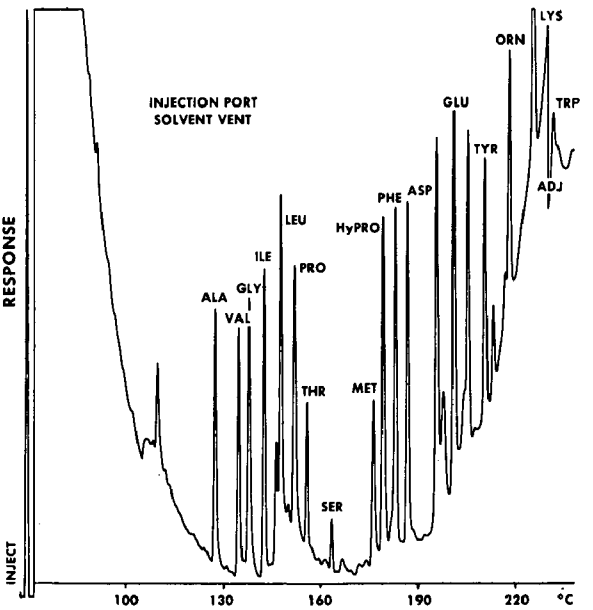

Fig. 12. Derivatization and GLC analysis of 50 ng of each amino acid. Derivatization: esterification, 100 μl of *n*-butanol with 3 *N* HCl, 100°, 30 min; acylation, 100 μl CH_2Cl_2–TFAA (2:1) 100°, 10 min; GLC analysis, sample injected, 25 μl; solvent vent time, 15 sec; injection port temperature, 180°; program rate 6°/min; final temperature, 230°; attenuation, 4×10^{-11} A.F.S. Column, 0.65 w/w% EGA on 80/100 mesh AW Chromosorb W, 1.5 m × 4 mm I.D. glass. Pre-column, 1.0 w/w% OV-17 on 80/100 mesh H.P. Chromosorb G, 4 in. × 4 mm.

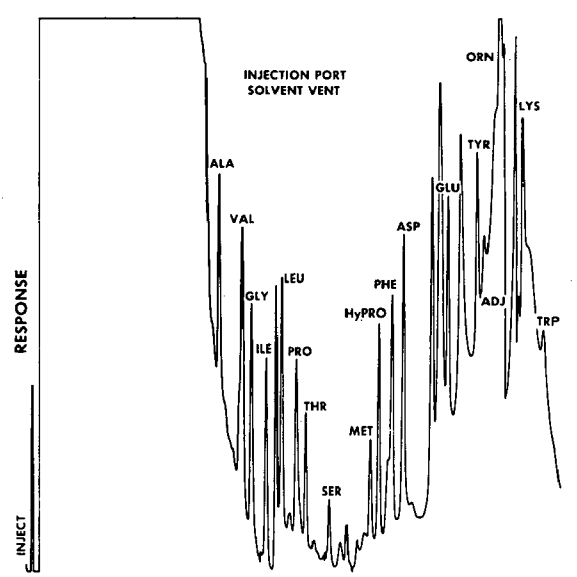

Fig. 13. Derivatization and GLC analysis of 10 ng of each amino acid. Derivatization: esterification, 50 μl *n*-butanol with 3 *N* HCl, 100°, 30 min; acylation, 50 μl CH_2Cl_2–TFAA (2:1), 100°, 10 min; GLC analysis, sample injected, 50 μl; solvent vent time, 15 sec.; injection port temperature, 180°, program rate, 6°/min; final temperature, 230°; attenuation, 32×10^{-12} A.F.S. Column, 0.65 w/w% EGA on 80/100 mesh AW Chromosorb W, 1.5 m × 4 mm I.D. glass. Pre-column, 1.0 w/w% OV-17 on 80/100 mesh H.P. Chromosorb G, 4 in. × 4 mm.

of some critical points in the derivatization and GLC analysis. A major obstacle associated with the GLC analysis of extremely small quantities of biological samples or samples containing very low concentrations of amino acids, has been the limited sample volume that could be injected. A solvent venting system has now been developed (patent applied for) which allows injection of the total derivatized sample (50 to 100 μl) on a standard packed analytical column. The device prevents the large volume of solvent and acylating reagent injected from traversing the EGA column, while allowing the essentially quantitative transport of amino acids present in the sample to the detector. Of particular importance in the analysis of nanogram amounts of amino acids is that this instrumental system eliminates the interfering TFA peak from the chromatogram. Fig. 5 presents a typical chromatogram obtained of a standard amino acid mixture at the macro level without the instrumental adaptation. Fig. 6 shows the effect of the venting device with the corresponding reduction of the solvent peak, and the absence of TFA throughout the chromatogram. Figs. 7 and 8 are similar comparisons with analysis of bovine blood plasma and soybean oil meal analyses are presented in Figs. 9 and 10.

Initial investigations of the system have shown great promise in the GLC analysis of nanogram amounts of amino acids. Fig. 11 presents the chromatogram obtained on derivatization and analysis of 100 ng of each amino acid. These initial studies were designed to evaluate the derivatization and chromatographic procedures, thus stringent precautions to exclude contaminants were not taken.

The derivatization and chromatography of samples containing 50 to 10 ng of each amino acid were also successfully conducted, with the chromatograms obtained presented in Figs. 12 and 13. Studies are currently underway to refine this technique further for the analysis of 1 ng of each amino acid taken through the complete chemistry and chromatographic methods.

CHROMATOGRAPHIC COLUMNS FOR ANALYSIS OF AMINO ACIDS AS N-TRIFLUOROACETYL *n*-BUTYL ESTER DERIVATIVES

Column I. Ethylene glycol adipate (EGA) on Chromosorb W, 0.65 w/w%

Materials

Column packing I* can be procured from Analytical Biochemistry Laboratories, P.O. Box 1097, Columbia, Mo., 65201 and Regis Chemical Company, 1101 N. Franklin Street, Chicago, Ill. 60610. Code No. 201033.

Ethylene glycol adipate, stabilized grade, (Analabs Inc., Hamden, Conn.).

Chromosorb W, 80/100 mesh, acid washed (Johns-Manville product, obtained from Applied Science, State College, Pa. or Fisher Scientific, St. Louis, Mo.).

Acetonitrile (anhydrous, "Nanograde") Mallinckrodt Chemical Works, St. Louis, Mo.

Adsorbent traps containing charcoal and molecular sieve 5A, Guild Corporation, P.O. Box 217, Bethel Park, Pa. 15102, Regis Chemical Company, and Supelco, Inc.

* The chromatographic packings described for columns I and II following, are the subject of a separate manuscript. Their use and application will be discussed in detail.

Procedure for column I

For preparation of 25 g of column packing I, 24.84 g of Chromosorb W are weighed into a 500 ml ridged round bottom flask, then anhydrous "Nanograde" acetonitrile is added until the liquid level is *ca.* $\frac{1}{4}$ in. above the Chromosorb W.

Ten milliliters of a solution containing 16.25 mg/ml of EGA in anhydrous "Nanograde" acetonitrile are then added to the flask containing the Chromosorb W. The flask is then rotated on a rotary evaporator, slowly removing the solvent at room temperature under partial vacuum for *ca.* 45 min. When the Chromosorb is still slightly damp, the vacuum is increased and the flask is immersed in a 60° water bath with continued rotation until the solvent is completely removed. At this point, no Chromosorb W packing should adhere to the inner wall of the flask during rotation.

At the end of this period, the dry, freely-flowing column packing is poured into clean, dry 1.5 m × 4 mm I.D. glass columns with gentle tapping. Dry silanized glass wool plugs are then placed in each end of the column to hold the packing in place. Prior to analytical use, the column is placed in the gas chromatograph and conditioned at 220° with a carrier flow of *ca.* 50 ml/min of pure N_2. Analyses can be made after conditioning for 1 h when 0.5 to 1 μg of each amino acid are injected. Longer conditioning times (8–24 h at 220°) are required for analyses at lower concentrations.

When not in use, the columns should be kept at 200° in the chromatograph with a carrier flow of 20–50 ml/min. If the columns must be removed from the instrument, the ends should be tightly closed during storage to exclude atmospheric moisture. The EGA columns must not be subjected at any one time to temperatures in excess of 225° for longer than 1 to 2 h.

Column II. Separation of His, Arg, Trp, and Cys (2.0 w/w% OV-17 + 1.0 w/w% OV-210 on Supelcoport)

Materials

Column packing II can be procured from Analytical BioChemistry Laboratories, P.O. Box 1097, Columbia, Mo. 65201.

OV-17 (Supelco, Inc., Bellefonte, Pa.) and OV-210 (Applied Science, State College, Pa.).

Supelcoport, 100/120 mesh (Supelco, Inc., Bellefonte, Pa.).

Prepare solutions containing: OV-17 in anhydrous "Nanograde" methylene chloride (20 mg/ml). OV-210 in "Nanograde" acetone (10 mg/ml). These solvents were obtained from Mallinckrodt Chemical Works, St. Louis, Mo.

Procedure for Column II

For preparation of 30 g of column packing II, 29.1 g of Supelcoport are weighed into a 500 ml ridged round bottom flask, then "Nanograde" acetone is added until the liquid level is *ca.* $\frac{1}{4}$ in. above the support material. Pipet 30.0 ml OV-17 solution (600 mg) and 30.0 ml of OV-210 solution (300 mg) into the flask. The solvent is removed in the manner described above for preparation of column I, and the dried column packing is placed in 1.5 m × 4 mm I.D. glass columns. The columns are then placed in the gas chromatograph, and conditioned overnight at 250° with a carrier flow of *ca.* 50 ml/min of pure N_2.

Comments

Column I, EGA on Chromosorb W, AW. Filters containing a high grade charcoal (an efficient adsorbent for hydrocarbons), and $CaSO_4$ and Linde 5A indicating molecular sieve for water should be placed in the N_2, H_2, and air lines to the gas chromatograph. The charcoal end of the filters is connected to the gas inlet side. The purity of the carrier gas is very important, especially when analyses are made at the submicrogram level.

Properly prepared columns should last *ca.* two months and give the desired separation for 17 amino acid derivatives, depending on the individual column and the types of samples injected. Signs of column degradation are: loss of the glycine–valine separation; loss of resolution in the methionine–hydroxyproline–phenylalanine region and loss of separation for the ornithine–*n*-butyl stearate pair. Also, the TFA peak will be eluted later in the chromatogram as the column deteriorates.

Column II, separation of basics and cystine. The OV-17, OV-210 mixed phase columns should last three to six months, depending on the types of samples analyzed. The first sign of column deterioration is usually a loss of quantitative elution of arginine and cystine indicated by a reduced $RWR_{a.a./I.S.}$

Note on chromatography and columns

In our previous publications[4,5], reference is made to the chromatographic separation of the amino acid derivatives. The packing composed of stabilized grade EGA and acid washed Chromosorb W (heated at 140° for 12 h) is an excellent one and gives effective separation of 17 amino acids. Column packing II, consisting of the mixed phase of OV-17 and OV-210 is a superior packing and shows highly efficient and effective separation of the basic amino acids plus cystine over that reported by us earlier. No longer is it necessary to make a computation for histidine as reported in ref. 6.

With these packings (columns I and II), as described above, one can now simultaneously analyze and separate all 20 of the protein amino acids on these two columns in 30 min with automatic electronic integration of all peaks.

In our recent studies on chromatographic separations of the amino acids, it was found that heating the Chromsorb W at 140° for 12 h was unnecessary. However, certain lots of Chromosorb W may still require a heat treatment for the removal of surface adsorbed water as described in ref. 5.

REFERENCES

1 R. W. ZUMWALT, D. ROACH AND C. W. GEHRKE, *J. of Chromatog.*, 53 (1970) 171.
2 C. W. GEHRKE, R. W. ZUMWALT AND K. KUO, *Symposium on Characterization of Proteins, 160th National Amer. Chem. Soc. Meetings Chicago, Ill., September, 1970. J. Agr. Food Chem.*, (1970) in press.
3 C. W. GEHRKE, D. ROACH, R. W. ZUMWALT, D. L. STALLING AND L. L. WALL, *Quantitative Gas–Liquid Chromatography of Amino Acids in Proteins and Biological Substances*, 1968, Analytical BioChemistry Laboratories, Inc., P.O. Box 1097, Columbia, Mo. 65201, U.S.A.
4 C. W. GEHRKE, R. W. ZUMWALT AND L. L. WALL, *J. Chromatog.*, 37 (1968) 398.
5 D. ROACH AND C. W. GEHRKE, *J. Chromatog.*, 43 (1969) 303.
6 D. ROACH, C. W. GEHRKE AND R. W. ZUMWALT, *J. Chromatog.*, 43 (1969) 311.

CHROM. 5183

AN EVALUATION OF THE GAS CHROMATOGRAPHIC ANALYSIS OF PLASMA AMINO ACIDS*

E. D. PELLIZZARI**, J. H. BROWN, P. TALBOT, R. W. FARMER AND L. F. FABRE, JR.
Section of Neuroendocrinology, Texas Research Institute of Mental Sciences, Houston, Texas (U.S.A.)

(First received October 6th, 1970; revised manuscript received December 1st, 1970)

SUMMARY

The accuracy and reproducibility of gas–liquid chromatography of plasma amino acids as their *n*-butyl N-trifluoroacetyl esters are statistically evaluated. Plasma is deproteinized with picric acid and amino acids are purified by microcolumn chromatography on Dowex 50 W-X12. Routine analysis requires only 0.2 ml of plasma with recoveries of 75–90% for the protein precipitation–ion exchange steps as determined by tracer methods.

The ester derivatives are injected directly onto 0.7% EGA or 1.0% OV-17 columns. Variability due to the use of different GLC columns is minimized by careful calibration. Replicate analysis of the same sample indicates that the overall reproducibility is satisfactory for clinical usuage. The range of normal concentration for amino acids in our clinical population is within agreement with values obtained by other methods.

A complete analysis can be accomplished within 12 h, however grouping samples allows processing of 8–10 plasma samples in one working day, greatly facilitating biochemical investigations such as metabolic disorders in retarded children.

INTRODUCTION

The repertoire for amino acid analysis generally involves column, paper, and thin-layer chromatography as well as a variety of electrophoresis, spectrophotometric and ion-exchange techniques. Unfortunately, the elegant automated amino acid analyzers that are commercially available remain expensive and have relatively limited application to other problems.

Within the past decade, gas–liquid chromatography (GLC) has been applied to many arduous separation problems. It is an expedient analytical tool with capabilities of extremely high sensitivity and resolution, which provides the opportunity to obtain qualitative and quantitive data simultaneously. The relatively low cost

* Address reprint request to Dr. L. F. Fabre, Jr., 1300 Moursund Avenue, Texas Research Institute of Mental Sciences, Houston, Texas 77025, U.S.A.

** USPHS Post-doctoral Fellow, Training Grant TO1MH12224-01.

of the instrument has allowed its extensive usage in biological studies. However, the technical difficulties involved in the preparation of volatile derivatives of amino acids has delayed its development in this area. A variety of suitable chemical subterfuges has been developed by GEHRKE AND STALLING[1] in which the amino, carboxyl and other functional groups are esterified whereby allowing gas chromatography. In addition, TALBOT *et al.*[2], have substantiated that standard amino acid mixtures can be quantitated accurately by GLC when columns are precisely calibrated.

The increasing need of an expedient method for quantitative analysis of plasma amino acids has prompted us to investigate further the potentiality of GLC. In previous studies, the purification, derivatization and resolution of each amino acid on a quantitative basis has not been adequately examined.

This report is a statistical evaluation of the accuracy and reproducibility for the quantification of plasma amino acids. Also, the results of the application of this technique is presented for determining the levels of individual plasma amino acids in retarded children who are suspected of carrying inborn errors of metabolism.

EXPERIMENTAL

Purification of amino acids from blood

Blood from retarded children was centrifuged to remove cells and a quantity of norleucine equivalent to 5 mg% was added as an internal standard. The purification of amino acids by ion-exchange is shown in Fig. 1. A volume of serum (0.2–0.5 ml)

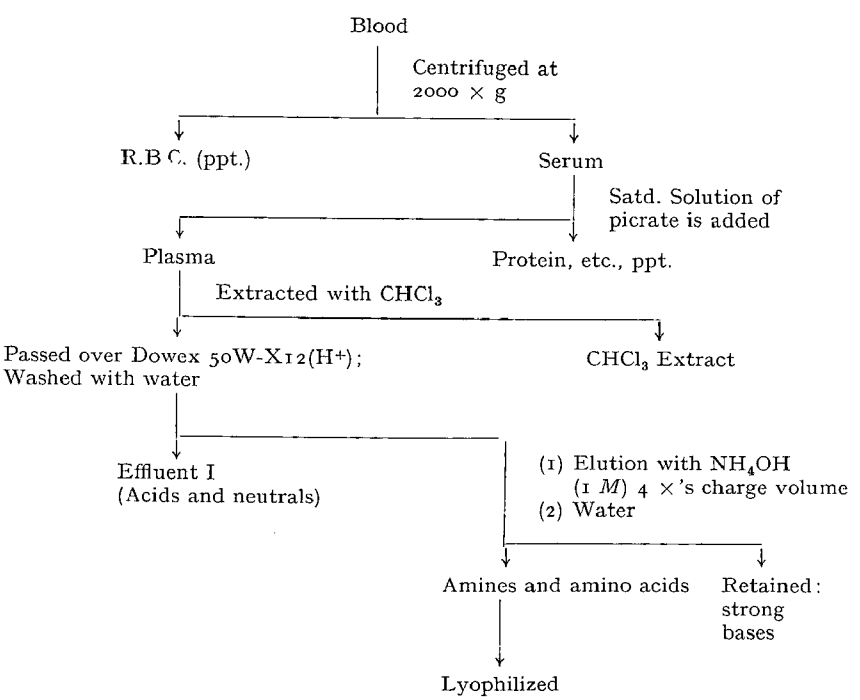

Fig. 1. Schematic diagram for the extraction of amino acids from blood.

was added to precipitate proteins and the precipitate was washed three times with fresh picric acid solution. The washings were combined and plasma was extracted three times with one-half the volume of $CHCl_3$. The aqueous extract was passed through a 6–9 ml bed-volume of Dowex 50 W-X12 (H^+) resin (50–100 mesh); followed by ten times the charge-volume with water; four times the bed-volume with 1 *M* NH_4OH; and again with water. The fraction containing amino acids and weak bases were lyophilized.

The percent recovery for each amino acid for the purification procedure was determined by adding 0.1 μCi of a uniformly labeled [^{14}C]amino acid to the serum and an aliquot from the final elution fraction was assayed for radioactivity with a Nuclear Chicago liquid-scintillation spectrometer. Samples were dissolved in 15 ml of Triton scintillation fluid and counted until a standard error of 0.2% was attained. The Triton scintillation fluid consisted of one part Triton X-100, two parts toluene scintillator solution containing 8.25 g PPO and 0.25 g Me_2POPOP per liter. Observed radioactivity was corrected for quenching by the channels ratio method. The percent recoveries were based on the added disintegrations per min.

Preparation of derivatives and gas–liquid chromatography

The method of GEHRKE AND STALLING[1] was modified to prepare the *n*-butyl N-trifluoroacetyl esters of the amino acids for GLC. Methyl esters were prepared by treating the lyophilized residue with 2.0 ml of dry methanol–HCl (1.25 *N*) solution for 30 min at ambient temperature. Excess solvent was removed under a nitrogen stream; the residue interesterified with 1.0 ml of *n*-butanol–HCl (1.25 *N*) for 2.5 h at 100° and the excess solvent removed. Trifluoroacetic anhydride (1.0 ml) was added to the *n*-butyl esters and heated to 100° for 1 h. Prior to analysis the remaining reagent was evaporated and the derivatives were resuspended in 0.5 ml of CH_2Cl_2.

Analyses were performed on a Microtek 220 and Barber-Coleman instruments equipped with flame ionization detectors. Two columns, 6 ft. × 4 mm (I.D.) were employed consisting of unsilanized glass tubes packed with 100–200 mesh heat-treated Chromosorb G (Supelco) coated with 1.0% OV-17 (phenyl, methylsilicone polymer) or 0.68% EGA (ethylene glycol adipate). The conditions for analyses were identical for both columns. The flash heater and the detector were maintained at 220° respectively. The columns were programmed from 100° to 220° at 5°/min. The carrier gas, nitrogen, hydrogen and air flow rates were 60, 55, and 480 ml/min respectively.

Quantification of amino acids

Each gas chromatographic column employed for quantification of amino acids was calibrated with the assistance of a Fortran IV program and IBM 7094 computer as described by TALBOT *et al.*[2]. Standard curves were generated for each amino acid with 95% confidence limits using the internal standardization method. The relative response ratio was calculated and plotted *versus* the concentration of each amino acid.

The area of each chromatographic peak was determined by triangulation (height × width at 1/2 peak height); the relative response ratio calculated and the unknown concentration of each amino acid was determined.

Quantitative data for plasma amino acids from replicate analysis and population sampling was statistically evaluated. Standard deviations, standard errors of the mean, and their confidence limits were calculated by computer means.

TABLE I

PERCENT RECOVERY OF AMINO ACIDS FROM HUMAN PLASMA

The data represents an average of four replications plus their standard deviations. To [^{14}C]Norleucine, a non-protein amino acid, carrier was added to give an equivalent concentration of 5 mg% when added to serum.

Amino acid	*% of added D.P.M. ± S.D.*	*Amino acid*	*% of added D.P.M. ± S.D.*
Norleu	77 ± 3.0	Glu	90 ± 2.0
Ala	87 ± 1.0	Asp	77 ± 3.0
Val	82 ± 1.0	Phe	89 ± 1.0
Gly	81 ± 7.0	Tyr	75 ± 10.0
Ile	83 ± 1.0	Lys	78 ± 3.0
Leu	90 ± 3.0	Arg	60 ± 10.0
Thr	89 ± 1.0	His	95 ± 3.0
Ser	86 ± 2.0	Try	73 ± 7.0
Pro	83 ± 1.0	Cys	61 ± 2.0

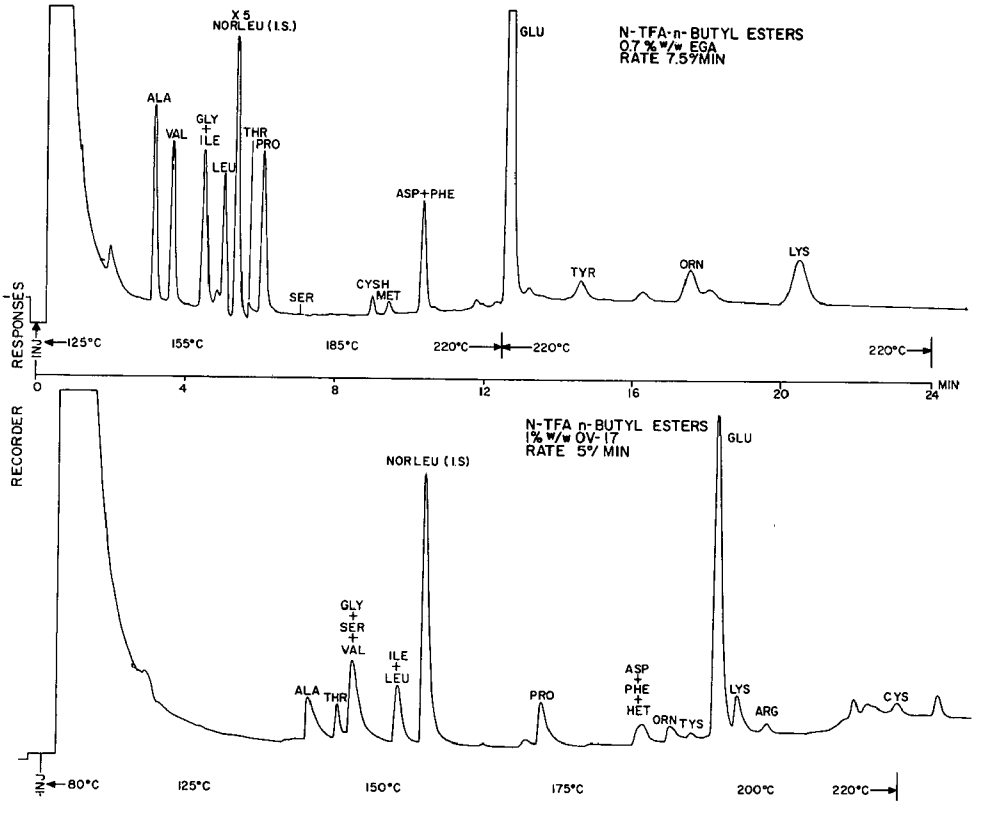

Fig. 2. Gas–liquid chromatograms for amino acids purified from human blood.

RESULTS AND DISCUSSION

The percent recoveries including standard deviations for each amino acid from plasma was determined using individually labeled compounds and these results are shown in Table I. Recoveries reported here are in agreement with other studies[3]. Arginine, tryptophan, and tyrosine were not as reproducible as the other amino acids studied. Tryptophan and possibly cystine may have been partially destroyed during acid precipitation of protein. Coprecipitation of basic amino acids such as arginine with proteins could not be alleviated by successive washing, an observation also noted by others[3] who employ acid denaturation techniques. The actual extent of amino acid loss has been shown to depend on the relative protein concentration, precipitating agent and is not greatly altered by variation in modes of precipitation. The lost amino acids are firmly bound to the precipitate and were not recovered by repeated washing.

Depicted in Fig. 2 are the gas–liquid chromatograms of the ester derivatives of amino acids from human plasma. The employment of two chromatographic columns containing EGA and OV-17 stationary phases provided satisfactory resolution and peak symmetry for their quantification by the triangulation method. However, the EGA coated support provides better separation and by judiciously selecting the gas chromatographic parameters, it is possible to isolate all of the amino acids in a relatively short period of 25 min. Since the *n*-butyl N-trifluoroacetyl ester derivative of arginine, histidine and cystine do not elute quantitatively from the EGA column, an OV-17 column is employed for their quantification. Limited use of the OV-17 to these amino acids is recommended since peak tailing does occur for some amino acids and this reduces the accuracy of peak area measurement.

The variability of amino acid analysis on several gas chromatographic columns employing the same stationary phase was investigated. Columns prepared and calibrated as described by TALBOT *et al.*[2] were used in this study. Amino acids were purified from a sample of plasma; derivatives were prepared and then injected onto two EGA and two OV-17 columns. The concentration (mg%) of each amino acid

TABLE II

VARIABILITY OF AMINO ACID ANALYSIS ON DIFFERENT GAS–LIQUID CHROMATOGRAPHIC COLUMNS
The concentration (mg%) of each amino acid from one sample of plasma was determined on different calibrated GLC columns. Standard deviation (S.D.) for the two EGA and OV-17 columns are given respectively.

Amino acid	*EGA*		±*S.D.*	*OV-17*		±*S.D.*
	I	*II*		*I*	*II*	
Ala	2.0	1.7	±0.15	0.9	1.3	±0.20
Pro	1.3	1.1	±0.10	1.2	1.1	±0.05
Lys	1.3	1.4	±0.05	1.2	1.4	±0.10
Val	7.6	7.0	±0.30	—	—	—
Gly + Ile	3.7	3.2	±0.25	—	—	—
Leu	3.5	3.2	±0.15	—	—	—
Thr	0.4	0.6	±0.10	—	—	—
Asp + Phe	1.7	1.3	±0.20	—	—	—
Glu	—	10.8	—	9.9	9.1	±0.40

TABLE III

REPRODUCIBILITY OF AMINO ACID ANALYSIS BY GAS–LIQUID CHROMATOGRAPHY

Amino acid	*Average + C.L.*[a]
Ala	2.07 ± 0.39
Val	3.44 ± 0.58
Leu	1.31 ± 0.29
Thr	1.66 ± 0.42
Pro	1.88 ± 0.34
Ser	1.49 ± 0.65
Glu + Gln	7.28 ± 0.80
Gly	0.52 ± 0.08
Ile	4.44 ± 1.35
Phe	1.52 ± 0.60
Asp	1.27 ± 0.38
Orn	1.16 ± 0.47
Lys	3.76 ± 1.56

[a] Values are in mg% and include standard error at the 95% confidence limits for five determinations.

was calculated and the mean of two determinations including their standard deviation are listed in Table II. These data indicate that careful calibration of gas chromatographic columns by the computer method[2] will provide reliable values when analyses are performed on different columns. The observed standard deviations can possibly be further diminished by employing more accurate techniques for peak area measurements, for example, disc, electronic or computer integration.

A study on the over-all reproducibility of amino acid analysis by employing ion-exchange purification, derivatization and gas chromatography was initiated. A single plasma sample was divided into five 0.1 ml aliquots and the amino acids recovered by ion-exchange. Derivatives were prepared in the usual manner and each sample analyzed by gas chromatography. The average concentration (mg%) for each amino acid plus the standard error at the 95% confidence limit is shown in Table III for the five determinations. These data indicate that analysis of a single sample of plasma by the procedure described here allows the determination of the levels of amino acids with a high degree of reproducibility.

The gas chromatographic and amino acid analyzer methods were compared as to their accuracy for the determination of amino acid concentrations in a synthetic mixture. The average values obtained from six determinations are depicted in Table IV. In most cases, the accuracy of the amino acid analyzer is higher, as reflected by the standard error of the mean and the calculated concentration of amino acid. However, the gas chromatographic method is a relatively accurate method for quantitation since the standard errors of the mean were low.

A comparative study was initiated to discern whether the concentrations of amino acids determined by GLC are in agreement with those reported by the conventional method. Several children with normal levels of amino acids in plasma were used to establish mean values with standard deviations. The results are given in Table V. Comparison of the average plasma values obtained by gas chromatography and the amino acid analyzer technique reveals a rather good correlation between

TABLE IV

COMPARATIVE ANALYSIS OF A SYNTHETIC AMINO ACID MIXTURE

Values are given in mg %.

Amino acid	*GLC*	*Calculated*	*Amino acid analyzer*
	Average S.E.		*Average S.E.*
Ala	1.62 ± 0.26	2.02	2.17 ± 0.06
Val	2.13 ± 0.36	2.81	3.15 ± 0.18
Leu	2.04 ± 0.20	2.10	2.21 ± 0.12
Thr	1.32 ± 0.13	1.50	1.51 ± 0.06
Pro	1.78 ± 0.27	2.31	3.05 ± 0.39
Ser	2.25 ± 0.30	2.01	1.96 ± 0.09
Glu	10.41 ± 0.66	8.51	7.94 ± 0.31
Gly	1.36 ± 0.11	1.51	1.55 ± 0.05
Phe + Asp	3.21 ± 0.31	2.41	2.56 ± 0.09
Lys	2.66 ± 0.36	2.40	2.33 ± 0.14
Tyr + His	7.83 ± 0.76	6.10	6.53 ± 0.18
Arg	2.23 ± 0.29	2.00	2.04 ± 0.07
Met	0.64 ± 0.09	0.50	0.53 ± 0.01
Orn	2.07 ± 0.29	1.20	1.36 ± 0.12
Ile	1.29 ± 0.20	1.51	0.67 ± 0.03
Cys	1.17 ± 0.16	1.00	—

TABLE V

COMPARISON OF GAS–LIQUID CHROMATOGRAPHIC AND AMINO ACID ANALYZER METHODS

Amino acid	*GLC*	*Amino acid analyzer*
	Average ± S.D.[a]	*Average ± S.D.*[b]
Ala	1.74 ± 0.60	2.42 ± 0.32
Val	2.63 ± 0.93	2.12 ± 0.24
Leu	1.92 ± 0.84	1.19 ± 0.17
Thr	1.59 ± 0.90	1.73 ± 0.19
Pro	1.21 ± 0.85	2.05 ± 0.38
Ser	1.29 ± 0.37	1.27 ± 0.15
Glu + Gln	7.87 ± 3.48	— —
Lys	0.84 ± 0.75	1.91 ± 0.29
Tyr	— —	0.83 ± 0.15
Arg	1.92 ± 0.59	1.49 ± 0.27
Met	0.47 ± 0.30	0.24 ± 0.05
Orn	1.25 ± 0.86	0.61 ± 0.11
Gly + Ile	2.91 ± 1.49	1.23 ± 0.33
Phe + Asp	1.39 ± 1.57	0.99 ± 0.13

[a] Plasma values (mg%) with standard deviations for 12 children who demonstrated normal levels when also analyzed by the amino acid analyzer method.

[b] Data taken from BRODEHL AND GELLISSEN[5] on a population of 12 normal children (ages 3–13 years).

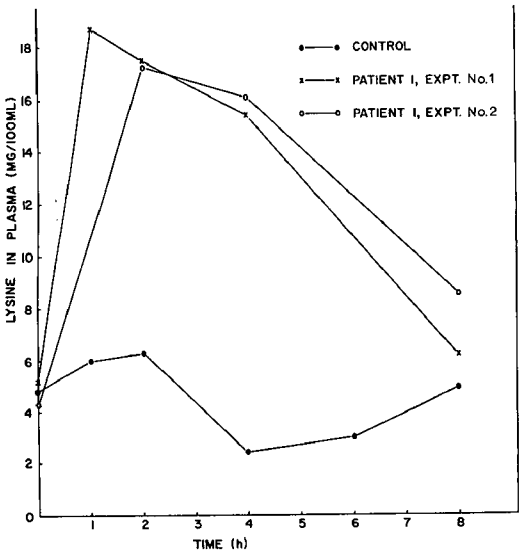

Fig. 3. Lysine concentration in plasma after oral administration.

the two methods since the population of individuals used in both cases was rather small.

As an example of the application of this method to a specific problem, at retarded patient with hyperlysinuria and hyperlysinemia[4] was chosen. The subject was given an oral lysine tolerance test and the results indicate the ability of this method to differentiate abnormal tolerance levels of lysine in the plasma (Fig. 3).

Studies of amino acid metabolism are facilitated by reliable ultramicro quantitative analytical methods. The gas chromatographic method described here is particularly attractive from this point of view since it allows for the analyses of amino acids in small volumes of plasma (0.1–0.5 ml). The preparation of the *n*-butyl N-trifluoroacetyl esters which have a high electron capture coefficient allows the possibility of extending the sensitivity even by an additional several orders of magnitude through the employment of electron capture detection. This is particularly important in clinical studies involving infants which restricts the investigator to extremely small quantities of plasma for analyses.

In order that an analytical procedure be acceptable for routine laboratory usage, it is imperative to demonstrate its accuracy and reproducibility. The variability of the gas chromatographic method due to employment of different columns can be minimized by careful calibration. The analytical method described here was statistically analyzed for its overall reproducibility and the results indicated that it is satisfactory for clinical usage. In addition, the range of normal concentrations in our clinical population is within agreement with values obtained by other methods.

ACKNOWLEDGEMENT

The amino acid analyzer analysis on a synthetic mixture by Dr. R. JOHNSON is gratefully acknowledged. The expert technical assistance of Mrs. C. RISING is also recognized.

REFERENCES

1 C. W. GEHRKE AND D. L. STALLING, *Separ. Sci.*, 11 (1967) 101.
2 P. TALBOT, E. D. PELLIZZARI, J. H. BROWN, R. W. FARMER AND L. F. FABRE, Jr., *J. Chromatog. Sci.*, in press.
3 L. Z. BITO AND J. DAWSON, *Anal. Biochem.*, 28 (1969) 95.
4 J. H. BROWN, G. L. FARRELL, E. D. PELLIZZARI AND L. F. FABRE, Jr., *Clin. Res.*, 2 (1970) 452.
5 J. BRODEHL AND K. GELLISSEN, *Pediatrics*, 42 (1968) 395.

CHROM. 5153

GAS CHROMATOGRAPHIC ANALYSIS OF TRYPTOPHAN METABOLITES

TOMOO NOGUCHI, HIROKI KASEDA, NORIHIKO KONISHI AND RYO KIDO
Department of Biochemistry, Wakayama Medical College, Wakayama 640 (Japan)

(Received September 29th, 1970)

SUMMARY

A procedure was developed for preparing the derivatives of tryptophan metabolites, which were classified into three groups; (A) kynurenine and its related compounds; (B) 2-aminoacetophenone and its related compounds; and (C) anthranilic acid and its related compounds. Groups A and B were converted to methoxy trifluoroacetylamino acetophenones and group C to methyl methoxy trifluoroacetylamino anthranilates. Each of these derivatives has proved to be useful for gas chromatographic separations using Apiezon grease L on Celite 545 SK with isothermal temperature.

INTRODUCTION

There have been intensive investigations of tryptophan metabolism. A number of metabolites of tryptophan have been shown to occur in the urine of various species under different conditions[1–24]. These metabolites have been isolated and identified by means of ion-exchange resin, paper and thin-layer chromatography. 3-Hydroxyanthranilic acid was studied by gas chromatography (GC) analysis by ROSE *et al.*[25]. However, there are few or no reports on the methods for GC analysis of the biologically important metabolites of tryptophan, including kynurenine, anthranilic acid, 2-aminoacetophenone and other related compounds. Therefore, attempts were made to prepare the derivatives of ten metabolites of tryptophan and to analyze the resulting derivatives by GC.

EXPERIMENTAL

Reagents

Anthranilic acid, 3-hydroxyanthranilic acid, 5-hydroxyanthranilic acid, DL-kynurenine, 3-hydroxy-DL-kynurenine and 5-hydroxy-DL-kynurenine were the same preparations as those used in previous studies[24,26]. 3,5-Dihydroxyanthranilic acid was generously provided by Dr. SHIRO SENOH, Institute for Food Chemistry, Osaka, Japan. 2-Aminoacetophenone, 2-amino-3-hydroxyacetophenone and 2-amino-5-hydroxyacetophenone were synthesized according to the methods described be-

fore[27–29]. Trifluoroacetic anhydride was obtained from Tokyo Chemical Industry Co. Ltd. Etherial diazomethane was prepared from N-methyl-N-nitrosotoluene-*p*-sulphonamide (Tokyo Chemical Industry Co. Ltd.). It remained stable at least for 3 weeks when stored over potassium hydroxide pellets at −10°.

Apparatus and working conditions

A Hitachi–Perkin-Elmer Model F-6 gas chromatograph with a flame ionization detector was used. The 6 ft. × 3 mm I.D. stainless-steel column used was packed with 10% (w/w) Apiezon grease L on Celite 545 SK (Nippon Chromatographic Industry Co. Ltd.). The column oven temperature was 230°, the detector and injection port temperatures, 270° and 250°, respectively. The gas flow rates of nitrogen, hydrogen and air were 70, 40 and 300 ml/min, respectively. The sample size was 2.0 μl. The chart speed was 1 cm/min.

Preparation of derivatives

Eleven tryptophan metabolites were classified into three groups. Each group is designated through the text of this paper as Group A, B or C. Group A contained DL-kynurenine, 3-hydroxy-DL-kynurenine and 5-hydroxy-DL-kynurenine. Group B contained 2-aminoacetophenone, 2-amino-3-hydroxyacetophenone and 2-amino-5-hydroxyacetophenone. Group C contained anthranilic acid, 3-hydroxyanthranilic acid, 5-hydroxyanthranilic acid and 3,5-dihydroxyanthranilic acid. Each group was a mixture of equal amounts (2 mg) of its respective components. Groups B and C were quantitatively converted to methoxy N-trifluoroacetyl derivatives and methyl methoxy N-trifluoroacetyl derivatives, respectively as follows. The mixture of Group B or Group C was placed in a glass-stoppered test tube with 1 ml of etherial diazomethane and left overnight in the dark at room temperature. After the solvent was removed under a stream of nitrogen gas *in vacuo*, 0.5 ml of chloroform and 0.2 ml of trifluoroacetic anhydride were added. The tube was sealed and allowed to stand in the dark at room temperature at least for 30 min. The solution was evaporated to dryness under a stream of nitrogen gas *in vacuo*. The dry residue was dissolved in a small volume of anhydrous ethyl acetate for GC examination.

DL-Kynurenine, 3-hydroxy-DL-kynurenine and 5-hydroxy-DL-kynurenine in Group C were converted to 2-aminoacetophenone, 2-amino-3-methoxy-acetophenone and 2-amino-5-methoxyacetophenone, respectively, as follows. The mixture of Group C was dissolved in 2 ml of methanol, and 4 ml of etherial diazomethane were added. After the solution stood overnight in the dark at room temperature, the solvent was removed under nitrogen *in vacuo*. The residue was heated for 1 h with 2 ml of 1 *N* HCl to hydrolyze the methyl esters on the boiling water bath. After the resulting yellow-brown solution was adjusted to pH 7.0 with 6 *N* NaOH, 0.2 ml of 0.1 *N* $Ba(OH)_2$ was added, and the solution was refluxed for 1 h at 100°. The solution was refluxed with 2.5 ml of 2 *N* NaOH for 1 h at 100°, and then was adjusted to pH 7.0 with 4 *N* HCl and shaken with three 30-ml portions of diethyl ether. The combined ether extract was evaporated to dryness *in vacuo*. The resulting methoxy aminoacetophenones were trifluoroacetylated by the procedure described above. The resulting derivatives were dissolved in a small volume of ethyl acetate for GC analysis.

RESULTS AND DISCUSSION

Eleven tryptophan metabolites were classified into three groups: (A) kynurenine and its related compounds; (B) 2-aminoacetophenone and its related compounds; (C) anthranilic acid and its related compounds, because each group can be isolated according to the procedure of ROY AND PRICE[30]. Groups B and C were quantitatively converted to methoxy N-trifluoroacetyl derivatives and methyl methoxy N-trifluoroacetyl derivatives respectively, by treating with diazomethane overnight and trifluoroacetic anhydride for 30 min at room temperature as described under EXPERIMENTAL. All the derivatives were stable under anhydrous condition at least for one week at room temperature. In the previous investigation, the resolution of two methoxy N-trifluoroacetyl derivatives of 2-amino-3-hydroxyacetophenone and 2-amino-5-hydroxyacetophenone in Group B, or two methyl methoxy N-trifluoroacetyl derivatives of 3-hydroxyanthranilic acid and 5-hydroxyanthranilic acid in Group C were not satisfactory using Silicone XE-60 on Diasolid (Nippon Chroma-

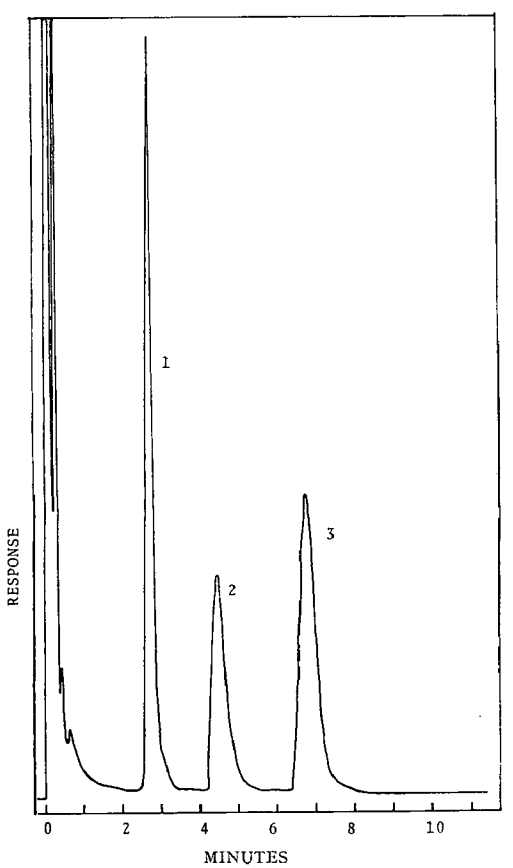

Fig. 1. Gas chromatogram of the derivatives of anthranilic acid and its related compounds. Working conditions are as described in the text. 1 = methyl 2-trifluoroacetylamino anthranilate; 2 = methyl 3-methoxy-2-trifluoroacetylamino anthranilate; 3 = methyl 5-methoxy-2-trifluoroacetylamino anthranilate; 4 = methyl 3,5-dimethoxy-2-trifluoroacetylamino anthranilate.

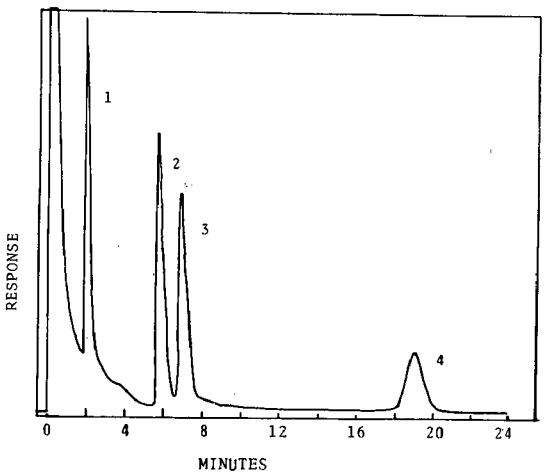

Fig. 2. Gas chromatogram of the derivatives of 2-aminoacetophenone and its related compounds. Working conditions are as described in the text. 1 = 2-trifluoroacetylamino acetophenone; 2 = 3-methoxy-2-trifluoroacetylamino acetophenone; 3 = 5-methoxy-2-trifluoroacetylamino acetophenone.

tographic Industry Co. Ltd.)[28]. In this work, the clear separation of these compounds was obtained by using Apiezon grease L on Celite 545 SK with isothermal temperature. The chromatogram of the derivatives from the mixture of the members, belonging to Group B is illustrated in Fig. 1. That of Group C is shown in Fig. 2. As shown in both figures, the peaks with good shapes characterized by specific retention time were obtained for each component. The separation was complete and no extraneous peaks were observed. Working conditions are described under EXPERIMENTAL. The use of several other conditions resulted in unsatisfactory separation. In previous experiments, we failed to prepare the volatile derivatives of Group A (kynurenine, 3-hydroxykynurenine and 5-hydroxykynurenine) by treating with diazomethane and trifluoroacetic anhydride. Subsequently, it was attempted to convert each component of Group A to the corresponding methoxy aminoacetophenones. This attempt was successful. The yield of each product was found to be complete from its molar absorption coefficient in ethyl alcohol (2-aminoacetophenone, $\varepsilon_{364\ m\mu} = 3500$; 2-amino-3-methoxyacetophenone, $\varepsilon_{370\ m\mu} = 3750$; 2-amino-5-methoxyacetophenone, $\varepsilon_{390\ m\mu} = 3800$). The methoxy aminoacetophenones were trifluoroacetylated prior to GC analysis. The retention times of three derivatives prepared were the same as those of trifluoroacetylamino acetophenone, 3-methoxy-2-trifluoroacetylamino acetophenone and 5-methoxy-2-trifluoroacetylamino acetophenone, respectively. Other important tryptophan metabolites, quinoline compounds such as kynurenic acid, xanthurenic acid, 6-hydroxykynurenic acid, quinaldic acid, 4-hydroxyquinoline, 4,6-dihydroxyquinoline, 4,8-dihydroxyquinoline and others were also subjected to GC analysis. The separation of these metabolites was not satisfactory because of the difficulty of quantitative conversion of these compounds to volatile derivatives. The GC analysis of quinoline compounds and determination of tryptophan metabolites are in progress.

REFERENCES

1 J. LIEBIG, *Ann. Chem. Liebigs*, 86 (1853) 125.
2 Y. KOTAKE AND J. IWAO, *Z. Physiol. Chem.*, 195 (1931) 139.
3 W. G. GORDON, R. E. KAUFMAN AND R. W. JACKSON, *J. Biol. Chem.*, 113 (1936) 125.
4 K. ICHIHARA AND S. GOTO, *Z. Physiol. Chem.*, 243 (1936) 257.
5 W. A. PERLZWEIG, F. ROSEN AND P. B. PEARSON, *J. Nutr.*, 40 (1950) 453.
6 C. E. DALGLIESH, W. E. KNOX AND A. NEUBERGER, *Nature*, 168 (1951) 20.
7 C. E. DALGLIESH, *Biochem. J.*, 52 (1952) 3.
8 C. E. DALGLIESH AND S. TEKMAN, *Biochem. J.*, 56 (1954) 458.
9 E. BOYLAND AND C. WILLIAMS, *Biochem. J.*, 60 (1955) V.
10 L. MUSAJO, C. A. BENASSI AND A. PARPAJOLA, *Nature*, 175 (1955) 855.
11 K. INAGAMI, *J. Sericult. Sci.*, 24 (1955) 295.
12 R. R. BROWN AND J. M. PRICE, *J. Biol. Chem.*, 219 (1956) 985.
13 J. M. PRICE AND L. M. DODGE, *J. Biol. Chem.*, 223 (1956) 699.
14 H. TAKAHASHI, M. KAIHARA AND J. M. PRICE, *J. Biol. Chem.*, 223 (1956) 705.
15 R. R. BROWN, *J. Biol. Chem.*, 227 (1957) 649.
16 H. TAKAHASHI AND J. M. PRICE, *J. Biol. Chem.*, 233 (1958) 150.
17 J. K. ROY, R. R. BROWN AND J. M. PRICE, *Nature*, 184 (1959) 1573.
18 J. K. ROY AND J. M. PRICE, *J. Biol. Chem.*, 234 (1959) 2759.
19 A. M. PAMUKCU, R. R. BROWN AND J. M. PRICE, *Zent. Veterinaermed.*, 6 (1959) 361.
20 A. M. PAMUKCU, J. M. PRICE AND R. R. BROWN, *Amer. J. Vet. Res.*, 20 (1959) 597.
21 K. MAKINO, *Biochem. Biophys. Res. Commun.*, 5 (1961) 481.
22 R. KIDO, T. TSUJI AND Y. MATSUMURA, *Biochem. Biophys. Res. Commun.*, 13 (1963) 428.
23 W. I. AUSTAD, J. R. CLAMP AND R. G. WESTALL, *Nature*, 207 (1965) 757.
24 R. KIDO, T. NOGUCHI, T. TSUJI AND Y. MATSUMURA, *Biochim. Biophys. Acta*, 136 (1967) 131.
25 D. P. ROSE AND P. A. TOSELAND, *Clin. Chim. Acta*, 17 (1967) 235.
26 R. KIDO, T. NOGUCHI, T. TSUJI AND Y. MATSUMURA, *Biochim. Biophys. Acta*, 141 (1967) 270.
27 R. KIDO, T. NOGUCHI, H. KASEDA AND Y. MATSUMURA, *Proc. Symp. Chem. Physiol. Pathol.*, 8 (1968) 65.
28 T. NOGUCHI, H. KASEDA, R. KIDO AND Y. MATSUMURA, *J. Biochem.*, 67 (1970) 113.
29 T. NOGUCHI, H. KASEDA, R. KIDO AND Y. MATSUMURA, *J. Biochem.*, 68 (1970) 245.
30 J. K. ROY AND J. M. PRICE, *J. Biol. Chem.*, 233 (1958) 150.

CHROM. 5164

DETERMINATION OF METABOLITES OF TYROSINE AND OF TRYPTOPHAN AND RELATED COMPOUNDS BY GAS–LIQUID CHROMATOGRAPHY

PHILLIP W. ALBRO AND LAWRENCE FISHBEIN

National Institute of Environmental Health Sciences, National Institutes of Health, Public Health Service and Department of Health, Education and Welfare, Research Triangle Park, N.C. 27709 (U.S.A.)

(Received November 17th, 1970)

SUMMARY

A one-step procedure for the simultaneous derivatization of acidic, neutral and basic metabolites of tyrosine and tryptophan has been developed. The derivatives of sixteen tryptophan metabolites, twelve tyrosine metabolites and several related compounds were quantitatively determined by gas–liquid chromatography using three stationary phases of varying selectivities.

INTRODUCTION

The metabolism of tryptophan and tyrosine is becoming of increasing interest[1–5] due primarily to the varied activities of their metabolites in the nervous system, but also due to the association of these metabolites with various disorders such as Kwashiorkor[6] and malignant carcinoid[7]. Metabolites of tryptophan and of tyrosine have been determined in a variety of ways, including gas–liquid chromatography (GLC) of acidic[8] and basic[9,10] components separately.

We have developed a procedure for the GLC analysis of sixteen tryptophan metabolites, twelve phenylalanine/tyrosine metabolites, the parent amino acids and a number of related compounds. Carboxy-, amino- and polyfunctional metabolites are determined simultaneously.

MATERIALS AND METHODS

Silylating agents were obtained from Pierce Chemical Co., Rockford, Ill. Reference amino acids and metabolites were from Sigma Chemical Co., St. Louis, Mo. Gas chromatography stationary phases and solid supports were from Applied Science Laboratories, State College, Pa., and from Supelco, Inc., Bellefonte, Pa.

Analyses were performed using Varian Aerograph Model 1200 and Hewlett-Packard Model 5750 gas chromatographs, both equipped with hydrogen flame ionization detectors. Injection port and detector temperatures were 260 and 300°, re-

spectively, while in all cases the helium flow rates were initially 45 ml/min measured at the column outlet. Hydrogen and air flows were 22 and 250 ml/min, respectively. Columns were 3.1 m × 3.2 mm O.D. stainless steel; they contained the packings and were temperature-programmed as described in Table I.

Reactions were carried out in 1-ml vials equipped with Teflon-lined screw caps

TABLE I

CONDITIONS FOR GAS CHROMATOGRAPHY

System	*Liquid phase*	*Solid support*	*Linear program*
A	7% OV-1	100/120 Gas-Chrom Q	120–265° at 6°/min.
B	10% OV-17	80/100 Supelcoport	150–270° at 6°/min.
C	10% OV-210	80/100 Supelcoport	150–245° at 6°/min.

(Reactivials, Pierce Chemical Co.). 3-μl samples of the reaction mixtures were injected directly into the gas chromatographs.

Studies with model compounds

Indole, hydroxyindole, 2-phenyl-ethylamine, indole-3-acetic acid, 5-hydroxytryptophan and 5-hydroxyindole-3-acetic acid were individually studied to compare the derivatizations of the various functional groups by different silylating reagents. Solutions or suspensions of the starting materials in pyridine were chromatographed to determine the retention times of those unreacted compounds capable of eluting.

Silylation reactions were run either at room temperature for 3 h, at 100° for 10 min, or at 100° for 10 min followed by overnight standing at room temperature. 1-mg samples of each compound to be derivatized were reacted with 50–300 μl quantities of: (1) trimethylsilylimidazole (TMSI), (2) N-trimethylsilyl diethylamine (TMSDEA), (3) hexamethyldisilazane–trimethylchlorosilane–pyridine (HMDS–TMCS–PYR), 10:5:25 (v/v/v), (4) HMDS–TMCS–Dimethylformamide, 10:5:25 (v/v/v), (5) bis-trimethylsilyltrifluoroacetamide (b-TMSTFA) containing 1% TMCS, (6) b-TMSTFA–TMCS–PYR, 99:1:250 (v/v/v), (7) TMSDEA–TMSI, 1:1 (v/v), (8) 30% TMSDEA in pyridine, (9) 30% TMSI in pyridine, (10) TMSDEA–TMCS, 8:1 (v/v), (11) b-TMSTFA–TMSDEA–TMCS–PYR, 99:30:1:100 (v/v/v/v).

Quantitative measurements

Peak areas were measured as height × width at half-height, and were expressed relative to the peak area of an internal standard, usually *n*-docosane. These measurements were used to determine relative molar response factors for the various compounds under the conditions used. It was found that the same relative molar response factors applied whether the Varian or the Hewlett-Packard gas chromatographs were used.

Assumptions

It was assumed that any silylating procedure that did not produce a silylated derivative with indole would not react with the indole nitrogen of tryptophan metabolites. Similarly, failure to derivatize phenylethylamine was assumed to indicate

that the reagent would not derivatize amino groups in the other test substances. These assumptions were used only to eliminate reagents from further consideration; therefore, the final results presented below do not depend upon the assumptions being valid.

Recommended procedures

Add *n*-docosane to reagent (11) above to give 50 μg/ml. Up to 2 mg of tryptophan and/or tyrosine metabolites may be derivatized in a sealed tube with 0.30 ml of reagent, preferably by heating at 100° for 10 min followed by letting stand overnight at room temperature. The resulting solution may be analyzed directly, chromatographing 3-μl aliquots on each of the columns described in Table I.

Application to biological materials

Up to 50 mg of lyophilized, finely pulverized tissue, bacterial cells, or lyophilized urine may be reacted directly with 1 ml of reagent as described above. Insufficient reagent usually results in the formation of a gel, in which case additional reagent may be added. It was found advisable to centrifuge these preparations prior to chromatography to avoid fouling the injection block. After complete silylation, all of the compounds discussed below were found to be soluble in the reagent. A somewhat similar procedure has been previously applied to dried urine for screening purposes[11].

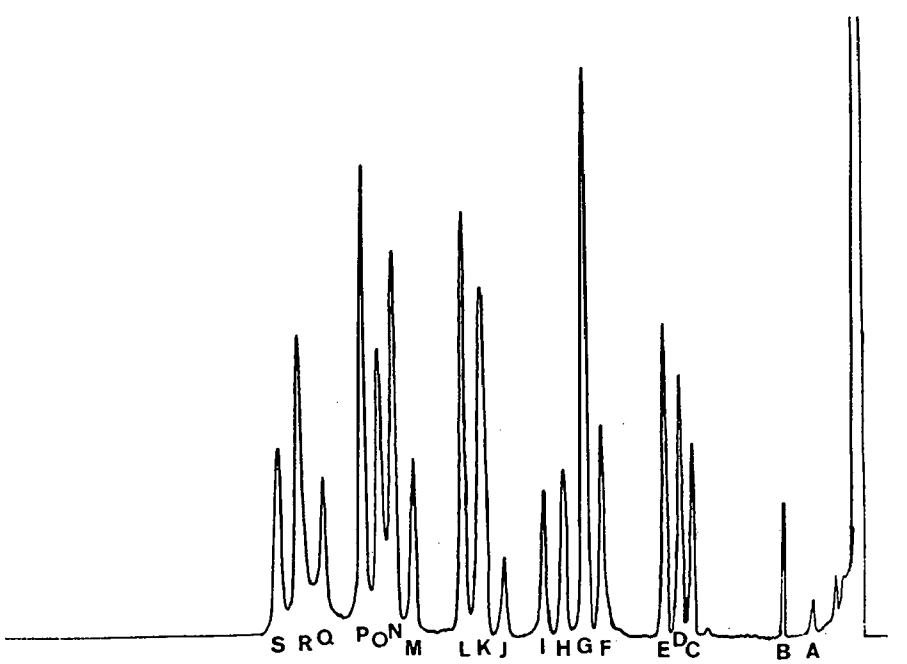

Fig. 1. Chromatography of silylated derivatives on OV-17. Identification of peaks: A = urea; B = nicotinic acid; C = nicotinamide; D = phenylalanine; E = *p*-hydroxyphenylacetic acid; F = 3-hydroxyanthranilic acid; G = homogentisic, homovanilic, and homoprotocatechuic acids; H = artifact; I = tyrosine; J = dopamine, K = Dopa plus *p*-hydroxyphenylpyruvic acid; L = indole-3-acetic acid; M = kynurenic acid; N = kynurenine; O = tryptophan plus serotonin; P = 5-hydroxyindole-3-acetic acid; Q = 3-hydroxykynurenine; R = 5-hydroxy-tryptophan; S = indole-3-pyruvic acid. For chromatographic conditions, see Table I.

RESULTS AND DISCUSSION

Model compounds

Reagents (1), (7) and (9) which contained TMSI gave multiple products with all of the model compounds. Reagents (3) and (4) gave two peaks with hydroxyindoleacetic acid when the products were chromatographed in the B system. Reagents (2) and (8) containing TMSDEA alone never gave quantitative silylation, possibly because the diethylamine produced was not removed from the reaction mixtures[12]. Reagents (5) and (6) generally gave quantitative results with the model compounds, but the derivatives of phenylethylamine partially decomposed on standing.

TABLE II

ELUTION AND RESPONSE PARAMETERS OF SILYLATED DERIVATIVES

Compound	*OV-1*[a]		*OV-17*		*OV-210*		*Rel. molar resp.*[b]
	R'_T *(min)*	E_T *(°C)*	R'_T *(min)*	E_T *(°C)*	R'_T *(min)*	E_T *(°C)*	
Urea	1.60	130.6	1.93	164.6	2.20	166.2	—
Nicotinic acid	4.04	145.2	2.62	168.7	3.37	173.4	0.058
Indole	6.30	158.8	5.05	180.3	4.48	179.8	0.117
Nicotinamide	6.96	162.8	5.80	187.8	7.88	200.6	0.093
Creatinine	9.56	178.4	4.73	181.4	4.66	181.0	—
Phenyllactic acid	9.62	178.7	5.74	187.4	5.02	183.1	0.174
Phenylalanine	10.40	183.4	5.90	188.4	5.75	187.5	0.196
p-Hydroxyphenylacetic acid	10.41	183.5	6.88	194.3	6.62	192.7	0.157
Tryamine	10.42	183.5	5.70	187.2	5.09	183.5	0.153
5-Hydroxyindole	12.75	197.5	10.00	213.0	9.00	207.0	0.152
Homovanilic acid	12.78	197.6	9.51	210.0	9.18	208.1	0.200
3-Hydroxyanthranilic acid	12.91	198.5	8.90	206.4	8.79	206.1	0.277
Homoprotocatechuic acid	14.37	207.2	9.51	210.0	9.25	208.9	0.546
Homogentisic acid	14.44	207.7	9.53	210.2	9.85	212.5	0.546
4-Pyridoxic acid	16.30	218.9	11.61	222.7	10.90	218.4	0.580
Indole-3-acetic acid	16.31	219.0	13.59	243.5	13.54	234.9	0.399
Tyrosine	16.40	219.4	10.60	216.6	10.63	216.8	0.213
L-Epinephrine	17.70	227.2	10.00	213.0	8.00	201.0	0.682
p-Hydroxyphenylpyruvic acid	18.38	231.3	12.90	230.4	12.50	228.0	0.206
Dopamine	19.19	236.1	12.15	225.9	11.22	221.0	0.438
Uric acid	19.20	236.2	14.52	240.1	11.04	219.0	—
Dopa	19.50	238.0	12.99	230.9	12.91	231.1	0.446
Tryptamine	19.83	240.1	12.37	220.5	11.62	222.8	0.068
Kynurenic acid	20.31	243.0	15.29	244.7	15.48	245	0.103
n-Docosane	20.61	244.8	13.67	235.0	10.71	217.4	1.000
Kynurenine	20.64	245.0	15.98	248.9	15.50	245	0.193
5-Methoxyindole-3-acetic acid	20.65	245.0	17.52	258.1	17.79	245	0.431
Xanthurenic acid	20.80	245.8	16.98	254.9	16.50	245	0.456
Serotonin	20.88	246.2	16.25	250.5	15.85	245	0.078
5-Hydroxyindole-3-acetic acid	20.90	246.4	16.98	254.9	16.93	245	0.467
Tryptophan	21.10	247.6	16.40	251.4	16.58	245	0.139
Indole-3-pyruvic acid	24.25	265	19.80	270	20.40	245	0.208
3-Hydroxykynurenine	24.37	265	18.32	262.9	18.38	245	0.206
5-Hydroxytryptophan	24.95	265	19.10	267.6	19.60	245	0.149
N-Acetyl-5-serotonin	25.23	265	23.60	270	24.01	245	0.129

[a] R'_T (min) = corrected elution time in minutes; E_T (°C) = temperature at peak elution.
[b] Molar response relative to *n*-docosane in terms of peak areas.

Reagents (10) and (11) were quite satisfactory for quantitative conversion of the model compounds into gas chromatographable derivatives. They differed in that reagent (10), TMSDEA–TMCS, 8:1, did not react with indole while reagent (11), b-TMSTFA–TMCS–TMSDEA–PYR, 99:1:30:100, did; thus the two reagents gave different derivatives with the various tryptophan metabolites. We were unable to find chromatographic conditions that would resolve all of those tryptophan metabolites derivatized by reagent (10); therefore, reagent (11) was finally selected as most suitable for our purposes.

Complex mixtures of tryptophan and tyrosine metabolites

Fig. 1 shows a typical chromatogram obtained with the OV-17 column in the Varian Aerograph chromatograph. This column did not separate the derivatives of tryptophan and serotonin, of Dopa and *p*-hydroxyphenylpyruvic acid, and of homovanilic, homogentisic, and homoprotocatechuic acids. These derivatives were, however, resolved on OV-210. OV-210 did not resolve hydroxyindole from homovanilic acid, while this separation could be accomplished on either OV-1 or OV-17. The dopamine–tryptamine pair was best resolved on OV-1.

Table II lists the compounds tested, their elution parameters for the three sets of conditions used, and their molar responses relative to that of *n*-docosane. It is clear from Table II that separation of all the compounds listed requires the use of all three columns.

Analysis of "spiked" urine

A water solution containing indole, dopamine, kynurenic acid, hydroxyindoleacetic acid, hydroxykynurenine, and N-acetylserotonin was prepared, representing various functional groups to be expected in biological materials. 1 ml of standard mixture was diluted with 1 ml of water, 1 ml of standard was mixed with 1 ml of rat urine, and 1 ml of rat urine was diluted with 1 ml of water after which the three solutions were freeze-dried and analyzed as described above. The ratios of the peak areas of the "spike" compounds to that of the internal standard (*n*-docosane) were compared as shown in Table III.

TABLE III

ANALYSIS OF SPIKED URINE

Compound	*Peak area ratios*[a]			
	Spike	*Control urine*	*Spiked urine*	
			Calc.[b]	*Found*
Indole	0.49	0.53	1.02	0.95
Dopamine	1.41	0.25	1.66	1.65
Kynurenic acid	0.06	0.08	0.14	0.15
Hydroxyindoleacetic acid	2.20	0.13	2.33	2.32
Hydroxykynurenine	0.04	0.11	0.15	0.13
N-Acetyl serotonin	0.79	0.15	0.94	1.01

[a] Peak area as fraction of *n*-docosane (internal standard) peak area.
[b] Sum of spike + control urine.

It is clear from Table III that the constituents of normal rat urine do not interfere with determination of the test metabolites. An unusually high amount of urea will interfere as has been indicated previously[11], but we found that a urea content high enough to exhaust the reagent inevitably resulted in formation of an obvious gel. In such a case it was necessary to add additional reagent and warm briefly.

REFERENCES

1 D. K. ZHELYASKOV, M. LEVITT AND S. UDENFRIEND, *Mol. Pharmacol.*, 4 (1968) 445.
2 H. VARLEY AND A. H. GOWENLOCK (Editors), *West-European Symposia on Clinical Chemistry*, Vol. 2. Elsevier, New York, 1963.
3 J. JACOB, *Proc. Eur. Soc. Study Drug Toxicity*, 8 (1967) 59.
4 J. J. SCHILDKRAUT AND S. S. KETY, *Science*, 156 (1967) 21.
5 C. L. GAZZULLO, A. MANGONI AND G. MASCHERPA, *Brit. J. Psychiat.*, 112 (1966) 157.
6 A. S. ABBASSY, M. M. ZEITOUN, E. A. HASSANEIN, G. A. ABDEL-TAWAB, T. S. KHOLIEF AND S. W. EL-SEWEDY, *Trans. Roy. Soc. Trop. Med. Hyg.*, 64 (1970) 27.
7 G. T. BRYAN, *Ann. Ind. Hyg. Ass. J.*, 30 (1969) 27.
8 M. G. HORNING, K. L. KNOX, C. E. DALGLIESH AND E. C. HORNING, *Anal. Biochem.*, 17 (1966) 244.
9 C. J. W. BROOKS AND E. C. HORNING, *Anal. Chem.*, 36 (1964) 1540.
10 E. C. HORNING, M. G. HORNING, W. J. A. VANDENHEUVEL, K. L. KNOX, B. HOLMSTEDT AND C. J. W. BROOKS, *Anal. Chem.*, 36 (1964) 1546.
11 R. F. COWARD AND P. SMITH, *J. Chromatog.*, 37 (1968) 111.
12 P. S. MASON AND E. D. SMITH, *J. Gas Chromatog.*, 4 (1966) 398.

CHROM. 5158

QUANTITATIVE ANALYSIS OF MALEIC AND CITRACONIC ANHYDRIDES BY GAS CHROMATOGRAPHY

ALDO DI LORENZO

Laboratorio di Ricerche sulla Combustione, C.N.R., Istituto di Chimica Industriale e Impianti Chimici dell'Università di Napoli, Naples (Italy)

(Received November 10th, 1970)

SUMMARY

A gas chromatographic technique has been developed for quantitative analysis of the maleic and citraconic anhydrides produced by catalytic vapor-phase oxidation of methylcyclopentane with air. The main difficulty in analysing samples as obtained from the catalytic reactor is that the above anhydrides are partially hydrated to acids in the presence of the condensed water. Maleic and citraconic acids cannot, as their anhydrides, be detected quantitatively by gas chromatography nor are they completely dehydrated using the usual temperature of the injection block and flow rate of the carrier gas. Gas chromatographic analysis of methyl esters derived from maleic and citraconic acids correctly gives the amount of anhydrides and acids initially present in the sample from the reactor. The di-2-ethylhexyl sebacate/sebacic acid column separates anhydrides, esters and their isomers, allowing the control of the completeness of esterification.

INTRODUCTION

During work on the vapor-phase oxidation of methylcyclopentane over vanadium–molybdenum catalyst[1] the problem of analysing mixtures consisting of methylcyclopentane, acetic acid, water, maleic and citraconic anhydrides in dioxane solution arose. The principal difficulty in measuring such mixtures arose from the coexistence of two anhydrides and water. Many methods for analysing anhydrides, utilizing various techniques such as conventional chemical, polarographic and GC analyses, have been described in the literature[2–16]. Several authors[2–4] estimated the maleic anhydride as barium maleate monohydrate by precipitation with $BaCl_2 \cdot 2H_2O$ in alcohol solution. Others[5,6] determined maleic anhydride, in the products arising from catalytic vapor-phase oxidation of benzene, by the bromine consumption. The polarographic analysis of anhydrides, described by various authors[7–10] has recently been optimized[11]. GC has been utilized in the catalytic vapor-phase oxidation processes of alkylaromatic hydrocarbons for quantitative determination of condensed products including maleic and citraconic anhydrides[12–15]. Finally, CUCARELLA AND CRESPO[16] have developed a GC method which allows a measurement of the impurities,

normally present in phthalic anhydride, which include maleic and citraconic anhydrides, after esterification with a sulfuric acid–methanol mixture.

EXPERIMENTAL

Preliminary experiments on methylcyclopentane oxidation have been made to study the composition of reaction products. The presence, in all the tests, of both maleic and citraconic anhydrides in the reaction products excluded the use of the Ba method, the Br method and polarographic analysis because these methods determine the total anhydrides but do not distinguish between them. Therefore, for quantitative determination, the previously known GC methods[12–16] have been tested.

Chemicals

Chromosorb P AW 60–80 mesh (John Manville Products Co.); di-2-ethylhexyl sebacate, didecyl phthalate, sebacic acid, phosphoric acid, methylcyclopentane, dioxane, acetic acid, *m*-xylene, maleic anhydride (Carlo Erba S.p.A.); citraconic anhydride, maleic, fumaric, citraconic, mesaconic and itaconic acids, maleic and itaconic acid dimethyl esters (Fluka AG Chemische Fabrik); fumaric, citraconic and mesaconic acid dimethyl esters were synthesized in this Laboratory by esterification of their corresponding acids with a sulfuric acid–methanol mixture and were subsequently purified.

Apparatus

All analyses were carried out with a Perkin-Elmer F 6 gas chromatograph equipped with a flame ionization detector (flow rates: hydrogen, 30 ml/min; air, 350 ml/min). The chromatograms were recorded with a Leeds & Northrup Speedomax 5 mV recorder at a chart speed of $\frac{1}{2}$ in./min. Helium was used as the carrier gas. Samples were injected with a 10-μl Hamilton syringe (Model No. 701 N).

In preliminary analyses, various columns, including those described in the literature for maleic and citraconic anhydride separation[12–14], were tested to select the most suitable working conditions for separating the products obtained from the reactor. Two columns were prepared from a 2-m length of $\frac{1}{4}$-in. stainless-steel tubing; the first was packed with 25% di-2-ethylhexyl sebacate and 10% sebacic acid on 60–80 mesh acid-washed Chromosorb P, and the second with 25% didecyl phthalate on 60–80 mesh acid-washed Chromosorb P, previously treated with 10% sulfuric acid as described in ref. 17. The operation was done isothermally at 120° and gave a good separation of methylcyclopentane, dioxane, acetic acid, *m*-xylene (used as internal standard in the quantitative evaluations), maleic and citraconic anhydrides. During the experiments it was noted that the didecyl phthalate–phosphoric acid column was not suitable for routine analysis, as it easily deteriorated, with drop in retention time for the various substances and consequent overlapping of the dioxane and acetic acid peaks.

A hydrogen flame ionization detection system was used because many dilute solutions (about 15 g of dioxane per g of condensed products) had to be analyzed. Water, not detectable with this system, was determined by Fischer's method.

Under the previously described experimental conditions synthetic mixtures of methylcyclopentane, acetic acid, *m*-xylene, maleic and citraconic anhydrides, pre-

pared by weighing the individual components and then dissolving them in dioxane, were analyzed. The analyses of these mixtures were still reproducible even after several days. On the contrary the same mixtures with water did not give good results. In particular, maleic anhydride behaved irregularly. If these mixtures were analyzed directly after preparation, the maleic anhydride values were approximately those obtained for mixtures without water. However, on repeating the analyses, the values gradually decreased until they were about half and then remained almost constant. Instead, the values for citraconic anhydride, always present in the products from the reactor and the synthetic mixtures in amounts lower than the maleic anhydride, did not alter. Such irregularity of maleic anhydride in the presence of water has not been hitherto reported in the literature[13–15].

Since GC analysis of maleic acid from a solvent solution gave a peak whose retention time corresponded to the maleic anhydride, while the area of the acid was about half with respect to that of the anhydride at the same concentration, the irregularity in the quantitative determination of maleic anhydride in the synthetic mixtures with water was attributed to its hydration into the acid. Thus complete dehydration from acid to anhydride was not possible with the ordinary injection block temperature and carrier gas flow rates.

On the other hand, maleic acid was always present in the mixtures from the reactor. In fact, by adding to these mixtures, after the first analysis, a solution of acetyl chloride and acetic acid to improve the dehydration of the acid to anhydride and then repeating the analysis, higher values of maleic anhydride were obtained.

Thus, the possibility of determining the maleic acid and anhydride as maleic acid dimethyl ester was studied. The esterification was preceded by a GC quantitative determination of methylcyclopentane, acetic acid and citraconic anhydride to avoid possible errors due to loss, especially of methylcyclopentane, in the methylation procedure. Then, citraconic anhydride was added to the solution to be utilized as an internal standard for determination of the maleic acid dimethyl ester.

In principle, our method was similar to that given in ref. 16. The methylation was carried out using a sulfuric acid–methanol mixture (1:4). The esters produced were extracted with ether; the ethereal solution was washed with Na_2CO_3 and Na_2SO_4 until neutral and was concentrated. A 2-μl sample was introduced into the gas chromatograph. But with these working conditions the maleic anhydride was not satisfactorily determined. A chromatographic check of the esterification procedure showed that the methylation was partial and extraction of esters with ether incomplete. Moreover, it was not possible to concentrate the solution because a water and an ether phase were obtained.

The presence of water in the products from the reactor and their considerable dilution in dioxane were among the reasons for non-quantitative esterification. Therefore, after the analysis of products in dioxane solution and the addition of citraconic anhydride, the solution was concentrated before the esterification to eliminate most of the dioxane, water and methylcyclopentane. A mixture of methanol and sulfuric acid (8:1) was added to the concentrate and was esterified by refluxing the solution on a water bath for 2 h. After cooling, the mixture was neutralized with a 20% aqueous solution of Na_2CO_3 and a 2-μl sample was injected into the gas chromatograph. By this procedure, the analysis of an alcoholic solution of dimethyl esters derived from maleic and citraconic acids gave the correct amount of maleic anhydride

TABLE I

RELATIVE RETENTION DATA

Column temperature, 120°; carrier gas flow rate, 90 ml/min; retention time of maleic anhydride, 14 min.

Sample	*Relative retention time*
Maleic anhydride	1.00
Fumaric acid dimethyl ester	1.38
Maleic acid dimethyl ester	1.47
Citraconic anhydride	1.61
Itaconic acid dimethyl ester	2.00
Citraconic acid dimethyl ester	2.11
Mesaconic acid dimethyl ester	2.21

and acid initially present in the sample from the reactor. The di-2-ethylhexyl sebacate–sebacic acid column separated anhydrides, esters and their isomers (Table I) and this enables control of the completeness of the esterification.

RESULTS

Both direct analysis of the products from the reactor dissolved in dioxane and determination of maleic anhydride and acid as maleic acid dimethyl ester were carried out with the column prepared from a 2-m length of $\frac{1}{4}$-in. stainless-steel tubing packed with 25% di-2-ethylhexyl sebacate and 10% sebacic acid on 60–80 mesh acid-washed Chromosorb P. The operation was done isothermally at 120° with a helium carrier gas flow rate of 90 ml/min.

Internal standards were used for quantitative analysis. Calibration curves of methylcyclopentane, acetic acid and citraconic anhydride were obtained by plotting the concentration for each compound *vs.* the ratio of its peak area to that of *m*-xylene (20% referred to weight of the products). In the same way the calibration curve for maleic anhydride was obtained using citraconic anhydride as an internal standard, obtained in small part from the reaction and the rest being added by weight to the mixture up to 10% referred to weight of the products. Curves were linear at the concentrations used.

Some mixtures of known composition were analyzed for control purposes. Table II shows, for example, a comparison between compositions valued in weight and those measured by GC giving the relative differences and percentage errors.

ACKNOWLEDGEMENT

The author acknowledges the help of Mr. SABATO MASI in obtaining the experimental data.

TABLE II

ANALYSIS OF METHYLCYCLOPENTANE, ACETIC ACID, MALEIC AND CITRACONIC ANHYDRIDES AND WATER IN DIOXANE SOLUTION

Column temperature, 120°; carrier gas flow rate, 90 ml/min.

Substance	*Theor. values*	*Exper. values*	*Differences*	*Errors (%)*	*Theor. values*	*Exper. values*	*Differences*	*Errors (%)*	*Theor. values*	*Exper. values*	*Differences*	*Errors (%)*
	Mixture 1				*Mixture 2*				*Mixture 3*			
Methylcyclopentane	14.60	14.85	+0.25	1.71	29.80	30.15	+0.35	1.17	44.00	43.30	−0.70	1.59
Acetic acid	3.48	3.40	−0.08	2.30	2.26	2.30	+0.04	1.72	1.85	1.83	−0.02	1.08
Maleic anhydride	24.62	24.70	+0.08	0.32	20.60	20.49	−0.11	0.53	14.90	14.60	−0.30	2.01
Citraconic anhydride	2.60	2.56	−0.04	1.54	3.24	3.27	+0.03	0.91	2.62	2.59	−0.03	1.14
Water[a]	54.70	54.60	−0.10	0.18	44.10	44.13	+0.03	0.07	36.63	36.71	+0.08	0.22
	Mixture 4				*Mixture 5*				*Mixture 6*			
Methylcyclopentane	52.50	52.20	−0.30	0.57	69.20	70.10	+0.90	1.30	80.20	80.05	−0.15	0.19
Acetic acid	1.15	1.08	−0.07	6.09	0.59	0.57	−0.02	3.39	0.35	0.36	+0.01	2.86
Maleic anhydride	10.40	10.60	+0.20	1.92	7.15	7.10	−0.05	0.70	4.05	4.10	+0.05	1.23
Citraconic anhydride	1.72	1.66	−0.06	3.48	0.84	0.83	−0.01	1.19	0.29	0.31	+0.02	6.91
Water[a]	34.23	34.19	−0.04	0.12	22.22	22.01	−0.19	0.89	15.11	15.21	+0.02	0.66

[a] Determined by Fischer's method.

REFERENCES

1 G. RUSSO, G. D'ANGELO AND S. MASELLI, *Chim. Ind. (Milan)*, 52 (1970) 465.
2 W. A. SKINNER AND D. TIESZEN, *Ind. Eng. Chem.*, 53 (1961) 557.
3 N. A. MILAS AND W. L. WALSH, *J. Amer. Chem. Soc.*, 57 (1935) 1389.
4 C. K. CLARK AND J. E. HAWKINS, *Ind. Eng. Chem.*, 33 (1941) 1174.
5 H. J. LUCAS AND D. PRESSMAN, *Ind. Eng. Chem., Anal. Ed.*, 10 (1938) 140.
6 C. G. BERTIL HAMMAR, *Svensk Kem. Tidskr.*, 64 (1952) 165.
7 P. J. ELVING, A. MARTIN AND I. ROSENTHAL, *Anal. Chem.*, 25 (1953) 1082.
8 P. J. ELVING AND C. TEITELBAUM, *J. Amer. Chem. Soc.*, 71 (1949) 3916.
9 C. RICCUITI, C. O. WILLETS, H. B. KNOGHT AND D. SEVERN, *Anal. Chem.*, 25 (1953) 933.
10 B. WARSHOWSKY, P. J. ELVING AND J. MANDEL, *Anal. Chem.*, 19 (1947) 161.
11 F. BERNARDINI, M. RAMACCI AND A. PAOLACCI, *Chim. Ind. (Milan)*, 47 (1965) 485.
12 C. J. NORTON AND T. E. MOSS, *Ind. Eng. Chem., Process Des. Develop.*, 2 (1963) 140.
13 H. PICHLER AND F. OBENAUS, *Brennstoff-Chem.*, 45 (1964) 97.
14 H. PICHLER AND F. OBENAUS, *Brennstoff-Chem.*, 46 (1965) 258.
15 H. TRACHMAN AND F. ZUCKER, *Anal. Chem.*, 36 (1964) 269.
16 M. C. H. CUCARELLA AND F. CRESPO, *J. Gas Chromatog.*, 6 (1968) 39.
17 G. EWALD AND H. ZECH, *Z. Anal. Chem.*, 215 (1966) 8.

CHROM. 5143

INDUSTRIAL ANALYTICAL APPLICATIONS OF RAPID ION-EXCHANGE SEPARATIONS OF WEAK ORGANIC ACIDS

NORMAN E. SKELLY AND WARREN B. CRUMMETT
Analytical Laboratories, The Dow Chemical Company, Midland, Mich. 48640 (U.S.A.)

(Received November 3rd, 1970)

SUMMARY

Rapid ion-exchange chromatography has been adapted to the separation of industrial mixtures of weak organic acids. Minor impurities can be determined with a sensitivity of 0.1%. A methanol solution of the sample is injected directly into a 2.8 × 500 mm acetate form ion-exchange column. Using a specially designed gradient elution apparatus separation is achieved with an acetic acid–methanol gradient. The eluate proceeds through a flow cell mounted in an ultraviolet spectrophotometer. Response of the spectrophotometer is monitored on a strip-chart recorder. Concentrations are calculated by comparing peak areas with those of standards. Separations are generally produced in thirty to sixty minutes. Products analyzed by this technique include: 2,4-dichlorophenol, 2,4,6-trichlorophenol, 2,2′, 6,6′-tetrabromobisphenol A, 2,6-dimethyl-4-pyridinol, 3,4′,5-tribromosalicylanilide, and 3,5,6-trichloro-2-pyridinol.

INTRODUCTION

In the past two years there has been rapid growth in the area of liquid chromatography. Various commercial instruments have been designed and placed on the market. However, a very limited number of publications have appeared illustrating the application of rapid liquid chromatography to the analysis of industrial products. Generally the authors have been concerned with the separation of components present in near-equal concentrations. It was the purpose of this work to develop a system that would be competitive with gas chromatography in respect to such operations as sample introduction, separation time, and column regeneration; and the application of this technology to the analysis of commercial products.

LOGIE[1] indicated the usefulness of acetate form resins for the separation of chlorophenols. This work was extended by SKELLY[2] who employed a gradient elution which gave increased resolution. Various automated systems have been developed for the separation of weak organic acids. These have employed either ion-exchange[3] or partition[4] chromatography for the mode of separation. DAVIES *et al.*[5] made a comprehensive study of the ion-exchange characteristics of a number of organic

acids. An unusual, though complex, gradient elution apparatus was recently reported by STEHLIK[6].

EXPERIMENTAL

Reagents

Methanol, ACS grade without further purification.

Glacial acetic acid.

Organic standards. All organic standards were prepared in The Dow Chemical Company Research Laboratories. Structure determination was accomplished by elemental analysis and rigorous IR, NMR, and MS examination.

Acetic acid–methanol solutions. All eluent solutions were prepared on a volume (v/v) basis.

Ion-exchange resin, AG1-X2, acetate form, 200–400 mesh, Bio-Rad Laboratories, 32nd and Griffin, Richmond, Calif. 94804. A portion of the resin was placed in a $\frac{1}{2}$-in.-diameter column and washed with 100 ml of glacial acetic acid. Following extrusion from the column, the resin was washed three times with methanol by decantation. It was then stored under methanol in a closed container until used.

Apparatus

Syringe, 10 μl, No. 701-N, The Hamilton Co., Whittier, Calif.

Pump, Milton Roy Instrument miniPump®, Catalog No. 196-31, St. Petersburg, Fla.

Chromatography columns and fittings. The 2.8 × 500 mm columns and fittings were obtained from Chromatronix Inc., 2743 Eight Street, Berkeley, Calif. 94710.

Column septum. A 6.5 mm disc was cut from Type W silicone rubber, Catalog No. 15414, Applied Science Laboratories Inc., State College, Pa. 16801.

Column monitoring unit. The basic unit consisted of a Gilford Model 222 power supply, Gilford Instrument Co., 132 Artino Street, Oberlin, Ohio 44074. This was used in conjunction with a Beckman model DU monochromator and Sargent recorder, Model SRG, Catalog No. X574180-15 with chart speeds of 3, 6, and 12 in./h; Sargent-Welch Scientific Co., 7300 North Linden Avenue, Skokie, Ill. 60076.

Flow cells. 1-cm path length optical cells with bubble traps (Gilford Catalog No. 203A) were used for all measurements.

Connections. $\frac{1}{8}$-in.-I.D. Teflon® tubing was connected to the inlet side of the pump with a Swagelok fitting (Crawford Fitting Co., 884 East 140 St., Cleveland, Ohio). On the outlet side, $\frac{1}{16}$-in.-I.D. Teflon tubing was connected to the pump with a Swagelok fitting. The same size tubing was used from the column to the flow cell and from the flow cell to waste.

Stepwise gradient cell. This unit is illustrated in Fig. 1. 1-mm capillary tubing was used throughout. Stainless-steel 0.072-in.-O.D. tubing was attached at the various inlet and outlet points with the exception of the methanol reservoir which had 0.125-in.-O.D. tubing. All two- and three-way stopcocks were of Teflon plastic construction. Mixing flasks were 38 × 140 mm with 29/42 S/T joints. 40 ml of methanol was added to each flask and a calibration line was marked on the glass. Joint seals were made with 29/42 Teflon sleeves.

Continuous gradient cell. Similar dimension glassware and related fittings were

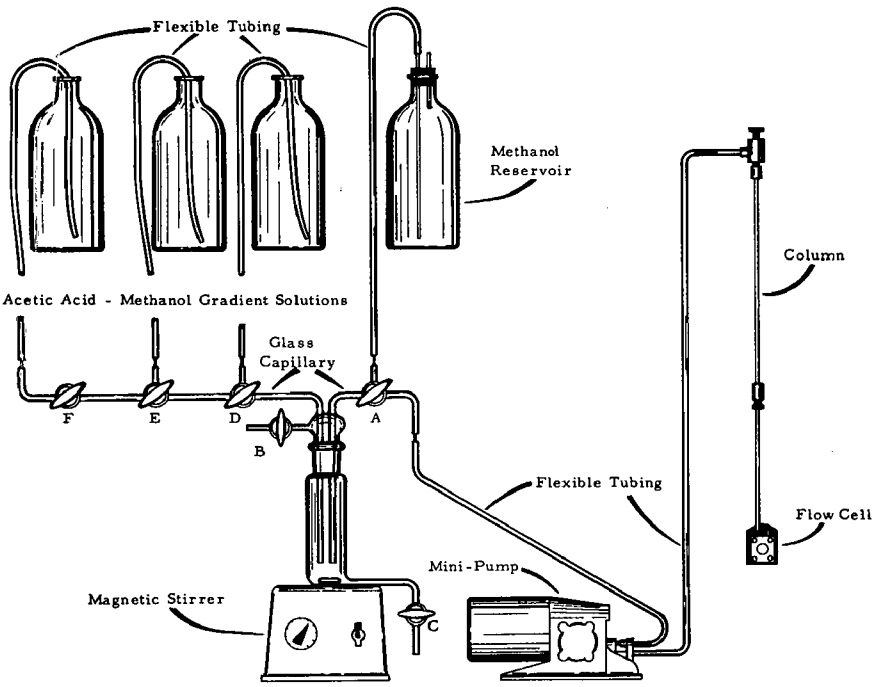

Fig. 1. Stepwise gradient cell.

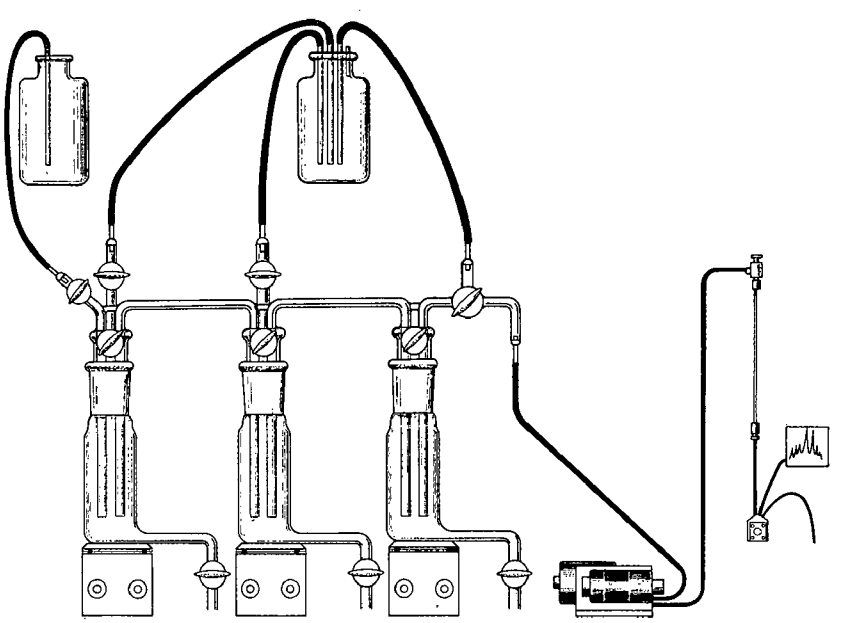

Fig. 2. Continuous gradient cell.

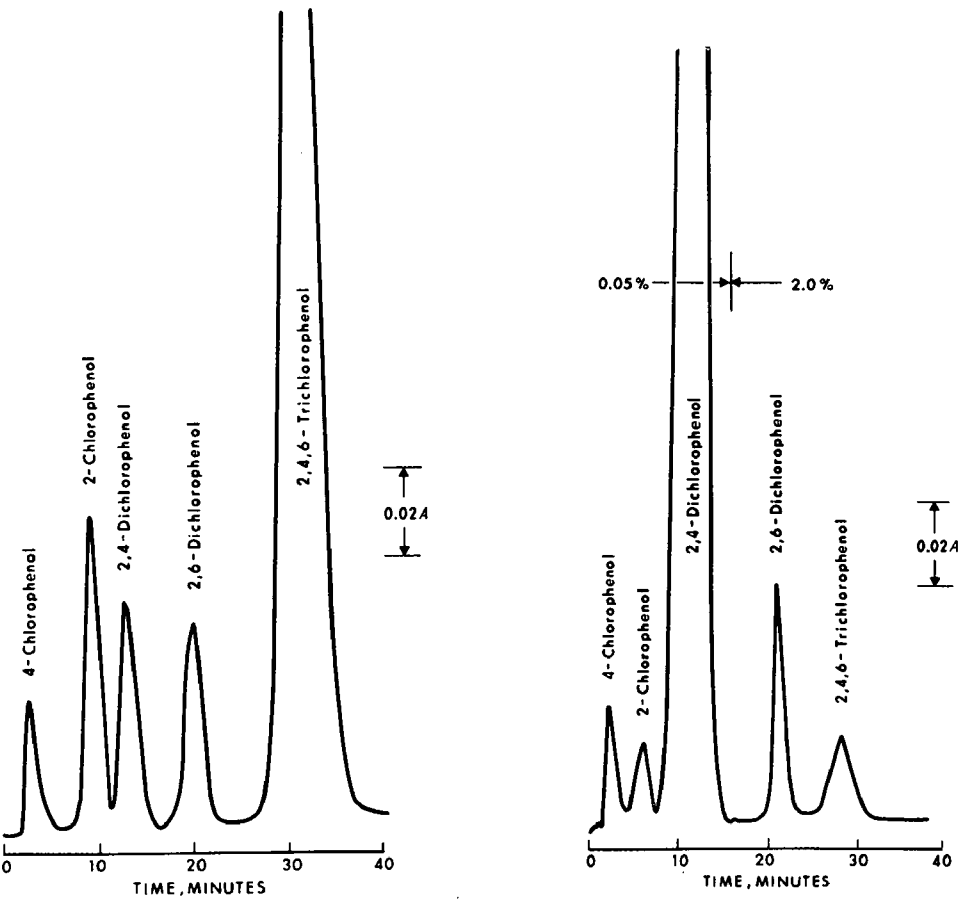

Fig. 3. Separation of 10 μl of a methanol solution containing 0.06% 4-chlorophenol, 0.13% 2-chlorophenol, 0.15% 2,4-dichlorophenol, 0.11% 2,6-dichlorophenol, and 2.52% 2,4,6-trichlorophenol on 2.8 × 500 mm AG1-X2 ion-exchange resin with 5% acetic acid–methanol, continuous gradient at 280 nm and a flow rate of 2.4 ml/min.

Fig. 4. Separation of 10 μl of a methanol solution containing 0.05% 4-chlorophenol, 0.04% 2-chlorophenol, 0.11% 2,6-dichlorophenol, 0.12% 2,4,6-trichlorophenol, and 3.0% 2,4-dichlorophenol on 2.8 × 500 mm AG1-X2 ion-exchange resin with a stepwise gradient of 0.05% and 2.0% acetic acid–methanol at 280 nm and a flow rate of 2.4 ml/min.

used in this unit which is illustrated in Fig. 2. A reinforcing glass rod was welded between the mixing chambers to give the apparatus added rigidity.

Column preparation

A plug of pyrex wool was placed at the bottom of the 2.8 × 500 mm tube. The membrane in the bed support disc was removed and the disc was replaced at the base of the column. Excessive back pressure was exerted by the membrane; therefore, the pyrex wool was used to hold the resin in place. A methanol slurry of the AG1-X2 resin was injected into the chromatography column through an 18-in. section of $\frac{1}{8}$-in.-I.D. Teflon tubing using a 10-ml hypodermic syringe and a luer lok

adapter. The luer lok adapter was removed and the final packing was accomplished with a flow of methanol under pump pressure.

Sample preparation

For a given analysis, 0.25–1.0 g samples are weighed into a 10-ml volumetric flask. The solid is dissolved and diluted to volume with methanol. Standard mixtures were prepared in a similar manner. Milligram amounts of the individual impurities were weighed into a 10-ml volumetric flask. 0.25-1 g of the major component was added to the flask. The sample was dissolved and diluted as before.

Procedure

The mixing flask was filled from the methanol reservoir with 40 ml of methanol through stopcock A, with drain stopcock C closed and vent stopcock D open. Eluent containers were filled with the desired concentration of acetic acid in methanol. The pump was turned on and methanol allowed to flow through the column. After select-

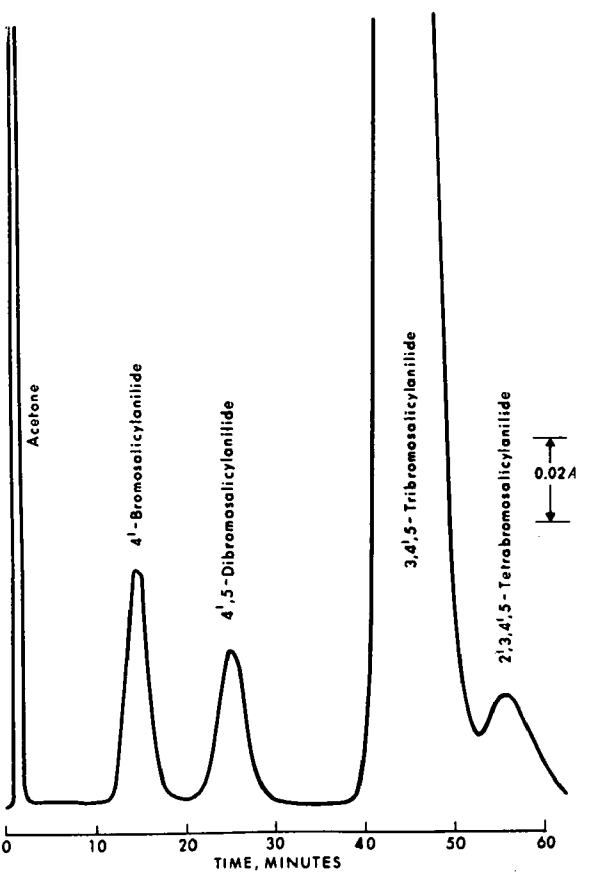

Fig. 5. Separation of 10 μl of an acetone solution containing 0.05% 4'-bromosalicylanilide, 0.05% 4',5-dibromosalicylanilide, 0.16% 2',3,4',5-tetrabromosalicylanilide, and 2.6% 3,4',5-tribromosalicylanilide on 2.8 × 500 mm AG1-X2 ion-exchange resin with a continuous gradient of 100% glacial acetic acid at 280 nm and a flow rate of 2.4 ml/min.

ing the appropriate wavelength, the instrument was nulled using the slit control knob and the null indicator. 10 μl of sample solution was injected directly into the resin through the silicone rubber septum. Vent stopcock D was closed, the magnetic stirrer activated and stopcocks D, E, or F were turned to the appropriate positions to allow the acetic acid–methanol solution to flow into the mixing flask. The eluent proceeds through the ion-exchange column and into the flow cell. Response of the spectrophotometer is monitored on a recorder.

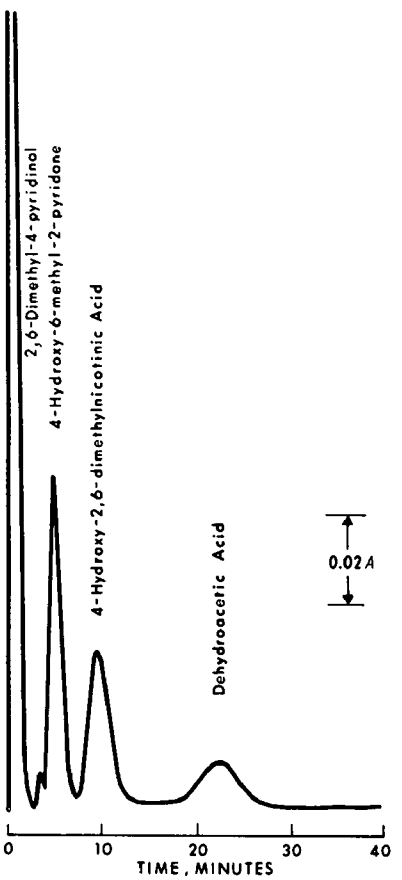

Fig. 6. Separation of 10 μl of a methanol solution containing 0.10% 4-hydroxy-2,6-dimethylnicotinic acid, 0.10% dehydroacetic acid, 0.05% 4-hydroxy-6-methyl-2-pyridone, and 5.0% 2,6-dimethyl-4-pyridinol on 2.8 × 500 mm AG1-X2 ion-exchange resin with a stepwise gradient elution of 1.0% acetic acid–methanol at 270 nm with a flow rate of 2.4 ml/min.

Concentration of the impurities was determined by measuring the areas in the resulting chromatogram and comparing these with standards. When the chromatogram was complete, stopcock A was turned to the methanol-wash position in preparation for the next run. Dual pumps, columns and gradient units make it possible to monitor one column while the other one is undergoing a wash cycle.

RESULTS AND DISCUSSION

Chromatograms for the separation of several industrial materials are given in Figs. 3–8. The components contained in the respective products may not necessarily be the same as that found in various production materials. This composition will be dependent upon the method of synthesis and the degree of purification.

The choice of elution system will depend on the pK range of the acid mixture to be separated. If the mixture contains acids having a wide range of pK values,

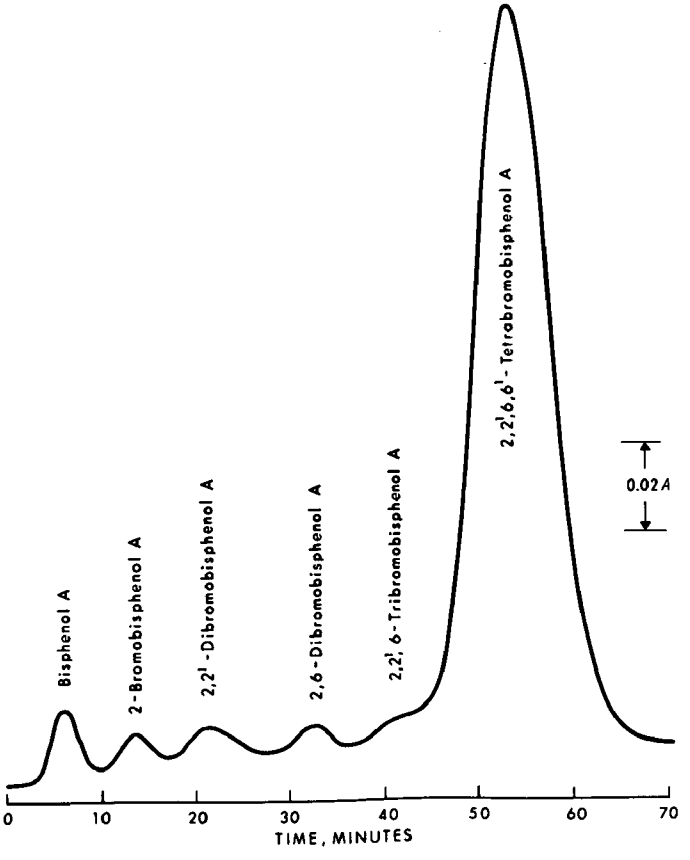

Fig. 7. Separation of 5 μl of a methanol solution containing 0.10% bisphenol A, 0.07% 2-bromobisphenol A, 0.10% 2,2'-dibromobisphenol A, 0.10% 2,6-dibromobisphenol A, 0.10% 2,2',6-tribromobisphenol A, and 5% 2,2',6,6'-tetrabromobisphenol A on 2.8 × 500 mm AG1-X2 ion-exchange resin with a continuous gradient elution of 1.0% acetic acid–methanol at 285 nm and a flow rate of 2.4 ml/min.

two choices of elution systems are available. Either a two or three step gradient elution using the stepwise unit may be used. Or, the continuous gradient cell may be preferred. The elution profile as obtained for the two units is illustrated in Fig. 9. 50% acetic acid–methanol was led into the mixing flask containing 40 ml of methanol. The column eluate was monitored at 256 nm. In the stepwise unit there is a rapid

buildup in the acetic acid concentration while the continuous cell allows a more gradual increase. Different sizes of mixing flasks may be substituted to change the gradient profile.

Neutral and basic compounds are not exchanged by the resin, but proceed directly into the eluate. If a mixture contains a neutral component as a minor impurity, the gradient can be started immediately following sample injection without causing this impurity and any weakly acidic impurities from emerging together. There is sufficient methanol in the column dead volume and tubing so that the effect of the gradient is delayed. However, if the major component is neutral, it may be necessary to elute this material with methanol before the gradient is started.

A sample solution that is acid by its very nature, or contains mineral acid, may require neutralization prior to introduction on the resin bed. Weakly acidic components may be eluted prematurely from this acid environment. In most in-

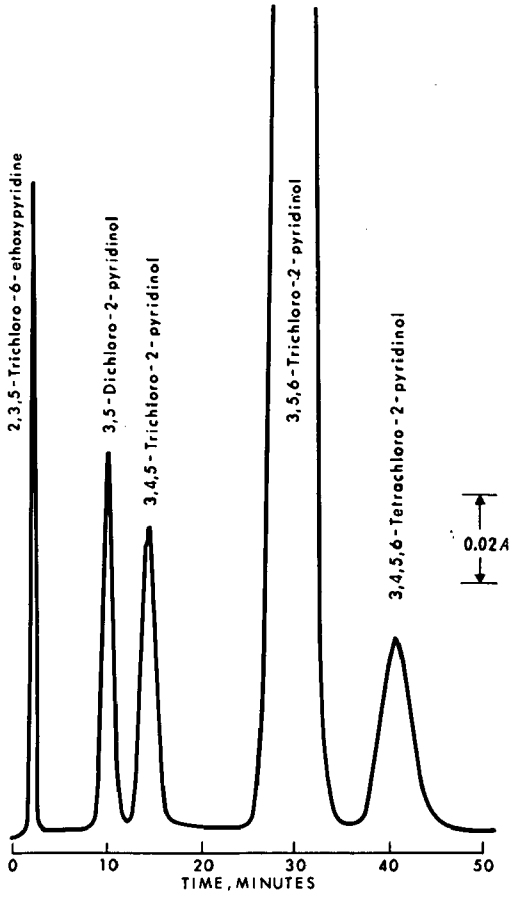

Fig. 8. Separation of 10 μl of a methanol solution containing 0.09% 2,3,5-trichloro-6-ethoxypyridine, 0.07% 3,5-dichloro-2-pyridinol, 0.09% 3,4,5-trichloro-2-pyridinol, 0.17% 3,4,5,6-tetrachloro-2-pyridinol, and 2.6% 3,5,6-trichloro-2-pyridinol on 2.8 × 500 mm AG1-X2 ion-exchange resin with a stepwise gradient elution of 100% glacial acetic acid at 310 nm and a flow rate of 2.4 ml/min.

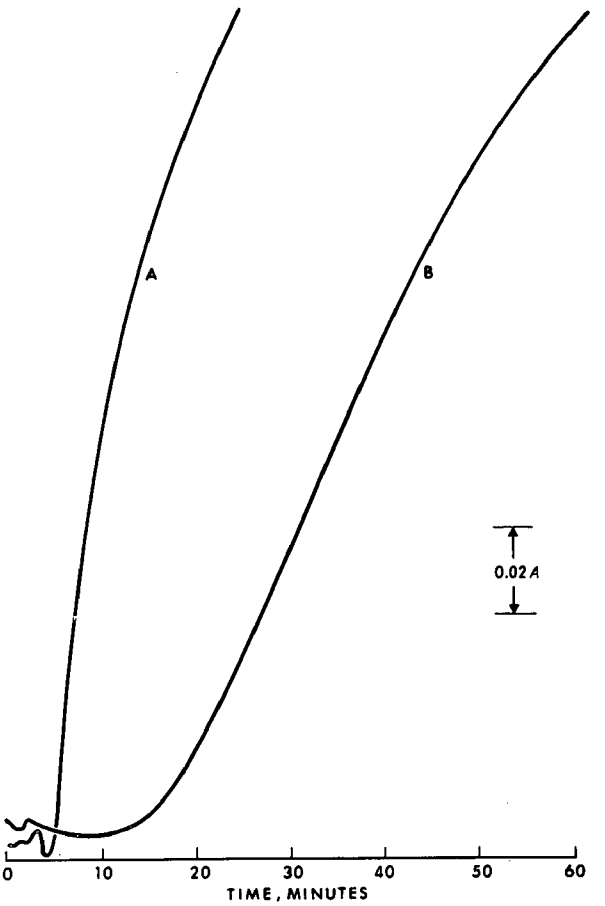

Fig. 9. Elution profile obtained by the stepwise gradient cell, A, and the continuous gradient cell, B, with 50% acetic acid–methanol monitored at 256 nm.

stances, with the use of μl sample sizes, the effect of the acidity is diluted out such that this does not present a problem.

Sensitivity of detection for the minor impurities is generally in the range of 0.1% relative to the major component. This will depend on how large a sample can be injected and on the degree of resolution for the components. On an absolute basis with compounds that have average UV sensitivity, 1 μg can be observed. Compounds that are eluted with difficulty and give long low peaks, will have a much higher limit of detection.

If the sample to be analyzed contains a diverse range of UV-absorbing species, a wavelength is chosen such that the components have near-equal sensitivity. Another factor that will influence this choice will be the relative concentrations of the impurities. If the sample contains a high concentration of one impurity and lesser amounts of others, it may be desirable to select a wavelength where the major impurity is insensitive and the minor impurities are extremely sensitive.

Samples that are sparingly soluble in methanol may also be analyzed by this

technique. Dissolution may be achieved with any neutral solvent. This will include UV radiation absorbing solvents. The UV-absorbing solvent will emerge with the solvent front and show up on the chromatogram as a sharp peak. Any neutral components present in the sample would be masked by the solvent. The separation of the brominated salicylanilides shown in Fig. 5 illustrates the use of a UV-absorbing solvent.

If the sample to be analyzed contains two neutral species, and they have different UV spectra, they can be analyzed by this technique. Duplicate injections are made in sequence with the spectrophotometer set at two different wavelengths. By making the appropriate calibrations and solving simultaneous equations the respective concentrations can be calculated.

Impurity concentrations are determined by either measuring peak height or peak area. Generally, the concentration of neutral and basic impurities, those which come through with the solvent front, are calculated from peak height measurements, while those compounds eluted with the gradient are calculated from peak areas. Peak heights and peak areas were found to obey Beer's law over the full scale absorbance range.

The use of special sample injection valve (Chromatronix Inc., SV-8031) allows the introduction of sample solutions above the microliter level. In fact, the limit is that of practicality. This makes it possible to concentrate on the resin weak acids from dilute solutions. Elution is then carried out in the normal manner. Chloroform extracts of aqueous solutions may be processed in this manner.

REFERENCES

1 D. LOGIE, *Analyst*, 82 (1957) 567.
2 N. E. SKELLY, *Anal. Chem.*, 33 (1961) 271.
3 O. SAMUELSON AND L. THEDE, *J. Chromatog.*, 30 (1967) 556.
4 L. KESNER AND E. MUNTWYLER, *Anal. Chem.*, 38 (1966) 1164.
5 C. DAVIES, R. D. HARTLEY AND G. J. LAWSON, *J. Chromatog.*, 18 (1964) 47.
6 G. STEHLIK, *J. Chromatog.*, 34 (1968) 128.

CHROM. 5159

A NEW COLUMN PACKING FOR THE SEPARATION OF CARBON MONO- AND DIOXIDE

KUNIO OHZEKI AND TOMIHITO KAMBARA
Department of Chemistry, Faculty of Science, Hokkaido University, Sapporo (Japan)

(Received November 10th, 1970)

SUMMARY

Amberlyst, Nickel form, packed in a gas chromatographic column, was reduced at 180° for 6 h by hydrogen flowing at a rate of 150 ml/min. The resulting column of Amberlyst with the reduced active nickel metal was found to be suitable for separation of carbon mono- and dioxide. The properties of the column are discussed.

INTRODUCTION

The sulfonic acid cation exchanger, Amberlyst 15, has a macroporous structure similar to those of conventional adsorbents such as alumina and bone char[1]. In this work, Amberlyst is tested as a column packing for the separation of a gas mixture.

BRECK *et al.*[2] proposed the separation of carbon monoxide from gases using a molecular sieve with reduced iron and nickel or cobalt that absorbs carbon monoxide to form carbonyl compounds. The present authors prepared a column packed with the Amberlyst support with reduced active atomic nickel and found that the column was suitable for separation of carbon mono- and dioxide. The separation properties are investigated from the heat of adsorption of the gases on the new column packing.

The heat of adsorption of a gas is determined by GC from the familiar relationship[3]

$$\frac{t_R - t_{R,0}}{t_{R,0}} = K \cdot \frac{F_S}{F} = B\exp\left(\frac{-\Delta H_a}{RT}\right)$$

where $t_{R,0}$ and t_R are retention times of air and component, respectively, K is the partition coefficient, F and F_S are volume fractions of the mobile and stationary phases, respectively, B and R are constants, H_a is the heat of adsorption, and T is the absolute column temperature. It is seen from the above equation that the plot of log $\{(t_R - t_{R,0})/t_{R,0}\}$ *vs.* $1/T$ should be linear and that the heat of adsorption for an eluted gas could be derived from the slope of the plot for a given column.

EXPERIMENTAL

Column packing

The commercially available Amberlyst 15 is sieved to a fraction of 42–60 mesh. The resin is first washed with ethyl alcohol to remove impregnated toluene, and then with water, treated with an aqueous hydrochloric acid solution, dried by suction and heated at 110° for 8 h. 31.89 g of the dried H-form Amberlyst 15 are swelled in ethyl alcohol to prevent breakage, washed with water, and treated with an aqueous solution of nickel nitrate. The resulting Amberlyst in the nickel form is washed with water until the washings show no color reaction with dimethylglyoxime, and is dried by suction at 110° for 8 h. The weight of the nickel form resin is 37.44 g, and the calculated exchange capacity of the resin for nickel is 5.9 mequiv./g of dried resin.

Apparatus

The gas chromatograph used is a Shimadzu GC-1B with a thermal conductivity detector. Dried Ni-form, Amberlyst 15, 42–60 mesh, is packed in a stainless-steel column of 0.4 mm I.D. The length of the packing is 1.5 m. Hydrogen at a flow rate of 150 ml/min is employed to reduce the nickel ion to a metallic state at 180° for 6 h. After cooling, the column is used to separate gas mixtures. Helium is used as carrier gas.

Samples

Sample gases, namely carbon monoxide, carbon dioxide, and a mixture thereof, are prepared according to the conventional chemical methods from formic acid, calcium carbonate and oxalic acid. The concentration of carbon monoxide and/or carbon dioxide in the gas samples is indirectly determined by determining air in the sample by means of the calibration curve for air.

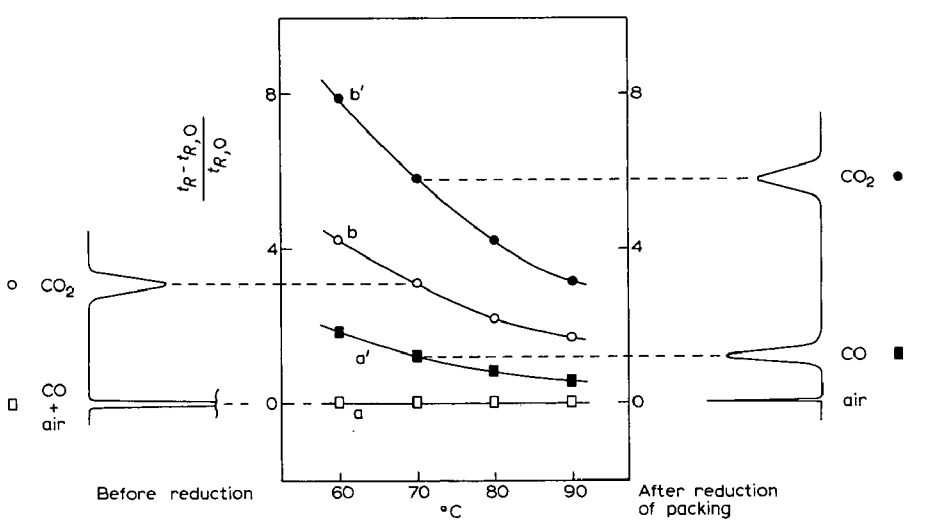

Fig. 1. The schematic gas chromatograms and the temperature dependences of the retention characteristics obtained before and after the reduction of the Ni-form Amberlyst 15 column, 42–60 mesh, 1.5 m long, 0.4 mm diameter. Flow rate of helium is 30 ml/min.

RESULTS AND DISCUSSION

Effect of nickel reduction

The gas chromatograms obtained before and after the reduction of the nickel column are shown in Fig. 1, together with the retention characteristics. Before the reduction, the dried Ni-form Amberlyst column is incapable of separating carbon monoxide from air, but separates carbon dioxide. After the reduction, however, the column excellently separates carbon mono- and dioxide from air.

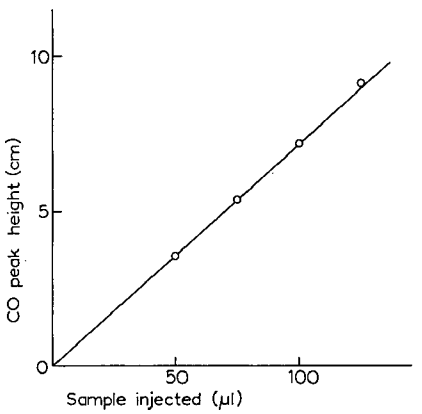

Fig. 2. Calibration curve for carbon monoxide. Column conditions are the same as given for Fig. 1. Column temperature is 70°. Sample: 66% CO + 34% air.

Proof that nickel carbonyl is not formed

It is now necessary to determine whether the separated peak in Fig. 1 is due to carbon monoxide itself or to nickel carbonyl. A sufficient amount of carbon monoxide, *viz.*, a 50-ml portion of a 30% carbon monoxide sample, is injected as a 0.4-ml portion, in succession, into the column of Amberlyst with reduced active nickel. The temperature of the column and detector is kept at 70°, and the cell current is cut off to prevent the possible decomposition of nickel carbonyl at the detector. The eluent gas is all trapped in a bubbler containing 6 ml of sulfuric acid, and the acid is neutralized with ammonia water before the solution is tested with dimethylglyoxime. No color of nickel dimethylglyoximate is developed. Thus, one may conclude that nickel carbonyl is not formed in the column. The analysis of the eluent gas by the molecular sieve 5A column also confirms that the second peak in Fig. 1 is due to carbon monoxide itself.

Calibration curve

Fig. 2 shows the calibration curve for the carbon monoxide. There is a good linearity between sample size injected and the peak height.

Heat of absorption

The retention data of carbon mono- and dioxide obtained before and after the reduction of the Ni-form Amberlyst column are shown as a function of temper-

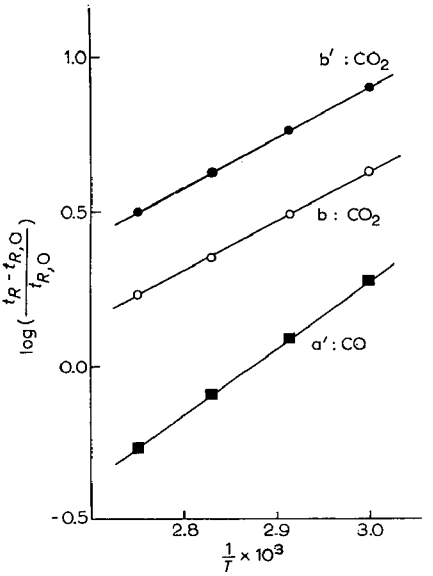

Fig. 3. Variation of logarithm of the corrected retention time relative to air with reciprocal of absolute temperature of the column. Closed and open circles correspond to the use of the Ni-form Amberlyst after and before the reduction of the nickel ion by hydrogen.

ature in Fig. 3. The slope of curve a' is $(2.17 \pm 0.07) \times 10^3$ at 95% confidence limits, thus the heat of absorption of carbon monoxide on the active nickel atom is (9.93 ± 0.32) kcal·mole^{-1}. The slopes of curves b and b' are $(1.60 \pm 0.05) \times 10^3$ and $(1.63 \pm 0.05) \times 10^3$, respectively. The difference in the two slopes cannot be regarded as significant. Therefore it can be concluded that carbon dioxide is not absorbed onto

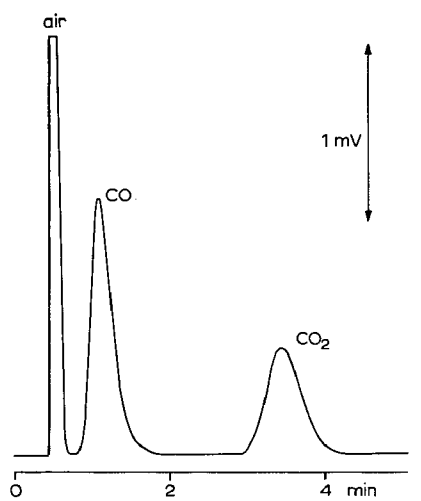

Fig. 4. The isothermal separation of carbon mono- and dioxide on the Amberlyst 15 column with reduced active metallic nickel. The column conditions are the same as given for Fig. 1. Column temperature 70°. 0.2 ml of the gas mixture of 20% CO, 20% CO_2 and 60% air is injected.

the active nickel metal. The heat of absorption of carbon dioxide on Amberlyst 15 is (7.46 ± 0.23) kcal·mole^{-1} which is similar to that obtained on the silica gel column by GREENE AND PUST[3].

Separation of carbon mono- and dioxide from air

Fig. 4 shows the isothermal separation of carbon mono- and dioxide. The sample gas is obtained by the decomposition of oxalic acid with sulfuric acid. It may be safe to say that carbon monoxide is retained by the active elementary nickel on the resin but carbon dioxide is retained by the molecular sieve structure of the Amberlyst. The separation power of the column is weakened by moisture, but it is easily restored by activating the column in a flow of hydrogen at 180° for 2–3 h.

REFERENCES

1 R. KUNIN, E. MEITZNER AND N. BORTNICK, *J. Amer. Chem. Soc.*, 84 (1962) 305.
2 D. W. BRECK, C. R. CASTOR AND R. M. MILTON, *U.S. Pat.* 3185540, May 25, 1965; *C.A.*, 63 (1965) 3930g.
3 S. A. GREENE AND H. PUST, *J. Phys. Chem.*, 62 (1958) 55.

CHROM. 5161

CONTINUOUS FLOW SEPARATION OF CAROTENOIDS BY LIQUID CHROMATOGRAPHY*

IVAN STEWART AND T. A. WHEATON
University of Florida Citrus Experiment Station, IFAS, Lake Alfred, Fla. 33850 (U.S.A.)

(Received November 12th, 1970)

SUMMARY

A liquid chromatographic system has been developed that gives good separation of complex mixtures of carotenoids. Carotenes are separated on magnesium oxide and xanthophylls on zinc carbonate. The columns are regenerated after each sample which virtually eliminates repacking. Submicrogram quantities of carotenoids are readily detected and many *cis–trans* isomers are separated. An antioxidant is included to reduce on-column losses and isomerization of carotenoids. The method is quantitative, reproducible, sensitive, moderately rapid, and suitable for routine analysis. Use of the system for the study of isomer formation of carotenoids and for the identification of citrus peel pigments is included.

INTRODUCTION

The technique of chromatography was developed in 1906 for the purpose of separating plant pigments. TSWETT, a Russian botanist, used columns of calcium carbonate and other materials for this purpose[1]. Later, KUHN AND LEDERER[2], STRAIN[3], CURL[4], and others developed improved procedures for separating carotenoids. More recently, thin-layer[5] and paper[6] chromatography have been used for rapid determinations.

DAVIES[7] and MONEGER[8] described continuous flow techniques for separating carotenoids. In our laboratory, however, we were unable to satisfactorily separate complex mixtures of citrus carotenoids with their techniques.

The purpose of this paper is to describe a liquid chromatographic system that is suitable for separation of carotenoid mixtures such as found in citrus peel. Standard adsorbents are used and the liquid chromatograph is assembled of materials and equipment readily available in many chromatographic laboratories. Careful attention to selection of adsorbents, methods of packing the column, selection of solvent systems, and inclusion of an antioxidant resulted in excellent separations of carotenoids and their isomers.

* Florida Agricultural Experiment Stations Journal Series No. 3796.

MATERIALS AND METHODS

Gradient systems

Several gradient devices were tried and found to be satisfactory. A simple linear gradient obtained by connecting two 125-ml erlenmeyer flasks together at their bottoms, using one as a reservoir and the other as a mixing chamber, gave good separations. A similar device using chambers of unequal size was also satisfactory (Kontes Glass Co., Vineland, N. J.). The reservoir and mixing chamber had diameters of 5.5 and 8.0 cm, respectively.

The most versatile gradient device was a nine-chamber assembly similar to the Technicon Chromatography Co. Autograd or the Phoenix Co. Varigrad, but constructed of material resistant to organic solvents. Ours was patterned after the Contigrad (Metaloglass, Inc., Boston, Mass.) but was machined from a block of aluminum 15 × 20 × 10 cm high. It was made with nine interconnected chambers each holding 90 ml of solvent. The gradient was mixed in each chamber by a metal paddle. In most separations, only the first three chambers were used. The added flexibility of this system allowed the production of nonlinear gradients tailored to the particular separation desired.

Pumps

A Milton Roy Chromatographic Mini pump, Model 196-31 (Milton Roy Co., St. Petersburg, Fla.), was used for most of these studies. This is a reciprocating plunger pump which uses either sapphire or Kennemetal plungers with various ring seals. Even with the recommended Rulon Tec ring seal, leakage around the plunger due to early failure of the seal was a problem under our operating conditions. The chromatograms shown in this paper were obtained with the sapphire plunger and solid teflon ring seal made in our machine shop. More recently we have been using a Milroyal D pump, Model HDB-1-30 R. This pump has adjustable graphite-impregnated teflon packing and sapphire ball checks and has worked well at 1800 p.s.i.

A Nester/Faust hi-pressure pump (Nester/Faust Mfg. Corp., Newark, Del.) was also tested. This pump uses digitally driven motors to drive pistons into stainless steel cylinders containing the solvents. By connecting two pumps in series and using one as the mixing chamber, a variety of gradients can be generated by regulating initial volumes and the relative speed of the two pumps. Although these pumps are rated at 2000 p.s.i., we have not yet achieved satisfactory operation without leaks. However, limited tests indicate the versatility of these pumps for generating various gradients and providing for more rapid separations of the carotenoids.

With both kinds of pumps, connections were made to a pressure gauge, and the column, using stainless steel tubing and Swagelok fittings. The pressure gauge (Frank W. Murphy Mfg., Inc., Tulsa, Okla., Model OPL-F-2000) was mounted on a diaphragm-seal transmitter and had both minimum and maximum pressure safety cut-off switches. A simple low-voltage latching circuit stopped the pump if either a high or low pressure setting was exceeded.

Columns

It has been traditional to use glass columns in the separation of plant pigments so that the various color bands could be observed as they were eluted. We found glass

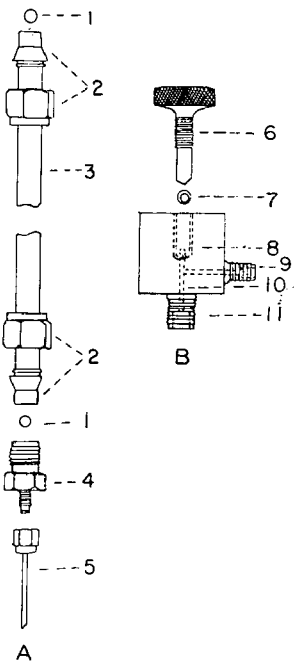

Fig. 1. (A) Chromatographic column (not drawn to scale). 1 = porous polyethylene disc; 2 = pressure fittings $^1/_4$ in.; 3 = stainless steel tubing $^1/_4$ in. O.D.; 4 = reducer $^1/_4$ in. to $^1/_{16}$ in.; 5 = polyethylene tubing 0.030 in. I.D. (B) Sample injection valve. 6 = thumb tightening screw $^1/_4$ in.; 7 = "O" ring; 8 = overflow spout $^1/_{16}$ in., open above "O" ring seat; 9 = inlet, threaded for pressure fitting; 10 = opening to column $^1/_{16}$ in.; 11 = column connection.

columns desirable for preliminary work in evaluating adsorbents and packing methods, and in fact used a 4 × 280 mm glass column for routine separation of the carotenes. However, stainless steel columns were preferable for routine work with the xanthophylls when higher operating pressures were encountered. The use of 1/4 in. tubing and standard Swagelok fittings provided columns that could be assembled or modified easily and provided leak-free operation up to 2000 p.s.i. (Fig. 1). The sample

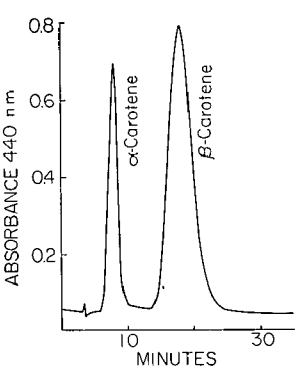

Fig. 2. Chromatogram from a carrot extract. Column: Sea Sorb 43, 4 mm I.D. × 280 mm long, glass; solvent: hexane containing 5% TPA; flow rate: 1.0 ml/min; temperature: room temperature.

injection valve was machined from brass, and although convenient, was not essential for satisfactory operation. Not shown is a water jacket for holding the column at a constant temperature of 15°. The use of the 1/4 × 1/16 in. reducer on the column and small diameter polyethylene tubing from the column to the detector gave minimum hold-up volume. Column lengths of 10–20 cm were satisfactory. Longer columns required excessive pressures for reasonable flow rates.

Detection and recording

Carotenoids in the column effluent were monitored with either a Beckman DB spectrophotometer and a Sargeant recorder, or a Technicon colorimeter and recorder. Both of these were satisfactory. The Beckman DB was used at 440 nm using a microflow cell with a 10 mm light path. A Sargeant SRL recorder with log gears was used to record absorbance with chart speeds of 0.1 or 0.2 in./min (Fig. 2).

The Technicon Model 1 colorimeter used an interference filter transmitting at 440 nm and a tubular flow cell with a 15 mm light path. The Bristol recorder supplied with the colorimeter was used to record absorbance at chart speeds of 0.1 or 0.2 in./min (Fig. 3).

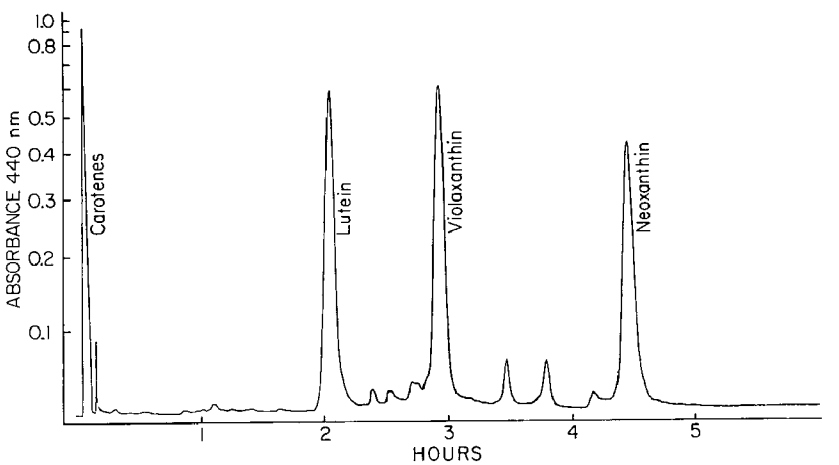

Fig. 3. Chromatogram of a spinach extract. Zinc carbonate column using a hexane TPA gradient. Column: $ZnCO_3$, 1/4 in. O.D. × 13.5 cm stainless steel. Solvent: chamber 1, 90 ml hexane, 1 g BHT; chamber 2, 89 ml hexane, 1 ml TPA; chamber 3, 65 ml hexane, 20 ml TPA. Flow rate: 1/2 ml/min; temperature: 15°.

With both types of equipment, the connection from the column to the flow cell was made with 0.03 in. I.D. polyethylene tubing. The length of this tubing was kept as short as possible to minimize mixing of the column effluent.

Adsorbents

A variety of adsorbents were tested for separation of carotenes and xanthophylls. These included silicic acid, infusorial earth, sugar, starches, cellulose, and several oxides, hydroxides, and carbonates of divalent cations.

Magnesium oxide (Sea Sorb 43, Fisher Scientific Co., S-120) was selected for the

separation of carotenes and was used as supplied. Precipitated zinc carbonate (Fisher Scientific Co., Z-29) was chosen for the separation of xanthophylls. Considerable variation existed in various batches of zinc carbonate giving materials of quite different physical and adsorptive characteristics. Lots were selected with fine, uniform particles. In using precipitated zinc carbonate for thin-layer or column chromatography, material from several sources should be obtained in order to compare their properties. Celite was tried as a diluent to increase flow rate. However, in each case resolution was greatly reduced.

Solvents

Separation of complex mixtures of carotenoids was achieved by gradually increasing the polarity of the solvent using a nonpolar and a polar solvent in one of the gradient devices described above. A variety of solvent combinations was tried. For the nonpolar solvent, petroleum ether, hexane, heptane, and higher boiling hydrocarbon fractions were evaluated. Freshly distilled hexane (b.p. 60–68°) was selected since the high volatility of petroleum ether created problems due to evaporation and formation of vapor bubbles in the system.

A number of alcohols were tested as polar solvents. Acetone, ethyl acetate, and some other commonly used solvents were not tested since portions of our liquid chromatograph did not have chemical resistance to these. Primary and secondary alcohols from methyl through hexyl were not entirely satisfactory and there was little difference in resolving properties among these. The tertiary alcohols, however, had unique properties for giving high resolution of carotenoids on both columns and thin layer plates. We used both *tert.*-butyl and *tert.*-pentyl alcohol (TPA). The TPA (Baker Chemical Co., 9046, *tert.*-amyl alcohol, reagent) was most satisfactory but had to be distilled over KOH before use to eliminate impurities (probably aldehydes) that absorbed light in the 300–350 nm range. TPA has a high boiling point (100°) but can be readily azeotroped at 30° in vacuum with benzene when it is necessary to concentrate carotenoid solutions.

Butylated hydroxytoluene (BHT) (Eastman Chemical Products, Tenox BHT) was routinely included in the solvent (1% w/v) to avoid losses and isomerization of carotenoids. Ethoxyquin (Monsanto Chemical Co.) was also effective as an antioxidant but was difficult to purify and caused some colorimetric interference because of its natural yellow color.

Packing the column

All of the standard methods of packing columns with dry and wet materials were tried. For the magnesium oxide and precipitated zinc carbonate finally selected, thick slurries in organic solvents packed rapidly and under pressure gave consistently good results. Since the initial loading of a column with a slurry under pressure presents certain technical difficulties, we used a simpler procedure.

This procedure started with a column that was three or four times longer than the final packed column. For glass columns, a standard 4 ft. length of glass tubing was used. For the stainless steel column, we attached a 4 ft. length of stainless steel tubing (same diameter as the column) to the column with a Swagelok coupling. The slurry was rapidly added to this extended column as a single charge and air pockets broken up with a piece of stiff plastic capillary tubing. The magnesium oxide slurry

was prepared in hexane and the zinc carbonate in hexane containing 5% TPA. The pump was then connected and solvent pumped as rapidly as possible to compact the column until the desired operating pressure was reached. The solvent was then pumped at a lower rate for about 1 h to complete packing of the adsorbent in the lower portion of the extended column. To provide the finished glass column, the tubing was broken in the lower packed region to provide a column of the desired length. For the stainless steel column, the upper tubing was removed leaving the lower column fully packed. A few mm of adsorbent was then removed from the top of the column and a thin porous polyethylene disc fitted on top of the packing.

Prior to running a sample of carotenoids, hexane containing BHT (1% w/v) was pumped through the column for 1 h. The same mixture was also used to regenerate the column after each sample had been run. It was found that with the use of this regeneration process, the column could be used repeatedly with little loss of resolution.

Loading the column

In order to make room for the sample, the excess solvent was removed from the top of the column. For loading, we used a microsyringe (No. 0010, Hamilton Co., Whittier, Calif.) with a No. 20 hypodermic needle. A piece of polyethylene tubing 0.030 in. I.D. and 36 cm long was attached to the end of the needle. The tubing was calibrated with water. Approximately 0.05 ml aliquots were used. The solvent used to dissolve the sample was very important in that good resolution could not be obtained with many common hydrocarbons and alcohols. The best results were obtained with ethyl ether. Following the application of the sample, the polyethylene tubing was washed with a small amount of hexane and the solvent was applied to the column.

Identification of carotenoids

The carotenoids, for the most part, were characterized from crystalline material and their properties compared with those from known sources[9–12]. Several kg of material was extracted with acetone and hexane. The esters were saponified and preliminary separations made with a 100 tube counter-current apparatus[4]. Further separations were made on large columns of Sea Sorb 43 or zinc carbonate using Celite as a diluent. The colored bands were collected in fractions and absorption spectra were determined on each. Fractions with similar spectra were combined, concentrated, and the carotenoids crystallized. Purity was also determined by monitoring on the column described in this paper. In this manner, good separation was achieved between the *trans* and *cis* isomers. All separations were carried out under low light intensity and whenever possible, systems were flushed with nitrogen. All materials were stored at −18°. However, in spite of these precautions it was obvious that artifacts formed profusely both in the counter-current apparatus and on the columns.

For identification purposes, some of the pigments were obtained from more than one source. The crystalline material was characterized with visible, IR and mass spectra[13]. The latter were made with a Bendix Time of Flight instrument with modifications to increase the resolution in the 400–700 mass range. In addition, identifications were based on TLC properties using the Hager method[5] and one developed in our laboratories using zinc carbonate. The zinc carbonate procedure consisted of

making plates from a slurry of precipitated $ZnCO_3$. They were heated in an oven at 110° for about 1 h or until thoroughly dry. The plates were then cooled slowly in order to prevent cracking, and were used immediately. The solvent consisted of hexane–triethylamine–TPA (90:5:5). The chromatograms were run at temperatures not exceeding 25°. This procedure gave very good resolution. The number of 5,6-epoxy groups were determined by the spectral shift following additions of HCl (ref. 14). Shifts in spectral curves due to isomerization were compared following treatment with iodine and light[14].

The chromatographic peaks of the "Dancy" tangerine extract (Fig. 4) were identified as follows:

Peak 1, carotene mixture and other unidentified compounds. Fraction chromatographed on Sea Sorb 43 column and on thin layer.

Peak 2, unknown.

Peaks 3, 4, unknown, probably cryptoxanthin *cis* isomers.

Peak 5, cryptoxanthin: crystallized from ethyl ether and methanol. Absorption maxima at 478, 452, and 426 nm in hexane. Mass 553. Cochromatographed on thin

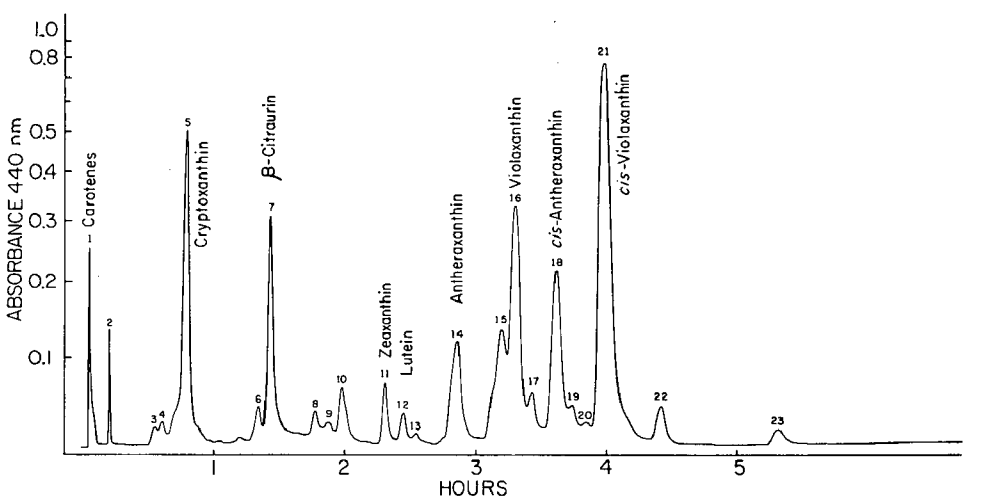

Fig. 4. Chromatogram of a Dancy tangerine peel saponified extract. Zinc carbonate column using a hexane–TPA gradient similar to that described in Fig. 3 except the flow rate was slightly lower.

layer with crystalline samples obtained from yellow papaya, egg yolks, and fruit of balsam apple (*Momordica charantia*).

Peak 6, unknown.

Peak 7, β-citraurin: crystallized from ethyl ether and hexane. Absorption maxima at 481, 454, and 429 (sh)nm. In ethanol, there was a smooth curve with no well-defined peaks. The IR spectrum showed peaks at 1665 and 1725 nm. The mass was 433.

Peaks 8, 9, 10, *cis* isomers of β-citraurin. We were unable to crystallize the compounds forming these peaks. Gels were formed in a mixture of ethyl ether and petroleum ether. Absorption maxima at 473, 447, and 428 nm. Impurities in all peel samples have interfered with the spectra in the *cis* region. When fractions collected from each peak were rechromatographed, all of the isomers including the trans were

formed. Similar absorption curves were obtained when the *trans* and the *cis* forms were treated with I_2 and light.

Peak 11, zeaxanthin: confirmation was based on absorption spectra, retention time of the *cis* isomers, R_F values, and color on thin layer. Comparisons were made with crystalline material obtained from yellow corn, balsam apple, and bacteria.

Peak 12, lutein: the column effluent gave absorption maxima at 473, 445, and 422 nm. The thin layer R_F values were similar to those obtained from crystalline samples obtained from spinach and orange marigold.

Peak 13, unknown.

Peak 14, antheraxanthin: fractions from the column had absorption maxima at 472, 443, and 423 (sh)nm. On treatment with HCl, the absorption maxima shifted to a shorter wavelength by 19 nm. This peak was formed when the effluent from peak 18 (*cis*-antheraxanthin) was treated with I_2 and light.

Peak 15, *cis*-violaxanthin: fractions from the column had absorption maxima at 457, 430, and 408 nm with a *cis* peak at 309 in ethanol. When treated with I_2 and light, the maximum shifted to a longer wavelength by 9 nm and had a similar absorption spectrum as the *trans* when treated in the same manner. When treated with HCl, the maximum shifted to a shorter wavelength by 32 nm.

Peak 16, Violaxanthin: absorption maxima of the column effluent in hexane was 470, 440, and 417 nm. When treated with HCl, the maximum shifted to a shorter wavelength by 44 nm. Chromatography on thin layer showed this compound to have similar R_F values to crystalline material obtained from spinach. This peak was formed when effluents from peaks 15, 21, or 22 were treated with iodine and light and rechromatographed.

Peak 17, unknown.

Peak 18, *cis*-antheraxanthin: the visible spectrum of crystalline material in ethanol was 469, 443, and 419 nm. There was no significant *cis* peak. However, it was not possible to obtain a pure *cis* form in that partial conversion to the *trans* (peak 14) took place in all samples. Following treatment with HCl, the maximum wavelength was 17 nm lower. When isomerized with I_2 and light, the absorption spectrum did not show a significant shift and the curve was similar to the *trans* when treated similarly. When the I_2-treated *cis* form was chromatographed on either thin layer or a $ZnCO_3$ column, the reversion to the *trans* form was observed. Because of the similarity between antheraxanthin and diadinoxanthin[15] additional steps were taken for identification. The IR spectra was not satisfactory for distinguishing these compounds. However, a high resolution mass spectra showed peaks at M 584.4229 and M-2 (loss of H_2).

Peaks 19, 20, unknown.

Peak 21, *cis*-violaxanthin: the crystalline material in hexane had absorption maxima at 468, 438, 415, and a small *cis* peak at 327 nm. When HCl in ethanol was added, the maximum shifted to a shorter wavelength by 39 nm. The absorption spectra of both *trans* and *cis* were similar when treated with I_2 and light. When the *cis* form was isomerized and rechromatographed, there was partial reversion to the *trans* as determined by retention time and absorption spectra. The mass was found to be 600.

Peak 22, *cis*-violaxanthin: the column eluate had absorption maxima at 463, 434, 410, and a high *cis* peak at 330 nm. When treated with I_2 and light, the amplitude

of the *cis* peak dropped and there was a shift of the maxima to a longer wavelength of 2 nm. The I_2-treated pigment had a similar spectrum to the *trans* which had been isomerized in the same way. When the isomerized *cis* form was again passed through the column, both the *trans* and *cis* forms separated.

Peak 23, unknown.

DISCUSSION

Basic requirements for the liquid chromatograph were: (a) a suitable gradient device; (b) a controlled volume pump capable of reproducible and leak-free operation at pressures up to 1000 or 2000 p.s.i.; (c) a jacketed column suitable for high pressures with minimal dead volume between column and detector; and (d) a low volume flow cell in a detector to monitor visible light absorption by the carotenoids. We used various types of standard and modified equipment with considerable success; the exact configurations described are mostly a matter of convenience and are probably not critical.

The adsorbents used, choice of solvents, and method of packing the columns were quite important, however. Magnesium oxide was the adsorbent of choice for the carotenes and zinc carbonate for the xanthophylls. Columns were packed rapidly with slurries of adsorbent in solvent under pressure. The most desirable solvent system was hexane containing TPA with BHT included as an antioxidant.

The method described gave excellent separation of the carotenes (Fig. 2) and xanthophylls (Figs. 3 and 4) in moderately short times. Separations like these were achieved routinely with leaf and citrus peel samples and also while monitoring the purity of preparative-scale samples for isolation and crystallization of individual pigments.

Most of our separations of complex mixtures of carotenoids such as that shown in Fig. 4 were done with a Milton Roy pump operating at approximately 800 p.s.i. Limited tests indicated that this time could be shortened considerably by using the Milton Roy pump at pressures up to 1600 p.s.i. or the Nester/Faust pump with pressures up to 2000 p.s.i. However, leakage became a serious problem at these higher operating pressures with the solvents used. These small leaks were difficult to detect but resulted in substantial changes in retention times.

The amounts of individual carotenoids were determined by measurement of peak areas on the chromatogram. Reproducibility of the system was demonstrated by running samples of a tangerine peel extract on the zinc carbonate column four times. Peak area measurements were made for the predominant carotenoids and absolute amounts calculated relative to standard areas obtained with crystalline pigments. The results shown in Table I demonstrate the ability of the method to determine quantitatively μg amounts with reproducible results. Retention times were also very reproducible. However, in order to make reproducible determinations on xanthophylls, it was necessary to maintain the column at a constant temperature. For this purpose, we used a water jacket through which water was circulated at 15°. Losses of carotenoids applied to the column were not studied extensively. Approximately 90% of two samples of lutein was recovered following standard chromatographic separation, but losses will undoubtedly vary among carotenoids.

TABLE I

RESULTS FROM 4 CHROMATOGRAMS OF DANCY TANGERINE PEEL EXTRACT SHOWING THE REPRODUCIBILITY OF THE METHOD

Zinc carbonate column with a hexane–TPA gradient.

Chromatogram	*Cryptoxanthin (μg)*	*β-Citraurin (μg)*	*cis-Antheraxanthin (μg)*	*cis-Violaxanthin (μg)*
1	2.49	1.72	1.34	9.17
2	2.52	1.72	1.36	9.78
3	2.44	1.59	1.24	8.76
4	2.55	1.66	1.20	9.13
Average	2.50	1.67	1.29	9.21
Std. error	± 0.02	± 0.03	± 0.04	± 0.21

Isomerization

The ease with which isomers are formed has long been a problem in carotenoid research. Although light, heat, iodine, and other agents are known to induce isomerization, the isomerization of pigments on the column has been disputed. ZECHMEISTER[16] maintained that isomerization of carotenoids was independent of the adsorption on an analytical column. "Indeed, it takes place spontaneously when a carotenoid solution is left at room temperature for several hours or days." Our research, however, indicates that carotenoids isomerized much more readily on columns than sitting on a laboratory bench. We also found that inclusion of an antioxidant in the solvent can greatly reduce this isomerization. The usefulness of our chromatographic

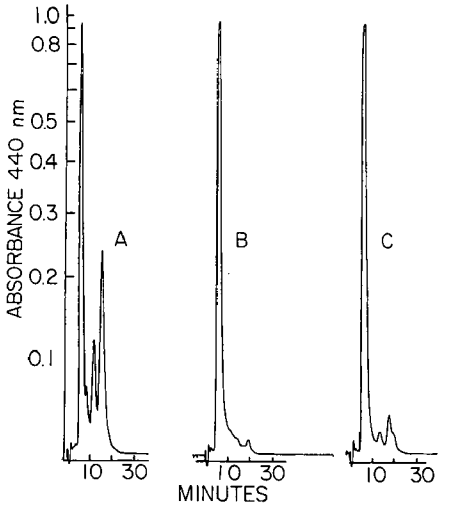

Fig. 5. Chromatogram of lutein using zinc carbonate column and 5% TPA in hexane. (A) *trans*-Lutein was put on the column and left for 2 h prior to developing the chromatogram. Note isomer formation. (B) *trans*-Lutein which remained on the laboratory bench while A was being run. (C) *trans*-Lutein which remained on the laboratory bench for about 4 h and was then adsorbed on the column, pretreated with BHT, for an additional 2 h. It was then run through the column with the above mentioned solvent containing 1 g BHT in 100 ml.

system in studying the formation of isomers and the benefits of adding an antioxidant were demonstrated with several pigments. Two examples follow: (a) a study of the on-column formation of lutein isomers and inhibition by antioxidants, and (b) the use of the chromatographic method for separation and identification of antheraxanthin isomers.

Demonstration of the formation of lutein isomers on the column was made using a nongradient chromatographic system that separated all the isomers observed in 25 min (Fig. 5). A sample of crystalline *trans*-lutein from marigold dissolved in ethyl ether and immediately run through the column gave a single peak. However, if the sample was adsorbed on the column, the pump turned off for 2 h, and the chromatogram then completed, at least three isomers were formed in substantial quantities (Fig. 5A). During the time the aliquot was on the column, the original sample was maintained in the dark at room temperature. Very little isomerization of this aged sample (about 3 h) occurred (Fig. 5B). We found that isomerization on the column could be greatly reduced by including 1% BHT (w/v) in the solvent. An aliquot of the lutein sample which had been in the dark at room temperature for about 4 h was adsorbed onto the column and allowed to remain for 2 h before completing the chromatogram (Fig. 5C). Much less isomerization occurred when an antioxidant was used.

Antheraxanthin isomers were also readily separated on the column. Treatment of *trans*-antheraxanthin with I_2 and light resulted in four peaks on the chromatogram (Fig. 6). The first was the *trans* and the last three were *cis*. The first two *cis* forms had similar absorption spectra and the last one had a very high *cis* peak at 332 nm. Proof that these last three peaks were actually antheraxanthin isomers was obtained by collecting them individually and treating them with iodine. Rechromatography showed that in each case a partial conversion back to the *trans* form had occurred. In addition, treatment with HCl shifted the absorption spectrum of each isomer downward about 20 nm indicating that these were isomers of antheraxanthin and not decomposition products.

Formation of isomers during extraction and chromatography is a major concern in attempting to establish the naturally occurring complement of pigments from

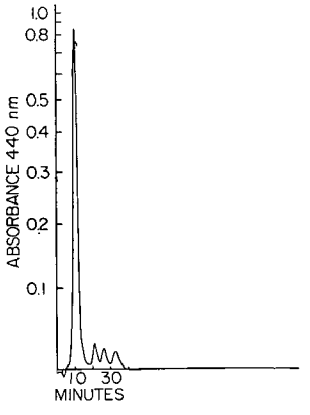

Fig. 6. Chromatogram of antheraxanthin following treatment with I_2 and light. Zinc carbonate column using 5% TPA in hexane. Left to right, *trans* and 3 *cis* isomers.

complex tissues such as citrus peel. Not only is it difficult to decide which are artifacts, but also large numbers of isomers result in incomplete separations during chromatography. We observed that highly purified extracts of citrus peel and crystalline carotenoids isomerized much more rapidly during chromatography than crude extracts. This probably is due to naturally occurring antioxidants that occur as contaminants in the less pure material. Incorporation of BHT as an antioxidant has greatly reduced problems related to isomer formation and has resulted in chromatographs with fewer artifacts.

Although the technique has been demonstrated to reduce isomerization, preliminary evidence would indicate that not all *cis*-isomers in citrus are artifacts (Fig. 4). Probably the predominant carotenoid in ripe citrus peel is *cis*-violaxanthin (peak 21). We have observed this from many cultivars with a variety of extraction procedures. This isomer has not been found in green peel, neither is it readily formed by treating the *trans* with iodine and light or by passing through a column.

Since carotenoids vary during a season, not all pigments found in tangerine peel are shown in Fig. 4. For example, we have isolated, crystallized, and characterized reticulataxanthin and found it to be the primary red pigment early in the season. Reticulataxanthin was readily separated from β-citraurin on the zinc carbonate column reported in this paper; the retention time of the latter pigment was slightly less than reticulataxanthin.

The method described here for the quantitative determination of carotenoids is simple and relatively rapid. It is believed that with slight modifications of gradients to give maximum resolution in minimum time for a particular mixture, the procedure can be used for routine determination of carotenoids from a variety of sources.

ACKNOWLEDGEMENTS

We thank the following for carotenoid samples: Dr. H. YOKOYAMA, Pasadena; Dr. G. BRITTON, Liverpool; and Dr. H. THOMMEN, Basle.

REFERENCES

1 H. H. STRAIN, *Chromatographic Adsorption Analysis*, Interscience, New York, 1945, pp. 1–7.
2 R. KUHN AND E. LEDERER, *Ber.*, 64 (1931) 1349.
3 H. H. STRAIN, *Leaf Xanthophylls*, Carnegie Institution of Washington, 1938.
4 A. L. CURL, *Agr. Food Chem.*, 8 (1960) 356.
5 A. HAGER AND T. MEYER-BERTENRATH, *Planta*, 69 (1966) 198.
6 A. JENSEN AND S. LIAAEN-JENSEN, *Acta Chem. Scand.*, 13 (1959) 1863.
7 B. H. DAVIES, *Biochem. J.*, 103 (1967) 51P.
8 R. MONÉGER, *Physiol. Veg.*, 6 (1968) 367.
9 P. KARRER AND E. JUCKER, *Carotenoids*, Elsevier, New York, 1950.
10 H. YOKOYAMA AND M. J. WHITE, *Phytochem.*, 5 (1966) 1159.
11 T. W. GOODWIN, *Chemistry and Biochemistry of Plant Pigments*, Academic Press, New York, 1965, pp. 127–142.
12 T. W. GOODWIN, *Carotenoids*, Chemical Publishing Company, New York, 1954.
13 C. R. ENZELL, G. W. FRANCIS AND S. LIAAEN-JENSEN, *Acta Chem. Scand.*, 23 (1969) 727.
14 B. H. DAVIES, in T. W. GOODWIN (Editor), *Chemistry and Biochemistry of Plant Pigments*, Academic Press, New York, 1965, pp. 489–532.
15 K. AITZETMÜLLER, W. A. SVEC, J. J. KATZ AND H. H. STRAIN, *Chem. Commun.*, 1 (1968) 32.
16 L. ZECHMEISTER, *Vitamins A and Arylpolenes*, Academic Press, New York, 1962, p. 230.

CHROM. 5090

GEL FILTRATION OF ABH BLOOD GROUP SUBSTANCES

I. FRACTIONATION OF ABH SUBSTANCES OF HUMAN SALIVA

A. FIORI, G. V. GIUSTI AND G. PANARI

Istituto di Medicina Legale e delle Assicurazioni, Università Cattolica del Sacro Cuore, 00168 Rome (Italy)

AND

G. PORCELLI

Istituto di Chimica, Università Cattolica del Sacro Cuore, 00168 Rome (Italy)

(First received August 20th, 1970; revised manuscript received September 25th, 1970)

SUMMARY

Human saliva from secretors of groups A, B, O and AB was gel filtered on Sephadex G-200 and G-100 columns, and on thin layers and the eluates were tested for A, B and H antigens by the haemagglutination inhibition method. A main excluded fraction (fraction 1) was detected in all the samples examined. A part of this fraction was also excluded from Sepharose 4B. The molecular weight of this fractions can be assumed to be between $2 \cdot 10^5$ and $5 \cdot 10^6$. In some samples of saliva, one or two group-specific subfractions were identified (fractions 2 and 3). Fraction 2 is excluded from Sephadex G-50 and probably has a molecular weight between 10 000 and 13 000. Fraction 3 is dialysable and has a lower molecular weight, probably no greater than 1500–2000. Fraction 1 is water-soluble and can be precipitated in alcohol, while fractions 2 and 3 are both water- and alcohol-soluble.

INTRODUCTION

Gel filtration on dextran gels or on crosslinked polyacrylamide has already been used for the purification and/or fractionation of ABH substances from various sources[1–10]. This method therefore seemed particularly useful for the study of ABH salivary substances, in which the presence of alcohol-soluble and alcohol-insoluble fractions has been recently demonstrated[11]. The present study deals with the results obtained by gel chromatography of untreated and alcohol-fractionated human saliva.

MATERIALS AND METHODS

Preparation of the samples

Samples of saliva from seven A, six B, five AB and five O secretors were examined. 10–15 ml of resting saliva, collected without preliminary stimulation, were

centrifuged, titred and then either immediately subjected to gel chromatography or submitted to alcohol or Rivanol fractionation before gel filtration. Secretors were considered those donors whose saliva clearly inhibited the specific serum at a dilution of 1/10 or greater.

The titre of the blood group specific substances on boiled and on unboiled samples was determined by the inhibition technique using freshly collected, diluted and centrifuged saliva, according to a slightly modified version of the method of BOORMAN AND DODD[12]. The samples examined had the following titres:

group A = 1/10; 1/50; 1/100; 1/400; 1/500; 1/1000; 1/2000
group B = 1/100; 1/100; 1/200; 1/400; 1/500; 1/1000
group O = 1/10; 1/50; 1/100; 1/100; 1/300
group AB = A 1/10, B 1/100; A 1/50, B 1/100; A 1/200, B 1/100; A 1/400, B 1/400; A 1/400, B 1/1000.

Untreated saliva, freshly collected and centrifuged, was used for thin-layer gel filtration experiments.

The samples to be examined by gel filtration on columns, in the first experiments were dialysed 24 h against Tris–HCl buffer, pH 7.3, (Tris–HCl 0.005 *M* containing 0.9% NaCl) and then concentrated to 3–4 ml in an air current at 4°. In successive experiments, dialysis was omitted to prevent loss of the lowest molecular weight fraction, and concentration was effected only on saliva from weak secretors.

In some experiments samples of saliva, usually 10 ml, were treated with 4.4 ml of 0.5% aq. Rivanol. After standing for 1 h the precipitated material was collected by centrifugation, washed five times with water, resuspended in water and, together with the supernatant, dialysed overnight against water in order to remove any excess Rivanol. After dialysis the precipitate became partially water soluble.

Samples of saliva (usually 10 ml) from the same donors were treated with absolute methyl alcohol or ethyl alcohol (1:4). After standing for 1 h, the precipitated material was collected by centrifugation, dried and suspended in saline. As a part of the precipitate was soluble in saline, the insoluble component was separated by centrifugation and once again suspended in saline for serological examination. The alcoholic supernatant solution was brought to dryness and dissolved in saline. The supernatants from Rivanol and ethanol or methanol precipitation, as well as the water-soluble part of the precipitate, were submitted to serological tests and then to gel filtration.

Gel filtration on columns

Gel filtration on Sephadex G-100 (fine) was performed using 1.5 × 36 cm columns, and 0.05 *M* Tris–HCl buffer (pH 7.3), which contained 0.9% NaCl. Flow rate was maintained at 15–20 ml/h and 1–1.5-ml fractions were collected.

Gel filtration on Sephadex G-200 (fine) was carried out using K 25/45 (bed dimensions, 2.5 × 32 cm) columns (Pharmacia, Uppsala) with the same buffer as eluant, at a flow rate of 15–20 ml/h and 2–3-ml fractions.

Bed dimensions of 2 × 80 cm for gel filtration on Sephadex G-50 and beds of 2.5 × 38 cm for Sephadex G-25 were used, at a flow rate of 15–20 ml/h and 2-ml fractions.

Gel filtration on Sepharose 4B (bed dimensions, 2.2 × 32 cm) was performed

with 0.025 *M* phosphate buffer (pH 7.2) at a flow rate of 15–20 ml/h, collecting fractions of 2–3 ml.

Packing of the columns and the void volumes were checked with Blue Dextran 2000, which had been freshly prepared (Pharmacia, Uppsala). Cytochrome *c* (mol.wt. 12 400), glucagon (mol.wt. 3485), oxytocin (mol.wt. 1007), bacitracin (mol.wt. 1400), and sucrose (mol.wt. 342) were also used as reference substances. The protein content of each fraction was determined by the LOWRY–FOLIN method[13] with an autoanalyser.

The fractions from Sephadex G-100, G-200, G-50 and G-25 were directly examined by the inhibition technique as described below. The fractions obtained from Sepharose 4B were made isotonic by adding 0.1 ml of 14.6% NaCl to 2 ml of eluate and then were submitted to serological analysis.

Thin-layer gel filtration

Thin-layer gel filtration was performed on Sephadex G-200 (superfine) and on Sephadex G-100 (superfine), swollen in 0.05 *M* Tris–HCl buffer (pH 7.3) containing 0.9% NaCl. To obtain 1-mm-thick layers of the gel on glass plates (20 × 20 cm), a strip of tape 1 cm wide was attached along the four edges of the surface of each plate. Into the centre of the glass surface (18 × 18 cm) so delimited, were poured 40 ml of a semifluid slurry of Sephadex that was then spread with a glass rod. A horizontal homogeneous surface was obtained by shaking the plate with caution. The excess water was absorbed by applying over the tape, along the four edges of the plate, four sheets of filter paper (20 × 20 cm). After 20–30 min, a convenient consistency was reached. The gel plates were then equilibrated overnight with Tris–HCl buffer by a descending development at an angle of 15° in a closed chamber. The flow rate was 2 cm/h, as measured by a completely excluded substance (Blue Dextran 2000). After the equilibration was completed, samples of saliva (80–100 μl) were applied to the starting line of the horizontal plate and chromatographed at an angle of 15°. As reference substances, Blue Dextran 2000, bovine serum albumin, chymotrypsin, cytochrome *c*, insulin and oxytocin were used. After completion of the run the uncoloured proteins were detected by covering the corresponding lane of the gel for a few minutes with a filter paper which was then dried for 10 min at 100° and stained with a methanolic solution of Amido Black. Insulin and oxytocin were eluted with distilled water and determined colorimetrically using the Folin–Ciocalteu reagent[14].

For the detection of active blood group substances by means of the inhibition technique, the gel was cut into 1 × 2 cm fractions (usually 16) beginning 1 cm before the starting line and continuing until the exclusion line. Each fraction of the gel was then transferred into separate test tubes and centrifuged; 0.2 ml of saline was added, and the elution prolonged overnight. After centrifugation 0.1 ml of the clear supernatant was transferred into another test tube and serologically examined by the inhibition test.

Haemagglutination inhibition test

Commercial anti-A and anti-B sera usually titred 1/4–1/8 were employed. Anti-H reagent of the same titre was prepared from seeds of *Ulex europaeus* according to BOORMAN AND DODD[12]. 0.1 ml of the antiserum was added to 0.1-ml samples of

the fractions eluted from the columns or from the thin-layer chromatograms. After 30 min of incubation at room temperature, 0.1 ml of a 2% suspension in saline of the appropriate red cells was added. The tubes were then centrifuged at 1000 r.p.m. for 1 min and finally vigorously shaken before reading the agglutination macroscopically. The results were scored in the following way: C = one clump, complete agglutination; +++ = very large clumps; ++ = large clumps; + = several clumps; ± = minimal clumps; and — = no agglutination, *i.e.* complete inhibition.

RESULTS

Sephadex G-100 and G-200 columns

All the samples of saliva filtered through Sephadex G-100 and G-200 columns contained a main fraction of blood group specific substance which was completely excluded from the gel. When zone broadening took place (*e.g.* in strong secretors) a control was made on the last fractions of the active peak. These fractions were pooled, dialysed overnight against distilled water, then concentrated to a small volume (2–3 ml) by an air current at 4° and recycled on the same column. A sharp

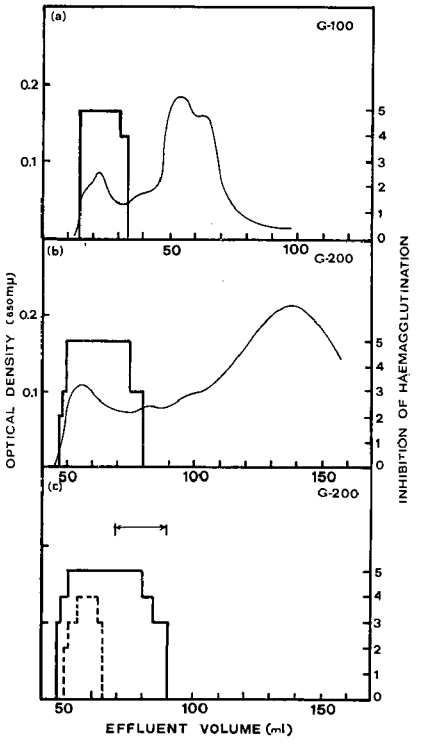

Fig. 1. Gel filtration of human saliva on Sephadex G-100 and G-200 columns. The serological activity is indicated by the thick line and the protein concentration by the thin line. The results of the inhibition of haemagglutination are scored as follows: 0 = one clump; 1 = +++; 2 = ++; 3 = +; 4 = ±; 5 = — (no agglutination). (a) Gel chromatogram of the saliva from a subject of group A (A titre: 1/200); (b) saliva from a group B subject (B titre: 1/800); (c) saliva from a group A_1 subject (A titre: 1/1000). The broken line shows a recycling experiment on the effluent indicated by the arrow.

excluded active peak was obtained. Fig. 1 shows the elution diagram of some typical experiments.

Sepharose 4B columns

The gel filtration on Sepharose 4B columns was performed with the aim of studying the spread of molecular weight of the active fraction of the blood group excluded from Sephadex G-100 and G-200. For this purpose specimens of whole saliva, having only the fraction excluded from Sephadex G-200 and G-100, were submitted to gel filtration on Sepharose 4B. Also excluded fractions isolated by means of a preliminary gel filtration through Sephadex G-200, then dialysed and concentrated to 2–3 ml, were examined in the same way.

All the samples examined were eluted as a broad zone of serological activity. The leading part of this zone was excluded from the gel, as shown in Fig. 2, where

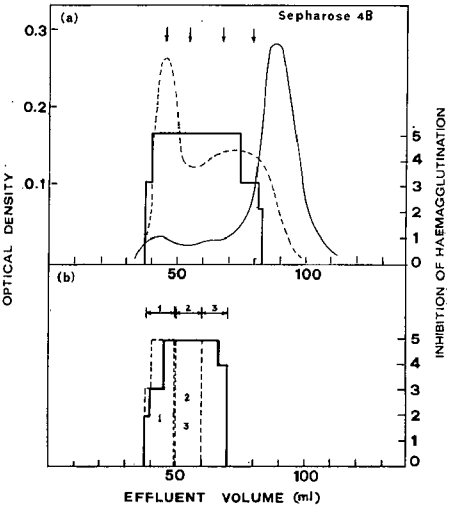

Fig. 2. Gel filtration on Sepharose 4B of a sample of saliva from a subject of group O (H titre: 1/200). The broken line of (a) is the UV absorption curve at 260 mμ of Blue Dextran 2000. In (b) recycling experiments are recorded. The arrows indicate the serological titration reported in Table I.

the elution curve is compared with that of Blue Dextran. The void volume is indicated by the leading peak of the UV absorption curve (at 260 mμ) of the Blue Dextran. The inhibition titre was determined on the eluate by the double dilution method. Maximum activity was found to coincide with the excluded part of the active zone.

In Table I the results of such a determination on four critical tubes of the case given in Fig. 2a are reported. A recycling of pooled fractions of the active zone was found necessary to ascertain if only one part of this zone was excluded. For this purpose three pools were prepared from the active zone. The first pool (40–50 ml) was made with the effluent of the leading part of the curve; the second (51–58 ml) and the third (59–68 ml) with the remaining part of the curve (Fig. 2b). The pooled solutions were dialysed 24 h against distilled water, then concentrated by an air current at 4° to 2–3 ml and separately recycled on Sepharose 4B. As shown by

TABLE I

SALIVA A GEL FILTERED ON SEPHAROSE 4B (SEE FIG. 2a)

To each dilution, 0.1 ml of serum anti-A titred 1/8 was added and, after 30 min, 0.1 ml of 2% red cells suspension. Agglutination is indicated by C (one clump), +++, ++, +, ±. No agglutination is indicated by —.

Sample (Test tube no.)	*Dilution of 0.1 ml of the eluate*							
	1/1	*1/2*	*1/4*	*1/8*	*1/16*	*1/32*	*1/64*	*1/128*
16 (46 ml)	—	—	—	±	±	+	+	+++
20 (55 ml)	—	—	±	+	+	++	C	C
24 (68 ml)	—	—	±	+	++	C	C	C
32 (80 ml)	+	++	C	C	C	C	C	C

Fig. 2b, the first pool is again excluded. The second pool had the same elution volume (50–59 ml) as in the first cycle. On the contrary the elution volume of the third pool was changed, becoming the same as the second pool (50–57 ml).

Eight samples of saliva (4 of group O; 3 of group A and 1 of group B) exhibited one or two additional active peaks on Sephadex G-100 and G-200 columns. The elution volumes of these two blood group subfractions were the following: 105 ml and 340 ml, respectively, on Sephadex G-200 and 55 ml and 78–80 ml on Sephadex G-100, with variations of 2–5 ml in relationship to the packing of the columns. The subfractions, especially the first one, had weak activity so that the 0.1 ml usually employed in serological tests sometimes gave complete inhibition, but more frequently incomplete inhibition (±; +).

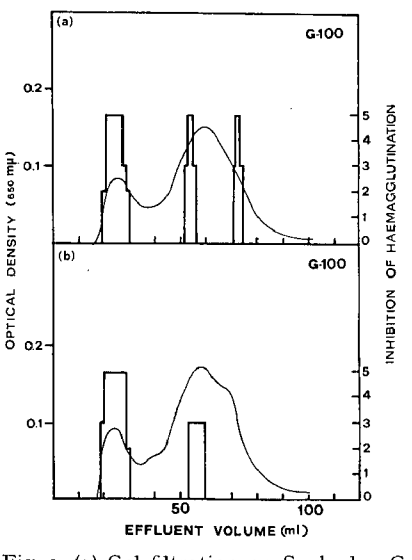

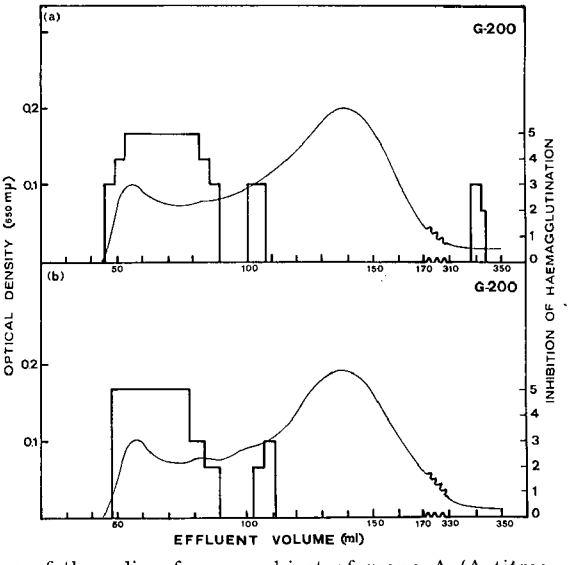

Fig. 3. (a) Gel filtration on Sephadex G-100 of the saliva from a subject of group A (A titre: 1/2000) with three group specific fractions; (b) The saliva from a secretor of group A (A titre: 1/800) with two group specific fractions.

Fig. 4. Gel filtration on Sephadex G-200 of the same samples of Fig. 3a and b.

Figs. 3 and 4 show the elution curves of salivas having one or two retained active fractions. In Table II a typical titration experiment is given in which the inhibition activity of the main excluded peak and that of the two subfractions are compared. Reproducible results were obtained in the same secretors reexamined at various times. No differences were observed in saliva preserved at −20° for a number of weeks.

TABLE II

GEL FILTRATION OF SALIVA A, TITRE 1/100

3 ml gel filtered on Sephadex G-100 column (36 × 1.5 cm), flow rate 8 ml/h.

Sample (Test tube no.)	*Dilution of 0.1 ml of the eluate*							
	1/1	*1/2*	*1/4*	*1/8*	*1/16*	*1/32*	*1/64*	*1/128*
Excluded effluent								
9	C	C	C	C	C	C	C	C
10	±	+	+	++	+++	C	C	C
13 (18 ml)	−	−	−	−	±	+	+++	C
16	−	−	−	−	−	±	+	+++
19 (24 ml)	−	−	−	−	−	−	+	+++
22	−	−	−	±	+	+++	C	C
26	−	±	+	+++	C	C	C	C
Non-excluded effluent								
54	C	C	C	C	C	C	C	C
55	+	+	+++	C	C	C	C	C
56 (62 ml)	±	+	+	++	C	C	C	C
57	+	+	++	C	C	C	C	C
58	C	C	C	C	C	C	C	C
70	C	C	C	C	C	C	C	C
71	+	+	+++	C	C	C	C	C
72 (80 ml)	−	−	−	−	±	+	+++	C
73	+	+	++	+++	C	C	C	C
74	C	C	C	C	C	C	C	C

Thin-layer chromatography on Sephadex G-200 and G-100

Thin-layer chromatography on Sephadex G-200 and G-100 allowed an easy separation of the two subfractions from the excluded fraction. As thin-layer gel filtration on Sephadex G-200 had no real advantages in comparison with Sephadex G-100, the latter was preferred throughout this work.

The main active fraction (fraction 1) was detectable in all the subjects examined. It migrated as the Blue Dextran spot, *i.e.* with the exclusion front. The faster subfraction (fraction 2) migrated 8–9 cm from the starting line (7–8 cm on Sephadex G-200) and had the same mobility as cytochrome *c*. The slow subfraction (fraction 3) was detected in a zone located in the first 2 cm after the starting line.

The R_{cy} values (ratio of the migration distance of the active fraction to that of cytochrome *c*) were the following:

fraction 1 (excluded) R_{cy} 1.65
fraction 2 R_{cy} 1
fraction 3 R_{cy} 0.10

In Fig. 5a and b, thin-layer gel chromatograms are given which were obtained from the same saliva as in Figs. 3 and 4; in Fig. 5d, a chromatogram from a saliva containing the 3 fractions, while in Fig. 5c the chromatogram is recorded of the same saliva as in Fig. 1a which was lacking in the subfractions.

The advantage of the thin-layer gel filtration is the possibility of running four samples of saliva in small amounts together with the reference substances. On the other hand the elution step is tedious and unpractical for routine work. In addition, false negative results when searching for subfractions could be obtained, due to the loss of material during elution.

Methanol or ethanol treatment

Methanol or ethanol treatment of saliva gave rise to a precipitate which was partially soluble in saline. The water-insoluble material was suspended in saline

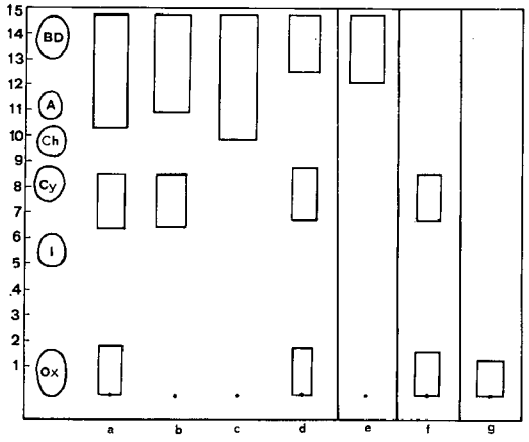

Fig. 5. Thin-layer gel filtration of saliva on Sephadex G-100. Reference substances: BD = Blue Dextran 2000; A = albumin; Ch = chymotrypsin; Cy = cytochrome *c*; I = insulin; Ox = oxytocin. The zones of blood group activity are represented by rectangles. (a) and (b): the same samples of Figs. 3 and 4; (c) the saliva of Fig. 1a; (d) another sample of saliva (group B) with three active fractions. For (e), (f) and (g) see explanation in RESULTS under *Methanol or ethanol treatment* and *Fraction 3*.

and serologically tested. It exhibited a strong activity. The water-soluble part of the precipitate was gel filtered on Sephadex G-200, G-100, Sepharose 4B columns and on thin layers of Sephadex G-100. Only the excluded blood group specific substance (fraction 1) was detectable on Sephadex G-200 and G-100, also in those samples of saliva containing subfractions (Fig. 5e). The elution profile on Sepharose 4B was very similar to that of untreated saliva, but the serological activity was very much lower.

The alcoholic supernatant was brought to dryness and dissolved in saline. It exhibited a clear blood group specific activity in those salivas having active subfractions (*i.e.* fractions 2 and 3). These specimens were gel filtered on columns

and on thin layers. The two subfractions were detected and they had the same elution volumes and R_{cy} values (Fig. 5f) as subfractions detected in untreated saliva.

The Rivanol treatment gave a precipitate which was partially soluble in saline after removal of Rivanol by dialysis. The solutions had blood group activity. Their main component in gel filtration was fraction 1. Gel filtration of the aqueous supernatant from Rivanol precipitation contained fractions 2 and 3.

Fraction 2

The behaviour of fraction 2 in dialysis experiments and in gel filtration on Sephadex G-50 columns was also investigated. For this purpose, salivas of secretors containing fraction 2 were gel filtered on Sephadex G-100 columns. The eluate from 48–58 ml was pooled and dialysed 24 h against distilled water. No blood group activity was detected in the dialysate whilst the retenate was clearly active. The latter was concentrated to 2 ml and gel filtered on a Sephadex G-50 column. Blood group activity was detected only as an excluded peak (elution volume 80 ml), while the reference substance cytochrome *c* was retained and had an elution volume of 104 ml.

Fraction 3

Specimens of saliva (30–100 ml) containing fraction 3 were dialysed 24 h in Visking tubes against distilled water, with three changes. The dialysate was evaporated to 2–5 ml. Only the dialysate exhibited a clear blood group activity. It was gel filtered on Sephadex G-100 and gave the same elution volume and R_{cy} value as fraction 3 of the untreated saliva (Fig. 5g).

The dialysate was also gel filtered on a Sephadex G-25 column. The elution volumes of the group specific substance (104 ml) and of some substances of known molecular weight are recorded in Fig. 6.

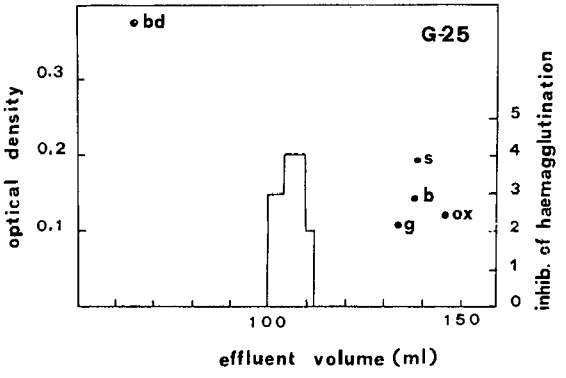

Fig. 6. Gel filtration on Sephadex G-25 of the fraction 3 isolated by dialysis of the saliva from a subject of group B. Reference substances: bd = Blue Dextran; g = glucagon; b = bacitracin; s = sucrose; ox = oxytocin.

DISCUSSION

In a previous paper it has been reported that some specimens of human saliva

can be fractionated into two main fractions by treating dried saliva with absolute methanol or ethanol. One fraction is denatured in the process and becomes water-insoluble; the other is water- and alcohol-soluble[11].

The present work is a development of these findings. In addition, some information is given on the polydispersity of the molecular weight of blood group substances from secretions.

Fraction 1

All the samples from secretors' saliva, which were examined without alcoholic treatment, had a main active peak which was excluded from Sephadex G-200 and G-100 columns and migrated with the exclusion front in thin-layer gel filtration experiments. These data are in agreement with gel filtration experiments of some other workers on ABH substances[2,4,7,9,10].

From the gel filtration behaviour of the main active fraction (fraction 1) it can therefore be assumed that this is the same substance as that isolated from secretions by the usual methods[15]. In fact, purified blood group substances from secretions are glycoproteins containing a high percentage of carbohydrate (about 85%) and have molecular weights greater than $2 \cdot 10^5$ (ref. 16), being therefore excluded from Sephadex G-200 (exclusion limit for dextrans: 200 000) as well as fraction 1 of untreated saliva. It is well known that the carbohydrate content has a strong effect on the gel filtration behaviour of proteins[17–19]. Gel filtration shows that some glycoproteins have a more expanded structure than the typical globular proteins. This may well be due to a greater hydration on solution of the carbohydrate chains[18,19]. Owing to their very high carbohydrate content blood group substances behave similarly to dextrans with regard to gel filtration behaviour.

Fraction 1 from gel filtration on Sephadex G-200 of untreated saliva also contains the larger macromolecules which form the sparingly soluble part of the group specific glycoproteins extracted from secretions by the phenol method[16,20]. These larger macromolecules probably are those excluded from Sepharose 4B.

The excluded fraction (fraction 1) is almost completely denatured, without loss of activity, when air dried and then treated by absolute methanol or ethanol. The treatment of fluid saliva with methanol or ethanol at the ratio of 1:4 gives a precipitate of fraction 1, part of which is irreversibly denatured and can not be gel chromatographed; part remains water-soluble and therefore can be studied by gel chromatography. No particular advantage is obtained by Rivanol precipitation which is incomplete and also more laborious.

The gel filtration studies on fraction 1 provided additional information on the polydispersity of the molecular weight of this fraction of the ABH blood group substances from secretions.

Values of molecular weight varying from $2 \cdot 10^5$ to $2 \cdot 10^6$ have been reported by some authors[15,16,21] from sedimentation velocity experiments carried out on ABH substances from ovarian cyst fluid.

DUNSTONE AND MORGAN[16] also studied the sparingly soluble part of the precipitate from phenol treatment of ovarian cyst fluid. This material exhibited no sharp boundaries, probably due to the high degree of polydispersity. The $S^0_{20,w}$ values of the fastest sedimenting component were greater than 15 S. This is considerably

higher than those generally found ($S^0_{20,w}$ 10–12 S) for the upper molecular range of values determined for the water-soluble blood group specific substances.

More recently, CREETH AND KNIGHT[22] gave qualitative evidence for a considerable spread of molecular weight of a B glycoprotein from ovarian cyst fluid, as demonstrated by the absence of a true plateau region in sedimentation velocity experiments.

Our gel filtration experiments on Sephadex G-200 confirmed that fraction 1 of untreated saliva has a molecular weight greater than 200 000, as discussed above.

The polydispersity of the molecular weight of this main fraction is suggested by its behaviour on Sepharose 4B. In fact, the elution profile of fraction 1 is similar to that of Blue Dextran 2000 which is known to contain some high-molecular-weight material excluded from Sepharose 4B, and other molecules which are not excluded from this gel. The leading peak of the UV elution profile of the coloured dextran contains the very large molecules and indicates the void volume. The exclusion limit for Sepharose 4B given now (1969) by the manufacturer is $20 \cdot 10^6$ for proteins and $5 \cdot 10^6$ for polysaccharides. Since the gel filtration behaviour of blood group substances is similar to that of polysaccharides, owing to their high carbohydrate content, it seems evident that the leading excluded peak of the salivary active substance has a molecular weight up to or over $5 \cdot 10^6$. The non-excluded part of the active zone is retained in the gel, as demonstrated by recycling experiments. In other words, gel filtration on Sephadex G-200 and on Sepharose 4B supported the results of DUNSTONE AND MORGAN[16] on glycoproteins from ovarian cyst fluid.

It must be emphasised that our data have been obtained mainly on untreated saliva. When the saliva is fractionated by alcohol, the water-soluble part of the precipitate is still excluded from Sepharose 4B but a great loss of substance occurs. It is therefore reasonable to think that many among the procedures used for the isolation of blood group substance produce a considerable denaturation especially of the larger molecules. This could explain the fact that many workers in the field have suggested molecular weights not greater than $1 \cdot 10^6$. It is probable, on the contrary, that the molecular weight of the main salivary blood group substance is within the range of $2 \cdot 10^5$ to $5 \cdot 10^6$.

Fractions 2 and 3

Some salivas contain one or two additional fractions, termed fraction 2 and fraction 3, which are both water- and alcohol-soluble. The blood group activity of these fractions, especially of fraction 2, is very low in comparison with that of fraction 1. In addition, the active peak eluted from the columns is usually very sharp. On the other hand, in thin-layer experiments, the active zones are usually elongated especially in specimens very rich in mucus. Fractions 2 and 3, as well as fraction 1, have a specific inhibitory activity, as controlled in each case by performing the serological test with anti-A, anti-B and anti-H sera. More complex is the problem of the results obtained with anti H serum on the eluates of saliva from A, B and AB subjects. This problem will be considered in a future paper.

The molecular weight of fraction 2 and fraction 3 can be approximately indicated by gel filtration and dialysis experiments. Fraction 2 is eluted with cytochrome *c* in gel filtration on Sephadex G-200 and G-100 columns or thin layers, while gel filtration on Sephadex G-50 columns separates fraction 2, which is excluded,

from cytochrome *c*, which is retained. This could be explained assuming that fraction 2 is a glycoprotein with a high carbohydrate content and therefore behaves on Sephadex G-50 as dextrans for which the exclusion limit of this gel is 10 000. Cytochrome *c* is, on the contrary, a carbohydrate-free protein (mol.wt. 12 400) which is not excluded, as the exclusion limit of Sephadex G-50 for proteins is 30 000. Thus fraction 2 probably has a molecular weight greater than 10 000, but no greater than that of cytochrome *c*. It should also be noted that fraction 2 was not dialysable through dialysis tubes which retained 30–40% insulin (mol.wt. 5734).

Fraction 3 is completely dialysable through a Visking membrane, as are also bacitracin (mol.wt. 1400) and oxytocin (mol.wt. 1007). In gel filtration on Sephadex G-200 and G-100 columns it has elution volumes much greater than fraction 2 (Figs. 3 and 4), migrates with oxytocin in thin-layer gel filtration on Sephadex G-100, and is not excluded from Sephadex G-25. In this gel some peptides have been used as reference substances of known molecular weight (Fig. 6) but the gel chromatographic behaviour of fraction 3, which should be considered mainly a carbohydrate in nature, can be better compared to that of a sugar as sucrose. On the basis of all these considerations, the molecular weight of fraction 3 could be assumed no greater than 1500–2000.

It is interesting to note that naturally occurring ABH substances with low molecular weights have been isolated in recent years in some secretions and also in urine. LUNDBLAD AND BERGGARD[6] reported the isolation from urine of A- and B-specific oligosaccharides. KANAZAWA[3] described several active fractions in saliva chromatographed on CM- and DEAE-cellulose, then filtered on Sephadex G-100. HIRANO *et al.*[23] isolated some ABH glycopeptides from human colostrum.

ACKNOWLEDGEMENTS

We are indebted to Dr. J. AMERIO for revising the english manuscript. We also thank Mrs. M. RANIERI, Mr. M. DI IORIO and Mr. V. GENTILE for helpful technical assistance.

This work was supported in part by the Consiglio Nazionale delle Ricerche.

REFERENCES

1 N. K. KOCHETKOV, V. A. DEREVITSKAYA AND S. G. KARA-MURZA, *Carbohyd. Res.*, 3 (1967) 403.
2 G. HRISTOVA, *Z. Immunitätsforsch. Allerg. Klin. Immunol.*, 135 (1968) 146.
3 T. KANAZAWA, *Hirosak. Med. J.*, 20 (1968) 1.
4 R. HAVEZ, P. ROUSSEL, P. DEGAND, Y. DELMAS-MARSALET AND G. BISERTE, *Bull. Soc. Chim. Biol.*, 51 (1969) 245.
5 N. TSUGAWA, *Jap. J. Leg. Med.*, 22 (1968) 515.
6 A. LUNDBLAD AND I. BERGGARD, *Biochim. Biophys. Acta*, 57 (1962) 129.
7 F. A. GREEN, *J. Immunol.*, 99 (1967) 56.
8 P. ZAHLER, *Vox Sang.*, 15 (1968) 81.
9 N. B. WHITTEMORE, N. C. TRABOLD, C. F. REED AND R. I. WEED, *Vox Sang.*, 17 (1969) 289.
10 I. LIOTTA, M. QUINTILIANI, L. QUINTILIANI, A. BUZZONETTI AND E. GIULIANI, *Vox Sang.*, 17 (1969) 11.
11 A. FIORI AND P. BENCIOLINI, *Boll. Soc. Ital. Biol. Sper.*, 45 (1969) 1483.
12 K. BOORMAN AND B. DODD, *Blood Group Serology*, 2nd ed., Churchill, London, 1961.
13 O. H. LOWRY, N. J. ROSEBROUGH, A. L. FARR AND R. J. RANDALL, *J. Biol. Chem.*, 193 (1951) 265.
14 R. M. HERRIOTT, *Proc. Soc. Exper. Biol. Med.*, 46 (1941) 642.

15 E. A. KABAT, *Blood Group Substances*, Academic Press, New York, 1956.
16 J. R. DUNSTONE AND W. T. J. MORGAN, *Biochim. Biophys. Acta*, 101 (1965) 300.
17 J. R. WHITAKER, *Anal. Chem.*, 35 (1963) 1950.
18 P. ANDREWS, *Biochem. J.*, 91 (1964) 222.
19 P. ANDREWS, *Biochem. J.*, 96 (1965) 595.
20 W. T. J. MORGAN AND H. K. KING, *Biochem. J.*, 37 (1943) 640.
21 W. M. WATKINS, *Science*, 152 (1966) 172.
22 J. M. CREETH AND C. G. KNIGHT, *Biochem. J.*, 105 (1967) 1135.
23 S. HIRANO, H. HAYASHI, T. TERABAYASHI, K. ONODERA, T. NAKAGAKI, N. YOGY, Y. NOGAI, N. KOCHIBE, S. ISEKI AND T. IMAGAWA, *J. Biochem. (Tokyo)*, 64 (1968) 563.

CHROM. 5091

GEL FILTRATION OF ABH BLOOD GROUP SUBSTANCES

II. INDIVIDUAL GEL CHROMATOGRAPHIC PATTERNS OF ABH SUBSTANCES IN THE SALIVA OF SECRETORS AND NON-SECRETORS

A. FIORI, G. V. GIUSTI AND G. PANARI

Istituto di Medicina Legale e delle Assicurazioni, Università Cattolica del Sacro Cuore, 00168 Rome (Italy)

(First received August 20th, 1970; revised manuscript received October 17th, 1970)

SUMMARY

The saliva from 605 donors was gel chromatographed on Sephadex G-100 and was examined serologically for ABH blood group specific fractions termed fractions 1, 2 and 3. All secretors had the main active excluded fraction (fraction 1) alone or associated with fraction 2 and/or fraction 3. The saliva from non-secretors lacked fraction 1 and had fraction 2 and/or fraction 3. In some non-secretors, no active fraction was detected (true non-secretors). Eight gel filtration patterns for each of the A, B and H antigens were therefore identified.

A standardised technique on small Sephadex G-100 columns was developed and the frequencies of each gel filtration type determined in the last 199 secretors and 32 non-secretors were examined. The gel filtration pattern of H substance in group A, B and AB subjects was also studied. In some of these subjects, gel filtration patterns of the single antigens had been found which differ from each other. The ABH salivary gel filtration pattern of a single subject is a stable individual characteristic and probably is genetically determined.

INTRODUCTION

In a previous paper[1] it has been shown that the saliva from secretors contains a main active fraction of blood group specific substances (fraction 1) which is excluded from Sephadex G-200 and G-100 and only partially excluded from Sepharose 4B. It has also been reported that saliva from secretors can contain one or two blood group specific subfractions of low molecular weight (fraction 2 and fraction 3). The subfractions appeared to be associated with each other and with fraction 1, giving four gel filtration ABH patterns.

In this paper the results of a more extensive study are presented in which the saliva of non-secretors is also included. Several individual ABH gel filtration patterns were detected among secretors and non-secretors and the frequency of this character determined.

MATERIALS AND METHODS

Preparation of the samples

The samples of saliva were collected without preliminary stimulation and immediately centrifuged at 3000 r.p.m. for 10 min. Gel filtration of the supernatant was performed no later than 12 h after or, otherwise, the supernatant was preserved at −20° until gel chromatographed.

The titre of blood group substances was determined before gel filtration on unboiled saliva, using a slight modification of the technique described by BOORMAN AND DODD[2]. Secretors were considered the subjects whose saliva inhibited the specific serum at a dilution of 1/10 or more.

Gel filtration

Thin-layer gel filtration on 1-mm-thick layers of Sephadex G-100 (superfine) was performed on 20 × 20 cm plates prepared as previously described[1]. After the run was completed, the gel chromatogram was cut into several 1-cm sections, eluted with 0.2 ml of saline and the eluate serologically determined for A, B and H substances. To allow this determination, three separate spots of the same saliva were usually run on the same plate.

Gel filtration on columns was carried out on 36 × 1.5 cm beds of Sephadex G-100 with 0.05 *M* Tris–HCl buffer (pH 7.3) containing 0.9% NaCl as eluant. Flow rate was maintained at 15–20 ml/h and fractions of 1–1.5 ml were collected. 2.5–3-ml samples of saliva were usually used for gel filtration.

For routine purposes, smaller columns were found to be more practical. In fact 20 × 1.2 cm beds, with a flow rate of 6 ml/h and 1-ml fractions, allowed a satisfactory separation of the three active specific fractions. 1-ml specimens of saliva were gel filtered through these small columns, using a timed-flow fraction collector with six concentric rows of 100 holes each; in this way six samples were examined simultaneously.

Haemagglutination inhibition test

The inhibition test was performed using undiluted commercial sera (Ortho Pharm. Co., Raritan, N.J.) titred 1/4–1/8 and having a high binding constant (K_0) between 10^6–10^8 and a heterogeneity index of about 0.5. In this way the macroscopic reading of the agglutination after a very short centrifugation (30 sec at 1000 r.p.m.) was facilitated by the formation of one unbroken clump in the tubes where no inhibition occurred. An anti-H serum titred 1/8 was prepared in our laboratory from *Ulex europaeus* seeds, using the method of BOORMAN AND DODD[2].

Three 0.1-ml amounts from the contents of each test tube were transferred into separated test tubes and tested for inhibition with anti-A, anti-B and anti-H sera, respectively, as described in a previous paper[1]. The thin-layer gel chromatograms obtained with three separate spots of the same saliva were eluted as previously described[1] and examined serologically using anti-A, anti-B and anti-H sera.

Analyses

The proteins and the peptides of the eluate were determined by the LOWRY–FOLIN method[3], in most cases using an autoanalyser. The fucose content was measured

by the method of DISCHE AND SHETTLES[4] on 0.5–0.7 ml taken from the content of each tube.

RESULTS

This work deals with the saliva from 605 healthy adults (501 secretors and 104 non-secretors). As many subjects were examined a number of times, over a thousand gel chromatographic determinations will be discussed.

Thin-layer gel filtration

In the first phase of the research, most cases were studied by thin-layer gel filtration on Sephadex G-100. However, subsequent controls showed certain drawbacks in the method. In some experiments on very viscous saliva from secretors, the excluded fraction seemed to be absent, while it was detectable on columns where the viscosity of the sample had no great effect on the elution volumes. In many other cases fractions 2 and 3 had been erroneously undetected, probably due to the loss of the active material during the elution step. As a consequence, the frequency of the ABH gel filtration patterns which had been calculated on secretors on the basis of the results obtained by thin-layer gel filtration (given in a preliminary communication in 1969, ref. 5) must now be considered invalid.

Gel filtration on columns

A standardised gel filtration technique on 20 × 1.2 cm columns was used and only 231 cases (199 secretors; 32 non-secretors) were utilised in calculating the frequencies of ABH gel filtration patterns. Samples taken at random were also gel filtered on 36 × 1.5 cm columns as a control.

Secretors. All the secretors examined (501 subjects) had the main active fraction excluded from Sephadex G-100 (fraction 1). The elution volume of this fraction in 36 × 1.5 cm columns was the same as determined in a previous study[1], *i.e.* about 25 ml. In the smaller columns the elution volume was about 8–9 ml.

In weaker secretors the blood group activity of fraction 1 was weaker than in stronger secretors, and the active peak covered only a few tubes in column gel filtration. A large zone of activity was on the contrary observed in strong secretors. In some of these subjects, especially of group B, zones of activity from the 22th to the 60th ml in 36 × 1.5 cm beds were detected. In these cases the last part of the active fraction was recycled to confirm its exclusion from the gel. For this purpose the contents of the last tubes of fraction 1 were pooled, dialysed 24 h against distilled water, concentrated to 2 ml and recycled. The blood group activity was always present in the excluded effluent. Fraction 2 and fraction 3 were also found to be present in the saliva of many secretors, either singly or together.

The elution volume on Sephadex G-100 beds (36 × 1.5 cm) was about 55 ml for fraction 2 and 80 ml for fraction 3. In the smaller columns the elution volumes were 18 ml and 26 ml, respectively. It should be noted that the elution volumes of fraction 2 and fraction 3 of the same saliva on a single gel chromatogram frequently exhibited an incomplete overlapping of A, B and H activity. In some cases these slight differences in the elution volumes of the subfractions were clearer, *i.e.* A, B and H activities were displaced with respect to each other at times by as much as

one test tube. Some examples taken from small column determinations could better illustrate these findings.

Case No. 410: group A, saliva A (A-1,2,3/H-1,2,3)
fraction 2 = A activity at the 18th ml; H: 17th ml
fraction 3 = A activity at the 27th ml; H: 26th ml
Case No. 398: group AB, saliva AB (A-1,2,3/B-1,2,3/H-1,2,3)
fraction 2 = A activity at the 14th and 15th ml; B: 17th ml; H: 17th–18th ml
fraction 3 = A activity at the 23rd–24th ml; B: 23rd–24th ml; H: 24th–25th ml
Case No. 482: group AB– saliva AB (A-1,2,3/B-1,2,3/H-1,2,3)
fraction 2 = A activity at the 16th–17th ml; B: 15th–16th ml; H: 16th–17th ml
fraction 3 = A activity at the 24th–25th ml; B: 25th–26th ml; H: 26th–27th ml

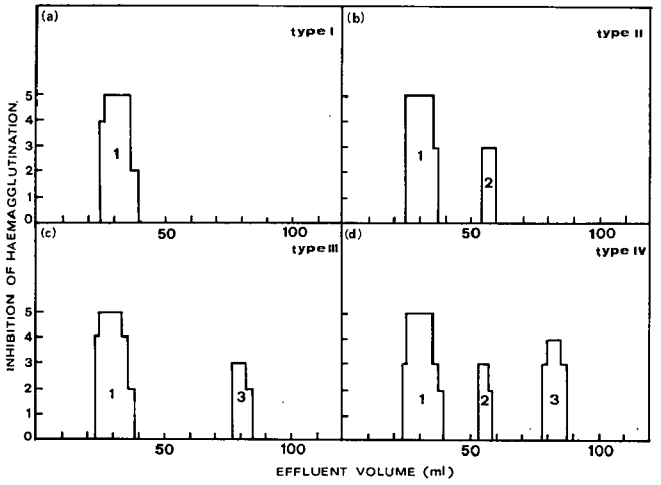

Fig. 1. The four salivary ABH gel filtration types as determined on a Sephadex G-100 36 × 1.5 cm column in the saliva from four secretors of group A. The blood group activity is indicated by the solid line. The results of the inhibition of haemagglutination are scored as follows: 0 = one clump; 1 = +++; 2 = ++; 3 = +; 4 = ±; 5 = – (no agglutination).

The four ABH gel filtration patterns which were observed in group A, B, O and AB secretors are shown schematically in Figs. 1 and 3a. In Table I the frequency of the four ABH gel filtration patterns in the saliva from 199 group A,B and O secretors, as determined by the standardised small column method, are reported. In Table IIa, the salivary gel chromatographic patterns of AB subjects are given, and in Table IIb are the H patterns of each subject. In two persons the B substance was absent, in agreement with the data given by some authors[6,7].

In conclusion, each of the A, B and H substances can be present in the saliva from secretors in four types of gel filtration patterns that have been called Type I, Type II, Type III and Type IV (see Table III).

So-called non-secretors. The saliva of so-called non-secretors does not contain the excluded fraction, *i.e.* fraction 1. This had been determined in the first phase of the present study and was later confirmed by the standardised small column method. In the preliminary experiments non-secretors had also been examined for fractions 2

TABLE I

FREQUENCIES OF THE VARIOUS GEL FILTRATION PATTERNS IN 199 SECRETORS AND 32 NON-SECRETORS
The numbers in parentheses are the percentages.

Gel filtration pattern	*Blood group*			*Totals*
	A	*B*	*O*	
Secretors				
Type I	16	6	29	51
(fraction 1)	(17.58)	(20.68)	(26.12)	(22.07)
Type II	9	3	11	23
(fractions 1, 2)	(9.89)	(10.34)	(9.90)	(9.95)
Type III	17	5	17	39
(fractions 1, 3)	(18.68)	(17.24)	(15.31)	(16.38)
Type IV	35	10	41	86
(fractions 1, 2, 3)	(38.46)	(34.48)	(36.93)	(37.22)
Subtotals	77	24	98	199
	(84.61)	(82.72)	(88.36)	(84.14)
Non-secretors				
Type V	4	—	4	8
(fraction 2)	(4.39)		(3.60)	(3.46)
Type VI	3	—	1	4
(fraction 3)	(3.29)		(0.90)	(1.73)
Type VII	7	2	6	15
(fractions 2, 3)	(7.69)	(6.89)	(5.40)	(6.49)
Type VIII	—	3	2	5
(no fraction)		(10.34)	(1.80)	(2.16)
Subtotals	14	5	13	32
	(15.37)	(17.23)	(11.70)	(13.86)

and 3, but frequently negative results had been obtained due to the use of thin-layer gel filtration. These data have therefore been discarded.

The results of only 33 cases will be reported here which have all been obtained by the small column method. No variation in the gel filtration pattern was observed

TABLE II

GEL FILTRATION PATTERNS FOR A, B AND H SUBSTANCES IN 10 AB SECRETORS AND 1 NON-SECRETOR (NS)

AB case No.	*a*				*b*	
	A		*B*		*H*	
	Type	*Fractions*	*Type*	*Fractions*	*Type*	*Fractions*
1 (NS)	VII	2, 3	VIII	—	VII	2, 3
2	IV	1, 2, 3	IV	1, 2, 3	IV	1, 2, 3
3	III	1, 3	VIII	—	III	1, 3
4	II	1, 2	I	1	III	1, 3
5	I	1	IV	1, 2, 3	II	1, 2
6	IV	1, 2, 3	IV	1, 2, 3	IV	1, 2, 3
7	IV	1, 2, 3	I	1	III	1, 3
8	I	1	I	1	I	1
9	III	1, 3	III	1, 3	III	1, 3
10	II	1, 2	I	1	II	1, 2
11	III	1, 3	I	1	III	1, 3

TABLE III

TYPES OF GEL FILTRATION PATTERNS FOR EACH OF THE A, B AND H SUBSTANCES IN SECRETORS AND SO-CALLED NON-SECRETORS

Type	*Gel filtration pattern (fractions)*	*Symbol for each antigen*		
Secretors				
I	1	A-1	B-1	H-1
II	1, 2	A-1, 2	B-1, 2	H-1, 2
III	1, 3	A-1, 3	B-1, 3	H-1,3
IV	1, 2, 3	A-1, 2, 3	B-1, 2, 3	H-1, 2, 3
So-called non-secretors				
V	2	A-2	B-2	H-2
VI	3	A-3	B-3	H-3
VII	2, 3	A-2, 3	B-2, 3	H-2, 3
VIII	—	A-	B-	H-

in random samples of saliva examined on 36 × 1.5 cm beds. The data showed that the saliva from some non-secretors contained only fraction 2. Fraction 3 was present in other non-secretors and both fractions 2 and 3 in others. Finally, a small number of subjects had no active fraction and so behaved as true non-secretors.

The gel filtration patterns, as detected in columns and thin-layer experiments on non-secretors, are shown schematically in Fig. 2 and Fig. 3b. In Table I the frequencies are reported of the different gel filtration patterns in 32 non-secretors; in Table II (No. 1) the pattern of an AB non-secretor is given.

In conclusion, each of the A, B and H substances was found to be secreted in saliva of non-secretors according to three types of gel filtration patterns, which have been called Type V, Type VI and Type VII. The term Type VIII was used for the absence in the saliva of the considered blood group substance (Table III). The number of secretors examined being relatively small, it was not surprising that in our samples Type V and Type VI among group B subjects and Type VIII in group A

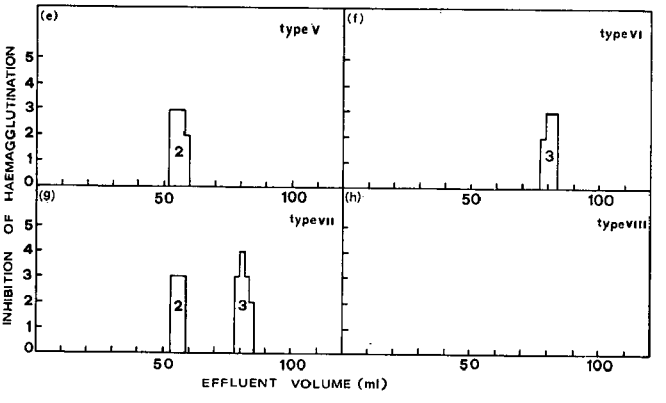

Fig. 2. The salivary ABH gel filtration types of non-secretors as determined on Sephadex G-100 36 × 1.5 cm beds. e, g, h = non-secretors of group A; f = non-secretor of group B.

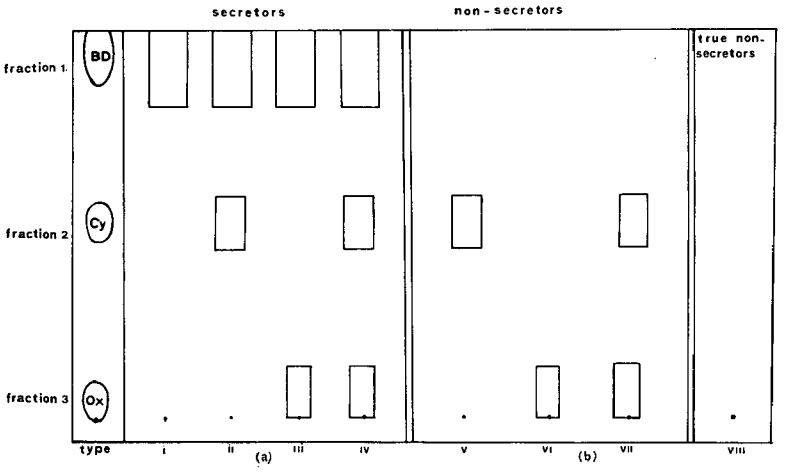

Fig. 3. Schematic representation of the eight ABH gel filtration types determined by thin-layer chromatography on Sephadex G-100 (superfine). Reference substances: BD = Blue Dextran 2000; Cy = cytochrome *c*; Ox = oxytocin.

subjects were absent. The eight types of gel filtration patterns which are possible for each of the A, B and H substances are given in Table III. Types V and VI for group B and Type VIII for group A are, of course, hypothesised.

H substance in the saliva of group A, B, O and AB subjects

The secretion titre of the H substance was determined in all the samples of saliva before gel filtration. The results of this preliminary study will be reported elsewhere[8]. The frequencies of the salivary gel filtration pattern of H substance in group O secretors and non-secretors are given in Table I.

The gel filtration patterns of the H substance were also studied in the saliva of group A, B and AB subjects. In these salivas the H substance was also found to be secreted according to the seven gel filtration types. Type VIII, which is the term used for the absence of any active fraction, was also detected. The various combinations of gel filtration patterns of A and B substances with the H substance patterns are reported in Table IV and Table V, respectively. The gel filtration patterns of H

TABLE IV

CORRELATION BETWEEN A AND H GEL FILTRATION PATTERNS
The number of cases is recorded.

	H-1	*H-1, 2*	*H-1, 3*	*H-1, 2, 3*	*H-2*	*H-3*	*H-2,3*	*H-*
A-1	13	1	2					
A-1, 2	1	7		1				
A-1, 3	3		14					
A-1, 2, 3	5			27		3		
A-2					4			
A-3						3		
A-2, 3							7	
A-								

TABLE V

CORRELATION BETWEEN A AND H GEL FILTRATION PATTERNS
The number of cases is recorded.

	H-1	*H-1, 2*	*H-1, 3*	*H-1, 2, 3*	*H-2*	*H-3*	*H-2, 3*	*H-*
B-1	3		3					
B-1, 2		1			2			
B-1, 3			4			1		
B-1, 2, 3	2			7			1	
B-2								
B-3								
B-2, 3							2	
B-								3

substance in the saliva of group AB subjects are given in Table IIb. The results indicate, as a general rule, a close relationship between the salivary patterns of the A and B substances and those of the H substance in the so-called non-secretors. In the saliva of secretors, a similar relationship was also found in most cases, but in 26 cases among A, B and O subjects the H substance gel filtration pattern was different from that of the group specific A or B substances. In seven of these cases, the H substance had only fractions 2 and 3 and lacked fraction 1.

Group AB subjects presented a still clearer example of the possible independence of A, B and H gel filtration patterns in the same subject. In this group two cases were observed in which the three ABH substances exhibited a completely different pattern (Table IIa and b, case No. 4,5,7).

The problem of the individuality of the H substance with respect to the A and B substances of a given saliva was also investigated. As the anti-H serum is known to react also with A and B substances, the hypothesis could be advanced that in a subject typed for example as A-1,2,3/H-1,2,3 the H pattern was due to a non-specific inhibition of anti-H serum by the three A active fractions.

The following type of experiment was developed in which saliva lacking fraction 1 was used to ensure a complete saturation of blood group antigens by the antibodies. 0.5 ml of anti-A serum titred 1/4 was added to 0.7 ml of saliva A-2,3/H-2,3. After incubation for 1 h, the solution was gel filtered through a small Sephadex G-100 column with the usual buffer. The haemagglutination inhibition test was then performed with both anti-A and anti-H sera as usual. Only fractions 2 and 3 of the H substance were detected with the usual elution volume. The same saliva was incubated with anti-H serum (0.7 ml : 0.5 ml) and then gel filtered on Sephadex G-100. The inhibition test revealed the disappearance of the H fractions while A fractions 2 and 3 were still present.

Constancy of the ABH salivary gel filtration patterns

The use of the standardised method on 20 × 1.2 cm Sephadex G-100 beds permitted a careful control of the technical reproducibility of the data. In fact the elution volumes of each fraction showed negligible variations (*e.g.* 1 tube) in all the experiments performed on a given column. In addition, the constancy of the secretory pattern was verified in the saliva of a number of subjects (32 medical students) who were examined many times in various physiological conditions.

The influence of the preservation of the samples of saliva before gel filtration on the reproducibility of the data was also investigated. Saliva maintained at 4° for 48 h, or at −20° for several months, preserved its original gel filtration group specific pattern. On the other hand preservation at 4° for 3–4 days or more resulted in a decrease of blood group activity and in erroneous data with respect to fractions 2 and 3.

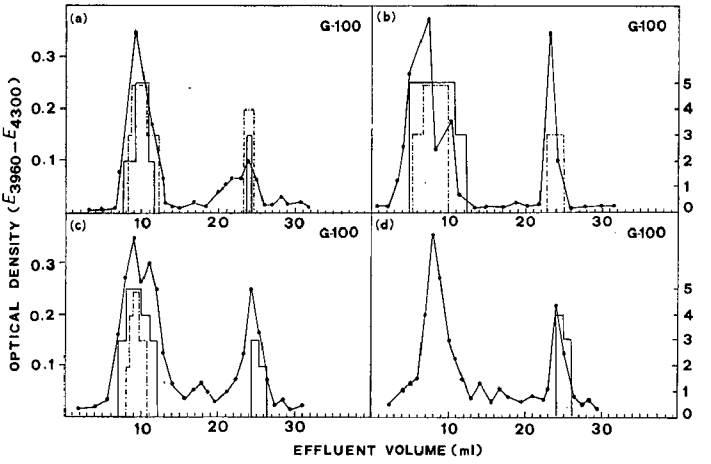

Fig. 4. Some results of fucose analyses on the eluates from gel filtration of saliva on Sephadex G-100 columns (20 × 1.2 cm). The solid line represents the group specific activity of the main antigen of the subject and the broken line the specific activity of the associated H substance. The curve indicates the optical density for fucose. (a) saliva A-1,3/H-1,3; (b) saliva B-1/H-1,3; (c) saliva A-1,3/H-1; (d) saliva H-3.

Fucose analyses

Fucose determinations on the eluates from column gel filtration of the various types of saliva were performed with the aim of giving an indirect support to the data obtained by the serological method. Positive reactions were obtained at the elution volumes of the three active peaks, *i.e.* fraction 1, fraction 2 and fraction 3. The fucose reaction is common to A, B and H substances and this could explain some of the results, *e.g.* the presence of a fucose peak with the elution volume of fraction 2 in an A subject who secreted fractions 1 and 3 only, but had fraction H-2.

In Fig. 4 some gel chromatograms are given showing the different results which can be obtained. It should be noted that the fucose peak at the elution volume of fraction 2 frequently had a very low optical density value. In addition, it was sometimes displaced by one tube from the tube containing the active substance. The excluded fucose peak was detectable also in the saliva of the so-called non-secretors lacking an active fraction 1, due probably to some other salivary excluded glycoproteins.

DISCUSSION

Salivary ABH gel filtration patterns

The data presented here show that, besides the well-known ABH blood group

specific fraction excluded from Sephadex G-100 or G-200 (refs. 1, 9, 10), that we termed fraction 1, two additional ABH subfractions occur in the saliva of secretors (fraction 2 and fraction 3). The saliva from non-secretors lacks fraction 1 but can have one or both of the subfractions.

The approximate molecular weights of fractions 2 and 3 have been previously estimated by gel filtration[1] as being between 10 000 and 13 000, and no greater than 1500–2000, respectively. The chemical nature of these subfractions is under investigation.

The three fractions of each of the A, B and H antigens can be variously represented and associated in saliva, thus giving rise to eight gel filtration patterns for each antigen (Figs. 1–3 and Table III). This pattern is a stable character and can be determined by a satisfactorily reproducible method.

As the subjects of group A, B and AB usually also secrete the antigen H in their saliva, the association of the patterns of each antigen in a single subject forms the individual salivary ABH gel filtration pattern. It should be noted that in some subjects gel filtration patterns of the single antigens have been found which differed from each other (see Tables II, IV, V).

Symbols are proposed which indicate the whole ABH gel filtration pattern of a given person, as in the following examples taken from our cases:

O (H-1,2,3)	A (A-1,2/H-1,2)
O (H-1,3)	A (A-1,2,3/H-1,2,3)
O (H-2)	A (A-1,2,3/H-1)
O (H-1)	A (A-1,2/H-1,2,3)
O (H-1,2)	A (A-2/H-2)
B (B-1,3/H-1,3)	AB (A-1/B-1/H-1)
B (B-1/H-1)	AB (A-1,2/B-1/H-1,3)
B (B-1/H-1,3)	AB (A-1,2,3/B-1/H-1,3)
B (B-2,3/H-2,3)	AB (A-1,3/B-/H-1,3)
B (B-/H-)	AB (A-2,3/B-/H-2,3)

The group of the considered subject is indicated with capital letters. The gel filtration pattern of each of the A, B and H antigens is reported in brackets; the gel chromatographic fractions of each antigen are indicated by 1, 2, 3. Since it was interesting to see whether the three active fractions of each of the A, B and H substances were or were not present in the erythrocyte membrane, experiments were carried out on solubilised red-cell stroma. The three fractions were always present, in a water-soluble form, irrespectively of the secretor status of the subject. A subsequent paper in this journal will deal with these findings[11].

As a consequence of the recent studies on the ABH substances of the red cell membrane[11–16] and of the discovery of the water- and alcohol-soluble fractions 2 and 3 from saliva[1] and red cells[11], it appears evident that the distinction of FRIEDENREICH AND HARTMANN[17] between water-soluble and alcohol-soluble ABH substances is no longer valid. We believe that blood group substances from secretions and red cells have the same basic chemical nature; different isolation methods are required owing to the bindings of the group specific substances with other components of the red cell membrane.

New approach to the problem of secretors and non-secretors

Our results suggest that the old problem of secretion of ABH substances in saliva should be reconsidered. Since the discovery of YAMAKAMI[18], it has been known that A and B antigens are present in saliva. LEHRS[19] and PUTKONEN[20] realised that this character is dimorphic and two classes of individuals were identified, *i.e.* secretors and non-secretors. The inheritance according to a Mendelian system was demonstrated by SCHIFF AND SASAKI[21]. Later FRIEDENREICH AND HARTMANN[17] suggested a distinction of ABH antigens into two forms: the water-soluble substances of the secretions and the alcohol-soluble substances from the tissues and the red cells. GRUBB[22] gave evidence that ABH secretion is associated with the Lewis blood groups. The importance of Hh genes was also elucidated[23].

The main problem, especially in disputed paternity cases, was a reliable distinction between secretors and non-secretors. This distinction is very easy in persons having a good titre of ABH antigens in saliva or those lacking specific activity. On the other hand the distinction is difficult between weak secretors and the non-secretors whose saliva is not completely devoid of blood group specific activity. This could explain the fact that the frequency reported for secretors and non-secretors vary with different workers and with different ABO group for the same workers[6,7,24]. To overcome those drawbacks, it has been therefore recommended to use a rigorously standardised quantitative method and a histogram of each individual antiserum[17,25].

The method reported here allows a good qualitative distinction between secretors and non-secretors. In addition, the previously unexplained reasons of the weak activity of many non-secretors seem to be satisfactorily elucidated. Secretors can now be considered those persons who have in their saliva the main active fraction 1, which is excluded from Sephadex G-200 and G-100. This fraction is secreted alone or in association with fraction 2, fraction 3 or with both fractions 2 and 3.

The so-called non-secretors always lack fraction 1. They have fraction 2, fraction 3, or both, these being the cases in non-secretors whose saliva has a very weak group specific inhibitory activity. This activity, apparently, is due to the specific fractions 2 and/or 3.

A few non-secretors lack any active fraction in their saliva, and therefore this saliva is free of group specific activity. These subjects could be termed true non-secretors. Since eight salivary patterns of each of the A, B and H antigens have been identified in place of the previously known dimorphic character, family studies were undertaken in order to determine whether these patterns are inherited molecular phenotypes. The results have shown that this is the case and the details will be reported elsewhere[26].

Recommended method

A brief comment on the drawbacks of thin-layer gel chromatography and on the recommended procedure on small Sephadex G-100 columns seems useful here. Thin-layer gel chromatography was abandoned after some hundred determinations because of the following drawbacks. The method is much too laborious as the plates must be prepared each time; three spots of each specimen of saliva must be run to allow the examination of the three ABH antigens and the elution step is tedious and unpractical. In addition, the method can give rise to serious errors. In viscous salivas

the migration of fraction 1 is sometimes retarded so that the subject can be erroneously considered a non-secretor; fractions 2 and 3 can be erroneously left undetected, due to the loss of the active material during the elution step.

Gel filtration on small 20 × 1.2 cm Sephadex G-100 beds is on the contrary a very practical and valid technique for routine purposes. 1-ml samples of centrifuged, unboiled saliva are sufficient for the detection of the three ABH fractions. The results are not affected by the viscosity of the saliva. If a timed-flow fraction collector with six or more concentric circular rows of at least 50–60 holes is used, six or more Sephadex columns can be employed simultaneously. This is particularly useful for family studies.

The total effluent volume usually collected at room temperature in about 6 h is only 35 ml divided into 32–35 test tubes.

A critical step of the method is the serological identification of fraction 2 and fraction 3 for which an adequate experience and suitable antisera are required due to their weak inhibitory activity. In fact the specific inhibition for fraction 1 is strongly positive in 4–5 tubes, while for fractions 2 and 3 it is confined to 1–3 tubes and is also usually incomplete.

To avoid errors, a correct macroscopic reading of the inhibition of the haemagglutination should be performed by means of a standardised technique. Fresh red cells should be used. Antisera should have low titre, *e.g.* 1/4, to allow antibodies to be absorbed as much as possible by the weaker antigens. At the same time the antisera should have a high binding constant (K_0) which should be between 10^6–10^8 with a heterogeneity index of about 0.5. This is required because the inhibition test is performed on the contents of each tube by an all-or-none method. It is therefore indispensable that the tubes which do not contain active material give a strong agglutination. In other words, after a short centrifugation, a single clump should be formed which is not easily broken when the tube is vigorously shaken. Under the above-mentioned conditions even an incomplete inhibition (±; +) can be assumed as evidence for the presence of an active group specific fraction in the tube under examination.

ACKNOWLEDGEMENTS

We are grateful to Prof. A. SERRA for helpful criticism and advice and to Dr. J. AMERIO for revising the English manuscript. We are also indebted to Miss M. T. A. FLORIS and to Mr. V. GENTILE for technical assistance.

This work was in part supported by the Consiglio Nazionale delle Ricerche.

REFERENCES

1 A. FIORI, G. V. GIUSTI, G. PANARI AND G. PORCELLI, *J. Chromatog.*, 55 (1971) 337.
2 K. BOORMAN AND B. DODD, *Blood Group Serology*, 2nd ed., Churchill, London, 1961.
3 O. H. LOWRY, N. J. ROSEBROUGH, A. L. FARR AND R. J. RANDALL, *J. Biol. Chem.*, 193 (1951) 265.
4 Z. DISCHE AND L. B. SHETTLES, *J. Biol. Chem.*, 175 (1948) 595.
5 A. FIORI, G. V. GIUSTI AND G. PANARI, *Med. Leg. Domm. Corpor.*, 2 (1969) 364.
6 T. G. FORMAGGIO, *Minerva Medicolegale*, 71 (1951) 157.
7 A. ANDERSEN, *Acta Path. Microbiol. Scand.*, 31 (1952) 448.

8 G. V. GIUSTI, G. PANARI AND M. T. FLORIS, *Acta Med. Romana*, in press.
9 W. M. WATKINS, *Science*, 152 (1966) 172.
10 E. A. KABAT, *Blood Group Substances*, Academic Press, New York, 1956.
11 A. FIORI, G. V. GIUSTI AND G. PANARI, *J. Chromatog.*, 55 (1971) 365.
12 F. A. GREEN, *J. Immunol.*, 99 (1967) 56.
13 P. ZAHLER, *Vox Sang.*, 15 (1968) 81.
14 N. B. WHITTEMORE, N. C. TRABOLD, C. F. REED AND R. I. WEED, *Vox Sang.*, 17 (1969) 289.
15 I. LIOTTA, M. QUINTILIANI, L. QUINTILIANI, A. BUZZONETTI AND E. GIULIANI, *Vox Sang.*, 17 (1969) 11.
16 M. D. POULIK AND P. K. LAUF, *Clin. Exp. Immunol.*, 4 (1969) 165.
17 V. FRIEDENREICH AND G. HARTMANN, *Z. Immun. Forsch.*, 92 (1938) 141.
18 K. YAMAKAMI, *J. Immunol.*, 12 (1926) 185.
19 H. LEHRS, *Z. Immun. Forsch.*, 66 (1930) 175.
20 T. PUTKONEN, *Acta Soc. Med. Fenn. Duodecim*, Ser. A, 14, No. 12 (1930) 113.
21 F. SCHIFF AND H. SASAKI, *Klin. Woch.*, 11 (1932) 1426.
22 R. GRUBB, *Nature*, 162 (1948) 933.
23 R. R. RACE AND R. SANGER, *Blood Groups In Man*, 5th ed., Blackwell Scientific Publications, Oxford, 1968.
24 R. T. SIMMONS, N. M. SEMPLE AND J. J. GRAYDON, *Med. J. Aust.*, 1 (1951) 105.
25 G. HARTMANN, *Group Antigen In Human Organs*, Munksgaard, Copenhagen, 1941.
26 A. FIORI, A. SERRA, G. PANARI AND G. V. GIUSTI, in preparation.

CHROM. 5092

GEL FILTRATION OF ABH BLOOD GROUP SUBSTANCES

III. ABH GEL FILTRATION PATTERN OF SOLUBILISED RED CELL STROMA

A. FIORI, G. V. GIUSTI AND G. PANARI

Istituto di Medicina Legale e delle Assicurazioni, Università Cattolica del Sacro Cuore, 00168 Rome (Italy)

(Received August 20th, 1970)

SUMMARY

Human red cell stroma were solubilised with the nonionic detergent Triton-X-100. By gel filtration of the solubilised material on Sephadex G-200 and G-100, three group specific fractions of each of the A, B and H substances were detected. Fraction 1 is water-soluble and can be precipitated with alcohol, while fractions 2 and 3 are water- and alcohol-soluble. The three active fractions had the same gel filtration and thin-layer chromatographic behaviour as fractions 1, 2 and 3 detected in saliva and reported in a previous paper. The probable identity of the stromal fraction 3 with the blood group specific glycolipid isolated by many investigators from erythrocytes is suggested.

INTRODUCTION

It has been shown in a previous work[1] that seven gel filtration patterns (Types I–VII) of the A, B and H substances can be detected in human saliva. Only a small number of subjects have no salivary ABH antigens (Type VIII, *i.e.* true non-secretors). The various patterns are formed by three serologically active fractions of each antigen, termed fractions 1, 2 and 3, which can be easily detected by gel filtration on small Sephadex G-100 columns owing to their quite different molecular weights. Each of these fractions is secreted in saliva alone or associated with one or both of the other fractions[1].

It was of interest to determine whether the three naturally occurring fractions of the ABH substances were also present in the red cell stroma. From the data presented in this report, it seems evident that three active fractions of each of the A, B and H substances are normally present in red cells and have the same gel chromatographic and solubility behaviour as the salivary ABH fractions.

MATERIALS AND METHODS

Preparation of the samples

The blood of 31 donors (nine group A; sixteen O; four B and two AB) was

examined. 10 ml of whole blood were usually employed. The blood was centrifuged for 30 min at 3000 r.p.m. and the red cells were washed three times with saline. The washed cells were haemolysed in 10 vol. of 0.005 *M* phosphate buffer (pH 7.4) and centrifuged for 40 min at 20 000 × *g*. The supernatant was carefully decanted and the ghost button was resuspended in the same volume of fresh buffer. The operation was repeated three or more times until the supernatant was free of haemoglobin. Finally, the clear white precipitate surrounding the small central-buff-coloured portion of the button was aspirated and suspended in 2 ml of 0.05 *M* Tris–HCl buffer (pH 7.3). In some cases the ghosts were resuspended in saline or in 0.005 *M* phosphate buffer.

The solubilisation of red cell stroma was then performed by adding 20 μl of concentrated Triton-X-100 (BDH, Ltd.) to each millilitre of suspension. The suspension clarified immediately on shaking. The solubilisation of the ghosts was controlled by a phase-contrast microscope. The solution was directly employed for gel filtration experiments or submitted to methanol fractionation of the blood group substances, followed by gel filtration.

Gel filtration

Gel filtration was performed on Sephadex G-200, G-100, G-50, G-25 and Sepharose 4B columns as previously described[1,2]. Bed dimensions of 36 × 1.5 cm or 20 × 1.2 cm; 32 × 2.5 cm; 80 × 2 cm; 38 × 2.5 cm; 32 × 2.2 cm were used, respectively. 0.05 *M* Tris–HCl buffer (pH 7.3) containing 0.9% NaCl was employed as eluant for Sephadex G-200, G-100, G-50 and G-25, and 0.025 *M* phosphate buffer (pH 7.2) for Sepharose 4B. In some particular experiments on Sephadex G-50 and G-25, the Tris–HCl buffer was replaced by distilled water.

Column packing and the void volumes were checked using a freshly prepared dilute solution of Blue Dextran 2000 (Pharmacia, Uppsala). Cytochrome *c*, insulin, glucagon, bacitracin, oxytocin and sucrose were used as reference substances of known molecular weight.

The fractions eluted from Sephadex G-200, G-100, G-50 and G-25 were directly examined by the technique of haemagglutination inhibition. Only for the tubes containing haemolytic material was an additional treatment required as described below.

The contents of the tubes from Sepharose 4B gel filtration experiments were made hysotonic by adding 0.1 ml of a 14.6% solution of NaCl to 2 ml of eluate and then were submitted to serological analysis. The fractions obtained from Sephadex G-50 and G-25 with distilled water as eluant were used for some TLC experiments.

Thin-layer chromatography

Silica Gel G (Merck, Darmstadt) plates (20 × 20 cm), 250 μ thick, activated at 110° for 1 h, were developed once or twice with chloroform–methanol–water (65:25:4) (solvent I) or with petroleum ether–ethyl ether–acetic acid (90:10:1) (solvent II). The samples were applied as separate spots or, when small-scale preparative runs were required, by streaking the sample along the whole origin line. The spots or the bands were revealed by exposure of the plates to iodine vapours. Carbohydrates were detected by spraying the plate with 1.6% aq. orcinol–60% sulphuric acid solution (1:7.5) and heating 10 min at 110°. The blood group specific activity was

determined on the untreated chromatograms by scraping the silica gel layer at various levels and by eluting with solvent I. After standing overnight, the suspension was centrifuged and the supernatant evaporated to dryness. The residue was finally dissolved in 0.2 ml of saline and serologically determined. Protein and carbohydrate tests were also performed in some eluates with the Folin–Ciocalteu reagent[3] and the orcinol reagent[4], respectively.

Haemagglutination inhibition test

The technique described in a previous paper was employed for testing ABH activity[2]. Where haemolysis was present, *i.e.* in the zone of the gel chromatograms in which Triton-X-100 was eluted, the detergent was eliminated as described below.

RESULTS

Sephadex G-100 gel filtration

Gel filtration of solubilised red cell stroma on Sephadex G-100 columns gave a pattern for each of the A, B and H substances as shown in Fig. 1. Three active fractions were detected for each antigen. The first fraction was eluted with the

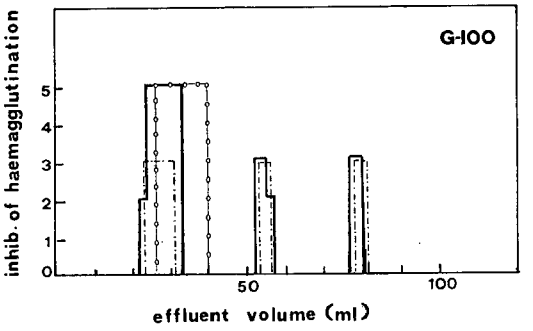

Fig. 1. Gel filtration of solubilised red cell stroma (group A) on Sephadex G-100 (36 × 1.5 cm bed). The solid line indicates the A blood group activity and the broken line the H activity. The results of the inhibition of haemagglutination are scored as follows: 0 = one clump; 1 = ++++; 2 = +++; 3 = +; 4 = ±; 5 = − (no agglutination); ○—○ represents the haemolytic effluent.

excluded effluent. Only one or two of the leading tubes of the first peak were free of haemolytic substance and were therefore serologically determined without any preliminary treatment. Because the contents of the other tubes were haemolytic (Fig. 1), Triton-X-100 was eliminated by precipitating the blood group substances. For this purpose, four volumes of absolute ethanol were added to the content of each tube. The supernatant was discarded, and the precipitate was washed with 80% methanol, suspended in saline and serologically tested. Blood group activity was detected both in the insoluble precipitate and in that part of the precipitate which was still soluble in saline. A strong specific inhibition occurred in the leading part of the haemolytic zone which was excluded from the gel (Fig. 1).

A second active fraction was detected with an elution volume of 56–57 ml in 36 × 1.5 cm columns, and of 18 ml in 20 × 1.2 cm columns. A third specific fraction

was identified with elution volumes of 78–80 ml in larger columns and of 27 ml in smaller ones. The two subfractions had a relatively weaker activity, which was confined to two or three tubes.

The three active fractions were termed fraction 1, fraction 2 and fraction 3, respectively, as the gel chromatographically similar fractions of the saliva[1,2].

Each of the A, B and H antigens had the three active fractions in all the blood samples examined. In subjects of group O only fractions 1, 2 and 3 for H substance were identified. In persons of group A, B and AB the three fractions were represented for each of the group antigens as well as for the H antigen. Only slightly quantitative differences in the inhibition test were observed between A_1 and A_2 subjects; in our cases A_1 subjects were detected by absorbed human anti-A serum and also gave a weak agglutination with anti-H from *Ulex europaeus*. The elution volumes for the different antigens in the same sample were sometimes identical or sometimes only similar as also observed in saliva[1,2].

Sephadex G-200 gel filtration

An easier detection of fraction 1 was realised by gel filtration on Sephadex G-200. This dextran gel allowed a nearly complete separation between the main excluded fraction (fraction 1) and the haemolytic zone (probably a Triton–lipoprotein complex) which is retained (Fig. 2). Only in the determination of H substance was a

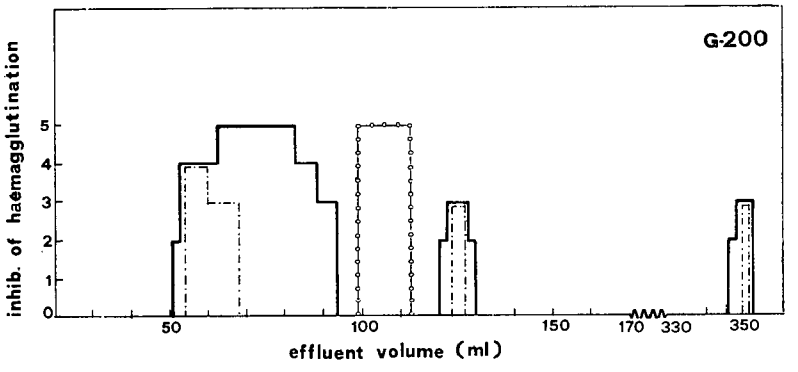

Fig. 2. Gel filtration of solubilised red cell stroma (group A) on Sephadex G-200. The haemolytic effluent (○—○) is completely separated from the blood group specific fractions A and H.

negligible overlapping of the haemolytic zone with the last part of the excluded peak frequently observed.

Fraction 1 had an elution volume of about 65–70 ml, and the haemolytic zone was located immediately after it, having an elution volume of approx. 108 ml and usually covering 20 ml. The elution volumes of fractions 2 and 3 were 125 and 350 ml, respectively.

The haemolytic zone was investigated for the presence of the specific active substances. For this purpose, the content of each tube exhibiting haemolysis was brought to dryness and absolute methanol was added to the residue. The precipitate was washed with methanol, dried and suspended in 0.4 ml of saline and serologically determined. Specific inhibition was observed in a few tubes of the last part of the excluded peak only in some group O samples.

In some cases another control was performed by eliminating Triton-X-100 through TLC on silica gel plates. The contents of the haemolytic tubes were concentrated on the whole origin of the plate by the streaking method and developed with solvent I. Triton-X-100 was detected by iodine vapour as a large yellow band near the front. The remaining area of the chromatogram was divided into three zones which were eluted with solvent I and serologically determined, giving constantly negative results.

Relationship between ABH patterns of red cell stroma and saliva

To study the relationship between the ABH gel filtration patterns of the solubilised red cell stroma with those of the saliva, the stroma of some subjects whose saliva lacked fraction 1 (so-called non-secretors), and had fraction 2 and/or fraction 3, were examined by gel filtration on Sephadex G-200 and G-100. In each subject all three fractions were found in solubilised stroma, irrespective of the secretor status of the individual.

Sepharose 4B gel filtration

The relation between fraction 1 detected in solubilised stroma and fraction 1 from saliva was also investigated by gel filtration on Sepharose 4B. The results of a

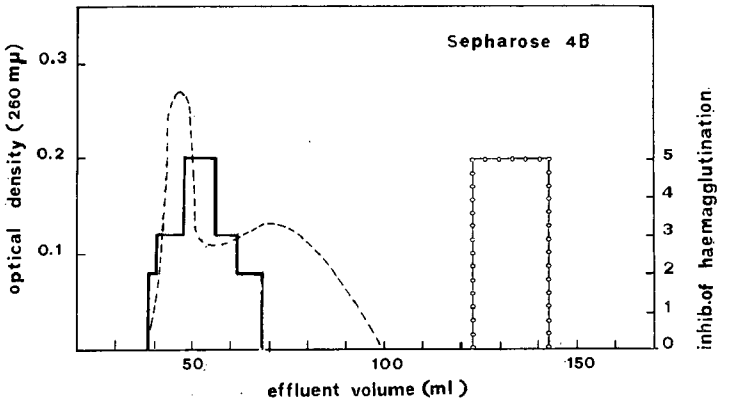

Fig. 3. Gel filtration of solubilised stroma (group O) on Sepharose 4B. The broken line represents the elution profile of Blue Dextran 2000. (○—○) indicates the hemolytic effluent.

typical experiment are shown in Fig. 3. The elution curve of the active substance from red cell stroma was practically the same as that for fraction 1 from saliva. Only a part of the active substance was excluded from Sepharose 4B; the remaining part was retained as shown by recycling experiments. The haemolytic material was eluted later. Broadening of the haemolytic zone was observed in detecting the H substance, so that the active fraction 1 was almost immediately followed by the haemolytic effluent.

Fraction 1

Samples of fraction 1 from Sephadex G-200 columns were treated to obtain the group specific substance free from lipids. The excluded effluent was brought to

dryness and 80% methanol was added to the residue. The precipitate was suspended in chloroform–methanol (1:1). The precipitate again formed was dried and washed with chloroform. The final precipitate was only partially soluble in saline. The undissolved part had a strong group specific activity but the aqueous supernatant also was clearly active.

TLC on Silica Gel G of the aqueous supernatant and of the chloroform–methanol and chloroform extracts was performed using solvent I (for neutral lipids) and solvent II (for phospholipids). After exposure of the plates to iodine vapour, yellow spots were located only in the chromatograms of chloroform–methanol and chloroform extracts. On the other hand, the aqueous supernatant exhibited a strong positive reaction with the orcinol–sulphuric acid reagent at the starting line (Fig. 4a).

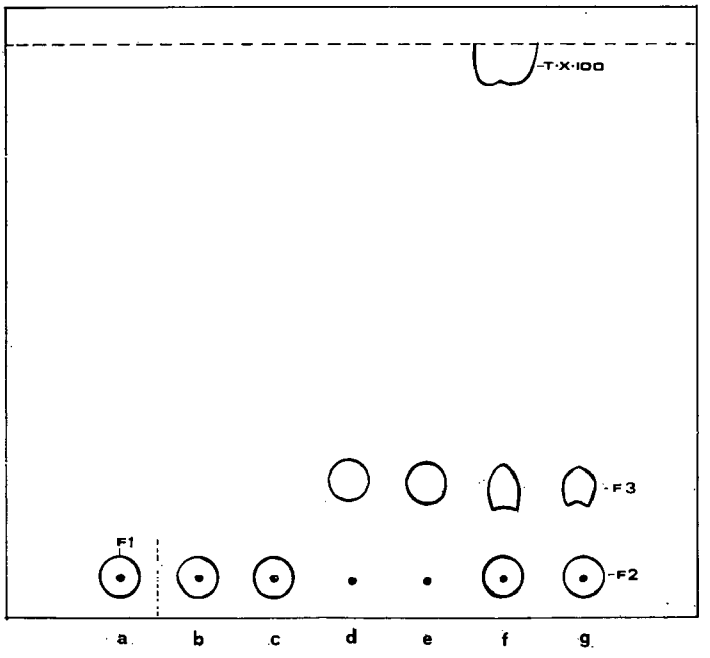

Fig. 4. Thin-layer chromatography on Silica Gel G of ABH blood group specific fractions Solvent: chloroform–methanol–water (65:25:4). (a) lipid-free fraction 1 from solubilised stroma; (b) fraction 2 and (d) fraction 3 from solubilised stroma; (c) fraction 2 and (e) fraction 3 from saliva; (f) fractions 2 and 3 from methanol extraction of solubilised stroma. Triton-X-100 on the solvent front; (g) fractions 2 and 3 from methanol extraction of saliva of Type IV.

In the same place the untreated chromatogram had a clear specific activity. The orcinol and the serological tests were negative on the chromatograms of chloroform–methanol and chloroform extracts.

Fraction 2

Fraction 2 was also characterised by gel filtration on Sephadex G-50. The effluent from Sephadex G-100 gel filtration of solubilised stroma was pooled in the zone containing fraction 2. After dialysis overnight against distilled water and concentration to 2 ml, the samples were gel filtered on a Sephadex G-50 column.

The blood group specific activity was detected only in the excluded effluent. On the other hand cytochrome *c* was retained, as reported in a previous work[2].

Fraction 3

Fraction 3 was characterised in a similar way by gel filtration on Sephadex G-25. Blue Dextran 2000, cytochrome *c*, insulin, glucagon, bacitracin, oxytocin and sucrose were used as references of known molecular weight. The blood group specific activity had an elution volume of 104–105 ml, *i.e.* the same elution volume as fraction 3 from saliva[2].

Samples of fraction 3 isolated by gel filtration on Sephadex G-100 were dialysed against distilled water. The concentrated dialysate exhibited a clear specific activity while the retenate was free of blood group activity. Fraction 3 from solubilised stroma is therefore dialysable as fraction 3 from saliva[2].

Fractions 2 and 3

The TLC behaviour of fractions 2 and 3 from solubilised red cell stroma was determined and compared with that of fractions 2 and 3 from human saliva. Samples of fractions 2 and 3 from saliva of type IV (*i.e.* containing fractions 1, 2 and 3) and from solubilised stroma were isolated by gel filtration on Sephadex G-100. Fraction 2 was then dialysed against distilled water, brought to dryness and finally dissolved with 80% methanol. Fraction 3 was desalted by gel filtration on Sephadex G-25, then concentrated and dissolved with 80% methanol. The samples were chromatographed on silica gel by a double development with solvent I. The spots were revealed with iodine vapour followed by spraying with the orcinol–sulphuric acid reagent. The blood group specific substances were also detected on untreated chromatograms by the serological test on the eluates. For this purpose the silica gel was scraped, eluted with solvent I, the eluate was centrifuged and the solvent evaporated. The dried residue was dissolved with 0.2 ml of saline and serologically tested. Fraction 2 from saliva and from stroma did not move from the starting line, while fraction 3 migrated about 3 cm (Fig. 4b, c, d, e).

A similar investigation was carried out on fractions 2 and 3 extracted directly from saliva of Type IV and from solubilised stroma by treatment with four volumes of absolute methanol. Since it was known from a previous work[2] that the salivary fraction 1 can be precipitated in alcohol and fractions 2 and 3 are alcohol soluble, it seemed obvious that stromal fractions 1, 2 and 3 behave in the same manner. The precipitates from the methanol treatment of saliva and of solubilised stroma were therefore discarded. Some of the methanol extracts were then brought to dryness, the residue was dissolved with saline and gel chromatographed on small 20 × 1.2 cm Sephadex G-100 columns. Fractions 2 and 3 were identified at the usual elution volumes both in salivary and stromal extracts.

Some of the other methanol extracts were concentrated to 0.2–0.3 ml and then chromatographed on silica gel plates by two developments with solvent I. The spots were revealed as described above. The results are recorded in Fig. 4f, g. Triton-X-100 migrated as a large spot with the solvent front and gave a yellow colour with iodine vapour. Fraction 2 did not move from the starting line and fraction 3 migrated about 3 cm.

DISCUSSION

Three blood group specific fractions of each of the A, B and H substances were detected by gel filtration of solubilised red cell stroma. The fractions have been called fraction 1, fraction 2 and fraction 3, respectively. The same nomenclature used to indicate the active fractions of ABH substances identified in saliva of secretors and non-secretors[1] was adopted because the blood group specific fractions from red cell stroma had a gel chromatographic behaviour identical to the active fractions from saliva.

Gel filtration on Sephadex G-200 is preferable for studying fraction 1 of solubilised stroma because the haemolytic material is completely separated from this and the other fractions, so that no particular treatment is required for the serological determination in the relevant tubes. Since a large volume of effluent is required to elute fraction 3 from Sephadex G-200 columns, we have found it very practical, throughout the work, to detect fractions 2 and 3 by gel filtration on small 20 × 1.2 cm beds of Sephadex G-100.

A polydispersity of molecular weight for stromal fraction 1 was demonstrated in the same way as for salivary fraction 1 (ref. 2). Gel filtration of solubilised stroma on Sepharose 4B showed that only the leading part of the first active peak, *i.e.* of fraction 1, is excluded. The exclusion limit for polysaccharides on Sepharose 4B is $5 \cdot 10^6$ ($20 \cdot 10^6$ for proteins); therefore it can be assumed that the molecular weight of that part of fraction 1 which is excluded from Sepharose 4B is up to or over $5 \cdot 10^6$. The final part of the active peak is retained, as shown by recycling experiments, and apparently has a lower molecular weight. Stromal fraction 1 was also completely excluded from Sephadex G-200 (exclusion limit for dextran: 200 000) as well was fraction 1 from saliva.

Fraction 2 was not dialysable and had the same elution volumes on Sephadex G-200 and G-100 as salivary fraction 2. It was also excluded from Sephadex G-50. It is therefore reasonable to assume that its molecular weight is of the same order as that of salivary fraction 2.

Fraction 3 was dialysable and had elution volumes on Sephadex G-200, G-100 and G-25 as salivary fraction 3. For this fraction it also seems reasonable to assume a molecular weight near to that of the salivary fraction 3.

The evidence of a relationship between the three active fractions of stromal origin and the three salivary fractions leads us to the conclusion that the solubilisation of the red cell stroma by the nonionic detergent Triton-X-100 does not produce artifacts with respect to ABH blood group substances. In fact these are brought in solution in three active fractions which have a gel chromatographic behaviour identical to active blood group fractions occurring naturally in untreated saliva.

The red cell stroma of the subjects examined always contained three fractions of the corresponding antigen, irrespective of their secretor status. In particular, fractions 1, 2 and 3 were detected in solubilised stroma of subjects who only had fraction 2 in their saliva, or fraction 3 or both fractions 2 and 3 but lacked salivary fraction 1.

The donors of group O had in their stroma only three fractions of H substance. Donors of groups A and B had three fractions for A or B antigens and three fractions for H and finally donors of the AB group had three fractions for A, B and H sub-

stances. In contrast with the findings of GREEN[5] and WHITTEMORE *et al.*[6] and in agreement with the data reported by LIOTTA *et al.*[7], H activity was also detected in solubilised stroma from A_1 and A_1B subjects. This is not surprising since it is well known that a weak reactivity to anti-H lectin is usually also exhibited by A_1 erythrocytes.

The present study gives only general information on the nature of the blood group substances from red cells. However some preliminary considerations can be made, also on the basis of more recent literature in this field.

The A, B and H substances had been extracted from erythrocytes chiefly by ethanol until solubilisation procedures of the stroma were worked out in more recent years. This leads to the conclusion that the substances from red cells were alcohol-soluble and chemically different from the water-soluble substances of secretions (see ref. 8).

The work carried out by YAMAKAWA AND IIDA[9], YAMAKAWA *et al.*[10–12], HAKOMORI[13], RADIN[14], HAKOMORI AND JEANLOZ[15], HANDA[16] and KOSCIELAK[17,18] established that A and B substances from red cells are glycolipids. More recently it was demonstrated by HAKOMORI AND STRYCHARZ[19] that the material extracted with ethanol from red cell stroma is a sphingoglycolipid with a single carbohydrate chain. On the other hand, some attempts have been made to obtain the ABH substances from red cells by means of extractions with aqueous solutions of diluted ethanol[20–23]. The data of STEPANOV *et al.*[23] were assumed by KABAT[8] as an indication of the similarity between ABH group specific substances from saliva and those from red cells.

A water-soluble blood group specific substance was also detected in the red cell haemolysate and electrophoretically characterised in agar gel by FIORI *et al.*[24]. POULIK AND LAUF[25] reported the isolation of group A specific material from stroma exposed to pH 2–2.2 and extracted with a two phase system (butanol–water). The material was excluded from Sephadex G-200. A similar technique was employed by WHITTEMORE *et al.*[6] and A, B and H activities were detected in aqueous extracts. The material was free of lipids and the extracted blood group substances were considered a glycoprotein with a molecular weight greater than $3 \cdot 10^5$ or probably greater than $1 \cdot 10^6$. LIOTTA *et al.*[7] extracted from red cell stroma a phenol-soluble and water-soluble A specific substance, using the phenol method of MORGAN AND KING[26]. The group specific material was excluded from Sephadex G-200.

More recent studies have given strong support to the hypothesis that blood group specific substances from red cells are glycoproteins as well as group substances from secretions. ZAHLER *et al.*[27] demonstrated A activity in glycolipids as well as in erythrocyte membrane proteins solubilised with 2-chloroethanol and gel filtered on Sephadex LH-20 to separate lipids.

The solubilisation of the red cell stroma was realised by GREEN[5] by means of 2% sodium dodecyl sulphate. Removal of the detergent was obtained by passing the solubilised membranes over a Dowex column. After removal of the detergent, the group specific material was found to be excluded from Bio-Gel P 300.

In the present study a simple method is proposed for the isolation of blood group substances from red cell stroma. A complete solubilisation of stroma is obtained by the nonionic surfactant Triton-X-100 and the detergent is separated from the active material by gel filtration on Sephadex G-200. Gel filtration on Sephadex G-100 separates the haemolytic material from only the active fractions 2 and 3. By this

method, loss of the material is prevented and artifacts are minimised. 4 to 5 ml of packed red cells are sufficient to obtain active material for microanalytical determinations and serological tests. By this method it has been determined that fraction 1 excluded from Sephadex G-200 is water-soluble and is precipitable, and in great part denaturable, by 80% methanol or ethanol. It should be considered a glycoprotein–lipid complex from which lipids can be removed without loss of the specific activity of the molecule. This fraction is therefore the same as that which has been recently isolated from red cell stroma[5–7,25,27]. Its easy denaturation by ethanol explains the unsuccessful attempts to extract this fraction from red cell stroma by many workers on the subject.

The active fractions 2 and 3 which have been isolated from solubilised stroma have gel and thin-layer chromatographic characters quite similar to fractions 2 and 3 from saliva. Both are water- and alcohol-soluble and are mainly carbohydrates in nature. Fraction 2 is not dialysable while fraction 3 is dialysable. Of course, a complete characterisation of these fractions requires further chemical study.

It seems evident, from our data and from the recent studies[5–7,25,27], that the substance chiefly responsible for the ABH blood group specific activity of the red cells is not the low-molecular-weight glycolipid isolated by the Japanese workers[9–12] and recently analysed by HAKOMORI AND STRYCHARZ[19], but on the contrary is a glycoprotein which has a molecular weight within the range of $2 \cdot 10^5$ to $5 \cdot 10^6$ as the group specific glycoproteins from secretions[2]. In the red cells, the glycoprotein probably is linked to the lipids of the membrane. The problem arises whether the glycolipid isolated by the Japanese workers is an artifact. The experiments reported here would support the hypothesis that the group specific glycolipid is the stromal fraction we called fraction 3. In fact this fraction is easily extracted from red cells by ethanol or methanol and can be eluted from silicic acid by chloroform–methanol. Fraction 2 can be extracted in the same way but it is strongly adsorbed to silicic acid (Fig. 4). Finally, fraction 1 is precipitated and in great part denatured by ethanol. As the methods used for the purification of the ethanol extracts of red cell stroma involved column chromatography on silicic acid and elution with chloroform–methanol[9–19], it is probable that only fraction 3 was present in the purified solutions.

On the basis of these considerations and taking into account the structure of the glycolipid as determined by HAKOMORI AND STRYCHARZ[19], it seems reasonable to think that this compound is the same as stromal fraction 3 and also the same as the salivary fraction 3, with respect to the group specific part of the molecule. The difference between fraction 3 from red cells and saliva might consist only, in our opinion, in the fact that in the red cells the group specific substance is linked to the lipids of the membrane.

ACKNOWLEDGEMENTS

We are grateful to Mr. G. ROSSI and to Mr. V. GENTILE for helpful technical assistance.

This work was supported by the Consiglio Nazionale delle Ricerche.

REFERENCES

1 A. FIORI, G. V. GIUSTI AND G. PANARI, *J. Chromatog.*, 55 (1971) 351.

2 A. FIORI, G. V. GIUSTI, G. PANARI AND G. PORCELLI, *J. Chromatog.*, 55 (1971) 337.
3 R. M. HERRIOTT, *Proc. Soc. Exper. Biol. Med.*, 46 (1941) 642.
4 H. E. WEINER AND J. R. MOSHIN, *Am. Rev. Tuberculosis*, 68 (1952) 594.
5 F. A. GREEN, *J. Immunol.*, 99 (1967) 56.
6 N. B. WHITTEMORE, N. C. TRABOLD, C. F. REED AND R. I. WEED, *Vox Sang.*, 17 (1969) 289.
7 I. LIOTTA, M. QUINTILIANI, L. QUINTILIANI, A. BUZZONETTI AND E. GIULIANI, *Vox Sang.*, 17 (1969) 11.
8 E. A. KABAT, *Blood Group Substances*, Academic Press, New York, 1956.
9 T. YAMAKAWA AND T. IIDA, *Jap. J. Exptl. Med.*, 23 (1953) 327.
10 T. YAMAKAWA, R. OTA, Y. ICHIKAWA AND J. OZAKI, *Compt. Rend. Soc. Biol.*, 152 (1958) 1288.
11 T. YAMAKAWA, R. IRIE AND N. IWANAGA, *J. Biochem. (Tokyo)*, 48 (1960) 490.
12 T. YAMAKAWA, S. NISHIMURA AND M. KAMIMURA, *Jap. J. Exptl. Med.*, 35 (1965) 201.
13 S. HAKOMORI, *Tohoku J. Exptl. Med.*, 60 (1954) 331.
14 N. S. RADIN, *Fed. Proc.*, 16 (1957) 825.
15 S. HAKOMORI AND R. W. JEANLOZ, *J. Biol. Chem.*, 236 (1961) 2827.
16 S. HANDA, *Jap. J. Exptl. Med.*, 33 (1963) 347.
17 J. KOSCIELAK, *Nature*, 194 (1962) 751.
18 J. KOSCIELAK, *Biochim. Biophys. Acta*, 78 (1963) 313.
19 S. HAKOMORI AND G. D. STRYCHARZ, *Biochemistry*, 7 (1968) 1279.
20 T. A. J. PRANKERD, K. I. ALTMAN AND J. R. ANDERSON, *Nature*, 174 (1954) 1146.
21 C. HOWE, *J. Immunol.*, 66 (1951) 9.
22 M. MOSKOWITZ, W. B. DANDLIKER, M. CALVIN AND R. S. EVANS, *J. Immunol.*, 65 (1950) 383.
23 A. V. STEPANOV, A. KUSIN, Z. MAKAJEVA AND P. N. KOSSJAKOW, *Biokhimiya*, 5 (1940) 547.
24 A. FIORI, P. BENCIOLINI, L. VETTORE AND A. BONADONNA, *Acta Med. Romana*, 6 (1968) 146.
25 M. D. POULIK AND P. K. LAUF, *Clin. Exp. Immunol.*, 4 (1969) 165.
26 W. T. J. MORGAN AND H. K. KING, *Biochem. J.*, 37 (1943) 640.
27 P. ZAHLER, D. H. F. WALLACH AND E. F. LUESCHER, *Protides of the Biological Fluids*, Elsevier, Amsterdam, 1967, p. 69.

CHROM. 5160

AN IMPROVED TECHNIQUE FOR THE ANALYSIS OF AMINO ACIDS AND RELATED COMPOUNDS ON THIN LAYERS OF CELLULOSE

PART IV. THE QUANTITATIVE DETERMINATION OF AMINO ACIDS IN URINE

J. G. HEATHCOTE, D. M. DAVIES, C. HAWORTH AND R. W. A. OLIVER
Department of Biochemistry, The University, Salford (Great Britain)

(Received October 27th, 1970)

SUMMARY

A new method is described for the accurate quantitative determination of amino acids in urine using thin-layer chromatography. Interfering salts and peptides are first removed from the urine by passing it through a column of an ion-retardation resin. The urine is then chromatographed on thin layers of cellulose and the amino acids are determined quantitatively by the method of HEATHCOTE AND HAWORTH.

Several normal and pathological urines have been examined by this technique and quantitative recovery of standard amino acids has been obtained. The results obtained with individual urine samples agree well with those determined by the automatic ion-exchange method of analysis. The method seems to hold considerable promise for the analysis of amino acids in urine.

INTRODUCTION

Thin-layer chromatography (TLC) is potentially the most simple and rapid method for the analysis of amino acids in urine.

Unfortunately, when the method is applied to unmodified urine, even using the improved separation techniques of HAWORTH AND HEATHCOTE[1,2] (Parts I and II of this series), distorted chromatograms are obtained. This makes the precise quantitative determination of each amino acid impossible.

We have found this distortion to be caused not only by the presence of inorganic salts but also by the presence of oligopeptides of a basic nature[3] which markedly distort the final pattern on the thin-layer plate. We have recently carried out a survey of available desalting techniques[3] and have found that, though these remove the inorganic salts, none of them results in a completely clear pattern because of the failure to remove the basic peptides. If it were possible to overcome this difficulty, then the advantages afforded by TLC would make it automatically the method of choice for the analysis of amino acids in urine.

We have accordingly developed a new method of treatment of the urine samples which effectively removes these peptides as well as inorganic salts and which enables a clear distortion-free chromatogram to be produced.

The de-salting step consists essentially in passing the urine through a column of ion-retardation resin under standard, specified conditions.

TLC on cellulose may now be applied both to the screening of large numbers of urine samples, which at present cannot be carried out by ion-exchange methods and to the quantitative analysis of a selected number of samples.

MATERIALS AND EQUIPMENT

Urine samples

Several normal and pathological urine samples were obtained from children of both sexes after a period of overnight fasting. The samples were desalted as soon as possible after arrival in the laboratory.

Ion-retardation resin

The ion-retardation resin used was Bio-Rad AG11A8 50–100 mesh (Batch No. 5145-16 B-2198, obtained from Calbiochem)*.

Cellulose powder

The cellulose powder used in this investigation was MN-300 (without binder)**; it was washed by the technique described previously in Part I of this series[1].

*Solvents for chromatographic development****

The 2-methylbutanol-2 was of G.P.R. grade and the butanone and propanone of M.F.C. grade. All other solvents were of Analar grade.

Detections reagents

Ninhydrin–cadmium acetate (0.2% w/v) reagent was used for the detection and determination of amino acids and isatin–cadmium acetate (0.2% w/v) for the imino acids. These were prepared as described previously[2].

Chromatographic equipment

Shandon§ equipment was used throughout this work for the preparation and development of the cellulose thin layers.

Chromatographic columns for desalting were prepared from glass tubing (1.5 × 30 cm). Indentations were made about 1 cm from one end in order to support a glass wool plug which in turn supported the ion-retardation resin. The flow rate was controlled by means of a Hoffmann screw clip attached to a length (2 cm) of rubber tube at the base of the column.

---

* Calbiochem Ltd., 10, Wyndham Place, London W.1.

** Macherey, Nagel and Co. Ltd., Agents Camlab (Glass) Ltd., Cambridge.

*** Hopkins & Williams Ltd., Freshwater Road, Chadwell Heath, Essex.

§ Shandon Scientific Co., 65 Pound Lane, London N.W.10.

Densitometer

The instrument used was the Joyce Loebl "Chromoscan" double beam densitometer with thin-layer attachment and the reflectance mode of operation was used throughout this work.

METHODS

Preparation of desalting column

The column was prepared from an aqueous suspension of Bio-Rad AG11A8 to the required dimensions (1.5 × 12.5 cm). The resin was then washed with distilled water (100 ml), to remove impurities.

Operation of desalting column

After removal of excess water from the surface of the resin the urine sample (2 ml) was applied carefully to the inside of the tube by means of a pipette so that the surface of the resin was not disturbed. The urine was then washed onto the column with distilled water (1 ml) which was allowed to pass through the column until the resin surface was again just free from water. The amino acids and related compounds were eluted from the resin with distilled water (19 ml) at a flow rate of about 2 ml/min.

The first 13 ml of the eluate was discarded and the next 6 ml, which contained the amino acids, was collected.

In order to prepare the column for re-use it was then washed with distilled water (100 ml) at a fast flow rate (10 ml/min).

Preparation of thin layers

Thin layers of cellulose, initially 400 μ thick, were spread on 20 × 20 cm glass plates as described previously by HAWORTH AND HEATHCOTE[1].

Development of thin-layer chromatograms[1]

The amount of desalted, peptide-free urine applied to the thin layer varied with the concentration of amino acids in the urine but 20 to 40 μl was usually sufficient with most urines to show about 15 different amino acids. It is important to keep the spot size as small as possible for successful chromatography and for this reason samples were applied using capillary pipettes (5 μl) with intermediate drying in a stream of warm air. The solvent systems used were 2-propanol–butanone–1 *N* hydrochloric acid (60:15:25, v/v) for development in the first dimension and 2-methylbutanol-2–butanone–propanone–methanol–water–(0.88) ammonia (50:20:10:5:15:5, v/v) for development in the second dimension. The chromatograms were developed in the first dimension until the solvent front was 13 cm from the origin (2.5 h). Then the plates were removed from the tank, dried in a stream of cool air for 15 min and heated in a convection oven at 60° for 15 min to remove final traces of solvent. Rapid cooling was effected by standing the plate in a current of cold air for 5 min.

When cool, the chromatograms were developed in the second dimension, at right angles to the first dimension, until the solvent front had again reached 13 cm from the origin. The solvent was removed by heating the plate in a convection oven at 60° for 15 min.

Detection of amino acids. When cool, the plates were sprayed with the ninhydrin–cadmium acetate chromogenic reagent until they appeared translucent. After heating at 60° for 15 min in the convection oven, the treated plates were allowed to stand in a dark, ammonia-free atmosphere for 4 h.

During this time the coloured amino acid complexes develop their strongest and most consistent colour value[2]. For the detection of proline and hydroxyproline the plates were similarly treated with isatin–cadmium acetate chromogenic reagent. This was followed by heating at 90° for 10 min and allowing them to stand for 1 h. A separate plate was used for the detection of proline and hydroxyproline since we have found this to give more consistent results[2].

Densitometry. In the case of the amino acid spots stained red by ninhydrin–cadmium acetate reagent, the filter used was 490 nm in wavelength while the spots staining blue by isatin–cadmium acetate reagent were scanned at 620 nm. The area under the densitometric curve was measured using the relationship

$$\text{area} = \text{peak height} \times \text{width at half height.}$$

The value for the area obtained was then related to the amount of amino acid present by reading from prepared standard graphs for each amino acid as described in ref. 2.

TABLE I

AMINO ACIDS EXCRETED BY NORMAL SUBJECTS

Amino acid	*Concentration (μg/ml of urine)*							
	1		*2*		*3*		*4*	
	TLC	*Ion exchange*	*TLC*	*Ion exchange*	*TLC*	*Ion exchange*	*TLC*	*Ion exchange*
Alanine	22.9	23.3	36.0	37.5	51.0	52.0	60.0	62.2
Arginine	7.5	7.6	14.2	14.0	12.2	12.0	12.0	13.0
Aspartic acid	3.8	4.1	4.1	4.0	2.0	2.2	4.4	4.7
Cysteic acid[a]	72.0	71.0	46.0	52.0	80.8	87.5	74.0	72.2
Glutamic acid[b]	23.0	24.4	7.4	8.7	2.0	1.8	3.6	3.8
Glutamine	105.3	116.7	82.4	87.0	99.7	107.0	73.0	78.0
Glycine	180.0	177.1	135.0	140.0	150.0	157.0	142.0	151.0
Histidine	132.0	130.0	112.0	115.0	138.0	141.0	200.0	201.0
Homocystine	0	0	0	0	0	0	0	0
Isoleucine	25.7	27.1	16.0	15.3	7.2	7.3	29.9	32.0
Leucine	17.4	17.1	9.1	10.0	10.9	10.7	23.7	25.0
Lysine	51.0	54.3	8.2	8.0	25.0	24.6	35.1	34.0
Methionine	2.7	3.0	0.7	0.8	1.4	1.0	2.9	3.0
Ornithine	5.7	6.2	0	0	0	0	13.9	14.0
Phenylalanine	18.6	17.9	18.0	18.7	25.2	24.0	53.1	51.0
Proline	12.1	12.2	3.7	4.0	5.5	6.0	1.4	1.4
Serine	40.1	35.2	18.8	19.4	24.2	26.0	18.2	18.0
Threonine	24.2	24.6	10.9	11.3	16.3	17.0	13.1	14.0
Tryptophan	2.8	2.9	1.8	1.8	6.7	6.7	3.6	3.7
Tyrosine	17.8	18.1	26.8	28.7	19.4	20.0	75.0	74.0
Valine	5.0	4.7	3.1	3.3	1.8	1.8	11.1	11.0

[a] The separate values obtained for cysteine, cysteic acid and cystine have been combined as "cysteic acid".

[b] Phenylacetylglutamine is not separated from glutamic acid by either technique and is therefore estimated as such.

TABLE II

AMINO ACIDS EXCRETED BY PATHOLOGICAL SUBJECTS

Amino acid	*Concentration (μg/ml of urine)*							
	Homocystinuria		*Generalized amino aciduria*		*Phenylketonuria*		*Lysinuria*	
	TLC	*Ion exchange*	*TLC*	*Ion exchange*	*TLC*	*Ion exchange*	*TLC*	*Ion exchange*
Alanine	62.0	59.1	40.5	44.1	3.2	3.1	19.5	17.1
Arginine	0	0.7	15.7	15.1	0	0	156.0	142.0
Aspartic acid	0	0.2	12.5	12.6	0	0	0	0
Cysteic acid[a]	33.9	23.2	44.6	30.1	0	0	37.5	42.0
Glutamic acid[b]	3.0	2.7	13.5	12.9	275	280	0	0
Glutamine	0	0	88.5	92.1	0	0	0	0
Glycine	47.5	56.0	55.0	50.0	13.0	13.4	126	140
Histidine	78.0	72.0	440	405	6.4	6.6	0	0
Homocystine	10.8	11.5	0	0	0	0	0	0
Isoleucine	0	0	0	0	0	0	0	0
Leucine	5.0	4.8	4.2	4.3	12.5	12.1	15.0	14.3
Lysine	12.1	8.1	23.0	19.1	3.2	2.4	315	289
Methionine	1.4	1.2	4.8	4.6	0	0	0.2	0
Ornithine	0	0	11.7	12.1	0	0	9.8	8.2
Phenylalanine	10.0	11.4	5.5	6.0	285.0	299.0	0	0
Proline	14.0	12.2	16.4	17.8	5.1	4.2	0	0
Serine	12.5	11.7	37.0	37.7	5.2	6.2	85.5	92.0
Threonine	10.0	10.0	27.5	30.9	6.2	7.7	16.5	18.8
Tryptophan	1.1	0.8	0	0	2.7	2.9	3.5	3.0
Tyrosine	11.2	12.9	8.0	9.7	2.5	3.4	18.0	19.0
Valine	10.0	9.1	4.0	3.8	12.5	11.1	0	0

[a] The separate values obtained for cysteine, cysteic acid and cystine have been combined as "cysteic acid".

[b] Phenylacetylglutamine is not separated from glutamic acid by either technique and is therefore estimated as such.

TABLE III

RECOVERY OF ADDED AMINO ACIDS AND UREA FROM URINE

Amino acid	*% recovery*	*Amino acid*	*% recovery*
Alanine	98	Leucine	97
Arginine	99	Lysine	98
Aspartic acid	93	Methionine	96
Cysteine	98	Phenylalanine	99
Glutamic acid	91	Proline	100
Glutamine	95	Serine	97
Glycine	101	Threonine	99
Histidine	93	Tyrosine	91
Isoleucine	98	Valine	97
Taurine	13	Urea	5

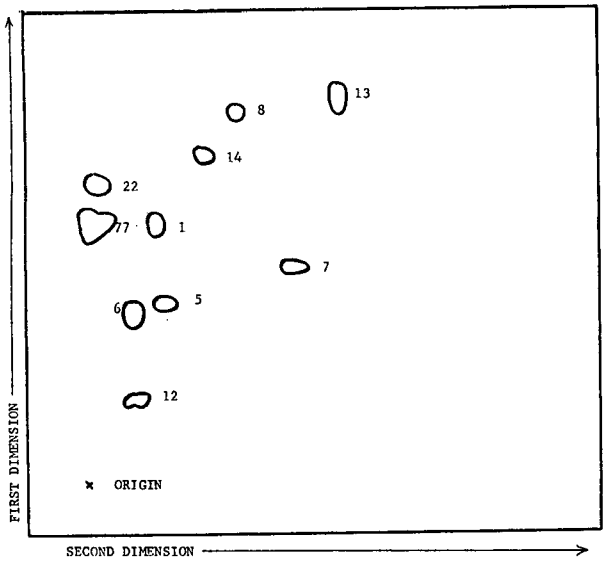

Fig. 1. Separation of amino acids in urine of phenylketonuric subject. The amino acids are numbered in accordance with Parts I and III of this series. 1 = alanine; 5 = serine; 6 = glycine; 7 = threonine; 8 = valine; 12 = lysine; 13 = phenylalanine; 14 = tyrosine; 22 = α-aminoadipic acid; 77 = phenylacetyl glutamine.

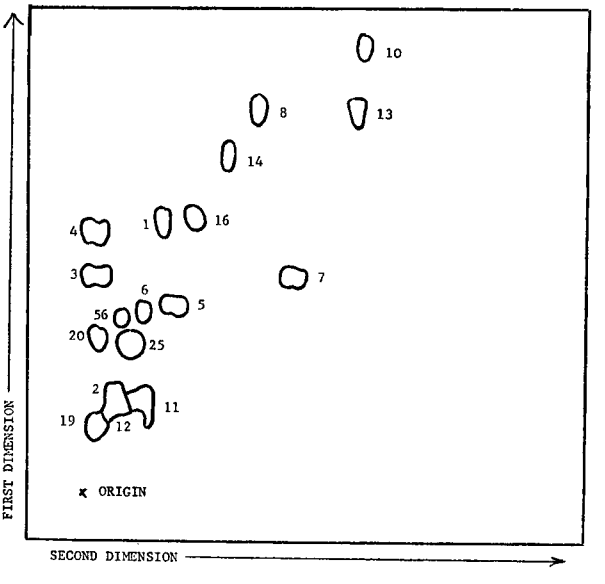

Fig. 2. Separation of amino acids in urine of subject with generalized hyperaminoaciduria. The amino acids are numbered in accordance with Parts I and III of this series. 1 = alanine; 2 = arginine; 3 = aspartic acid; 4 = glutamic acid; 5 = serine; 6 = glycine; 7 = threonine; 8 = valine; 10 = leucine; 11 = histidine; 12 = lysine; 13 = phenylalanine; 14 = tyrosine; 16 = proline; 19 = cystine; 20 = cysteic acid; 25 = glutamine; 56 = citrulline.

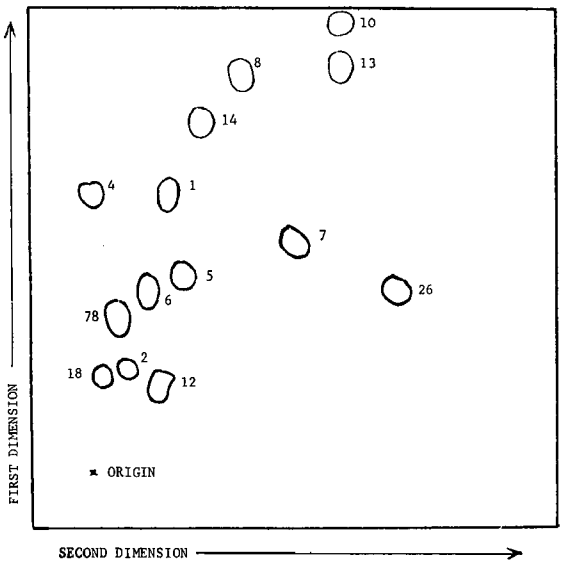

Fig. 3. Separation of amino acids in urine of homocystinuric subject. The amino acids are numbered in accordance with Parts I and III of this series. 1 = alanine; 2 = arginine; 4 = glutamic acid; 5 = serine; 6 = glycine; 7 = threonine; 8 = valine; 10 = leucine; 12 = lysine; 13 = phenylalanine; 14 = tyrosine; 18 = cysteine; 26 = ethanolamine; 78 = homocystine.

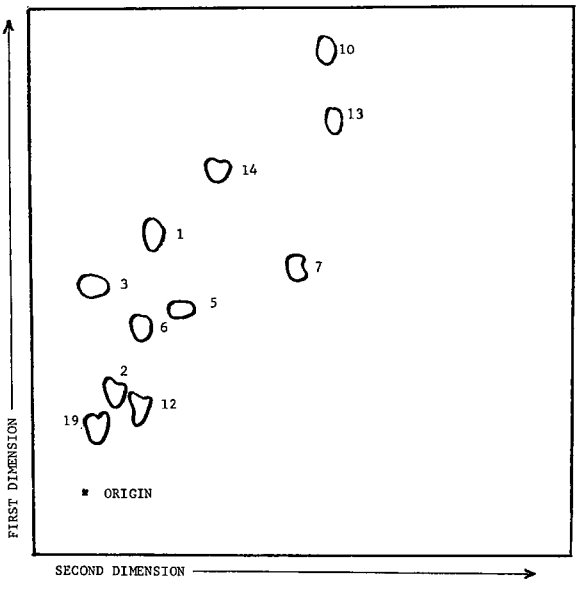

Fig. 4. Separation of amino acids in urine of lysinuric subject. The amino acids are numbered in accordance with Parts I and III of this series. 1 = alanine; 2 = arginine; 3 = aspartic acid; 5 = serine; 6 = glycine; 7 = threonine; 10 = leucine; 12 = lysine; 13 = phenylalanine; 14 = tyrosine; 19 = cystine.

RESULTS AND DISCUSSION

This investigation has resulted in a method which is highly suited to the quantitative determination of amino acids in urine samples. The urines of four normal and four pathological subjects have been examined by this procedure and by the automatic ion-exchange technique (Technicon). It is noted that the results obtained by the present thin-layer procedure agree well with those obtained by the standard column method (Tables I and II). The recoveries of the amino acids, of taurine, and of urea, have been determined by adding known amounts of these compounds to the urine samples. After desalting, the recoveries of the amino acids were found to be quantitative but those of taurine and urea were extremely low (Table III). Both of these latter compounds were almost completely removed by the desalting procedure but this removal enabled all the other amino acids to be identified unambiguously. Examples of the thin-layer chromatograms obtained for normal and pathological urines by this method are shown in Figs. 1–4.

It is important to note that the initial volume of eluate from the desalting column which is discarded contains the interfering basic peptides. That is why this initial volume is accurately measured for the column used. The conditions described here are those which apply to the exact volume of resin and flow rate given above. If the volume of the resin bed or the flow rate were altered from the given conditions it would be necessary to recalibrate the individual column.

The efficiency of the resin is impaired after about fifty samples have been passed through the column. This is due to colloidal material, present in the urine which accumulates on the column. It is therefore necessary to repack the column from time to time after washing the resin in a beaker with distilled water (3×100 ml).

Although the method described in this paper has been developed for the quantitative determination of amino acids in urine samples, more frequently only qualitative screening is required. For such unambiguous screening of samples it is possible to develop the ninhydrin colour immediately after chromatography. In this way large numbers of urine samples may be examined by a single operator during one working day.

REFERENCES

1 C. HAWORTH AND J. G. HEATHCOTE, *J. Chromatog.*, 41 (1969) 380.
2 J. G. HEATHCOTE AND C. HAWORTH, *J. Chromatog.*, 43 (1969) 84.
3 J. G. HEATHCOTE, D. M. DAVIES, C. HAWORTH AND R. W. A. OLIVER, to be published.

CHROM. 5156

A SCREENING METHOD FOR ORGANOCHLORINE AND -PHOSPHORUS PESTICIDE RESIDUES IN VEGETABLES USING THIN-LAYER CHROMATOGRAPHY

S. SANDRONI AND H. SCHLITT
Chemistry Division, Euratom Joint Research Center, 21020 Ispra (Italy)

(Received October 26th, 1970)

SUMMARY

A screening method is described for the semi-quantitative determination of the contamination level of organochlorine and -phosphorus pesticides in fruit and vegetables using thin-layer chromatography. The separations and R_F values are reproducible using this method that is sensitive and useful in confirmation of identity of the most widely used and typical pesticides; common organochlorine and organophosphorus pesticides are selectively eluted from extracts without a preliminary purification procedure and detected. The method allows one to determine whether a vegetable is contaminated below the tolerance limits, detecting residues as low as 0.05 p.p.m. of organochlorine and p.p.b. of organophosphorus pesticides.

INTRODUCTION

In the framework of our collaboration with the "European Economic Community (EEC) Committee for Standardisation of Analytical Methods for Pesticide Residues", we developed a screening method in fruit and vegetables using thin-layer chromatography (TLC) in parallel to gas chromatographic (GC) procedures. In our opinion, the aims of such a screening method are (a) to show whether a vegetable is contaminated above a certain level, (b) to determine by which class of pesticides it is contaminated, (c) to identify, if possible, the contaminating pesticides, and (d) to determine if the contamination level is lower than the tolerance limits allowed by law (Table I).

Several methods have been proposed in literature for separation and identification of different pesticides. Each method, generally, separates a chosen mixture of one single class by developing a series of chromatograms on different adsorbents, by different eluents (also binary and tertiary mixtures of different ratios) and, what is worse, with non-reproducible results, always needing spots of single components for the identification.

By the method described here a contaminated vegetable is examined by separating 16 out of 17 more representative and used pesticides on two plates under re-

TABLE I

TOLERANCE LIMITS (in p.p.m.) PROPOSED BY EEC FOR SOME OF THE MOST WIDELY USED PESTICIDES[1]

Pesticide	*Tolerance (p.p.m.)*
Azinphos-ethyl	0.4
Malathion	3.0
Parathion	0.5
Methylparathion	0.5
Paraoxon	0.5
pp'-DDT	1.0
Lindane	2.0
Aldrin	0.2
Dieldrin	0.2
Carbaryl	3.0

producible conditions. The method that we propose is perhaps more time-consuming than classical TLC procedures, but, in our opinion, this drawback is greatly compensated for by the additional information obtained and the excellent sensitivity.

In practice, we studied a chromatographic method that was able (a) to elute organochlorine and organophosphorus pesticides; (b) to have the lowest detection limits; (c) to have the best possible resolution for some of the most widely used and typical pesticides used for vegetables; (d) to be easily reproducible.

For (a) we observed that hexane on alumina eluted only organochlorine while methylene chloride on silica gel brought these substances to the solvent front, separating the organophosphorus compounds. The differentiation between the two classes is also favoured by using the detection methods on alumina, incorporating $AgNO_3$, as described by ABBOTT *et al.*[2] for organochlorine, and of the cholinesterase inhibition of organophosphorus pesticides as described by ACKERMANN[3]. Condition (b) the sensitivity of the two methods was 50 ng and approx. 0.5 ng respectively. To satisfy condition (c), only activity gradient techniques aid in separation of complex sample mixtures with components varying widely in polarity; for such a purpose we found the Vario-KS-Chamber* (ref. 4) useful because it permits several possibilities of gradients and a continuous development. Regarding condition (d), reproducible results are guaranteed by using the same adsorbent, controlling its activity[5] via relative humidity in a specially adapted chromatographic chamber. If R_F values are reproducible, the R_{st} and R_k values and the separation are reproducible as well[6]. In Figs. 2 and 4 the influence of a change in relative humidity (which controls the layer activity) is shown.

To characterise a contamination, we have chosen 17 pesticides (8 chlorinated, 8 phosphorated and 1 carbamate), and we looked for the best selective separation. Using a test solution (Table II) containing the above-mentioned pesticides, we spike pesticide-free extracts to the tolerance limits. The spiked extracts are used as reference for a simultaneous analysis of several samples under investigation. A comparison of the corresponding spot dimensions permits one to estimate the contamination level in a semi-quantitative way.

* Manufactured by Camag (Muttenz, Schweiz).

TABLE II

TEST SOLUTION (IN DISTILLED CHLOROFORM) USED FOR SPIKING THE EXTRACTS

Solution	*mg/l*	*Solution*	*mg/l*
Aldrin	4.0	Parathion	10.0
pp'-DDE	20.0	Methylparathion	10.0
op'-DDT	20.0	Malathion	60.0
pp'-DDT	20.0	Azinphos-ethyl	8.0
pp'-DDD	20.0	Carbaryl	60.0
Lindane	40.0	DDVP	10.0
Endrin	4.0	Paraoxon	10.0
Dieldrin	4.0	Malaoxon	60.0
Ethion	10.0		

EXPERIMENTAL

Extraction

The extracts are prepared according to the EEC method actually under investigation. Basically this method is a twofold acetonitrile /water–chloroform/ chloroform extraction, but any other extraction method can be used as well. Starting with a 100-g sample, we obtain a final 5-ml volume of extract in chloroform.

Spiked samples

Based on the proposed[1] tolerance limits (adding some arbitrary ones when not given in ref. 1) we prepare the test solution of the composition given in Table II. The contamination is such that when mixing the test solution and extract (1:1), the vegetable has a resulting contamination of the tolerance limits.

First plate: organochlorine pesticides

A 250-μ thick layer of Alumina DS-5 (Camag) is prepared from a slurry formed by shaking 55 g of adsorbent with 60 ml of 0.4% (w/v) aqueous silver nitrate solution (dose for five 20 × 20 cm plates) for 2 min. The prepared plates are dried in an oven at 110° for 1 h. On the cooled plate, 10 μl of the sample solution are spotted as a single application and an equal amount of extract, spiked to the tolerance limits, is spotted nearby. The plate is afterwards placed on a Vario-KS-Chamber for conditioning for 60 min at 18% rel. humidity, over conditioning trays filled uniformly with 60.6% sulphuric acid solution. Then the plate is eluted continuously (no front line was made) for 1.5 h. For the detection, the plate is exposed to moisture for some minutes before irradiating with a germicidal UV light source (Philips TUV, 15 W); within 20 min pesticides will appear as black spots on a white background.

Second plate: organophosphorus pesticides

At first, it is necessary to prepare (a) a rat liver homogenate (To 1 part of rat liver 3.5 parts (w/v) of iced distilled water are added and the mixture is homogenised at 3000 r.p.m. for 10 min. The solution is filtered on paper and the filtrate is centrifuged at 3000 r.p.m. for 15 min before decantation. To maintain the initial activity, the homogenate is stored in 1-ml tubes in a freezer.); (b) a bromine-saturated solution

in distilled water, freshly prepared; (c) a freshly prepared solution containing 4 ml of 2-naphthyl acetate solution (125 mg/100 ml of ethanol) and 16 ml of Fast Blue B solution (20 mg in 16 ml of distilled water).

1 μl of the sample solution is spotted on a 250-μ thick Silica Gel G (Merck) plate with an equal amount of extract spiked to the tolerance limits as reference. The plate is placed on a Vario-KS-Chamber arranged with the conditioning trays for an "anti-parallel" humidity gradient as shown in Fig. 3. 3, 3, 3, 3, 3, 13, 47, 58, 64 and 72% rel. humidities correspond to 77, 77, 77, 77, 77, 64.7, 45, 40, 36 and 33% sulphuric acid solutions. After conditioning for 60 min, chromatography is carried out using methylene chloride, the solvent front travelling 15 cm from the start. After evaporation of the solvent, the detection is obtained in four steps[3]. (1) The pesticides are activated by spraying lightly with solution (b). (2) When the odour of bromine is no longer present on the plate, it is sprayed with about 10 ml of liver homogenate (a) previously diluted with distilled water (1:3). (3) The plate is stored in a climatized atmosphere at 37°, having a high humidity (80–90%), for 30 min. (4) Then it is vapourized with about 5 ml of solution (c). Pesticides will appear as white spots on a violet background.

RESULTS AND DISCUSSION

Up to ten extracts can be simultaneously analysed on the two plates having as reference the corresponding extract spiked to the tolerance limits. The first plate gives information about the contents of organochlorine pesticides. In Fig. 1 extracts of lettuce, apple, cabbage and carrot are compared with the corresponding ones spiked

TABLE III

MIGRATION DISTANCES (IN CM) OF THE REFERENCE COMPOUNDS AS IN FIG. 1

References compounds	*cm*
pp'-DDE	11.5
op'-DDT	10.4
pp'-DDT	9.1
Aldrin	7.5
Lindane	3.5
pp'-DDD	3.0
Endrin	1.9
Dieldrin	1.4

to the tolerance limits; the migration distances (in cm) of the reference pesticides are listed in Table III with a standard deviation of 0.5 cm.

In Fig. 1 the relative spot dimensions are in relation to the tolerance limits (*e.g.* 2 p.p.m. for Lindane, 0.2 p.p.m. for Aldrin).

The detection limit for each reference chlorinated pesticide is 50 ng. For our extracts (20 g of sample per ml chloroform), spotting 50 μl, a contamination as low as 0.05 p.p.m. is easily detectable.

For organochlorine pesticides the best adsorbent is Alumina DS-5 (Camag).

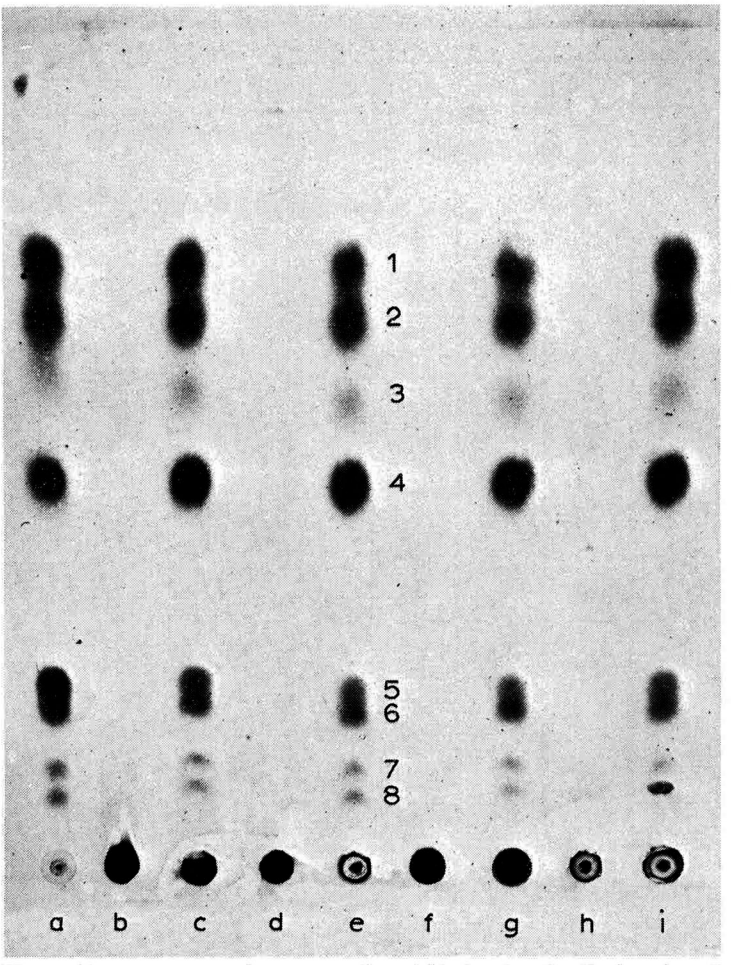

Fig. 1. Chromatogram of 4 extracts "pesticide free" and spiked to the tolerance limits with organochlorine pesticides: (a) test solution; (b) lettuce; (c) spiked lettuce; (d) apple; (e) spiked apple; (f) cabbage; (g) spiked cabbage; (h) carrot; (i) spiked carrot. All spots, 10 μl: (1) DDE, (2) *op'*-DDT, (3) *p,p'*-DDT, (4) Aldrin, (5) Lindane, (6) *pp'*-DDD, (7) Endrin and (8) Dieldrin. Alumina DS-5 (Camag) incorporating $AgNO_3$ conditioned 60 min at 18% relative humidity, Vario-KS-Chamber, 90 min continuous elution with cyclohexane.

We preferred this adsorbent because of its particular selectivity* towards the separation of DDE and Lindane and for the slower tendency to darken also during the irradiation process. In Fig. 2 the importance of controlling the humidity is shown; going from 65 to 18% rel. humidity the order is modified twice, passing from Aldrin–*pp'*-DDT–*pp'*-DDD–Lindane to *pp'*-DDT–Aldrin–Lindane–*pp'*-DDD. An elution time twice the normal one (15 cm elution) is required for ameliorating the separation.

The second plate gives information about the content of organophosphorus pesticides. In Fig. 3 extracts of lettuce, apple, cabbage and carrot are chromato-

* This selectivity was observed to be fading from one charge to another, perhaps due to different degrees of hydration of the gypsum binder.

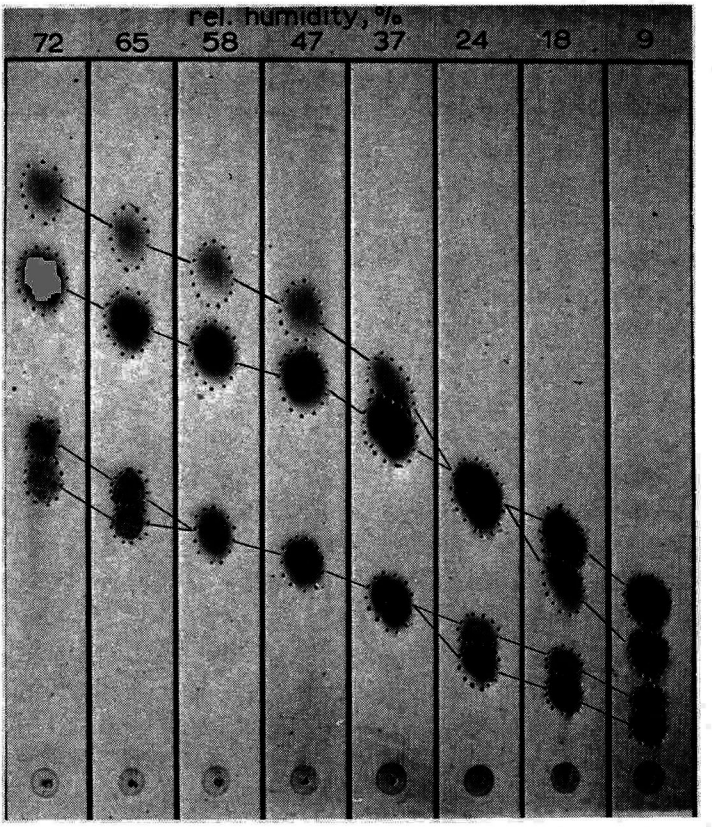

Fig. 2. Influence of humidity on the separation of chlorinated pesticides. Order of separations at 9% relative humidity: *pp'*-DDT, Aldrin, Lindane, *pp'*-DDD; at 72% relative humidity: Aldrin, *pp'*-DDT, *pp'*-DDD, Lindane. Alumina DS-5 (Camag) incorporating $AgNO_3$, Vario-KS-Chamber, orthogonal humidity gradient, cyclohexane.

graphed with the corresponding extracts spiked to the tolerance limits. The nine phosphorus pesticides* are listed in Table IV with the corresponding R_F values (standard deviation 5 hR_F) and sensitivities.

Pigments and other vegetable substances do not generally interfere seriously since they have different R_F values and bright colours, but difficult cases cannot be excluded.

In order to justify the experimental technique used for separating the organophosphorus pesticides, some considerations have to be made. A standard TLC plate (15 cm distance) has just sufficient space for the separation of, let us say, 10–15 spots, if these are equidistant from each other, which, of course, never happens. In the literature[3,7–11] R_F values of more than 80 organophosphorus pesticides are listed. Hence, it is impossible to separate all of them on a single TLC plate. Thus, for example, ACKERMANN[3] chose different mixtures as benzene–acetone or *n*-hexane–benzene–

* Carbaryl (Sevin), a carbamate pesticide, is here considered as an organophosphorus pesticide because of its similar chromatographic properties and its ability to inhibit cholinesterase[3].

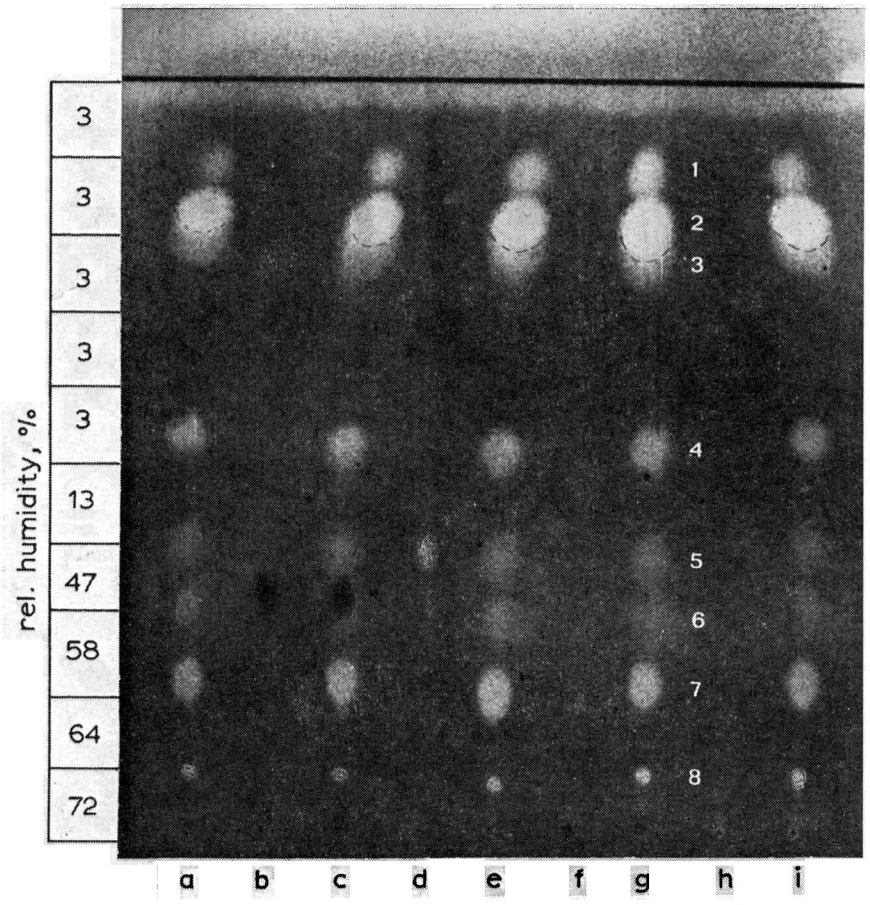

Fig. 3. Chromatograms of 4 extracts "pesticide free" and spiked to the tolerance limits with organophosphorus pesticides: (a–i) as in Fig. 1. Spot 0.5 μl: (1) Ethion, (2) Parathion, (3) Methylparathion, (4) Malathion + Azinphos-ethyl, (5) Carbaryl, (6) DDVP, (7) Paraoxon and (8) Malaoxon. Silica Gel G (Merck), Vario-KS-Chamber, antiparallel humidity gradient, methylene chloride.

TABLE IV

hR_F VALUES AND SENSITIVITIES OF REFERENCE ORGANOPHOSPHORUS PESTICIDES, AS IN FIG. 3

Pesticide	hR_F	*Sensitivity (ng)*
Ethion	89	1.0
Parathion	81	0.2
Methylparathion	77	0.2
Malathion	48	0.2
Azinphos-ethyl	48	0.2
Carbaryl	37	0.5
DDVP	28	0.2
Paraoxon	19	0.2
Malaoxon	7	10.0

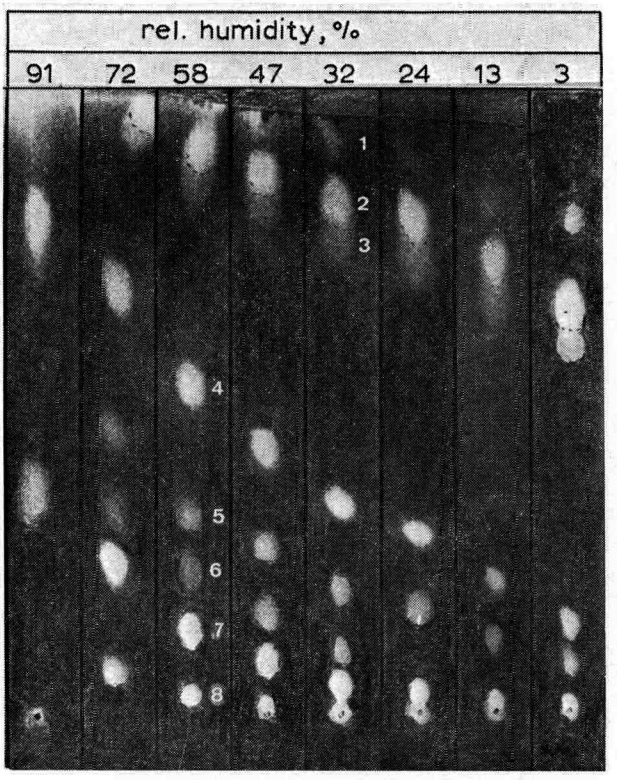

Fig. 4. Influence of humidity on the separation of organophosphorus pesticides. The order of separation is as in Fig. 3. Silica gel G (Merck), Vario-KS-Chamber, orthogonal humidity gradient, methylene chloride.

acetone of different composition, each of them separating* some (4–5) of the 38 compounds investigated, but never all of them. Other authors made other selections of compounds and hence had to use other solvents[7–11]. Therefore it is not astonishing that the separation of the 9 organophosphorus compounds chosen in the EEC list is not obtained by any of the forementioned methods. For example, by using an N-chamber and acetone–benzene mixture[3] or hexane–acetone mixture[7,10] as eluents, dependent on the solvent composition, the compounds are poorly resolved either in the upper or in the lower part of the plate, or, at the best, divided in two narrow regions, one in the upper and the other in the lower part of the plate. Thus we had to look for another technique. In Fig. 4 the influence of relative humidity on the separation is shown; only at a humidity as low as 3%, are Ethion, Parathion and Methyl parathion separated, while only at a higher humidity (62%) are the other five compounds satisfactorily separated. So, if we arrange a chromatographic system having in the lower part of the plate a high humidity, there the low-lying 5 compounds will separate; if the upper part of the plate is conditioned at 3% rel. humidity, the remaining 3 fast moving compounds will be resolved. Both regions are linked by steps of inter-

* The criterion for separation is a mean distance of 5 hR_F.

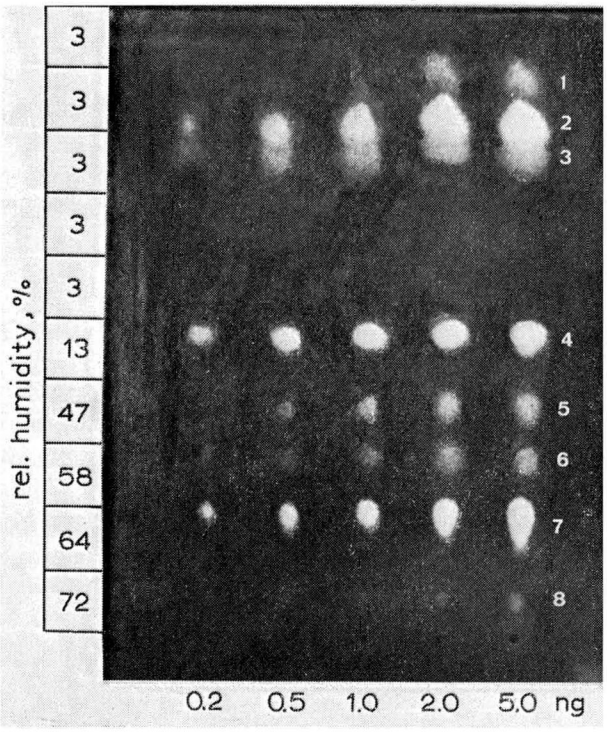

Fig. 5. Sensitivity test for organophosphorus pesticides: concentrations in ng/compound (Malaoxon is 10 times more concentrated). Silica Gel G (Merck), Vario-KS-Chamber, antiparallel humidity gradient as in Fig. 3, methylene chloride.

mediate humidities. Thus on the same plate in a single development we have well separated 8 or 9 spots (and there is space for others, if necessary!). Such an arrangement (humidity decreasing, *i.e.* increasing activity in the direction of the solvent flow) is a so-called "anti-parallel" activity gradient*, which has proved to be one of the more promising ways for separating a complex mixture of compounds varying widely in polarity[6,13].

In Fig. 5 a sensitivity test for the reference pesticides is shown at equal concentrations under identical chromatographic conditions. From these data, it is demonstrated that for a pesticide with 0.5 ng sensitivity, a contamination as low as the p.p.b. level can be easily detected.

Occasionally, as in Fig. 3, we observe that our unspiked apple extract contains a pesticide with a hR_F value equal to that of Carbaryl.

CONCLUSIONS

Detection methods

We have tested, as far as possible, all methods described in the literature balancing sensitivity and simplicity. For organochlorine pesticides, in our opinion,

* "Antiparallel" related to the solvent flow[12].

the method of ABBOTT *et al.*[2] is the most sensitive and simple. For organophosphorus pesticides, several papers have been published on the cholinesterase inhibition by MENDOZA *et al.*[7,14], ACKERMANN[3], WINTERLIN *et al.*[15] and quite recently by ERNST *et al.*[16]. Although for some single pesticides other enzymatic sources (*e.g.* honeybee brains[16]) seem to give a higher sensitivity, we preferred to use rat liver because rats are frequently used in biological laboratories. Experiments made with beef liver gave no better results.

Layer thickness

In contrast to what has been suggested in literature[3,7,14–16] we have found no remarkable advantage by using 450-μ instead of 250-μ-thick silica gel layers; thus we preferred to use the traditional 250 μ layer.

"Pesticide free" extracts

We had some problems in obtaining "pesticide free" extracts. Although the vegetables we used were not directly treated with pesticides, an unintentional contamination was present in apples and cabbages. Fortunately, a comparison with fortified samples showed that the contamination level was about 10% of the tolerance limits and so, nevertheless, we used them as "pesticide free" extracts.

Quantitative approach

By direct visual comparison, spots differing in size by 30% from the reference are easily distinguished. Therefore for fruit and vegetable samples, a decision (accepted or not accepted) can be taken if the contamination level is far enough from the tolerance limits. In doubtful cases, a GC or specific colorimetric determination has to be made.

ACKNOWLEDGEMENT

We are grateful to Dr. F. GEISS for the helpful discussion and for the interest shown in the work.

REFERENCES

1 Anonymous, J. Offic. Commun. Européennes, C 139/23 du 28 déc. 1968 and C 97/23 du 28 juillet 1969.
2 D. C. ABBOTT, J. O'G. TATTON AND N. F. WOOD, *J. Chromatog.*, 42 (1969) 83.
3 H. ACKERMANN, *J. Chromatog.*, 44 (1969) 414; *ibid.*, 36 (1968) 309.
4 F. GEISS AND H. SCHLITT, *Chromatographia*, 1 (1968) 392.
5 S. SANDRONI AND F. GEISS, *Chromatographia*, 2 (1969) 165.
6 F. GEISS, *Die Parameter der Dünnschichtchromatographie*, Friedr. Vieweg, Braunschweig, 1971.
7 C. E. MENDOZA, P. J. WALES, H. A. MC.LEOD AND W. P. MC.KINLEY, *Analyst*, 93 (1968) 34, 173.
8 J. ASKEW, J. H. RUZICKA AND B. B. WHEALS, *Analyst*, 94 (1969) 275.
9 K. C. WALKER AND M. BEROZA, *J. Ass. Offic. Anal. Chem.*, 46 (1963) 250.
10 D. C. ABBOTT, A. S. BURRIDGE, J. THOMSON AND K. S. WEBB, *Analyst*, 92 (1967) 170.
11 M. RAMASAMY, *Analyst*, 94 (1969) 1078.
12 A. NIEDERWIESER, *Chromatographia*, 2 (1969) 32.
13 F. GEISS, S. SANDRONI AND H. SCHLITT, *J. Chromatog.*, 44 (1969) 290.
14 C. E. MENDOZA AND J. B. SHIELDS, *J. Chromatog.*, 50 (1970) 92.
15 W. WINTERLIN, G. WALKER AND H. FRANK, *J. Agr. Food Chem.*, 16 (1968) 808.
16 G. F. ERNST AND F. SCHURING, *J. Chromatog.*, 49 (1970) 325.

CHROM. 5110

ELUTION REQUIREMENTS FOR ION-EXCHANGE SEPARATION OF URANIUM ISOTOPES

K. GONDA, A. OHNISHI, D. NARITA AND T. MURASE
Power Reactor and Nuclear Fuel Development Corporation, Tokai, Ibaraki (Japan)

(First received October 13th, 1970; revised manuscript received November 3rd, 1970)

SUMMARY

The necessary flow rate and the effective bed length for the ion-exchange separation of uranium isotopes have been calculated using ROSEN's theory. The applicability of ROSEN's theory was verified using the isotope exchange of ^{235}U–^{238}U between the anion-exchange resin bed and 8.4 M hydrochloric acid. The effective feed rate and the estimated column bed length were 8.6×10^{-3} cm/sec and 3.4×10^{2} cm, respectively, for the linear isotherm system of U(IV) using 8.4 M hydrochloric acid and the anion-exchange resin, Diaion SA10.

INTRODUCTION

Breakthrough operation has been frequently used for ion-exchange separation of isotopes since TAYLOR AND UREY[1] used the method to separate lithium isotopes with an inorganic ion exchanger, Zeolite. A method to estimate the degree of separation was derived for the breakthrough operation system by GLUECKAUF[2] who introduced "the number of theoretical plates" as the number of stages in the fixed resin bed in equilibrium with the eluent. GLUECKAUF's theory is expressed in eqn. 1 as the relative concentration of effluent, C/C_0,

$$\frac{C}{C_0} = \frac{1}{2} - A_\varepsilon\left\{\frac{N-M}{\sqrt{M}}\right\} + \exp(2N)\left[\frac{1}{2} - A_\varepsilon\left\{\frac{N+M}{\sqrt{M}}\right\}\right] \quad (1)$$

Here, $A_\varepsilon(t)$ is the area of the normal curve of error defined by

$$A_\varepsilon(t) = \frac{1}{\sqrt{2\pi}}\int_0^t \exp\left(-\frac{t^2}{2}\right) dt \quad (2)$$

N is the number of theoretical plates up to the point x,

M is the number of theoretical plate elution volumes contained in volume V.

However, GLUECKAUF's theoretical equation with a linear isotherm estimates neither the number of theoretical plates nor the degree of separation without first using practical separation.

A more rigorous theoretical expression for breakthrough curve for the linear equilibrium system had been derived earlier by ROSEN[3] who considered the presence

of both the fluid film and intraparticle diffusion resistance. ROSEN's expression uses the time required for the fluid to flow a distance and the time measured from an instant point reached by the fluid.

$$\frac{C}{C_0} = \frac{1}{2} + \frac{2}{\pi}\int_0^\infty \exp\{-XH_1(\lambda, \nu)\} \sin\{Y\lambda^2 - xH_2(\lambda, \nu)\} \frac{d\lambda}{\lambda}$$

$$H_1(\lambda, \nu) = \frac{H_1(\lambda) + \nu\{H_1(\lambda)\}^2 + \nu\{H_2(\lambda)\}^2}{\{1 + \nu H_1(\lambda)\}^2 + \{\nu H_2(\lambda)\}^2}$$

$$H_2(\lambda, \nu) = \frac{H_2(\lambda)}{\{1 + \nu H_1(\lambda)\}^2 + \{\nu H_2(\lambda)\}^2} \tag{3}$$

$$H_1(\lambda) = \frac{\lambda(\sinh 2\lambda + \sin 2\lambda)}{\cosh 2\lambda - \cos 2\lambda} - 1$$

$$H_2(\lambda) = \frac{\lambda(\sinh 2\lambda - \sin 2\lambda)}{\cosh 2\lambda - \cos 2\lambda}$$

The relative concentration can be given as a function of the three dimensionless parameters as follows:

$$\nu = \frac{D_s K}{r k_F}, \quad X = \frac{3D_s K(1-\varepsilon)}{r^2} \cdot \frac{z}{u}, \quad Y = \frac{2D_s}{r^2}\left(t - \frac{z}{u/\varepsilon}\right) \tag{4}$$

The nomenclature is shown in Table I.

In this paper, the applicability of ROSEN's equation is discussed to predict the column performance of the isotopes of U(IV) in 8.4 M hydrochloric acid with an

TABLE I

EXPERIMENTAL CONDITIONS

Symbols	*Nomenclature*	*U(IV)*	*Methods or formulae*
R	radius of column	1.27/2 (cm)	
	ion-exchange resin	Diaion SA10A (50 ~ 100 mesh)	
r	radius of resin particles	1.09×10^{-2} (cm)	
z	bed length	90.0 (cm)	
ε	void fraction	0.3 (—)	
C_0	inlet concentration of solute in liquid	22.7 (g/l)	
	concentration of hydrochloric acid	8.4 M	
u	linear velocity	4.53×10^{-3}	
		1.78×10^{-2} (m/sec)	
t	temperature	30 (°C)	
q	concentration of U in resin	192 (g/l-resin)	
K	equilibrium constant	8.45 (—)	q/C_0
ϱ	density of fluid	1.15 (—)	
μ	viscosity of fluid	1.38×10^{-2} (g/ml sec)	Ostwald's method
D_L	diffusivity of solute in liquid	1.80×10^{-6} (cm^2/sec)	Ref. 11
a_v	surface area of particle per unit volume of bed	1.80×10^2 (cm^2/ml)	$4\pi r^2/\frac{4}{3}\pi r^3$
Re	Reynolds number	8.24×10^{-3}	
		3.24×10^{-2} (—)	$Ru\varrho/2\mu$
Sc	Schmidt number	6.67×10^3 (—)	$\mu/\varrho D_L$
k_F	fluid film mass transfer coefficient	2.95×10^{-4}	
		5.88×10^{-4} (—)	$1.15\,(Re/\varepsilon)^{-1/2}Sc^{-2/3}\mu/\varepsilon$

anion-exchange system. Some effects of isotope separation have been previously found in this system[4].

EXPERIMENTAL

A column (100 cm long, 1.27 I.D.) was used. A jacket was installed around the column to keep the experimental temperature constant, with 30° water circulating from a thermostat. The anion-exchange resin, Diaion SA10 (made by Mitsubishi Kasei Co. Ltd., Tokyo; corresponding to Dowex 1 X8), was employed. The experiments were carried out on the linear adsorption isotherm system of U(IV). 8.4 *M* hydrochloric acid was passed through the ion-exchange resin bed prior to each experiment. Feed solution I containing depleted uranium (the isotope fraction of $^{235}U = 0.355\%$) was fed into the column until a uranium solution having the same concentration as feed solution I was eluted from the column. Feed solution II containing natural uranium (the isotope fraction of $^{235}U = 0.730\%$) was fed into an anion-exchange resin column pre-saturated with feed solution I. The concentrations of uranium and H^+ in solutions I and II were made equal to each other, within analytical errors. The Reynolds number, the Schmidt number and the coefficient for fluid film mass transfer are necessary for the discussion of the applicability of ROSEN's equation. These values and their calculation are listed together with other experimental values and conditions in Table I. The void fraction is the value measured on the column saturated with depleted uranium. The surface area of the particle per unit volume of the bed was calculated from the mean radius of the resin particles used and the void fraction. The diffusivity value of U(IV) in 8.4 *M* hydrochloric acid was used instead of the self-diffusivity.

A solution of natural uranium tetrachloride was prepared by dissolving pure metal chips in hydrochloric acid under cooling after washing the chips with ethanol, dilute nitric acid and water. A solution of depleted uranium tetrachloride was prepared by the electrical reduction of the uranyl chloride solution. These uranium tetrachloride solutions were refined by passing them through an anion-exchange resin bed to remove uranyl chloride. Uranous ion concentration was analyzed by titration with potassium bichromate. The isotope ratios were determined by thermoionization, using an Atlas mass spectrometer model CH4 equipped with a single collector[5].

RESULTS AND DISCUSSION

The process in which natural U(IV) is substituted for depleted U(IV) presaturated by passing through the ion-exchange resin bed is as follows;

$$^{235}U(IV) + {}^{238}\bar{U}(IV) \rightleftharpoons {}^{238}U(IV) + {}^{235}\bar{U}(IV)$$

ROSEN's theoretical breakthrough curve was given by the relative effluent concentration expressed as a function of time, Y/X, for bed length X, and for film resistance v/X. Several numerical solutions were computed for the several values of bed length and film resistance selected by ROSEN[6]. The film resistance parameter v/X of this study can be calculated from the experimental data listed in Table I. The approximate value of the bed length was obtained from the curve fitting the numerical solutions which had been computed for various values of the bed length with OKITAC 9050

by KAWAZOE *et al.*[7]. The effective diffusion coefficient of U(IV) in spherical particles assumed constant by ROSEN was calculated from the value of X obtained from the curves. The effective diffusion coefficient of U(IV) was calculated as 1.5×10^{-9} cm^2/sec for the linear velocities, 4.5×10^{-3} and 1.8×10^{-2} cm/sec used in this study. Therefore, the applicability of ROSEN's theoretical equation to the systems employed in this study was confirmed. The experimental breakthrough curves of natural uranium were obtained from the isotope ratios of the effluent. The experimental points and the breakthrough curves calculated with the effective diffusion coefficients obtained are shown in Fig. 1.

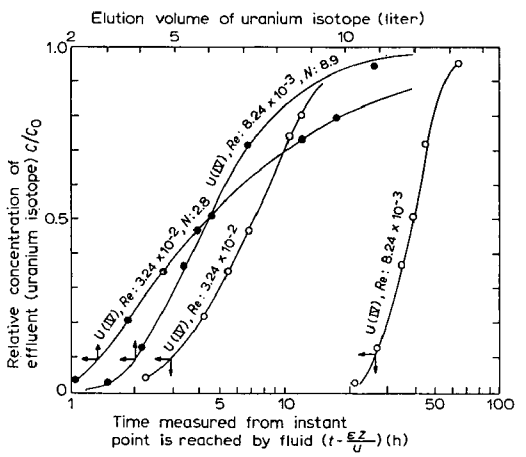

Fig. 1. Breakthrough curves of uranium isotopes. ○ and ●, observed points; ———, theoretical line.

For $X \geqq 50$ and $\nu \leqq 0.01$, the following expression, accurate to 1%, can be obtained directly from the integral of eqn. 3.

$$\frac{C}{C_0} = \frac{1}{2}\left[1 + \operatorname{erf}\left\{\frac{3Y/2 - X}{2\sqrt{X/5}}\right\}\right] \tag{6}$$

Substituting parameter E for $(3Y/2 - X)/2\sqrt{X/5}$ in eqn. 6, the following equation is obtained.

$$t - \frac{z}{u/\varepsilon} = \sqrt{\frac{4Kz\,(1-\varepsilon)\,r^2}{15uD_s}}\,E + \frac{K\,(1-\varepsilon)\,z}{u} \tag{7}$$

The parameter E can be calculated from the relative effluent concentration of natural uranium, using eqn. 6. The numerical values in the square root of eqn. 7 are constant, so that the effective diffusion coefficient can be evaluated from the slope obtained, plotting E *vs.* time, $t - \varepsilon z/u$. Fig. 2 is the graphical representation of the parameter E *vs.* time for the U(IV) system. The effective coefficients obtained were 1.4×10^{-9} and 1.6×10^{-9} cm^2/sec for the linear flow velocities of 4.5×10^{-3} and 1.8×10^{-2} cm/sec, respectively. These values agreed well with that obtained from the exact solution.

For $N > 3$, the second term of eqn. 1 becomes almost negligible. Eqn. 1 therefore is given by

$$\frac{C}{C_0} = \frac{1}{2} - A_\varepsilon \{\sqrt{N}\frac{\bar{V} - V}{\sqrt{\bar{V}V}}\} \tag{8}$$

where $\bar{V}$ is the elution volume of the center of the S-shaped elution curve ($C = C_0/2$). We read the value of $\bar{V}$ and also the column volume V' of the concentration given by

$$\frac{C}{C_0} = \frac{1}{2} - A_\varepsilon \{1\} = 0.1587 \tag{9}$$

Then, the number of theoretical plates is obtained from eqn. 10.

$$N = \frac{\bar{V}V'}{(\bar{V} - V')^2} \tag{10}$$

The values obtained from the breakthrough curve which is represented by the effective effluent concentration of U(IV) *versus* the effluent volume in Fig. 1 were 2.8 and 8.9 for the linear flow velocities of 4.5×10^{-3} and 1.8×10^{-2} cm/sec, respectively. The breakthrough curves calculated using these numbers of theoretical plates, fitted the experimental points well. ROSEN's approximate equation and also GLUECKAUF's equation were verified to be possible within their assigned requirements.

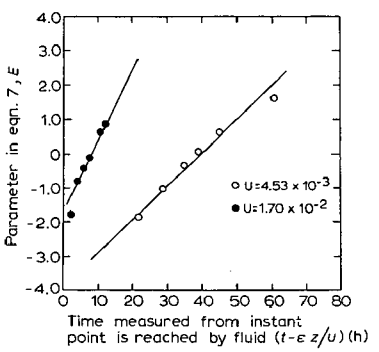

Fig. 2. Applicability of ROSEN's approximation (eqn. 4).

The ion-exchange separation factor of isotopes, α, is given by the ratio of the ion-exchange equilibrium constants of isotopes. Introducing an ion-exchange separation factor as follows,

$$\alpha = \frac{K_2}{K_1} - 1 = \frac{X_2}{X_1} - 1 \tag{11}$$

one can estimate the separation factor and also the degree of separation for a linear equilibrium system by the method of LONDON[8]. A local enrichment factor, S, will be estimated by the following equation derived by substituting α for the effective bed length X in eqn. 6, on the assumption that the effective diffusion coefficients of isotopes are identical.

$$_1^2S = \frac{^1C}{^1C_0} \cdot \frac{^2C_0}{^2C} = \frac{1 + \text{erf}\,\{(3Y/2 - X_1)/2\sqrt{X_1/5}\}}{1 + \text{erf}\,\{(3Y/2 - X_2)/2\sqrt{X_2/5}\}} = \frac{1 + \text{erf}\,(t_1)}{1 + \text{erf}\,(t_2)} \tag{12}$$

$$t_2 = \frac{1}{\sqrt{1 + \alpha}}\{t_1 - \alpha\sqrt{5X_1}/2\} \doteq t_1 - (\sqrt{5X_1}/2)\alpha$$

The parameter $\sqrt{5X_1}/2$ corresponds to the number of theoretical plates given by GLUECKAUF. The parameter is superior to that used by GLUECKAUF since it is expressed by the quantities exactly measurable as shown by eqn. 4.

Usually, for ion-exchange separation of isotopes, one employs the ion-exchange resin particles of 50–100 mesh of which the mean radius is 1×10^{-2} cm. The linear ion-exchange equilibrium constant of U(IV) using the anion-exchange resin SA10 and 8.4 M hydrochloric acid was measured as 40 up to 0.002 M U(IV). Substituting the values of the mean radius of the resin particles, the linear ion-exchange equilibrium constant and the effective diffusion coefficient of U(IV), 1.5×10^{-9} cm^2/sec, for the parameters, v and X, which are expressed by eqn. 4 and satisfy the requirements of eqn. 6, the following are obtained.

$$k_F \geqq 6 \times 10^{-4}, \quad z/u \geqq 4 \times 10^4 \tag{13}$$

Rewriting the coefficient of fluid film mass transfer with the Reynolds number and the Schmidt number[9], the above expression for k_F of ROSEN's approximate equation is described as follows.

$$1.15\,(\varrho/\mu)^{1/6}\,(2/\varepsilon R)^{1/2}\,D_L^{2/3}\,u^{1/2} \geqq 6 \times 10^{-4} \tag{14}$$

The feed rate and the effective column bed length are calculated from eqns. 12–14, using the experimental data listed in Table I. The following results are obtained.

$$u \geqq 8.6 \times 10^{-3} \text{ cm/sec}, \quad z \geqq 3.4 \times 10^2 \text{ cm} \tag{15}$$

The number of theoretical plates is inversely proportional to the feed rate, so that an estimated feed rate of 8.6×10^{-3} cm/sec and a calculated effective column bed length of more than 3.4×10^2 cm are optimal. The longitudinal diffusion will be neglected for the isotope separation system mentioned above so far as the estimated effective feed rate is employed[10].

CONCLUSIONS

The elution requirements for the separation of uranium isotopes were estimated by ROSEN's theory and verified by the use of ^{235}U–^{238}U exchange in the linear equilibrium system between the anion-exchange resin and the hydrochloric acid. The optimal linear flow velocity and the effective length of the column bed could be determined from an invariable Schmidt number and a variable Reynolds number fixed experimentally. This study showed the applicability of ROSEN's theory to the pre-computation of a local enrichment factor along the eluted partitions from a column.

ACKNOWLEDGEMENTS

The numerical integration was performed by the use of the routine programmed by KAWAZOE *et al.* The authors are indebted to Prof. KAWAZOE for computation and for comments on ROSEN's treatment.

REFERENCES

1 T. I. TAYLOR AND H. C. UREY, *J. Chem. Phys.*, 6 (1938) 429.
2 E. GLUECKAUF, *Trans. Faraday Soc.*, 51 (1955) 34.
3 J. B. ROSEN, *J. Chem. Phys.*, 20 (1952) 387.
4 H. KAKIHANA, K. GONDA, H. SATOH AND Y. MORI, *At. Energ. Soc., Japan*, 5 (1963) 990.
5 Y. MORI, T. KANZAKI AND H. KAKIHANA, *Jap. Analyst*, 12 (1963) 736.
6 J. B. ROSEN, *Ind. Eng. Chem.*, 46 (1954) 1590.
7 K. KAWAZOE, Y. TAKEUCHI, I. SUGIYAMA AND T. HASHIMOTO, *Kagaku Kogaku*, 31 (1967) 49.
8 H. LONDON, *Separation of Isotopes*, Newnes, London, 1961.
9 J. J. CARBERRY, *Amer. Inst. Chem. Eng. J.*, 6 (1960) 460.
10 E. GLUECKAUF, *Ion Exchange and Its Applications*, Society of Chemical Industry, London, 1955, p. 34.
11 M. C. BROOKS AND R. M. BADGER, *J. Phys. Colloid Chem.*, 52 (1948) 1890.

Notes

CHROM. 5140

Analysis of some hydroxy fatty compounds as their trimethylsilyl ethers by gas–liquid chromatography

In the gas–liquid chromatography (GLC) analysis of hydroxy fatty esters either as such or as their acetates, their high polarity and low volatility gave rise to long retention times and thus made quantitation somewhat unsatisfactory. The introduction of trimethylsilyl (TMS) ethers has allowed the analysis of a large number of these acids. Thus WOOD *et al.*[1] reported good resolutions of mono- and diglycerides as their TMS ethers. The retention times of various ricinoleic acid derivatives showed that the TMS derivative eluted approximately four times faster than the acetylated derivative and five times faster than the methyl ester[2]. A comparison of the GLC resolution of diastereoisomeric polyhydroxystearates as TMS and trifluoroacetyl derivatives revealed that the trifluoroacetyl derivatives were more useful for the analysis of hydroxy derivatives especially for resolving *erythro* and *threo* isomers[3]. There are a few more reports on the analysis of fatty alcohols as their TMS ethers[4,5]. In continuation of our work on the GLC of TMS ethers of hydroxy compounds[6], we now report the analysis of some long-chain hydroxy fatty acids.

Experimental

The hydroxy derivatives were prepared by established procedures of hydroxylation, lithium aluminium hydride and catalytic reductions, etc.[7]. The procedure of WOOD *et al.*[1] was employed for silylation. Thus the hydroxy ester (20 mg) taken in pyridine (0.5 ml) was treated with hexamethyldisilazane (0.2 ml) and trimethylchlorosilane (0.1 ml). After a reaction time of 30 sec during which the contents were intimately mixed, the reaction mixture was kept for 5 min. After addition of 5 ml of water, the silylated mixture was extracted with light petrol (b.p. 40–60°). The petroleum ether extracts were washed with water and dried, and solvent was removed on a steam bath. GLC of this material was carried out in an F & M model 1609 GLC unit provided with a flame ionisation detector. A 3% SE-30, silicone gum rubber, packed with Chromosorb W, 45–60 mesh, in a 2 ft. × 3/16 in. stainless-steel column was used. Other conditions of analysis were: hydrogen flow rate, 40 ml/min; nitrogen flow rate, 100 ml/min; air, 300 ml/min; injection port temp., 310°; block temp., 300°; attenuation, 1600; and chart speed, 4 min/in. Programming was carried out for the various TMS derivatives of different chain lengths from temperatures ranging from 130 to 220° at 5°/min.

Results and discussion

Table I gives the elution temperatures and retention times of various hydroxy fatty compounds analysed as their TMS ethers. Undecanol, undecanediol and undecanetriol had progressively higher retention temperatures and were well separated from each other. Among the C_{18} monohydroxystearates, the 2-hydroxy ester emerged first from the column followed by 9(10)-hydroxy and 12-hydroxy esters. But 18-hydroxystearate which carries a primary hydroxyl group is distinctly separable from

TABLE I

RETENTION TIMES OF VARIOUS TMS ETHERS OF HYDROXY FATTY COMPOUNDS

TMS ether	*Elution temp. (°C)*	*Absolute retention time (min)*
Temp. programming from 160 to 180° at 5°/min		
Methyl 2-hydroxystearate	183	4.8
Methyl 9(10)-hydroxystearate	185	5.0
Methyl 12-hydroxystearate	186	5.2
Methyl 18-hydroxystearate	192	6.4
Temp. programming from 180 to 220° at 5°/min		
Methyl *threo*-9,10-dihydroxystearate	195	3.0
Methyl *erythro*-9,10-dihydroxystearate	196	3.2
Methyl 9,10,12,13-tetrahydroxystearate	206	5.2
Methyl 13(14)-hydroxydocosanoate	209	5.8
Methyl 2-hydroxydocosanoate	209	5.8
Methyl *erythro*-2,3-dihydroxydocosanoate	212	6.6
Methyl *erythro*-13,14-dihydroxydocosanoate	214	6.8
Methyl *threo*-13,14-dihydroxydocosanoate	214	6.8
1,13,14-Docosanetriol	220	8.0
Temp. programming from 130 to 180° at 5°/min		
Undecanol	142	2.4
1(10),11-Undecanediol	158	5.6
1,10,11-Undecanetriol	168	7.6

compounds carrying a secondary hydroxyl group and has a longer retention time. The TMS derivatives of positional isomers obtained by catalytic hydrogenation of *cis*-9,10-epoxystearic acid, *viz.*, 9- and 10-hydroxystearates, were not resolvable from each other as has been earlier observed for acetoxy analogues by TULLOCH[8].

Among the di- and polyhydroxy derivatives, the *threo* and *erythro* isomers are not separable. Tetrahydroxy derivatives had a longer retention time (5.2 min) than the dihydroxystearates (3.2 min). Similarly the hydroxy compounds of C_{22} series had higher elution temperatures than those of the C_{18} and C_{11} derivatives. The *threo*- and *erythro*-13,14-dihydroxydocosanoates were not separable and had higher retention times than the corresponding 2,3-dihydroxy isomers (2,3-dihydroxy, 6.6 min; 13,14-dihydroxy, 6.8 min). 1,13,14-Docosanetriol had the highest retention time (8.0 min) of all the compounds of C_{22} series analysed by GLC. Analysis on a polyester column was attempted to separate the stereoisomers but could not be used due to the bleeding of the stationary phase from the column at temperatures above 210°.

The silylation technique for the analysis of hydroxy isomers was used in the identification of the formoxylation product of *trans*-2-docosenoic acid. As the 2- and 3-hydroxy groups are in closer proximity to carboxyl than in other centrally located hydroxy fatty acids, the former pair were separated. Thus GLC analysis of the formoxylated product after methylation and silylation showed it to consist of 78% of 3-hydroxy- and 22% of 2-hydroxydocosanoic acids, respectively[7].

Conclusions

Hydroxy compounds with C_{11}, C_{18} and C_{22} chain lengths show significant differences in their retention times and are easily separable.

Mono-, di-, tri- and tetrahydroxy esters can be separated, their retention times increasing in the order stated. However *threo* and *erythro* isomers are not separable.

Methyl 18-hydroxystearate has a longer retention time than either the 12-hydroxy or 9(10)-hydroxy isomers and is separable from them.

Regional Research Laboratory,
Hyderabad-9 (India)

R. KANNAN*
A. RAJIAH
M. R. SUBBARAM
K. T. ACHAYA

1 R. WOOD, P. K. RAJU AND R. REISER, *J. Amer. Oil Chem. Soc.*, 42 (1965) 81.
2 R. WOOD, P. K. RAJU AND R. REISER, *J. Amer. Oil Chem. Soc.*, 42 (1965) 161.
3 R. WOOD, E. L. BEVER AND F. SNYDER, *Lipids*, 1 (1966) 399.
4 R. WOOD, *J. Gas Chromatog.*, 6 (1968) 94.
5 W. J. ESSELMAN AND C. O. CLAGETT, *J. Lipid Res.*, 10 (1969) 234.
6 A. RAJIAH, M. R. SUBBARAM AND K. T. ACHAYA, *J. Chromatog.*, 38 (1968) 35.
7 R. KANNAN, *Ph. D. Thesis*, Osmania University, 1968.
8 A. P. TULLOCH, *J. Amer. Oil Chem. Soc.*, 41 (1964) 833.

Received October 22nd, 1970

* Present address: Department of Medical Chemistry, Royal Veterinary College, Stockholm-50, Sweden.

CHROM. 5152

Polyvinylpyrrolidone column chromatography of strawberry, rhubarb, and raspberry anthocyanins

We have been interested in isolating substantial quantities of pure anthocyanin pigments for use in study of reactions involved in their degradative reactions. Using column chromatography on insoluble polyvinylpyrrolidone (PVP), Polyclar AT, HRAZDINA[1] successfully separated the 3,5-diglucosides of peonidin, petunidin, cyanidin, malvidin, and delphinidin from grapes. These 5 pigments differ in number of methoxyl and/or phenolic groups and therefore are particularly well suited for a separation system employing Polyclar AT, which has a high affinity for phenolic groups. BLUNDSTONE AND CREAN[2] used column Polyclar AT chromatography for isolating the anthocyanins of strawberry, raspberry, cherry, black currant and plum which they subsequently identified by thin-layer chromatography. The degree to which the different anthocyanin systems were resolved was not reported.

This communication reports the conditions used for Polyclar AT column separation of strawberry, rhubarb, and raspberry anthocyanins, the latter two containing anthocyanins having the same phenolic pattern and differing in the glycosidic moiety.

Experimental

Column chromatography. Columns were prepared according to the procedure of HRAZDINA[1]. The Polyclar AT (GAF Corp., New York, N.Y.) was sieved and particles larger than 80 mesh were suspended in 10% aqueous HCl, boiled 10 min, let settle for $7\frac{1}{2}$ min, and the supernatant decanted. The PVP was resuspended in distilled water, allowed to settle and this procedure repeated until the supernatant was clear (30–40 times). The following column sizes were employed: 50 × 2.4 cm, 36 × 5.0 cm, 35 × 1.5 cm, and 70 × 1.5 cm. Columns were water-jacketed (23–25°) and all had flow rates of 2.7–3.0 ml/min when washed with water. Both gravity flow and a pump (LKB miniflow precision micropump) were employed.

Thin-layer chromatography. The procedure of QUARMBY[3] was followed in preparing 5 × 20 cm PVP plates. Modifications in his procedure included using 100–200 mesh dry-sieved PVP and elimination of the water sieving step.

Cellulose plates of 0.25 mm thickness were also utilized.

Solvent systems. PVP column and thin-layer chromatography: The solvent used by HRAZDINA[1] (30% aqueous ethanol containing 1 ml of 1 *N* HCl/l) was used. Numerous other systems were investigated employing methanol (MeOH) and/or ethanol (EtOH), HCl, and water. MeOH systems varied from 30–100%, HCl from 0.01–4%, the remaining percentage being water. EtOH systems varied from 30–100% and HCl from 0.0083–0.1%. Cellulose TLC: (1) glacial acetic acid–water–HCl (15:82:3) (AWHCl); (2) *n*-butanol–water–HCl (5:1:2) (BuWHCl 512); (3) water–formic acid–HCl (8:1:4) (WFHCl 814); (4) *n*-butanol–water–acetic acid (6:1:2) (BuWHAc 612); (5) propanol–water–HCl (3:10:2) (PrWHCl 3102); (6) upper phase of *n*-butanol–benzene–formic acid–water (100:19:10:25) (BuBFW).

Pigment isolation. Strawberries (Northwest variety), rhubarb (crimson cherry), and red raspberries (Willamette) were obtained from the OSU Horticulture Department. Anthocyanins were extracted with water, filtered through celite, and further purified by adsorption onto PVP (WROLSTAD *et al.*[4,5]). The methanolic–HCl antho-

cyanin concentrate was precipitated with diethyl ether three times (1 vol. methanol to 10 vol. ether) and the precipitate air dried and stored in a desiccator.

Results and discussion

The anthocyanins of strawberry, pelargonidin-3-glucoside (pgd-3-glu) and cyanidin-3-glucoside (cyd-3-glu), differ in number of phenolic groups and should be easily separated using PVP column chromatography. 1 l of clarified strawberry juice was applied to the column and separated using HRAZDINA's procedure. Most fractions were contaminated, however, and rechromatography was necessary to obtain pure fractions. We found two procedural changes which resulted in improved separation, eliminating the need for rechromatography. We could obtain a very compact band by applying a dried anthocyanin isolate to the column bed and then washing with water to adsorb the pigments. Using 0.1% HCl in MeOH as a developing solvent gave better resolution, faster development time, and speeded concentration.

We were interested in separating the anthocyanins of rhubarb, cyd-3-glu and cyanidin-3-rutinoside (cyd-3-rut), as it is much richer in cyd-3-glu than strawberry (WROLSTAD AND HEATHERBELL[6]). The two pigments, having the same phenolic pattern, would presumably have the same affinity for PVP. The pigments could be resolved by PVP TLC using either methanolic or ethanolic HCl systems provided that water content was at least 50%. Best resolution was obtained with 0.1% HCl in MeOH–H_2O (60:40). The pigments were successfully separated by column chromatography (Table I) using either 0.1% HCl in 60% MeOH–H_2O or 0.1% HCl in 30% EtOH–H_2O. The ethanolic system is preferred as a shorter column is required for resolution.

TABLE I

PARAMETERS FOR PVP COLUMN CHROMATOGRAPHY OF ANTHOCYANINS

Sample	*Ether precipitate (mg)*	*Column size (cm)*	*Solvent*[a]	*Development time (h)*	*Resolution*
Strawberry	200	40 × 5	100% MeOH	3	Very good
	20	35 × 1.5	30% EtOH	5	Poor
Rhubarb	30–40	35 × 1.5	100% MeOH	3	Good
	30–40	35 × 1.5	30% EtOH	7	Very good
	30–40	70 × 1.5	100% MeOH	7	Very good
Raspberry	25	30 × 1.5	70% MeOH	4	Good

[a] 0.1% HCl included in all solvents.

Fig. 1 is a thin-layer chromatogram showing the purity of the fractions obtained from the rhubarb column. Only 2 spots were detected when the original rhubarb anthocyanin isolate was separated by two-dimensional cellulose TLC using solvent systems 2 and 3, and 4 and 5 (NYBOM[7]). The concentration resulting from column chromatography shows presence of two additional anthocyanins, Pigment A present in fractions 1 through 7, and Pigment B present in fractions 26 through 48. FULEKI[8] using paper chromatography reported presence of 2 additional minor pigments in rhubarb, reporting one to be a cyanidin bioside.

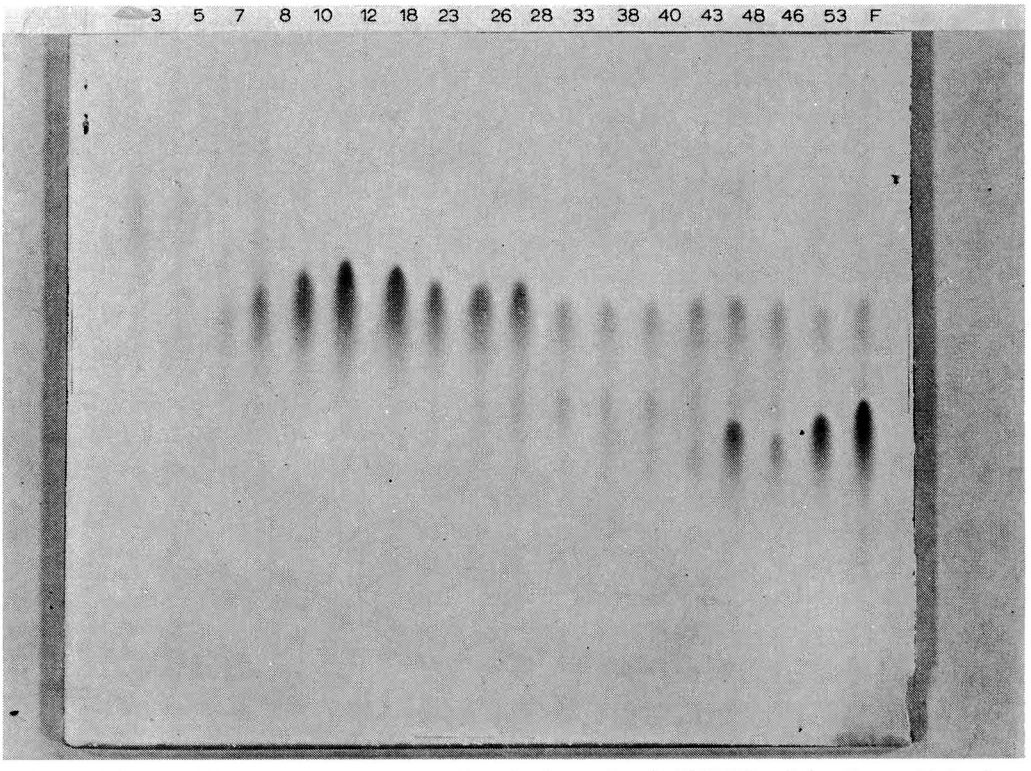

Fig. 1. Cellulose thin-layer chromatogram (developing solvent AWHCl) of fractions obtained from PVP column chromatography of rhubarb anthocyanins. Developing solvent, 30% EtOH containing 0.1% HCl; column size, 35 × 1.5 cm.

When a cellulose thin-layer chromatogram (solvent 1) of a fraction containing Pigment B was sprayed with molybdate spray (ALBACH *et al.*[9]) it gave a much more intense blue color than did the cyanidin pigments. Pigment B was extremely labile being particularly light-sensitive. We succeeded in purifying it by preparative PC. Its wavelength of maximum absorption (537 nm) and spectral shift with $AlCl_3$ (37 nm) would be more in accordance with delphinidin than with cyanidin, malvidin, or petunidin anthocyanins (HARBORNE[10]). The lack of a shoulder at 440 nm in the absorption spectrum suggests the possibility of substitution in 5th position. This could also account for its chromatographic behavior on PVP as the additional phenolic group in the B ring should give increased retention on PVP; substitution in the 5th position conceivably could compensate for this. Pigment A was present in low quantities and no spectral data was obtained. Its chromatographic properties were similar to the minor pigment in strawberries described by WROLSTAD *et al.*[11].

Red raspberries contain cyd-3-glu, cyd-3-rut, cyanidin-3-sophoroside (cyd-3-soph), and cyanidin-3-(2^G glucosylrutinoside) with some species containing the corresponding pelargonidin glycosides[12]. The anthocyanins from Willamette variety could be separated into five spots by two-dimensional cellulose TLC using solvent systems 2 and 3 and into five bands using one-dimensional chromatography on BuBFW. The best separation with PVP TLC was achieved with 0.1% HCl in MeOH–H_2O (70:30)

giving three spots. Examination by cellulose TLC (BuBFW) of different fractions obtained by PVP column chromatography (0.1% HCl in MeOH–H_2O, 70:30) revealed presence of seven different pigments. Mono-, di-, and tri-glucosides could be separated from each other; while diglucosides were not well resolved, the concentration effected would now permit separation by preparative paper or further column chromatography for identification work.

These studies show that column PVP chromatography can be utilized in separating not only anthocyanins which differ in number of phenolic groups but also those which differ in number of glycosides. PVP TLC is extremely useful in selecting suitable solvent systems for column separation of anthocyanin mixtures. Columns can be regenerated by washing with 10% HCl in MeOH, followed by distilled water to a neutral pH. The column should be prewashed with distilled water immediately before use, as in one experiment we obtained a new band which eluted very quickly from the column. Subsequent TLC analysis showed it to contain the slower moving anthocyanins and soluble PVP. PVP on a cellulose TLC plate fluoresces white when examined under UV light. Apparently some PVP was solubilized on standing in water; this adsorbed anthocyanins and eluted with the developing solvent.

PVP columns can be heavily loaded and the high recovery of pigments makes them very useful for preparative work. The concentration effect gives fractions rich enough in minor pigments to allow characterization after purification by some other method such as preparative paper chromatography.

This work was supported by a Future Leader Grant to the senior author from The Nutrition Foundation, Inc.

The authors thank L. BLECHER of General Aniline and Film, New York, for supplying the Polyclar AT.

Department of Food Science and Technology,
Oregon State University,
Corvallis, Ore. 97331 (U.S.A.)

R. E. WROLSTAD
BARBARA J. STRUTHERS

1 G. HRAZDINA, *J. Agr. Food Chem.*, 18 (1970) 243.
2 H. A. W. BLUNDSTONE AND D. E. C. CREAN, *The Pigments of Red Fruits*, Fruit and Vegetable Preservation Research Association, Chipping Campden, England, 1966.
3 C. QUARMBY, *J. Chromatog.*, 34 (1968) 52.
4 R. E. WROLSTAD AND T. P. PUTNAM, *J. Food Sci.*, 34 (1969) 154.
5 R. E. WROLSTAD, T. P. PUTNAM AND G. W. VARSEVELD, *J. Food Sci.*, 35 (1970) 448.
6 R. E. WROLSTAD AND D. A. HEATHERBELL, *J. Food Sci.*, 33 (1968) 592.
7 N. NYBOM, *J. Chromatog.*, 38 (1968) 382.
8 T. FULEKI, *J. Food Sci.*, 34 (1969) 365.
9 R. F. ALBACH, R. E. KEPNER AND A. D. WEBB, *J. Food Sci.*, 28 (1965) 69.
10 J. B. HARBORNE, *Biochem. J.*, 70 (1958) 24.
11 R. E. WROLSTAD, K. I. HILDRUM AND J. F. AMOS, *J. Chromatog.*, 50 (1970) 311.
12 J. B. HARBORNE, *Comparative Biochemistry of Flavonoids*, Academic Press, New York, 1967, p. 157.

Received November 9th, 1970

CHROM. 5147

High-speed liquid chromatography of glucuronide and sulfate conjugates

High-speed liquid chromatography is a relatively new form of liquid chromatography in which the column is operated at high pressures (> 1000 p.s.i.g.) permitting rapid analyses to be made. Systems capable of operation under these conditions have been described by several authors[1–5]. These systems have been employed in biochemical studies for the analysis of nucleotides and related compounds[1,4,6–8], carbohydrates[9], amino acids[10] and urinary constituents[11,12]. Recently high-speed liquid chromatography has been applied to the analysis of various drugs including benzodiazepines[13], phenacetin metabolites[14] and barbiturates, diphenylhydantoin and their hydroxylated metabolites[15].

Few methods are available for the qualitative and quantitative analysis of drug conjugates in biological samples. For example, thin-layer chromatography has been employed for the analysis of the glucuronide and sulfate conjugates of *p*-hydroxyacetanilide[16] and gas chromatography has been utilized in glucuronide analysis[17–19]. No methods have been described for the direct gas chromatographic analysis of sulfate conjugates although derivatives of these compounds can be analyzed by this technique[20]. The success obtained with the use of high-speed liquid chromatography in the analysis of various compounds of biochemical interest suggested that this technique could be useful for the analysis of sulfate and glucuronide conjugates. The present paper describes conditions for the analysis of sulfate and glucuronide conjugates in urine using high-speed liquid chromatography; a preliminary report of this work has been presented elsewhere[21].

Experimental

Chemicals. Phenol, *p*-nitrophenol, catechol, *p*-hydroxyacetanilide, phenyl glucuronide, *p*-nitrophenyl glucuronide, *p*-nitrophenylsulfate, formic acid and potassium chloride were used as obtained from the suppliers. Modifications of the methods of DUSZA *et al.*[22] and HEARSE *et al.*[23] were employed for the synthesis of N-acetyl-*p*-aminophenyl sulfate (acetanilide sulfate) and catechol monosulfate. N-Acetyl-*p*-aminophenyl glucuronide (acetanilide glucuronide) was isolated by thin-layer chromatography (*n*-butanol–acetic acid–water (8:1:1); acetone–*n*-butanol–water (5:4:1)[16] from the urine of rats given 150 mg/kg *p*-hydroxyacetanilide intraperitoneally or from the urine of adult human males given 15 mg/kg *p*-hydroxyacetanilide (Tylenol®) orally. Spots corresponding to acetanilide glucuronide on thin-layer chromatograms showed a positive reaction to the naphtharesorcinol test for glucuronides. Similarly, peaks corresponding to acetanilide glucuronide collected from the liquid chromatograph were glucuronide positive using the method of MEAD *et al.*[24]. Acetanilide glucuronide and sulfate peaks showed the presence of *p*-aminophenol after collection and analysis[25,26].

Apparatus. A Varian LCS-1000 high-speed liquid chromatograph equipped with an ultraviolet photometer monitoring absorbance at 254 mμ was employed. The stainless-steel column (1 mm I.D. × 250 cm long) contained a pellicular anion-exchange resin[2] (type LSF); the column was maintained at 80°. Inlet pressures in the range of 800–1000 p.s.i.g. provided a flow rate of 30 ml/h. Exact instrumental operating parameters are given in the tables and figures.

Procedure. Experiments were conducted employing both non-gradient and gradient modes of operation. When conditions were varied, the system was flushed and the column purged with the new solution for at least 30 min. Formic acid, 10.0 m*M*, pH 3 containing 1.0 *M* potassium chloride served as the eluent when non-gradient elution was employed. The following conditions were employed in most gradient elution experiments: high concentrate solution: 1.0 m*M* formic acid, pH 4, containing 2.0 *M* potassium chloride; gradient chamber solution: 1.0 m*M* formic acid, pH 4; initial volume of 1.0 m*M* formic acid in gradient chamber: 50 ml; high concentrate flow rate into the gradient chamber: 15 ml/h and column flow rate: 30 ml/h. These conditions yield a linear gradient of potassium chloride.

Sample preparation. Reference materials were dissolved in double distilled water for analysis. Collected urine was immediately passed through an ultrafiltration membrane (Centriflo®, Amicon Corp.) and the ultrafiltrates stored frozen until analyzed by direct injection into the liquid chromatograph.

Results and discussion

The non-gradient mode of operation was selected for initial experiments dealing with the high-speed liquid chromatography of phenols and their glucuronide and sulfate conjugates. Trials with eluents of differing molarity and pH were performed. Formate, acetate, and phosphate buffers of pH greater than 5.0 and varying in molarity from 1.0 m*M* to 1.0 *M* failed to adequately resolve phenols and their corresponding glucuronides; in addition poor peak shape was observed. These buffers did not elute sulfate conjugates. Addition of potassium chloride to the above buffers did not significantly improve resolution. Failure of the previously mentioned buffers to elute sulfate conjugates led to the use of eluents of lower pH and increased ionic strength. Formic acid solutions, pH 3.0, containing 1.0 *M* potassium chloride successfully eluted sulfate conjugates as well as phenols and glucuronides (Fig. 1 and Table I).

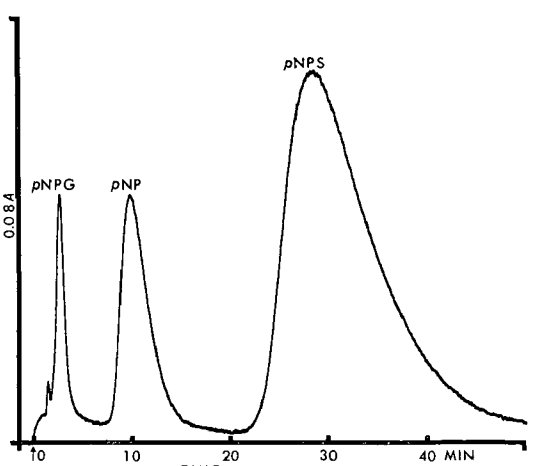

Fig. 1. Chromatography of *p*-nitrophenol (*p*NP, 100 nmoles), *p*-nitrophenyl glucuronide (*p*NPG, 50 nmoles) and *p*-nitrophenyl sulfate (*p*NPS, 150 nmoles). Mode: non-gradient; eluent: 10.0 m*M* formic acid, pH 3, containing 1.0 *M* potassium chloride; column temperature: 80°; flow rate: 30 ml/h; inlet pressures: 800–1000 p.s.i.g.

TABLE I

RETENTION VALUES OF PHENOLS AND THEIR CORRESPONDING GLUCURONIDE AND SULFATE CONJUGATES

Compound	*Non-gradient mode, retention time (min)*[a]	*Gradient mode, retention time (min)*[b]
Phenol	5.0	5.0
Catechol	4.7	4.7
p-Nitrophenol	15.5	13.9
p-Hydroxyacetanilide	3.6	3.4
Phenyl glucuronide	3.1	9.7
Catechol glucuronide	2.7	3.1
p-Nitrophenyl glucuronide	4.5	3.7
Acetanilide glucuronide	2.7	8.5
Phenyl sulfate	12.5	—[c]
Catechol monosulfate	14.7	—[c]
p-Nitrophenyl sulfate	38.5	—[c]
Acetanilide sulfate	9.5	37.5

[a] Conditions: 10.0 m*M* formic acid, pH 3, containing 1.0 *M* potassium chloride, 80°, 30 ml/h.

[b] Conditions: Low concentrate chamber: 1.0 m*M* formic acid, pH 4. High concentrate chamber: 1.0 m*M* formic acid, pH 4, containing 2.0 *M* potassium chloride. Flow of high concentrate into gradient chamber: 15 ml/h. Column flow: 30 ml/h. Initial volume: 50 ml. Temperature: 80°.

[c] No compound eluted within 90 min.

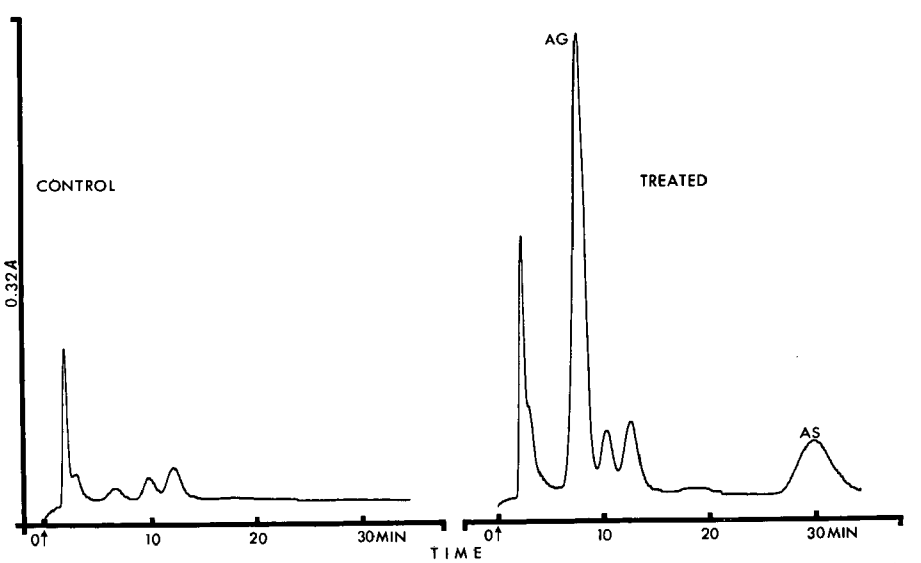

Fig. 2. Chromatography of *p*-hydroxyacetanilide metabolites in human urine. Subject was normal adult human male given 15 mg/kg *p*-hydroxyacetanilide (Tylenol®) orally. One microliter of ultrafiltrate from control and 0–5 h urine samples was injected into the liquid chromatograph: AG = acetanilide glucuronide, AS = acetanilide sulfate. Mode: gradient; eluent: 1.0 m*M* formic acid, pH 4 to 1.0 m*M* formic acid, pH 4, containing 2.0 *M* potassium chloride; temperature: 80°; flow rate: 30 ml/h; inlet pressures: 800–1000 p.s.i.g.

It should be noted, though, that the non-gradient system did not satisfactorily retain glucuronide conjugates on the column.

Experiments using gradient elution techniques were undertaken in an attempt to provide satisfactory analytical conditions for glucuronides. A linear gradient formed by mixing 1.0 m*M* formic acid, pH 4.0, with 2.0 *M* potassium chloride in 1.0 m*M* formic acid, pH 4, separated phenols and glucuronides (Table I). Gradient elution also resolved a mixture of *p*-hydroxyacetanilide, acetanilide glucuronide and acetanilide sulfate. This gradient system did not elute phenyl, *p*-nitrophenyl or catechol sulfate. The data in Table I shows that relatively little difference in retention times of phenols was observed between non-gradient and gradient modes of operation; similar results were obtained with *p*-nitrophenyl or catechol glucuronide. In contrast to the results obtained with non-gradient operation, the gradient system retained phenyl and acetanilide glucuronides longer than the corresponding phenols.

The methods described above have been applied to the estimation of conjugates in biological fluids. Specifically, non-gradient elution techniques have been used to measure sulfate conjugates in chicken urine following the infusion of catechol and *p*-nitrophenol as well as phenyl sulfate itself[27]. Gradient elution permitted analysis of phenyl glucuronide in chicken urine following its infusion. In other experiments acetanilide glucuronide and sulfate have been identified and quantitated in both rat and human urine following the administration of *p*-hydroxyacetanilide (Fig. 2). Urine samples were prepared and analyzed as described in the *Experimental* section. Previously BURTIS *et al.*[14] have reported the liquid chromatography of phenacetin metabolites. They observed the presence of glucuronide conjugates of *p*-hydroxyacetanilide and 3-methoxy-4-hydroxyacetanilide. However, sulfate conjugates were not detected and the elution time for acetanilide glucuronide was approximately 23 h. In contrast, the method reported in this paper permits quantitative estimation of acetanilide glucuronide and sulfate in urine in less than 40 min. These results suggest that high-speed liquid chromatography should be useful for monitoring glucuronide and sulfate conjugates of drugs in clinical situations.

ACKNOWLEDGEMENTS

This work was supported by U.S. Public Health Service Grant No. GM 17511 and GM 15477.

Department of Pharmacology,
University of Minnesota,
Minneapolis, Minn. 55455 (U.S.A.)

M. W. ANDERS
JENNINE P. LATORRE

1 C. D. SCOTT, J. E. ATTRILL AND N. G. ANDERSON, *Proc. Soc. Exp. Biol. Med.*, 125 (1967) 181.
2 C. G. HORVATH, B. A. PREISS AND S. R. LIPSKY, *Anal. Chem.*, 39 (1967) 1422.
3 H. FELTON, *J. Chromatog. Sci.*, 7 (1969) 13.
4 A. C. BURTIS, M. N. MUNC AND F. R. MACDONALD, *Clin. Chem.*, 16 (1970) 667.
5 R. E. MAJORS, *J. Chromatog. Sci.*, 8 (1970) 338.
6 C. HORVATH AND S. R. LIPSKY, *Anal. Chem.*, 41 (1969) 1227.
7 J. J. KIRKLAND, *J. Chromatog. Sci.*, 8 (1970) 72.
8 G. BROOKER, *Anal. Chem.*, 42 (1970) 1108.
9 D. S. YOUNG, *Amer. J. Clin. Pathol.*, 53 (1970) 803.

10 G. ERTINGHAUSEN, H. J. ADLER AND A. S. REICHLER, *J. Chromatog.*, 42 (1969) 355.
11 C. A. BURTIS AND K. S. WARREN, *Clin. Chem.*, 14 (1968) 290.
12 C. D. SCOTT, *Clin. Chem.*, 14 (1968) 521.
13 C. G. SCOTT AND P. BOMMER, *J. Chromatog. Sci.*, 8 (1970) 446.
14 C. A. BURTIS, W. C. BUTTS AND W. T. RAINEY, JR., *Amer. J. Clin. Pathol.*, 53 (1970) 769.
15 M. W. ANDERS AND J. P. LATORRE, *Anal. Chem.*, 42 (1970) 1430.
16 H. BÜCH, K. PFLEGER AND W. RUDIGER, *Z. Klin. Chem. Klin. Biochem.*, 5 (1967) 110.
17 T. IMANARI AND Z. TAMURA, *Chem. Pharm. Bull.*, 15 (1967) 1677.
18 J. B. KNAAK, J. M. ELDRIDGE AND L. J. SULLIVAN, *J. Agr. Food Chem.*, 15 (1967) 605.
19 E. C. HORNING, M. G. HORNING, N. IKEKAWA, E. M. CHAMBAZ, P. I. JAAKONMAKI AND C. J. W. BROOKS, *J. Gas Chromatog.*, 5 (1967) 283.
20 G. D. PAULSON AND C. E. PORTNOY, *J. Agr. Food Chem.*, 18 (1970) 180.
21 M. W. ANDERS AND J. P. LATORRE, *Pharmacologist*, 12 (1970) 273.
22 J. P. DUSZA, J. P. JOSEPH AND S. BERNSTEIN, *Steroids*, 12 (1968) 49.
23 D. J. HEARSE, A. H. OLAVESEN AND G. M. POWELL, *Biochem. Pharmacol.*, 18 (1969) 173.
24 J. A. MEAD, J. N. SMITH AND R. T. WILLIAMS, *Biochem. J.*, 68 (1958) 61.
25 B. B. BRODIE AND J. AXELROD, *J. Pharmacol. Exp. Ther.*, 94 (1948) 22.
26 T. SHIMAZU, *Biochim. Biophys. Acta.*, 105 (1965) 377.
27 A. J. QUEBBEMANN AND M. W. ANDERS, *Pharmacologist*, 12 (1970) 273.

Received November 5th, 1970

CHROM. 5144

A sensitive method for the detection of adenine compounds separated by paper or thin-layer chromatography

Purine compounds separated by paper chromatography (PC) or thin-layer chromatography (TLC) are most often detected by means of their fluorescence in UV light[1]. Purines can also be detected by PC by directing UV light at chromatograms pinned over a sheet of photographic paper; upon development of the photographic paper, the UV absorbing purines appear as white spots against a dark background[2]. Location reagents are less sensitive than the above techniques for locating purines[1]. One location reagent is the silver nitrate–Bromphenol Blue reagent of WOOD[3]. This reagent forms a blue purine-silver-dye complex which, under optimum conditions, can detect 0.05 μmole of purine derivatives.

In the present communication paper chromatograms are first dipped in an acidic vanillin reagent; they are then dried and dipped in a modified silver nitrate–Bromphenol Blue reagent. Adenyl compounds appear as pink spots on a gold background. The method is considerably more sensitive than any of the methods described above and specifically detects adenyl purines only. The same method can be applied to TLC by spraying instead of dipping. The specificity and sensitivity of the method are discussed.

Materials and methods

All the materials and reagents used were commercially available. The chromatographic paper used was Whatman No. 1. Microcrystalline cellulose, vanillin and silver nitrate were obtained from Merck AG, Darmstadt, G.F.R. Bromphenol Blue was obtained from May & Baker Ltd., Dagenham, Great Britain.

Reagent 1 consisted of 3.0 g of vanillin in 100 ml ethanol plus 0.5 ml sulphuric acid (*d* 1.84). Reagent 2 consisted of aqueous silver nitrate 2.5% mixed with an equal quantity of Bromphenol Blue 0.5% in acetone.

Paper chromatograms containing purines were first dipped in reagent 1, then immediately placed on filter paper in an oven at 90° for 5 min. They were then dipped in reagent 2, allowed to dry in air for 10 min, then placed in an oven at 90° for approximately $1\frac{1}{2}$ min.

The presence of adenyl compounds on paper chromatograms was indicated by a characteristic pink spot on a gold background. The colour was stable for at least several months.

Results and discussion

The location method was most sensitive for ATP and adenine, which could be detected on chromatograms spotted with as little as 0.0005 and 0.0001 μmole respectively (Table I). Other adenine compounds could be located in spots containing a minimum of 0.01 μmole. Higher concentrations of inosine were needed for detection. Deamination of the purine nucleus as occurs in the conversion of adenine to hypoxanthine (Fig. 1) failed to decrease the sensitivity of the compound to colour development since spots containing 0.01 μmole hypoxanthine could still be detected (Table I). However, sensitivity to colour development is lost in the conversion of hypoxanthine to xanthine since the latter compound could not be detected in spots containing as much as 10 μmole (Table I). The conversion of hypoxanthine to xanthine involves substitution on carbon 2 of the purine nucleus (Fig. 1). It should be noted that guanine and its nucleotides also have a substituent on carbon 2 of the purine nucleus and also failed to be detected by this location method in relatively higher concentrations (Table I, Fig. 1). The pyrimidines cytosine, thymine and uracil were not detected in concentrations as high as 0.1 μmole. The nature of the coloured

TABLE I

MINIMUM QUANTITIES OF PURINES DETECTED BY LOCATION REAGENTS

Compound	*μmole*
ATP[a]	0.0005
ADP[a]	0.01
AMP[e]	0.01
Cyclic 3′,5′-AMP[a]	0.01
Adenosine[c]	0.01
Inosine[b]	0.05
Adenine[c]	0.0001
Guanine[c]	5.0 (not detected)
GMP[e]	2.0 (not detected)
Hypoxanthine[d]	0.01
Xanthine[d]	10.0 (not detected)
Uric acid[d]	10.0 (not detected)

[a] Calbiochem, Los Angeles, U.S.A.
[b] Nutritional Biochemicals Corp., Cleveland, Ohio, U.S.A.
[c] The British Drug Houses Ltd., Poole, Great Britain.
[d] Koch-Light Laboratories, Ltd., Colnbrook, Bucks., Great Britain.
[e] Fluka AG, Buchs SG, Switzerland.

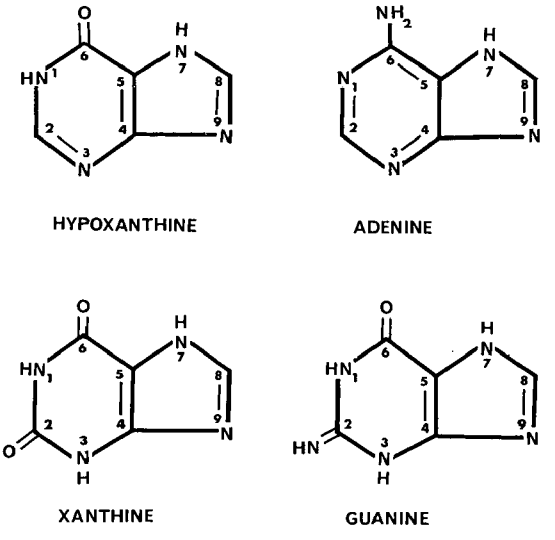

Fig. 1. The structures of hypoxanthine, adenine, xanthine and guanine.

TABLE II

COLOUR REACTIONS BY NON-PURINE COMPOUNDS

Spots contained 10 μmole of compound unless otherwise specified.

Compound	*Colour reaction*
Uracil[c,d]	—
UMP[e,f]	—
Thymine[c,h]	—
Cytosine[c,d]	—
DL-Phenylalanine[d]	brown
DL-Alanine[d]	—
Glycine[e]	—
Taurine[d]	—
DL-Leucine[d]	—
L(+)-Lysine[d]	—
Sucrose[e]	green
KCl[e]	—
Urea[b]	—
Noradrenaline[g]	green
Histamine[e]	—
5-Hydroxytryptamine[a,f]	—
Creatine[e]	—
Orcinol[e]	purple
Pyrogallol[e]	brown-purple
Cholesterol[e]	green

[a] Purple spot visible only after first dip.
[b] Yellow spot visible only after first dip.
[c] Spot contained 0.1 μmole.
[d] Koch-Light Laboratories Ltd., Colnbrook, Bucks., Great Britain.
[e] The British Drug Houses Ltd., Poole, Great Britain.
[f] Calbiochem, Los Angeles, U.S.A.
[g] Sterling Pharmaceuticals Ltd., Sydney, Australia.
[h] Nutritional Biochemicals Corp., Cleveland, Ohio, U.S.A.

complex is at present under investigation and will be the subject of a further communication.

A limited range of organic compounds was spotted on to the chromatogram and dipped in the location reagents in order to determine the specificity of the method. None of the compounds tested gave a pink spot, although in certain cases spots of other colours were observed (see Table II).

Non-phosphorylated adenyl compounds could be detected with sensitivity equal to that described above by omitting the step of heating the chromatogram in an oven at 90° for 5 min after dipping in Reagent I. This step was initially introduced because the phosphorylated adenyl compounds present on the chromatogram dipped in the acid Reagent I were hydrolysed upon heating and could be detected in smaller amounts.

The method has been applied to PC and microcrystalline cellulose coated TLC developed in a variety of solvent systems. However, it should be noted that solvents which are either strongly acidic or strongly alkaline may interfere with the location method.

Department of Zoology,
University of Melbourne,
Parkville 3052, Victoria (Australia)

MARY E. WRIGHT
D. G. SATCHELL

1 I. SMITH, *Chromatographic and Electrophoretic Techniques*, Vol. I, Heinemann, London, 1960
2 R. MARKHAM AND J. D. SMITH, *Nature*, 163 (1949) 250.
3 T. WOOD, *Nature*, 176 (1955) 175.

Received October 9th, 1970

J. Chromatog., 55 (1971) 413–416

CHROM. 5149

Quantitative analysis of tropane alkaloids in pharmaceutical preparations*

The problem of tropane alkaloid determination in mixtures is familiar to the drug analyst. The present paper describes procedures for the determination of scopolamine in injection solutions containing, in addition to scopolamine hydrobromide, morphine hydrochloride and sodium bisulphite and for the determination of atropine sulphate in coated tablets containing phenobarbitone and ergotamine tartrate. To our knowledge the few analytical methods elaborated so far for these mixtures are based on the determination of tropane alkaloids only after double extraction procedures in separation funnels or by ion exchange.

For the determination of scopolamine hydrobromide in a mixture with morphine hydrochloride, SVENSEN[1] proposed UV spectrophotometric assay after double shaking-out from the solution. SJÖSTRÖM AND RANDALL[2] separated scopolamine from morphine by passing the solution through a column filled with the strongly basic Dowex resin. The phenolic morphine was quantitatively retained on the column while the non-phenolic alkaloid passed through the resin and was determined in the effluent by colorimetry.

To obtain a rapid separation we thought that TLC separation known for its simplicity, high separation efficiency and accuracy might be useful for solving this problem. It must be borne in mind that in medical preparations the tropane alkaloids are usually present in microamounts in relation to other components present, which was another reason to choose TLC for this purpose.

Experimental

Reagents. Dragendorff–Munier reagent was made by mixing 1 part of a solution containing 17 g of bismuth nitrate and 200 g of tartaric acid in 800 ml of water with 1 part of a solution containing 160 g potassium iodide in 400 ml of water. Before use 100 g tartaric acid and 500 ml of water were added to 50 ml of this mixture. Hydrochloric acid was 10%; ethanol was 10%; sodium nitrite solution was a freshly prepared 1% water solution; ammonium sulphamate solution was a 2.5% water solution; N-naphthylethylenediamine dihydrochloride solution was a 1% water solution. The standard solution consisted of 7.5 mg of scopolamine hydrobromide (B.P. 1968) dissolved in 50 ml of water; the solvent system was chloroform–25% ammonia (100:0.15).

Apparatus. The TLC apparatus used was fitted with a thickness regulation spreader (Desaga, Heidelberg, G.F.R.).

Preparation of plates. The layer thickness was 0.5 mm. Activation required 3 h at 130°. The adsorbent was Aluminium Oxide G (Merck A.G., Darmstadt, G.F.R.).

Determination of scopolamine hydrobromide in scopolamine–morphine injection solutions

By means of a micropipette twice 150 μl of the injection solution (about 45 μg

* A communication of a part of this work has been given at the Annual Meeting of the Commission of Drug Control Laboratories F.I.P. in Montpellier, Sept. 1967.

of scopolamine·HBr) and 150 μl of the standard solution were applied separately along the starting line as 4-cm horizontal bands. The chromatogram was run by the ascending technique in a chamber previously saturated with solvent for 1 h. After 1 h, the plate was removed from the chamber and dried, and the alkaloid was located by means of the guide chromatogram sprayed with the Dragendorff–Munier reagent. The corresponding zones containing the alkaloid on the sample chromatogram and that of the standard were marked and quantitatively scraped off the plate into 50-ml flasks. The alkaloid was extracted by stirring for 30 min with 10 ml of chloroform, and the solution was centrifuged (5 min at 5000 r.p.m.). 5 ml of the clear supernatant solutions were each pipetted into 50-ml beakers and evaporated to dryness on a boiling water bath. The residues were allowed to cool and thereafter 1 ml of fuming nitric acid was added and evaporated to dryness in the same way as before. The residues were dried for 10 min at 100°. After cooling to room temperature, 2 ml of hydrochloric acid, 0.1 g of zinc powder and 10 ml of ethanol were added. After heating for 10 min at 100° and cooling on ice, each solution was filtered through a white band filter paper ($2r$ = 4.5 cm) into a 25-ml volumetric flask, and each residue on the filter was thereafter washed with three 2-ml portions of water. To the filtrates 1 ml of sodium nitrite solution and 1 ml of ammonium sulphamate solution were added. The solutions were stirred for 10 min, *i.e.* until liberated oxygen was completely expelled. After addition of 1 ml of N-naphthylethylenediamine dihydrochloride solution the reacting solution was mixed well, filled up to the mark with water and after 30 min the absorbances were measured at 545 nm in a 2-cm glass cell against water as a blank. The percentage of scopolamine hydrobromide was calculated from the mean value of the absorbances of both samples relative to that of the standard.

Determination of atropine sulphate in coated tablets containing ergotamine tartrate and phenobarbitone

Reagents. Dragendorff–Munier reagent, sodium nitrite solution, ammonium sulphamate solution, N-naphthylethylenediamine solution were as prescribed for the determination of scopolamine. Tartaric acid solution was a 1% water solution. Sulphuric acid–ethanol was a mixture of 100 ml of ethanol (96%) and 1 ml of sulphuric acid (16%).

Preparation of plates. Layer thickness was 0.5 mm. Activation required 3 h at 130°. The sorbent was Kieselgel G (Merck A.G., Darmstadt, G.F.R.).

Standard solution. 6.0 mg of atropine sulphate (B.P. 1968) was dissolved in the mixture of chloroform–methanol (4:1). The solvent was used to bring the volume to 25 ml. Solvent system was benzene–chloroform–ethanol (1:4:2).

After removing the coating from 20 tablets, the dried tablets were finely powdered. The quantity of the powder equivalent to about 1 mg of atropine sulphate, 3 mg of ergotamine tartrate and 200 mg phenobarbitone were mixed thoroughly for 2 min with 5 ml of 0.1 N H_2SO_4 and then with 7 ml of 0.1 N NaOH. The mixture was quantitatively transferred into a 100-ml separatory funnel with 3 times 3-ml portions of water. Extraction was carried out with six 10-ml portions of chloroform and the extract was filtered through a white band filter paper over anhydrous Na_2SO_4. After washing the filter with 5 ml of chloroform, the chloroform extracts were evaporated *in vacuo* at 40° to dryness. The residues were dissolved in 5 ml of a mixture of 40 ml

of chloroform and 10 ml of methanol (sample solution). By means of a micropipette, 200 μl of about 40 μg of atropine sulphate of the sample solution and 200 μl of the standard solution were applied twice as about 4-cm horizontal bands along the starting line. The chromatogram was run by the ascending technique until the solvent moved 10 cm from the start. The plate was removed from the chamber, air dried and the alkaloid detected on the guide chromatogram by spraying with the Dragendorff–Munier reagent. The corresponding zones with atropine on the samples and standard chromatogram were marked and quantitatively scraped off the plate into 50-ml flasks. To each flask 10 ml of sulphuric acid–ethanol were added, and the contents of the flask were mixed for 20 min and thereafter centrifuged (5 min at 5000 r.p.m.). 5 ml of the clear supernatant solution were pipetted each into 50-ml beakers and processed as directed for the determination of scopolamine. The percentage of atropine sulphate in the sample was calculated relative to the concentration of the alkaloid in the standard solution.

Results and discussion

For the separation of scopolamine hydrobromide from morphine hydrochloride, various solvent systems were checked. Owing to the phenolic character of morphine, various alkaline solvent systems were primarily used such as chloroform–diethylamine (90:10), chloroform–ammonia (100:0.15), cyclohexane–chloroform–diethylamine (50:40:10), using Aluminium Oxide G coated plates. Best separation was obtained with the solvent system chloroform–ammonia (100:0.15).

In choosing an appropriate solvent system for the separation of atropine sulphate from ergotamine tartrate and phenobarbitone, special care had to be taken to use a solvent system which would quantitatively separate atropine from ergotamine and phenobarbitone but cause no isomerisation of ergotamine which was then determined separately off the same plate. The solvent mixture chloroform–benzene–ethanol (40:10:20) met these requirements. Plates were coated with Silica Gel G and visualisation of the separated alkaloids was carried out using the Dragendorff–Munier reagent.

TABLE I

ANALYSIS OF A STANDARD SOLUTION OF SCOPOLAMINE–MORPHINE

Analysis No.	*Scopolamine hydrobromide found (mg) (0.3 mg present)*
1	0.281
2	0.276
3	0.300
4	0.279
5	0.310
6	0.292
7	0.301
Mean	0.291
Standard deviation ($P = 0.05$)	0.014
Limits of error	± 4.8%

TABLE II

ANALYSIS OF ATROPINE–ERGOTAMINE TARTRATE–PHENOBARBITONE TABLET

Analysis No.	*Atropine sulphate found (mg) (0.1 mg present)*
1	0.095
2	0.098
3	0.104
4	0.106
5	0.093
6	0.093
7	0.104
Mean	0.099
Standard deviation ($P = 0.05$)	0.052
Limits of error	± 5.2%

In spite of various methods published so far, the quantification of minute quantities of tropane alkaloids seems still to be a problem. Methods described in the literature for this purpose make use mainly of UV spectrophotometric[1], colorimetric[3–6] or IR[7] procedures of determination. The most frequently used method is that making use of the Vitali–Morin colorimetric test[3]. For the purpose of attaining stability of the violet colour formed, this method has been submitted for years to various investigations and modifications. However in spite of all precautions proposed and technical improvements introduced, such as the strict control of the water content of the solvent or introducing solvents other than acetone as for instance pyridine[8], isopropylamine[9], dimethylformamide[10], ethyl methyl ketone[11], the quick fading of the colour caused poor reproducibility of the results.

TABLE III

ANALYSIS OF COMMERCIAL TROPANE ALKALOID SAMPLES

Atropine sulphate (0.1 mg quantity claimed)		*Scopolamine hydrobromide (0.3 mg quantity claimed)*	
Found (mg)	*Difference (%)*	*Found (mg)*	*Difference (%)*
Sample A			
0.105	+5	0.100	+3.3
0.103	+3	0.295	−1.6
Sample B			
0.095	−5	0.300	—
0.100	—	0.310	+3.3
Sample C			
0.111	+11	—	—
0.112	+12		
0.113	+13		

For all these reasons the modified Bratton–Marshall colorimetric method[3,12] seemed to be the method of choice. This method includes nitration of the alkaloid, subsequent reduction of the obtained nitroproduct to the corresponding amino compound that is coupled after diazotisation with N-naphthylethylenediamine dihydrochloride to produce a red-violet colour having a maximum at 550 nm. Although this reaction includes four operations, the reaction product is stable and results are reproducible.

To confirm the accuracy and reproducibility of the procedures, determination of scopolamine hydrobromide and atropine sulphate, respectively, were carried out with standard mixtures containing all components in the same quantities as those of preparations commonly used in therapy. Results were statistically treated and as can be seen in Tables I and II satisfactory limits of error were obtained. Results of determinations with commercial samples of both mixtures are given in Table III.

ACKNOWLEDGEMENTS

The author is greatly indebted to Mrs. BLANKA PAVELIĆ and Mrs. ANDJELA HARAPIN for their excellent technical assistance.

Institute for the Control of Drugs,
Zagreb (Yugoslavia)

TATJANA BIĆAN-FIŠTER

1 R. SVENSEN, *Farm. Rev.*, 57 (1958) 147.
2 E. SJÖSTRÖM AND A. RANDALL, *J. Amer. Pharm. Ass., Sci. Ed.*, 48 (1959) 445.
3 B. KAKAČ AND Z. VEJDELEK, *Handbuch der Kolorimetrie*, B.I.G.Fischer Verlag, Jena, 1962, p. 105.
4 P. HORAK AND J. ZYKA, *Česk. Farm.*, 12 (1963) 394.
5 A. S. SAINT-FIRMIN AND R. R. PARIS, *J. Chromatog.*, 31 (1967) 252.
6 R. ADAMSKI, J. LUTONSKI AND J. WISNIEWSKI, *Deut. Apoth. Ztg.*, 107 (1967) 185.
7 R. S. BROWNING, S. E. WIBERLEY AND F. C. NACHOD, *Anal. Chem.*, 27 (1955) 7.
8 M. G. ASHLEY, *J. Pharm. Pharmacol.*, 4 (1952) 181.
9 I. GROSFELD-NIR AND E. WEISSBERG, *Drug Standards*, 25 (1945) 18.
10 W. O. JAMES AND M. ROBERTS, *Quart. J. Pharm. Pharmacol.*, 18 (1945) 29.
11 F. M. FREEMAN, *Analyst*, 80 (1955) 520.
12 A. C. BRATTON AND E. K. MARSHALL, *J. Biol. Chem.*, 128 (1939) 537.

Received October 1st, 1970

CHROM. 5181

Thin-layer chromatography of epoxy plasticizers

It has been reported[1] that plasticizers lend themselves satisfactorily to thin-layer chromatography (TLC) analysis using Silica Gel G plates with high moisture content. The developing solvent used was benzene–methylene chloride (2:1). However, it was hard to differentiate between an epoxidized tallate, an epoxidized soya oil or an epoxidized linseed oil. To improve the results, HUBER AND WIMMER[2] suggested a mixture consisting of petroleum ether (boiling range 40–80°)–ethyl ether–glacial acetic acid (80:20:1). However, this too was not satisfactory in accomplishing complete separation. Epoxy plasticizers are based on epoxidized triglycerides (soybean oil, linseed oil) or alkyl stearate[1]. Only the latter, however, can be detected by gas chromatography, since triglycerides cannot be evaporated without decomposing them[1]. Our studies have revealed that epoxidized triglycerides lend themselves satisfactorily to analysis by TLC on Silica Gel G plates of 500 μ thickness.

In our studies, we have found that the best developing solvent system to distinguish between different types of epoxidized plasticizers (soya from linseed or tallate types) was: hexane–ethyl ether–glacial acetic acid (70:40:3). This solvent system also differentiated oils from primary plasticizers such as adipates, phthalates, and from the phosphate type plasticizers. The R_F value of the epoxy plasticizer was much smaller than the primary and phosphate plasticizers, so one can easily distinguish between the different types.

Experimental

Plates coated with 500 μ thick Silica Gel G (E. Merck A.G.) are spotted with 5 μl of 0.5% w/w of known plasticizers in methylene chloride. The plate is developed in a solvent mixture of hexane–ethyl ether–glacial acetic acid (70:40:3), all ACS reagent grade. The traveling distance of the solvent front should be 15 cm. After the marked end point has been reached, the plate is dried for 15 min at 105°. Visualization is accomplished with one of the following spraying reagents: (1) Concentrated H_2SO_4 or chromic acid–concentrated H_2SO_4 followed by charring in the oven at 125–130°. (2) 10 g of $SbCl_5$ (5 ml of $SbCl_5$) in 40 ml carbon tetrachloride—heat for 30 min in an air oven at 100°. (3) 20% alcoholic solution of phosphomolybdic acid, followed by heating for 20 min at 130–140°. Upon cooling of the plate, immerse in a chamber saturated with ammonium hydroxide for a few seconds.

The above three spraying reagents have been found to be best suited for this type of work.

Results and discussion

Fig. 1 shows the results obtained. It is of interest to observe that this simple technique can differentiate between an epoxy type oil of the soya family, the tallate family and that of the linseed oil family. The 20% phosphomolybdic acid spraying reagent gives a better visualization of the spots than the concentrated H_2SO_4 or $SbCl_5$ solution. In Fig. 1, the plate was sprayed with phosphomolybdic acid. The important part of this technique is that, even if one can separate the epoxidized oil by another technique and follow it by IR analysis, the IR spectra do not differentiate

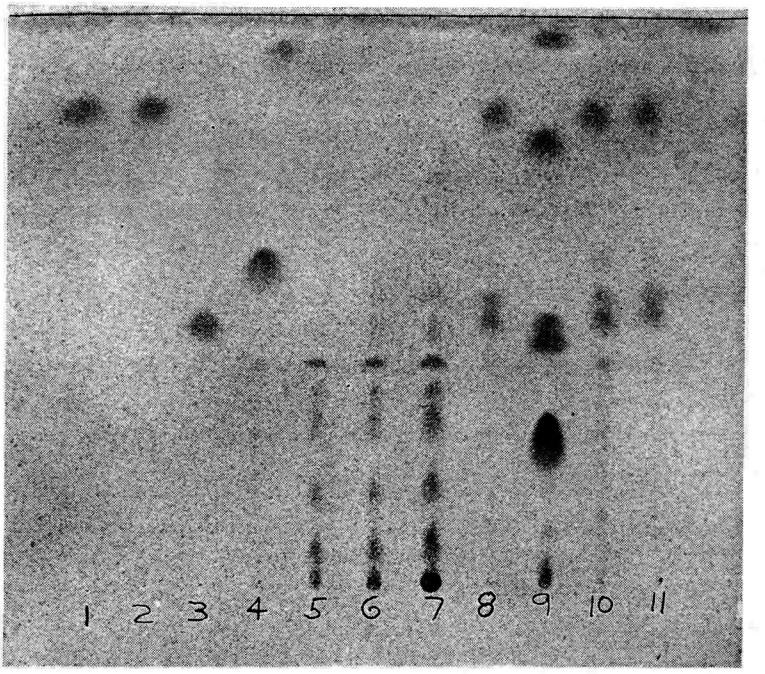

Fig. 1. Thin-layer chromatogram of epoxidized and non-epoxidized plasticizers. 5-μl spottings of 0.5% by weight concentration on 500 μ thick coating of Silica Gel G. 1 = dioctyl phthalate (DOP); 2 = dioctyl adipate (DOA); 3 = Santicizer 141 (octyl diphenyl phosphate); 4 = stearic acid; 5 = Paraplex G-62 (epoxidized soya oil); 6 = Admex 711 (epoxidized soya oil); 7 = Flexol EPO (epoxidized soya oil 1% by weight); 8 = Santicizer S-73 (epoxidized tallate oil); 9 = Epoxol 8-2B (butyl epoxidized linseed oil); 10 = Drapex 4.4 (octyl epoxy stearate); 11 = Admex 746 (epoxidized octyl tallate).

between a tallate epoxidized oil, a linseed epoxidized oil, or an epoxidized soya oil, whereas TLC does accomplish this in a very simple way.

The author wishes to thank the Goodyear Tire and Rubber Company for permission to publish this work.

Chemical Materials Development,
The Goodyear Tire and Rubber Company,
Akron, Ohio 44316 (U.S.A.)

ZALMAN RONEN

1 L. VERES, *Kunstst.*, 59 (1969) 241.
2 H. HUBER AND J. WIMMER, *Kunstst.*, 58 (1968) 786.

Received November 6th, 1970

CHROM. 5146

Rapid staining of proteins and peptides in starch gels by chlorination

The detection of proteins and peptides by chlorination has become a standard procedure in paper electrophoresis and chromatography. Direct extension of this method to gel media presents difficulties because of the time required to wash out the excess of chlorinating agent. Recently, however, BOREL *et al.*[1] have applied the reaction in a peptide analyser by destroying excess hypochlorite with hydrazinium sulphate. As will be shown below, this modification is applicable to starch-gel electropherograms in the absence of urea and other interfering substances.

Materials

Sodium hypochlorite solution was a commercial product (Lab. Supply, Melbourne). Other chemicals were laboratory reagent grade except hydrazinium sulphate, which was of analytical reagent grade (BDH). Hydrolysed starch was obtained from Connaught Laboratories, Toronto.

Procedure

After electrophoresis the starch gel is cut to give slices 1.5 mm thick. Hypochlorite solution is diluted to approximately 0.1 *M* with 0.2 *M* sodium phosphate buffer, the pH being adjusted to about 7. The gel slice is agitated in this solution for 1 min, the solution is replaced with an aqueous 1% solution of hydrazinium sulphate and agitation is continued until a corner cut from the gel no longer stains in potassium iodide solution (about 2–3 min at 20°). The hydrazinium sulphate is replaced with aqueous 10% potassium iodide, which finally is replaced with deionized water. The stain is stable for several days.

If the formation of bubbles of nitrogen in the gel is to be avoided, the gel slice can be soaked for 1 min in 1% sodium dithionate after chlorination. Alternatively, an almost bubble-free gel can be obtained if the hydrazinium sulphate solution is cooled to 0°.

Results and discussion

With this staining procedure, the result of a separation by starch-gel electrophoresis can be observed about 5 min after the gel is sliced. A clear background is obtained except for the presence of the bubbles referred to above, and of small blue-black spots due possibly to impurities in the starch.

Quantitative aspects of the reaction were not studied, but it seems to be somewhat less sensitive to protein detection than staining with Nigrosine dye. However, the reaction conditions used may not be the optimum ones. Thus proteins stain more intensely if the excess hypochlorite is removed by repeated washing in 1% trichloroacetic acid instead of with hydrazinium sulphate.

This method of detection is relatively non-specific, so that buffers must be carefully selected. Care must also be taken to avoid contamination in the preparation and handling of the gels, since otherwise a heavy background stain may result. A partial list of interfering substances is given by BOREL *et al.*[1]. On the other hand, the method should be applicable to most proteins with roughly the same sensitivity. Several small

peptides, including glycylglycine, could also be detected after starch-gel electrophoresis in 1 *M* acetic acid at 40 V/cm, although the zones were up to 5 mm wide after ½ h.

I wish to thank Mr. M. FRENKEL for technical assistance.

Division of Protein Chemistry, CSIRO, R. L. DARSKUS
Parkville (Melbourne), Victoria 3052 (Australia)

1 J. P. BOREL, M. DESANTI, G. GUILLAUME AND J. L. BARASCUT, *Bull. Soc. Chim. Biol.*, 50 (1968) 2165.

Received November 5th, 1970

CHROM. 5148

Two dimensional paper chromatography for the detection of oxidation of maltose by glucose oxidase

The present report describes a novel paper chromatographic procedure for studying the action of glucose oxidase on glucosyl oligosaccharides. With this technique, it has been shown conclusively that maltose is oxidized to maltobionic acid by glucose oxidase. Other methods for following glucose oxidase action are based on oxygen uptake[1,2] or hydrogen peroxide production[3,4] and are not suitable for use with oligosaccharides since the primary carbohydrate products cannot be identified. Further, since glucose oxidase preparations may contain contaminating glucosidase and transferase activities[4], conversion of oligosaccharides to glucose followed by oxidation of glucose may occur and may be interpreted erroneously as indicative of oligosaccharide oxidation[5]. By separating the products of glucose oxidase action on maltose on paper chromatograms, then utilizing a specific glucosidase for hydrolyzing the products directly on the chromatogram, and finally separating the products of the glucosidase reaction by chromatography in a second direction, it has been shown that maltobionic acid is the carbohydrate product of glucose oxidase action on maltose.

Materials and methods

The maltose used in all experiments was prepared from amylose via β-amylase and was free of glucose[6]. Reference maltobionic acid was synthesized by oxidation of maltose with bromine[7]. The maltobionic acid thus produced was purified by a paper chromatographic procedure using the *n*-butanol–pyridine–water solvent system to remove unoxidized maltose. Glucose and gluconic acid were obtained from commercial sources. Glucose oxidase (EC 1.1.3.4), obtained from Miles Laboratories, was purified according to the procedure described by PAZUR AND KLEPPE[8]. This glucose oxidase preparation did not contain any contaminating α-glucosidase activity. Glucoamylase (α-1,4-glucan glucohydrolase, EC 3.2.1.3) was prepared according to the methods described by PAZUR AND ANDO[9].

Paper chromatography was carried out at room temperature using Whatman No. 1 filter paper. The two solvent systems employed in this study were *n*-butanol–pyridine–water, 6:4:3 by volume, and isobutyric acid–1 *N* NH_4OH, 10:6 by volume.

A typical incubation mixture for checking the activity of glucose oxidase on maltose contained 10 mg of maltose dissolved in 80 μl of 0.05 *M* sodium acetate buffer, pH 5.0, to which 20 μl of a solution of glucose oxidase (5.6 mg/ml) were added. A crystal of thymol was placed in the final solution to prevent bacterial contamination. After 24 h of incubation at room temperature, a 5 μl aliquot of the incubation mixture was placed on a 9 × 9-in. paper chromatogram and subjected to a single ascent in the *n*-butanol–pyridine–water solvent system followed by a second ascent in the same direction in an isobutyric acid–1 *N* NH_4OH solvent system. The region of the chromatogram containing the maltose and maltobionic acid was then sprayed with a solution of glucoamylase (0.5 mg/ml). This area of the chromatogram was maintained in a moist condition for approximately 2 h by spraying the chromatogram every 15 min with the glucoamylase solution. The chromatogram was allowed to dry and

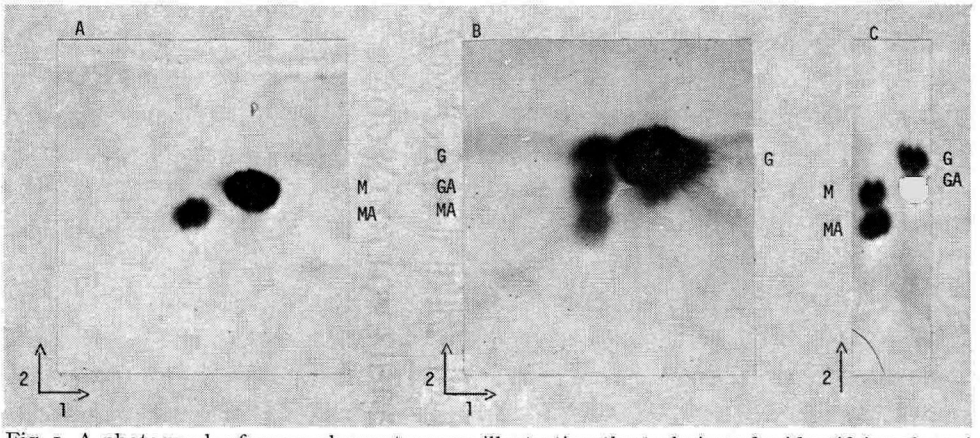

Fig. 1. A photograph of paper chromatograms illustrating the technique for identifying the primary carbohydrate product present in an incubation mixture of maltose and glucose oxidase. Part A of the figure illustrates the mobility of the carbohydrate components found in a 24-h digest. Part B shows the new carbohydrates that appear when the chromatogram is treated with glucoamylase before development in the second direction. Part C illustrates mobility in the second direction of pertinent reference compounds. Abbreviations are: G, glucose; GA, gluconic acid; M, maltose, and MA, maltobionic acid.

then subjected to two ascents in the second direction in the isobutyric acid–1 *N* NH_4OH solvent system. The compounds were located on the chromatograms by a silver nitrate procedure[10] (see Fig. 1).

The acidic product obtained from oxidation of maltose with glucose oxidase was isolated by placing the total content of the final incubation mixture in a band along the base line of a chromatogram. The chromatogram was developed by 2 ascents in the *n*-butanol–pyridine–water solvent system. After detection by the silver nitrate procedure, two carbohydrate components were observed. One cochromatographed with maltose and the other, the product of the oxidation, cochromatographed with gluconic and maltobionic acids. The material cochromatographing with authentic

gluconic acid and maltobionic acid was eluted with water from the chromatogram. An aliquot of this material was placed as a single spot on a chromatogram. Glucoamylase (0.5 mg/ml) was spotted at the same location, and this area of the chromatogram was again maintained in a moist condition for 1 h by repeated applications of the glucoamylase solution. After spotting the appropriate reference compounds at different locations along the origin, the chromatogram was subjected to two passes in the isobutyric acid–1 N NH_4OH solvent system. The compounds present on the chromatogram were again located by the silver nitrate procedure (see Fig. 2).

Results and discussion

The information presented in Figs. 1 and 2 clearly illustrates that glucose oxidase oxidizes maltose to maltobionic acid. The chromatograms reproduced in Fig. 1 illustrate that the product of the glucose oxidase reaction has the same R_F value as maltobionic acid and a lower R_F value than maltose or gluconic acid. Fig. 1B illustrates that the product is hydrolyzed by glucoamylase indicating an α-glucosidic linkage. In addition, the products of the glucoamylase action on the compound co-chromatographed with glucose and gluconic acid. Enzymatic hydrolysis of maltobionic

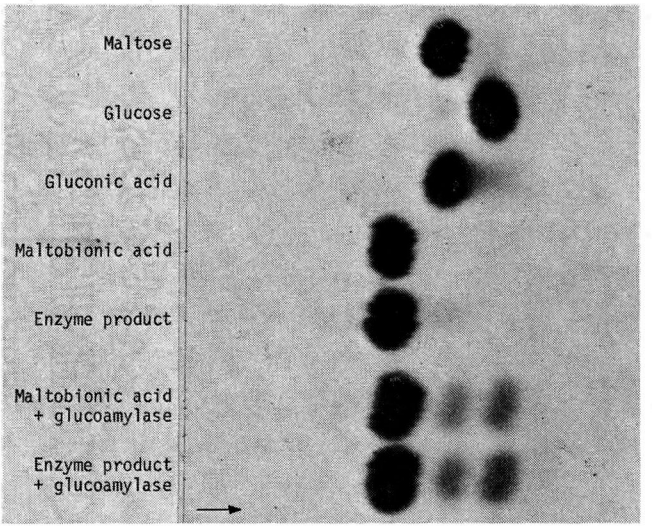

Fig. 2. A photograph of a paper chromatogram comparing both the relative mobilities of maltose, glucose, gluconic acid, maltobionic acid, and enzyme product, and the effect of glucoamylase on maltobionic acid and the enzyme product. Enzyme product refers to the product isolated from the maltose–glucose oxidase incubation mixture.

acid by glucoamylase has been demonstrated in an earlier report from this laboratory[11]. Utilizing this property of glucoamylase, further evidence demonstrating that maltobionic acid is the oxidation product of maltose is presented in Fig. 2. The chromatogram reproduced in this figure shows the mobility of different compounds that may be found in the assay mixture as well as the product of the glucose oxidase reaction. Also presented are results following treatment of the enzymatically produced maltobionic acid and chemically synthesized maltobionic acid with glucoamylase directly

on the chromatogram. In both cases, glucose and gluconic acid are the products of the hydrolase activity. The data in Fig. 2 also show that the rates of hydrolysis of maltobionic acid and the glucose oxidase product are very similar.

Thus, that maltobionic acid is the product of the action of glucose oxidase on maltose has been demonstrated by both cochromatography and by enzymatically characterizing maltobionic acid by direct application of glucoamylase to the chromatograms. The solvent systems selected for this study effected appropriate separation of the products, resulting in the reaction. The *n*-butanol–pyridine–water solvent system allowed the separation of unoxidized maltose from the possible oxidation products, maltobionic acid, and gluconic acid. Separation of maltobionic acid from gluconic acid was achieved using the isobutyric acid–1 *N* NH_4OH solvent system. The inclusion of the enzymatic hydrolysis step directly on the chromatogram aided in the final characterization of the small amount of maltobionic acid present in the reaction mixture.

This work was supported in part by grants from the National Institutes of Health (AM-10822), Bethesda, Md. and the Corn Refiners Association, Washington, D.C.

Department of Biochemistry,
Pennsylvania State University,
University Park, Pa. 16802 (U.S.A.)

H. R. KNULL*
J. H. PAZUR

1 D. KEILEN AND E. F. HARTREE, *Biochem. J.*, 42 (1948) 230.
2 D. SCOTT, *J. Agr. Food Chem.*, 1 (1953) 727.
3 L. A. UNDERKOFLER, *Proc. Intern. Symp. Enzyme Chem., Tokyo-Kyoto*, (1958) 486.
4 E. E. SMITH AND W. J. WHELAN, *Biochem. Prep.*, 10 (1963) 126.
5 N. O. KAPLAN, *Methods Enzymol.*, III (1957) 107.
6 J. H. PAZUR AND R. M. SANDSTEDT, *Cereal Chem.*, 31 (1954) 416.
7 C. FITTING AND E. W. PUTMAN, *J. Biol. Chem.*, 199 (1952) 573.
8 J. H. PAZUR AND K. KLEPPE, *Biochemistry*, 3 (1964) 578.
9 J. H. PAZUR AND T. ANDO, *J. Biol. Chem.*, 234 (1959) 1966.
10 F. C. MAYER AND J. LARNER, *J. Amer. Chem. Soc.*, 81 (1959) 188.
11 J. H. PAZUR AND K. KLEPPE, *J. Biol. Chem.*, 237 (1962) 1002.

Received October 19th, 1970

* Present address: Department of Biochemistry, Michigan State University, East Lansing, Mich. 48823, U.S.A.

CHROM. 5173

The identification of the five main histone fractions by comparative electrophoresis in polyacrylamide gel

The histones, the basic proteins associated with DNA in the nuclei of most multicellular organisms are thought to control transcription in some way. Five main fractions have been isolated and characterised from calf thymus, and designated F1, F2B, F2A2, F2A1 and F3 (ref. 1). It is now known that these five fractions also occur in bird[2], fish[3] and plant[4] somatic cells.

Methods for their preparation in large quantities[5,6] and for their characterisation by amino acid analyses[7] and polyacrylamide gel electrophoresis[8] have also been described. More recently we have described a simple method for running two proteins on one gel for comparative electrophoresis[9] and this paper shows how this method can be used for the identification of each of the five main histone fractions.

Polyacrylamide gel electrophoresis was carried out essentially as described previously[8,10] but with the addition of urea to the gel to a final concentration of 2 *M*. The application of two samples to one gel was also carried out as described previously[9].

The results obtained are shown in Fig. 1. It can be seen that each histone fraction can be identified with a corresponding band in the whole histone pattern. Frac-

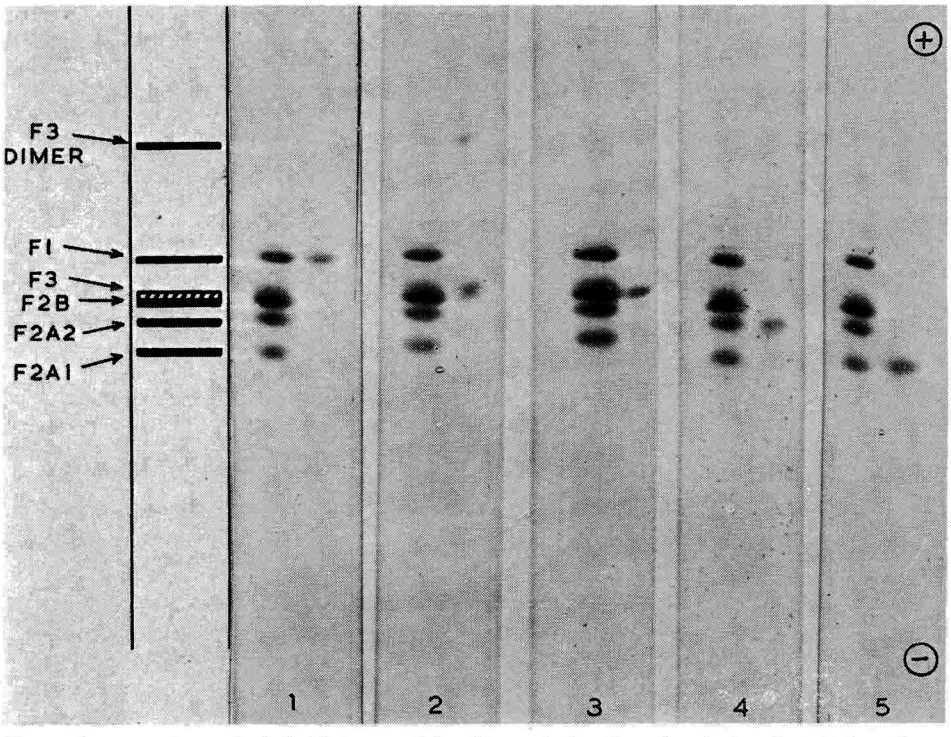

Fig. 1. A comparison of whole histone and the five main fractions by electrophoresis in polyacrylamide gel at pH 2.4. The fractions are on the right-hand side of the gels and are compared with whole histone on the left-hand side. 1 = F1; 2 = F3; 3 = F2B; 4 = F2A2; 5 = F2A1.

tions F3 and F2B run close together but are easily differentiated because of the unique dimer formation of F3 (ref. 11). F3 is the only histone fraction to contain cysteine (1 residue per mole) and partial dimer formation occurs by oxidation under these conditions giving a band of approximately half the mobility of F3. This does not occur with any other histone fraction. F3 and F2B can of course be better separated by extending the length of migration.

Using this method, any histone fraction or mixture of fractions can be identified and characterised, and if quantitative methods are subsequently employed[8] the relative amounts of each fraction can be determined.

Chester Beatty Research Institute,
Institute of Cancer Research,
Royal Cancer Hospital,
Fulham Road, London, S.W. 3 (Great Britain)

E. W. JOHNS
S. FORRESTER

1 E. W. JOHNS, in G. E. W. WOLSTENHOLME AND J. KNIGHT (Editors), *Homeostatic Regulators*, Churchill, London, 1969, p. 128.
2 G. VIDALI AND J. M. NEELIN, *Eur. J. Biochem.*, 5 (1968) 330.
3 J. PALAU AND J. A. V. BUTLER, *Biochem. J.*, 100 (1966) 779.
4 D. M. FAMBROUGH AND J. BONNER, *Biochemistry*, 5 (1966) 2563.
5 E. W. JOHNS, *Biochem. J.*, 92 (1964) 55.
6 E. W. JOHNS, *Biochem. J.*, 105 (1967) 611.
7 J. A. V. BUTLER, E. W. JOHNS AND D. M. P. PHILLIPS, *Advan. Biophys. Mol. Biol.*, 10 (1968) 209.
8 E. W. JOHNS, *Biochem. J.*, 104 (1967) 78.
9 E. W. JOHNS, *J. Chromatog.*, 42 (1969) 152.
10 C. DICK AND E. W. JOHNS, *Biochim. Biophys. Acta*, 174 (1969) 380.
11 S. PANYIM, R. CHALKLEY, S. SPIKER AND D. OLIVER, *Biochim. Biophys. Acta*, 214 (1970) 216.

Received November 23th, 1970

J. Chromatog., 55 (1971) 429–430

CHROM. 5168

Electrophoretic heterogeneity of crystalline insulin: A comparison of methods

The heterogeneity of crystalline insulin has been demonstrated by a number of methods. On paper[1] or cellulose acetate[2] electrophoresis with high concentrations of urea present to dissociate aggregated proteins, about six fractions may be separated, which apparently correspond to a series of deamidated insulins. MIRSKY AND KAWAMURA[3] studied crystalline insulins from eleven species by polyacrylamide gel electrophoresis, and found marked heterogeneity in each case, all the separated fractions having the biological properties of insulin. The presence of 8 *M* urea, however, had no effect on the electrophoretic pattern, so aggregated insulin molecules may have been absent. Other separation techniques have nevertheless shown the presence of molecules very different in size from insulin: gel filtration of bovine insulin on Sephadex G-50 resulted in the separation of several fractions one of which, with a molecular

weight of *ca.* 9,300, was identified as the single chain insulin precursor, proinsulin[4]. The present work compares the results obtained when crystalline insulin samples were fractionated using electrophoresis on conventional and gelatinised cellulose acetate membranes and polyacrylamide gels. The molecular weights of some of the fractions present have been estimated by introducing sodium dodecyl sulphate and iodoacetamide into the acrylamide gel electrophoresis buffers.

Materials and methods

Three different crystalline samples of bovine insulin (standard grade, *ex* English pancreas; standard grade, *ex* American pancreas; Isophane grade) were kindly donated by Boots Pure Drug Co. Ltd., and others were obtained from Mann Research Laboratories, Calbiochem and Sigma; a sample of porcine insulin was also obtained from Mann Research Laboratories. All samples had activities of *ca.* 25 I.U. per mg.

Cellulose acetate electrophoresis was carried out using a Tris–barbiturate buffer, pH 9.0, $I = 0.025$, using both conventional (Millipore U.K. Ltd. and Shandon Scientific Co. Ltd.) and gelatinised ("Cellogel RS", Arnold R. Horwell Ltd.) membranes. 2–3 μl samples at 2% w/w concentration were used with the conventional strips, and 20 μl samples at 8% w/w concentration with Cellogel RS. Protein fractions were stained with 0.5% w/v Ponceau S (Ed. Gurr Ltd.) in 5% trichloroacetic acid and densitometric traces of the stained membranes were obtained by reflectance using a Joyce-Loebl "Chromoscan". Disc electrophoresis on 7.5% w/w polyacrylamide gels at pH 8.5 were performed according to ORNSTEIN AND DAVIS[5]. Experiments were performed at ambient temperatures of 3° and 22° and the temperature in the gels monitored using a calibrated thermocouple. The gels were stained with Amido Black and scanned by transmission densitometry in the Chromoscan. Molecular weight determinations on 10% w/w polyacrylamide gels were performed using the method of WEBER AND OSBORN[6]. The buffer contained 1% w/v sodium dodecyl sulphate and 0.002 *M* iodoacetamide (British Drug Houses, Ltd.). Bovine serum albumin, pepsin, trypsin, β-lactoglobulin, lysozyme, cytochrome *c* and protamine sulphate (B.D.H. Ltd. and Sigma) were used as molecular weight markers and the protein bands were stained with 0.6% w/v Coomassie Blue in methanol–acetic acid (3:1).

All the insulin samples examined were revealed to be heterogeneous by all the methods used. With each method, however, the electrophoresis patterns given by the different insulins were similar and it was not possible to distinguish individual samples.

Results and discussion

Electrophoresis on conventional cellulose acetate was not a very satisfactory method of analysis; not more than four weakly-stained and poorly-separated bands could be distinguished. The use of Cellogel RS gelatinised cellulose acetate, however, produced superior resolution. A typical densitometer trace is shown in Fig. 1(a). Fig. 1(b) shows the results of the analysis of the same insulin sample by polyacrylamide gel electrophoresis. Although the protein bands are sharper and better resolved in the latter case there is an unmistakable similarity between the two traces, approximately six fractions being separated in each case. Since separations effected by polyacrylamide gel electrophoresis are normally due in part to a molecular sieving effect, which is presumably absent in cellulose acetate membranes[7], these results

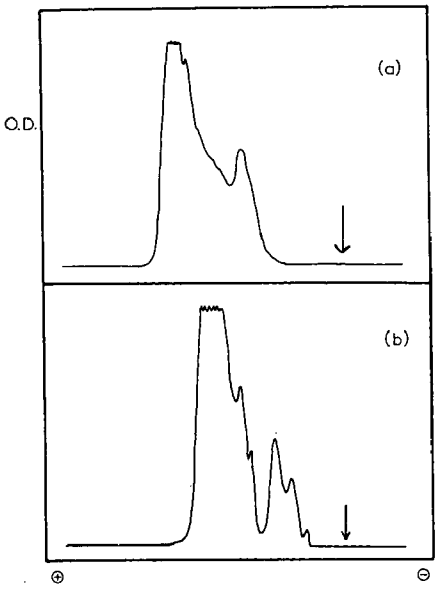

Fig. 1. Electrophoretic separation of crystalline insulin (Boots Pure Drug Co. Ltd., *ex* English pancreas) on (a) Cellogel RS gelatinised cellulose acetate, and (b) 7.5% polyacrylamide gel. Densitometer traces of stained protein bands. Arrows mark the position of sample application.

indicate that most of the separated fractions may have molecular weights similar to that of native insulin, *i.e.* that they are modified insulins. Because of the possibility of different dyebinding capacities in the separated fractions no attempt was made to estimate their relative concentrations.

When gel electrophoresis runs were performed at an ambient temperature of 3° rather than 22°, there was no improvement in the separations obtained. The thermocouple showed that the gel temperature after the first few minutes of the run was not greatly dependent on the ambient temperature. In all experiments, the temperature at first rose sharply but reached a constant value after 40–50 min. With a constant current of 5 mA per gel this final temperature was *ca.* 43° when the ambient temperature was 3°, and *ca.* 46° when the ambient temperature was 22°. Representative data are given in Table I. Similar temperature increases for runs at room temperature were recently reported by KNUDSEN *et al.*[8].

The presence of contaminants with molecular weights different from that of insulin was established by incorporating sodium dodecyl sulphate and iodoacetamide in the polyacrylamide gel electrophoresis buffers. In these conditions a linear relationship was found between the mobilities and the logarithms of the molecular weights of the marker proteins, whose molecular weights lie in the range 3,000–66,000. Other workers have found that the linear relationship does not hold over the whole of this range[9]. Staining of the protein bands in these experiments was found to be difficult possibly because of competition between dye and sodium dodecyl sulphate molecules for sites on the protein surface. When the insulin samples were examined, three bands were observed, whose mobilities corresponded to molecular weights of approximately 3,000, 6,000 and 22,000. The second of these figures is close to the

TABLE I

TEMPERATURE VARIATIONS IN ACRYLAMIDE GEL COLUMNS DURING GEL ELECTROPHORESIS

Time after start of experiment (min)	*Temperature (°C)*	
	Ambient temperature 3°	*Ambient temperature 22°*
1.5	16.0	—
3	17.0	25.5
6	19.0	27.0
9	20.5	28.0
12	22.5	29.5
15	25.0	—
18	27.0	31.5
24	31.5	35.0
30	37.0	39.0
36	41.5	43.0
42	42.5	46.0
48	—	46.0
54	—	46.0
60	43.5	46.0

molecular weight (5,750) of insulin itself, but the other two bands represent contaminants which may be quite distinct proteins. No band corresponding to the molecular weight of proinsulin could be detected, perhaps because of the poor staining.

It was concluded that the crystalline insulin samples studied contained both modified insulin molecules and contaminants of very different molecular weights. It was also found that electrophoresis on gelatinised cellulose acetate was a satisfactory method for the analysis of such samples.

Department of Chemistry,
University of Technology,
Loughborough, Leics. (Great Britain)

L. A. GIFFORD
J. N. MILLER
R. J. STRETTON

1 F. SUNDBY, *J. Biol. Chem.*, 237 (1962) 3406.
2 F. H. CARPENTER AND S. L. HAYES, *Biochemistry*, 2 (1963) 1272.
3 I. A. MIRSKY AND K. KAWAMURA, *Endocrinology*, 78 (1966) 1115.
4 H. ZÜHLKE AND J. BEHLKE, *FEBS Letters*, 2 (1968) 130.
5 L. ORNSTEIN AND B. J. DAVIS, *Ann. N.Y. Acad. Sci.*, 121 (1964) 321, 404.
6 K. WEBER AND H. OSBORN, *J. Biol. Chem.*, 244 (1969) 4406.
7 G. B. DEL CAMPO, *Clin. Chim. Acta*, 22 (1968) 475.
8 P. U. KNUDSEN, H. E. KNUDSEN AND J. GORSEN, *Anal. Biochem.*, 36 (1970) 192.
9 A. K. DUNKER AND R. R. RUECKERT, *J. Biol. Chem.*, 244 (1969) 5074.

Received November 16th, 1970

Book Review

CHROM. 5229

Active Carbon, Manufacture, Properties and Applications, M. SMIŠEK AND S. ČERNÝ, Elsevier, Amsterdam, 1970, V + 479 pp., price Dfl. 95.00.

This book is a revised and updated version of a 1964 Czech edition. It deals with the manufacture, structure and applications of active carbon (charcoal), the theory of adsorption on active carbon, specific methods for evaluating the properties of active carbon, and a general treatment of adsorption dynamics. The emphasis throughout is on the industrial uses of active carbon. Specific references to charcoal chromatography occur in Chapters 5 (Applications) and 7 (Methods for Studying the Properties of Active Carbons). Applications of charcoal chromatography receive quite brief treatment (six pages total) and the references are mainly to work published before 1960. The measurement of adsorption isotherms by gas chromatography is treated in greater detail (15 pages total), and the references cited are more recent (about half since 1960, two since 1965).

The chromatographer who picks up this book will be generally disappointed. Liquid column chromatography on charcoal has played an important historical role, and the technique retains significant advantages for some applications. However, the reader must look elsewhere for a good review of charcoal chromatography, or for a clear understanding of its uniquely useful features. Recent work on the separation of higher boiling mixtures by gas–solid chromatography on graphitized carbon (as summarized in KISELEV's book, *Gas-Adsorption Chromatography*) is not cited, and the separation of anything except gases by gas chromatography is not discussed. Those aspects of adsorption theory which receive attention are pertinent mainly to industrial applications, and their extension to the specialized systems of chromatography can prove misleading.

Union Research Center, Union Oil Company of California, Brea, Calif. (U.S.A.) L. R. SNYDER

Author index

Subject index

Errata

J. Chromatog., 50 (1970) 10–18

Page 14, Table III(a), line 7 in the table should read

	30°				40°			
	PF	*PM*	*GCI*	*SI*	*PF*	*PM*	*GCI*	*SI*
trans-1,2-DCEth	$\bar{1}$.805	$\bar{1}$.773	$\bar{1}$.809	$\bar{1}$.797	$\bar{1}$.793	$\bar{1}$.776	—	$\bar{1}$.788
	50°				60°			
	PF	*PM*	*GCI*	*SI*	*PF*	*PM*	*GCI*	*SI*
trans-1,2-DCEth	$\bar{1}$.781	$\bar{1}$.751	—	$\bar{1}$.786	$\bar{1}$.782	$\bar{1}$.742	—	—

J. Chromatog., 54 (1971) 413–421

Page 418, Fig. 8 and page 419, Fig. 9: "Trichloroacetic acid (ml/100 ml)" should read "Acetic acid (ml/100 ml)".